Alkaline Earth and Cerium Compounds

A Thesis Presented by

Stewart Anthony Miller

In partial fulfilment of the requirements
for the award of the degrees of

Doctor of Philosophy
of the
University of London
and
Diploma of Imperial College

Department of Chemistry
Imperial College of Science, Technology and Medicine
London SW7 2AY

August 1995

Abstract

Chemical vapour deposition (CVD) principally involves the thermal conversion of a metal-organic precursor (such as metal alkoxides and β-diketonates) to a thin film of the metal oxide. Homoleptic β-diketonates often have solubility problems due to oligomerization. They can be made more soluble by the appropriate choice of alkyl group e.g. t-butyl and CF_3, which block coordination sites. The metal centres may not be completely coordinatively saturated by these chelating ligands and aggregates often result.

On the addition of an appropriate Lewis base, these aggregates are cleaved to form soluble, molecular species which may be preformed in the solid state or alternatively the Lewis base is added to the CVD carrier gas. These ligands give improved volatility and mass transport properties. Part one describes the synthesis and characterization of a number of complexes which have shown some of the properties necessary for CVD precursors. The use of multidentate glymes and amines as Lewis bases has resulted in the isolation of air / moisture stable, low melting, hydrocarbon soluble, volatile complexes.

Although there are many studies on lanthanide (III) carboxylates, there is a dearth of work relating to cerium (IV) and that which has been done is limited to the smaller carboxylates. Chapter five describes the synthesis and characterization of a range of novel cerium (IV) carboxylates using larger straight chain and branched acids. These compounds are synthesized from cerium ammonium nitrate in either aqueous or anhydrous media. The compounds synthesized are shown to be hexameric with a common Ce_6O_8 core framework around which the carboxylate ligands coordinate. These compounds form the basis to the rest of the Thesis.

The reaction of these carboxylates with various neutral and potentially charged coordinating ligands has been investigated in Chapters six (hydrocarbyl) and seven (perfluoro), the very different chemistries of the two species necessitating the division.

Cerium is the only lanthanide element which has numerous stable (3+) and (4+) compounds. Chapter eight describes the interchangeability of the Ce^{3+}/Ce^{4+} oxidation states. Firstly the cerium (IV) carboxylates are light sensitive and photoreduce to Ce(III) species in either sunlight or ultraviolet light. Secondly cyclic voltammetric studies of the Ce^{3+}/Ce^{4+} couple has been investigated. Finally chemical oxidation of Ce (III) carboxylates with peracetic acid has been shown to give similar Ce (IV) species to those produced *via* the aqueous route.

Acknowledgements

Primarily, I would like to thank Dr Simon Drake, for giving me the chance to study and helping me realise more of my potential. I would also like to express my thanks to Professor Mike Mingos who took over the 'Drake group' and threw himself into a whole new world of chemistry. Belated thanks go to John Graham (CV), the NMR (Dick Sheppard and Paul Hammerton), mass spectrometry (John Barton and Geoff Tucker) and microanalysis (Hilary O'Callaghan) departments of I.C. who have been made to struggle under the sheer weight of submissions. Thanks too go to the solid-state NMR service at U.C.L. and Simon Bastians at I.C. for the Raman spectra. In the same vein I would like to express my sincerest thanks to the crystallographic departments at both Imperial College (David Williams and Andy White) and especially Cardiff (Prof. Mike Hursthouse, Abdul Malik and Ian Baxter) for allowing me to learn a little about what it is you all get up to.

To my industrial sponsors Rhone-Poulenc chemicals (Manchester and Lyon) and more especially Dr. Ian Hawkins, thanks for a) the money, b) the football tips and c) the chance to see what chemistry is really like in the outside world. I hope this Thesis goes some way to answering any questions you may have had about what my end of the bargain was. Thanks too to Dr. Tim Leedham (InorgTech) for the numerous gifts of chemicals and hardware.

To all my chemistry colleagues in the DMPM group over the years, especially John, Janni, JAD (he of the dancing loins), Booma, Kevin, Dave, Alan, Paul, Izoldi and also to the Inorganic staff especially Bill Griffith and Brent Young, a big thankyou goes out for keeping me entertained, sustained and well explained over the last three (six!) years.

Salutations to the (too) numerous (to mention) members of the Royal College of Science rugby team with whom I have enjoyed many sober and 'alternative' hours over the years. Both the magistrate of a certain province of central London and I would like to thank you all, especially Glenn, Vince, Bas, Rhid, Darren and all the other cheerful (beerful) funsters I've had the pleasure of playing with over six years. Cheers and beers to all of you and don't forget to keep 'the woman in red' warm for me lads!

Finally thanks to Claire for getting me up, out and over the bench.

"Peace, bread, war and freedom are the best we can achieve, but wearing badges is not enough, in days like these"

Billy Bragg 'days like these' 1985.

Contents

List of Tables

List of Figures

Abbreviations

A.E.	alakaline earth
amu	atomic mass unit
β-diket	β-diketonate
β-diketF	fluorinated β-diketonate
bdmap	1,3-bis(dimethylamino)propan-2-ol
benz	benzoate
br	broad (IR and NMR)
^{t}Bu	tertiary butyl
^{t}BuEE	tertbutoxy-ethoxyethane
bzpd-H	1-benzyl-1,3-butanedione
calcd.	calculated
CAN	cerium ammonium nitrate
cek	3,5-dimethylheptanoate (cekanoate)
CPMAS	Cross Polarisation Magic Angle Spinning
18-C-6	18-crown-6
δ(IR)	in plane bending vibration
δ(NMR)	chemical shift in ppm
dch18-C-6	dicyclohexano-18-crown-6
diglyme	$CH_3(OCH_2CH_2)_2OCH_3$
diki	^{t}BuC(O)CHC(CH_3)N(CH_2)$_2$O(CH_2)$_2$OCH_3
2,4-di^{i}Pr	2,4-diisopropyl
2,6-di^{i}Pr	2,6-diisopropyl-
dipic	pyridine-2,6-dicarboxylate
2,4-di^{t}Bu	2,4-ditertiarybutyl-
2,6-di^{t}Bu	2,6-ditertiarybutyl-
dmb	2,2-dimethylbutyrate
dme	dimethoxyethane (monoglyme)
dmf	dimethylformamide
dmop	2,9-dimethyl-1,10-phenanthroline
dmp	2,2-dimethylpentanoate
dmso	dimethyl sulphoxide
dppd-H	1,3-diphenylpropanedione
DSC	Direct Scanning Calorimetry
DTG	first derivative of TGA curve
ε	molar extinction coefficient
eb	2-ethylbutyrate
edta	ethylenediaminetetraaceticacid
eh	2-ethylhexanoate (octoate)
EI+	Electron Impact positive ion mode (Mass Spectrometry)
emb	2-ethyl,2-methylbutyrate
en	$H_2NCH_2CH_2NH_2$: ethylenediamine
ESR	electron spin resonance
Et_2O	diethyl ether
EtOH	ethanol
FAB+ve	Fast Atom Bombardment positive mode(Mass spectrometry)
fdhd-H	6,6,6-trifluoro-2,2-dimethyl-3,5-hexanedione
fhd-H	1,1,1,2,2,6,6,7,7,7-decafluoro-3,5-heptanedione
fod-H	1,1,1,2,2,3,3-heptafluoro-7,7-dimetyl-4,6-octanedione
heptaglyme	$CH_3(OCH_2CH_2)_7OCH_3$
hfpd-H	1,1,1-5,5,5-hexafluoro-2,4-pentanedione

hmdz	hexamethyldisilazide
HMPA	hexamethylphosphoramide
hmteta	$(CH_3)_2NCH_2CH_2N(CH_3)CH_2CH_2N(CH_3)CH_2CH_2N(CH_3)_2$: hexamethyltriethylenetetraamine
HOAr'	2,4,6-tritertbutylphenol
isopentane	2-methylbutane
iva	isovalerate (3-methylbutyrate)
Ln	lanthanide element (non-specific)
mb	2-methylbutyrate
$MeCO_3H$	peroxyacetic acid (peracetic acid)
MeOH	methanol
MOCVD	Metal Organic Chemical Vapour Deposition
m-Ph	*meta* substituted phenyl
mv	2-methylvalerate
ν(IR)	stretching vibration
OAc	acetate
oct	octanoate
o-Ph	*ortho* substituted phenyl
π(IR)	out of plane bending vibration
Pc	phthalocyanate
pdfo	pentadecafluorooctanoate
pd-H	2,4-pentanedione (acac)
pfb	heptafluorobutyrate
pfp	pentafluoropropionate
phen	1,10-phenanthroline
phenol'	substituted phenol
pmdeta	$(CH_3)_2NCH_2CH_2N(CH_3)CH_2CH_2N(CH_3)_2$
p-Ph	*para* substituted phenyl
Pr^i	iso-propyl
Pr^iOH	isopropanol
py	pyridine
sar	sarcophagine (3,6,10,13,19-Hexaazabicyclo[6.6.6]icosane)
STA	Similtaneous Thermal Analysis
$TBAPF_6$	n-tertbutyl ammonium hexafluorophosphate
^tBu	tert-butyl
tdfnd-H	1,1,1,2,2,3,3,7,7,8,8,9,9,9-tetradecafluoro-4,6-nonanedione
terpy	2,2',2''-terpyridine
tetraglyme	$CH_3(OCH_2CH_2)_4OCH_3$
tfa	trifluoroacetate
tfdh-H	1,1,1-trifluoro-5,5-dimethyl-2,4-hexanedione
tfpd-H	1,1,1-trifluoro-2,4-pentanedione
TGA	Thermal Gravimetric Analysis
tgme	triethylene glycol monomethyl ether
thf	tetrahydrofuran
tmeda	$(CH_3)_2NCH_2CH_2N(CH_3)_2$: tetramethylethylenediamine
tmhd-H	2,2-6,6-tetramethyl-3,5-heptanedione
tmnd	1,8-bis(dimethylamino)naphthalene
TMS	tetramethylsilane
triglyme	$CH_3(OCH_2CH_2)_3OCH_3$
triki	$^tBuC(O)CHC(CH_3)N(CH_2)_2O(CH_2)_2O(CH_2)_2OCH_2CH_3$
VT	variable temperature (NMR)
XPD	X-ray Powder Diffraction
XPS	X-ray Photoelectric Spectroscopy

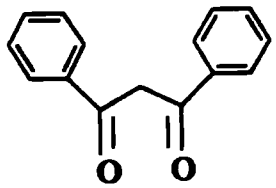

dppd-H

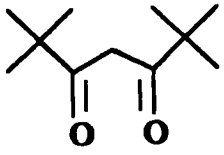

tmhd-H

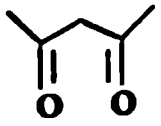

pd-H

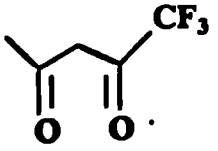

tfpd-H

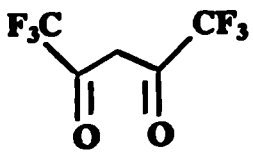

hfpd-H

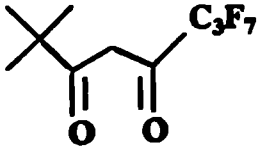

fod-H

Pictoial representation of β-diketones used within this Thesis

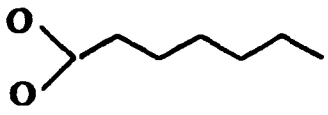

heptanoate (hept)

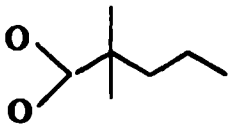

2,2-dimethylpentanoate (dmp)

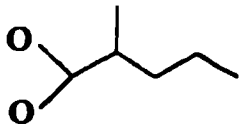

2-methylvalerate (mv)

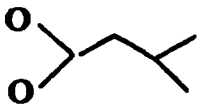

isovalerate (iv)

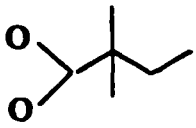

2,2-dimethylbutyrate (dmb)

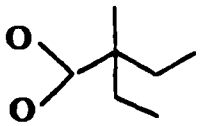

2-ethyl,2-methylbutyrate (emb)

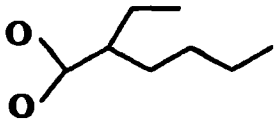

2-ethylhexanoate (eh)

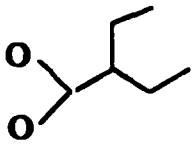

2-ethylbutyrate (eb)

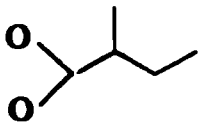

2-methylbutyrate (mb)

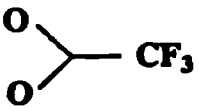

trifluoroacetate (tfa)

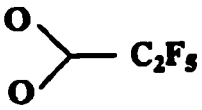

pentafluoropropionate (pfp)

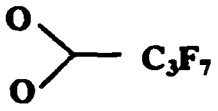

perfluorobutyrate (pfb)

Pictoial representation of the carboxylates used within this Thesis

PART 1 :

THE STABILIZATION OF ALKALINE EARTH METAL β-DIKETONATES BY MULTIDENTATE OXYGEN AND NITROGEN DONOR LIGANDS

Chapter 1

AN INTRODUCTION TO METAL ALKOXIDE AND β-DIKETONATE COMPLEXES

The principal aim of this Thesis was to synthesize stable complexes from the air and moisture sensitive Group 2 homoleptic β-diketonate complexes. This objective was achieved using multidentate oxygen and nitrogen donor ligands. The physical and chemical properties of these compounds have been studied as a prelude to an investigation of their suitability as metal oxide film precursors in MOCVD experiments.

1.1 Overview

Although inorganic 'ceramics' have been used for many thousands of years their application in industry today has increased significantly. Compounds based on metal oxides, nitrides, borides and carbides have all found recent applications. The properties of these materials include hardness and wear resistance, mechanical strength, high thermal and chemical stability and low density. Therefore, some of these compounds have found applications as electrical and thermal insulators. Many also show semiconducting (SiC) and piezoelectric ($Pb_xTi_{1-x}O_3$ and $BaTiO_3$) properties. The latter group of mixed metal oxides is particularly important in the context of this project.

Alkoxides have been known since the mid nineteenth century and the first reported compound, silicon tetra-iso-amyloxide was synthesized by Ehbelman in 1846.[1] Alkoxide derivatives of at least seventy elements are known and have found applications as paints, catalysts and coatings.[2] The importance of metal alkoxides for making ultra-high purity ceramics is rather more recent. Not only do they form well characterized ceramic powders, but they are also important as precursors for films and gels.[3]

Single or multicomponent oxide thin films are of interest for electronic and optoelectronic devices, catalysts, high T_c superconductors, corrosion protectors, etc. The preparation of thin films is usually achieved using one of two traditional routes, either the hydrolytic (sol-gel) or pyrolytic (metal organic chemical vapour deposition (MOCVD)) conversion of precursors. In order to form metal oxide films it is desirable that the precursor has a M-O bond already in place, therefore, metal alkoxides and β-diketonates are ideal from this point of view.[4]

The sol-gel process has been used for metal alkoxides and alkoxysilanes for many years.[5] A homogeneous solution of the precursor is prepared by dissolving the material in the parent alcohol. Controlled hydrolysis is then performed producing a gel containing the hydrated metal oxide. One such technique is dip coating which involves the immersion of the substrate into the precursor solution, and its removal at a controlled rate. This leaves a

film on both sides of the substrate which is left open to the atmosphere so that further hydrolysis can occur. The gel is then dried, compacted and fired to produce a ceramic material at a temperature much lower than that required for conventional melting processes. The advantages of this process resides in the high purity of the metal alkoxide precursors, the homogeneity of the components and the low processing temperature.[6]

Evaluation of appropriate precursors for MOCVD applications is based on volatilization temperatures which are studied in part by TGA and DSC techniques. Metal β-diketonates are generally solids, but despite this difficulty they are more widely used as precursors for MOCVD than alkoxides. This is a result of their increased hydrolytic stability and higher volatility compared with metal alkoxides.[7] For CVD conversions solid or liquid coordination compounds are evaporated, entrained in a carrier gas and then thermally decomposed on a hot substrate to form the required (mixed) metal oxide (or nitride, fluoride etc.) film.

β–diketonate derivatives are thermally converted into metal oxides in the case of oxyphilic alkaline earth and lanthanide metals, whereas the later transition metals form metallic films. Thermolysis in the presence of hydrogen appears to be a means of improving the purity of the deposited film as well as decreasing the temperatures for the deposition. Fluorinated ligands are observed to enhance volatility, but the formation of metal fluoride in addition to the oxide (as is observed for hfpd, fod and tfpd ligands for example) is often problematical. Barium fluoride may be converted to the oxide either by aqueous washing or by introducing a flow of oxygen over the film.[8]

1.2 Synthesis of metal alkoxides

In general the choice of a synthetic route to a metal alkoxide is dictated by the electronegativity of the metal(s) involved. For electropositive metals, e.g. alkali and alkaline earth metals, direct reaction with the alcohol may be used. For rather less reactive metals, e.g. aluminium and beryllium, a catalyst may be needed. The halides of relatively electronegative elements, e.g. boron and silicon, may be reacted with alcohols in the presence of a base such as pyridine, ammonia or alkylamides, to synthesize the required alkoxide and ensure complete halide replacement.

Due to the moisture and air sensitivity of alkoxides, which lead to their ready decomposition, the solvents and ligands, etc. used in the syntheses must be rigorously dried and purified before use. Some more detailed aspects of metal alkoxide syntheses are

described below.

1.2.1 Reaction of the bulk metal with alcohols [9]

Due to the low pK_a values of alcohols and phenols only the very electropositive alkali and alkaline earth metal alkoxides can be synthesized by this method. The addition of a Group 1 or 2 metal to a pre-distilled and dried alcohol, in an inert atmosphere, yields the alkoxide, e.g.

$$M + ROH \longrightarrow MOR + 1/2\ H_2 \quad \text{(i)}$$
$$(M = Li, Na, K)$$

The rate of the reaction is highly dependent on the nature of the alcohol. Very large sterically demanding alcohols react considerably more slowly, as the rate is partly dependent on the relative acidity of the hydroxylic hydrogen atom.

The heavier alkaline earth metal alkoxides (Ca, Sr and Ba) have, with few exceptions, remained largely uninvestigated.[10-11] This is due to a number of reasons;

(a) The levels of oxide and hydroxide contamination of the metal.

(b) The presence of other metals in quantities >1%, resulting in the poor activities of commercially available metals.

(c) The inherent air and moisture sensitivity of the products, which caused considerable handling problems in early studies.

(d) Thermal sensitivity and insolubility in many organic solvents, due to their polymeric nature.

The heavier Group 2 metals react directly with ethanol forming pure ethoxide products providing rigorous anaerobic techniques are employed and the metal has been prewashed in ethanol.[12] e.g.

$$M + \text{xs. EtOH} \longrightarrow [M(OEt)_2(EtOH)_4]_n \quad \text{(ii)}$$
$$(M = Mg, Ca, Sr \text{ and } Ba)$$

This prewash method cleans the surface of the metal, freeing it of any oxide or hydroxide

impurities, thereby ensuring the formation of a pure compound.

Pertinent to this report is the stabilization by the parent alcohol of the metal ethoxides. These compounds are fine crystalline powders which were formerly considered to be non-volatile and insoluble in non polar solvents.[12] We have shown that their solubility is greater than previously recognized when the complexes are isolated as pure needle like crystals. The degree of oligomerization has not yet been established as these compounds are highly sensitive to the atmosphere and as such are as yet impossible to characterize by crystallographic means. Turova *et al.*, have structurally characterized the related calcium oxo- ethoxide complex $[Ca_6O_2(OEt)_8].14EtOH$ made by refluxing calcium ethoxide in air. This compound is air stable and soluble in aromatic solvents.[13]

For less electropositive metals the reaction with bulk metals will not proceed readily, due to the presence of an inert oxide film. If a catalyst is added, e.g. I_2 or $HgCl_2$, this will clean the metal surface or alternatively form an intermediate halide derivative which may then undergo a facile reaction with the alcohol,[14] e.g.

$$Sr + 2ROH \xrightarrow[\text{catalyst}]{I_2} [Sr(OR)_2]_n + H_2 \qquad \text{(iii)}$$

Mercury halides are generally used in the syntheses of alkoxides of the lanthanide metals, however, the mercury used must be kept to a low concentration (10^{-3} - 10^{-4} equivalents) to avoid any secondary reactions which lead to impurities that are often difficult to remove and also ligand cleavage reactions.[15]

A related route involves alcohol interchange. In general the ease of exchange follows the order: tertiary < secondary < primary, i.e. t-butoxides of titanium, for example, will undergo rapid exchange with ethanol and methanol.[16]

1.2.2 Reaction with metal halides

This route is more significant in terms of the number of elements which can form alkoxides and the relative cheapness of the starting materials. With the less electropositive elements, such as the p block elements, alcoholysis of the chloride goes to completion with the elimination of HCl.[17]

$$MCl_n + nROH \longrightarrow M(OR)_n + nHCl_{(g)} \qquad \text{(iv)}$$

(M = B, Si and P)

With lanthanides, which are considerably more electropositive, the addition of the

alcohols to chlorides results in the formation of solvates, unless an ammoniacal base is also present,[18] e.g.

$$LaCl_3 + 3\ Pr^iOH \text{ ----------> } LaCl_3(Pr^iOH)_3 \qquad (v)$$

However, a potential problem with this type of synthesis is the possible reaction of the liberated HCl with the alcohol, thereby generating water and a mixture of other organic products. Nelles[19] found that in the preparation of titanium alkoxides, the addition of ammonia ensured the production of an adduct free alkoxide of the formula $Ti(OR)_4$, with ammonium chloride as a byproduct. Applying the same method to zirconium tetrachloride, Bradley and Wardlaw succeeded in preparing zirconium tetralkoxides directly.[20]

$$TiCl_n + nROH \xrightarrow{NH_3} Ti(OR)_n + nNH_4Cl_{(ppt)} \qquad (vi)$$

1.2.3 Reaction with metal oxides and hydroxides

These syntheses are limited to the oxides and hydroxides of electropositive metals. Alkali and p block metal alkoxides may be prepared by dissolving the metal hydroxide in the alcohol,[21] e.g.

$$NaOH + EtOH \text{ ----------> } NaOEt + H_2O \qquad (vii)$$

$$MO + 2nROH \text{ ----------> } M(OR)_n + nH_2O \qquad (viii)$$
$$(M = B, Si \text{ and } Sn)$$

The water may then be removed as an azeotrope *via* co-distillation with benzene or toluene.

1.2.4 Reaction of metal alkyls and metal hydrides with alcohols

Metal alkyls with a high degree of ionic character react with alcohols or phenols to give alkoxides and aryloxides respectively, often in excellent yields. These reactions are important as they form the basis of the calorimetric measurement of a large number of metal-alkyl bond dissociation energies.[22]

This synthetic route is very convenient because the volatility of the hydrocarbon side products leads to a simple purification of the products.

$$MR_2 + R'OH \dashrightarrow RMOR' + RH \quad \text{(ix)}$$

This method has been successfully employed for the syntheses of alkoxides of Be, Mg and Zn.[23] Metal hydrides will also react, providing that the M-H bond is not too strong, e.g. aluminium hydride will react with the weakly acidic hydroxyl groups of alcohols and phenols to evolve hydrogen and produce an alkoxide,[24] e.g.

$$AlH_3 + nROH \dashrightarrow Al(RO)_nH_{3-n} + H_2(g) \quad \text{(x)}$$

1.2.5 Via substituted amides

The trimethylsilamide complex $Sr(NR_2)_2(thf)_2$ is a possible starting material into alkaline earth metal alkoxides, given its facile preparation from the metal in thf / NH_3 in the presence of $HN\{Si(Me_3)_2\}_2$.[25] Both of these materials can be used in an alcoholysis reaction, e.g.

$$Sr\{N(SiMe_3)_2\}_2(thf)_2 + 2ROH \dashrightarrow [Sr(OR)_2]_n + HN(SiMe_3)_2 \quad \text{(xi)}$$

A range of other synthetic routes are available to the inorganic chemist, e.g. metal vapour / alcohol co-condensation,[26] transesterification[27] or phenolysis of sulphides.[28]

1.3 Reactions of metal alkoxides

1.3.1 Reactions with Lewis bases

The reactivity of the metal alkoxides relies in part on the relative Lewis acidity of the metal centre, which is the main reason for oligomerization in these complexes and also on the volatility of the liberated alcohol which may be easily removed under reduced pressure. For Group 1 and 2 metals and the lanthanides, typical adducts involve coordinating O-donors such as Et_2O, thf and water. In some cases too, nitrogen donor bases may coordinate in a similar fashion,[29] e.g.

$$LiOAr + L \dashrightarrow [Li(OAr)(L)]_2 \quad \text{(xii)}$$

(where L = Et_2O, pyridine or thf)

1.3.2 Insertion reactions

Insertion reactions involving CO_2 or RCNO for example, have been observed for a number of metal alkoxides. The ligand resulting from the insertion can adopt a didentate bonding mode e.g. eqn (xiii),[30]

$$MOR + X{=}C{=}Y \longrightarrow MX\text{-}C(Y)\text{-}OR \quad \text{(xiii)}$$

(where X and Y = O or NR)

$$Mo_2(OR)_6 + 2\,CO_2 \longrightarrow Mo_2(OR)_4(O_2COR)_2 \quad \text{(xiv)}$$

Alkaline earth metal alkoxides may also undergo insertion reactions,[31] e.g.

$$[Mg(OMe)_2]_n + CO_2 \xrightarrow{MeOH} [Mg_9(CO_3)(O_2COMe)_7(OMe)_9(MeOH)_{14}] \quad \text{(xv)}$$

These alkoxides may be of use in the oil industry as additives. The insertion of such gases is important because the reactions are relevant to chemical processes which occur in petrol engines.

1.3.3 Protonolysis reactions

An important class of reactions of alkoxides and aryloxides is the substitution of an OR group by protonation and the elimination of the alcohol or phenol,[32] e.g.

$$L_nM(OR) + HX \longrightarrow L_nM(X) + HOR \quad \text{(xvi)}$$

A large number of molecules can react in this way; typically HX contains a H-S or H-O bond or else is a hydrohalic acid. The mechanism of the reaction rarely involves the direct protonation of the M-OR bond. Instead, initial coordination of HX via the lone pairs of electrons on X is necessary prior to transfer of the proton. Hence the rate of reaction is dependent on the steric encumbrance of both HX and the metal coordination site and the electronic donor-acceptor qualities of the two species.

1.3.4 Reactions with β-diketones

As has been suggested, metal alkoxides are not alone in their suitability for precursors of electroceramic materials, metal β-diketonates too play a very valuable role. Another example of the reactivity of metal alkoxides is the reaction of the alkaline earth

metal ethoxides, with β-diketones in an inert atmosphere, to produce either unadducted or solvent adducted complexes which are the basis to this Thesis,[33] e.g.

$$[M(OEt)_2(EtOH)_4]_n + 2\ \beta\text{-diket-H} \dashrightarrow [M(\beta\text{-diket})_2]_m + 6nEtOH \quad \text{(xvii)}$$

(where M = Ca, Sr or Ba; β-diket = tmhd, fod, tfpd, hfpd or dppd)

1.4 Coordination modes of metal alkoxides

The Lewis acidity and consequent electron deficiency of the alkaline earth metal centres in their alkoxide complexes enables these metals to form oligomers which utilize the bridging properties of the alkoxide ligand. The degree of oligomerization is dependent on a number of factors, including;

(a) The size of the metal. The larger ionic radius of the metal leads to greater ability to expand its coordination number and form bridging alkoxide species.

(b) Oligomerization becomes more pronounced as the metal becomes more electron deficient. Electropositive metals, therefore, often form larger aggregates.

(c) The steric effects of the alkoxide substituent. Generally the larger the substituent group, the lower the degree of polymerization.

Thus alkoxides of alkaline earth metals containing less bulky alkyl groups tend to form oligomers, while larger more sterically demanding ligands form complexes with significantly lower molecular weights. The simple methoxides $[M(OMe)_2]_n$ and ethoxides $[M(OEt)_2]_n$ often exhibit a high degree of oligomerization, with n being 2, 3 or 4, due to the bridging properties of the alkoxide groups, *via* the formation of conventional two-electron polar covalent bonds to give a μ-2 or μ-3 species, e.g.

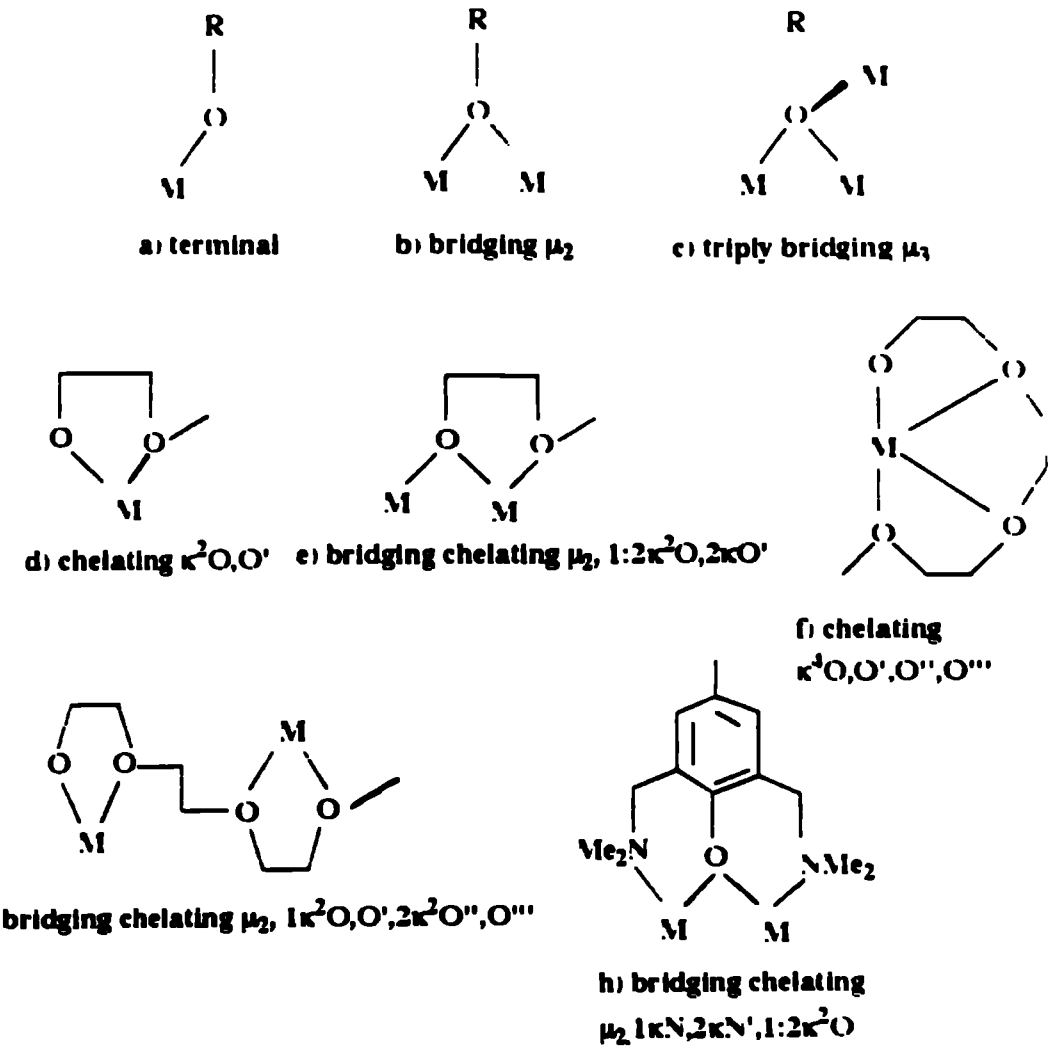

Figure 1.1 : Coordination modes for alkoxides and related ligands

The driving force for aggregation is the tendency of the metal to expand its coordination number.[4] Electropositive metals such as the alkaline earth metals, have high charge density to size ratios. For calcium, a coordination number of six is typical and the ligands generally surround the metal to generate an octahedral geometry. Coordination numbers of less than six are observed, however, for $[Ca(OAr')_2(thf)_3]$ and $[Ca(OAr')_2(thf)]_2$ where the coordination numbers are five and four respectively.[3,4] In these cases the presence of bulky aryl and Lewis base groups are sufficient to resist the formation of aryloxide bridges. For the majority of alkoxides, the strength of the alkoxide bridge is sufficiently great to preclude another mechanism of aggregation, e.g. the addition of another ligand L, containing a donor ligand.

Mass spectrometric evidence has been used to show that some oligomeric metal alkoxides retain their structures in the vapour state. Much more energy is generally required to vaporize an oligomeric species than is needed for a monomeric one and this often leads to complex decomposition processes in the gas phase.

Bridging may also be prevented by utilizing bulky alkyl groups to give a relatively volatile metal alkoxide, e.g. tertiary butoxides. The metal radius also plays a vital role in the coordination geometry. Using larger aryl groups may also have the effect of reducing aggregation. Chisholm *et al.* have reported the thf soluble complex, $[Sr_4(OPh)_8(PhOH)_2(thf)_6]$ formed from the reaction of strontium metal in thf and phenol.[35] In this complex all the metals have a coordination number of six, and a rare μ_3-phenol ligand is observed. A detailed account of the synthesis, physical and chemical properties and industrial applications of metal alkoxides is given in Mehrotra's book.[36]

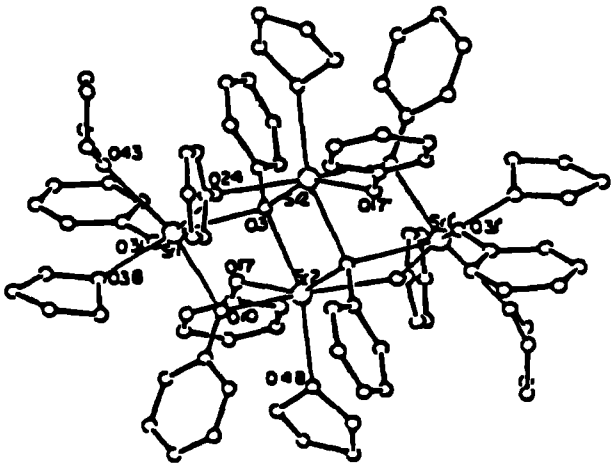

Figure 1.2 : X-ray crystal structure of $[Sr_4(OPh)_8(PhOH)_2(thf)_6]$

1.5 Synthesis of metal β-diketonates

The metal β–diketonates $M(RCOCHCOR')_x$ (where R and R' are alkyl, aryl or fluorinated alkyl etc.) are one of the most widely studied inorganic compounds. The variation of metals and R groups are almost limitless and both of these factors help to give these compounds their desirable properties. Metal β-diketonates have higher volatilities than alkoxides and as such are more appropriate for MOCVD precursors. However, the M-O bond is less rapidly hydrolysed than alkoxides; therefore, they are of less use as sol-gel precursors.

1.5.1 From metal alkoxides

As mentioned in section 1.3.4. previously, metal alkoxides undergo full or partial exchange with β-diketones in a stoichiometric manner. Providing anhydrous conditions and non-oxygenated solvents are used throughout, pure materials may be isolated.[37]

$$[Ti(OPr^i)_4] + n(\beta\text{-diket}) \xrightarrow{\text{hexane}} [(Pr^iO)_{4-n}Ti(\beta\text{-diket})_n]_m + nPr^iOH \quad \text{(xviii)}$$

1.5.2 From metal salts

The reaction of metal salts with β-diketones generally gives rise to metal β-diketonate derivatives and free acid, which attain equilibrium unless the β-diketonate derivative is highly insoluble in the reaction medium. In this way carbonates, acetates, nitrates and sulphates may be used for a range of metals,[38] e.g.

$$Al_2(SO_4)_3 + 6\,NH_4pd \longrightarrow 2\,Al(pd)_3 + 3\,(NH_4)_2SO_4 \quad \text{(xix)}$$

1.5.3 Direct methods

The direct synthesis of metal β-diketonates may be achieved by many routes e.g. M, MO_x, MCl_x and MH_x. Reaction between a metal halide and a β-diketone results in either a mixed halide or a homoleptic β-diketonate complex depending on the nature of the metal halide employed,[39] e.g.

$$BCl_3 + 2\,pdH \longrightarrow [B(pd)_2]^+Cl^- + 2\,HCl \quad \text{(xx)}$$

$$AlCl_3 + 3\,pdH \longrightarrow Al(pd)_3 + 3\,HCl \quad \text{(xxi)}$$

Generally the same conditions and limitations apply for the β-diketonates as for the aforementioned alkoxides.

1.6 Reactivity of metal β-diketonates

The chemical properties of the β-diketonate complexes have only been studied in detail recently. These investigations have led to many novel structures and also encouraged the development of new preparative methods.

1.6.1 Electrophilic substitution

Many electrophilic substitution reactions, e.g. halogenation, nitration, thiocyanation and acetylation, can be carried out under the required conditions without degrading the metal β-diketonate chelate rings which are acid labile.[40] These reactions are more widely observed with transition metals,[41] e.g.

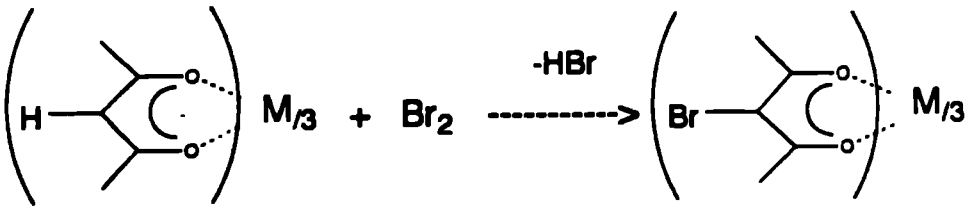

Figure 1.3 : Electrophilic substitution of β-diketonates

Electrophilic substitution generally occurs to place the electrophile at the carbon between the two C=O groups as above.

1.6.2 Adduct formation

The central metal atom in many β-diketonate complexes has a high tendency to increase its coordination number by complex formation. These reactions are common in alkaline earth metal chemistry due to the high acidity of the metal centre. Ligands such as water, ammonia, pyridine and CO_2 are often employed, e.g. $Mg(pd)_2SO_2$,[42] Mg(pd)(OMe).nMeOH[43] and $Mg(pd)_2$.1,8-*bis*(dimethylamino)naphthalene.[44]

1.6.3 Substitution reactions

With this group of reactions the nature of the reactants and reaction conditions are all important. Some transition metal 2,4-pentanedionates undergo replacement reactions with anhydrous hydrogen halides to form mixed species,[45] e.g.

$$M(pd)_3 + HX \xrightarrow[\text{benzene}]{\text{ether}} MX(pd)_2 \qquad \text{(xxii)}$$

(M = Mn^{III}, Fe^{III}, X = Cl, Br, I)

These chelates may then be capable of adduct formation with, for example, pyridine-N-oxide (L) to form $MX_2(pd).L_2$ type species.[46]

Nesemeyanov *et al.* reported that Fe^{III} and Zr^{IV} 2,4-pentanedionato complexes undergo replacement reactions with higher β-diketones, esters and alcohols,[47] e.g.

$$Zr(pd)_4 + 4\,AH \xrightarrow[\text{chloroform}]{\text{benzene}} Zr(A)_4 + pdH \qquad \text{(xxiii)}$$

(AH = benzoylpentanedione or salicyaldehyde)

$$Zr(pd)_2(NO_3)_2 + 2\,bzpdH \xrightarrow{\text{benzene}} Zr(bzpd)_2(NO_3)_2 + 2\,pdH \qquad \text{(xxiv)}$$

1.7 Coordination modes of β-diketonates

Oligomerization may be prevented and the formation of monomeric species favoured, by coordinatively saturating the metal centre. This is achieved by using ligands that can coordinate through more than one donor atom, e.g. chelating ligands. Substituted alcohols, furans and β-diketones are some of a long list of such chelating ligands which considerably reduce the polymerization of alkoxides.[48]

The additional donor atoms bind to the metal utilizing the chelate effect, while the bulky substituent groups provide the steric size needed for the prevention of molecular aggregation.[49] The reduced number of ligands provides the stability against decomposition and also reduces some of the problematical interactions with external Lewis bases blocking vacant coordination sites, i.e. labile ligands and the complications that arise from their incorporation into the product, an inherent problem with these species.

β-diketones are weak acids, which in the presence of a base form a chelating anion. This anion has a delocalized π-electron system. When the anion is protonated, there are three sites at which the proton may be bound. Two of these, the oxygens, are equivalent, but the other, the central carbon atom of the O-C-C-C-O ring, is different. The β-diketone molecule, therefore, exists in two different forms, depending on the site of protonation. 2,4-pentanedione, for instance, is an equilibrium mixture of these forms. They are rapidly interconverting, but each has a real existence. These forms are known as tautomers and this particular form of tautomerism is known as keto-enol tautomerism.

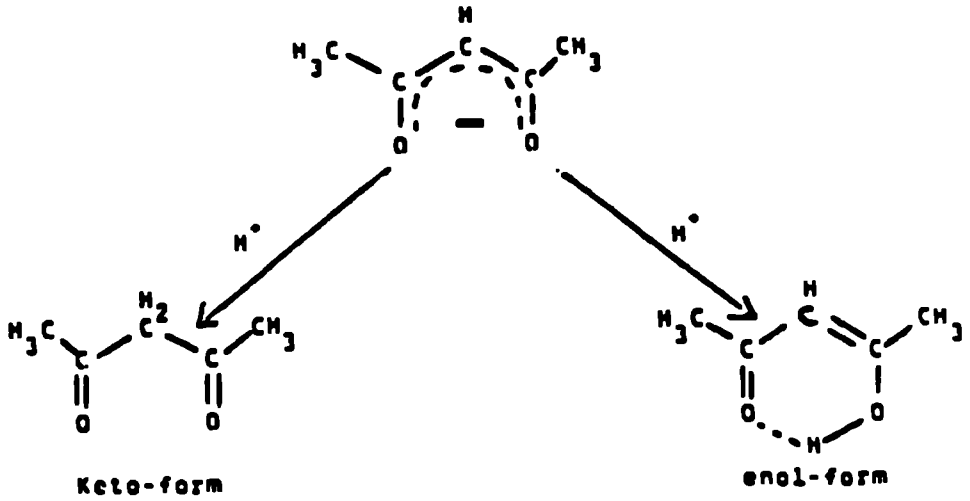

Figure 1.4 : Tautomeric forms of pd-H

Metal β-diketonate complexes are often very stable due to the favourable electron donation of the oxygen atoms in the chelate ring and the delocalization of the negative charge over the whole anionic ring. The size of the β-diketonate ligand helps to prevent oligomerization providing that bulky substituent groups, e.g. CF_3 and ^tBu, are employed. There is also the possibility of solvent coordination due to the high Lewis acidity of the metal and this may lead to difficulties in characterization. The presence of Lewis bases may also be a problem as we need to balance the advantages of polymerization limitation and complex stability, with possible contamination by excess carbon and fluorine atoms of the daughter product in the thin films produced by MOCVD.[4]

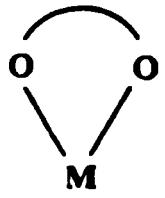

a) chelating κ^2O,O'

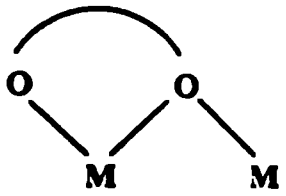

b) chelating bridging μ_2, $1\kappa O,1{:}2\kappa^2O'$

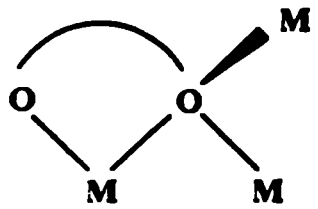

c) chelating bridging μ_3, $1\kappa O$, $1{:}2{:}3\kappa^3O'$

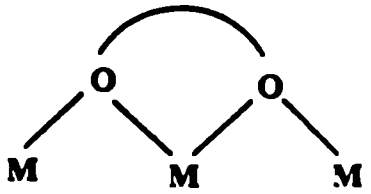

d) chelating bridging μ_3, $1{:}2\kappa^2O$, $2{:}3\kappa^2O'$

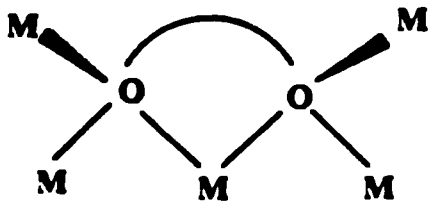

e) chelating bridging μ_5, $1{:}2{:}3\kappa^3O,3{:}4{:}5\kappa^3O'$

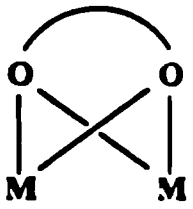

f) double chelating bridging μ_2, $1{:}2\kappa^2O,1{:}2\kappa^2O'$

Figure 1.5 : β-diketonate coordination modes

1.8 Molecular precursor design

Homoleptic β-diketonates are often rather insoluble due to the aggregation of the metal - ligand ensemble. They can be made more soluble by the appropriate choice of alkyl or aryl group e.g. t-butyl, CF_3, or phenyl. The use of these sterically bulky groups to block coordination sites increases the solubility even in hydrocarbon solvents. The metal centres may not be completely coordinatively saturated by these chelating ligands, however, and aggregates often result. Hollander *et al.* have shown this by the synthesis of $[Sr_4(dppd)_8(acetone)_2]$ from strontium nitrate, ethanol and an ethanolic solution of dppd (see Figure 1.6).[50]

On the addition of an appropriate Lewis base, these aggregates are cleaved to form soluble, molecular species. Lewis bases which have been employed include thf[51] and Et_2O[29] solvents, phosphines,[52] multidentate glyme[53] and amine[54] ligands and crown ethers.[55] These molecular entities may be preformed in the solid state and may be used directly as precursors to CVD. An alternative strategy is the addition of Lewis base additives to the carrier gas flow of the CVD apparatus. Typical additives to the homoleptic β-diketonates include tmhd-H,[48] NH_3[56] and other amines. These ligands result in the improvement of volatility and mass transport properties. In the case of multidentate glymes and amines, the isolated complexes are also seen to be air / moisture stable, whereas their precursors are air sensitive. Chapters 2 and 3 describe the syntheses and characterization of a number of air and moisture stable complexes which have shown some of the properties necessary for CVD precursors.

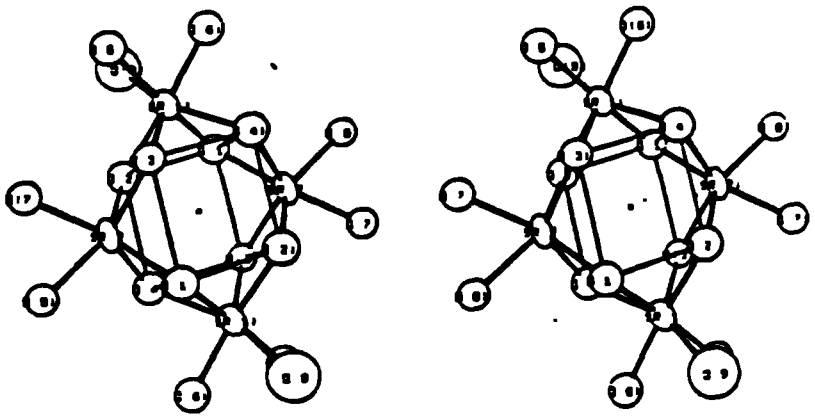

Figure 1.6 : Stereoscopic view of the X-ray crystal structure of $[Sr_4(dppd)_8(acetone)_2]$

Chapter 2

STABILIZATION OF GROUP II β-DIKETONATES BY OXYGEN DONOR LIGANDS

2.1 Introduction

Probably the primary obstacle to the widespread application of MOCVD to the growth of high T_c superconducting oxide thin films (e.g. $YBa_2Cu_3O_{7-x}$), is the absence of effective alkaline earth metal and in particular barium precursors.[57] The large ionic radius of Ba results in the preference for high coordination numbers; therefore, any lack of saturation leads to them being strongly associated in the solid state, significantly reducing their volatilities.

A major disadvantage of these precursors is that sufficient volatility is only attained in excess of 200°C. At these temperatures oligomerization and decomposition tend to occur, resulting in the formation of non-volatile metal species. The only commercially available barium compounds which shows significant volatility without decomposition are based on $[Ba(fod)_2]_n$ compounds.[58] Thin films have been laid down using $[Ba(fod)_2]_n$ itself as a precursor both at ambient pressure (and *ca.* 300°C), and at low (5 Torr) pressure. The latter shows that the sublimation temperature is significantly reduced (170°C).[59] It is clear therefore, that an alternative barium source with a lower evaporation temperature and higher thermal stability is needed.

The ideal characteristics of a molecular precursor for CVD applications are;

(a) It would need to be a crystalline solid of known stoichiometry.
(b) The material should be easy to handle and manipulate.
(c) Easy large scale synthesis is necessary for industrial scale up.
(d) The compound should be soluble in a range of organic solvents especially hydrocarbon solvents, to allow reactions to occur at low temperatures.
(e) The reaction should proceed in high yield, resulting in a pure product and without the need for expensive precautions.

Homoleptic metal β-diketonates, although generally less soluble than metal alkoxides in non-polar solvents, can be made soluble by the appropriate choice of the substituent alkyl groups.[60] This effect is due to a reduction of intermolecular interactions in the solid state. The increased volatility of β-diketonates over alkoxides is also due to the decrease in molecular complexity, owing to the bidentate nature of the diketonate ligand, and its potential to act as a chelating rather than a bridging entity.[49]

A typical problem encountered in the synthesis of these molecules is the contamination of the end products by water, the products being very prone to solvent uptake. If the reaction is carried out in aqueous media, then hydrated products such as $[Ba_5(tmhd)_9(H_2O)_3(OH)]$ are obtained.[61] The hydrogen bonding water molecules decrease the volatility of the complex and also lead to the contamination of thin films deposited by CVD.

Although alkaline earth metal homoleptic complexes of the tmhd ligand have been known for many years, only recently have they been structurally characterized. The barium complex is tetrameric with bridging ligands. The strontium complex is trimeric with a neutral tmhd-H ligand associated with it.[62] In this structure each of the metals is seen to have a different coordination numbers which range from 6-8. The calcium complex also consists of a triangular array of metals, each of which is six coordinate.[63] In these complexes the tmhd ligands adopt bridging, which satisfy the coordination requirements of the metal.

Complexes of fluorinated ligands such as hfpd and fod, often have greater volatilities than their hydrogen analogues,[55,64] while aryl groups tend to have lower .[4] A disadvantage of using fluorinated ligands, however, is that the Lewis acid characteristics of the barium metal are increased by the addition of a fluorinated substituents, therefore, its tendency to adduct formation is greater. For example, Bradley *et al.* have synthesized $[Ca(hfpd)_2(H_2O)_2]_2$ and $[Ba(hfpd)_2(H_2O)]_n$[65] from the reactions of the metal hydroxide and hfpd-H in aqueous solution.

2.1.3 Lewis base stabilised metal β-diketonates

It has previously been noted that an important criterion for β-diketonate complexes, which are useful as molecular precursors for MOCVD is the coordinative saturation of the metal centres. This is achieved through the addition of sterically demanding organic ligands.[4] Given the high coordination numbers of the metal centres in this type of complex a great deal of choice remains in the type of ligands.

In the absence of a Lewis base, homoleptic metal β-diketonates generally form polymeric insoluble materials. On the addition of a suitable Lewis base, the polymeric ensembles are cleaved to form simpler molecular species. The use of closed chain macrocyclic ligands such as crowns, torrands and cryptands, e.g.[Ba(hfpd)$_2$(18-crown-6)][55] provide specific examples. It may also be seen that carrying the reaction out in non-aqueous media yields Lewis base stabilised β-diketonates with high purities, e.g. $[Ba_2(tmhd)_4(Et_2O)_2]$.[66]

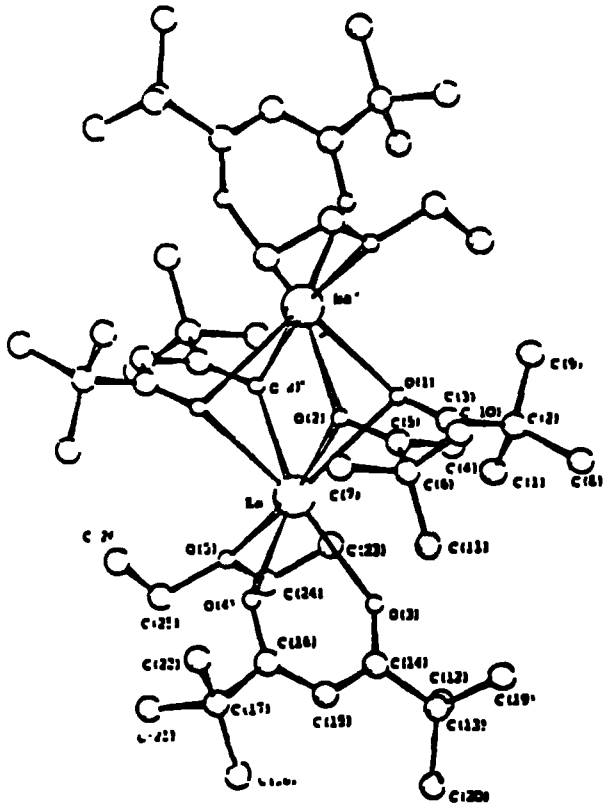

Figure 2.1 : X-ray crystal structure of $[Ba_2(tmhd)_4(Et_2O)_2]$

β-diketonates act mostly as chelating ligands, or as chelating and bridging ligands and, therefore, often result in a decrease in the degree of oligomerization, and greater volatilities. They do not tend to form air stable complexes with the alkaline earth metals, but many transition metal and rare earth metals do form stable β-diketonate complexes. The environment of these complexes is, therefore, modified by adding 'multi-pronged' Lewis bases, such as glymes or amines thereby filling vacant coordination sites.[53,67] Typical glyme ligands have between two and eight oxygen donor sites which they can use to bind to the metal centre, thereby excluding the chance of water coordination. The glyme ligands are generally only chelating and effectively reduce the metal's degree of oligomerization. More rare is the observation of a bridging - chelating glyme ligand.

Recently Marks[68] *et al.* combined a pendant Lewis base chain with a diketonate group in an attempt to form more volatile species. They have structurally characterized the monomeric compounds $Ba(diki)_2$ and $Ba(triki)_3$ amongst others, (where diki, and triki are β-ketoiminate ligands containing appended polyether lariats). These compounds have

proven, however, not to be as volatile as many previously studied β-diketonate complexes, due in part to the imbalance between both O- and N- donors of the same ligand chelating to one metal centre.

Water free glyme stabilized complexes have recently been synthesized by Gardiner *et al.*,[53] where β-diketones were added to a suspension of barium hydride in tetraglyme at room temperature; however low yields (*ca.* 40%) were observed. Another route into these complexes is to dissolve barium hydroxide in a Lewis base solvent e.g. dme or diglyme, prior to adding the β-diketonate, to yield $[Ba(tmhd)_2(dme)_2]_n$ and $[Ba(tmhd)_2(diglyme)]_n$ respectively.[69] Timmer *et al.* have formed similar complexes, e.g.$[Ba(hfpd)_2(tetraglyme)]$ where the metal centre is nine coordinate.[70] Very few crystal structures of these complexes exist; however, Drozdov *et al.*, [71] in attempting to improve the storage capability of $[Ba(tmhd)_2]_4$, added both tetraglyme and diglyme and isolated $[Ba(tmhd)_2(tetraglyme)]$ and $[Ba(tmhd)_2(diglyme)]_2(\mu\text{-}H_2O)$ respectively, the strontium analogue of the latter compound is described in this Thesis.

As far as MOCVD is concerned, the addition of a range of Lewis base additives, e.g. ammonia, amines and glymes, to the carrier gas flow, or the introduction of preformed stabilized compounds, results in the improvement of both volatility and mass transport properties. Indeed studies have shown they improve the volatility of $[Ba(hfpd)_2]_n$, which is not itself volatile below 200°C (10^{-5} Torr), whilst $[Ba(hfpd)_2(18\text{-crown-}6)]$[55] and $[Ba(hfpd)_2(tetraglyme)]$[53] sublime at 150-180°C and 120°C at 10^{-3} torr respectively. The related $[Ba(tdfnd)_2(tetraglyme)]$[72] is cleanly vaporized at 90°C (10^{-2}mmHg) from the liquid phase.

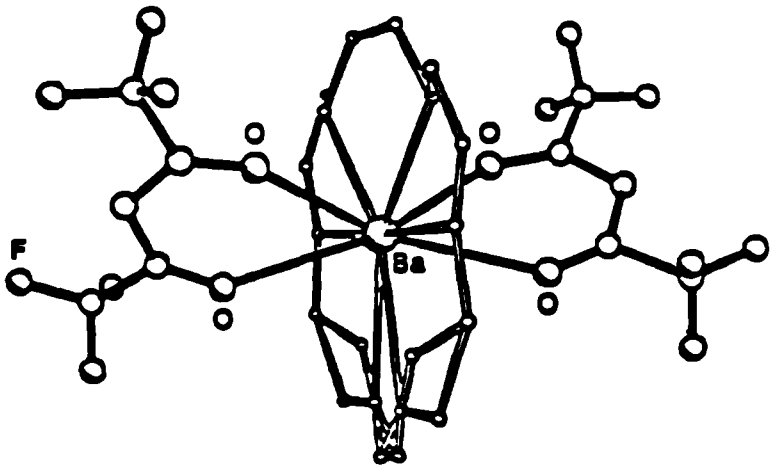

Figure 2.2 : X-ray crystal structure of $[Ba(hfpd)_2(18\text{-crown-}6)]$

As far as Group 2 β-diketonate complexes are concerned, the coordination of three β-diketonate ligands has not been achieved previously, although it has been proposed that the '*tris*' species are formed in the transfer process. Sievers'[73] approach to CVD is to add vapours of tmhd-H to the carrier gas and thereby increase and stabilize the vaporization rate of $[Ba(tmhd)_2]_4$ so that its vapour pressure remains constant for several hours. It also stabilizes the compound against decomposition during evaporation at temperatures as high as 300°C.

In gas chromatography the addition of fod-H to the helium carrier gas stream improves the shapes of the peaks observed for $[Ca(fod)_2]_n$ and $[CaBa(fod)_4]_n$ (the latter of which is formed only in the vapour phase).[74] Also with gas chromatography / mass spectrometry analysis, the introduction of liquid fod-H has a profound effect on the observed results for $[Ba(fod)_2]_n$. As fod-H is more volatile than the Ba chelate they become separated, and are postulated to be in equilibrium with the *tris* species; however, this means that contact between the two species is only transient, and the *tris* species can only be considered to exist in the gas phase.

2.2 Synthesis of oxygen donor stabilized β-diketonates

It has previously been noted that the addition of Lewis base ligands to the homoleptic β-diketonates, reduces the degree of oligomerization and produces more discrete entities. In this Chapter we describe the syntheses of air and moisture stable complexes which were formed according to the general equation (i);

$$[M(OEt)_2(EtOH)_4]_n + 2\ \beta\text{-diketH} \xrightarrow{\text{hexane}} \text{`}[M(\beta\text{-diket})_2]_n\text{'} \xrightarrow{\text{L-L}} [M(\beta\text{-diket})_2(\text{L-L})]_n \quad \text{(i)}$$

(M = Ca, Sr, or Ba; β-diketonate = dppd, hfpd, fod, tmhd; L-L = glyme or β-diketonate)

The results which have been obtained are summarized in Figure 2.3. The compounds produced are all low melting crystalline solids, and are formed in high yields. Although the starting materials, i.e. the ethoxides, are air sensitive, the *in situ* addition of β-diketone and multidentate glyme ligands result in air stable complexes. The reactions are carried out at room temperature and produce compounds which are soluble in a range of organic solvents including hydrocarbons. This route has a number of advantages over

those which have previously been used by other workers. Firstly, the *in situ* procedure makes reaction times very short, high temperatures are needed only to remove excess ethanol solvent and yields are > 65%.

For compounds (1) - (2), (4) - (5) and (7) - (11), only one equivalent of glyme is needed; however, for the diglyme complexes (3) and (6), two equivalents are used to completely solubilize the homoleptic β-diketonate complex in hexane solution, which is taken as the indication of the reaction being complete. It is noteworthy too that the diglyme ligand does not produce monomeric species with Ba and Sr as do the larger glymes. This is presumably due to the diglyme ligand having only three oxygen donor sites and therefore not enough to saturate the Ba and Sr metal centres. Conversely only half an equivalent of heptaglyme was added for (11) as the heptaglyme ligand has eight oxygen donors and is, therefore, capable of bridging two [$M(\beta\text{-diket})_2$] entities.

In contrast to the addition of glymes, a third β-diketonate ligand was added in the case of (12) and (13). These *tris* species may, therefore, not only be formed in the gas phase and thereby promote volatility in CVD experiments, but also in the solid state *via* the ethoxide route which we have developed. Once again these compounds are observed to be crystalline low melting solids, although air and moisture stability is poorer than for the glyme species. Product yields are also observed to be lower in the case of (13).

These routes have been extended by using alternative precursors, in the form of metal oxides, carbonates or hydroxides and using 95% ethanol as the reaction solvent. Compound (14) [$Ca(fod)_2$(triglyme)] was made by this route. The reaction workup for this type of synthesis involves the use of cheap starting materials, which need not be purified before use. Reaction times are slightly longer than for the metal ethoxide route, and the reaction needs to proceed at refluxing temperatures. The advantages are that no expensive techniques are needed for this type of synthesis, e.g. no Schlenk lines or glove boxes. All the necessary equipment (e.g. round bottomed flasks and rotary evaporators) is readily and cheaply available. There are several noteworthy factors associated with the general synthetic method:

(i) This synthetic strategy of preparing glyme stabilized metal β-diketonates made *in situ* from a metal oxide or hydroxide is the first example for Group 2 complexes and generally leads to anhydrous complexes.

(ii) The coordinative saturation of the metal centre by the multidentate Lewis bases leads to air / moisture stable precursors of known stoichiometry, and thus is highly flexible since L-

L may be varied providing that it contains more than three donor atoms.

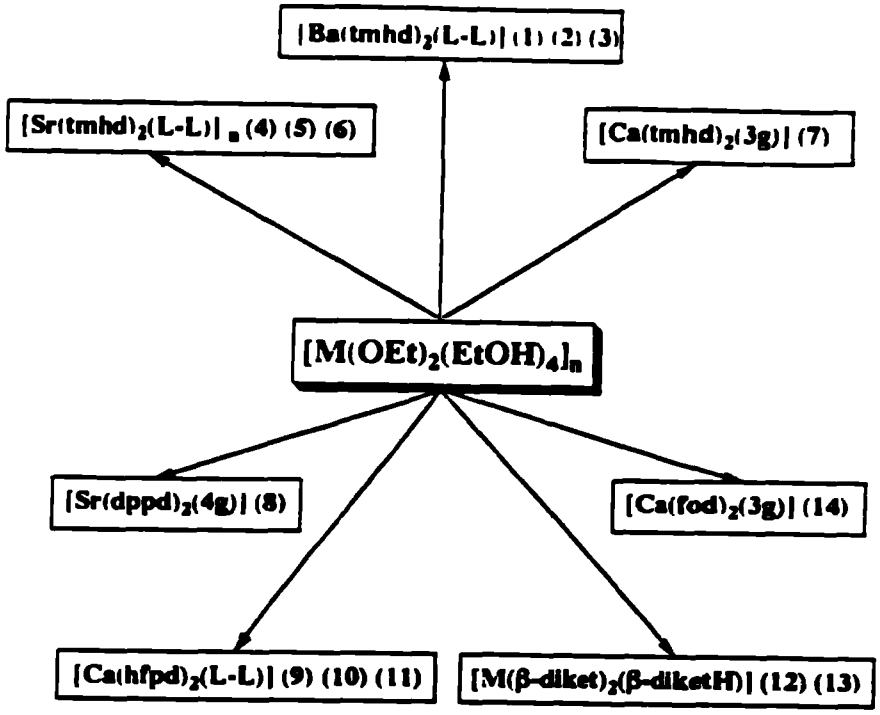

Figure 2.3 : Reaction scheme for glyme stabilized compounds (1) - (14)

Reaction Conditions : Two basic reactions conditions (A) and (B) have been employed; (A) The respective metal ethoxides (or in the case of compound (14) the oxide) were dissolved in n-hexane (chloroform (8), 95% ethanol (14)), to which was added two equivalents of the required β-diketone, the following multidentate glymes (L-L) were then added: tetraglyme (1), (4), (8), (9); triglyme (2), (5), (7), (10), (14); diglyme (two equivalents) (3), (6); heptaglyme (half equivalent) (11). (B) The respective metal ethoxides were dissolved in n-hexane (12) or chloroform (13), to which was added three equivalents of tmhd-H (12) or dppd-H (13).

The compounds which resulted from these syntheses and are discussed within this Chapter are:

(1) $Ba(tmhd)_2$(tetraglyme), (2) $Ba(tmhd)_2$(triglyme), (3) $[Ba(tmhd)_2(diglyme)]_2$,

(4) $Sr(tmhd)_2$(tetraglyme), (5) $Sr(tmhd)_2$(triglyme), (6)$[Sr(tmhd)_2(diglyme)]_2(\mu\text{-}H_2O)$,

(7) $Ca(tmhd)_2$(triglyme), (8) $Sr(dppd)_2$(tetraglyme), (9) $Ca(hfpd)_2$(tetraglyme),

(10) $Ca(hfpd)_2$(triglyme), (11) $[Ca(hfpd)_2]_2$(heptaglyme), (12) $Sr(tmhd)_2$(tmhd-H),

(13) $Ca(dppd)_2$(dppdH), (14) $Ca(fod)_2$(triglyme).

2.3 Spectroscopic characterization

2.3.1 Infrared analyses

Pertinent IR data for complexes (1) - (14) are summarized in Table 2.1 The IR spectra of complex (1) shows characteristic bands for the β-diketonate, with strong absorption bands at 1602cm^{-1} for C--O, and 1532 and 1504cm^{-1} for C--C. These results may be contrasted to the unadducted β-diketonates, where numerous peaks are found in this region. This is most likely due to the differing coordination modes of the β-diketonate ligand (i.e. chelating or bridging or a combination of both) in the base free compounds, whereas the structural orientations of the β–diketonate ligands are essentially equivalent in the Lewis base adducted complexes, because they are simply chelating. Due to the coupling of the vibrational modes, however, the precise assignments of the bands is not completely unambiguous.

The C--O stretch(es) of the tmhd complexes are generally observed between 1605 and 1580cm^{-1}, and the C--C stretch(es) at *ca.* 1535(±5), and *ca.* 1505(±5)cm^{-1}. The dimeric tmhd complexes, (3) and (6), all exhibit more vibrations (two C--O and two C--C stretches) in this region consistent with their formulation as dimeric units (see Figure 2.4).

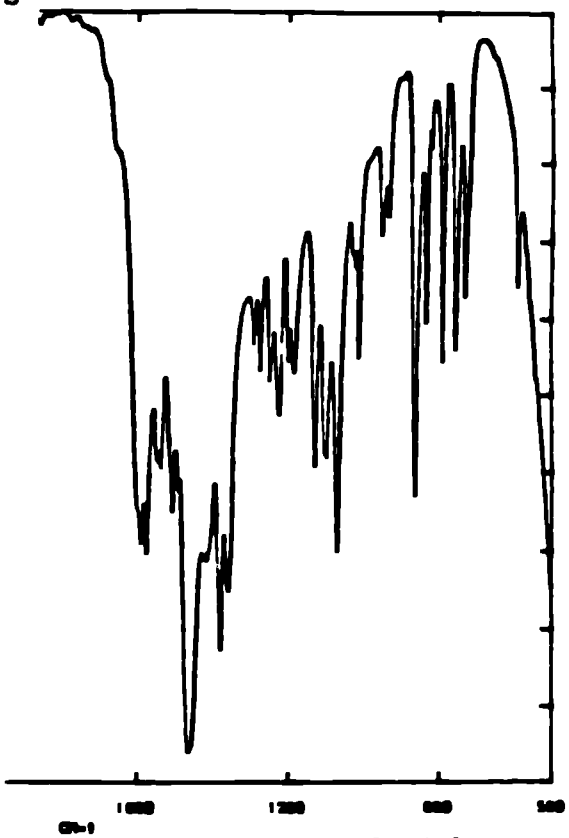

Figure 2.4 : Infrared spectrum of (3) between 2000-500cm^{-1} in nujol

Table 2.1 : Selected Infrared Data of Complexes (1) - (14) :

Compound	ν(C-H)[a]	ν(C=O)	ν(C=C)	ν(C-O-C)
(1)	2947	1602	1532, 15043	1354, 1099
(2)	2949	1587	1532, 1504	1356[a], 1099
(3)	2964	1571	1535, 1504	1356, 1126
(4)	2969	1591	1532, 1502	1356[a], 1104[a]
(5)	2949	1600	1532, 1502	1356[a], 1102[a]
(6)	2966	1586, 1574	1535, 1504	1356, 1105
(7)	2949	1594, 1575	1532, 1504	1349, 1101
(8)	2918	1620, 1582	1513	1324, 1108
(9)	2947	1658, 1594	1532, 1504	1349, 1101
(10)	2957, 2867	1658, 1589	1530	1366, 1140
(11)	2947, 2869	1661, 1590	1526	1368[a], 1355[a], 1338[a], 1143
(12)	2962, 2868	1725*, 1592 1579, 1561	1537, 1505	---
(13)	2958, 2926 2853	1732*, 1598	1557, 1523[a]	---
(14)	2954, 2837	1648	1538, 1502	1352, 1123

N.B. all spectra run at 20 C as nujol mulls except ([a]) which was run as a hexachlorobutadiene mull, * is actually C=O for *tris* species

For the dppd complex (8), hfpd complexes (9) - (11) and fod complex (14), a shift in frequency for the C=C and C=O stretching modes is observed. Comparing the relative β-diketonate ligands, we observe a clear tendency for the C=O and C=C stretches to shift to a higher frequency with fluorinated and aryl substituted ligands. Similar results have also been observed in other complexes of β-diketonate ligands.[58] This observation is due to the increased electron removal from the $M\text{-}O_2\text{-}C_3$ ring by the phenyl and fluorine groups when compared with the ^tBu groups. This has the effect of strengthening the C=O and C=C bonds and consequently their stretching frequencies are higher. Conversely, the M-O bonds are weakened with fluorinated substituents, therefore the frequencies are lower.

The general trend for C=O and C=O stretching frequencies is;

Tmhd < Fod < Dppd < Hfpd

For all the pure β–diketone ligands it can be seen that there is a peak between 1735-1770cm^{-1} corresponding to the C=O bond. These peaks are shifted to lower frequency when the ligands are complexed to a metal as the bond is weakened; consequently we observe the C=O stretching frequencies at ca 1600cm^{-1}. However, if we observe a peak in the 1750 - 1720cm^{-1} region for the *tris* species then we may postulate that there is a neutral β-diketone ligand complexed, and the *tris* complex is present, with the metal still in the 2+ oxidation state.

This β-diketone C=O stretch is observed for the two *tris* complexes (12) and (13) at 1725 and 1732cm^{-1} respectively. These two peaks are rather weak, however, and cannot be taken as direct evidence of the formation of a *tris* species by themselves. For example this band may be due to the presence of some excess β–diketone ligand.

The bands assigned as ν (C-O-C) for the glyme ligands occur at slightly lower frequencies than the same peaks for the free ligand, at 1354, and 1103cm^{-1}. The shifts from the free ligand are *ca.* ±20cm^{-1} which is indicative of coordinated glyme ligands. Secondly we note that there are more C-O-C stretches for the heptaglyme ligand in complex (11), in the region 1360-1100cm^{-1}. For the parent ligand there are two peaks, here we observe four. This is possibly due to the different coordination mode of the heptaglyme ligand i.e. both bridging and chelating, in comparison with the monomeric compounds in which the glyme ligands simply chelate.

2.3.2 ^{1}H NMR characterization

Selected features of the ^{1}H spectra for complexes (1) - (11) and (14) are summarized in Table 2.2. The spectroscopic data are in general accord with the structural data. There is no evidence of any ethanol from the starting material $[M(OEt)_2(EtOH)_4]_n$, nor is there any water from the atmosphere and only one characteristic signal for one type of β-diketonate and glyme environment is observed. A shift downfield of the methylene protons of the glymes ligands is observed on coordination to the alkaline earth metals, a fact which has been observed previously by other researchers.[53] This is induced by the electropositive metals withdrawing electron density from the glyme ligands, consequently the hydrogen atoms become more acidic and are shifted downfield.

The chemical shift of the methyl group of the tmhd ligand is observed not to change greatly between complexes (1) - (7); it has a very narrow range between δ 1.24 and 1.35. The range of the OCH_3 protons of the glyme ligands is also very small (δ 2.97 - 3.24). There is, however, a distinct trend in the tmhd complexes, in that the peak is observed to shift downfield in the order tetraglyme < triglyme < diglyme. No such trend is observed for the fluorinated ligands, but the narrow range of frequencies still applies.

The OCH_2 resonances of the glyme ligands are readily differentiated by NMR studies for all complexes except (11), which is rather complex due to the large number of resonances in this region. The ^{1}H NMR cannot readily differentiate between all seven different CH_2 resonances at 90MHz, with only five observed, one of which is a summation of three CH_2 groups. The respective methylene resonances can be identified according to Figure 2.5 which details the classification of tetraglyme methylene protons.

$$(CH_3OCH_2CH_2OCH_2CH_2)_2O$$

a b c d

Figure 2.5 : Identification of tetraglyme methylene groups.

For the other complexes, there is no clear trend in the shifts of the methylene protons as is observed with the OCH_3 protons. The only clear trend is observed between fluorinated and non-fluorinated ligands. The OCH_2 resonances of the hfpd complexes are generally shifted upfield with respect to the tmhd complexes by *ca.* δ 0.1 - 0.3.

Table 2.2 : Selected ^1H NMR Data of Complexes (1) - (11) and (14) :

Compound	CH_3	OCH_3	CH_2(a)	CH_2(b)	CH_2(c)	CH_2(d)	CH_2(e,f,g)	CH
(1)	1.35	3.07	3.26	3.33	3.36	3.39	---	5.83
(2)	1.32	3.13	3.15	3.20	3.31	---	---	5.79
(3)	1.28	3.18	3.17	3.20	---	---	---	5.80
(4)	1.24	3.10	3.21	3.24	3.36	3.39	---	5.70
(5)	1.34	3.15	3.04	3.24	3.31	---	---	5.80
(6)	1.24	3.20	3.17	3.18	---	---	---	5.77
(7)	1.32	3.16	3.11	3.28	3.47	---	---	5.80
(8)	----	3.23	3.41	3.42	3.48	3.51	---	6.57
(9)	----	3.05	2.95	3.12	3.14	3.18	---	6.30
(10)	----	2.97	2.71	2.93	3.24	---	---	6.29
(11)[a]	----	3.19	3.21	3.39	3.41	3.43	3.46	5.52
(14)	1.13	3.25	3.48	3.60	3.88	---	---	5.73

N.B. all spectra run at 270MHz, 20 C in C_6D_6 except ([a]) which was recorded at 90MHz, 20°C in d_6-dmso.

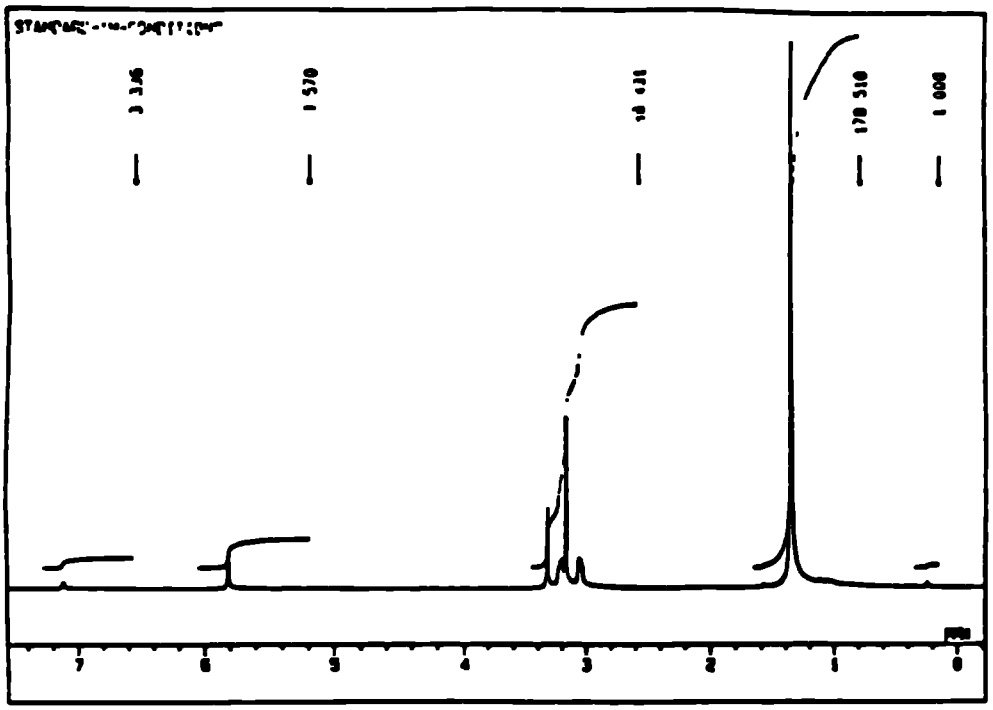

Figure 2.6 : ^{1}H NMR spectra of (5) in C_6D_6

The CH proton of the dppd ligand is, by its nature, very acidic due to the presence of two phenyl groups on the outside of the chelate ring and this explains the shift downfield of the CH proton of (8) to δ 6.57. The CF_3 groups are also sufficiently electron withdrawing to have a marked effect on the CH proton. A typical hfpd complex has a CH proton resonance at δ 6.30(±0.3), whereas that of the fod complex (14), is at δ 5.76 and that of the CH of a typical tmhd complex, δ 5.70(±0.3). This trend is consistent with the decreasing acidity of the methine proton, and the decreasing electron withdrawing capability of the substituent groups.

2.3.3 Solvent effects on ^{1}H NMR spectra of (12) and (13)

Pertinent ^{1}H and ^{13}C NMR data are shown in Tables 2.3 and 2.4 respectively. The NMR data correlates with melting point and infrared data in confirming that the complexes (12) and (13) exist as *tris* species.

For complexes (12) and (13) the NMR data can be observed in a wide range of solvents due to the exceptional solubility of these complexes in aromatic (benzene and toluene) and coordinating (dmso and chloroform) solvents. The ^{1}H NMR of (12) in dmso and toluene both show the presence of CH and CH_2 protons. In dmso solvent two CH

Table 2.3 : Selected ^1H NMR of (12) - (13) :

Compounnd	δ(CH_3)	δ(CH_2)	δ(CH)
(12)[a]	0.99	3.80	5.35
			6.21
(12)[b]	1.01	----	5.56
(12)[c]	1.34	3.60	5.97
(12)[d]	1.15	----	5.78
(13)[a]	----	4.88	7.34
(13)[b]	----	----	6.70
(13)[c]	----	----	6.51
(13)[d]	----	----	6.56

Table 2.4 : Selected ^{13}C NMR of (12) - (13) :

δ(CH_3)	δ(CH_2)	δ(CH)	δ(CO)
25.89, 28.69	----	86.67, 86.96	210.60
31.12	----	90.74	203.84
27.85	----	90.16	200.74
27.96	----	90.74	201.78
---	50.20	93.46	183.42
----	----	92.21	184.92

(a) spectra run at 20 C in d_6-dmso (b) run at 20°C in $CDCl_3$ (c) run at 20°C in C_7D_8 (d) run at 20°C in C_6D_6

resonances are observed at δ 5.35 and 6.21, and one CH_2 at δ 3.80. Integration reveals that there are two protons associated with both types of resonance. In toluene only one broad CH resonance is observed at δ 5.97 and also a very broad CH_2 resonance at δ 3.60. In both chloroform and benzene no CH_2 resonances are seen but integration of the CH peak defines it as a combination of both CH and CH_2 protons. No CH_2 resonances are observed in any solvent for ^{13}C NMR analysis. It is noteworthy, however, that two CH_3 and two CH resonances are observed in dmso, corroborating the results gained from ^1H NMR.

Complex (13) shows similar results in the different solvents. The ^1H NMR spectra in dmso shows the presence of both CH and CH_2 protons. The first sharp peak is at δ 7.34 and the CH_2 at δ 4.88. However, integration of these peaks gives a ratio of 3 : 1 and not the expected 1 : 1 as is seen for (12). ^{13}C NMR also shows a very weak signal for the CH_2 carbon at δ 50.2 in conjunction with a CH carbon at δ 93.46.

* In chloroform, toluene and benzene a single sharp CH proton is observed; once again integration suggests a combination of the two types of protons within the M-O-C ring. It is noteworthy too that compared with the proton of (13) in dmso, all the other three are shifted dramatically upfield by *ca.* δ 0.8(±0.1) in the less coordinating solvents. No CH_2 resonances are observed in the ^{13}C spectrum of the other solvents.

Dmso is probably acting as a non-innocent ligand, in that it can coordinate according to the following reaction equilibrium:

$$[Sr(tmhd)_2(tmhd\text{-}H)] \underset{}{\overset{dmso}{\rightleftharpoons}} [Sr(tmhd)_2(dmso)_n] + tmhd\text{-}H \quad (ii)$$

The dmso ligand is able to approach the metal and coordinate. Group 2 metals being oxophillic readily attract such molecules (this explains the water coordination problems and the need for such rigorous anaerobic techniques). Because the dmso ligand releases the β-diketonate ligands, both the keto and enol forms of tmhd-H are observed.

In contrast toluene is acting as an innocent solvent, in that it fails to coordinate sufficiently to the metal centres to interrupt the fluxional exchange. It is noticeable, however, that [Sr(tmhd)$_2$(tmhd-H)] (12) shows a CH and a very broad CH_2 peak in toluene. The two peaks are broad suggesting that we are nearing the coalescence point for

exchange, and the presence of a combined CH and CH_2 peak. The relative integration of this peak also suggests a combination of the two resonances.

Benzene and chloroform, as with toluene do not combine with the metal as a solvate; therefore we once again see rapid exchange and the presence of only one resonance. Another equilibrium is thus set up:

$$[Ca(dppd)_2(dppd\text{-}H)] \underset{C_6D_6}{\overset{C\text{-}D_8 \,/\, CDCl_3}{\rightleftharpoons}} [Ca(dppd)_2] + dppd\text{-}H \quad \text{(iii)}$$

Presumably this equilibrium lies well over to the left otherwise we would clearly see a separate CH and CH_2 peak. The ^1H NMR spectra of $[Ca(dppd)_2(dppd\text{-}H)]$ (13) in D_6-dmso and $CDCl_3$ are show below.

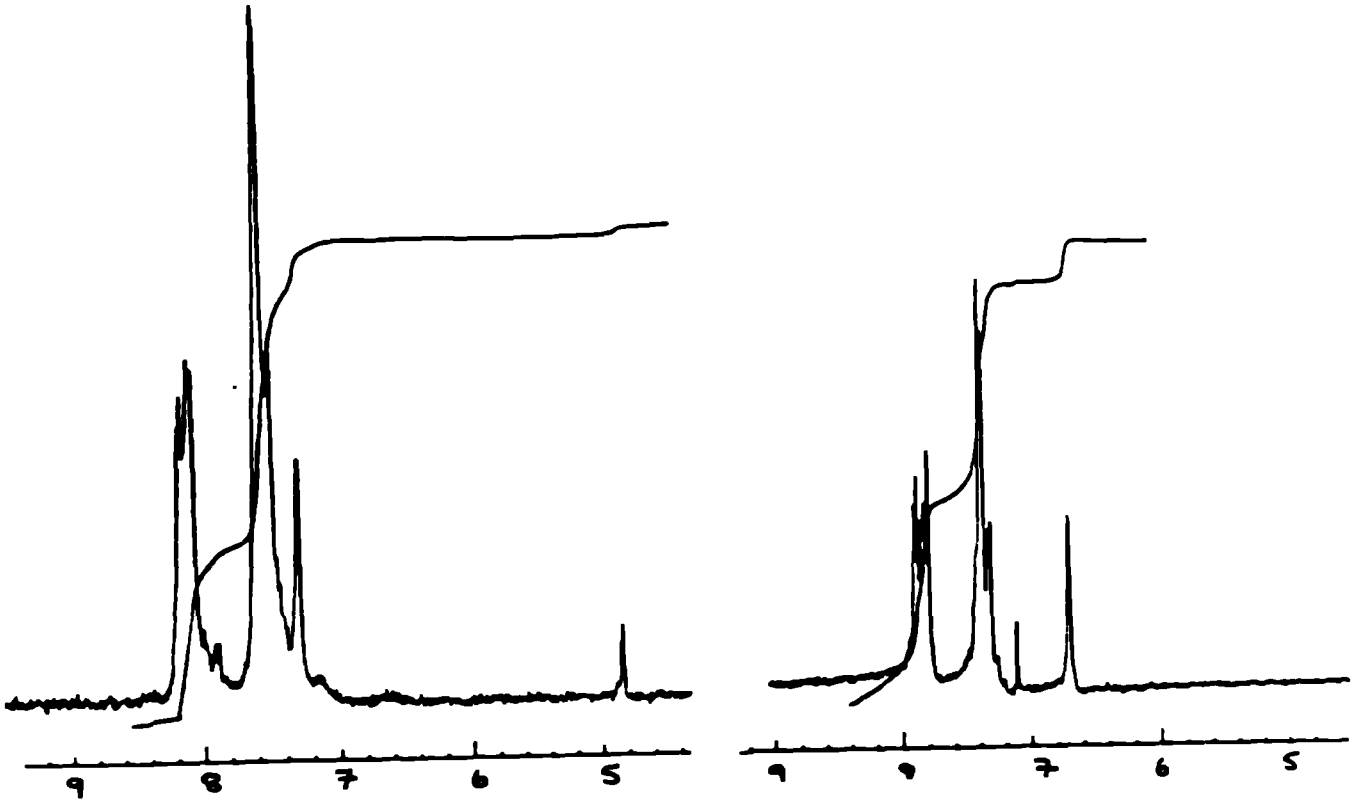

Figure 2.7 : ^1H NMR spectra of (13) in dmso (left) and $CDCl_3$ (right)

The reason why the integrals are not as theoretically predicted lies in the equilibrium reaction schemes above. The degree to which the equilibrium is set up determines the 'amount' of CH relative to the 'amount' of CH_2 observed. This explains why [Sr(tmhd)$_2$(tmhd-H)] (12) exhibits CH and CH_2 resonances in equal proportion in dmso (due to the steric relief given by the larger metal centre and the less demanding tmhd ligand, thus the dmso can coordinate and stop the rapid fluxional exchange), yet (13) in the same solvent has a smaller CH_2 peak with respect to a large CH peak (i.e. the dmso can not solvate as much due to steric problems of the dppd group and the smaller metal centre; consequently there is less hinderance for the rapid fluxional exchange process).

2.3.4 ^{13}C NMR characterization

Pertinent NMR data for complexes (1) - (11) and (14) are shown in Table 2.5. The ^{13}C NMR of the tmhd complexes shows a shift downfield of the CH_3 and $\underline{C}(CH_3)_3$ resonances, but a shift upfield of the CH and CO, with respect to the parent ligand. This effect has been observed previously and was ascribed to the formation of an electron rich M-O-C_3-O chelating ring system.[59] The electron density accumulates on the carbons within the ring (i.e. CH and CO), and therefore electron withdrawal from the tertiary butyl carbons is observed and a resulting deshielding occurs. As with the ^1H NMR the CH_3 and also the $\underline{C}(CH_3)_3$ resonances fall within a very narrow range (δ 28.26 - 29.43 and 40.46 - 41.84 respectively). Signals due to the tertiary butyl methyls are observed for the tmhd and fod complexes, and appear to be independent of the nature of the diketonate ligand. Only one peak is seen for each of these groups, signifying a single β-diketonate environment.

In contrast to the proton NMR, the OCH_3 resonance is seen to shift downfield following the order tetraglyme > triglyme > diglyme. This phenomenon is seen both for the tmhd and the hfpd complexes. The OCH_3 resonance also falls into a narrow range, irrespective of β-diketonate. No such trend is observed for the OCH_2 resonances, but once again it is easy to identify each one of the different environments. This is not the case for the heptaglyme complex (11), which has a very complex spectrum in this region.

The methine carbon is observed to shift a great deal when both the β-diketonates and glyme ligand are altered (the latter to a lesser degree). The decrease in electron density on the CH group of the fluorinated and aryl ligands results in a series where the CH resonance of these complexes is shifted downfield with respect to the tmhd ligand. The general order is;

Tmhd < Hfpd < Fod < Dppd

Table 2.5: Selected ^{13}C NMR Data for Complexes (1) - (11) and (14) :

Compound	CH_3	$\underline{C}(CH_3)_3$	CH_3	CH_2	CH	CF_3	CO
(1)	29.43	41.16	59.04	68.89, 69.31, 70.08, 70.87	87.11	----	196.42
(2)	28.26	40.66	58.24	69.09, 69.13, 70.58	87.20	----	196.78
(3)	28.74	41.84	58.13	69.41, 71.13	89.05	----	198.42
(4)	28.81	40.67	58.82	69.92, 69.97, 70.13, 71.64	86.90	----	196.55
(5)	28.91	40.67	58.62	69.20, 69.97, 70.51	86.90	----	196.93
(6)	28.52	40.46	58.64	69.45, 70.91	88.11	----	198.46
(7)	28.82	40.56	58.64	69.04, 69.45, 71.05	87.30	----	197.28
(8)	----	----	58.7	70.28, 70.48, 71.97, 72.12	92.36	----	182.53
(9)	----	----	59.79	68.64, 69.91, 70.31, 71.30	88.16	118.80	176.32
(10)	----	----	59.28	68.60, 69.37, 70.84	88.29	118.77	176.67
(11)[a]	----	----	57.44	69.03, 69.22(x5), 70.74	84.11	118.25	171.57
(14)[b]	28.02	41.74	59.32	68.62, 69.50, 71.26	89.74	*	170.59, 203.70

All spectra measured in C_6D_6, at 20°C and 67.94MHz, except ([a]) which was measured under the same conditions in d_6-dmso, and ([b]) which was measured under the same conditions in $CDCl_3$. * Indicates complex resonances which are discussed later in this Chapter.

It is noticeable that the CH resonance of (11), is significantly lower (δ 84.11) than the other complexes of the series. On changing from tetraglyme to triglyme to diglyme, we observe a shift of *ca.* δ +2, with the tetraglyme ligand appearing furthest downfield.

The CF_3 resonance of the hfpd complexes appears as a 1:3:3:1 quartet, between δ 118.25 and 118.80ppm. The ^1J (C-F) coupling constants are generally about 300(±10) Hz. The CO resonance also appears as a quartet in the fluorinated β-diketonate ligands, with a ^2J (C-F) *ca.* 30(±3) Hz.

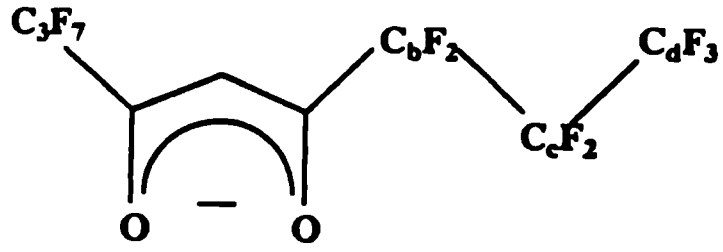

fod-H

Figure 2.8 : Pictorial representation of fod-H

The fod complex (14), shows three different environments for the carbon atoms of this region as shown in Figure 2.9. At lowest field is the $\underline{C}F_3$ carbon which is centred at δ 116.3. This is split by both the CF_2 group adjacent and the fluorines attached, forming a quartet of triplets with a ^1J coupling constant of 286Hz and a ^2J constant of 26Hz. The $O\underline{C}F_2$ carbon is also doubly split into a triplet of triplets by the attached fluorines and the adjacent $OCF_2\underline{C}F_2$ group and occurs at slightly higher field, δ 111.0. The final carbon atom, $OCF_2\underline{C}F_2$, appears at highest field at δ 109.6. The pattern observed is a complex one and overlaps the splitting pattern of the OCF_2 group to a degree. The coupling constants are similar to those observed for the $O\underline{C}F_2$ group. The CO adjacent to the C_3F_7 group is also split into a triplet and is centred at δ 170.59.

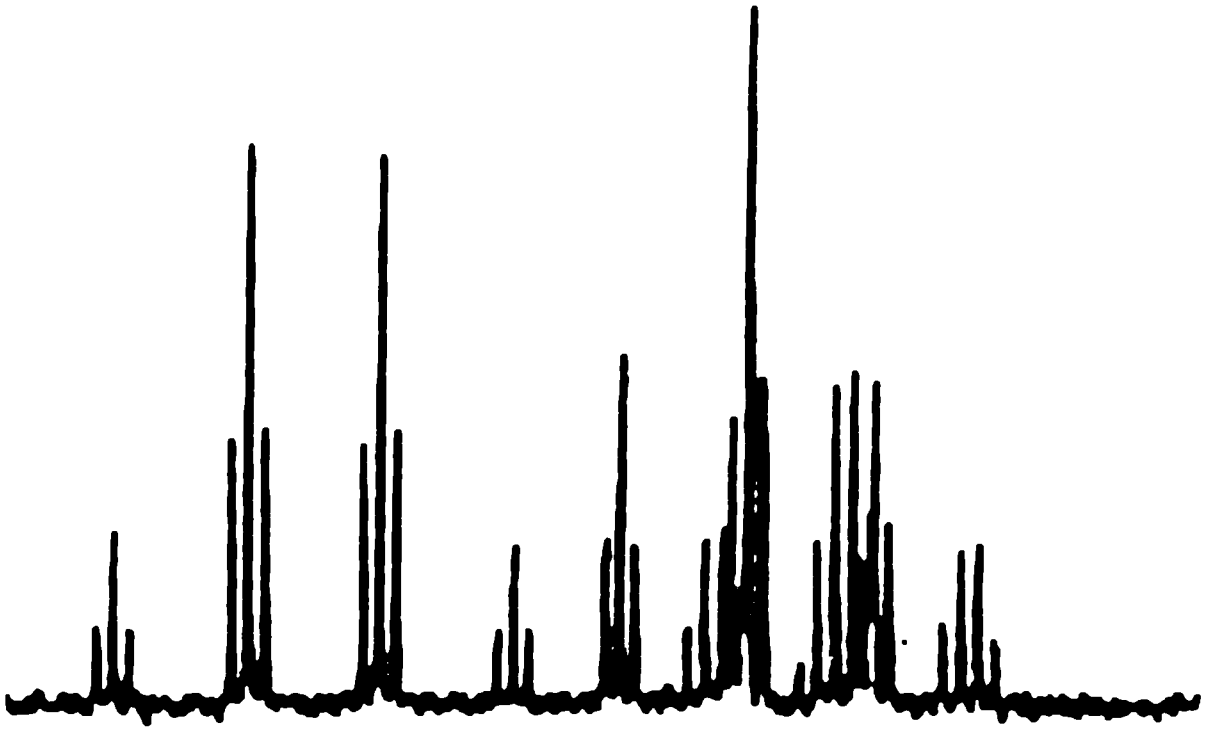

Figure 2.9 : CF region in the ^{13}C spectrum of (14) in $CDCl_3$

2.3.5 Mass spectrometry

Pertinent mass spectrometric data for complexes (1) - (14) are shown in Table 2.6. The isotope patterns of the metal containing complexes are consistent with those which may be predicted from natural abundance patterns. The m/z ratios which are given relate to the isotopes of greatest abundance, e.g. ^{40}Ca, ^{88}Sr and ^{137}Ba.

There is a wide variety of species observed for this series of compounds. In many cases the expected monomeric species are observed, confirming that they are monomers in both solution and the gas phase. These peaks (labelled ML_2N in Table (2.6) are not necessarily the most intense peaks in the spectrum. For the three Ba complexes (1) - (3) only the tetraglyme complex appears as a monomer in the gas phase with an ion observed at m/z 629 for [Ba(tmhd)$_2$(tetraglyme)]. One other complex (9), also has intact monomeric molecular ions in the gas phase.

A (MLN) ion is observed for most of the glyme complexes. These ions correspond to the monomeric final products with the loss of one diketonate ligand. These ions are

Table 2.6 : Selected Mass Spectrometry Results for complexes (1) - (14) :

Compound	ML	ML_2	M_2L_3	ML_2N	MLN	MN
(1)	321	505	----	629	541	----
(2)	321	504	825	----	----	----
(3)	321	448	827	----	----	271
(4)	271	397, 454	725		677	----
(5)	271	397, 454	----	----	450	262
(6)	271	397, 454	725	----	406	223
(7)	223	349, 422	629	----	----	---
(9)	247	----	----	607, 676	470	----
(10)	----	----	----	----	----	218
(11)	247	454	701	----	557, 601, 325	----
(12)	271	398, 454	726	---	---	---
(13)	---	---	766	---	---	---
(14)	336	---	972	810	513	---

N.B. all spectra measured under EI+ conditions.

Note : M – Metal, L – β diketonate ligand, N – glyme ligand.

observed for all except the Ba and Ca tmhd / triglyme and tmhd / diglyme compounds, and complex (10) which does not appear to be very volatile, only one ion being observed. These peaks are generally more intense than those of the complete monomeric molecular ions.

Complex (14) exhibits related behaviour with a clear molecular ion being observed at m/z 810 for [Ca(fod)$_2$(triglyme)], and then loss of a fod ligand to yield [Ca(fod)(triglyme)] at m/z 513 with the lowest clearly discernable molecular ion observed at m/z 336 for [Ca(fod)]. Complex (14) is more stable in the vapour phase than the tmhd complexes generally are, (i.e. there is little evidence of M_2L_3 (only 2%) or higher oligomeric ions) the monomeric Lewis base adducted complex evidently persists.

Vapour phase studies for (12) and (13) shows that they are sufficiently volatile to produce a mass spectrum. This is very encouraging especially for the dppd compound (13), as they are generally involatile due to the high carbon content. This involatility is seen for the glyme adducted complex (8). As for most of the β-diketonate species the oligomeric ML, ML_2 and M_2L_3 ions are observed.

The ML_2 ions of (12) show the fragmentations of the β-diketonate ligand clearly (see Figures 2.10 and 2.11). The tmhd ligand itself is shown to fragment firstly by losing a $C(CH_3)_3$ group, then the subsequent loss of each of the atoms in turn. Each of these fragments is observed in the mass spectrum of (12).

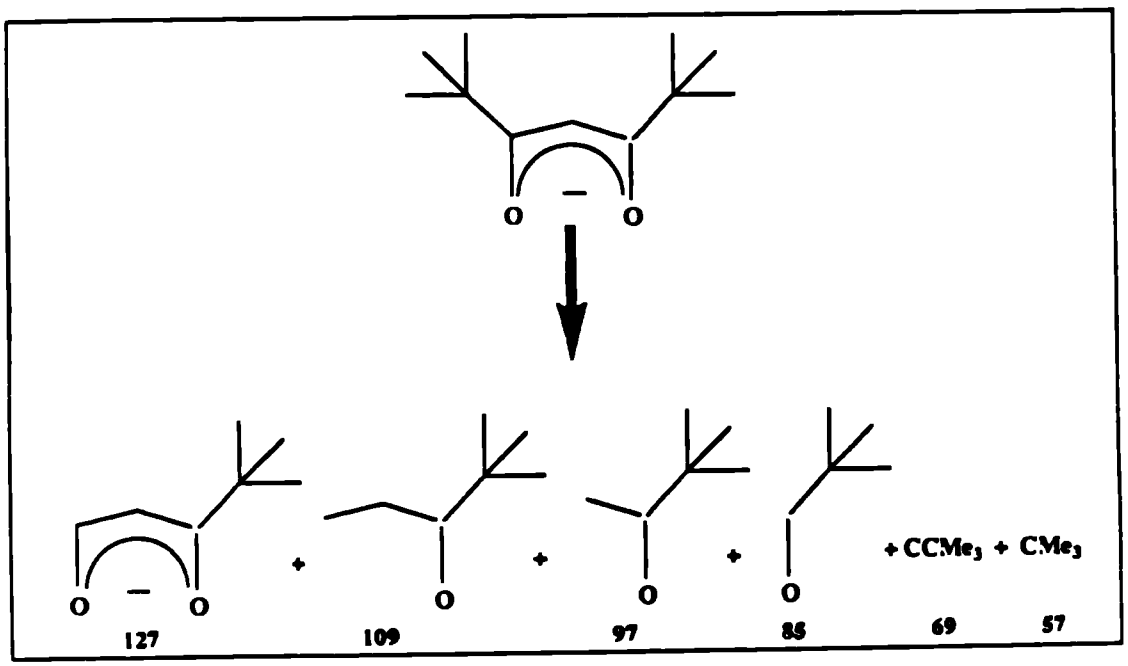

Figure 2.10 : Tmhd vapour phase fragmentations

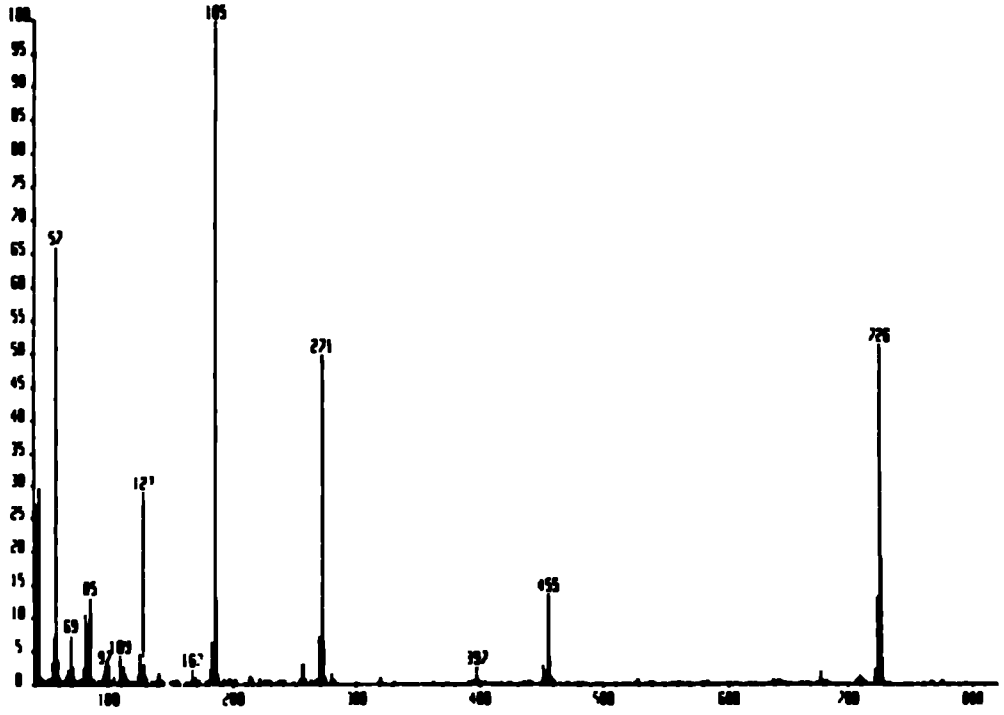

Figure 2.11 : EI+ mass spectrum of (12)

Compound (12) shows the regular disintegration of the tmhd ligand, a peak at m/z 398 corresponding to [Sr(tmhd)(ᵗBuCOCHCOH)] with the complete ML_2 ion occurring at m/z 454 for [Sr(tmhd)$_2$]. It is noticeable that the intensity of the ML ions are considerably larger than those of the ML_2 ions. ML_3 ions are observed for complex (13) which is the molecular ion and as such we may tentatively suggest that the compound remains fairly stable during a period of heating. However, as this ion has only an intensity of *ca.* (3%), not too much emphasis may be put on this observation.

Intense peaks are also observed for the oligomeric species ML, ML_2 and M_2L_3. The ML ion is observed for all complexes except (10), the [Ca(hfpd)] ion. This ion is observed; however, for complexes (9) and (11); complex (10) prefers to exist as an MN species only in the gas phase. The ML_2 ion is observed for all but the fluorinated β-diketonate complexes (except (11)). For the Ca and Sr tmhd complexes, two ions are observed corresponding to ML_2. These are due to the breakdown of the tmhd ligand to a fragment of m/z 127 for [(ᵗBuCOCHCOH)]. Compound (9) shows a similar breakdown of the hfpd ligand at m/z 607 for [Ca(hfpd)(CF_3COCHCO)(tetraglyme)]. This ligand

breakdown is rather more rare than for the tmhd ligand.

The presence of these ions was also noted by Sievers et al. for the Sr and Ca homoleptic tmhd compounds, they observed the ML, ML_2 and M_2L_3 ions in large abundance.[73] The ML and M_2L_3 fragments were found to be of greatest intensity (*ca.* 75 and 65% respectively) while the ML_2 ion was observed in a much smaller quantity (*ca.* 25%). Our findings are consistent with those reported previously.

The consistency of the M_2L_3 implies that the tmhd complexes readily form the oligomeric donor-Lewis base free complexes $[M(tmhd)_2]_n$. Such behaviour is important because the O-donor adducts deliver these materials into the gas phase at *ca.* 100°C lower than has previously been observed,[64] an important criterion for MOCVD purposes. The fod and hfpd complexes in general are far more stable in the vapour phase and the monomeric Lewis base adduct complex persists.

2.4 Physical properties

2.4.1 Melting points and solubilities

Table 2.7 : Melting points of glyme β-diketonate complexes (1) - (14) :

	Compound	M. Pt. (°C)
(1)	$[Ba(tmhd)_2(tetraglyme)]$	90-92
(2)	$[Ba(tmhd)_2(triglyme)]$	77-79
(3)	$[Ba(tmhd)_2(diglyme)]_2$	93-95
(4)	$[Sr(tmhd)_2(tetraglyme)]$	56-60
(5)	$[Sr(tmhd)_2(triglyme)]$	88-89
(6)	$[Sr(tmhd)_2(diglyme)]_2(\mu\text{-}H_2O)$	96-98
(7)	$[Ca(tmhd)_2(triglyme)]$	71-74
(8)	$[Sr(dppd)_2(tetraglyme)].0.5C_7H_8$	96-98
(9)	$[Ca(hfpd)_2(tetraglyme)]$	82-85
(10)	$[Ca(hfpd)_2(triglyme)]$	103-106
(11)	$[Ca(hfpd)_2]_2(heptaglyme)$	112-116

(12)	$[Sr(tmhd)_2(tmhd\text{-}H)]$	76-81
(13)	$[Ca(dppd)_2(dppd\text{-}H)]$	68-72
(14)	$[Ca(fod)_2(triglyme)]$	80-83

The most immediately noticeable feature of the melting points of these glyme adducted compounds is the large decrease observed in comparison to the unadducted homoleptic β-diketonates. $[Ba(tmhd)_2]_4$ is seen to melt at 194-197 C,[62] while compound (1) melts over 100 C lower than this at 90-92 C. Complex (2) melts 120 C lower than the base free compound at 77-79°C. This is a general finding for all the complexes in this series.

The base free homoleptic strontium compound $[Sr_3(tmhd)_6(tmhdH)]$ is observed to melt at 172-175°C.[62] Complexes (4) - (6) show a significant decrease often over 100 C. This feature is also noted for the calcium homoleptic analogue which melts at 242-246 C whereas its adducted complexes melt much lower.[63] This effect is due to the stabilization of the homoleptic complexes by the Lewis bases. The glyme ligand coordinates to the metal centre, saturating it. This has the effect of lowering the molecularity of the homoleptics, altering them from tetrameric and trimeric species, into simpler monomeric structures. The heat necessary to melt an oligomeric species is often more than that needed to melt a monomeric one.

There is no obvious trend in melting points as a function of the metal or the β-diketonate ligand. What is more noticeable, however, is the difference in melting point as we alter the glyme ligand from tetraglyme to diglyme. Both the tetraglyme and triglyme complexes melt at similar temperatures for most of the complexes. However, the diglyme complexes, (3) and (6), have higher melting points than their larger glyme analogues. This is due presumably to the dimeric nature of the Ba and Sr species. Complex (11) is a dimeric species too, and consequently has a higher melting point. The *tris* complexes (12) and (13) have low melting points and may therefore be expected to be monomeric or at least dimeric species. This is consistent with additional spectroscopic and crystallographic data.

The air / moisture stability of these complexes is extremely good in all cases. It may be considered that the complete saturation of the coordination sphere of the metal centre by the Lewis base ligands, has lead to the exclusion of any possible water coordination. This difference is extremely marked when we compare the stability of these complexes with the 'base free' complexes. The added advantage of air stability is a necessity for CVD

precursors, therefore, glyme stabilized complexes may be used in preference. The subsequent volatility of the O- donor ligands is all important when CVD applications are the ultimate goal.

The remarkable increase in solubility of the majority of these complexes over the homoleptics, also gives good reasons for suggesting this type of compound as a CVD precursor. All the compounds have high solubilities in coordinating solvents such as chloroform and dmso. This phenomena is also seen to a degree with the base free homoleptic compounds. However, in contrast to the homoleptics these compounds are all soluble in aromatic solvents (e.g. toluene and benzene) and most are soluble in aliphatic solvents (e.g. hexane) at room temperature. Complexes (8) and (13) are insoluble in hexane but more soluble in more polar solvents. The insolubility of (8) in hexane is typical of dppd complexes which show decreased solubilities even when in conjunction with Lewis base ligands; the reason for the insolubility is that dppd compounds (and more especially the phenyl rings) have a very high carbon content. With this type of compound the fluorinated compounds also appear to be slightly less soluble. Compound (11) is a dimeric entity and as such may be expected to be less soluble than the molecular complexes. The overall increased solubility over the base free homoleptics is undoubtedly due to the glyme ligands forming an organic 'sheath' around the metal centre.

2.4.2 Simultaneous Thermal Analysis (STA)

Thermal gravimetric analysis (TGA) has found extensive use in both molecular and non-molecular chemistry and materials science. The study of weight loss versus temperature may yield valuable information on the thermal behaviour of materials. Differential scanning calorimetry (DSC) allows the study of the enthalpy changes occurring during a controlled thermolysis, and most importantly whether a reaction is taking place (distinguishing between a melting point and a decomposition). In our apparatus both these techniques are performed simultaneously.

The DSC of the tmhd complexes (1) - (5) and (7) shows a sharp melting point at 75.4(4) - 108.1°C(3), this is noted as DSC(1) in Table (2.8). These melting temperatures do not comply exactly with those obtained by conventional methods, due to the different conditions applied. Two further isotherms are observed at higher temperatures. The first between 191.0(5) - 223.0°C(1) undoubtedly corresponds to the loss of the respective glyme ligand. This is an endothermic process as bonds are being broken and is represented as such by a curve downwards in the DSC. The second endotherm is between 350.5(7) - 396.6(1)°C and is ascribed to the end point of sublimation of the homoleptic $[M(tmhd)_2]_n$ compound. Complex (7) does not have the second DSC curve, the loss of the glyme ligand

Table 2.8 : TGA / DSC Results for Complexes (1) - (7) and (10) - (14) :

Compound	TGA 1(°C)	TGA 2(°C)	DSC 1(°C)	DSC 2(°C)	DSC 3(°C)	Res.(%)	$T_{50\%}$(°C)
(1)	170 225	250-410	103.8	223.0	396.6	6.00	380
(2)	123-250	300-420	88.2	197.6	395.8	8.48	360
(3)	120-171	240-402	108.1	219.7	393.2	6.05	365
(4)	150-260	260-382	75.4	215.5	370.9	2.05	350
(5)	153-224	316-383	101.6	191.0	376.4	5.78	330
(7)	134-323	324-359	78.5	----	350.5	2.05	330
(10)	140-264	----	59.56	126.2	251.9	0.64	236
(11)	309-333	----	123.6	292.1	----	8.13	330
(12)	90-193	270-390	70.8	92.7	384.2	3.43	350
(13)	229-275	344-411	79.2	265.9	----	2.60	255
(14)	271-326	----	84.5	272.8, 307.7*	330.0	4.27	291

TGA(1) = first weight loss: TGA(2) = second weight loss: DSC(1) = melting endotherm:
DSC(2) = loss of respective glyme ligand: DSC(3) = end point of sublimation: Res. = residue.
* – second value denotes separate loss of β diketonate ligands.

not proving to be a very endothermic process, presumably due to the lability of the triglyme ligand.

The DSC for [Ca(hfpd)$_2$(triglyme)] (10), also shows three inflexions but at considerably lower temperatures. The melting point endotherm is seen at 59.6 C with the two further isotherms at 126.2 and 251.9°C. This is evidence that the fluorinated complexes are more volatile than their hydrocarbon analogues and as such may be more valuable for CVD applications.

The TGA of the tmhd complexes has two clearly defined steps, the first generally between 120-171(3) - 170-225°C(1), probably represents the loss of the glyme ligand. The weight loss percentages are consistent with these observations. The second step is generally between 240-402(3) - 300-420°C(2) and is more than likely to be the intact sublimation of the [M(tmhd)$_2$]$_n$ fragment. There is generally a plateau between the loss of the glyme and the onset of sublimation; however, this is not seen for complexes (4) or (7), the two steps being in rapid succession. Complex (7) has a relatively low end point of sublimation (359°C) when compared to the rest of the series. Complex (10) is once again different to the tmhd complexes. In contrast to the others only one step is observed, the loss of the glyme and the sublimation being concurrent. The end point of sublimation for this complex is much lower (by over 100°C in most cases) than the tmhd analogues, the fluorinated complexes again proving to be more volatile.

A direct comparison between the barium tmhd complexes (1) - (3) shows a number of interesting results (see Figure 2.12). The DSC plots show very similar results for the triglyme and tetraglyme compounds, namely one single sharp inflexion at *ca.* 100°C. The diglyme complex shows this inflexion too and also a further large broad inflexion at 220°C. Finally there is also a very broad trough between 350-400°C for all three compounds. The TGA plots show similar results too. For this particular system the diglyme is lost at a lower temperature than the tetraglyme which is lost at a lower temperature than the triglyme. All three compounds convert to the homoleptic diketonate in the same order too. However, the $T_{50\%}$ and the sublimation of the homoleptic are all at very similar temperatures. This is an indication that at these elevated temperatures, the compounds are all the same species, i.e. the oligomeric homoleptic β-diketonate, indicating that a conversion from the monomer to the oligomer occurs at high temperatures.

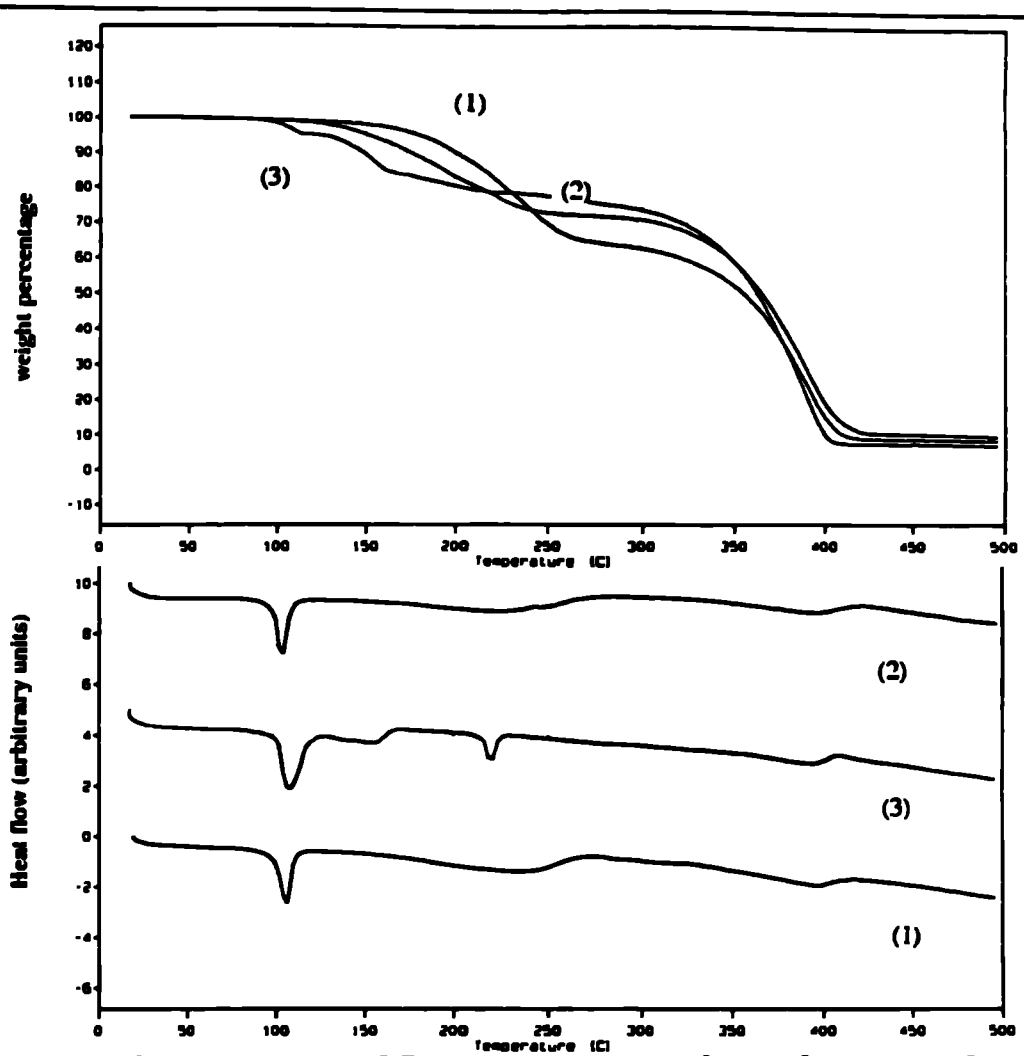

Figure 2.12 : TGA (top) and DSC (bottom) comparison of compounds (1), (2) and (3) : $[Ba(tmhd)_2(n\text{-glyme})]_x$

The residues of complexes (1) - (7) and (10) - (14) (< 8.8%) are only carbonaceous deposits, which is due to some thermal decomposition of the diketonate ligands. Whereas previous workers have had high residues at high temperatures, these complexes all have very low residues at much lower temperatures.[75,76] The residue of complex (10) is virtually negligible due to its high percentage of sublimation.

The $T_{50\%}$ is a measure of the point at which half the percentage weight of the complex has been lost. In order to be an ideal CVD precursor this value should be as low as possible; for the tmhd complexes it is still quite high (in the region of 330-380°C), but for the hfpd complex (10), it is only 236°C, a marked improvement over many other compounds.

The TGA data for the tmhd complexes reveals that they do not sublime intact (whereas the hfpd complex (10) does); however, they are important materials as they are

air stable precursors which will deliver the homoleptic tmhd complexes into the gas phase easily. Such materials are of importance if they can be obtained as liquids at, or just above room temperature. The very low melting point of $[Sr(tmhd)_2(tetraglyme)]$ (56-60°C), makes it an obvious choice for further analysis.

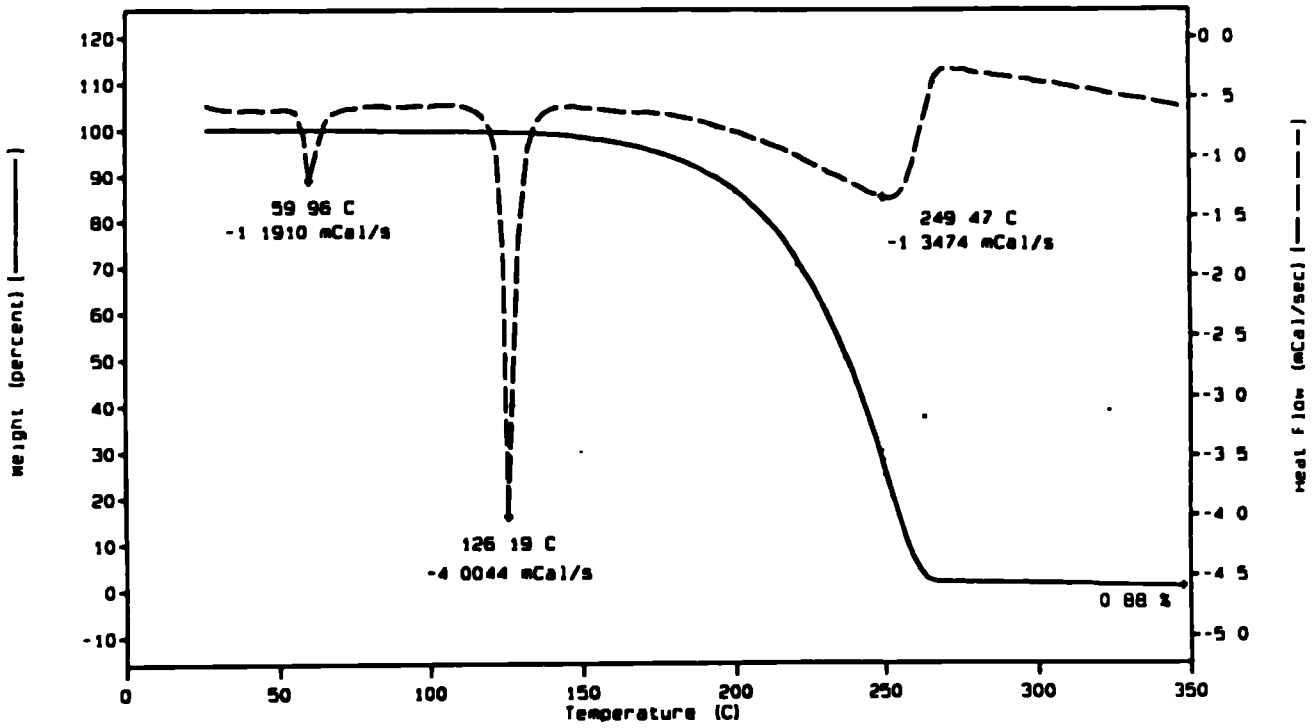

Figure 2.13 : TGA and DSC plots of (10)

The TGA of complex (12) gives definitive evidence that the *tris* species has been synthesized. There are two distinct steps, the first is between 90 and 193°C and probably corresponds to the loss of the tmhd-H ligand (observed 23.0%, expected 28.7%). The second step equates to the complete sublimation of the resultant *bis* species between 270 and 390°C. The residue of 3.43% is due to carbonaceous deposits with $T_{50\%}$ at 350°C. We may correlate this directly with the TGA of $[Sr_3(tmhd)_6(tmhd\text{-}H)]$,[62] which shows two steps also. The first between 90 and 240°C corresponds to the loss of the tmhd-H ligand and the second to the subsequent sublimation of the resultant material between 260 and 390°C. The residue level is low (*ca.* 6%) and is due also to carbon deposits from the tmhd ligand. The $T_{50\%}$ is slightly higher than that of the *tris* species at 370°C.

The DSC of (12) shows three peaks. The first at 70.8°C is the melting point and corresponds well with the 76-81°C obtained by normal methods. The second at 92.7 C corresponds to the loss of the tmhd-H ligand. The final endotherm at 384.2 C is the end point of sublimation of the $[Sr(tmhd)_2]_n$ species. The DSC of the *bis* species shows only two endotherms. The first at 110.5°C is a melting endotherm while the second at 387°C corresponds to the end point of sublimation of the *bis* species. The final endotherm is directly comparable to that observed for the *tris* complex. We may postulate therefore, that the *tris* complex rearranges to the *bis* species on the loss of the tmhd-H ligand; this also explains why three endotherms are observed in the DSC of the *tris* species and only two are noted for the *bis* complex.

The other *tris* complex (13) shows different behaviour. The TGA shows two steps, the first at 229-275°C is likely to equate to the loss of all carbon and hydrogen atoms to leave a Ca-O species, (observed 80.4, calculated 80.8%), the second at 344-411°C to the complete sublimation of the product, to leave a residue of 2.60% (carbon deposits), with a low $T_{50\%}$ at 255°C. The DSC shows a melting point at 79.2°C and only one other endotherm at 265.9°C which corresponds to the end point of sublimation to the calcium oxide species.

Compound (14) is consistent with the other fluorinated β-diketonate species. A single TGA step is noted between 271 and 326°C which corresponds to the complete sublimation of the product, to leave a carbonaceous residue of 4.3%. The $T_{50\%}$ is also low at 291°C. The DSC is more revealing indicating four individual steps. The melting endotherm appears at 84.5°C, while the other three endotherms are at 273, 308 and 330°C, corresponding to the loss of the triglyme, fod and complete sublimation of the end product respectively.

The TGA and DSC plots of the three $[M(tmhd)_2(triglyme)]$ complexes (2), (5) and (7) are shown in Figure 2.14 below. The DSC results show just major two inflexions, the first at about 100°C which follows the order Ca < Ba < Sr and corresponds to the melting points of the respective complexes. The final inflexion corresponds to the sublimation of the homoleptic at 350-400°C which, in contrast, follows the order Ca < Sr < Ba.

The TGA plots are all remarkably similar with respect to the loss of the triglyme ligand which essentially occurs between 123 and 250°C. The sublimation of the homoleptic occurs at slightly different temperatures for the three complexes with the calcium subliming before the strontium which subsequently sublimes before the barium complex. The final residues and $T_{50\%}$ values are also noted to follow the trend Ba > Sr > Ca.

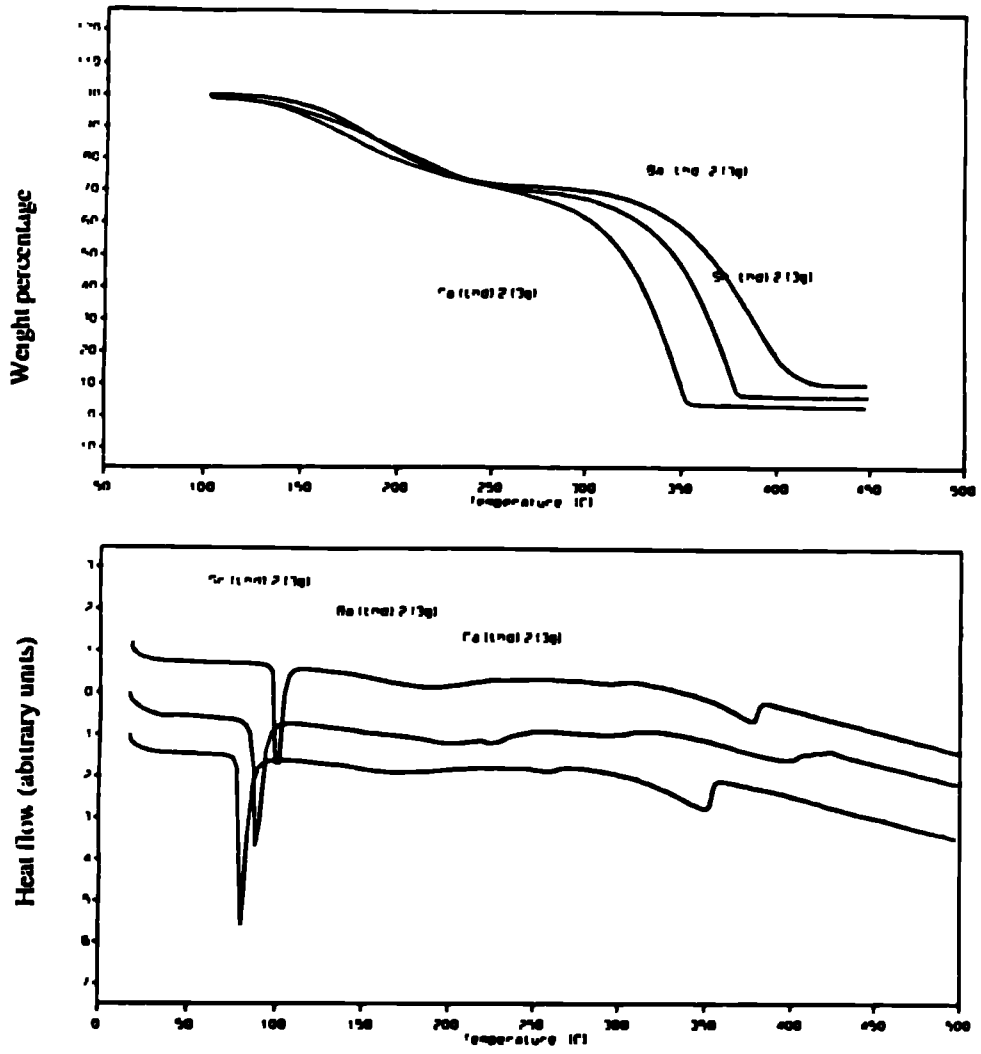

Figure 2.14 : TGA (top) and DSC (bottom) comparison of compounds (2), (5) and (7) : [M(tmhd)$_2$(triglyme)]

The above glyme complexes may be placed into two broad groups, namely those with fluorinated β-diketonate ligands and those with hydrocarbon ligands. The former generally have only one step in the TGA, corresponding to the complete loss of both diketonate and glyme ligands. The residues and $T_{50\%}$ temperatures are often very low, e.g. (10) whose $T_{50\%}$ is only 236°C compared with over 330°C for the tmhd compounds.

This result is comparable to the mass spectrometric observations that in the gas phase the tmhd compounds tend to dissociate and revert to the base free homoleptics, hence the first TGA step. This is then followed by the sublimation of the homoleptic at nearly the same temperature as is seen for the homoleptics themselves. With the fluorinated complexes, however, the increased volatility of the diketonate ligand leads to a one step

sublimation of the entire compound. This too, is observed in the mass spectra where the glyme ligands tend not to 'drop off' the metal β-diketonate molecules.

The increased volatility at lower operating temperatures of the glyme stabilized hydrocarbyl and more especially fluorinated complexes in comparison with the homoleptic β-diketonates may make these complexes more suitable as CVD precursors. Although these complexes are at first glance no more useful as precursors in terms of their sublimation temperatures than the base free homoleptics, they do have the added advantages of being air and moisture stable and reproducibly synthesized.

2.5 X-ray crystallography

The structures of a number of compounds described in this Chapter were solved by single crystal X-ray techniques. Crystallographic data and collection data for each of the compounds reported within this section may be found in Appendix 3 at the end of this Thesis.

[Ba(tmhd)$_2$(tetraglyme)] (1)

The unit cell and intensity data were obtained at 150 K using a Delft-Instruments FAST TV area detector diffractometer and graphite monochromated Mo-K_α radiation at (λ = 0.71069 Å), following previously described procedures.[77] The data were corrected for Lorentz and Polarisation effects, and also for absorption.[78] The crystal data and details of data collection and structure refinement are presented in the Appendix. The structures were solved *via* Patterson methods and refined by full-matrix least squares using the SHELX program system.[79] The non-hydrogen atoms were refined anisotropically.

For (1), the CH and CH_2 hydrogens were included in the idealized positions with a common U_{iso} value, but the methyl hydrogens were ignored. The methyl carbon of atoms one tert-butyl group were refined in two orientationally disordered tetrahedra with occupancies of 0.6 and 0.4.

The solid-state X-ray structure of (1) is shown in Figure 2.15. The structure is monomeric with a nine coordinate metal centre whose coordination geometry can be best described as a distorted dodecahedron with an additional atom coordinating along one edge.

As in most of the complexes of this section the glyme ligand wraps around the metal in a meridional plane with the two diketonates positioned either side of the plane. The M-O bonds fall into two categories, the first being to the tmhd ligands, where the bond average is 2.648(7)Å, and the second to the glyme ligand, with an average M-O length of 2.901(9)Å. These bond lengths are comparable to those found in $[Ba(hfpd)_2(tetraglyme)]^{-}$ whose $Ba\text{-}O_{(tmhd)}$ average bond length is 2.698(8) and $Ba\text{-}O_{(glyme)}$ is 2.952(7)Å. Similarly $[Ba(tdfnd)_2(tetraglyme)]^{-2}$ has average lengths of 2.68(7) and 2.81(8)Å respectively.

The glyme ligand adopts the conventional *anti / gauche* geometry around the C-O and C-C bonds respectively.[65] It binds in a five pronged mode with the pattern of two short and three long M-O bonds being observed, this is probably due to steric hinderance. The tmhd ligands are not co-planar with respect to each other, in fact a considerable fold is seen about the O...O axis, this dihedral angle is 22.9°.

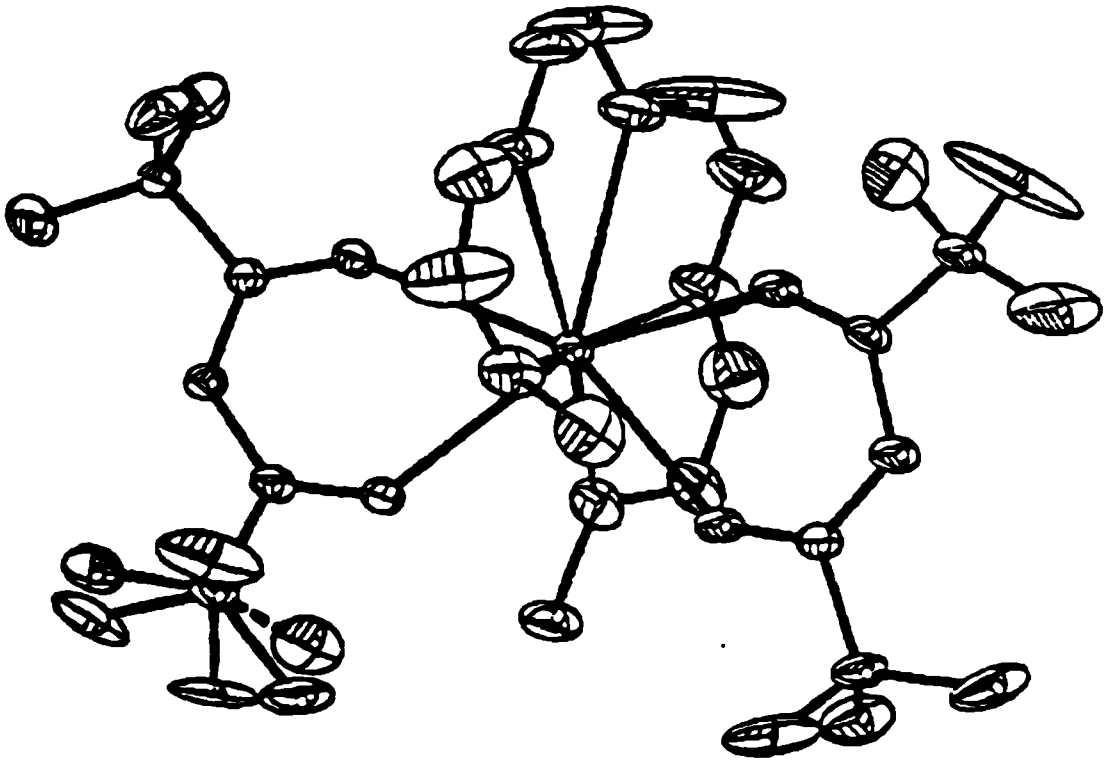

Figure 2.15 : X-ray crystal structure of $[Ba(tmhd)_2(tetraglyme)]$ (1)

[Ba(tmhd)$_2$(triglyme)] (2)

The crystal data of [$C_{30}H_{56}O_8Ba$] (2) are as follows : M = 682.1, monoclinic, spacegroup $P2_1/c$, a = 10.668(2), b = 23.614(6), c = 15.650(3) Å, β = 109.11(2)°, Z = 4, D_c = 1.216 g cm^{-3}, F(000) = 1424, μ(Mo-K_α) = 11.1, 293 K, R = 0.0502, Rw = 0.0471. 6561 Unique reflections were measured of which 3926 having $F > 4\sigma(F)$ were used in the refinement.

The crystal was mounted onto a glass fibre with epoxy resin and coated with epoxy to reduce any possible crystal decomposition during collection. The accurate unit cell parameters were obtained by least squares analysis of between 18 and 25 centred reflections. Data for (2) were collected on a Siemens P4/PC diffractometer with graphite monochromated Mo K_α radiation. The structure was solved by the heavy atom method and refined with the full-matrix least squares technique, using anisotropic thermal parameters for non-hydrogen atoms. In (2), there is rotational disorder in all tert-butyl groups; however, this disorder could not be resolved into alternative partial occupancy orientations.

The X-ray structure of (2) is shown in Figure 2.16. This shows it to be monomeric and eight coordinate as expected, with the glyme ligand in one plane and the tmhd ligands in a plane perpendicular to it, forming a distorted propellane type geometry. The coordination polyhedron of the metal can be best described as bicapped trigonal prismatic with O(2) and O(8) as the capping atoms. The principal change in geometry for compound (2) (the majority of the other eight coordinate complexes being square antiprismatic) is due to the steeply inclined relationship of the two tmhd ligands. These are inclined by *ca.* 70°. The mean plane of the glyme ligand is still essentially orthogonal to one of the tmhd ligands although of necessity the ends of the glyme chain are markedly displaced relative to the plane of one of the β-diketonate groups. In (2) the terminal methyl groups of the triglyme ligand are almost coincident with one of the ligand planes, whereas for (1), for instance, they are above and below the plane. The metal is completely encapsulated by the polyether ligand and adopts an eight coordinate environment. Again we observe two different M-O bond length groups, with those to the glyme being in the range 2.814(5) to 2.900(6)Å, and those to the tmhd, 2.621(5) to 2.643(5)Å.

The triglyme adopts a fairly conventional geometry with *anti* and *gauche* relationships around the C-O and C-C bonds respectively. It binds in a four pronged mode; however, the pattern of two short and two long M-O bonds is not observed, i.e. 2.856(9) - 2.900(6) for the outer Ba-$O_{(glyme)}$ and 2.814(6)- 2.889(5)Å for the inner.

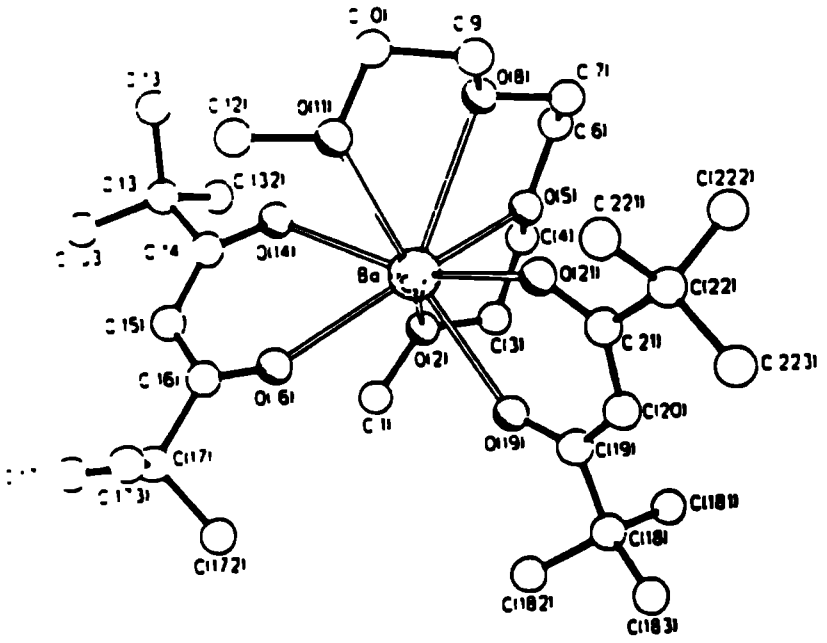

Figure 2.16 : X-ray crystal structure of [Ba(tmhd)$_2$(triglyme)] (2)

[Ba(tmhd)$_2$(diglyme)]$_2$ (3)

The X-ray measurements were made on a crystal mounted using silicone oil and transferred to a goniostat. The data were collected at 150K on a Delft Instruments FAST TV area detector diffractometer equipped with a rotating anode FR591 generator (50kV, 50mA), bufferboard and DEP image intensifier with Mo-Kα radiation (λ = 0.71069Å, graphite monochromator), and Oxford Cryostream low temperature cooling system, controlled by a microVax 3200 and driven by MADNES software. The orientation matrix and unit-cell parameters were determined *via* the ENDEX and REFINE routines of the MADONL software (the small molecule version of MADNES) using 50 reflections from two 5° FIND rotation ranges separated by 90° around the omega axis and subsequently refined during data processing using 250 reflections from each processed bach of data. Data evaluation was performed off-line on a Vax station 4000/60 clustered with the diffractometer driving computer with frames transfer and processing taking place simultaneously with data collection, the processing time not exceeding the exposure time. Slightly more than a hemisphere of data was collected (an ω rotation of 195° around an arbitrary axis at χ=0° plus two complementary 'cusps' of 70° each differing by 90° in φ at

χ=90°) with crystal-to-detector distance = 39.92mm, detector swing angle = 24.97°, between frames increment 0.20° and exposure time = 10 seconds. The data were corrected for Lorentz and Polarisation effects, and also for absorption using the program DIFABS, adapted for FAST geometry.[78] The structure was solved *via* the Patterson and Fourier methods and refined (on F) by full matrix least-squares (SHELX-80),[79] with a unit weighting scheme which gave acceptable variance analyses. All non-hydrogen atoms were refined anisotropically; the hydrogen atoms isotropically. All calculations were performed on a T800 transputer hosted by a IBM/AT personal computer.

In the solid state the complex exists as a centrosymmetric dimer, with a distorted square antiprismatic eight coordinate geometry at each metal centre. The stoichiometry of this complex is the same as some recently characterised complexes of the type $[Ba_2(tmhd)_4(L)_2]$.[53,66,80] In contrast to these complexes the tmhd ligands do not bridge the metal centres. Instead it is the diglyme which both chelates and bridges. For example, $[Ba_2(tmhd)_4(Et_2O)_2]$[66] has two bridging and two chelating tmhd ligands, with two chelating ethers. The $M\text{-}O_{(tmhd)}$ bond lengths of (3) are between 2.567(6) and 2.826(7)Å. In (3) the barium metal is coordinated by the three oxygen atoms of the diglyme in a classical chelating manner, with an average bond length of 2.859(8)Å. The terminal oxygen of the diglyme chain also binds to the second barium with a bond length of 3.173(6)Å, thus bringing the two metals closer together.

The bridging interaction of the glyme ligand maximises the coordination number of the metal centres, thus they achieve a higher coordination number than in a monomeric complex. The fact that the glyme ligands and not the tmhd ligands are bridging also explains why the Ba...Ba distance is so large (5.130(2)Å) when compared with other recent structures.[62] The four tmhd ligands are bound to the metal in a classical chelating manner, and again the M-O bond lengths are found to be *ca.* 0.2Å shorter (2.615(8)Å) than those of the glyme ligand.

It is also of note that the two tmhd ligands chelated to each barium show large deviations from planarity (atomic deviations of up to 0.072(1)Å from the mean plane of OCCCO) and significant buckling about the O--O axis [dihedral angle of 33.7(5)° between the Ba O(1) O(2) and O(1) C(2) C(3) C(4) O(2) planes and 20.4° between the Ba O(3) O(4) and O(3) C(13) C(14) C(15) O(4) planes]. These results suggest considerable flexibility of the tmhd ligands when chelated to a metal centre and may be attributed to several inter-ligand steric interactions between the tmhd oxygens and diglyme CH_2 / CH_3 groups. In

particular the non-bonded contacts O(1)---H(24A)/C(24) of 2.56(5)/3.356(8)Å, O(2)---H(28C)/C(28) of 2.73(7)/3.352(8)Å and O(4)---H(24B)/C(24') of 2.66(7)/3.251(8)Å are fairly short and would contribute towards the non-planarity and folding nature of the tmhd ligands observed in this complex.

Drozdov *et al.*[71] in trying to improve the shelf life of $[Ba_4(tmhd)_8]$ added diglyme but not under inert conditions, thereby synthesizing $[Ba(thd)_2(diglyme)]_2(\mu\text{-}H_2O)$. The structural data were, however, not published. Compound (3) has also been synthesized by other workers along with $[Ba(tmhd)_2(dme)_2]$ but its crystal structure was not reported.[69]

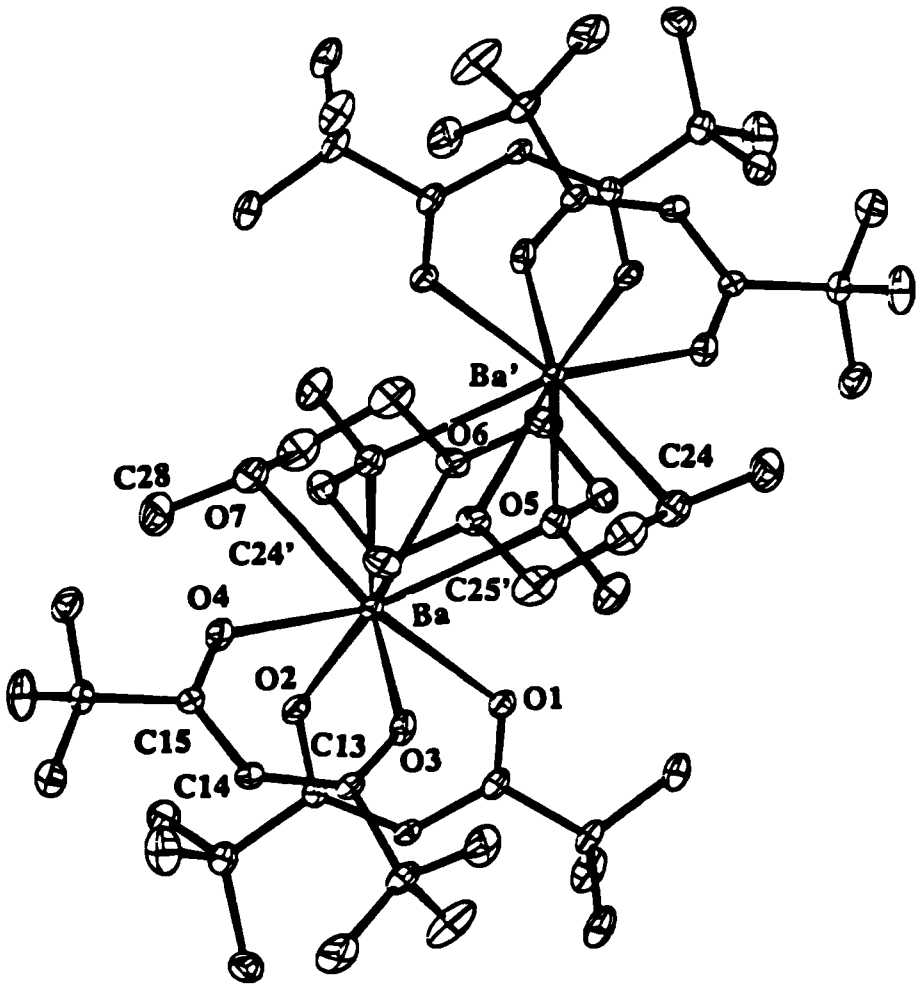

Figure 2.17 : X-ray crystal structure of $[Ba(tmhd)_2(diglyme)]_2$ (3)

Table 2.9 : Selected bond lengths (Å) and angles (°) for compound (3) :

O(1)-Ba	2.679(6)	O(2)-Ba	2.578(6)
O(3)-Ba	2.574(7)	O(4)-Ba	2.630(6)
O(5)-Ba	2.888(6)	O(5')-Ba*	3.173(6)
O(6)-Ba	2.819(6)	O(7)-Ba	2.870(7)
C(2)-O(1)	1.247(6)	C(4)-O(2)	1.271(6)
C(13)-O(3)	1.259(6)	C(15)-O(4)	1.263(6)
C(23)-O(5)	1.437(9)	C(24)-O(5)	1.440(7)
C(25)-O(6)	1.425(7)	C(26)-O(6)	1.434(9)
C(27)-O(7)	1.435(8)	C(28)-O(7)	1.410(8)
C(2)-C(1)	1.551(8)	C(6)-C(1)	1.530(10)
C(7)-C(1)	1.521(8)	C(8)-C(1)	1.531(8)
C(3)-C(2)	1.414(7)	C(4)-C(3)	1.387(8)
C(5)-C(4)	1.555(7)	C(9)-C(5)	1.533(9)
C(10)-C(5)	1.523(11)	C(11)-C(5)	1.526(10)
C(13)-C(12)	1.545(9)	C(17)-C(12)	1.516(10)
C(18)-C(12)	1.532(10)	C(19)-C(12)	1.520(9)
C(14)-C(13)	1.404(7)	C(15)-C(14)	1.414(8)
C(16)-C(15)	1.544(8)	C(20)-C(16)	1.517(9)
C(21)-C(16)	1.521(10)	C(22)-C(16)	1.534(8)
C(25)-C(24)	1.496(10)	C(27)-C(26)	1.500(10)
O(2)-Ba-O(1)	66.2(2)	O(3)-Ba-O(1)	86.2 (2)
O(3)-Ba-O(2)	103.4(2)	O(4)-Ba-O(1)	141.0(1)
O(4)-Ba-O(2)	92.2(2)	O(4)-Ba-O(3)	66.9 (2)
O(5)-Ba-O(1)	74.9(2)	O(5)-Ba-O(2)	138.4(1)
O(5)-Ba-O(3)	87.5(2)	O(5)-Ba-O(4)	128.4(2)
O(5')-Ba-O(1) *	138.0(2)	O(5')-Ba-O(2)	155.8 (2)
O(5')-Ba-O(3)	82.2(2)	O(5')-Ba-O(4)	68.1(2)
O(5')-Ba-O(5)	64.4(2)	O(6)-Ba-O(1)	78.1(2)
O(6)-Ba-O(2)	97.6(2)	O(6)-Ba-O(3)	146.0(1)
O(6)-Ba-O(4)	139 .1(1)	O(6)-Ba-O(5)	59 .4 (2)
O(6)-Ba-O(5')	89 .4 (2)	O(7)-Ba-O(1)	116.8 (2)
O(7)-Ba-O(2)	76.0(2)	O(7)-Ba-O(3)	152.9(1)
O(7)-Ba-O(4)	86.1(2)	O(7)-Ba-O(5)	111.2 (2)
O(7)-Ba-O(5')	88.4 (2)	O(7)-Ba-O(6)	58.5 (2)

* The primed atom belongs to one and the same dimer and relate to the unprimed one by the symmetry (-x, 1-y, -z).

[Sr(tmhd)$_2$(triglyme)] (5)

The crystal data for [$C_{30}H_{56}O_8Sr$] (5) are as follows : M = 632.39, monoclinic, spacegroup $P2_1/c$, a = 11.986(5), b = 19.705(3), c = 15.490(2) Å, α = 90, β = 96.24(2), γ = 90°, Z = 4, D_c = 1.155 g cm^{-3}, F(000) = 1352, μ(Mo-K_α) = 14.7, 298 K. 8588 Unique reflections were measured of which 2449 having $I > 3\sigma(I)$ were used in the refinement. The structure was solved *via* the heavy atom method and refined by full matrix least squares to R = 0.0453, Rw = 0.0478.

The X-ray crystal structure of (5) is shown in Figure 2.18. The solid-state structure of the colourless crystalline solid (5) grown from hexane, confirms the spectroscopic findings in that the complex exists as an anhydrous mononuclear strontium β-diketonate stabilized by a coordinated triglyme ligand. The strontium metal is coordinated by all eight oxygen donor atoms of the three ligands. The coordination polyhedron of the metal can be best described as a distorted square antiprism. The triglyme ligand partially encapsulates the metal in the equatorial plane with the two tmhd ligands sitting above and below this plane A space filling model of (5) shows extensive shielding of the large dipositive cation Sr^{2+} by the tmhd and triglyme ligands. The good solubilities of these complexes in organic (e.g. aliphatic, aromatic and coordinating) solvents may be attributed to this encapsulation which effectively forms an organic sheath around the Sr metal.

The β-diketonate ligands asymmetrically chelate to the metal centre, with Sr-$O_{(tmhd)}$ bond lengths ranging from 2.468(9)-2.519(9), with an average of 2.495(9)Å. The triglyme Sr-$O_{(glyme)}$ bond lengths range from 2.628(1)-2.715(1), with an average of 2.674(1)Å; however, one may note that the outer two glyme oxygens bind closer (by *ca.* 0.07Å) to the strontium than the other inner oxygens. This is due primarily to steric reasons and also the fact that the two oxygens on the end of the glyme chain are held less rigidly.

$[Sr(tmhd)_2(diglyme)]_2(\mu\text{-}H_2O)$ (6)

The crystal data for $[C_{56}H_{106}O_{15}Sr_2]$ (6) are as follows : M = 1194.689, monoclinic, spacegroup C2/c, a = 29.267(6), b = 10.565(2), c = 21.846(5) Å, β = 95.99(1), Z = 4, D_c = 1.181 g cm^{-3}, F(000) = 2552, μ(Mo-K_α) = 16.0 cm^{-1}, 298 K. 14296 Unique reflections were measured of which 3497 having $F > 3\sigma(F)$ were used in the refinement. The structure was solved by direct methods and refined by least squares to R = 0.0435, Rw = 0.0501.

In an attempt to form a crystalline product for X-ray analysis of the formula $[Sr(tmhd)_2(diglyme)]_n$ water was absorbed either from the solvent or air to yield regular colourless blocks in a high yield. The X-ray crystal structure of (6) is shown in Figure 2.19.

The structure of complex (6) shows it to be a centrosymmetric dimer, but with the coordination geometries of the strontium metals distorted. The coordinative saturation is satisfied by the bridging water molecule making each Sr metal eight coordinate. The coordination geometry of the metal can be best described as a distorted square antiprism. The β-diketonates bind asymmetrically to the metal with M-O bonds varying from 2.459(1) to 2.520(1), with an average of 2.489(6)Å. The angle between the two tmhd ligands is 93.45°. The diglyme ligand chelates to the metal centre with Sr-O(5), Sr-O(6) and SrO(7) distances of 2.686(7), 2.692(7) and 2.644(7) respectively, with an average bond length of 2.681(7)Å.

The water molecule sits symmetrically between the two $[Sr(tmhd)_2(diglyme)]$ units with a Sr-O(8) distance of 2.967(7)Å, this may be contrasted to the μ-H_2O observed in $[Ba(hfpd)_2(H_2O)]_n$[65] which has a longer bond length of 3.12Å. The water molecule in (6) presumably acts as a bridging ligand due to the sterically congested situation at the metal centre. In contrast, for $[Ba(hfpd)_2(H_2O)]_n$ there is ample room for both the bridging water molecules and Ba-F interactions in the one-dimensional chain. The water molecule may therefore be described as a very effective bridging ligand in both cases.

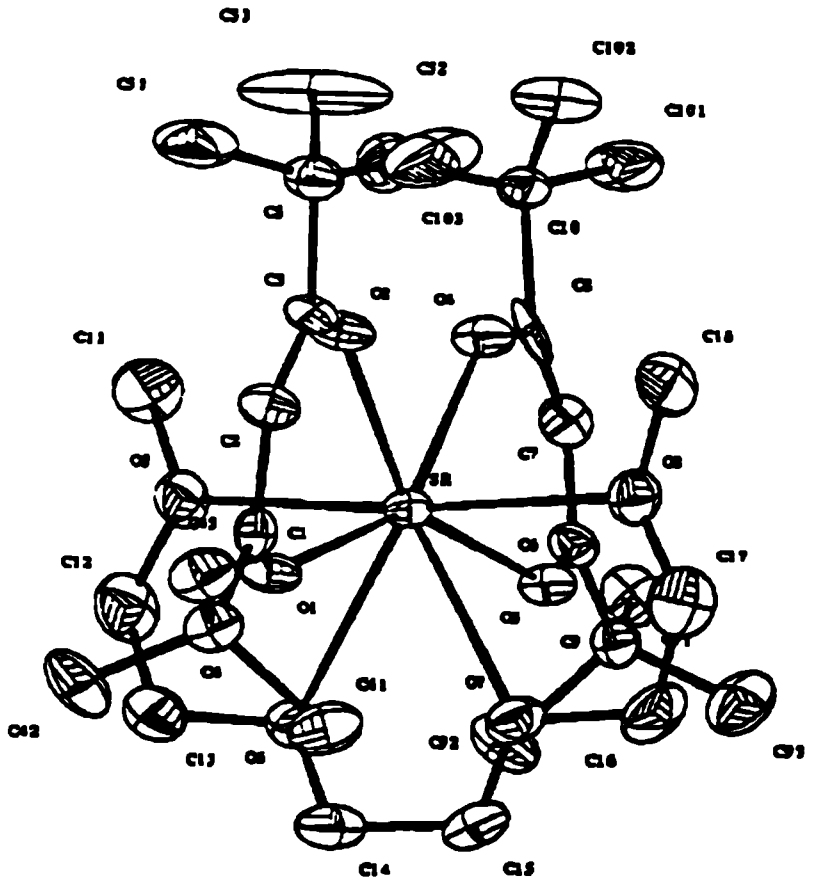

Figure 2.18 : X-ray crystal structure of [Sr(tmhd)$_2$(triglyme)] (5)

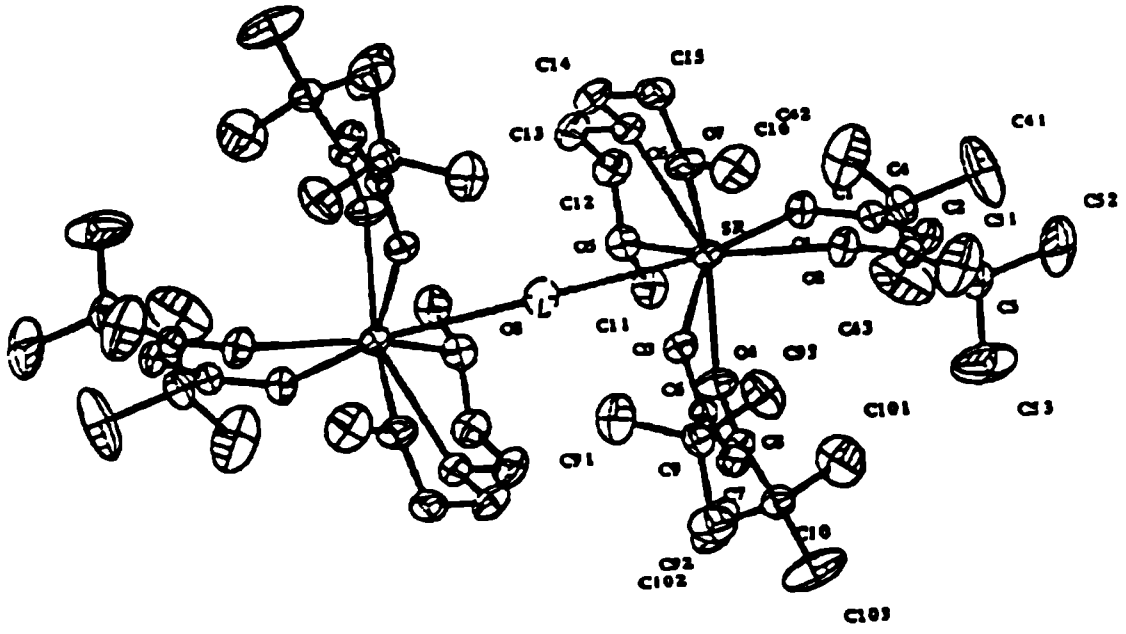

Figure 2.19 : X-ray crystal structure of [Sr(tmhd)$_2$(diglyme)](μH$_2$O) (6)

[Ca(tmhd)$_2$(triglyme)] (7)

The crystal data of [$C_{30}H_{56}O_8Ca$] (7) are as follows : M = 584.8, triclinic, spacegroup P-1, a = 10.378(3), b = 11.601(4), c = 15.483(3) Å, α = 84.03(3), β = 71.75(2), γ = 82.61(3)°, Z = 2, D_c = 1.109 g cm^{-3}, F(000) = 640, μ(Cu-K_α) = 18.8, 291 K, R = 0.0541, Rw = 0.0596. 4716 Unique reflections were measured of which 4146 having $F > 4\sigma(F)$ were used in the refinement.

The crystal was mounted onto a glass fibre with epoxy resin and coated with epoxy to reduce any possible crystal decomposition during collection. The accurate unit cell parameters were obtained by least squares analysis of between 18 and 25 centred reflections. Data for (7) were collected on a Siemens P3/PC diffractometer with graphite monochromated Cu K_α radiation. The structure was solved by direct methods. In (7), one of the tert-butyl groups (that attached to C(18)) displays rotational disorder, and two discrete orientations with occupancies of 0.75 and 0.25 were refined. The minor occupancy atoms were refined isotropically.

The solid state NMR of this complex provides primary evidence that this complex is monomeric. ^{13}C CPMAS experiments show the presence of only two types of CH_3 environment on the tertiary butyl groups of the tmhd ligand. This can be explained by the fact that the tmhd ligands are bound asymmetrically to the calcium metal and are not completely co-planar with each other. The observation of four CO resonances may be similarly interpreted. We are also able to differentiate between the four different CH_2 groups of the triglyme.

The X-ray crystal structure of (7) is illustrated in Figure 2.20. The structure of the colourless crystalline solid shows that the calcium metal is coordinated to all eight oxygen donor atoms of the three ligands. The triglyme ligand encapsulates the metal in the equatorial plane and above and below this plane sit the two tmhd ligands in an approximately orthogonal relationship, forming a distorted propeller. The coordination geometry of the Ca metal centre can best be described as a distorted square antiprism with O-O distances in the range 2.34(6) - 2.68(6)Å.

The Ca-O distances lie in two distinct groups, those for the tmhd ligand being in the range 2.348(2) (O19) to 2.379(2)Å (O21), while those of the triglyme are between 2.471(3) (O2) and 2.594(3)Å (O5). In contrast with compound (2), the two outer glyme oxygens O(2) and O(11), bind significantly closer [2.471(3) and 2.492(3)Å] to the metal than the two central atoms of the polyether chain O(5) and O(8) [2.578(2) and 2.594(3)Å]. The difference of *ca.* 0.1Å, is probably due to the different steric constraints imposed by the two equatorial tmhd ligands.

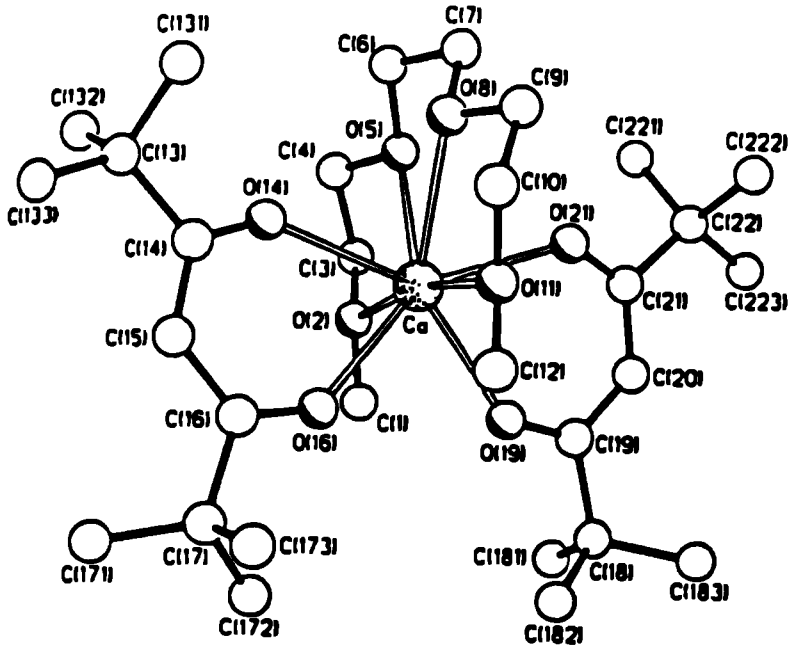

Figure 2.20 : X-ray crystal structure of [Ca(tmhd)$_2$(triglyme)] (7)

[Sr(dppd)$_2$(tetraglyme)].0.5C$_7$H$_8$ (8)

The unit cell and intensity data were obtained at 150 K using a Delft-Instruments FAST TV area detector diffractometer and graphite monochromated Mo-K$_\alpha$ radiation at (λ = 0.71069 Å), following previously described procedures. [77] The data were corrected for Lorentz and Polarisation effects, and also for absorption.[78] The crystal data and details of data collection and structure refinement are presented in Table 1. The structures were solved *via* direct methods and refined by full-matrix least squares using the SHELX program system.[79] The non-hydrogen atoms were refined anisotropically.

For (8) the methyl hydrogens on the tetraglyme were located from the difference map and included in the calculation of F_c; the methylene hydrogens on the tetraglyme and those on the dppd groups were allowed to ride on their parents in calculated positions (C-H = 0.96 Å); a common Uiso was refined for all hydrogens; the hydrogens on the disordered toluene were ignored.

The X-ray crystal structure of (8) is shown in Figure 2.21. X-ray crystallography shows that the strontium metal is in a nine coordinate environment, each of the oxygens of the three ligands coordinating to the metal centre. The geometry around the metal is again irregular and may be described as a distorted dodecahedron with an additional atom coordinating along one edge, in a similar fashion to (1).

The Sr-$O_{(dppd)}$ bond lengths range from 2.500(6) to 2.540(5)Å, while the Sr-$O_{(glyme)}$ lengths range from 2.708(6) to 2.791(5)Å, with an overall average of 2.66(6)Å. In comparison with compound (1), the variations in M-O distances involving tetraglyme ligands and β-diketonates appear to be a common phenomenon in alkaline earth metal complexes. Also in common with (1) we observe that the two diketonate ligands are not co-planar but make an angle of 12.0°, due to the steric encumbrance caused by the relatively large Lewis base ligand. The centrosymmetric dimer $[Sr(dppd)_2(CH_3COCH_3)]_4$,[50] has Sr-O bond lengths between 2.42(7) and 2.59(8)Å, with the Sr-$O_{(bridging)}$ lengths having a 2.55(8)Å average, and the Sr-$O_{(unshared)}$ lengths a 2.44(8)Å average.

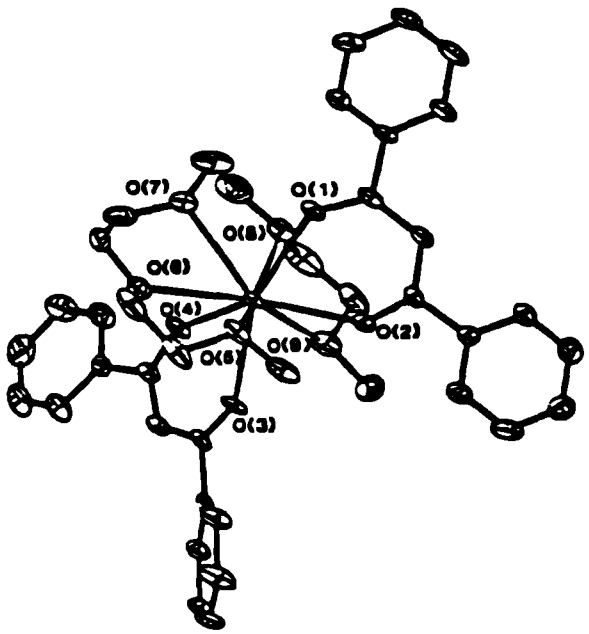

Figure 2.21 : X-ray crystal structure of $[Sr(dppd)_2(tetraglyme)]$ (8)

[Ca(hfpd)$_2$(tetraglyme)] (9)

The crystal data of [$C_{20}H_{24}O_9CaF_{12}$] (9) are as follows : M = 676.5, triclinic, spacegroup P-1, a = 9.453(2), b = 12.600(3), c = 13.215(4) Å, α = 70.30(2), β = 83.09(2), γ = 76.49(2)°, Z = 2, D_c = 1.561 g cm^{-3}, F(000) = 688, μ(Cu-K_α) = 30.3, 291 K, R = 0.0707, Rw = 0.0843. 3857 Unique reflections were measured of which 3616 having $F > 4\sigma(F)$ were used in the refinement.

The crystal was mounted onto a glass fibre with epoxy resin and coated with epoxy to reduce any possible crystal decomposition during collection. The accurate unit cell parameters were obtained by least squares analysis of between 18 and 25 centred reflections. Data for (9) were collected on a Siemens P3/PC diffractometer with graphite monochromated Cu K_α radiation. The structure was solved by direct methods. In (9), there is rotational disorder in three of the CF_3 groups (those attached to C(16), C(20) and C(21)). The occupancies for the orientations of the CF_3 group on C(16) are 0.6 and 0.4 and for C(20) and C(21) 0.7 and 0.3 occupancies were refined. The minor occupancy fluorine atoms on C(20) and C(21) were refined isotropically.

The X-ray crystal structure of (9) is shown in Figure 2.22. In stark contrast to the usual structures observed for these complexes we find that although the hfpd ligands are bound in a genuinely chelating manner, the glyme ligand coordinates with only four of the five oxygen atoms. The fifth oxygen is not bound at all and forms an essentially planar pendant arm, leaving the metal in an eight coordinate geometry. However, the uncoordinated portion of the tetraglyme ligand is rotated by *ca.* 86° about O(11) - C(12) relative to C(10) - O(11). It is noticeable that the normal *anti / gauche* sequence about the C-O and C-C bonds respectively, is destroyed, with the geometry about C(12) - C(13) being anti. Despite this, however, there is virtually no perturbation in the coordination geometry about the metal, which is a distorted square antiprism.

Again the Ca-O bond lengths fall into two classes. Those of the hfpd ligand are between 2.395(3) and 2.410(3)Å, whereas those of the glyme ligand are between 2.434(3) and 2.497(3)Å. The outer two oxygens of the tetraglyme ligand are slightly further away from the calcium metal by an average of *ca.* 0.054Å. There are no short C...F distances as have been found in the eight coordinate complex [Ca(hfpd)$_2$(H_2O)$_2$]$_2$,[65] presumably due to the coordinative saturation of the metal. The question arises why the calcium metal prefers to adopt an eight coordinate geometry and not a nine coordinate one, thereby coordinating to all the oxygen atoms available.

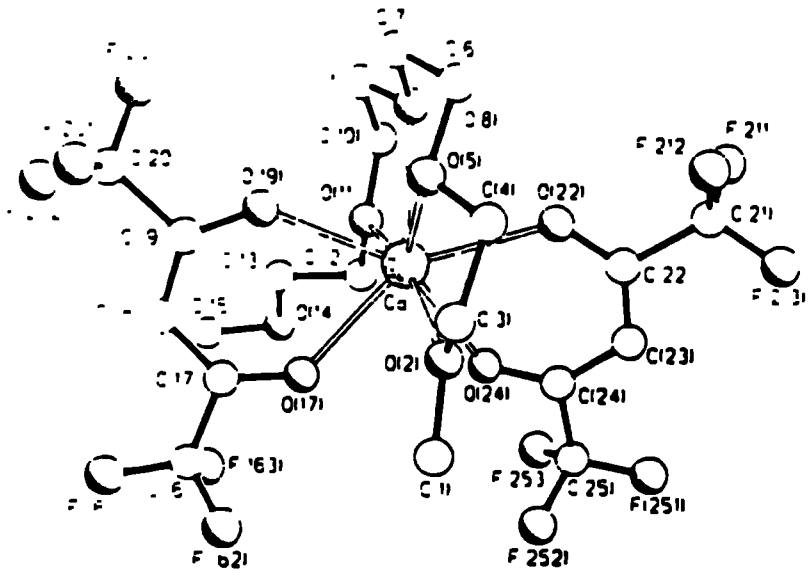

Figure 2.22 : X-ray crystal structure of [Ca(hfpd)$_2$(tetraglyme)] (9)

Due to the electron withdrawing nature of the CF_3 groups the electron density at the metal centre is reduced. Thus the Lewis acid character of the metal centre is increased and a stronger interaction with the Lewis base glyme occurs. This effect is obviously weaker with a non-fluorinated compound, but we may expect the dppd ligand to have a similar effect as the hfpd ligand. It may be the case therefore, that [Ca(dppd)$_2$(tetraglyme)] would also have a pendant arm. Complex (8) presumably does not have an uncoordinated arm due to the increase in ionic radii of the respective metals. The average Ca-$O_{(\beta\text{-diket})}$ bond length for the hfpd complex is 2.401(6)Å, and it would appear that this does not provide enough room for the tetraglyme ligand to coordinate completely. It may be noted too that the two hfpd ligands are not co-planar but are at 14° to each other.

A study of the space-filling model of (7) indicates that the coordination of an additional glyme oxygen centre is sterically prohibited. The van der Waals circumference is not large enough to accommodate an additional meridional coordination site without significantly altering the coordination geometry about the calcium centre.

$[Ca(hfpd)_2]_2$(heptaglyme) (11)

The crystal data for (11) are as follows : $[Ca_2(C_5HF_6O_2)_4(C_{16}H_{34}O_8)]$: $C_{36}H_{38}Ca_2F_{24}O_{16}$, M_r = 1262.82, Monoclinic, $P2_1/c$, a = 10.288(2), b = 24.335(5), c = 11.011(2) Å, β = 109.660(12)°, U = 2596.0(9) Å^3 (by least squares refinement of diffractometer angles for 250 reflections within θ = 2.0 - 30.0°, λ = 0.71069 Å), space group $P2_1/c$ (no. 14), Z = 2, D_c = 1.616 gcm^{-3}, F(000) = 1276, μ = 0.368 mm^{-1}. T = 150K. colourless prism, crystal size 0.20 x 0.13 x 0.13 mm^3.

The data were collected and processed on a Delft instruments FAST TV area detector diffractometer positioned at the window of rotating anode generator, Mo-K_α radiation, 13154 reflections measured ($2.26 < \theta < 29.92°$; index ranges $-12 < h < 14$; $-27 < k\ 32$; $-10 < l < 14$), 6533 unique [merging R = 0.0783 after absorption (max. and min. absorption correction factors = 0.846, 1.196)].

The structure was solved by direct methods and refined by full matrix least-squares on Fo^2 using all 6533 unique data and 403 parameters (non-hydrogen atoms anisotropic, hydrogens in idealised positions with U_{iso} free to refine) to wR_2 (on F^2) = 0.1411 and R_1 (on F) = 0.0723. The corresponding wR_2 and R_1 values for 3707 data with $I>2\sigma(I)$ were 0.1155 and 0.0464 respectively. Three of the four unique CF_3 groups were orientationally disordered; the F atoms of these groups were refined with partial occupancies. The weighting scheme used was $w = 1/\sigma^2(Fo)^2$, which gave satisfactory agreement analysis. An extinction coefficient refined to a final value of 0.015(1). Minimum and maximum residual electron density = -0.37 and 0.41 eÅ^{-3}, maximum shift / esd = 0.010; goodness of fit on Fo^2 = 0.541. The diagram was drawn by the program SNOOPI.[81] Atom scattering factors as in SHELXL-93.[82] All calculations were performed on a 486DX2/66 personal computer.

The yield of heptaglyme complexes is generally comparatively low (68%) by the standards set by the rest of the compounds in this series. The reason for this becomes apparent when we discover that this complex is dimeric with only one heptaglyme ligand bonded. Much of the product is a rather oily solid which suggests that the compound is soluble in an excess of uncoordinated glyme ligand.

The single crystal X-ray structure of this complex is shown in Figure 2.23 and shows it to consist of two $Ca(hfpd)_2$ moieties linked by a heptaglyme ligand involving an unusual coordination mode. The two Ca metals are formally related by a two fold axis. Both calcium metals are eight coordinate and are in a distorted square antiprismatic geometry. The glyme ligand is acting as both a chelating and a bridging ligand *via* the

central ethylene bridge, with four of the oxygens coordinating to one metal and the other four to the second metal. The Ca-O bond lengths differ greatly in the molecule as may be expected. The Ca(1) - O(13) bond length of 2.481(5)Å is *ca.* 0.12Å shorter than that of Ca(1) - O(14) which is 2.597(6)Å; this is most likely due to O(13) carrying the pendant methyl group, which can bind tightly to the metal centre. In contrast O(14) must bend back with a fairly acute angle of 64.0(3)°, to create the chelate. Similar bonding is also observed at the other end of the compound.

As the hfpd ligands are shown to be coordinating in a classical, almost symmetrical manner it is not surprising that their bond lengths are very different from those of the glyme ligands, ranging from 2.224(6) to 2.348(6)Å. This structure is similar in nature to the recently characterised [{(tmhd)$_3$Ln}$_2$(triglyme)] (where Ln = Eu, Y, Tb etc.), which also contains an unusual chelate bridge.[83]

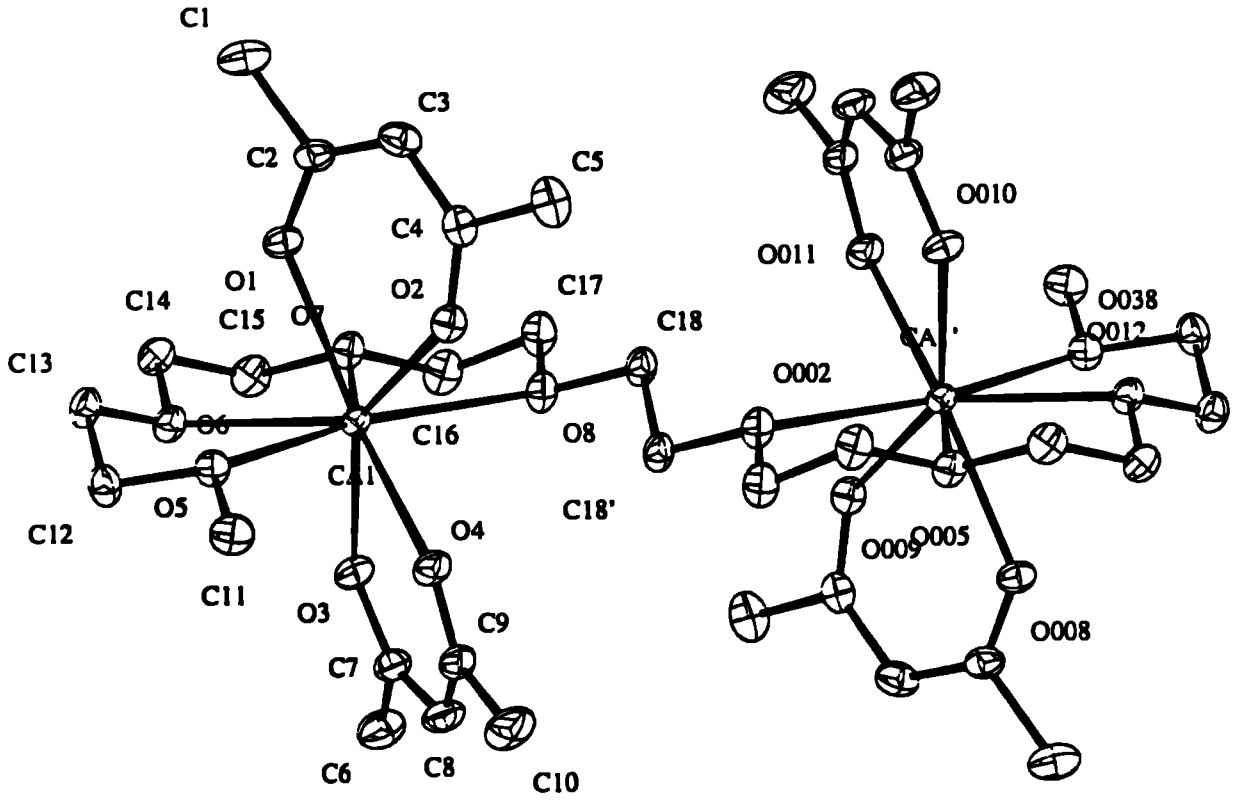

Figure 2.23 : X-ray crystal structure of [Ca(hfpd)$_2$(heptaglyme)] (11)

[Ca(dppd)$_2$(dppd-H)] (13)

The crystal data for [Ca(dppd)$_2$(dppd-H)] (13) are as follows : M = 710.84, triclinic, spacegroup P-1, a = 9.775(3), b = 10.620(3), c = 17.811(2) Å, α = 92.77(1), β = 94.75(1)^0, γ = 107.14°, V = 1755.64 Å^3, Z = 4, D_c = 1.345 g cm^{-3}, F(000) = 744, μ(Mo-K_α) = 2.2 cm^{-1}. 150 K. 7907 unique reflections were measured using [Mo-K_α] radiation on a FAST TV area detector diffractometer, of which 3652 having Fo > 4σ(Fo) were used in the refinement. The structure was solved by direct methods and refined by full matrix least squares to R = 0.0741 and Rw = 0.0966.

The single crystal X-ray structure of [Ca(dppd)$_2$(dppd-H)] (13) is shown in Figure 2.24. The calcium atom has a six-coordinate geometry with the three bidentate chelating diphenylpentanedione β-diketonates arranged around it in an octahedral structural motif. The Ca-O bond distances in this compound lie in an unusually narrow range 1.858(7) - 1.882(7)Å, [1.874(5) Å average] with the β-diketonate ligands binding in a slightly asymmetric chelating manner. The average Ca-O distance is considerably shorter (ca 0.5 Å) than the corresponding average observed for the recently reported trimeric complex [Ca_3(tmhd)$_6$][63] 2.35(5) Å, and in the complexes [Ca_4(dppd$_8$(EtOH)$_2$][75] 2.37(6)Å and also [Ca(pd)$_2$(H_2O)$_2$].H_2O 2.33(6)Å.[65] This substantial difference in bond-lengths may be attributed to the observation that in (13) all three diketone / diketonate ligands bond in a classical chelating manner, whereas in other calcium complexes they are present in a diverse range of coordination modes, leading to an effective overall increase of Ca-O bond lengths.

The O-Ca-O average chelate angle of 90.2(3)±2.0° in (13) is unique, being a direct result of the near perfect octahedral geometry, with no other similar alkaline earth compounds known. A systematic search of both Ca-O, C-O and C-C bond lengths and angles did not reveal the unique β-diketone dppd-H ligand. It appears that the methylene proton is disordered over all three ligands resulting in nearly identical Ca-O bond lengths and angles.

Table 2.10 : Selected bond lengths (Å) and angles (°) for (13) :

O(1) - Ca	1.875(7)	O(2) - Ca	1.882(7)
O(3) - Ca	1.881(7)	O(4) - Ca	1.882(7)
O(5) - Ca	1.869(7)	O(6) - Ca	1.858(7)
C(7) - O(1)	1.291(9)	C(9) - O(2)	1.278(8)

C (22) - O (3)	1.275(8)	C (24) - O (4)	1.276(8)
C (37) - O (5)	1.287(8)	C (39) - O (6)	1.286(8)
C (7) - C (8)	1.387(10)	C (8) - C (9)	1.387(9)
C (22) - C (23)	1.391(10)	C (23) - C (24)	1.393(10)
C (37) - C (38)	1.386(10)	C (38) - C (39	1.404(10)

O (2) - Ca - O (1)	89.3(3)	O (3) - Ca - O (1)	91.2(3)
O (3) - Ca - O (2)	88.9(3)	O (4) - Ca - O (1)	91.2(3)
O (4) - Ca - O (2)	179.1(2)	O (4) - Ca - O (3)	90.3(3)
O (5) - Ca - O (1)	176.2(2)	O (5) - Ca - O (2)	87.3(3)
O (5) - Ca - O (3)	87.3(3)	O (5) - Ca - O (4)	92.4(3)
O (6) - Ca - O (1)	90.5(3)	O (6) - Ca - O (2)	92.9(3)
O (6) - Ca - O (3)	177.5(2)	O (6) - Ca - O (4)	87.9(3)
O (6) - Ca - O (5)	91.1(3)		

C (9) - O (2) - Ca	129.4(5)	C (22) - O (3) - Ca	127.5(5)
C (24) - O (4) - Ca	127.8(5)	C (22) - O (3) - Ca	127.5(5)
C (39) - O (6) - Ca	129.3(5)	C (37) - O (5) - Ca	127.9(5)
C (7) - C (8) - O (1)	124.0(7)	C (8) - C (9) - O (2)	124.1(7)
C (22) - C (23) - O (3)	124.2(7)	C (23) - C (24) - O (4)	123.1(7)
C (37) - C (38) - O (5)	123.0(7)	C (38) - C (39) - O (6)	123.0(7)
C (7) - C (8) - C(9)	121.6(7)	C (22) - C (23) - C(24)	122.7(7)
C (37) - C (38) - C(39)	122.9(7)		

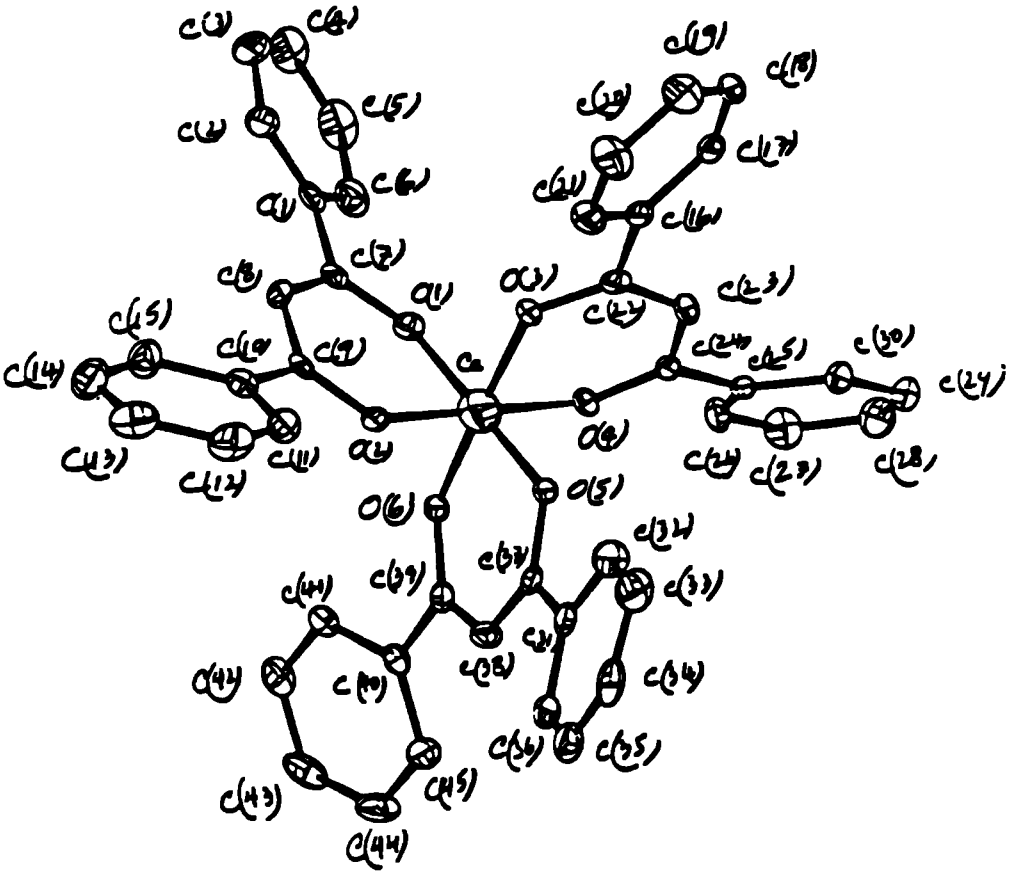

Figure 2.24 : X-ray crystal structure of [Ca(dppd)$_3$] (13)

[Ca(fod)$_2$(triglyme)] (14)

A single crystal of complex (14) was obtained directly from a saturated n-hexane solution. The crystal was mounted onto a glass-fibre and coated with epoxy resin to reduce any decomposition during data collection. The accurate unit cell parameters for complex (14) were obtained by means of least squares analysis between 18-25 centred reflections. Data for complex (14) were measured on a Siemens P4-PC diffractometer with graphite monochromated Mo-K_α radiation. Two standard reflections were monitored every 50 and showed no significant variation over the data collection. The structure of complex (14) was solved by direct methods and refined with full matrix least squares technique, using anisotropic thermal parameters for non-hydrogen atoms.

The X-ray structure shows that the calcium atom has a high coordination number of eight, with all of the oxygens of both the fod ligands and the triglyme bound to the metal atom. In this complex, the triglyme ligand is lying in a meridional plane, with the fod ligands positioned on either side of this plane in an orthogonal relationship, in a similar manner previously observed in [Ca(tmhd)$_2$(triglyme)](7). The coordination geometry around the calcium atom is highly irregular in nature being a distorted square antiprismatic with Ca-O distances in the range 2.365(3) - 2.514(4)Å.

The metal oxygen bonds fall into distinct categories, those to the β-diketonate, with Ca-$O_{(fod)}$ bonds ranging from 2.365(3) [O(8) / (8A)] to 2.374(3) [O(10) / (10A)], while those to the glyme, Ca-$O_{(glyme)}$ are in the range 2.491(4) [(O)2 / (2A)] to 2.514(4)Å [O(5) / (5A)]. These Ca-O distances are comparable with the corresponding Ca-$O_{(β\text{-}dik)}$ and Ca-$O_{(glyme)}$ values for [Ca(tmhd)$_2$(triglyme)](13), 2.348(6) - 2.379(6) and 2.471(5) - 2.594(5)Å respectively. It may be noted in this context that variations in the M-O distances involving the β-diketonate and glyme ligands appear to be a common phenomenon in alkaline earth metal complexes.

It is noteworthy that the two outer glyme oxygens O(2) and O(2A) bind slightly closer [2.491(4)Å] to the calcium than the two central oxygens of the polyether chain O(5) and O(5A) [2.514(4)Å]. This effect has previously been attributed to the steric constraints imposed by the two equatorial fod ligands.

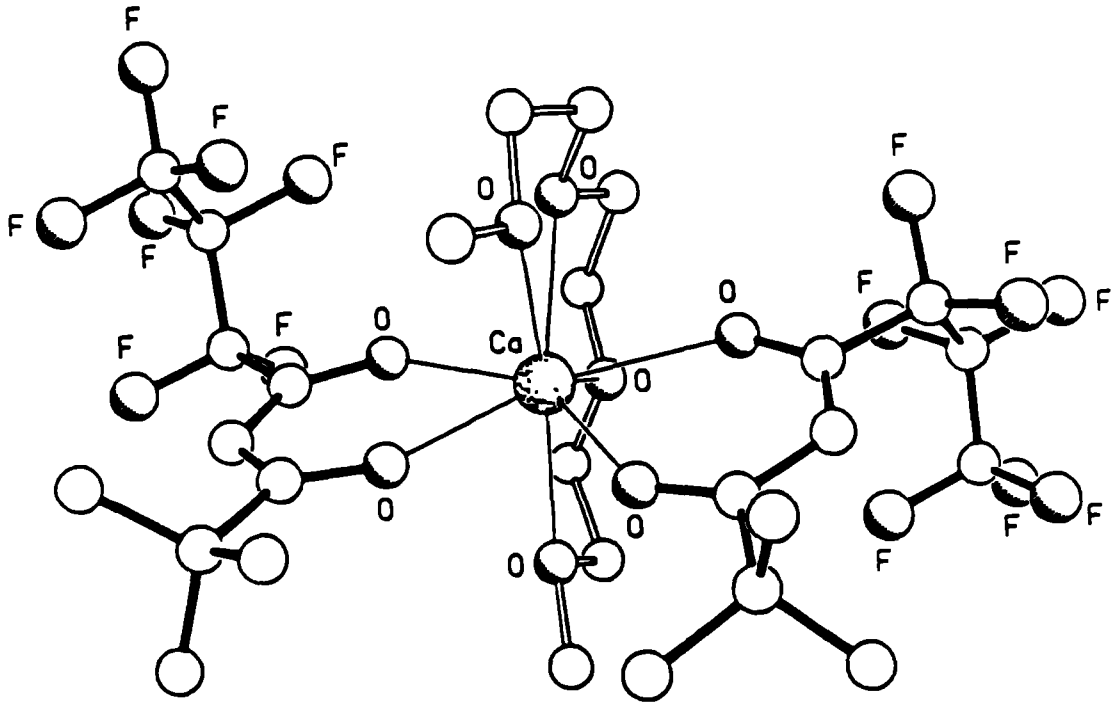

Figure 2.25 : X-ray crystal structure of [Ca(fod)$_2$(triglyme)] (14)

2.5.1 Crystallographic summary

A number of general points about the crystal structures of the glyme stabilized complexes of this Chapter may be noted from an analysis of the structural data. Firstly the majority of them are monomeric implying that the coordinative saturation requirements of the metals are met by the combination of glyme and β-diketonate ligands. Those that are not monomeric but dimeric fall into two categories; those with the heptaglyme and those with the diglyme ligand. The former are dimeric due to the fact that there are an excess of oxygen donor atoms on the glyme ligand making it susceptible to further bonding to a second metal centre, thereby satisfying the coordination requirements of two metals. The latter, however, exhibit completely the opposite properties. They have only three oxygen donor atoms and as such cannot saturate the metals fully; this explains the need for two diglyme molecules in (3) and the presence of a bridging water molecule in (6).

Secondly the metal - oxygen bond lengths fall into two distinct categories, those to the diketonate and those to the glyme. The latter is further split up into two classes, the outer metal - oxygen bonds being significantly shorter than the inner M-O bonds, this phenomenon is most likely to be due to steric crowding which is at a maximum at the terminal oxygens of the Lewis base ligands. Table 2.11 below collates the average metal - oxygen bond lengths for the monomeric complexes described in this Chapter.

Table 2.11 : M-O bond lengths of monomeric complexes (average) (Å) :

Compound	$M\text{-}O_{(\beta\text{-diket})}$	$M\text{-}O_{(glyme\ inner)}$	$M\text{-}O_{(glyme\ outer)}$
(1) $Ba(tmhd)_2(tetraglyme)$	2.648(7)	2.912(9)	2.868(9)
(2) $Ba(tmhd)_2(triglyme)$	2.632(6)	2.900(6)	2.814(5)
(5) $Sr(tmhd)_2(triglyme)$	2.494(10)	2.709(10)	2.639(10)
(7) $Ca(tmhd)_2(triglyme)$	2.362(3)	2.594(5)	2.471(5)
(8) $Sr(dppd)_2(tetraglyme)$	2.540(6)	2.791(5)	2.708(6)
(10) $Ca(hfpd)_2(tetraglyme)$	2.401(6)	2.497(6)	2.434(6)
(14) $Ca(fod)_2(triglyme)$	2.365(3)	2.514(4)	2.491(4)

Comparing the $M\text{-}O_{(tmhd)}$ bond lengths of compounds (1) and (2) we note that the tetraglyme complex has longer bonds. This is probably due to the increase in steric crowding afforded by the larger glyme ligand on the same metal - diketonate ensemble. Similarly both the $M\text{-}O_{(glyme)}$ bond lengths are shorter for the triglyme complex, this can be explained by the same reasoning.

Comparing the three tmhd / triglyme complexes (2), (5) and (7), we note a decrease in all three M-O bonds in the order Ca < Sr < Ba. This is consistent for both diketonate and glyme ligands (and also the difference between the outer and inner oxygen donors of the glyme ligands) and can be rationalized by the increasing ionic radii of the metals from Ca - Ba.

The $M\text{-}O_{(\beta\text{-diket})}$ bond lengths of the three, eight coordinate Ca complexes (7), (10) and (14), may also be directly compared. The bond lengths follow the trend; tmhd < fod <

hfpd, with respect to the β-diketonates. This phenomenon can be explained by the relative acidities of the β-diketonate ligands. Due to the electron withdrawing nature of the CF_3 groups of the hfpd ligands the M-O bond has less electron density associated. In contrast the fod ligand has both an electron withdrawing (C_3F_7) and an electron donating (^tBu) group; therefore, more electron density is imparted. The tmhd ligand has two electron donating groups and as such renders the M-O-C ring very electron dense.

This has the consequence of increasing the C=O bond lengths for tmhd (average 1.247(4)Å) (as is corroborated in infrared and NMR analyses) and subsequently decreasing the M-O bond lengths. Conversely the C=O bond lengths for the hfpd complexes are decreased by the extra electron density (average 1.241(5)Å) while the M-O bonds are lengthened. This factor would also expect to be seen with the dppd complexes [$Ca(dppd)_2$(n-glyme)] the diketonate ligand of which is also very acidic.

It is noteworthy too that the $M\text{-}O_{(\beta\text{-diket})}$ bond lengths are all considerably shorter than the corresponding $M\text{-}O_{(glyme)}$ bond lengths. This is hardly surprisingly when we realize that the diketonate ligands have a formal negative charge and thus are better donors. This difference in bond length ranges from 0.03(10)Å to 0.22(1)Å. It is noteworthy that there is a trend in the difference between the two sets of ligands following the order, Ba > Sr > Ca. This is most likely to be due to the increasing ionic radii from Ca - Ba, which allows the glyme ligands to stretch further away with the larger metals.

2.5.2 Dihedral angles in glyme stabilized β-diketonates

In all of the aforementioned monomeric glyme complexes a common structural phenomenon is noted. The two β-diketonates are observed to be on opposite sides of the metal centre with the glyme ligand separating the two, binding in a roughly planar coordination mode. However, the β-diketonates are not co-planar with respect to each other and a considerable fold is seen about the O...O axis. This angle between two planes is known as the dihedral angle and it is said to be zero when the planes are parallel. This deviation in planarity is a general feature but appears to be dependent on the nature of the metal, glyme and β-diketonate (see Table 2.12).

Table 2.12 : Dihedral angle (°) between β-diketonates in monomeric glyme complexes :

	Compound	Dihedral angle ( )
(1)	$Ba(tmhd)_2$(tetraglyme)	22.9
(2)	$Ba(tmhd)_2$(triglyme)	20.0
(5)	$Sr(tmhd)_2$(triglyme)	15.8
(7)	$Ca(tmhd)_2$(triglyme)	11.0
(8)	$Ca(tmhd)_2$(triglyme)	12.0
(10)	$Ca(hfpd)_2$(tetraglyme)	14.0
(14)	$Ca(fod)_2$(triglyme)	7.8

The tetraglyme compound (1), has a dihedral angle of 22.9° whereas (2), which has a smaller glyme, has an angle of only 20.0°. It is likely, therefore, that the tmhd ligands of (1) need to twist further away from the tetraglyme than with the smaller glyme due simply to steric size.

Comparing compounds (2), (4) and (7), which are all [$M(tmhd)_2$(triglyme)] species, we note a decrease in the dihedral angle in going from Ba > Sr > Ca; 20.0 , 15.8° and 11.0° respectively. These changes in coordination geometry are attributed to the different ionic radii (Ca = 1.03, Sr = 1.27 and Ba = 1.43Å). Thus in (2) there is a larger hemisphere of space around which the ligands may orient themselves.

Only one compound does not appear to follow this trend, namely compound (8), which has a dihedral angle of only 12°. However, when we consider that the phenyl substituents of the dppd ligands are essentially planar, whereas those of the tmhd and hfpd ligands are more tetrahedral, it is likely that the dppd ligand need not twist so much in order to relieve steric crowding.

Finally a study of complex (14) in terms of the dihedral angle between the planes of the fod ligands and their disposition with respect to the metal centre was made. The angle between the planes formed by O(8A)-Ca-O(10A) and O(8)-Ca-O(10) is *ca.* 7.8°. This fold about the axis is considerably less than for (7) which is 11°, the difference may be due to the tmhd ligand being more sterically crowded nearer the metal, whereas the fod ligand

has the bulk of its steric encumbrance further from the M-O bonds. As an example of this, Figure 2.26 below, shows perspective views of complexes (2), (7) and (10), showing the different twists of the β-diketonate ligands (the ^{t}Bu and CF_3 ligands have been omitted for clarity).

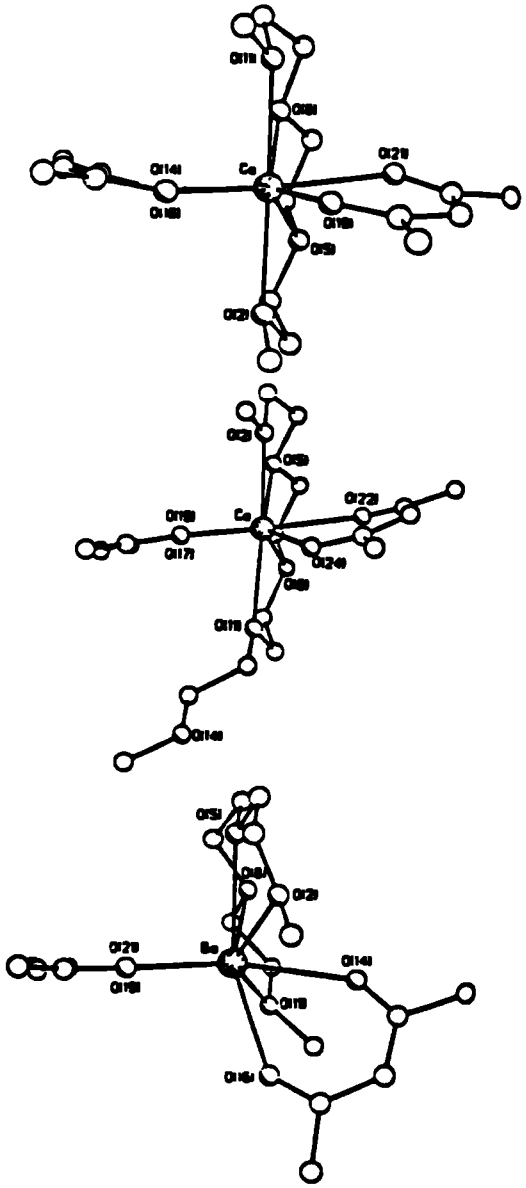

Figure 2.26 : Perspective views of (2), (7) and (10) (top to bottom) showing the dihedral angles of the β-diketonate ligands relative to the plane of the glyme ligands

2.6 Experimental section

(i) General Procedures

All manipulations (except for the synthesis of (14)) were carried out under an atmosphere of dry (molecular sieves) nitrogen using standard glove-box (Miller-Howe) and Schlenk techniques (using 'greaseless' J. Young's joints/valves). All hydrocarbon solvents were rigorously pre-dried and then distilled first over calcium oxide, and then redistilled over calcium metal by standard techniques. Chlorinated solvents were pre-dried and distilled over calcium hydride while alcohols were pre-dried and distilled over magnesium turnings. Elemental analyses were performed by the microanalytical department of Imperial College. The melting points were measured under argon in sealed capillaries and are uncorrected values.

(ii) Instrumentation

Infrared spectra were recorded on a Perkin Elmer FTIR 1720 spectrometer as either nujol or hexachlorobutadiene mulls between 25 x 4 mm KBr plates. The nujol and hexachlorobutadiene were both pre-dried with 4A molecular sieves prior to use (and stored in the glove-box); the samples were protected from the atmosphere by an O-ring-sealed Presslok holder (available from Aldrich chemicals).

NMR spectra were recorded on a Jeol GS 270 MHz NMR spectrometer, using the protio impurities of the deuterated solvent as reference for ^{1}H spectra and the ^{13}C resonance of the solvent as a reference for ^{13}C spectra. All chemical shifts are reported positive to high frequency of the standard. Mass spectra were run on a Kratos MS30 using the instrument in electron impact positive ion mode at the Royal School of Pharmacy Mass Spectrometry service, University of London. Thermal analyses of the complexes was investigated using a Polymer Laboratories 1500H simultaneous thermal analyzer, controlled by a Omni Pro 486DX-33 PC connected to a Rioch 1200 laser printer. The measurements were carried out in alumina crucibles under an atmosphere of flowing (30 ml/min) nitrogen gas, using heating rates of 5 °C/min.

Solid-state NMR spectra can provide valuable information with regards to the number of unique carbon environments in the solid state. It is often considered to be equivalent of running the solution spectra at very low temperatures. The use of magic angle spinning (MAS) where the sample is rotated at 54.7° to the permanent magnetic field, removes isotropic interactions observed in the solid state. CPMAS sequences reduce side spinning bands in the spectra. The NQS TOSS sequence removes all carbon signals from the $^{13}C\{^{1}H\}$ NMR spectra that have a strong dipolar coupling to protons.

Synthesis of [Ba(tmhd)$_2$(tetraglyme)] (1)

[Ba(OEt)$_2$(EtOH)$_4$]$_n$ (2.65 g, 6.45 mmol) was weighed into a Schlenk tube and n-hexane (25 mL) added. To the resulting clear solution was added tmhd-H (2.7 mL, 12.9 mmol) and the reaction left to stir for 5 mins., then tetraglyme (1.43 mL, 6.45 mmol) added, and the reaction left to stir for a further 10 mins.. The solvent and liberated ethanol were then removed under vacuum to yield a white solid, which was redissolved in n-hexane (20 mL), and left to crystallize at -20°C. **Yield** 100%. **M.pt.** 90-92°C

Microanalyses : Found, C, 52.39; H, 5.98 ; Calcd for $BaO_9C_{32}H_{60}$, C, 52.97; H, 8.27 %.

Infrared (Nujol ν cm^{-1}) : 1602(s), 1532(s), 1503(s), 1354(s), 1287(m), 1224(m), 1179(s), 1099(s), 1026(s), 953(s), 858(s), 788(m), 744(s), 731(m), 590(w), 532(w).

Infrared (Hexachlorobutadiene ν cm^{-1}) : 2947(s), 1532(s), 1503(m), 1430(s), 1386(s), 1268(m), 1224(s), 1103(s), 1024(m), 746(m), 731(m), 590(w).

^{1}H NMR (270 MHz, C_6D_6, 20°C) : δ 1.35 (36H, s, CH_3), 3.07 (6H, s, OCH_3), 3.26 (4H, s, OCH_2 a), 3.33 (4H, s, OCH_2 b), 3.36 (4H, s, OCH_2 c), 3.39 (4H, s, OCH_2 d), 5.83 (2H, s, CH).

^{13}C NMR (67.94 MHz, C_6D_6, 20°C) : δ 29.43 (s, CH_3), 41.16 (s, $\underline{C}(CH_3)_3$), 59.04 (s, OCH_3), 68.89 (s, OCH_2 a), 69.32 (s, OCH_2 b), 70.08 (s, OCH_2 c), 70.87 (s, OCH_2 d), 87.11 (s, CH), 196.42 (s, CO).

Mass Spectrometry (EI+) : 629 [Ba(tmhd)(Bu^{t}COCHCOH)(tetraglyme)](15%), 541 [Ba(tmhd)(tetraglyme)](41%), 505 [Ba(tmhd)$_2$](43%), 321 [Ba(tmhd)](100%).

Solubility : soluble in aliphatic (hexane), aromatic (toluene) and coordinating (chloroform and dmso) solvents.

STA data : TGA: 170-225°C(37.6%), 250-410 C(56.0%), Residue (6.00%), $T_{50\%}$ (380°C); DSC: 103.8°C, 223.0°C, 396.6°C.

Synthesis of [Ba(tmhd)$_2$(triglyme)] (2)

[Ba(OEt)$_2$(EtOH)$_4$]$_n$ (3.28 g, 7.98 mmol) was weighed into a Schlenk tube and n-hexane (25 mL) added. To the resulting clear solution was added tmhd-H (3.35 mL, 15.96 mmol) and the reaction left to stir for 5 mins., then triglyme (1.0 mL, 7.98 mmol) added, and the reaction left to stir for a further 10 mins.. The solvent and liberated ethanol were then removed under vacuum to yield a white solid, which was redissolved in n-hexane (18 mL), and left to crystallize at -20°C. **Yield** 100%. **M.pt.** 77-79°C

Microanalyses : Found, C, 52.99; H, 7.95 ; Calcd for $BaO_8C_{30}H_{56}$, C, 52.86; H, 8.22 %.

Infrared (Nujol ν cm^{-1}) : 1587(s), 1532(s), 1504(s), 1269(m), 1224(m), 1185(s), 1099(s), 1031(s), 950(s), 865(s), 832(m), 788(m), 748(s), 731(m), 590(w), 553(w).

Infrared (Hexachlorobutadiene ν cm^{-1}) : 2949(s), 1425(s), 1356(m), 1224(s), 1100(s), 1023(m), 748(m), 731(m), 591(w).

^{1}H NMR (270 MHz, C_6D_6, 20 C) : δ 1.32 (36H, s, CH_3), 3.13 (6H, s, OCH_3), 3.15 (4H, s, OCH_2 a), 3.20 (4H, s, OCH_2 b), 3.31 (4H, s, OCH_2 c), 5.79 (2H, s, CH).

^{13}C NMR (67.94 MHz, C_6D_6, 20 C) : δ 28.26 (s, CH_3), 40.66 (s, $\underline{C}(CH_3)_3$), 58.24 (s, OCH_3), 69.09 (s, OCH_2 a), 69.13 (s, OCH_2 b), 70.58 (s, OCH_2 c), 87.20 (s, CH), 196.78 (s, CO).

Mass Spectrometry (EI+) : 825 [$Ba_2(tmhd)_3$](35%), 504 [$Ba(tmhd)_2$](5%), 321 [Ba(tmhd)](100%).

Solubility : soluble in aliphatic (hexane), aromatic (toluene) and coordinating (chloroform and dmso) solvents.

STA data : TGA: 123-250 C(27.9%), 300-420 C(62.8%), Residue (8.48%), $T_{50\%}$ (360 C); DSC: 88.2 C, 197.6 C, 395.8 C.

Synthesis of $[Ba(tmhd)_2(diglyme)]_2$ (3)

$[Ba(OEt)_2(EtOH)_4]_n$ (3.29 g, 8.02 mmol) was weighed into a Schlenk tube and n-hexane (25 mL) added. To the resulting clear solution was added tmhd-H (3.40 mL, 16.03 mmol) and the reaction left to stir for 5 mins., then diglyme (1.56 mL, 16.03 mmol) added, and the reaction left to stir for a further 10 mins.. The solvent and liberated ethanol were then removed under vacuum to yield a white solid, which was redissolved in n-hexane (20 mL), and left to crystallize at -20°C. **Yield** 3.02g (86%) **M.pt.** 93-95°C

Microanalyses : Found, C, 52.89; H, 7.87 ; Calcd for $BaO_7C_{28}H_{52}$, C, 52.75; H, 8.16 %.

Infrared (Nujol ν cm^{-1}) : 1588(s), 1571(m), 1535(s), 1504(s), 1356(m), 1289(m), 1272(m), 1248(m), 1224(m), 1184(s), 1126(w), 1093(s), 1066(m), 1010(s), 950(s), 858(s), 833(m), 788(m), 757(s), 731(m), 593(w).

Infrared (Hexachlorobutadiene ν cm^{-1}) : 2964(s), 1505(w), 1451(s), 1414(m), 1358(m), 1289(m), 1272(m), 1248(m), 1224(s), 1184(w), 1126(m), 1093(s), 1066(m), 1010(m), 757(m), 731(m).

^{1}H NMR (270 MHz, C_6D_6, 20 C) : δ 1.28 (36H, s, CH_3), 3.18 (6H, s, OCH_3), 3.17 (4H, s, OCH_2 a), 3.20 (4H, s, OCH_2 b), 5.80 (2H, s, CH).

^{13}C NMR (67.94 MHz, C_6D_6, 20 C) : δ 28.74 (s, CH_3), 41.84 (s, $\underline{C}(CH_3)_3$), 58.13 (s, OCH_3), 69.41 (s, OCH_2 a), 71.13 (s, OCH_2 b), 89.05 (s, CH), 198.42 (s, CO).

Mass Spectrometry (EI+) : 827 [$Ba_2(tmhd)_3$](90%), 448 [Ba(tmhd)($Bu^tCOCHCOH$)](7%), 321 [Ba(tmhd)], 271 [Ba(diglyme)](100%).

Solubility : soluble in aliphatic (hexane), aromatic (toluene) and coordinating (chloroform and dmso) solvents.

STA data : TGA: 120-171 C(21.3%), 240-402 C(72.0%), Residue (6.05%), $T_{50\%}$ (365 C); DSC: 108.1 C, 219.7 C, 393.2 C.

Synthesis of [Sr(tmhd)$_2$(tetraglyme)] (4)

[Sr(OEt)$_2$(EtOH)$_4$] (2.72 g, 8.13 mmol) was weighed into a Schlenk tube and n-hexane (25 mL) added. To the resulting clear solution was added tmhd-H (3.46 ml, 16.25 mmol) and the reaction mixture left to stir for 5 min., tetraglyme (1.96 ml, 8.13 mmol) was then added, and the reaction left for a further 10 min. The solvent and liberated ethanol were then removed under vacuum to yield a waxy solid, which was re-dissolved in hot n-hexane (20 mL), and stored at -25°C. Crystals were obtained over a period of 3 days. **Yield** 4.1 g (66%) **M.pt.** 56-60 C

Microanalyses : Found, C, 56.64; H, 9.14 ; Calcd for $SrO_9C_{32}H_{60}$, C, 56.80; H, 8.88 %.

Infrared (Nujol υ cm^{-1}) : 1591(s), 1532(s), 1502(s), 1222(s), 1179(m), 1081(m), 1025(m), 952(s), 874(s), 855(m), 840(m), 788(m), 745(s), 729(s), 592(w), 469(w).

Infrared (Hexachlorobutadiene υ cm^{-1}) : 2969(s), 1505(s), 1452(s), 1425(s), 1356(s), 1272(m), 1224(s), 1104(s), 1068(m), 1012(m), 748(m), 731(m), 591(w).

^{1}H NMR (270 MHz, C_6D_6, 20 C) : δ 1.24 (36H, s, CH_3), 3.10 (6H, s, OCH_3), 3.21 (4H, s, OCH_2 a), 3.24 (4H, s, OCH_2 b), 3.36 (4H, s, OCH_2 c), 3.39 (4H, s, OCH_2 d), 5.70 (2H, s, CH).

^{13}C NMR (67.94 MHz, C_6D_6, 20 C) : δ 28.81 (s, (CH_3)), 40.67 (s, $\underline{C}(CH_3)_3$), 58.82 (s, OCH_3), 69.92 (s, OCH_2 a), 69.97 (s, OCH_2 b), 70.13 (s, OCH_2 c), 71.64 (s, OCH_2 d), 86.90 (s, CH), 196.55 (s, CO).

Mass Spectrometry (EI+) : 725 [Sr$_2$(tmhd)$_3$](41%), 677 [Sr(tmhd)(tetraglyme)](15%), 454 [Sr(tmhd)$_2$](14%), 397 [Sr(tmhd)(Bu^{t}COCHCOH)](15%), 271 [Sr(tmhd)](61%).

Solubility : soluble in aliphatic (hexane), aromatic (toluene) and coordinating (chloroform and dmso) solvents.

STA data : TGA: 150-260 C(32.5%), 260-382 C(58.1%), Residue (2.05%), $T_{50\%}$ (350 C); DSC: 75.4 C, 215.5 C, 370.9 C.

Synthesis of [Sr(tmhd)$_2$(triglyme)] (5)

[Sr(OEt)$_2$(EtOH)$_4$]$_n$ (2.72 g, 8.13 mmol) was weighed into a Schlenk tube and n-hexane (25 mL) added. To the resulting clear solution was added tmhd-H (3.46 mL, 16.25 mmol) and the reaction left to stir for 5 mins., then triglyme (1.79 mL, 8.13 mmol) added, and the reaction left to stir for a further 10 mins.. The solvent and liberated ethanol were then removed under vacuum to yield a white solid, which was redissolved in n-hexane (20 mL), and left to crystallize at -20°C. **Yield** 100%. **M.pt.** 88-89 C

Microanalyses : Found, C, 56.95, H, 9.31 ; Calcd for $SrO_8C_{30}H_{56}$, C, 56.96; H, 8.86 %

Infrared (Nujol ν cm^{-1}) : 1600(s), 1532(s), 1502(s), 1251(m), 1222(m), 1199(s), 1179(m), 1129(m), 1025(s), 952(s), 874(s), 855(m), 840(m), 788(s), 745(m), 719(w), 592(w).

Infrared (Hexachlorobutadiene ν cm^{-1}) : 2949(s), 1965(w), 1428(s), 1356(m), 1222(s), 1102(s), 1025(m), 749(m), 727(m), 589(w).

^1H NMR (270 MHz, C_6D_6, 20 C) : δ 1.34 (36H, s, CH_3), 3.15 (6H, s, OCH_3), 3.04 (4H, s, OCH_2 a), 3.24 (4H, s, OCH_2 b), 3.31 (4H, s, OCH_2 c), 5.80 (2H, s, CH).

^{13}C NMR (67.94 MHz, C_6D_6, 20 C) : δ 28.91 (s, CH_3), 40.67 (s, $\underline{C}(CH_3)_3$), 58.62 (s, OCH_3), 69.20 (s, OCH_2 a), 69.97 (s, OCH_2 b), 70.51 (s, OCH_2 c), 86.90 (s, CH), 196.93 (s, CO).

Mass Spectrometry (EI+) : 454 [Sr(tmhd)$_2$](15%), 450 [Sr(tmhd)(triglyme)](3%), 397 [Sr(tmhd)($Bu^tCOCHCOH$)](31%), 271 [Sr(tmhd)](60%), 262 [Sr(triglyme)](1%).

Solubility : soluble in aliphatic (hexane), aromatic (toluene) and coordinating (chloroform and dmso) solvents.

STA data : TGA: 153-224 C(30.3%), 316-383 C(65.4%), Residue (5.78%), $T_{50\%}$ (330 C); DSC: 101.6 C, 191.0 C, 376.4 C.

Synthesis of $[Sr(tmhd)_2(diglyme)]_2(\mu\text{-}H_2O)$ (6)

$[Sr(OEt)_2(EtOH)_4]_n$ (1.99 g, 5.92 mmol) was weighed into a Schlenk tube and n-hexane (25 mL) added. To the resulting clear solution was added tmhd-H (2.52 mL, 11.84 mmol) and the reaction left to stir for 5 mins., then diglyme (1.70 mL, 11.84 mmol) added, and the reaction left to stir for a further 10 mins.. The solvent and liberated ethanol were then removed under vacuum to yield a white solid, which was redissolved in n-hexane (20 mL), and left to crystallize at 0°C. **Yield** 3.95g (79 %) **M.pt.** 96-98°C

Microanalyses : Found, C, 56.81; H, 8.93 ; Calcd for $Sr_2O_{15}C_{56}H_{106}$, C, 56.28; H, 8.88 %

Infrared (Nujol ν cm^{-1}) : 3347(m), 1732(m), 1586(s), 1574(m), 1535(s), 1504(s), 1356(m),1272(m), 1248(m), 1224(m), 1184(s), 1129(w), 1105(s), 1066(m), 866(s), 835(m), 790(m), 757(s), 731(m), 595(w).

Infrared (Hexachlorobutadiene ν cm^{-1}) : 3341(m), 2966(s), 1588(m), 1505(w), 1477(s), 1451(s), 1429(m), 1388(m), 1358(m), 1272(m), 1226(m), 1184(w), 1103(m), 1066(m), 1014(m), 757(m), 731(m), 594(w).

^1H NMR (270 MHz, C_6D_6, 20 C) : δ 1.24 (36H, s, CH_3), 3.20 (6H, s, OCH_3), 3.17 (4H, s, OCH_2 a), 3.18 (4H, s, OCH_2 b), 3.34 (1H, br, H_2O), 5.77 (2H, s, CH).

^{13}C NMR (67.94 MHz, C_6D_6, 20 C) : δ 28.52 (s, CH_3), 40.46 (s, $\underline{C}(CH_3)_3$), 58.64 (s, OCH_3), 69.45 (s, OCH_2 a), 70.91 (s, OCH_2 b), 88.11 (s, CH), 198.46 (s, CO).

Mass Spectrometry (EI+) : 725 [Sr_2(tmhd)$_3$](6%), 454 [Sr(tmhd)$_2$](34%), 406 [Sr(tmhd)(diglyme)](16%), 397 [Sr(tmhd)($Bu^tCOCHCOH$)](15%), 271 [Sr(tmhd)](51%), 223 [Sr(diglyme)](13%).

Solubility : soluble in aliphatic (hexane), aromatic (toluene) and coordinating (chloroform and dmso) solvents

Synthesis of [Ca(tmhd)$_2$(triglyme)] (7)

[Ca(OEt)$_2$(EtOH)$_4$]$_n$ (2.78 g, 8.87 mmol) was weighed into a Schlenk tube and n-hexane (25 mL) added. To the resulting solution was added tmhd-H (3.78 mL, 17.76 mmol) and the reaction left to stir for 5 mins., then triglyme (1.60 mL, 8.87 mmol) added, and the reaction left to stir for a further 10 mins.. The solvent and liberated ethanol were then removed under vacuum to yield a white solid, which was redissolved in n-hexane (20 mL), and left to crystallize at -20°C. **Yield** 100%. **M.pt.** 71-74 C

Microanalyses : Found, C , 61.80; H, 9.73 ; Calcd for $CaO_8C_{30}H_{56}$, C, 61.64; H, 9.59 %.

Infrared (Nujol ν cm^{-1}) : 1594(s), 1575(s), 1532(s), 1504(s), 1349(m), 1261(m), 1234(m), 1224(s), 1199(s), 1178(m), 1132(m), 1101(s), 1083(s), 1025(s), 953(m), 877(s), 856(m), 840(m), 788(m), 744(s), 731(s), 594(w), 545(w).

Infrared (Hexachlorobutadiene ν cm^{-1}) : 2949(s), 1590(m), 1534(s), 1505(s), 1425(s), 1386(m), 1356(m), 1261(m), 1224(s), 1100(s), 1023(m), 749(m), 731(m), 594(w).

^{1}H NMR (270 MHz, C_6D_6, 20 C) : δ 1.32 (36H, s, CH_3), 3.16 (6H, s, OCH_3), 3.11 (4H, s, OCH_2 a), 3.28 (4H, s, OCH_2 b), 3.47 (4H, s, OCH_2 c), 5.80 (2H, s, CH).

^{13}C NMR (67.94 MHz, C_6D_6, 20 C) : δ 28.82 (s, CH_3), 40.56 (s, $\underline{C}(CH_3)_3$), 58.64 (s, OCH_3), 69.04 (s, OCH_2 a), 69.45 (s, OCH_2 b), 71.05 (s, OCH_2 c), 87.30 (s, CH), 197.28 (s, CO).

Mass Spectrometry (EI+) : 813 [Ca_3(tmhd)$_4$](4%), 727 [Ca_2(tmhd)$_3$($Bu^tCOCHCOH$)](15%), 629 [Ca_2(tmhd)$_3$](83%), 422 [Ca(tmhd)$_2$(H_2O)](20%), 349 [Ca(tmhd)($Bu^tCOCHCOH$)](55%), 223 [Ca(tmhd)](100%).

Solubility : soluble in aliphatic (hexane), aromatic (toluene) and coordinating (chloroform and dmso) solvents.

STA data : TGA: 134-323 C(30.1%), 324-359 C(71.0%) Residue (2.05%), $T_{50\%}$ (330 C); DSC: 78.5 C, 350.5°C.

Synthesis of [Sr(dppd)$_2$(tetraglyme)].0.5 C_7H_8 (8)

[Sr(OEt)$_2$(EtOH)$_4$]$_n$ (2.51 g, 7.45 mmol) was weighed into a Schlenk tube and chloroform (25 mL) added. To the resulting clear solution was added dppd-H (3.34 g, 14.90 mmol) and the yellow solution was left to stir for 5 mins., then tetraglyme (1.64 mL, 7.45 mmol) added, and the reaction left to stir for a further 10 mins.. The solvent and liberated ethanol were then removed under vacuum to yield a yellow solid, which was redissolved in hot toluene (20 mL), and left to crystallize at 20°C. **Yield** 100%. **M.pt.** 96-98 C

Microanalyses : Found, C, 64.81; H, 6.14 ; Calcd for $SrO_9C_{43.5}H_{48}$, C, 65.09; H, 5.99 %.

Infrared (Nujol ν cm^{-1}) : 1620(s), 1582(s), 1513(s), 1324(s), 1222(m), 1108(s), 935(s), 870(s), 733(m).

580(w), 513(w).

Infrared (Hexachlorobutadiene ν cm^{-1}) : 2918(s), 1471(w), 1425(s), 1299(m), 1224(s), 1113(s), 1026(m), 748(m), 731(m), 690(w), 579(m).

^1H NMR (270 MHz, C_6D_6, 20 C) : δ 3.23 (6H, s, OCH_3), 3.41 (4H, s, OCH_2 a), 3.42 (4H, s, OCH_2 b), 3.48 (4H, s, OCH_2 c), 3.51 (4H, s, OCH_2 d), 6.57 (2H, s, CH), 7.40, 7.98 (20H, m, phenyl protons)

^{13}C NMR (67.94 MHz, C_6D_6, 20 C) : δ 58.70 (s, OCH_3), 70.28 (s, OCH_2 a), 70.48 (s, OCH_2 b), 71.97 (s, OCH_2 c), 72.12 (s, OCH_2 d), 92.36 (s, CH), 128.87 (m, phenyl protons), 182.52 (s, CO).

Mass Spectrometry (EI+) : Shows only ligand decomposition

Solubility : soluble in aromatic (toluene) and coordinating (chloroform and dmso) solvents.

Synthesis of $[Ca(hfpd)_2(tetraglyme)]$ (9)

$[Ca(OEt)_2(EtOH)_4]_n$ (2.46 g, 7.83 mmol) was weighed into a Schlenk tube and n-hexane (25 mL) added. To the resulting clear solution was added hfpd-H (2.21 mL, 15.66 mmol) and the reaction left to stir for 5 mins., then tetraglyme (1.73 mL, 7.83 mmol) added, and the solution was left to stir for a further 10 mins.. The solvent and liberated ethanol were then removed under vacuum at room temperature to yield a white solid, which was redissolved in n-hexane (15 mL), and left to crystallize at 20°C. **Yield** 100% **M.pt.** 82-85°C

Microanalyses : Found, C, 35.61; H, 3.72 ; Calcd for $CaO_9C_{20}F_{12}H_{24}$, C, 35.49; H, 3.55 %.

Infrared (Nujol ν cm^{-1}) : 1658(s), 1594(s), 1532(s), 1504(m), 1349(m), 1261(s), 1234(m), 1224(m), 1199(m), 1178(m), 1130(m), 1101(m), 1083(m), 1026(m), 953(s), 877(s), 856(m), 840(w), 794(s), 744(m), 732(w), 594(w), 545(w).

Infrared (Hexachlorobutadiene ν cm^{-1}) : 2947(s), 1660(s), 1590(s), 1534(w), 1505(s), 1425(m), 1386(m), 1356(m), 1261(s), 1225(m), 1100(m), 1023(m), 748(m), 731(m) 594(m).

^1H NMR (270 MHz, C_6D_6, 20 C) : δ 2.95 (4H, s, OCH_2 a), 3.05 (6H, s, OCH_3), 3.12 (4H, s, OCH_2 b), 3.14 (4H, s, OCH_2 c), 3.18 (4H, s, OCH_2 d), 6.30 (2H, s, CH).

^{13}C NMR (67.94 MHz, C_6D_6, 20 C) : δ 59.79 (s, OCH_3), 68.64 (s, OCH_2 a), 69.91 (s, OCH_2 b), 70.31 (s, OCH_2 c), 71.30 (s, OCH_2 d), 88.16 (s, CH), 118.80 (q, CF_3 ^1J = 296Hz), 176.32 (q, CO ^2J = 32Hz).

Mass Spectrometry (EI+) : 676 [Ca(hfpd)$_2$(tetraglyme)](15%), 607 [Ca(hfpd)($CF_3COCHCO$)(tetraglyme)](9%), 470 [Ca(hfpd)(tetraglyme)](26%), 247 [Ca(hfpd)](52%).

Solubility : soluble in aliphatic (hexane), aromatic (toluene) and coordinating (chloroform and dmso) solvents.

Synthesis of [Ca(hfpd)$_2$(triglyme)] (10)

$[Ca(OEt)_2(EtOH)_4]_n$ (2.50 g, 7.96 mmol) was weighed into a Schlenk tube and n-hexane (25 mL) added. To the resulting clear solution was added hfpd-H (2.25 mL, 15.92 mmol) and the reaction left to stir for 5 mins., then triglyme (1.84 mL, 7.96 mmol) was added, and the solution left to stir for a further 10 mins.. The solvent and liberated ethanol were then removed under vacuum at room temperature to yield a white solid, which was redissolved in n-hexane (15 mL), and left to crystallize at 20°C. **Yield** 2.98 g (60%) **M.pt.** 103-106 C

Microanalyses : Found, C, 34.28; H, 3.28 ; Calcd for $CaO_8C_{18}F_{12}H_{20}$, C, 34.18; H, 3.16 %.

Infrared (Nujol ν cm^{-1}) : 1658(s), 1589(s), 1530(s), 1366(m), 1253(s), 1192(m), 1140(m), 1086(m), 1066(m), 1026(m), 949(s), 877(s), 850(m), 832(w), 794(s), 758(m), 732(w), 580(w).

Infrared (Hexachlorobutadiene ν cm^{-1}) : 2957(s), 2867(w), 1658(s), 1530(w), 1475(s), 1455(m), 1366(m), 1353(m), 1252(s), 1185(m), 1145(m), 1088(m), 1066(m), 1027(m), 876(m), 758(m) 580(m).

^{1}H NMR (270 MHz, C_6D_6, 20 C) : δ 2.71 (4H, s, OCH_2 a), 2.93 (4H, s, OCH_2 b), 2.97 (6H, s, OCH_3), 3.24 (4H, s, OCH_2 c), 6.29 (2H, s, CH).

^{13}C NMR (67.94 MHz, C_6D_6, 20°C) : δ 59.28 (s, OCH_3), 68.60 (s, OCH_2 a), 69.37 (s, OCH_2 b), 70.84 (s, OCH_2 c), 88.29 (s, CH), 118.77 (q, CF_3 ^1J = 289Hz), 176.67 (q, CO ^2J = 33Hz).

Mass Spectrometry (EI+) : 218 [Ca(triglyme)](12%).

Solubility : soluble in aliphatic (hexane), aromatic (toluene) and coordinating (chloroform and dmso) solvents.

STA data : TGA: 140-264 C(98.6%), Residue (0.64%), $T_{50\%}$ (236°C); DSC: 59.56 C, 126.2 C, 251.9 C.

Synthesis of [Ca(hfpd)$_2$]$_2$(heptaglyme) (11)

$[Ca(OEt)_2(EtOH)_4]_n$ (4.00 g, 11.83 mmol) was weighed into a Schlenk tube and n-hexane (25 mL) added. To the resulting clear solution was added hfpd-H (3.35 mL, 23.66 mmol) and the reaction left to stir for 5 mins., then heptaglyme (1.61 mL, 5.91 mmol) added, and the solution left to stir for a further 10mins.. The solvent and liberated ethanol were removed under vacuum to yield a colourless oil, which was held under vacuo for 1h at 80°C. This was redissolved in n-hexane (20 mL), and left to crystallize at 20 C. **Yield** 6.13g (68%) **M.pt.** 112-116 C

Microanalyses : Found, C, 34.45, H, 2.72 , Calcd for $Ca_2O_{16}C_{36}F_{24}H_{38}$, C, 34.23; H, 3.01 %.

Infrared (Nujol ν cm^{-1}) : 1661(s), 1590(s), 1526(s), 1356(m), 1260(s), 1195(m), 1143(m), 1085(m), 1066(m), 1032(m), 1021(m), 957(s), 872(s), 856(m), 795(s), 738(m), 722(w), 661(m), 580(w).

Infrared (Hexachlorobutadiene ν cm^{-1}) : 2947(s), 2869(s), 1660(s), 1611(w), 1589(m), 1526(s), 1487(s),

1447(m), 1455(m), 1368(m), 1355(m), 1338(m), 1316(m), 1261(s), 1187(m), 1143(m), 1085(m), 1066(m), 1033(m), 1022(m), 872(w), 763(m), 739(m) 581(m).

^{1}H NMR (90 MHz, d_6-dmso, 20 C) : δ 3.19 (6H, s, OCH_3), 3.21 (4H, s, OCH_2 a), 3.39 (4H, s, OCH_2 b), 3.41 (4H, s, OCH_2 c), 3.43 (4H, s, OCH_2 d), 3.46 (12H, s, OCH_2 e, f, g), 5.52 (4H, s, CH)

^{13}C NMR (22.61 MHz, C_6D_6, 20 C) : δ 57.44 (s, OCH_3), 69.03 (s, OCH_2 a), 69.22 (s, OCH_2 b, c, d, e, f) 70.74 (s, OCH_2 g), 84.11 (s, CH), 118.25 (q, CF_3 ^1J = 296Hz), 171.57 (q, CO ^2J = 28Hz).

Mass Spectrometry (EI+) : 701 [$Ca_2(hfpd)_3$](20%), 601 [Ca(hfpd)(heptaglyme)](100%), 557 [Ca(hfpd)(heptaglyme-$O(CH_2)_2$)](25%), 513 [$Ca(hfpd)_2(CH_2CH_2O_2)$](5%), 454 [$Ca(hfpd)_2$](5%), 325 [$Ca(hfpd)(CH_2CH_2O_3)$](5%), 247 [Ca(hfpd)](7%).

Solubility : soluble in aromatic (toluene) and coordinating (chloroform and dmso) solvents.

STA data : TGA: 309-333 C(79.9%), Residue (8.13%), $T_{50\%}$ (330 C); DSC: 123.6 C, 292.1 C.

Synthesis of $[Sr(tmhd)_2(tmhd\text{-}H)]$ (12)

$[Sr(OEt)_2(EtOH)_4]_n$ (4.71 g , 14.2 mmol) was added to 25 ml hexane and stirred at room temp for 10 mins, tmhd-H (10 ml, 45.0 mmol) was added to the reaction mixture which completely dissolved. The solution was stirred for a further 10 mins and then the solvent removed under vacuo to yield a colourless viscous liquid which was held under vacuum for 1h at 80°C. 8 ml of hexane was added and the soluble solution placed at 0 C to crystallize. A large number of colourless crystals were collected. The hexane was then removed from the filtrate and the product placed at 0°C to yield a second crop of crystals.

Yield. 6.21 g (69%) M.Pt. 76-81 C

Microanalyses : Found ; C, 61.98 ; H, 8.67 ; Calcd. for $SrC_{33}O_6H_{58}$; C, 62.07 ; H, 9.09%

Infrared (nujol ν cm^{-1}) ; 1725 (w), 1592 (s), 1579 (s), 1561 (m), 1537 (m), 1505 (s), 1425 (m), 1361 (m), 1276 (m), 1245 (m), 1222 (m), 1185 (m), 1132 (m), 1024 (m), 956 (w), 867 (m), 793 (m), 756 (w), 736 (m), 596 (w), 564 (m), 476 (m), 386 (w).

Infrared (Hexachlorobutadiene ν cm^{-1}): 2962 (s), 2868 (m), 1722 (w), 1592 (s), 1578 (s), 1538 (m), 1505 (s), 1416 (m), 1390 (m), 1359(m), 1261 (m), 1245 (m), 1222 (m), 1185 (m), 1133 (m), 1061 (m), 1022 (m), 758 (w), 736 (m), 655 (w), 595 (w).

^{1}H NMR (90 MHz, 20 C, d_6-dmso) : δ 0.99 (s, 54H, CH_3), 3.80 (s, 2H, CH_2), 5.35 & 6.21 (s, 2H, CH).

^{1}H NMR (90 MHz, 20 C, $CDCl_3$) : δ 1.01 (s, 54H, CH_3), 5.56 (br, 4H, CH/CH_2).

^{1}H NMR (90 MHz, 20 C, C_7D_8) : δ 1.34 (s, 54H, CH_3), 3.60 (br, 2H, CH_2), 5.97 (br, 2H, CH)

^{1}H NMR (270 MHz, 20 C, C_6D_6) : δ 1.15 (s, 54H, CH_3), 5.78 (br, 4H, CH).

^{13}C NMR (22.61 MHz, 20 C, d_6-dmso). δ 25.89, 28.69 (s, CH_3), 46.15 (s, $\underline{C}(CH_3)_3$), 86.67, 86.96 (s,

CH), 210.60 (s, CO).

^{13}C NMR (22.61 MHz, 20 C, $CDCl_3$). δ 31.12 (s, CH_3), 43.70 (s, $\underline{C}(CH_3)_3$), 90.74 (s, CH), 203.84 (s, CO).

^{13}C NMR (22.61 MHz, 20 C, C_7D_8). δ 27.85 (s, CH_3), 40.48 (s, $\underline{C}(CH_3)_3$), 90.16 (s, CH), 200.74 (s, CO).

^{13}C NMR (67.94 MHz, 20 C, C_6D_6). δ 27.96 (s, CH_3), 40.52 (s, $\underline{C}(CH_3)_3$), 90.74 (s, CH), 201.78 (s, CO).

Mass Spectrometry : 726 [Sr_2(tmhd)$_3$](52%), 454 [Sr(tmhd)$_2$](16%), 398 [Sr(tmhd)(OCCHOCC$(CH_3)_3$)](5%), 271 [Sr(tmhd)](52%), 185 [thd](100%), 127 [OCCHOCC$(CH_3)_3$](29%), 109 [CCHOCC$(CH_3)_3$](5%), 97 [CHOCC$(CH_3)_3$]](3%), 85 [OCC$(CH_3)_3$](13%), 69 [CC$(CH_3)_3$](8%), 57 [C$(CH_3)_3$](66%).

Solubility : soluble in aliphatic (hexane), aromatic (toluene) and coordinating (chloroform and dmso) solvents.

STA data : TGA: 90-193 C(23.0%), 270-390 C(74.6%), Residue (3.43%), $T_{50\%}$ (350 C); DSC: 70.8 C, 92.7 C, 384.2 C.

Synthesis of [Ca(dppd)$_2$(dppd-H)] (13)

[$Ca(OEt)_2(EtOH)_4]_n$ (1.40 g, 4.54 mmol) was added to 30 ml chloroform and dppd-H (3.05 g, 13.6 mmol) added to the reaction which turned yellow and fully soluble. The solution was stirred for 50 mins. and the solvent was removed under vacuo to yield a yellow solid which was held under vacuum for 1h at 80°C. Then 30 ml of boiling toluene was added to dissolve all the solid, on slow cooling a pale orange precipitate formed. The solid was filtered and the filtrate placed at -25°C. **Yield.** 1.34g (25%) Mpt. 68-72 C

Microanalyses : Found ; C, 75.28; H, 4.83 ; Calcd. for $CaC_{45}O_6H_{43}$; C, 76.06 ; H, 4.65%.

Infrared (nujol ν cm^{-1}) ; 1732 (w), 1598 (s), 1557 (br), 1309 (m), 1261 (m), 1094 (m), 1024 (m), 802 (m), 756 (m), 723 (m), 700 (w), 682 (m), 609 (m).

Infrared (Hexachlorobutadiene ν cm^{-1}) ; 2958 (s), 2926 (m), 2855 (m), 1730 (w), 1611 (m), 1523 (s), 1481 (s), 1455 (m), 1403 (m), 1305 (m), 1261 (m), 1225 (m), 1171 (m), 1135 (m), 1071 (m), 1024 (m), 754 (w), 726 (m), 655 (w), 609 (w), 548 (w).

^{1}H NMR (90 MHz, 20 C, $CDCl_3$). δ 6.70 (s, 4H, CH), 7.30-7.90 (m, 30H, Ph).

^{1}H NMR (270 MHz, 20 C, d_6-dmso). δ 4.88 (s, 1H, CH_2), 7.34 (s, 3H, CH), 7.53-8.18 (m, 30H, Ph).

^{1}H NMR (90 MHz, 20 C, C_6D_6). δ 6.56 (s, 4H, CH), 7.01-7.85 (m, 30H, Ph).

^{1}H NMR (90 MHz, 20 C, C_7D_8). δ 6.51 (s, 4H, CH), 6.90-7.81 (m, 30H, Ph).

^{13}C NMR (67.94 MHz, 20 C, d_6-dmso). δ 50.20 (s, CH_2), 93.46 (s, CH), 127.53 (s, p-Ph), 128.92 (s,

m-Ph), 133.11 (s, o-Ph), 139.84 (m, i-Ph), 183.42 (s, CO).

^{13}C NMR (22.61 MHz, 20 C, C_7D_8). δ 92.21 (s, CH), 125.13 (s, p-Ph), 126.29 (s, m-Ph), 130.17 (o, Ph), 136.40 (s, i-Ph), 184.92 (s, CO).

Mass Spectrometry : 766 [$Ca_2(dppd)_3(H_2O)$](8%), 727 [$HCa(dppd)_3(H_2O)$](5%).

Solubility : soluble in aromatic (hot toluene) and coordinating (chloroform and dmso) solvents.

STA data : TGA: 229-275 C(80.4%), 344-411 C(14.9%), Residue (2.60%), $T_{50\%}$ (255 C); DSC: 79.2 C, 265.9 C.

Synthesis of [Ca(fod)$_2$(triglyme)] (14)

CaO (0.5 g, 8.93 mmol) was weighed into a flask and 95% ethanol (45 ml) and water (3 ml) added. To the resulting solution was added fod-H (4.16 ml, 17.86 mmol) and the reaction mixture left to stir for 5 min. and then triglyme (1.61 ml, 8.93 mmol) was added, the reaction was refluxed for 4 h during which time all the solid dissolved. The solvent was then removed on a rotary evaporator to yield a white solid which was held at 100 C for 1h. The resulting material was dissolved in warm n-hexane (30 ml), filtered, then placed at -25 C. Crystals were obtained over a period of 14 h. **Yield** 6.15 g (84%) **M.pt.** 80-83 C

Microanalyses: Found, C, 41.38; H, 4.37 ; Calcd for $CaO_8F_{14}C_{28}H_{38}$, C, 41.58; H, 4.70 %.

Infrared (Nujol υ cm^{-1}) : 1648(s), 1538(s), 1502(s), 1366(w), 1352(m), 1261(m), 1224(s), 1171(m), 1156(m), 1145(m), 1123(m), 1096(w), 1061(m), 1021(m), 966(s), 874(s), 851(m), 801(m), 791(m), 745(s), 725(s), 659(w), 534(w).

Infrared (Hexachlorobutadiene υ cm^{-1}) : 2954(s), 2837(m), 1647(s), 1501(s), 1468(s), 1444(s), 1392(m), 1351(s), 1278(m), 1205(s), 1171(m), 1157(m), 1144(m), 1120(s), 1094(m), 1060(m), 1021(m), 893(m), 737(w), 655(m).

^{1}H NMR (270 MHz, $CDCl_3$, 20°C) : δ 1.13 (18H, s, CH_3), 3.25 (6H, s, OCH_3), 3.48 (4H, m, OCH_2 a), 3.60 (4H, s, OCH_2 b), 3.88 (4H, s, OCH_2 c), 5.73 (2H, br, CH).

^{13}C NMR (67.94 MHz, $CDCl_3$, 20 C) : δ 28.02 (s, CH_3), 41.74 (s, $\underline{C}(CH_3)_3$), 59.32 (s, OCH_3), 68.62 (s, OCH_2 a), 69.50 (s, OCH_2 b), 71.26 (s, OCH_2 c), 89.74 (s, CH), 109.6 (m, $CF_3\underline{C}F_2$), 111.0 (t of t, $CO\underline{C}F_2$), 116.3 (q of t, CF_3), 170.59 (t, $\underline{C}OCF_2$), 203.70 (s, CO).

Mass Spectrometry (EI+) : 972 [$Ca_2(fod)_3$](2%), 810 [$Ca(fod)_2$(triglyme)](9%), 513 [Ca(fod)(triglyme)](23%), 336 [Ca(fod)](2%).

Solubility : soluble in aliphatic (warm hexane), aromatic (toluene) and coordinating (chloroform and dmso) solvents.

STA data : TGA: 271-326 C(92.7%), Residue (4.27%), $T_{50\%}$ (291 C); DSC: 84.5 C, 272.8 C, 307.7 C, 330.0 C.

Chapter 3

AMINE ADDUCTS OF ALKALINE EARTH METAL β-DIKETONATES

3.1 Introduction

Inorganic compounds which involve the direct linkage of a metal and a nitrogen donor ligand are numerous in materials chemistry. They may be used not only as isolable examples of metal amines, but also as precursors to further materials. They can be found in conjunction, for instance, with alkoxides, e.g. $[Ba_6(OPh)_8(tmeda)_2]$,[84] or with acetates, e.g. $[Cu_4(OAc)_6(bdmap)_2(H_2O)_6]_n$,[85] the latter of which is a two dimensional hydrogen bonded network, placing the copper metal in a five coordinate geometry.

The reaction of the heavier alkaline earth metals with hexamethylsilazide (hmdz) in a solvent system comprising ammonia and toluene at -40°C, produces NH_3 adducts of $[M\{N(SiMe_3)_2\}_2]_2$ which may be converted to the homoleptic species by toluene reflux. Tetramethylethylenediamine (tmeda) has been found to be very reactive with the electropositive metals, especially lithium.[86,87] For example, the reaction of the former $[Li\{N(SiMe_3)_2\}_2]_2$ with tmeda in a non polar solvent, e.g. pentane, results in the formation of the monomer, $[Li\{N(SiMe_3)_2\}tmeda]$. In polar solvents such as thf a dimeric species, $[Li\{N(SiMe_3)_2\}thf]_2$ is formed.

A variety of transition metal, main group and lanthanide β-diketonato amides have recently been synthesized. $[Ce(tmhd)_3phen]$ and $[Ce(tfdh)_3phen]$ have both been prepared as possible CVD precursors.[88] Interesting results from the reactions between AlH_3 and GaH_3 with hfpd-H and $N(CH_3)_3$ have yielded both metallation and reduction products, either exclusively or combined.[89] The product derived from $H_3AlN(CH_3)_3$ and hfpd-H is based on deprotonation and reduction of the β-diketone to form $[Al_2\{OC(CF_3)=CHCH(CF_3)O\}_3(N(CH_3)_3)_2]$, whereas the Ga compound is only reduced to give $[Ga_2\{OCH(CF_3)CH_2CH(CF_3)O\}_3(N(CH_3)_3)_2]$. Ni^{II} and Cu^{II} amine compounds with pd-H, tmhd-H, tfpd-H and hfpd-H have been synthesized using hexamethyltriethylenetetraamine (hmteta).[90,91] The reaction of a 1:2:1 mixture of $[M(ClO)_4.6H_2O]$ and the corresponding β-diketone and amine in ethanol results in the formation of a number of noteworthy compounds. Most of these are dimeric species of the form $[M_2(\beta\text{-diket})_4(hmteta)]$; however, one monomeric compound, $[Ni(tmhd)(hmteta)]ClO_4$, has also been prepared.

Alkaline earth metal complexes are altogether more rare. In the early 1970's, Fenton *et al.* synthesized four calcium β-diketonate amides, including $[Ca(phen)(hfpd)_2.H_2O]$, $[Ca(bipy)(hfpd)_2]$ and $(tmndH)^+_2[Ca(hfpd)_4]^{2-}$.[92a] The related $\{(tmndH)^+[Mg(hfpd)_3]^-\}$

compound has been structurally characterized and shows the presence of discrete $[Mg(hfpd)_3]$ ions.[92b] Further advances in this area have been made by Sievers *et al.* who has successfully prepared $\{(enH_2)_{1.5}[Ba(hfpd)_5].C_2H_5OH\}$ (see Figure 3.1) from a barium hydroxide metal source and an ethanolic solution of hfpd.[93] The crystal structure of the complex reveals that the barium atom is coordinated by nine oxygen atoms from five surrounding hfpd enolates, forming the complex anion $[Ba(hfpd)_5]^{3-}$. There are one and a half fully protonated ethylenediamine molecules situated between the molecules which balance the charges.

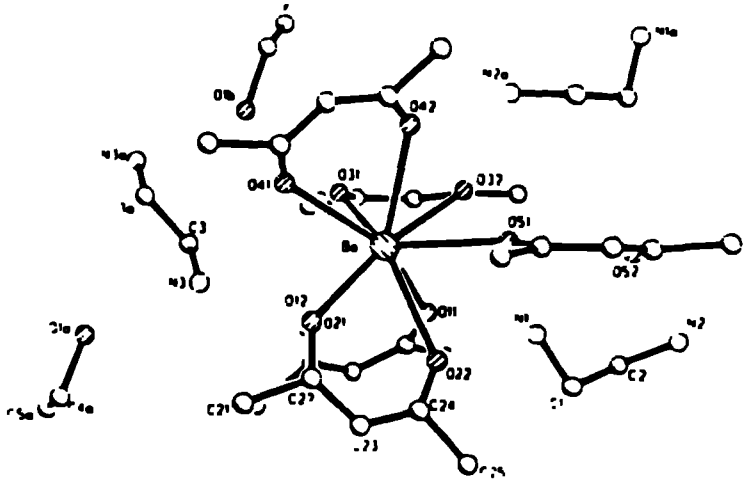

Figure 3.1 : X-ray crystal structure of $\{(enH_2)_{1.5}[Ba(hfpd)_5].C_2H_5OH\}$

It was previously thought that no stable, isolable complexes could be obtained with barium β-diketonates and amines;[94,95] however, this has recently been disproved by us and others. Hubert-Pfalzgraf[96] has isolated $[Ba(tmhd)_2(tmeda)_2]$ which purports to be monomeric, both in the solid state and in solution, melting at 130°C. Rees has reported the low molecularity barium complex, $[Ba(tmhd)_2.2NH_3]_2$ which was formed by the direct addition of excess ammonia to $[Ba(tmhd)_2]_4$[80].

The ability of the group II homoleptic β-diketonates to form adducts has already been discussed in Chapter 2. They may not only be preformed solid complexes though: various potential ligands such as thf,[51] tmhd-H,[48] NH_3 and other amines,[56] have been added to the carrier gas flow of the CVD apparatus, to improve mass transport and thermal stability.

The most dramatic changes in volatility and stability of Group 2 β-diketonate

complexes are observed when nitrogen bases are added to the gas flow, instead of an oxygen donor.[94] Barron *et al.* have studied the addition of numerous primary, secondary and tertiary amines with $[Ba(tmhd)_2]_4$. The homoleptic compound is found to decompose at 200-170 C failing to sublime without decomposition. In the presence of amine vapours, it melts between 70-100 C and sublimes with negligible decomposition, between 70-190 C, the best results being obtained with ammonia as the carrier gas.[95]

The nitrogen donor acts as a transport agent without, in many cases, the formation of a distinct complex. Nitrogen-free films of barium oxides have been deposited at 500 C under ambient pressure with NEt_3 vapour added to the N_2 / O_2 carrier gas, with the $[Ba(tmhd)_2]_4$ component at 130 C.[94]

The process of applying amine adducts of barium metal to CVD sources *via* this route has a number of advantages.

(i) The depression of the melting point relative to the homoleptic compounds allows for a liquid CVD source at moderate temperatures.

(ii) The dramatic decrease in sublimation temperatures allows the barium source to be at a similar temperature to the Y and Cu sources needed for the $YBa_2Cu_3O_{7-x}$ system. This enhances the thermal stability of the barium complex.

(iii) No nitrogen contaminants are observed (by XPS) in the films deposited.

(iv) Barium complexes which can not otherwise be volatilized, e.g. $[Ba(pd)_2]$, can now be sublimed at moderate temperatures and atmospheric pressure.

The experimental details are different depending on whether a gaseous or a liquid amine is employed.[95] For a gaseous amine such as ammonia, the nitrogenous base is added directly to the carrier gas, commonly oxygen. They are thus combined and bubbled through the β-diketonate precursor. The amount of amine added can be controlled by flow meters.

If a liquid amine, e.g. tmeda, is employed, the method involves a carrier gas being passed through a bubbler containing the liquid amine. The amine saturated carrier is subsequently passed through a second bubbler containing the β-diketonate precursor.

3.2 Synthesis of amine stabilized group II β-diketonates

The synthesis of air and moisture stable isolable Group 2 complexes with amines has been investigated. They are all low melting solids with a high degree of solubility. It has been previously noted that the reaction of the heavier alkaline earth metal ethoxides and two equivalents of β-diketonate in the presence of a multidentate oxygen donor ligand yields either monomeric or dimeric complexes of the general form $[M(\beta\text{-diket})_2(L)_m]_n$. These findings have now been extended by the replacement of the glyme ligands with the multidentate nitrogen donor ligands, tmeda, pmdeta and hmteta. The results are summarized in Figure 3.2.

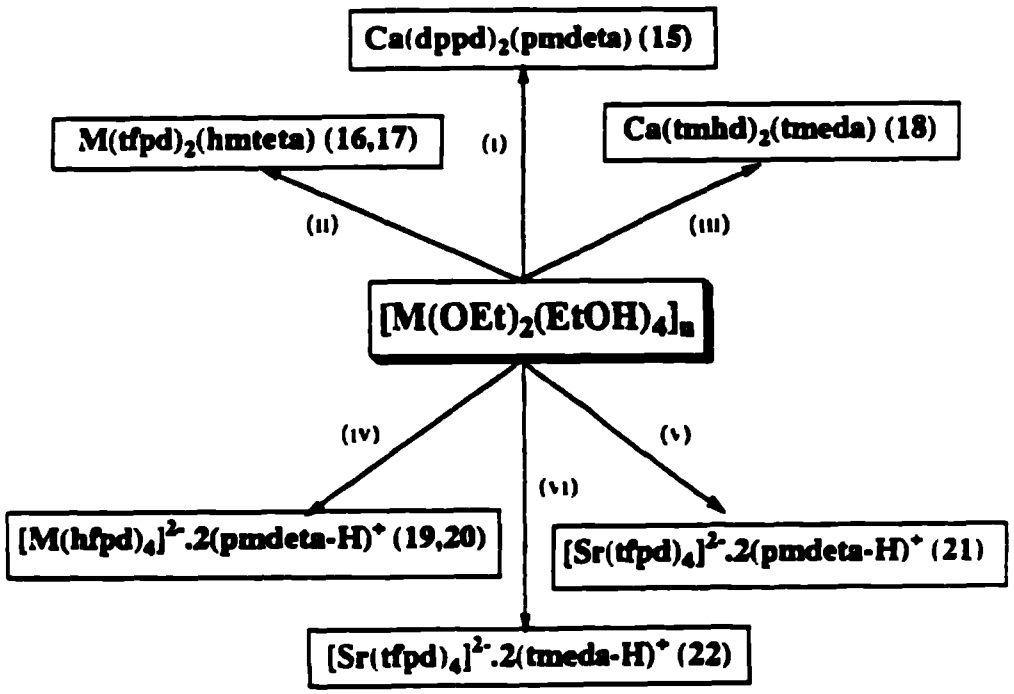

Figure 3.2 : Reaction scheme for compounds (15) - (22)

Reaction Conditions: (A) Reactions carried out at R.T. in chloroform (15) or n-hexane (16 - 18) at R.T. with 10 mins. stirring after addition of amine ligand. (i) dppd-H and pmdeta (15); (ii) tfpd-H and hmteta, M = Ba (16), Sr (17); (iii) tmhd-H and tmeda (18). (B)

Reactions carried out at R.T. in toluene (19 - 20) or n-hexane (21 - 22) at with 10 mins. stirring after addition of amine ligand. (iv) hfpd-H and pmdeta, M = Ca (19), Ba (20); (v) tfpd-H and pmdeta (21); (vi) tfpd-H and tmeda (22). See experimental section for further details.

The complexes described within this Chapter are:
(15) $Ca(dppd)_2(pmdeta)$, (16) $Ba(tfpd)_2(hmteta)$, (17) $Sr(tfpd)_2(hmteta)$,
(18) $Ca(tmhd)_2(tmeda)$, (19) $[Ca(hfpd)_4.2(pmdetaH)]$, (20) $[Ba(hfpd)_4.2(pmdetaH)]$,
(21) $[Sr(tfpd)_4.2(pmdetaH)]$ and (22) $[Sr(tfpd)_4.2(tmedaH)]$.

Unlike the glyme complexes described in Chapter 2, the amine complexes always appear to be monomeric, independent of the nature of the metal, β-diketonate or amine. All reactions take place at room temperature and are fully complete within a few minutes. Compounds (15) - (18) are all soluble in aromatic (toluene), halogenated (chloroform) and coordinating (dmso) solvents and are produced in high (>60%) yield.

Unlike the amine adducts previously mentioned, the reaction between $[M(\beta\text{-diketF})_2]_n$ and tmeda or pmdeta does not form a simple monomeric species. The reaction proceeds *via* the proton transfer from the fluorinated diketone in the *in situ* reaction, to the multidentate amine ligand. This forms a tight cation - anion pair, of the form $[M(\beta\text{-diketF})_4]^{2-}.2(LH)^+$. These complexes are air and moisture stable as are the aforementioned monomeric adducts. The reaction is very exothermic and is seen to be a general reaction for fluorinated β-diketonates in conjunction with the smaller amines, tmeda and pmdeta. A similar reaction is not observed for complexes (16) or (17) which utilize the larger tetradentate hmteta amine.

The yields of complexes (19) - (22) are all less than 50%, due to the fact that only half the metal equivalent of the ligands has been added. When three equivalents of diketone ligand are added to the metal in conjunction with an amine ligand, the tight cation anion pair complex is formed in preference to the Lewis base adduct complexes in slightly lower yields. These solids also tend to be 'wet' as the excess diketone ligand is still present in the Schlenk tube to a certain extent. However, when the correct amounts of metal and ligand (i.e. a 1 : 4 : 2 ratio of metal : β-diketone : amine) are added, the yield is seen to increase in line with the other amine complexes to *ca.* 80%.

3.3 Spectroscopic analyses

3.3.1 Infrared spectroscopy

The complexes (15) - (22) were studied as both Nujol and hexachlorobutadiene mulls between KBr windows. Selected infrared data are shown in Table 3.1. A typical infrared spectrum of these amine adducts is shown in Figure 3.3 for compound (22).

Generally either three or four sharp peaks or a range of broader peaks are observed in the 1675-1500cm^{-1} region which may be attributed to the C=O and C=C stretches and are indicative of monomeric species, a factor which is confirmed by X-ray crystallography. As has previously been shown, a shift in frequency is observed on altering the substituent groups on the β-diketonate ligand. With the electron donating ^{t}Bu group, the C=O and C=C bonds are relatively long in comparison (the M-O bonds being conversely shorter and stronger) and as such are weaker and resonate at a lower wavenumber. In contrast, fluorinated substituents are electron withdrawing and strengthen the C=O and C=C bonds, causing a shift to higher frequency.

The order of shift observed in Chapter 2, *viz.* hfpd > fod > dppd > tmhd, is also applicable to the amine complexes. With the amine adducts the hfpd compounds have peaks in the 1665±3 and 1605cm^{-1} (19) for the C=O, and 1550±8 and 1535±8cm^{-1} for the C=C. For the tfpd compounds these stretches are noted at 1635±2, 1612±1 and 1541(22), 1510±5cm^{-1} ((16), (17), (21)). In contrast the corresponding tmhd stretches of (18) are noted at 1589, 1577 and 1536, 1506cm^{-1}. The largest shift is observed for the high frequency C=O stretching vibration which is observed to shift downfield by *ca.* 70cm^{-1} on changing β-diketonate ligand from hfpd to tmhd.

The C-N-C stretches are in very similar positions to the C-O-C stretches of the glyme complexes. The stretches at *ca.* 1115cm^{-1} essentially remain within a narrow region, between 1103 and 1146cm^{-1}. However the higher frequency band undergoes larger variations. With the simple monomers (15) - (18), the frequency is between 1347 and 1357cm^{-1}. With the tight cation anion pair complexes (19) - (22), the wavenumber is shifted upfield to 1355 - 1384cm^{-1}, the difference being due to the fact that in complexes (19) - (22), the amine ligand is not directly bound to the metal, and therefore acts more like a free ligand. As with the compounds in Chapter 2, no peaks which could be assigned to OH or H_2O were observed in any of the spectra.

Finally a weak N-H stretch is observed at *ca.* 3435±25cm^{-1} for compounds (19) - (22), consistent with their formulation as cation - anionic compounds [M(β-diket)$_4$].2[(L-LH)]$^+$ with protonated amine ligands.

Table 3.1 : Selected Infrared data (cm^{-1}) for Amine Complexes (15) - (22) :

Compound	ν(CH)[a]	ν(C=O)	ν(C=C)	ν(C-N C)
(15)	3057, 2962, 2867	1610, 1601	1555, 1511	1347[a],1134
(16)	3042, 2859	1635, 1614[a]	1515	1357[a], 1134[a]
(17)	2969	1635, 1613[a]	1515[a]	1354[a], 1133
(18)	2964, 2904	1589, 1577	1536, 1506	1357, 1132
(19)	3027, 2960, 2917	1664, 1605	1542[a], 1527	1377, 1146
(20)	2960, 2917	1664	1558, 1540	1368[a], 1126
(21)	3027, 2960, 2917	1635, 1612[a]	1505	1384[a], 1132
(22)	3037, 2923	1638	1541	1355, 1126

All spectra run as nujol mulls except ([a]) which was run as a hexachlorobutadiene mull

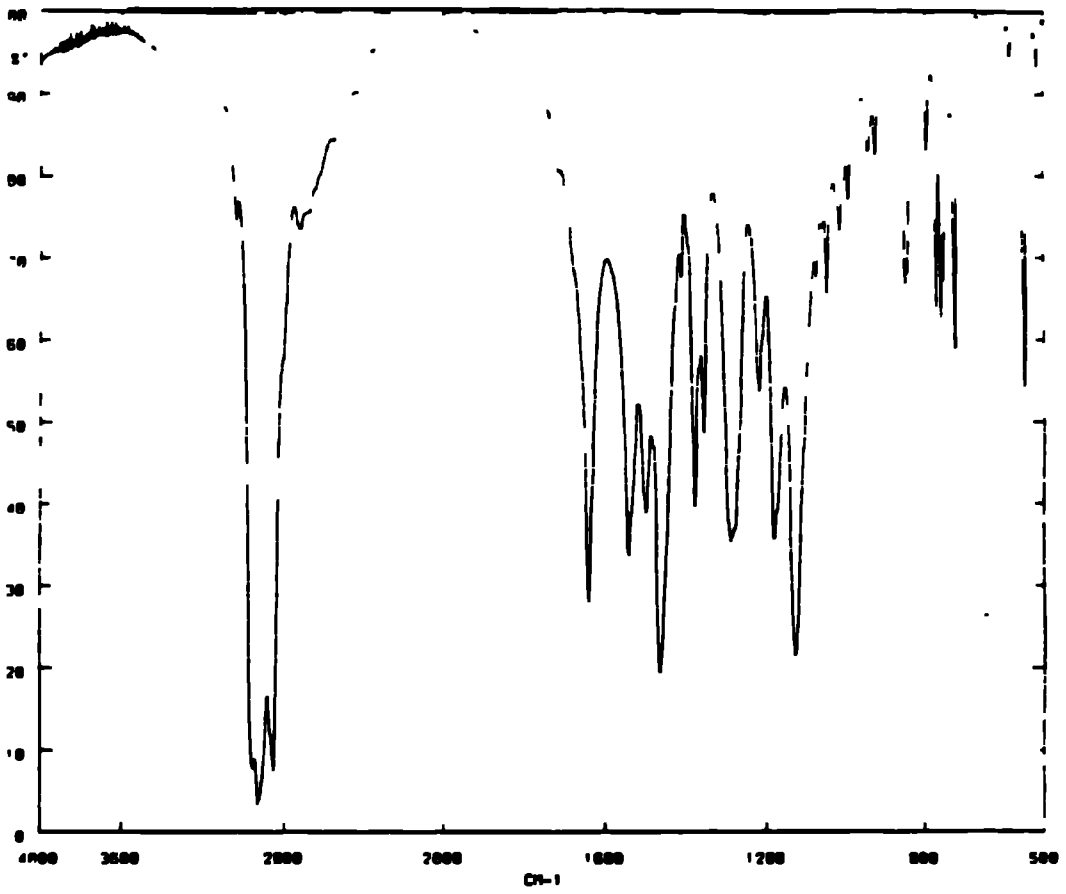

Figure 3.3 : Infrared spectrum of compound (22) in nujol

3.3.2 ^{1}H NMR spectroscopy

The ^{1}H NMR spectra of complexes (15) - (22) in either C_6D_6 (18) or d_6-dmso (15) - (17) and (19) - (22) at room temperature, show the presence of only one set of resonances for both the amine and the β-diketonate ligands, indicating only one environment for each ligand. This is consistent with the crystallographic results. The principle data are recorded in Table 3.2 overleaf.

The methyl group resonance of the tmhd complex (18), is shifted downfield by *ca.* δ 0.2 (with respect to the glyme complexes of Chapter 2), to δ 1.15. Two trends are noted for the $N(CH_3)_2$ and NCH_3 amine resonances. The monomeric complexes (15) - (17) show the NCH_3 further downfield than the $N(CH_3)_2$ (except for (17) where the chemical shifts have very similar values). The NCH_3 resonances of the cation - anion complexes (19) - (22), in contrast, are upfield with respect to the $N(CH_3)_2$ resonances. This factor

may be due to the amine ligands not being coordinated to the metal in the latter complexes. From crystallographic data it can be seen that the M-NCH_3 bond length is shorter than the M-$N(CH_3)_3$ bond in the monomeric complexes. This accounts for the $N(CH_3)_2$ resonance being further upfield. In contrast, for the ionic complexes there are no M-N bonds, thus the amine resonances are similar to the free ligand with the $N(CH_3)_2$ resonance downfield of the NCH_3.

Secondly there is a trend concerning the nature of the metal centre. For compounds (19) - (22) a shift downfield for both the NCH_3 and $N(CH_3)_2$ resonances is observed with increasing ionic radius in the order Ca < Sr < Ba. For the pmdeta complexes (19) - (21), a shift of ca. δ 0.8 for $N(CH_3)_2$ and *ca.* δ 0.9 for $N(CH_3)$ is observed following this sequence.

Each of the chemically inequivalent CH_2 groups present in the amine ligands give rise to distinct resonances, however, it is not possible to correlate exact CH_2 groups with specific chemical shifts. Only with complex (17) is this differentiation not possible, the spectrum containing only a very broad multiplet at δ 2.23. As with the $N(CH_3)_2$ and $N(CH_3)$ resonances, similar trends are seen for the CH_2 groups, i.e. a notable shift downfield with increasing ionic radii.

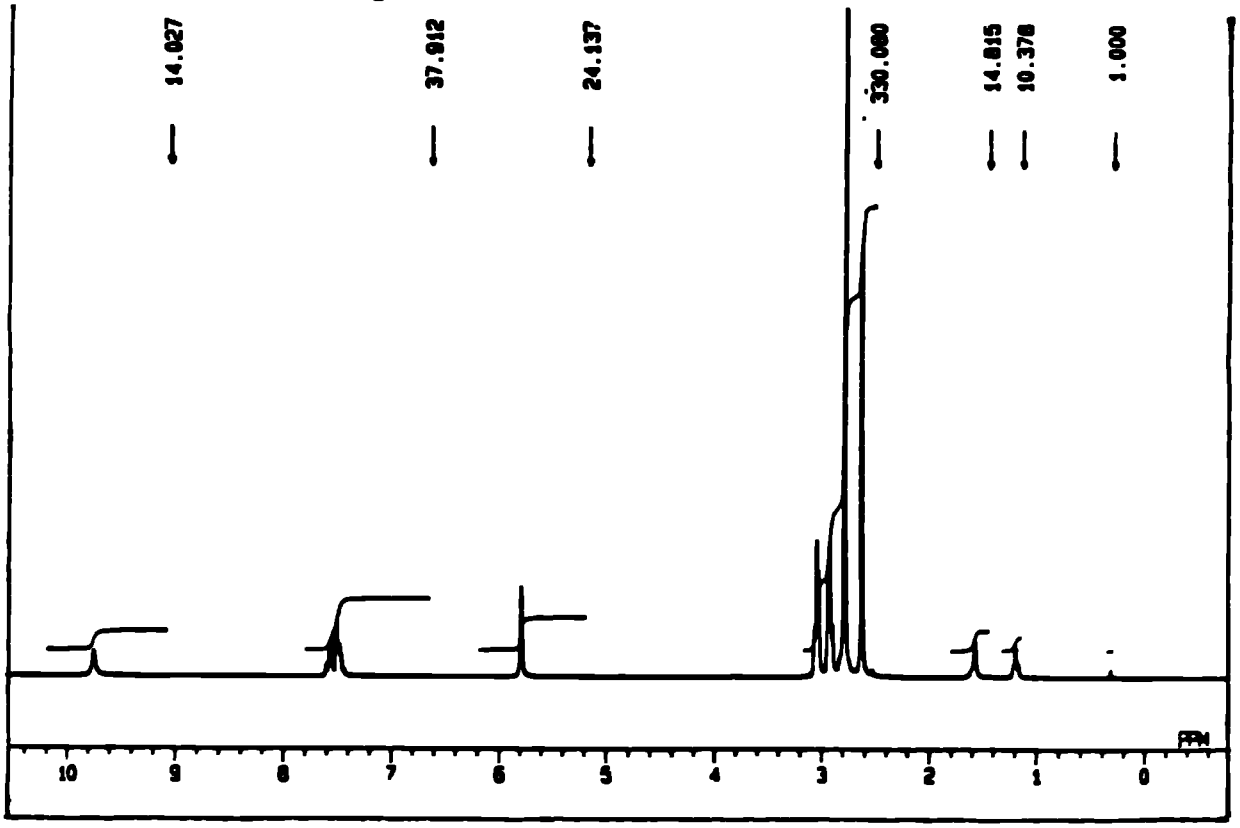

Figure 3.4 : ^1H NMR spectrum of (20) in D_6-dmso (residual toluene)

A shift of the CH proton occurs when changing the β-diketonate ligands as before, but it is not as pronounced as for the glymes complexes. The dppd complex (15), has a very acidic β-diketonate proton and consequently its resonance is at δ 6.80, there is no apparent difference between the CH resonances of the tmhd, tfpd or hfpd complexes; however, complex (19) also has a rather more acidic CH proton than expected, appearing at δ 6.23.

For the cation - anion complexes (19) - (22), a small broad peak is observed at very low field (see Figure 3.4). The proton, as is shown by X-ray crystallography, is bound to one of the nitrogen donors of the amine ligand and is in close proximity to one of the oxygen donors of the fluorinated β-diketonate. Hence, the hydrogen atom is very acidic and consequently appears between δ 9.74 and 11.31. This spectrum provides strong evidence that the tight cation anion pair complexes are formed in preference to the more general monomeric Lewis base adducted complexes [M(β-diket)$_2$L]. The resonance of the NH proton is also noticeably further downfield for the two tfpd complexes, than for the two hfpd complexes. This may be due to the steric encumberence being less for the tfpd complexes.

3.3.3 ^{13}C NMR spectroscopy

The principal data for complexes (15) - (22) are listed in Table 3.3. In contrast to the ^{1}H NMR spectra of complexes (16) and (17), ^{13}C NMR shows a shift downfield of the $N(CH_3)_2$, $N(CH_3)$ and CH_2 groups with decreasing ionic radii, (i.e. Sr > Ba). The tight cation anion pair pmdeta complexes (19) - (21) show an unusual trend which does not correspond to those previously seen. For $N(CH_3)_2$, $N(CH_3)$ and CH_2, the shift in resonance is seen to follow the order Sr < Ca < Ba. The fact that the amine is not directly coordinated to the metal centre in these complexes bears little difference on their spectra when compared to the other complexes.

Again one can differentiate between the CH_2 groups of the amine ligand. All three resonances are also observed for complex (17), whereas in the ^{1}H NMR spectrum only one broad peak was observed. The difference in timescales between the two NMR techniques is sufficiently large to account for this, the fluxionality of the CH_2 carbon atoms being less on the ^{13}C timescale.

Table 3.3 : ^{13}C NMR data for Amine Complexes (15) - (22) :

Compound	$\delta(CH_3)$	$\delta(N(CH_3)_2)$	$\delta(NCH_3)$	$\delta(NCH_2)$	$\delta(CH)$	$\delta(CO)$
(15)	----	46.26	43.28	56.30, 57.81	93.16	184.38
(16)	29.86	44.13	40.78	52.42, 54.12	93.06	169.43
				54.70		193.58
(17)	28.05	44.78	41.13	54.22, 54.32	93.51	170.13
				54.74		194.21
(18)[a]	28.21	44.51	----	55.98	88.75	199.10
(19)	----	45.26	43.17	54.95, 56.71	88.83	176.80
(20)	----	44.65	42.86	52.81, 56.10	84.19	172.40
(21)	28.94	43.54	41.36	52.41, 55.29	93.82	176.80
						193.98
(22)	28.79	43.90	- -	54.45	94.11	169.05

All spectra were recorded at 67.94 MHz in D_6, dmso at R.T., except ([a]) which was recorded at 22.61 MHz in C_6D_6 at R.T.

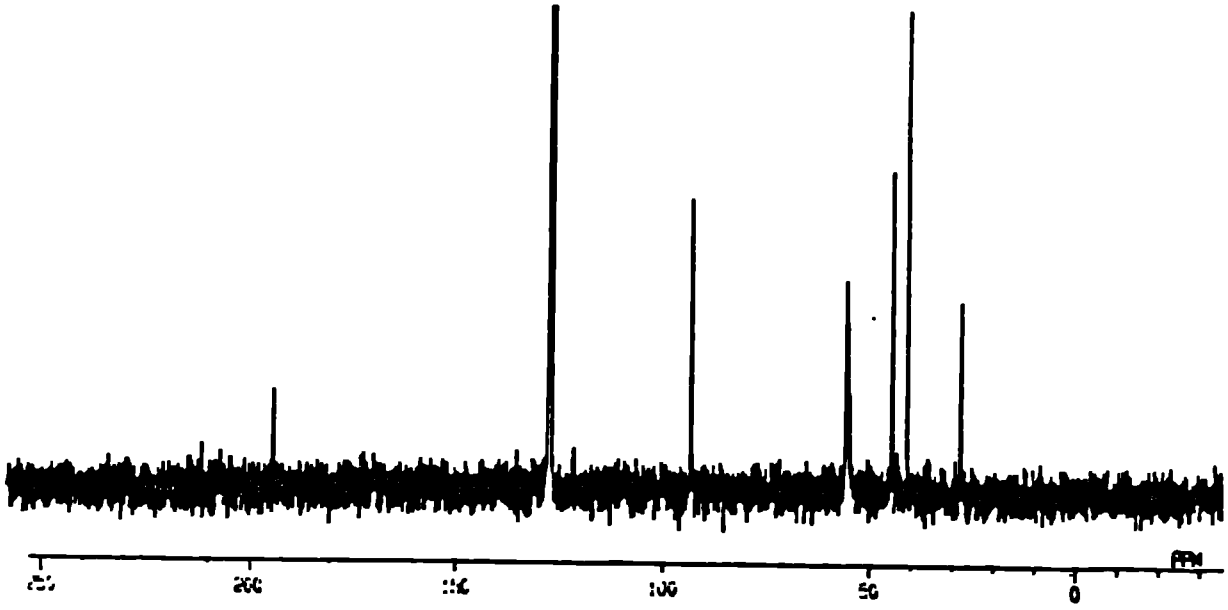

Figure 3.5 : ^{13}C NMR spectrum of (16) in C_6D_6

The CH carbon resonance of the complex is shifted downfield when the β-diketonate is either tfpd or dppd, to a singlet at δ 93.06 - δ 94.11 (for (16) and (22) respectively). For the tfpd compounds where the amine is coordinated to the metal ((16) and (17)), the CH resonance is at a slightly lower wavenumber by *ca.* δ 1.0; this may be insignificant, however. For both the tmhd and hfpd compounds, the CH resonance is distinctly lower. This is consistent for the tmhd compounds described in Chapter 2, but not necessarily for the hfpd compounds.

The appropriate 1:3:3:1 quartets are observed for the CF_3 resonances of the fluorinated β-diketonate complexes centred at *ca.* δ 115 with a ^1J (C-F) coupling constant of *ca.* 300Hz. This quartet is also noted for the carbonyl adjacent to the CF_3 group in the tfpd (δ 169.43 - δ 176.80) and hfpd (δ 172.40 - δ 176.80) complexes with an average ^2J (C-F) coupling constant of 30Hz . Consistent with their formulations, the tfpd compounds show two carbonyl resonances; the second is further downfield, and may be compared to that of the tmhd complex (18), whose singlet CO resonance appears at δ 199.10. The carbonyl resonance of the dppd complex (15) is, as usual, between these two groups of resonances, at δ 184.38.

3.3.4 Mass spectrometry

The principal data for complexes (15) - (22) are recorded in Table 3.4 overleaf. All mass spectra data for complexes (15) - (22) were accumulated under electron impact conditions (EI+) which tended to disclose better results than other available techniques. A range of both oligomeric and molecular ions were observed in the gas phase as they were with the glyme complexes of Chapter 2. The frequently observed species ML, ML_2 and the oligomeric ion, M_2L_3 are observed in most cases, as is the MLN ion for both the simple monomers and the tight cation anion pair complexes.

The diphenylpentanedionato complex (15), differs from that of [Sr(dppd)$_2$(tetraglyme)] (8), in that it is volatile enough to produce a mass spectrum, a feature which appears to be quite rare. The ML and M_2L_3 ions occur at m/z 263 (100%) and 749 (6%) respectively. A weak ML_3 ion is also observed at m/z 709 for [Ca(dppd)$_3$]. This compound may be considered to be a poor precursor due to its low thermal stability at elevated temperatures (i.e. the loss of both the amine and β-diketonate ligands). This is not surprising due to its high carbon content.

The hmteta complexes (16) and (17), both show the same type of ions. The highest mass ion is monomeric [M(tfpd)($Me_2NCH_2CH_2$)], with subsequent loss of amine fragments to produce peaks corresponding to [M(tfpd)(Me_2NCH_2)] and [M(tfpd)] also observed. All of these ions have relatively low intensities (<12%).

Complexes (18) and (19) show both monomeric and oligomeric ions for ML, ML_2 and M_2L_3. The ML ion is very intense (27% and 100%) as is the M_2L_3 ion (45% and 100% respectively). The molecular MLN ions at m/z 343 for [Ca(tmhd)(tmeda)] (5%) and m/z 415 for [Ca(hfpd)(pmdeta)] (45%) are also observed.

Complex (20) shows molecular ions at m/z 518, 575 and 709 for [Ba(hfpd)(pmdeta)], [Ba(hfpd)(pmdeta)($N(CH_3)_2$)] and [Ba(hfpd)(pmdeta)$_2$(H_2O)] respectively. The latter two are MLN_2 based ions. Complexes (21) and (22) are both strontium tfpd compounds and as such show similar oligomeric ions with similar intensities. Two molecular ions at m/z 416 for [Sr(tfpd)(pmdeta)] (15%) and m/z 357 for [Sr(tfpd)(tmeda)] (40%) are seen for the MLN ions of (21) and (22) respectively. For (22) also a weak ML_4 ion at m/z 699 (2%) is also present.

Table 3.4 : Selected Electron Impact Mass Spectra data for Complexes (15) - (22) :

Compound	ML	ML_2	M_2L_3	MLN	ML_2N	MLN_2	ML_n (n=3 or 4)
(15)	263	----	749	----	----	----	709 (3)
(16)	278, 291	----	----	351, 362	----	----	----
(17)	228, 241	----	----	301, 312	----	----	----
(18)	223	349	630	343	----	----	----
(19)	247	561	701	420	----	----	----
(20)	345	552	----	518	----	575, 709	----
(21)	241	393	634	416	586	500	----
(22)	241	325, 394	634	357	----	----	699 (4)

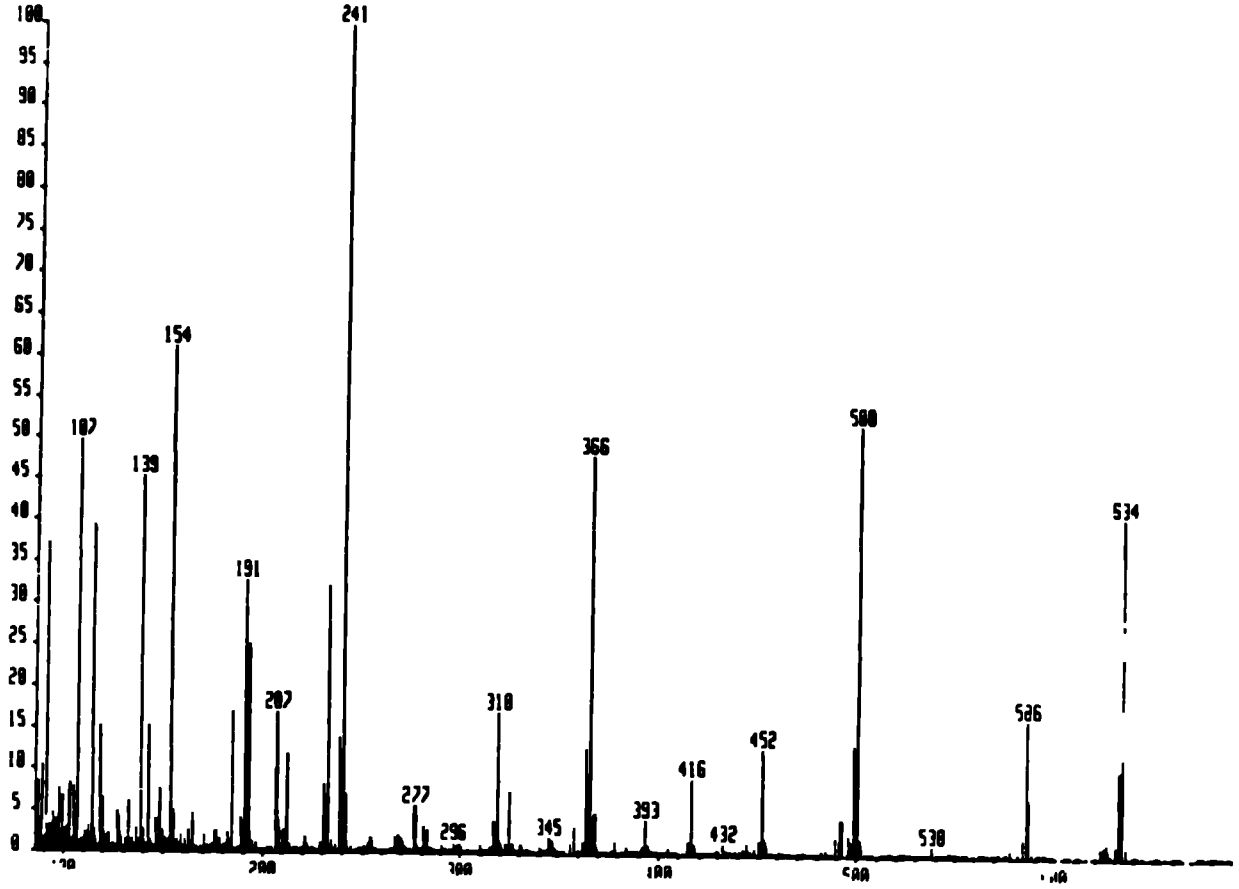

Figure 3.6 : The electron impact mass spectrum of (21)

There are a number of general trends as regards intensities of the relative ions. For the tight cation anion pair complexes (19) - (22), the molecular ion MLN is observed to be much more intense than that observed in the simple monomers. The ML_2 and M_2L_3 ions are also more apparent with these complexes. Almost exclusively, the most intense peak is the monomeric ML ion, normally ca.100%. This is not observed in (18), where the M_2L_3 ion is the most abundant, a factor which is often seen in tmhd complexes (see Chapter 2).

3.4 Physical properties

3.4.1 Solubilities and melting points

Table 3.5 : Melting points of complexes (15) - (22) :

	Compound	M. Pt.(°C)
(15)	$[Ca(dppd)_2(pmdeta)]$	143-145
(16)	$[Ba(tfpd)_2(hmteta)]$	143-147
(17)	$[Sr(tfpd)_2(hmteta)]$	69-72
(18)	$[Ca(tmhd)_2(tmeda)]$	117-119
(19)	$[Ca(hfpd)_4].2[(pmdeta-H)]$	83-86
(20)	$[Ba(hfpd)_4].2[(pmdeta-H)]$	53-56
(21)	$[Sr(tfpd)_4].2[(pmdeta-H)]$	98-102
(22)	$[Sr(tfpd)_4].2[(tmeda-H)]$	86-88

In direct line with the glyme adducted complexes of Chapter 2, it is found that on coordination of a multidentate amine ligand to the homoleptic β-diketonate complexes a significant decrease in melting point is observed, the degree of oligomerization being successfully broken down by the coordinated nitrogen donor ligand.

The crystal structure of $[Ca(dppd)_2(EtOH)_{0.5}]_4$ has previously been solved[75] showing it to be tetrameric. It melts at 274°C, whereas compound (15) melts over 130°C lower at 143-145°C. This temperature is higher than many of the glyme complexes, however, diphenylpentanedionato compounds often have higher melting points due to the intermolecular phenyl ring interactions. X-ray crystallography has proved that (15) and (16) are monomeric and as such are expected to have low melting points. The strontium analogue of (16), complex (17), is expected to be monomeric by direct comparison. It is noted, however, that there is a significant difference in the melting points of these two compounds, the strontium complex being *ca.* 75°C lower.

If compound (18) were monomeric, the metal would only be 6-coordinate; however, it is air stable which would suggest that the coordination number might be at least seven (that being the number suggested for this type of complex to be air stable, as dictated

by complex (15)). The melting point is higher than most of the glyme complexes to which it is related (e.g. [Ca(tmhd)$_2$(triglyme)] (7) melts at 71-74 C). It may be, therefore, reasonable to conclude that compound (18) is dimeric, in line with [Ba(tmhd)$_2$(diglyme)]$_2$ (3). [Ca(dppd)$_2$(dppd-H)] (13) was discussed in Chapter 2 and is an air stable six coordinate calcium complex which owes its monomeric nature to the steric encumbrance of the dppd ligands. It would appear that complex (18) might also have a large degree of steric interaction from the bulky tmhd and multidentate amine ligands, dictating a monomeric structure.

The related compounds, (19) - (22), all show distinctly lower melting points than their parent compounds. These materials are all air stable but have decreased solubilities in hydrocarbon solvents with respect to the complexes outlined in Chapter 2; they are all completely insoluble in hexane even at boiling temperatures. This is consistent with the X-ray structure of (22), which shows the possible difficulties encountered by the solvent molecules in trying to encompass the metal centre.

The stability of these compounds to air and moisture is very pronounced. The majority are produced as crystalline solids and remain so on exposure to the atmosphere. Further, infrared analyses on the aerated products reveal that they are identical to the water free complexes synthesized by the anhydrous ethoxide route.

The solubility of the amine adducts is not as marked as the glyme complexes. Whereas the latter were all soluble in aliphatic solvents (e.g. hexane), the amine complexes are not, except for the tmhd complex (18) (tmhd compounds are often more soluble in such solvents due to the large size of the substituent group on the β–diketonate ligand). All the amine complexes show appreciable solubilities in aromatic solvents (e.g. toluene); similarly they are all soluble in coordinating solvents (e.g. thf and dmso).

3.4.2 STA analyses

The TGA of compound (20) shows only one clearly discernible weight loss between 234-277°C with a weight loss percentage of 75.3%. This is most likely to correspond to the loss of the amine and partial loss of the hfpd ligands to leave BaF_2 along with some carbonaceous deposits (Calc. 13.4%, Found 16.2%). The $T_{50\%}$ of 256°C is relatively low compared with the glyme complexes but not when compared to the fluorinated complex (10), whose $T_{50\%}$ is 236°C. Thus the volatility advantages of fluorinated ligands over hydrocarbyl ligands persist in this type of compound as well.

The DSC shows two inflexions. The first, an endotherm, is at 193°C and most likely corresponds to the onset of the loss of the amine ligand. The second, an exotherm at 263°C, probably corresponds to the severing of the Ba-$O_{(hfpd)}$ bonds and the subsequent formation of Ba-F bonds to leave the BaF_2 residue.

Compound (17) conversely shows two TGA peaks at 223-251 and 268-285°C, corresponding to the loss of the hmteta ligand, and the partial loss of the tfpd ligands respectively. The residue is 24.8% and more than likely corresponds to SrF_2 (Calc. 20.2%) and carbon deposits. Two DSC inflexions are noted at 98.1°C, which is very sharp and corresponds to the melting point, and also at 269.5°C (endothermic), which as before is most likely to be due to the cleavage of the Sr-O bonds, and the subsequent formation of the SrF_2 residue.

Complex (15) has a very complicated TGA plot showing at least five separate weight losses. The first at about 100°C is due to the loss of a small amount of solvent; however, the second is far more significant. This occurs between 128.5 and 278.9°C with a percentage weight loss of 37.6%. This may correspond to the loss of the amine ligand and one of the phenyl groups of the dppd ligand (expected 38.9%). The third weight loss is between 425.7 and 467.3°C (14.7%) and is most likely to be due to the loss of the remaining phenyl group of the first dppd ligand (expected 12.0%). The fourth weight loss is again substantial (25.9%) and is between the temperatures of 522.2 and 570.6°C. This weight loss may be due to the loss of the remaining carbon atoms (of which there are three), and one of the oxygen atoms of the first dppd ligand thus leaving only one oxygen atom remaining. This is combined with the loss of another dppd ligand minus one of the phenyl groups. The final weight loss occurs between 704.9 and 785.1°C and corresponds to the loss of the final phenyl group. The residue of 10.8% is most likely to be due to CaO (expected 8.7%) and some carbonaceous deposits.

The DSC plot is similarly complex with exothermic peaks corresponding to the first two weight losses at 122.2 and 213.6°C respectively. The third and fourth inflexions are both endothermic and correspond to the loss of a phenyl group at 455.6°C and the combined dppd and carbon and oxygen fragments detailed above at 566.7°C. The final exotherm corresponds to the loss of the final phenyl group and the formation of the calcium oxide residue at 766.7°C.

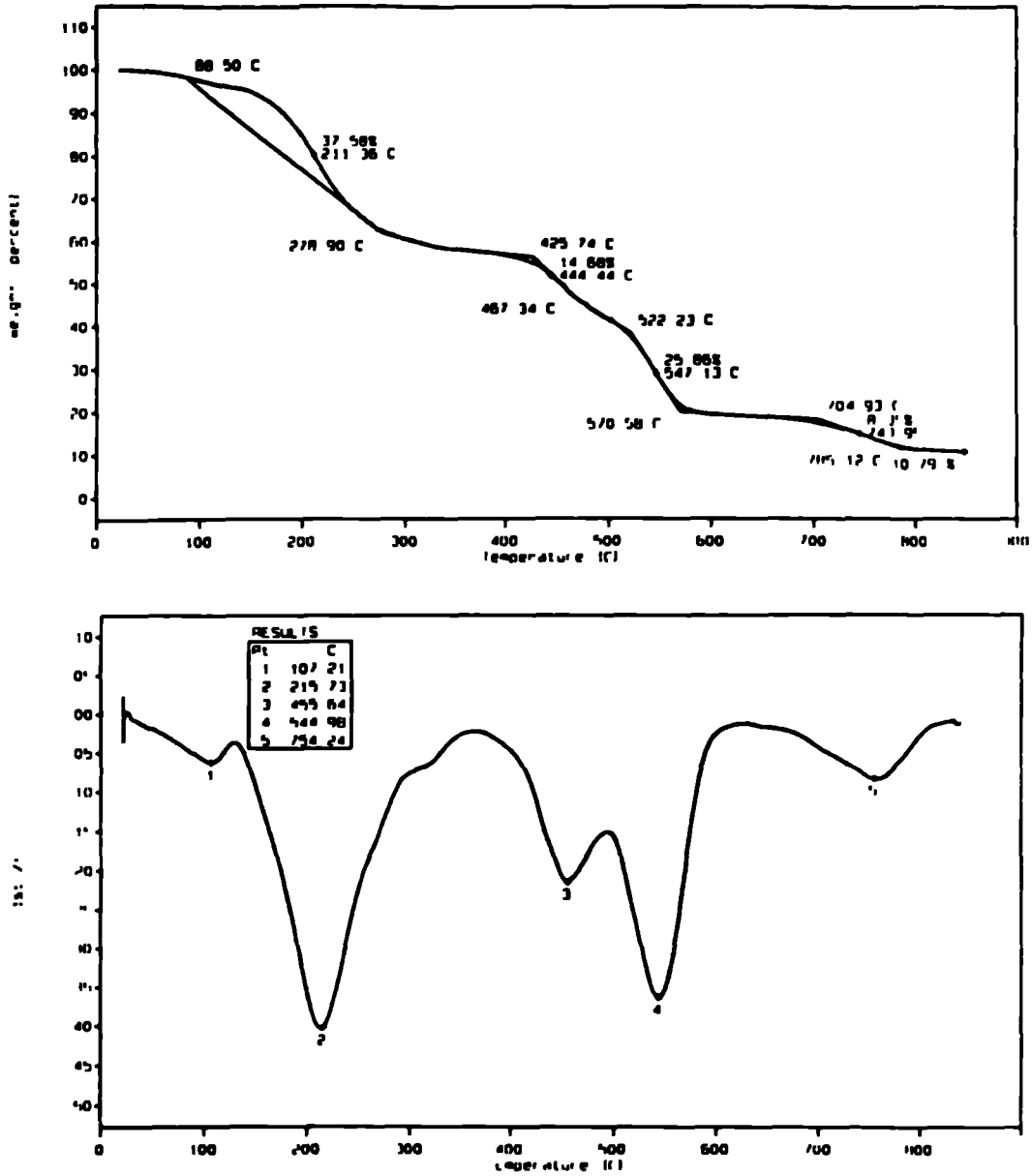

Figure 3.7 : TGA (top) and first derivative of TGA (bottom) plots of (15)

Two noteworthy points in comparing the amine complexes to the glyme complexes of the previous Chapter are, (i) the fact that the residues are larger in these complexes and in fact correspond to more than just carbonaceous deposits, either the metal fluorides or oxides and (ii) that the weight losses in the TGA generally occur at slightly higher temperatures than in the analogous glyme complexes.

3.5 X-ray crystallography

The crystal structures of a number of compounds described within this Chapter were solved by single crystal X-ray techniques. Crystal and collection data together with details of bond lengths and angles appear in the Appendix section.

[Ca(dppd)$_2$(pmdeta)] (15)

Crystal data for [Ca(dppd)$_2$(pmdeta)] (15) : M = 659.88, monoclinic, spacegroup C2/c (No 5), a = 50.531(7), b = 17.625(5), c = 12.230(3) Å, α = 90, β = 101.84(1)^0, γ = 90°, V = 10660.41 Å^3, Z = 12, D_c = 1.233 g cm^{-3}, F(000) = 4224, μ(Mo-K_α) = 2.1 cm^{-1}. 150 K. 6796 unique reflections were measured using [Mo-K_α] radiation on a FAST TV area detector diffractometer, of which 4949 having Fo > 4σ(Fo) were used in the refinement. The structure was solved by direct methods and refined by full matrix least squares to R = 0.0600 and Rw = 0.0665. The full crystal-data and details of bond lengths and angles appear in the appendix.

The single crystal X-ray structure of complex (15) shows that the central metal atom is seven coordinate with a distorted capped octahedral geometry. The tridentate amine lies in one plane with the dppd ligands in totally different planes to produce a twisted propellane structure. The average Ca-O distance is 2.317(5)Å and the O-Ca-O chelate angle is 75.7(2)°. The steric hinderance of both the phenyl groups and the amine methyl groups, cause these values to be larger than those discussed in the complexes described in Chapter 2. Comparisons may be made with [Ca$_4$(dppd)$_8$(EtOH)$_2$][75] and [Ca(dppd)$_2$(dppd-H)] whose Ca-$O_{(dppd)}$ bond lengths lie in the range 2.256(2) - 2.508(2) and 1.858(7) - 1.882(7)Å respectively. The former is a centrosymmetric dimer with four calcium atoms, two of which are six coordinate, the other two being seven coordinate.

The pmdeta chelates to the metal in a tridentate manner with an average Ca-N distance of 2.633(7)Å. The two terminal chelating N(CH$_3$)$_2$ groups bind slightly closer to the metal (as in the glyme complexes) than the central N(CH$_3$) group, due to steric reasons. This compound provides plausible evidence that in order to have an air / moisture stable monomeric complex of this type, the lowest possible coordination number is seven, and not eight, as is represented by the glyme complexes, where [Ca(tmhd)$_2$(triglyme)] (7) is the

lowest coordinated monomeric complex. The most likely reason for this effective lowering of coordination number is the fact that there is more steric crowding, imparted by the methyl groups, surrounding the nitrogen donors than there is around the oxygen atoms of the multidentate glyme ligands.

Unlike the bonding of the related glyme complexes, compound (15) has a different disposition of ligands about the metal centre. Previously it was noted that the diketonate ligands were opposite each other and the glyme ligand wrapped around the meridional plane. However, in this case the diketonates are not opposite but adjacent to each other with the amine ligand lying in a plane which is neither parallel nor perpendicular. This is most likely to be a result of the extra steric crowding imparted by both the phenyl ligands and the multidentate tertiary amine.

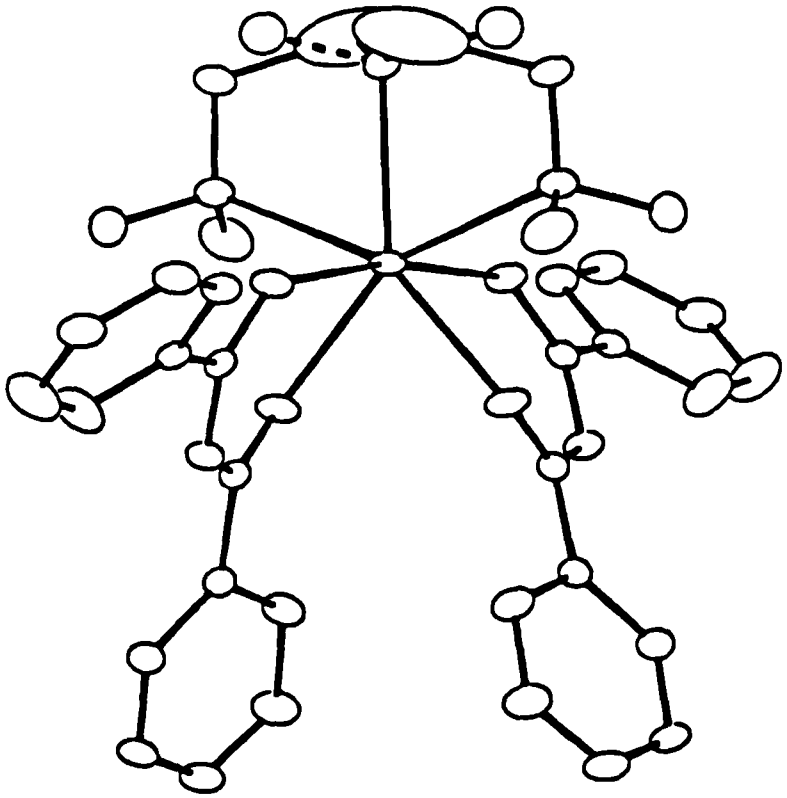

Figure 3.8 : X-ray crystal structure of [Ca(dppd)$_2$(pmdeta)] (15)

[Ba(tfpd)$_2$(hmteta)] (16)

Crystal data for (16) : The X-ray measurements for complex (16) were made on a colourless crystal of approximate dimensions 0.30 x 0.20 x 0.18 mm^3 which was mounted onto a fibre using silicon oil and transferred to the goiniostat. The unit cell parameters and intensity data were obtained at 150 K using a Delft-Instruments FAST TV area detector diffractometer and graphite monochromated Mo-K_α radiation, λ= 0.71069 Å, following previously described procedures.[78]

The total of 9140 intensities measured within a θ range 2.0 - 24.8°, corresponding to slightly more than one hemisphere, yielded 3608 unique and 2208 observed [$F_0 > 3\sigma(F)$] reflections [merging R = 0.040]. The data were corrected for Lorentz and polarisation effects, and also for absorption using the program DIFABS, adapted for FAST geometry.[78] The structure was solved *via* the Patterson and Fourier methods and refined (on F) by full-matrix least-squares (SHELX-80)[79] to give a final R-value of 0.0384 for 2208 observed data and 334 parameters. All non-hydrogen atoms were treated anisotropically; the hydrogens atoms were all located from difference maps; these were not refined, but included in the calculation of F_c with a common U_{iso} assigned to all [0.05 Å^2]. The collection data and details of bond lengths and angles appear in the appendix.

In compound (16) the barium ion, as shown by X-ray crystallography, is eight coordinate with a distorted square prismatic geometry. The tetradentate amine lies in one plane, while the tfpd ligands are in totally different planes to produce a twisted propellane structure. The Ba-$O_{(tfpd)}$ distances lie between 2.665(9) and 2.688(11) with an average of 2.677(9)Å and the average O-Ba-O chelate angle is 64.6(3)°. The distances are slightly different to those of the recently reported complex [Ba(tfpd)$_2$(tetraglyme)][53] which has an average Ba-$O_{(tfpd)}$ distance of 2.691(3)Å and an O-Ba-O angle of 64.4(1)°. The small differences in bond lengths and angles may be attributed to the steric hinderance from the methylated amines on the multidentate Lewis base for (16).

The amine ligand chelates to the metal in a four pronged coordination mode with Ba-N ranging between 2.963(1) and 3.022(1), with an average bond length of 2.983(7)Å. The two terminal chelating N(CH$_3$)$_2$ groups bind slightly closer to the metal (as with (15)) probably due to steric reasons. These lengths and angles may be contrasted with [Ba$_2$(tmhd)$_4$(bipy)$_2$][97] whose Ba-O bond lengths lie in the region 2.62(3) - 3.01(4)Å and Ba-N distances are between 2.87(5) and 2.93(5)Å. In this latter compound the barium

metal is eight coordinate with all tmhd ligands bridging. Comparable too is $[Ba(tmhd)_2.2NH_3]_2$ whose seven coordinate barium metal has Ba-O bond distances of 2.595(6) - 2.874(7) and Ba-N lengths of 2.888(8) and 2.923(8)Å.[80]

The binding mode of the amine is similar to that of the tetraglyme ligand in $[Ba(hfpd)_2(tetraglyme)]$.[67] In contrast to the glyme complexes described in Chapter 2, however, we do not observe the same relative disposition of the ligands. For the glyme complexes we note that the diketonate ligands are *trans* to each other, with the glyme ligand wrapping around the metal centre. This is not the case, as may be expected, for the water bridged complex (6) or indeed the diglyme bridged dimer (3) where the ligands are essentially *cis*, compound (16) too has β-diketonate ligands which have a *cis* formation.

Table 3. 6 : Selected bond lengths (Å) and angles (°) for compound (15) :

O(1)-Ba	2.687(9)	O(2)-Ba	2.669(10)
O(3)-Ba	2.665(9)	O(4)-Ba	2.688(10)
N(1)-Ba	2.972(10)	N(2)-Ba	2.975(11)
N(3)-Ba	3.022 (10)	N(4) -Ba	2.963 (11)
C(5)-F(1)	1.323(12)	C(5)-F(2)	1.334(13)
C(5)-F(3)	1.330(13)	C(10)-F(4)	1.296(14)
C(10)-F(5)	1.319(15)	C(10)-F(6)	1.316(14)
C(2)-O(1)	1.242(12)	C(4)-O(2)	1.258(12)
C(7)-O(3)	1.256(12)	C(9)-O(4)	1.261(13)
C(11)-N(1)	1.465(15)	C(12)-N(1)	1.476(13)
C(13)-N(1)	1.451(13)	C(14)-N(2)	1.466(13)
C(15)-N(2)	1.474(13)	C(16)-N(2)	1.459(14)
C(17)-N(3)	1.455(14)	C(18)-N(3)	1.478(14)
C(19)-N(3)	1.487(13)	C(20)-N(4)	1.481(13)
C(21)-N(4)	1.467(13)	C(22)-N(4)	1.476(13)
C(2)-C(1)	1.524(15)	C(3)-C(2)	1.411(14)
C(4)-C(3)	1.362(14)	C(5)-C(4)	1.532(15)
C(7)-C(6)	1.488(15)	C(8)-C(7)	1.419(15)
C(9)-C(8)	1.353(16)	C(10)-C(9)	1.532(17)
C(14)-C(13)	1.512(16)	C(17)-C(16)	1.505(16)
C(20)-C(19)	1.479(16)		
O(2)-Ba-O(1)	65.2(3)	O(3)-Ba-O(1)	79.5(3)
O(3)-Ba-O(2)	104.4(3)	O(4)-Ba-O(1)	94.7(3)
O(4)-Ba-O(2)	159.1(2)	O(4)-Ba-O(3)	64.1(3)
N(1)-Ba-O(1)	72.9(3)	N(1)-Ba-O(2)	97.3(3)
N(1) -Ba-O(3)	133.3(2)	N(1) -Ba-O(4)	81.3 (3)
N(2)-Ba-O(1)	134.5(2)	N(2)-Ba-O(2)	124.4(3)
N(2)-Ba-O(3)	127.9(3)	N(2)-Ba-O(4)	73.5(3)
N(2)-Ba-N(1)	62.1(3)	N(3)-Ba-O(1)	131.8(2)
N(3)-Ba-O(2)	71.7 (3)	N(3)-Ba-O(3)	133.1(2)

N(3)-Ba-O(4)	129.1(3)	N(3)-Ba-N(1)	92.8(3)
N(3)-Ba-N(2)	59.7(3)	N(4)-Ba-O(1)	129.3(3)
N(4)-Ba-O(2)	82.5(3)	N(4)-Ba-O(3)	71.7(3)
N(4)-Ba-O(4)	108.1(3)	N(4)-Ba-N(1)	153.1(2)
N(4)-Ba-N(2)	95.7(3)	N(4)-Ba-N(3)	61.4(3)
C(2)-O(1)-Ba	138.9(6)	C(4)-O(2)-Ba	135.4(5)
C(7)-O(3)-Ba	141.4(7)	C(9)-O(4)-Ba	136.0(6)
C(11)-N(1)-Ba	111.4(7)	C(12)-N(1)-Ba	103.4(6)
C(12)-N(1)-C(11)	109.5(9)	C(13)-N(1)-Ba	113.0(6)
C(13)-N(1)-C(11)	110.8(9)	C(13)-N(1)-C(12)	108.5(9)
C(14)-N(2)-Ba	107.8(7)	C(15)-N(2)-Ba	104.0(7)
C(15)-N(2)-C(14)	108.8(9)	C(16)-N(2)-Ba	115.7(7)
C(16)-N(2)-C(14)	110.5(9)	C(16)-N(2)-C(15)	109.7(9)
C(17)-N(3)-Ba	112.5(7)	C(18)-N(3)-Ba	107.0(7)
C(18)-N(3)-C(17)	110.7(9)	C(19)-N(3)-Ba	107.5(6)
C(19)-N(3)-C(17)	111.5(9)	C(19)-N(3)-C(18)	107.5(9)
C(20)-N(4)-Ba	113.9(6)	C(21)-N(4)-Ba	114.6(7)
C(21)-N(4)-C(20)	109.9(9)	C(22)-N(4)-Ba	100.5(7)
C(22)-N(4)-C(20)	109.1(9)	C(22)-N(4)-C(21)	108.2(8)
C(1)-C(2)-O(1)	116.6(10)	C(3)-C(2)-O(1)	125.6(10)
C(3)-C(2)-C(1)	117.8(10)	C(4)-C(3)-C(2)	123.8(10)
C(3)-C(4)-O(2)	130.8(9)	C(5)-C(4)-O(2)	111.(9)
C(5)-C(4)-C(3)	117.7(10)	F(2)-C(5)-F(1)	107.2(10)
F(3)-C(5)-F(1)	106.1(9)	F(3)-C(5)-F(2)	105.2(9)
C(4)-C(5)-F(1)	112.0(9)	C(4)-C(5)-F(2)	114.4(9)
C(4)-C(5)-F(3)	111.4(9)	C(6)-C(7)-O(3)	118.1(12)
C(8)-C(7)-O(3)	122.8(10)	C(8)-C(7)-C(6)	119.1(11)
C(9)-C(8)-C(7)	124.9(10)	C(8)-C(9)-O(4)	129.7(11)
C(10)-C(9)-O(4)	112.0(11)	C(10)-C(9)-C(8)	118.3(11)
F(5)-C(10)-F(4)	104.9(11)	F(6)-C(10)-F(4)	109.4(13)
F(6)-C(10)-F(5)	103.8(11)	C(9)-C(10)-F(4)	112.5(11)
C(9)-C(10)-F(5)	111.6(11)	C(9)-C(10)-F(6)	114.0(11)
C(14)-C(13)-N(1)	115.1(9)	C(13)-C(14)-N(2)	114.7(9)
C(17)-C(16)-N(2)	113.4(9)	C(16)-C(17)-N(3)	113.7(9)
C(20)-C(19)-N(3)	114.1(9)	C(19)-C(20)-N(4)	115.3(9)

The crystal structure of the related transition metal complex, $[Cu_2(hfpd)_4(hmteta)]$, shows each Cu^{II} ion to be at the centre of an elongated N_2O_4 octahedron. This compound is soluble both in polar and non polar solvents. Nickel chelates based on the same formulae are generally less soluble, especially in polar solvents; however, with tmeda, e.g. $[Ni(tmhd)_2(tmeda)]$, solubility is increased.[90]

The strontium analogue of this species, complex (17), is presumably monomeric and eight coordinate, from spectroscopic considerations. Both barium and strontium have previously been shown to exist as stable 8-coordinate complexes in $[Ba(tmhd)_2(triglyme)]$ (2) and $[Sr(tmhd)_2(triglyme)]$ (5).

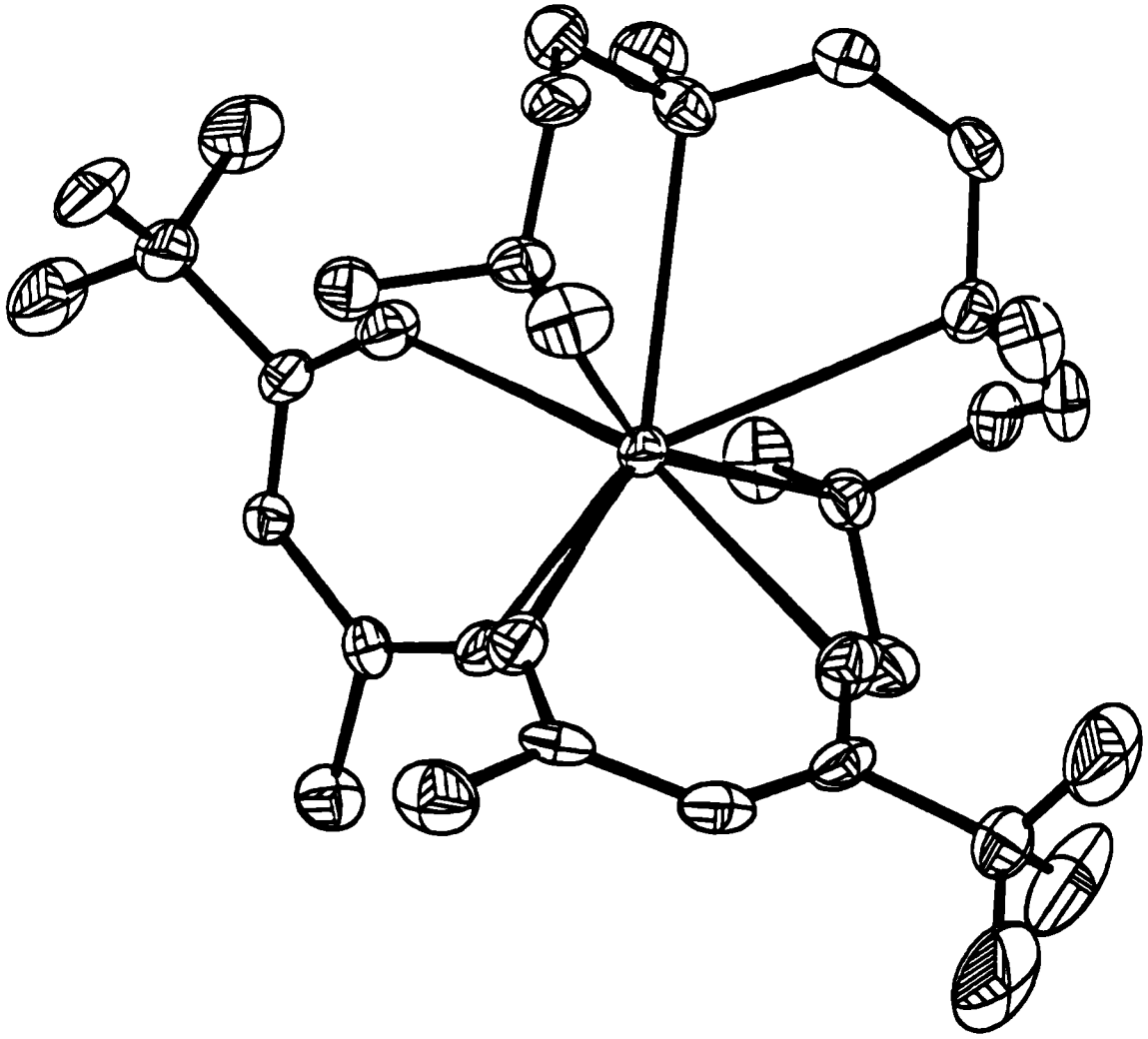

Figure 3.9 : X-ray crystal structure of [Ba(tfpd)$_2$(hmteta)] (16)

[Sr(tfpd)$_4$]$^{2-}$.2[(tmeda-H)]$^+$ (22)

Crystal data for [Sr($C_5H_4O_2F_3$)$_4$].2($C_6H_{17}N_2$): F.W. = 934.38, Orthorhombic, a = 27.095(4), b = 28.416(3), c = 11.154(1)Å, U = 8588(2)Å^3 (by least squares refinement of diffractometer angles for 250 reflections within θ = 2.9-29.9°, λ = 0.71069Å), space group Fdd2 (no. 43), Z = 8, D_c = 1.445 g cm^{-3}, F(000) = 3840, μ = 13.56 cm^{-1}, T = 150K, colourless parallelpiped, crystal size 0.40 x 0.20 x 0.15mm^3.

The data collection and processing were performed on a Delft Instruments FAST TV area detector diffractometer positioned at the window of rotating anode generator, Mo-K_α radiation and an Oxford Cryostream low-temperature cooling system; 11417 reflections measured (index ranges $-29 < h < 37$; $-38 < k < 33$; $-15 < l < 14$), 5491 unique (merging R = 0.0376 after absorption correction using DIFFABS; max. and min. absorption correction factors = 0.892, 1.199).

The structure was solved *via* direct methods (SHELX-S)[79] (most of the atoms in the $[Sr(tfpd)_4]^{2-}$ moiety) followed by the difference syntheses. Full-matrix least squares refinement on F using SHELX-80[79] with all non-hydrogen atoms anisotropic resulted in a model which appeared to be chemically correct but the conventional R value was rather high (ca. 0.09). The refinement was continued using the program SHELXL-93[82] employing the unique F^2 data, which immediately suggested that the working model was the wrong enantiomorph. The correct enantiomorph was then obtained by transforming the existing atom coordinates by (0.25-x, 0.25-y, 1-z). The hydrogen atoms were all located from difference maps. The refinement finally converged at $\omega R_2 = [\Sigma\{\omega(\Delta(F^2)^2)\}/\Sigma\{\omega(Fo^2)^2\}]^{1/2} = 0.0842$ and $R_1 = \Sigma(\Delta F)/\Sigma(Fo) = 0.0428$ for all 5491 data and 358 parameters (hydrogen atoms isotropic, others anisotropic; ρ_{min}, ρ_{max} −0.22, 0.51eÅ^{-3}; $(\Delta/\sigma)_{max}$ 0.035). The corresponding ωR_2 and R_1 values for 3486 data with $Fo > 4\sigma(Fo)$ were 0.0585 and 0.0262 respectively. The weighting scheme used was $\omega = 1/\sigma^2(Fo)^2$, which gave acceptable agreement analyses. The Flack's parameter was-0.015(5) confirming that the absolute structure was determined correctly. The calculations were done on a 486DX2/66 personal computer. The collection data and details of bond lengths and angles appear in the appendix.

The single crystal X-ray structure of (22) shows that the complex is monomeric, the structure being in good agreement with the spectroscopic data. The strontium atom is bound to all four didentate tfpd ligands, but not directly to the two amine ligands, thereby producing a dianionic $[Sr(tfpd)_4]^{2-}$ species. Thus the strontium atom clearly prefers to adopt a coordination number of eight rather than a possible number of ten or twelve. The geometry around the metal centre consists of a severely distorted square antiprism. The Sr-$O_{(tfpd)}$ bond lengths [2.526(4) - 2.582(6)Å] can be contrasted with those of the comparable Sr compounds $[Sr(tmhd)_2(triglyme)]$(5), and $[Sr(dppd)_2(tetraglyme)]$(8) which are 2.494(10) and 2.540(6)Å respectively; this is most likely due to the electron donating (^{t}Bu,

making the M-O bonds longer) and withdrawing (phenyl, making the M-O bonds of a similar length) nature of the diketonate ligands.

One of the most interesting features of complex (22) is the observation that the amine ligands do not bind directly to the metal as might have been expected. Instead, the protonated nitrogen, N(2) (on the cationic amine ligand) comes into close contact with one of the tfpd oxygens, O(2), with a bond length of 2.75(4)Å. This 'short' term bond implies the presence of an intramolecular hydrogen bond HN(2) - O(2) of 1.79(4)Å. Clearly, the central $[Sr(tfpd)_4]^{2-}$ moiety has the β-diketone ligands wrapped around in a preferred square antiprismatic orientation, because this allows not only the hydrogen bonding between the tfpd ligand and protonated tmeda to occur, but also for the amine nitrogen N(1) to orientate itself near to the tfpd [O(3) and O(4)] bearing the carbon C(6) carrying the CF_3 group with a non-bonded F-H(CH_3) contact distance of 2.38(5)Å.

Clearly, the situation which results in what may be termed a tight cation anion pair alleviates the excess negative charge in the strontium. This mode of bonding of the protonated amine to the carbonyl group of one of the tfpd ligands, appears to be a rare and unusual example of hydrogen bonding and a fascinating and unexpected structural motif. All of the cation - anionic complexes (19) - (22) are likely to have the same basic structural geometry, as indicated by spectroscopic data, in particular ^1H NMR.

Table 3.7 : Bond lengths (A) and angles (°) for compound (22) :

Sr-O(1)	2.577(2)	Sr-O(2)	2.583 (2)
Sr-O(3)	2.530(2)	Sr-O(4)	2.593 (2
F(1)-C(1)	1.320(4)	F(2)-C(1)	1.329(4)
F(3)-C(1)	1.318(4)	F(4)-C(6)	1.338(4)
F(5)-C(6)	1.326(4)	F(6)-C(6)	1.331(4)
O(1)-C(2)	1.237(3)	O(2)-C(4)	1.266(3)
O(3)-C(9)	1.243(3)	O(4)-C(7)	1.257(3)
N(1)-C(12)	1.452(5)	N(1)-C(13)	1.462(5)
N(1)-C(11)	1.468(4)	N(2)-C(15)	1.484(4)
N(2)-C(16)	1.486(4)	N(2)-C(14)	1.495(4)
C(1)-C(2)	1.541(4)	C(2)-C(3)	1.397(4)
C(3)-C(4)	1.407(4)	C(4)-C(5)	1.501(4)
C(6)-C(7)	1.538(4)	C(7)-C(8)	1.383(4)
C(8)-C(9)	1.421(5)	C(9)-C(10)	1.502(4)
C(13)-C(14)	1.513(5)		

O(3) #1-Sr-O(3)	90.37(9)	O(3) -Sr-O(1) #1	152.15(6)
O(3)-Sr-O(1)	76.75(6)	O(1)#1-Sr-O(1)	124.62(8)
O(3) #1-Sr-O(2)	109.20(6)	O(3) -Sr-O(2)	136.35(7)
O(1) #1-Sr-O(2)	71.49(6)	O(1) -Sr-O(2)	67.89(6)
O(2)-Sr-O(2)#1	83.42(8)	O(3)-Sr-O(4)#1	70.14(7)
O(1)-Sr-O(4)#1	127.26(6)	O(2)-Sr-O(4)#1	153.12(6)
O(3)-Sr-O(4)	68.25(7)	O(1)-Sr-O(4)	82.11(6)
O(2)-Sr-O(4)	81.97(7)	O(4)#1-Sr-O(4)	119.49(9)
C(2)-O(1)-Sr	126.5(2)	C(4)-O(2)-Sr	128.8(2)
C(9)-O(3)-Sr	133.4(2)	C(7)-O(4)-Sr	127.9 (2)
C(12)-N(1)-C(13)	110.4(3)	C(12)-N(1)-C(11)	109.7(3)
C(13)-N(1)-C(11)	111.0(3)	C(15)-N(2)-C(16)	111.6(3)
C(15)-N(2)-C(14)	110.9(3)	C(16)-N(2)-C(14)	112.7(3)
F(3)-C(1)-F(1)	106.7(3)	F(3)-C(1)-F(2)	106.5(3)
F(1)-C(1)-F(2)	105.4(3)	F(3)-C(1)-C(2)	114.9(3)
F(1)-C(1)-C(2)	110.9(3)	F(2)-C(1)-C(2)	111.8(3)
O(1)-C(2) -C(3)	130.5(3)	O(1) -C(2)-C(1)	113.3 (3)
C(3)-C(2)-C(1)	116.1(2)	C(2)-C(3)-C(4)	124.0(3)
O(2)-C(4)-C(3)	124.1(2)	O(2)-C(4)-C(5)	118.4(2)
C(3)-C(4)-C(5)	117.6(3)	F(5)-C(6)-F(6)	106.4(3)
F(5)-C(6)-F(4)	107.2(3)	F(6)-C(6)-F(4)	106.3(3)
F(5)-C(6)-C(7)	111.6(3)	F(6)-C(6)-C(7)	110.7(2)
F(4)-C(6)-C(7)	114.2(3)	O(4)-C(7)-C(8)	130.O(3)
O(4)-C(7)-C(6)	112.0(3)	C(8)-C(7)-C(6)	118.O(3)
C(7)-C(8)-C(9)	124.4(3)	O(3)-C(9)-C(8)	123 .7(3)
O(3)-C(9)-C(10)	117.7(3)	C(8)-C(9)-C(10)	118.6(3)
N(1)-C(13)-C(14)	111.1(3)	N(2)-C(14)-C(13)	113.4(3)

Symmetry transformations used to generate equivalent atoms: #1 -x+1/2, -y+1/2, z.

A direct comparison with another tight cation - anion complex, $\{[Ba(hfpd)_5]^{2-}.2(enH)^+\}$ may be made.[93] In this complex the metal coordinates to nine of ten possible oxygen donor sites of the β-diketonates ligands with Ba-O bond lengths ranging between 2.73(5) - 2.86(6)Å. There is also a Ba-F interaction at 3.29(8)Å. Also the reaction of tmnd with hfpd-H gives the salt, hfpd-tmnd-H+. The addition of this salt to group II hfpd's gives anionic complexes, e.g. with calcium, $[Ca(hfpd)_3]$-[tmnd-H]+.$2H_2O$ and $\{2.(tmnd-H)^+[Ca(hfpd)_4]^{2-}\}$.[92a] No N-H signals are observed in the ^1H NMR for either of these complexes in contrast with complexes (19) - (22). The crystal structure of the magnesium equivalent $[Mg(hfpd)_3]$-(tmnd-H)+, shows the presence of discrete anions.[92b]

3.5.1 Crystallographic summary :

Comparing the amine complexes described in this Chapter with the glyme complexes described in the previous Chapter we note a number of inherent differences. Firstly the coordination numbers are generally lower for the amine complexes. A specific

example is [Ca(tmhd)$_2$(triglyme)] (7) which is eight coordinate, while [Ca(dppd)$_2$(pmdeta)] (15) is only seven coordinate. This difference is most likely to be due to the added steric crowding imparted by the extra terminal methyls groups on the amine ligand. In order for the glyme complexes to be seven coordinate, the diglyme ligand must be employed. However, this results in the formation of either dimeric (3) or water bridged (6) complexes. Noteworthy, however, is the fact that the pattern of the terminal M-N bond lengths to the amine are shorter than for the inner M-N bonds. This pattern is also noted in the crystallographic data of the majority of the glyme complexes.

Also the β-diketonate ligands generally have different dispositions about the metal centre when the monomeric complexes are compared. This factor too may be due to the added steric crowding.

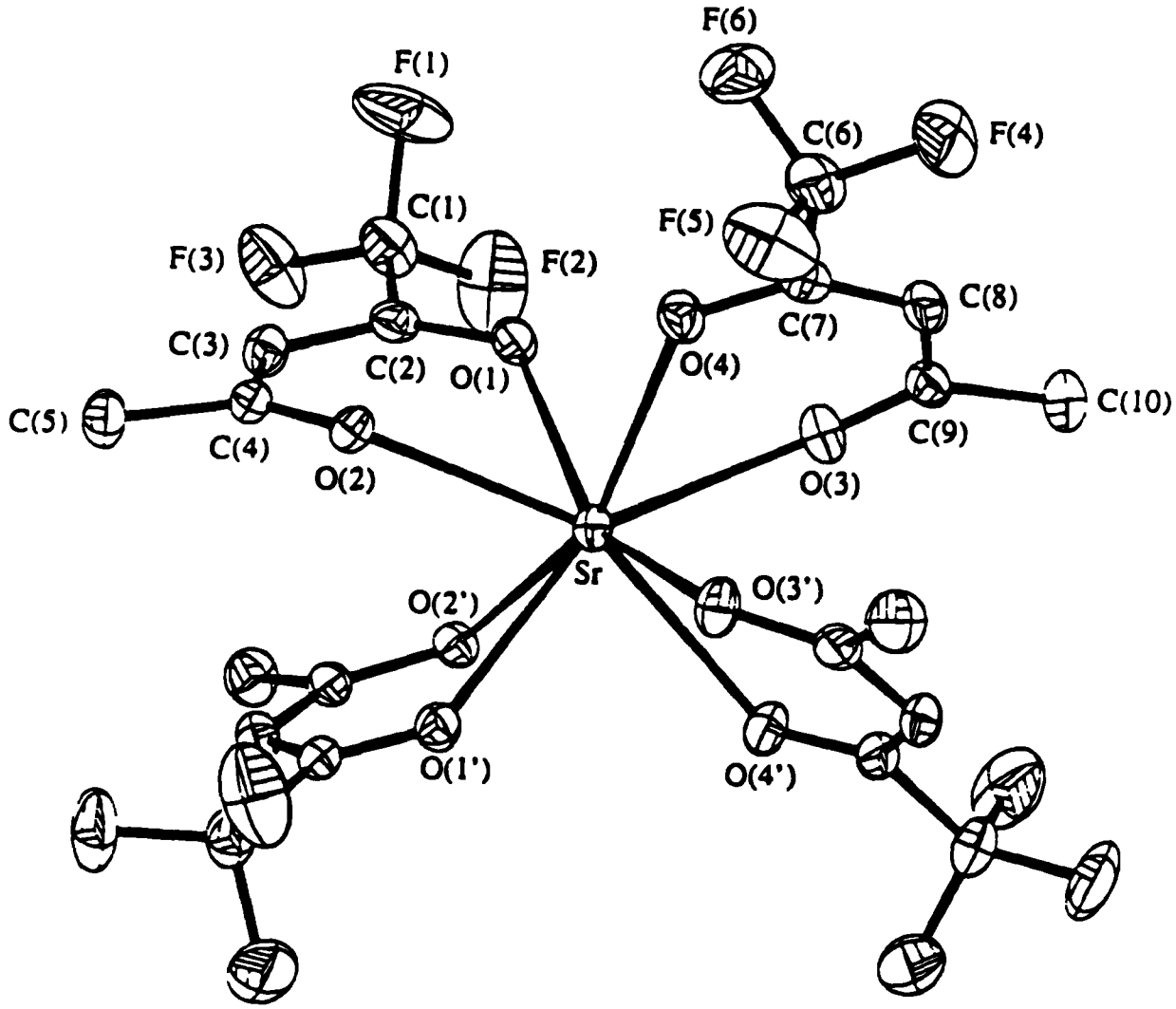

Figure 3.10 : X-ray crystal structure of the [Sr(tfpd)$_4$]$^{2-}$ dianion (22)

3.6 Experimental section

Synthesis of [Ca(dppd)$_2$(pmdeta)] (15)

[Ca(OEt)$_2$(EtOH)$_4$]$_n$ (1.92 g, 6.16 mmol) was dissolved in chloroform (25 mL) in a Schlenk and dppd-H (2.73 g, 12.32 mmol) added to yield a soluble yellow coloured solution. Pmdeta (3.0 mL, 14.0 mmol) was added and the solution stirred at R.T. for 10 mins.. The solvent was removed *in vacuo* to yield a yellow solid. This was redissolved in toluene (25 mL) and placed at 0°C to crystallize as large colourless crystals. **Yield** 2.78g (68.5%) **M. Pt.** 143-145 C.

Microanalyses : Found, C, 71.31 ; H, 6.93 ; N, 6.19 ; Calcd for $CaC_{39}H_{45}O_4N_3$, C, 71.02 ; H, 6.83 ; N, 6.37%.

Infrared (Nujol ν cm^{-1}) : 1610(w), 1601(m), 1555(m), 1511(m), 1412(m), 1302(w), 1261(s), 1219(m), 1134(m), 1068(m), 1022(s), 964(w), 938(m), 898(m), 797(m), 780(m), 750(w), 723(m), 693(m), 619(w), 610(w).

Infrared (Hexachlorobutadiene ν cm^{-1}) : 3057(w), 2962(m), 2867(m), 1611(s), 1602(s), 1513(m), 1470(s), 1412(s), 1347(m), 1303(w), 1261(m), 1219(s), 1177(m), 1103(m), 1069(m), 1022(s), 939(m), 751(w), 693(m), 619(w), 610(w).

^{1}H NMR (270 MHz, d_6-dmso, 20°C) : δ 2.26 (12H, s, $N(CH_3)_2$), 2.29 (3H, s, NCH_3), 2.40 (4H, m, NCH_2), 2.52 (4H, s, NCH_2), 6.80 (2H, s, CH), 7.55, 8.12 (20H, m, phenyl protons).

^{13}C NMR (67.94 MHz, d_6-dmso, 20°C) : δ 43.28 (s, NCH_3), 46.26 (s, $N(CH_3)_2$), 56.30 (s, NCH_2), 57.81 (s, NCH_2), 93.16 (s, CH), 128.29 (s, p-Ph), 129.32 (s, m-Ph), 133.29 (s, o-Ph), 143.12 (s, i-Ph), 184.38 (s, CO).

Mass Spectrometry (EI+) : 749 [Ca$_2$(dppd)$_3$](6%), 709 [Ca(dppd)$_3$](2%), 263 [Ca(dppd)](100%).

Solubility : Soluble in thf, chloroform, dmso and hot toluene, insoluble in hexane.

STA data : TGA : 128.5-278.9°C(37.6%), 425.7-467.3°C(14.7%), 522.2-570.6°C(25.9%), 704.9-785.1°C(8.35%), Res. 10.8%, $T_{50\%}$ 420°C. DSC : 122.2, 213.6, 455.6, 566.7, 766.7°C.

Synthesis of [Ba(tfpd)$_2$(hmteta)] (16)

[Ba(OEt)$_2$(EtOH)$_4$]$_n$ (1.90 g, 4.92 mmol) was dissolved in n-hexane (25 mL) in a Schlenk and tfpd-H (1.12 g, 9.84 mmol) added to yield a soluble yellow coloured solution. Hmteta (1.34 mL, 4.92 mmol) was added and the solution stirred at R.T. for 10 mins.. The solvent was removed *in vacuo* to yield a yellow - orange liquid. This was redissolved in boiling toluene (10 mL), then n-hexane (15 mL) was added and the solution was placed at R.T. to crystallize as large pale orange crystals. **Yield** 2.34g (71%). **M. Pt.** 143-147 C.

Microanalyses : Found, C, 40.03 , H, 5 14 , N, 7 96 : Calcd for $BaC_{22}H_{38}F_6O_4N_4$, C, 39.20 , H, 5 64 ; N, 8.32%.

Infrared (Nujol ν cm^{-1}) : 1635(m), 1515(m), 1281(s), 1212(m), 1181(m), 1115(m), 1043(s), 1022(w), 983(m), 934(m), 845(m), 773(m), 723(m).

Infrared (Hexachlorobutadiene ν cm^{-1}) : 3042(w), 2859(m), 1634(m), 1614(s), 1357(m), 1281(m), 1222(s), 1184(m), 1134(m), 716(w).

^{1}H NMR (270 MHz, C_6D_6, 20 C) : δ 1.89 (6H, s, CH_3), 2.30 (12H, s, $N(CH_3)_2$), 2.64 (6H, s, NCH_3), 2.93 (4H, m, CH_2), 3.03 (4H, t, CH_2), 3.28 (4H, t, CH_2), 5.40 (2H, s, CH).

^{13}C NMR (67.94 MHz, C_6D_6, 20 C) : δ 29.86 (s, CH_3), 40.78 (s, NCH_3), 44.13 (s, $N(CH_3)_2$), 52.42 (s, NCH_2), 54.12 (s, NCH_2), 54.70 (s, NCH_2), 93.06 (s, CH), 169.43 (q, CO ^2J = 30Hz), 193.58 (s, CO).

Mass Spectrometry (EI+) : 362 [Ba(tfpd)($Me_2NCH_2CH_2$)](10%), 351 [Ba(tfpd)(Me_2NCH_2)](2%), 291 [Ba(tfpd)](4%), 278 [Ba($CF_3COCHCO$)](5%).

Solubility : Soluble in thf, chloroform, dmso and hot toluene, insoluble in hexane.

Synthesis of [Sr(tfpd)$_2$(hmteta)] (17)

$[Sr(OEt)_2(EtOH)_4]_n$ (1.90 g, 5.65 mmol) was dissolved in n-hexane (25 mL) in a Schlenk and tfpd-H (1.36 g, 11.30 mmol) added to yield a pale yellow coloured solution. Hmteta (1.54 mL, 5.65 mmol) was added and the solution stirred at R.T. for 10 mins.. The solvent was removed *in vacuo* to yield an orange liquid. This was redissolved in boiling toluene (10 mL), then n-hexane (15 mL). The solution was placed at R.T. to crystallize. Small pale orange crystals were produced. **Yield** 2.18g (62%) **M. Pt.** 69-72 C.

Microanalyses : Found, C, 42.57 ; H, 6.34 ; N, 9.16 ; Calcd for $SrC_{22}H_{38}F_6O_4N_4$, C, 42.31 : H, 6.09 ; N, 8.97%.

Infrared (Nujol ν cm^{-1}) : 1635(s), 1281(s), 1181(m), 1133(m), 1022(w), 842(m), 799(m), 768(m), 722 (w), 548 (w).

Infrared (Hexachlorobutadiene ν cm^{-1}) : 2969(m), 1637(m), 1613(s), 1515(m), 1461 (m) 1354(m), 1281(m), 1158(s), 1182(m), 1133(m), 1026(m), 894(m), 723(w), 549(m).

^{1}H NMR (270 MHz, d_6-dmso, 20 C) : δ 1.73 (6H, s, CH_3), 1.96 (6H, s, NCH_3), 2 02 (12H, s, $N(CH_3)_2$), 2.23 (12H, br, CH_2), 5 67 (2H, s, CH).

^{13}C NMR (67.94 MHz, d_6-dmso, 20 C) : δ 28.05 (s, CH_3), 41.13 (s, $N(CH_3)_2$), 44.78 (s, NCH_3), 54 22 (s, NCH_2), 54.32 (s, NCH_2), 54.74 (s, NCH_2), 93 51 (s, CH), 170.13 (q, CO ^2J = 29Hz), 194 21 (s CO).

Mass Spectrometry (EI+) : 312 [Sr(tfpd)($Me_2NCH_2CH_2$)](12%), 301 [Sr(tfpd)(Me_2NCH_2)](4%), 241 [Sr(tfpd)](5%), 228 [Sr($CF_3COCHCO$)](6%).

Solubility : Soluble in thf, chloroform, dmso and toluene, insoluble in hexane.

STA data : TGA : 223-251°C(45.9%), 268-285°C(27.3%), Res. 24.8%, $T_{50\%}$ 248°C. DSC : 98.1, 247.2, 269.5°C.

Synthesis of $[Ca(tmhd)_2(tmeda)]$ (18)

$[Ca(OEt)_2(EtOH)_4]_n$ (2.27 g, 7.22 mmol) was dissolved in n-hexane (25 mL) in a Schlenk and tmhd-H (3.09 mL, 14.44 mmol) added to yield a clear solution. Tmeda (1.10 mL, 7.22 mmol) was added and the solution stirred at R.T. for 10 mins.. The solvent was removed *in vacuo* to yield a white solid. This was redissolved in n-hexane (8 mL) and placed at 0 C to crystallize as large colourless needles. **Yield** 2.56 g (67%) **M. Pt.** 117-119 C.

Microanalyses : Found, C, 64.21 ; H, 10.12 ; N, 5.31 ; Calcd for $CaC_{28}H_{54}O_4N_2$, C, 64.37 ; H, 10.34 ; N, 5.36%.

Infrared (Nujol ν cm^{-1}) : 1589(w), 1577(m), 1536(m), 1506(m), 1421(m), 1405(w), 1357(m), 1291(m), 1261(s), 1224(m), 1181(m), 1132(m), 1098(m), 1017(s), 964(w), 938(m), 898(m), 797(m), 780(m), 750(w), 723(m), 693(m), 619(w), 610(w).

Infrared (Hexachlorobutadiene ν cm^{-1}) : 2964(w), 2904(m), 1588(s), 1577(s), 1538(m), 1506(s), 1492(s), 1478(m), 1419(m), 1406(m), 1357(m), 1291(w), 1244(m), 1225(s), 1183(m), 1133(m), 1069(m), 1022(s), 939(m), 751(w), 693(m), 619(w), 600(w).

^{1}H NMR (90 MHz, C_6D_6, 20 C) : δ 1.15 (18H, s, CH_3), 1.95 (4H, m, CH_2), 2.14 (12H, s, $N(CH_3)_2$), 5.80 (2H, s, CH).

^{13}C NMR (22.61 MHz, C_6D_6, 20 C) : δ 28.21 (s, CH_3), 40.36 (s, $\underline{C}(CH_3)_3$), 44 51 (s, $N(CH_3)_2$), 55.98 (s, NCH_2), 88.75 (s, CH), 199.10 (s, CO).

Mass Spectrometry (EI+) : 1033 $[Ca_3(tmhd)_5]$(55%), 630 $[Ca_2(tmhd)_3]$(100%), 349 [Ca(tmhd)(^{t}BuCOCHCOH)](14%), 343 [Ca(tmhd)(tmeda)](5%), 223 [Ca(tmhd)](27%).

Solubility : Soluble in thf, chloroform, dmso, hexane and toluene.

Synthesis of $[Ca(hfpd)_4]^{2-}$ .2[(pmdeta-H)]$^+$ (19)

$[Ca(OEt)_2(EtOH)_4]_n$ (2.00 g, 6.37 mmol) was dissolved in toluene (25 mL) in a Schlenk and hfpd-H (1.28 mL, 12.75 mmol) added to yield a clear solution. Pmdeta (2.52 mL, 12.75 mmol) was added and the solution stirred at R.T. for 10 mins.. On addition of the amine the reaction was observed to be very exothermic. The solvent was removed *in vacuo* to yield a pale orange oil. This was redissolved in toluene (25 mL) and placed at

20 C to crystallize as small yellow crystals. **Yield** 2.98g (39%) **M. Pt.** 83-86 C.

Microanalyses : Found, C, 36.93 ; H, 4.16 ; N, 6.84 ; Calcd for $CaF_{24}C_{38}H_{52}O_8N_6$, C, 37.50 ; H, 4.28 ; N, 6.91%.

Infrared (Nujol ν cm^{-1}) : 3427(w), 1664(m), 1605(m), 1527(m), 1458(m), 1377(m), 1256(w), 1146(s), 1030(s), 987(w), 932(m), 797(m), 765(m), 737(w), 728(m), 660(m), 578(w).

Infrared (Hexachlorobutadiene ν cm^{-1}) : 3027(w), 2960(m), 2917(m), 1671(s), 1542(s), 1493(m), 1467(s), 1414(s), 1377(m), 1255(w), 1147(m), 1083(m), 1029(m), 895(m), 751(w), 729(m), 695(w), 579(w).

^{1}H NMR (270 MHz, d_6-dmso, 20 C) : δ 1.75 (3H, s, NCH_3), 1.94 (4H, m, CH_2), 1.95 (12H, s, $N(CH_3)_2$), 2.12 (4H, s, CH_2), 6.23 (2H, s, CH), 9.86 (1H, s, NH).

^{13}C NMR (67.94 MHz, d_6-dmso, 20 C) : δ 43.17 (s, NCH_3), 45.26 (s, $N(CH_3)_2$), 54.95 (s, NCH_2), 56.71 (s, NCH_2), 88.83 (s, CH), 118.10 (q, CF_3 ^1J = 297Hz), 176.80 (d, CO ^2J = 29Hz).

Mass Spectrometry (EI+) : 701 [Ca_2(hfpd)$_3$](12%), 561 [Ca(hfpd)($CF_3COCHCOH$)](10%), 420 [Ca(hfpd)(pmdeta)](45%), 247 [Ca(hfpd)](100%).

Solubility : Soluble in thf, chloroform, dmso and toluene, insoluble in hexane.

Synthesis of $[Ba(hfpd)_4]^{2-}$ .2[(pmdeta-H)]$^+$ (20)

$[Ba(OEt)_2(EtOH)_4]_n$ (3.03 g, 7.37 mmol) was dissolved in toluene (25 mL) in a Schlenk and hfpd-H (2.10 mL, 14.74 mmol) added to yield a soluble solution. Pmdeta (2.55 mL, 14.70 mmol) was added and the solution stirred at R.T. for 10 mins.. On addition of the amine the reaction was observed to be very exothermic. The solvent was removed *in vacuo* to yield a pale orange oil. This was redissolved in toluene (25 mL) and placed at 20 C to crystallize as small yellow crystals. **Yield** 3.78g (39%) **M. Pt.** 53-56 C.

Microanalyses : Found, C, 34.54 ; H, 3.78 ; N, 6.22 ; Calcd for $BaF_{24}C_{38}H_{52}O_8N_6$, C, 34.73 ; H, 3.96 ; N, 6.40%.

Infrared (Nujol ν cm^{-1}) : 3436(w), 1664(m), 1558(m), 1540(m), 1414(m), 1256(w), 1192(s), 1126(s), 1079(m), 1023(m), 998(w), 943(m), 799(m), 765(m), 737(w), 728(m), 660(m), 578(w).

Infrared (Hexachlorobutadiene ν cm^{-1}) : 2960(m), 2917(m), 1668(s), 1467(s), 1414(s), 1368(m), 1255(w), 1186(m), 1147(m), 1083(m), 1024(m), 895(m), 754(w), 729(m), 695(w), 584(w).

^{1}H NMR (270 MHz, d_6-dmso, 20 C) : δ 2.62 (3H, s, NCH_3), 2.77 (12H, s, $N(CH_3)_2$), 2.91 (4H, m, CH_2), 3.03 (4H, s, CH_2), 5.78 (2H, s, CH), 9.74 (1H, s, NH).

^{13}C NMR (67.94 MHz, d_6-dmso, 20 C) : δ 42.86 (s, NCH_3), 44.65 (s, $N(CH_3)_2$), 52.81 (s, NCH_2), 56.10 (s, NCH_2), 84.19 (s, CH), 118.14 (q, CF_3 ^1J = 293Hz), 172.40 (d, CO ^2J = 29Hz).

Mass Spectrometry (EI+) : 709 [Ba(hfpd)(pmdeta)$_2$(H_2O)](21%), 575

[Ba(hfpd)(pmdeta)($N(CH_3)_2$)](100%), 552 [$Ba(hfpd)_2$](12%), 518 [Ba(hfpd)(pmdeta)](45%), 345 [Ba(hfpd)](100%).

Solubility : Soluble in thf, chloroform, dmso and toluene, insoluble in hexane.

STA data : TGA : 233.7-276.8°C(75.3%), Res. 16.2%, $T_{50\%}$ 256 C. DSC : 192.8, 263.1°C.

Synthesis of $[Sr(tfpd)_4]^{2-}.2[(pmdeta\text{-}H)]^+$ (21)

$[Sr(OEt)_2(EtOH)_4]_n$ (2.00 g, 5.88 mmol) was dissolved in n-hexane (25 mL) in a Schlenk and tfpd-H (1.42 mL, 11.72 mmol) added. Pmdeta (2.33 mL, 11.72 mmol) was added and the solution stirred at R.T. for 10 mins.. On addition of the amine the reaction was observed to be very exothermic. The solvent was removed *in vacuo* to yield a pale orange oil. This was redissolved in toluene (15 mL) and placed at 20 C to crystallize. After two days the solution was layered with n-hexane (15 mL). Small yellow crystals were produced within a few hours. **Yield** 2.65g (43%). **M. Pt.** 98-102 C.

Microanalyses : Found, C, 43.44 ; H, 5.97 ; N, 7.87 ; Calcd for $SrF_{12}C_{38}H_{64}O_8N_6$, C, 43.51 ; H, 6.11 ; N, 8.02 %.

Infrared (Nujol ν cm^{-1}) : 3458(w), 1635(m), 1505(m), 1285(m), 1181(m), 1132(s), 1033(m), 961(w), 932(m), 843(m), 765(m), 723(m), 694(m), 548(w).

Infrared (Hexachlorobutadiene ν cm^{-1}) : 3027(w), 2960(m), 2917(m), 1612(s), 1460(s), 1384(s), 1282(m), 1130(w), 1030(m), 895(m), 723(w), 695(m), 605(w), 548(w).

^1H NMR (270 MHz, d_6-dmso, 20 C) : δ 1.85 (6H, s, CH_3), 1.87 (3H, s, NCH_3), 2.08 (12H, s, $N(CH_3)_2$), 2.26 (4H, m, CH_2), 2.28 (4H, s, CH_2), 5.67 (2H, s, CH), 11.31 (1H, s, NH).

^{13}C NMR (67.94 MHz, d_6-dmso, 20°C) : δ 28.94 (s, CH_3), 41.36 (s, NCH_3), 43 54 (s, $N(CH_3)_2$), 52.41 (s, NCH_2), 55.29 (s, NCH_2), 93.82 (s, CH), 119.70 (q, CF_3 ^1J = 297Hz), 176.80 (q, CO ^2J = 29Hz), 193.98 (q, CO).

Mass Spectrometry (EI+) : 634 [$Sr_2(tfpd)_3$](46%), 586 [$Sr(tfpd)_2$(pmdeta)F](16%), 500 [Sr(tfpd)(pmdeta)($Me_2NCH_2CH_2N$)](50%), 416 [Sr(tfpd)(pmdeta)](15%), 393 [$Sr(tfpd)_2$](8%), 366 [Sr(pmdeta)($(Me_2NCH_2CH_2N)$F](48%), 318 [Sr(tfpd)($COCF_2$)](17%), 241 [Sr(tfpd)](100%).

Solubility : Soluble in thf, chloroform, dmso and hot toluene, insoluble in hexane.

Synthesis of $[Sr(tfpd)_4]^{2-}$ .2[(tmeda-H)]$^+$ (22)

$[Sr(OEt)_2(EtOH)_4]_n$ (1.92 g, 5.68 mmol) was dissolved in n-hexane (25 mL) in a Schlenk and tfpd-H (1.32 mL, 11.36 mmol) added to yield an orange soluble solution. Tmeda (1.72 mL, 11.42 mmol) was added and the solution stirred at R.T. for 10 mins.. On addition of the amine the reaction was observed to be very exothermic. The solvent was removed *in vacuo* to yield a pale orange oil. This was redissolved in toluene (15 mL) and placed at 20°C to crystallize. After two days the solution was layered with n-hexane (15 mL). Small yellow crystals were produced within a few hours. **Yield** 2.32g (48%). **M. Pt.** 86-88 C.

Microanalyses : Found, C, 40.84 ; H, 5.29 ; N, 5.89 ; Calcd for $SrF_{12}C_{32}H_{50}O_8N_4$, C, 41.11 ; H, 5.35 ; N, 6.00%.

Infrared (Nujol ν cm^{-1}) : 1638(m), 1541(m), 1496(m), 1355(m), 1285(m), 1181(s), 1126(m), 1043(m), 1009(w), 938(m), 919(m), 792(m), 604(m), 584(m), 548(w).

Infrared (Hexachlorobutadiene ν cm^{-1}) : 3410(w), 3037(w), 2923(m), 1637(s), 1384(s), 1355(s), 1275(m), 1125(w), 1043(m), 895(m), 756(m), 723(w), 605(w), 548(w).

^{1}H NMR (270 MHz, d_6-dmso, 20 C) : δ 1.89 (6H, s, CH_3), 2.10 (12H, s, $N(CH_3)_2$), 2.26 (4H, m, CH_2), 5.69 (2H, s, CH), 10.91 (1H, s, NH).

^{13}C NMR (67.94 MHz, d_6-dmso, 20 C) : δ 28.79 (s, CH_3), 43.90 (s, $N(CH_3)_2$), 54.45 (s, NCH_2), 94.11 (s, CH), 123.45 (q, CF_3 ^1J = 300Hz), 169.05 (q, CO ^2J = 30Hz).

Mass Spectrometry (EI+) : 760 $[Sr(tfpd)_4(NCH_2CH_2N)]$(30%), 699 $[Sr(tfpd)_4]$(2%), 634 $[Sr_2(tfpd)_3]$(48%), 394 $[Sr(tfpd)_2]$(16%), 357 [Sr(tfpd)(tmeda)](40%), 325 $[Sr(tfpd)(CH_3COCHCOH)]$(13%), 241 [Sr(tfpd)](76%).

Solubility : Soluble in thf, chloroform, dmso and hot toluene, insoluble in hexane.

PART 2:

THE CHEMISTRY OF CERIUM (IV) CARBOXYLATES

Chapter 4

AN INTRODUCTION TO LANTHANIDE CARBOXYLATES

The aims of this section of the Thesis were directed towards the synthesis and characterization of oxo-*bis* cerium(IV) carboxylate complexes by a range of spectroscopic and analytical methods. The chemistry of these compounds was also studied, in particular their ability to form coordination compounds, their propensity to photoreduce to Ce(III) compounds and their electrochemical properties. were investigated and the results obtained are presented in subsequent Chapters.

4.1 Overview

Naturally occurring carboxylic acids are, with only a few exceptions, straight chain unsubstituted acids of the form ($C_nH_{2n+1}CO_2H$) with an even number of carbon atoms. The only odd numbered acids that occur naturally are isovaleric and formic acids. However almost all of the straight chain acids up to C_{38} have been synthetically made, together with many branched, unsaturated, alicyclic, aromatic and substituted acids. The lower members of the saturated series are liquids at room temperature but on increasing the number of carbons, the liquids become more and more viscous, indeed those above C_{10} are generally solids. Substituted and aromatic acids may be solids with smaller numbers of carbon atoms, e.g. pivalic acid (2,2-dimethylpropionic acid) melts at 33°C while *para*tert-butylbenzoic acid is a high melting solid.

Metal organics have been known for many centuries, the carboxylates being recognized for the longest time. In ancient and medieval times many 'soaps' were used regularly. These early soaps were alkali metal carboxylates which are soluble in water, in contrast many metallic soaps of other polyvalent elements are insoluble in water. These metallic soaps are complexes which have the formula $M(O_2CR)_n$ where M is a metal in oxidation state 'n' and R is a linear organic chain containing at least six carbon atoms.

Carboxylates are interesting from a number of academic and industrial points of view. A diverse range of industrial applications utilize metal carboxylates, including many lubricants, paints, catalysts,[98,99] paint drying agents and greases.[100,101] For instance, aluminium salts of the higher fatty acids have found commercial applications in the lubrication industry and also in incendiary Napalm bombs used during the Second World War. From an academic point of view the variety of bonding modes which carboxylates may adopt has attracted great interest. As will be shown many strongly electropositive metals form ionic carboxylates, while others may have unidentate carboxylate ligands, e.g. Li(OAc).[102] A didentate chelating carboxylate may also be observed but this is rarer due to

the small 'bite' angle. Most carboxylate ligands adopt bridging modes, this leads to many compounds being polymeric. This is especially true for transition metal carboxylates.

Interesting magnetic effects between metals are observed in numerous cases because the bridging nature of many carboxylates brings the metals into close contact. For instance, magnetic exchange interactions between paramagnetic copper metals in dimeric copper acetate hydrate, suggested that there was a significant metal-metal interaction, which has also been borne out by absorption spectrometry.[103,104] Further, the addition of electronegative substituent groups, e.g. halogens, have been shown to weaken the metal-metal interaction and even, as in the case of $Cu(tfa)_2$, lead to the formation of monomers .[105]

4.2 Synthesis of metal carboxylates

Two routes are generally employed for the synthesis of metal carboxylates, the fused and precipitative methods.[100] The latter involves the reaction of a soluble salt of the metal with an alkaline solution of the carboxylic acid in water, whereas the former involves either (i) a neutralization reaction between a metal oxide / hydroxide with a fatty acid, or(II) a metathetic displacement reaction in which the carbonate or acetate, for example, is treated with an acid. The fused method, in which the reaction is undertaken in an inert non-aqueous solvent, such as benzene, often gives anhydrous products, whereas the precipitative route may yield hydrolysed products.

4.2.1 Reactions in aqueous media

Metal carboxylates may be synthesized by the reaction of aqueous or alcoholic solutions of a variety of metal salts, with stoichiometric amounts of carboxylates,[106] e.g.

$$MX_n + nRCO_2M' \dashrightarrow M(O_2CR)_n + nM'X \qquad \text{(i)}$$

(where M' = Na, K, NH_4 : X = Cl, NO_3)

Under the above conditions a metathetical reaction occurs and the insoluble metallic carboxylate is precipitated. In order to obtain high yields and good quality products the solutions for the precipitation of the metal carboxylates should be fairly dilute, the addition

of the basic carboxylate should be slow and be accompanied by vigourous stirring and finally, the pH and reaction temperature should be adjusted in order that the solution is slightly alkaline.[106]

This method is applicable to transition metal [107,108] and lanthanide [109-111] elements, however, for group (I) and(II) complexes (and also lanthanides and actinides) metal oxides, carbonates and hydroxides are generally employed.[100] Here the metal salts are dissolved in an aqueous solution of the required carboxylic acid and the resultant solution allowed to evaporate and crystallize. These compounds often result in hydrated compounds, however, they may be dehydrated by heating them at *ca.* 100°C *in vacuo*. Alternatively, crystallization of the hydrated species from dry organic solvents such as benzene may be preferred.

4.2.2 Reactions in non-aqueous media : Fusion Method

Electropositive metals react directly with the carboxylic acid to form the metallic salts,[100] these findings may be further extended to the neutralization of the oxides, hydroxides or carbonates of most metals, with a stoichiometric amount of acid, e.g. for a Group 2 metal.

$$MO + 2\,RCOOH \text{ ----------> } M(OOCR)_2 + H_2O \qquad \text{(ii)}$$

These reactions are easily performed with the byproducts (water, and water and carbon dioxide in the case of the carbonates) being easily removed. These reactions are not specific to the oxides and carbonates, in fact other salts such as the acetates, chlorides and nitrates have been used in the knowledge that the liberated acid can be volatilized out. Paul *et. al* [112] have employed this technique in the preparation of a number of lanthanide carboxylates. However, the tendency for acetic acid retention is high and this route is generally not favoured. In a similar vein cerium(III) carboxylates with linear acids of the form $Ce(OOCR)_3$ (where the number of carbon atoms in the chain is between 5 and 9) have been prepared by the reaction of cerium nitrate with the appropriate acid,[113] e.g.

$$Ce(NO_3)_3 + 3\,RCOOH \text{ --------> } Ce(OOCR)_3 + 3\,HNO_3 \qquad \text{(iii)}$$

For metal carboxylates which are strongly hydrolysed in aqueous media and for mixed carboxylates, some of the following preparative methods may be used.

4.2.3 Reactions with metal halides

The double decomposition of soluble metal halides and soluble metal carboxylates in a suitable organic solvent may yield the required metal carboxylate. However, the solvent used must be chosen so that at least one of the products is insoluble, e.g.

$$MX_n + nRCOOM' \text{ ----------> } M(OOCR)_n + nM'X(ppt) \quad \text{(iv)}$$

By this method the carboxylates of p,[114] d,[115,116] and f[117-119] block metals have been successfully synthesized. Not only may the simple metal halides (usually chlorides) be used in the above synthesis, but organometallic and carbonyl halides may also form the same products. *Tris* (carboxylato) derivatives of mono(cyclopentadienyl)titanium(IV) are normally prepared by the addition of a metal salt of a carboxylic acid in benzene,[120] e.g.

$$CpTiCl_3 + 3\ Ag(O_2CPh) \text{ ----------> } CpTi(O_2CPh)_3 + 3\ AgCl \quad \text{(v)}$$

4.2.4 Reactions with metal hydrides, alkyls and aryls

With metal hydrides it is the hydride displacement which provides the driving force for the formation of the carboxylates, while in the case of the alkyls and aryls it is a readily cleaved metal-carbon bond that is the impetus, as long as the bond is sufficiently polar. With less polar bonding, higher temperatures are needed to facilitate the reaction. Using R_4Sn (where R is a vinyl group) as a starting material, many organotin carboxylates have been synthesized.[121]

$$(CH_2{=}CH)_4Sn + nRCO_2H \text{ ---> } (CH_2{=}CH)_{4-n}Sn(O_2CR)_n + nCH_2{=}CH_2 \quad \text{(vi)}$$

Generally the cleavage of one or more vinyl groups by the acid occurs in preference to addition across the double bond. The trend is that vinyl groups are more easily cleaved than alkyl groups but less readily removed than aryl groups.[121] One of the most widely used acids used in this type of synthesis is trifluoroacetic acid, where, for example, Peruzzo *et al.*[122] synthesized $[(CH_2{=}CH)_3Sn(tfa)]$ by the reaction of SnR_4 with sodium trifluoroacetate.

4.2.5 Reactions with metal hydroxides and oxides

Anhydrous compounds may be synthesized by refluxing, for example, the tellurium(III) oxide in a solvent composed of 20% water in acetic acid and then subsequent recrystallization in diethyl ether.[123] Any water may then be removed by azeotropic distillation with benzene. This technique is a fairly general one, e.g.

$$[R_2SnO]_n + 2\,R'CO_2H \dashrightarrow R_2Sn(O_2CR')_2 + H_2O \qquad \text{(vii)}$$

Anhydrides may also be used in metal carboxylate syntheses. As(III) and Sb(III)[124] acetates and benzoates have been made by the reaction of their oxides with the respective anhydrides in dry distilled benzene. Perfluorocarboxylate anhydrides too may be used, for example in the synthesis of $VO_2(O_2CCF_3)$.[125]

4.2.6 Reactions with metal alkoxides

One of the advantages of using this method over some of the described above is that the side products of the reaction are comparatively unreactive alcohols in contrast to the water and HX byproducts formed in other reactions. The reaction of alkoxides with both acids and anhydrides, often using benzene as the reaction media, have been extensively studied for the preparation of metal carboxylates, e.g.

$$M(OR)_n + nR'COOH \dashrightarrow M(OOCR')_n + nROH \qquad \text{(viii)}$$

$$M(OR)_n + n(R'CO)_2O \dashrightarrow M(OOCR')_n + nRCOOR' \qquad \text{(ix)}$$

Mehrotra and Narain[126] investigated the reactions of numerous secondary and tertiary silicon alkoxides with some of the shorter chain anhydrides. They discovered that with the reactants in an equimolar ratio the product was always a trialkoxysilicon monocarboxylate, but with a 1 : 2 or higher ratio of anhydride, the product was a volatile monomeric dialkoxysilicon dicarboxylate, i.e.

$$Si(OR)_4 + 2\,(R'CO)_2O \dashrightarrow Si(OR)_2(OOCR')_2 + 2.R'COOH \qquad \text{(x)}$$

4.2.7 Exchange of lower metal carboxylates

The replacement of lower metal carboxylates with carboxylic acids can be achieved with higher and substituted acids. Usually the acetates of the metals are used and by performing the reaction in toluene, the resultant acetic acid may be removed azeotropically. Mixed metal carboxylates can also be synthesized by these means. Paul *et al.* have used this

technique in the preparation of some higher carboxylates of the lanthanide metals.[112,127,128]

$$M(O_2CR)_n + R'COOH \text{ --------> } M(O_2CR)_{n-x}(O_2CR')_x + xRCOOH \quad (xi)$$

Other synthetic methods include the use of metal carbonyls and thiolates, electrolysis of main group metals in a carboxylic acid solution, and also the insertion of carbon dioxide into the metal-carbon bond of compounds such as methyl-bis(triphenylphosphine)copper etherate.[129] Alkali metal formates have been synthesized by the addition of carbon monoxide to the alkali hydroxide under reduced pressure.[106]

4.3 Coordination modes of metal carboxylates

The nature of the carboxylate bonding in metal complexes can be sub-divided into four classes according to the type of M-O_2CR interaction.

4.3.1 Ionic or uncoordinated

Crystallographic authentication for this type of bonding mode is somewhat scarce, however, from solution and solid state spectra it appears that there is little cation-anion interaction in alkali metal carboxylates. The carboxylates of sodium and potassium are reported to be ionic with similar structures to that shown below for sodium formate.[130] There is resonance between the two C-O bonds making them equivalent, therefore, only one ν(C-O) band is observed for both the anti- and symmetric stretching vibrations in such compounds.[131] As will be shown later infrared analysis can be a very useful tool for the elucidation of the nature of the carboxylate bonding.

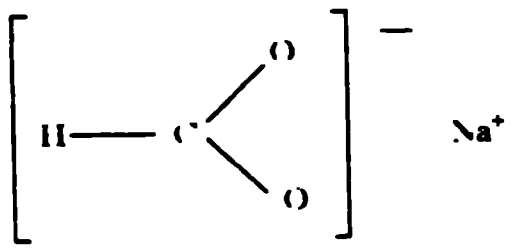

Figure 4.1 : Ionic carboxylate bonding mode in sodium formate

4.3.2 Unidentate

These species are better understood than the ionic complexes due to the larger number of crystal structures which have been reported. There remain, however, only a limited number of examples. The acetate ion in lithium acetate dihydrate functions as a unidentate ligand. Similarly a number of cobalt compounds have unidentate coordinated acetate ligands, e.g. $[Co(OAc)_2.4H_2O]$[132] and $[Co(NH_3)_5(OAc)]$.[133] The infrared spectra of these compounds reveals a large increase in the antisymmetric COO stretching and a comparable decrease in the symmetric COO stretching frequency when compared to the ionic species. These two frequencies approximate to C=O and C-O respectively, e.g. in the spectra of $As(tfa)_3$[134] the two stretches are at 1744 and 1355cm^{-1}. The solid state crystal structure of this compound reveals that the tfa ligands bond to the arsenic in a unidentate fashion, the overall structure around arsenic being a trigonal pyramid.

The best evidence, however, comes from the group 14 acetates, $R_3X(OAc)$. The decrease in the separation between the two COO^- frequencies ($\Delta\nu$) as the group is descended (C(523cm^{-1}) - Pb(312cm^{-1})) may be due to the increased polarity in the M-O bond, leading to a bonding situation which is closer to that of the free ion. Alternatively it may indicate that with increasing size of M, a weak interaction with the second oxygen atom becomes possible, and the compounds move from unidentate to unsymmetrical didentate chelating. The ($\Delta\nu$) is generally an indication of the structure, however, it is dangerous to rely solely on this as a definition of the coordination mode as a number of other factors can influence their separation.

4.3.3 Didentate chelating

Due to the small bite angle of the OOC system, this class of compounds is not well established. A four membered $M\text{-}O_2C$ ring may be formed either symmetrically, as in the uranyl[135] and zinc[136] acetates, or asymmetrically as in the tin[137] complex. The latter does not have enough space for all four acetato ligands to bond efficiently with the result that one of the acetate groups binds asymmetrically, one of the Sn-O bonds being the regular distance while the other is substantially longer. A theoretical infrared study of didentate acetates by Grigor'ev has given some useful conclusions.[138] He argued that the O-C-O angle would be smaller in didentate than in bridging acetates. This is reasonable as we can expect a decrease in the first case due to inter-ligand repulsions, but in bridging acetates an increase above 120° is likely because few pairs of metal atoms will be only 2.2Å apart, the separation of the oxygens in the acetate anion. This is confirmed by structural evidence. He found that increasing the angle should decrease $\nu_{(sym)}COO^-$ and increase $\nu_{(asym)}COO^-$

thereby increasing the separation ($\Delta\nu$), thus $\Delta\nu$ is smaller for chelating than bridging acetates.

4.3.4 Didentate bridging

By far the most common mode of carboxylate bonding is the didentate bridging mode, however, there are a number of different ways in which this bridge can form. These bonding modes are illustrated below.

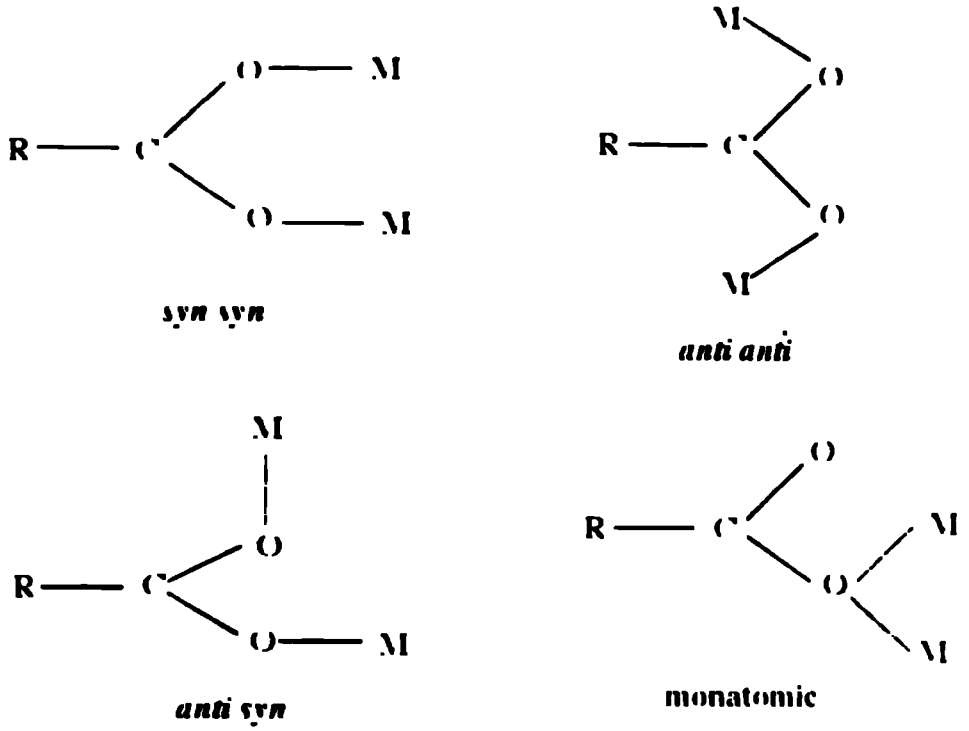

Figure 4.2 : Didentate carboxylate bridging modes

In polynuclear carboxylates both oxygens are generally involved in forming bridges. The *syn syn* geometry brings the metals close enough together to form metal - metal bonds. Both the *anti syn* and the *syn syn* arrangements may lead to polymeric structures while monatomic bridges are often found in conjunction with the other modes. For example the polymeric complex $[Cu_2(OAc)_2]$[139] has a structure in which one oxygen from each acetate group forms a monatomic bridge to another copper atom, while a *syn syn* bridging mode is also observed.

4.4 Structural aspects of metal carboxylates

Alkali metal carboxylates are predominantly ionic in nature, for instance, from infrared considerations $Li(OAc).2H_2O$ has a monodentate acetate rather than the ionic mode observed in the analogous sodium compound, the CO bond lengths in LiOAc are 1.33 and 1.22Å for C-OLi and C=O respectively.[140]

The Be carboxylates are made under anaerobic conditions because in the presence of water they form the more stable oxocarboxylates.[141,142] Be acetate is insoluble in inert solvents, but on the addition of NH_3, $Be(OAc)_2.2NH_3$ is formed. Similar reactions have been observed for primary amines.[143-145] The proposed structures consists of a six membered ring with intramolecular hydrogen bonding. Numerous aluminium carboxylates have been discussed by Mehrotra *et al.*, these materials include mixed alkoxide / carboxylates such as $[Al(OPr^i)(O_2CR)_2]_2$.[146]

Structures of $InR_2(OAc)$ (where R = methyl and ethyl) are polymeric. The metal is six coordinate and has a didentate acetate group. It is coordinated to the acetate groups of two neighbouring units. $Me_2In(OAc)$ reacts with neutral Lewis base ligands such as pyridine and dmso to give $Me_2In(OAc)L$, which are five coordinate dimers in solution. With didentate ligands such as ethylenediamine (en), monomeric six coordinate compounds are observed, however with the more crowded bipy and phen ligands, $[Me_2In(OAc)]_2L$ complexes result.[147] Similar complexes have been observed with tin, e.g. tribenzyltinacetate[148] and trimethyltintrifluoroacetate.[149]

For the trifluoroacetate group three of the possible carboxylate bonding modes have been observed by diffraction studies. The $NH_4(tfa)$ is composed of ions linked by hydrogen bonds, $(Ph_4As)_2[Co(tfa)_4]$ and $[CuOH(quin)_2(tfa)_3]_2$ contain unidentate tfa groups, the latter also containing *syn syn* bridging groups which have also been identified in $[(Cp)V(tfa)_2]_2$. As yet no compounds have been shown by diffraction studies to have symmetrically didentate trifluoroacetate groups, although they may be likely to exist for $[Th(tfa)_4]$.[150]

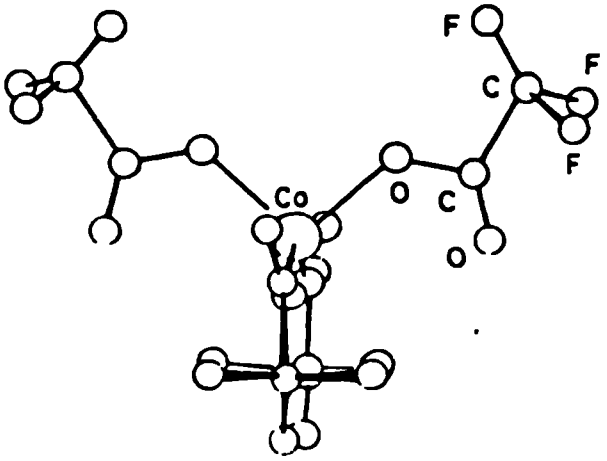

Figure 4.3 : X-ray crystal structure of the $(Ph_4As)_2[Co(tfa)_4]$ anion

The group fifteen complexes $M(O_2CCF_3)_3$ (M = P, As, Sb or Bi) have two distinct types of structures.[134] For P and As the indication from infrared analysis is that the tfa groups are unidentate with As (or P) in a three coordinate pyramidal geometry. The difference between νCOO asymmetric and νCOO symmetric is about 400cm^{-1}, while for Sb and Bi it is between 190 and 225cm^{-1}, indicating that the latter two are more likely to have bridging tfa groups.

The dimeric Ti (III) carboxylates $[CpTi(O_2CR)_2]_2$ (where R = CF_3, CH_3, C_2H_5 or phenyl) have been obtained by the reaction of the metal chloride with sodium carboxylate in thf.[151] The most likely structure of these dimers is shown below, ESR characterization also lends support to this formulation.

Similarly Cp derivatives of vanadium can be prepared, e.g. $[CpV(O_2CF_3)_2]_2$ which is a dimer with the V(III) ions bridged by four tfa groups, there are no direct metal-metal interactions as the separation is *ca.* 3.7Å.[152]

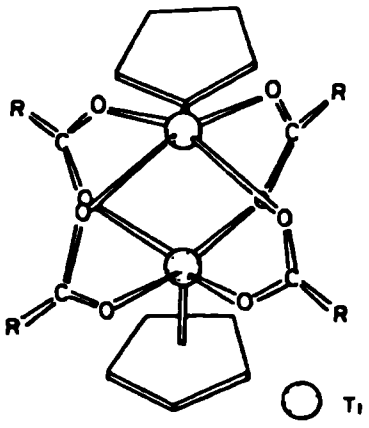

Figure 4.4 : Proposed crystal structure of $[CpTi(O_2CR)_2]_2$

Many Cr (III) (and other tervalent transition metals) form trinuclear carboxylates which have structures based on a triangular cluster $[M_3L_3O(O_2CR)_6]^+$. They contain carboxylate bridges about octahedrally coordinated metal ions which are arranged in a triangle around a central μ_3-oxo ligand (see Figure 4.5).

Examples of this include $[Fe_3(H_2O)_3O(OAc)_6]^+ClO_4^-$ [153] and $[Mn_3(py)_3O(OAc)_6]$.[154] For divalent metals the cluster may be modified such that there are no axial ligands and no central oxygen atom.[155]

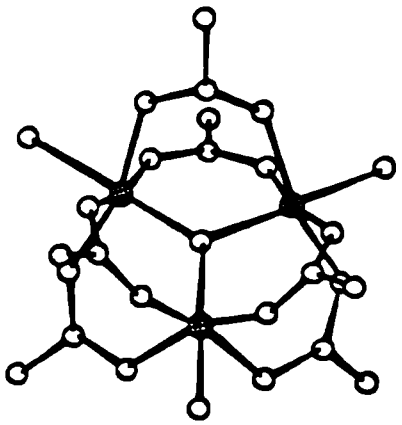

Figure 4.5 : The $[M_3L_3O(O_2CR)_6]^+$ cluster

Numerous rhenium compounds may be obtained by reacting $ReCl_3$ with, for example, isobutyric acid in the presence of O_2. The structure of this complex reveals that it is $[Re_2Cl_2(O_2CC_3H_7)_3]^+$ cation.[156] Rhenium complexes with strong metal-metal bonds can be synthesized from $Re_2X_8^{2-}$, which has a quadruple bond that remains partially intact on reaction with carboxylates, to yield $Re_2(O_2CR)_4X_2$ and $Re_2(O_2CR)_2X_4(H_2O)_2$, both of which have strong Re-Re bonds.[157]

Co (III) acetate dihydrate contains unidentate acetate groups which are strongly hydrogen bonded to a coordinated water molecule.[158] The structure of the more complex adduct $[Co_2(quinoline)(O_2CPh)_4]$, has been determined and is a centrosymmetric dimer bridged by four benzoate anions with two oxygens of each group bonded to different Co ions. Each metal has a square pyramidal geometry.[159]

Zinc is similar to beryllium in that it forms two types of carboxylate complexes, $Zn_4O(O_2CR)_6$ and $Zn(O_2CR)_2$. The dihydrated normal acetate is more stable than the Be analogue and contains chelating acetate groups which form a distorted octahedron in conjunction with the water molecules.[160]

Carboxylate compounds with the actinide metals are more rare, however, there are a number with thorium and more especially uranium (IV). The homoleptic acetate of both Th[161] and U[162] show them to be ten coordinate with two acetate ligands behaving as tridentate entities. The more soluble $Th(tfa)_4$ compounds have been shown to form adducts with oxygen donor ligands such as dmso and amides, e.g. $MeCONMe_2$ (DMA).[163] Diaquouranyl diacetate is made by warming UO_3 with acetic acid.[164] X-ray crystallography shows the product to be a seven coordinate species with a polymeric chain structure, e.g.

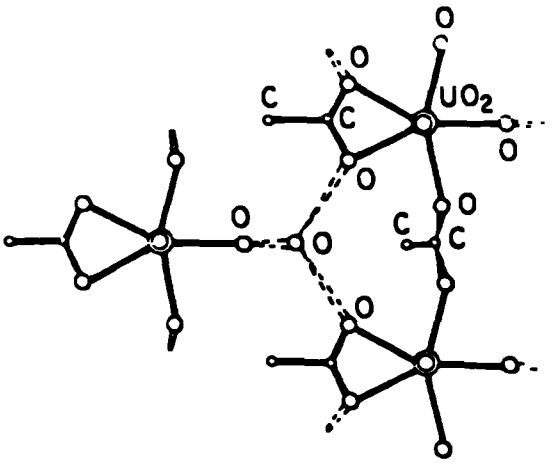

Figure 4.6 : Chain structure of diaquouranyl diacetate

4.5 Applications of lanthanide carboxylate complexes

The applications of metal carboxylates rely largely on their physical properties, stabilities, solubilities in common organic solvents and volatilities. Metal carboxylates with good thermal stabilities and labilities may be used as homogeneous catalysts for the synthesis of organic compounds. Pb, Co, Mn and Zn 2-ethylhexanoate salts are used as drying agents for lacquers and enamels, whereas the Fe, Ni and Co analogues are used as silicon stabilizers. The Cu material is used as a marine fungicide.[165] The palladium acetate complex is another example and is used to synthesize vinyl acetate from ethylene and acetic acid.[166] Industrial processes take advantage of the properties of carboxylates by applying them in the soap, paint, pharmaceutical, paper and textile industries.[106] Organotin,[167] lead[168] and silicon[169] carboxylates find applications both in industry and biology. All three are used as stabilizers for PVC resins and also as pesticides and wood preservatives.

Soaps are metallic salts (usually sodium or potassium) of carboxylates (and their derivatives) containing between eight and eighteen carbon atoms and are obtained by the saponification of fats with alkalis. The structural feature of a soap is that its salt end is water soluble and oil insoluble, while the hydrocarbon end has the opposite properties. The number and variety of synthetic detergents is vast, however the most widely used soaps are sodium salts of alkylated aromatic sulphonic acids, i.e. $ArCH_2SO_3Na$. Cerium carboxylates have been used as fuel additives for the reduction of diesel particulate emissions in motor engines (see Chapter 5 for further discussion).[170]

Ceric carboxylates may also be used as catalysts in organic syntheses. For example, the reaction between ceric acetate and styrene in the presence of glacial acetic acid gives a γ-lactone (70% yield) and an ester (<1%).[171] However, with longer chain acids such as propionic and isobutyric a smaller amount of lactone (60 and 3% respectively) is observed with a similar amount of ester (0.2-1%). In this way the carboxylates are seen to react in a similar manner to cerium ammonium nitrate (CAN), with respect to their catalytic capabilities.[172]

Although all tetrapositive lanthanides are potentially one-electron oxidizing agents, Ce(IV) salts are used almost exclusively because they are relative inexpensive and readily availabile. The oxidizing abilities of the Ce(IV) compounds are largely dependent on the reaction medium. The oxidation potential usually increases with an increasing acid

concentration, but the extent depends on the nature of the acid. For instance, a relatively high oxidation potential is observed in perchloric acid compared with nitric acid. This factor is ascribed to the higher coordination ability of nitrate to the Ce^{4+} ion.[173] Oxidative reactions include the direct alkoxylation of anthracene by treatment with $Ce(tfa)_4$ in alcohol (*ca.* 75% yield), a considerable amount of anthraquinone is formed as a major by-product, however.[174]

NMR spectroscopic characterization of carboxylates is limited by the relatively low sensitivity of the chemical shifts of the protons to changes in the environments of molecules. The application of paramagnetic lanthanide β-diketonates as lanthanide shift reagents is well documented.[175] The rare earth complexes form coordination compounds with the organic molecules that are being investigated by NMR. During this process the paramagnetic metal ion causes a change in the chemical shifts of the protons (or other nuclei) by transferring electron density from the metal to the affiliated nuclei or by magnetic effects associated with the unpaired electron. Lanthanide β-diketonates are especially useful for this as they cause insignificant line broadening. Examples of these compounds include $Eu(tmhd)_3$,[176] and also the more widely used fluorinated compounds $Ho(fod)_3$ [177] and $Ln(fhd)_3$.[178]

Laser chelates of lanthanides are compounds which, when irradiated by ultraviolet radiation, emit visible light at a wavelength characteristic of the metal ion. The rare earth chelate compounds are normally either Eu, Tb, Sm or Dy tervalent β-diketonates. However, the first case of lanthanide laser action was found in the europium complex $[Eu(bzac)_3]$ in the early 1960's where it was found to fluoresce at 6130Å.[179] Weissman made an in depth study on the fluorescence of a range of europium complexes and discovered that the radiation is absorbed by the organic ligand and is subsequently emitted as a line spectrum by the metal ion, i.e. there is an internal energy transfer between the ligand and the Eu ion.[180]

Metal alkoxides also find applications as heat resistant paints,[181] water repellents,[182] paint drying agents[183] and as ceramics.[184] The hydrolytic susceptibility of metal alkoxides makes them especially useful in producing high quality oxide films, which are used in the electronics industry.

4.6 Lanthanide carboxylate complexes

Cerium and thorium alkoxides are less volatile than those of the transition metals, indeed the methoxide and ethoxides are completely non-volatile solids. The isopropoxide and tertiary alkoxides volatilize under reduced pressure.[185] They are also less soluble than transition metal tervalent alkoxides due to their ionic nature. Without a X-ray structural determination the molecular complexity of lanthanide alkoxides is difficult to assess. The complexities of cerium n-propoxide and n-pentyloxide are 4.2-4.3 in refluxing benzene while in toluene they are 3.4. It appears that increasing the chain length of the straight chain alkoxides of Ce does not alter the degree of polymerization. However, with secondary and tertiary alkoxides the chain length does have a significant effect, $Ce(OCMeEtPr^n)_4$ for example is monomeric.[186] Mixed ligand compounds of alkoxides and β-diketonates have been synthesized with both Pr and Nd isopropoxides.[187] The reaction between the alkoxide and either dppd-H or bzpd-H results in the formation of either [M(β-diket)$_3$] or [M(β-diket)$_x$(RO)$_y$] depending on the molar ratios used.

For a given class of metal ions, the volatility of, for example, the rare earth tmhd chelates (i.e. with a common ligand) increases with a decrease in the ionic radius of the central metal ion. Also tetravalent chelates of the rare earth metals show increased volatilities and thermal stabilities over the tervalent chelates, which are generally thermally unstable. Indeed some, e.g. $Lu(hfpd)_4$ and $pyHLu(hfpd)_4$ show a very high degree of volatility and are completely volatilized without prior decomposition, a rarity for lanthanide complexes.[188]

Numerous studies exist concerning the crystal structures of rare earth β-diketonates and their coordination compounds with, for example, multidentate glymes and quinolines. $Ce(pd)_4$ is especially notable as it exists in two forms. The α- form is isomorphous with the Th and U pentanedionates in that it belongs to the space group $P2_1/_C$ and has a distorted antiprismatic arrangement with an average Ce-O bond length of 2.40Å and O-Ce-O angle of 72°.[189] The β- form is once again a distorted antiprism, but it crystallizes in the $C2/_C$ space group with an average Ce-O bond length of 2.32Å and O-Ce-O angle of *ca* 72°.[190]

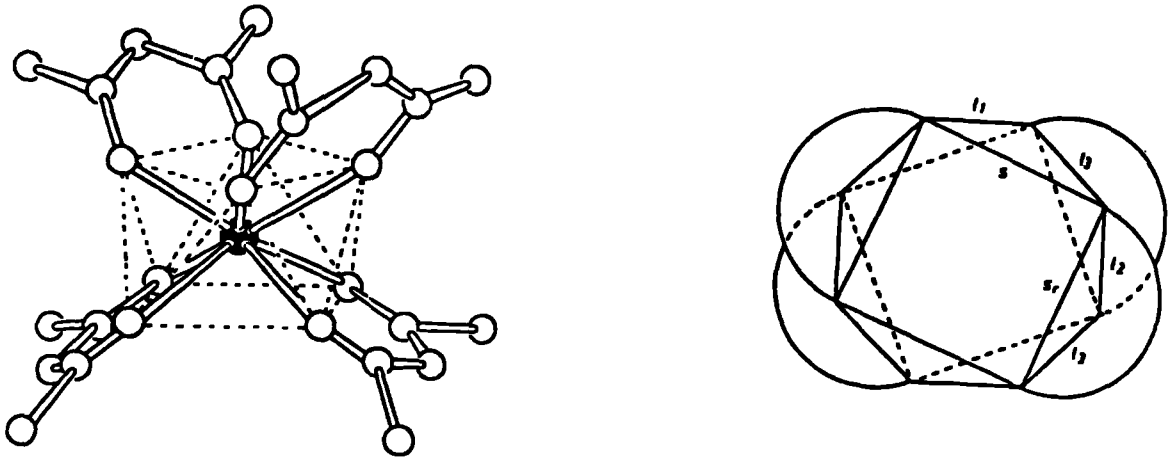

Figure 4.7 : The two structural forms of $Ce(pd)_4$, α (left) and β (right)

Work by Drake *et al.* into lanthanide β- diketonate species has yielded a number of interesting results. The reaction between $TbCl_3.6H_2O$ and Na(hfpd) in aqueous media gives a compound with three entities in the unit cell, one dimer and two monomers.[191] The dimer is $[Tb_2(hfpd)_4(\mu_2\text{-}O_2CCF_3)_2(H_2O)_4]$ and the monomer $[Tb(hfpd)_3(H_2O)_2]_2$ both of which have eight coordinate metal ions. Further, the reaction between the related $Tm(tmhd)_3.H_2O$ and triglyme gives the dimeric species [{Tm(tmhd)$_3$}(triglyme)], while with Pr a mixed dimer / monomer is formed, *viz.* [{Pr(tmhd)$_3$}(triglyme)] and [Pr(tmhd)]$_2$(triglyme) both of which have eight coordinate metal centres.[192]

The majority of research on metal carboxylate complexes of lanthanides has tended to concentrate on the smaller chain acids, e.g. formates and especially acetates. Very little has been done with respect to the larger (> C_5) acids. In neutral carboxylates of the trivalent lanthanides the coordination number of the central metal is often eight or nine because of the ligand's ability to chelate and bridge. Structures based on monomeric, centrosymmetric dimeric or chain polymeric units are known.

Rare earth formates have been prepared by the reaction of formic acid with the respective hydroxides[193] or carbonates,[194] to yield either $M(HCO_2)_3$ (M = La to Ho, except Ce and Pm)[193] or $M(HCO_2)_3.2H_2O$ with Tm, Yb and Lu.[195] Yttrium formate is based on the latter formulation and has an eight coordinate square-antiprismatic geometry, with all formate groups didentate bridging.[196] The Tb, Dy, Ho, Er and Tm complexes are

isostructural. The Yb (and higher lanthanide) formates, however, have only one didentate bridging and two didentate cyclic formate groups.[197] The reason for the different structures is that the lanthanide contraction, which causes a decrease in ionic radii across the group, is enough for the transformation from didentate bridging to didentate cyclic to occur, the latter needing less space to orientate itself about the metal. One Ce (IV) complex has been synthesized from H_2CeCl_6, formic anhydride and formic acid, to give the yellow solid complex $Ce(HCO_2)Cl_3.H_2O$. The acetate, propionate and butyrate analogues have been formed in a similar fashion.[198]

The anhydrous acetates may be made by the reaction of acetic anhydride with the hydrated lanthanide nitrate,[199] or by the dissolving the oxides in ammonium acetate.[200] Anhydrous acetates of Pr and Nd may also be produced by heating the chloride salt in acetic acid under reflux.[201] The related $[Ce(OAc)_3.H_2O]$ complex is nine coordinate, with all three acetates bridging, linking the Ce atoms in extended chains.[202] One acetate is didentate bridging while the other two are tridentate bridging cyclic. The average Ce-O bond lengths are 2.53Å. In contrast $[Er_2(OAc)_6.4H_2O]$ is a nine coordinate centrosymmetric dimer, with an average Er-O length of 2.45Å.[203] The ionic complex $[Ce_2(OAc)_8(H_2O)_2]^{2-}$ formed by the evaporation of a solution of Ce (III) and guadinium acetates, is a ten coordinate dimer, with two acetates didentate chelating and two tridentate bridging chelating.[204]

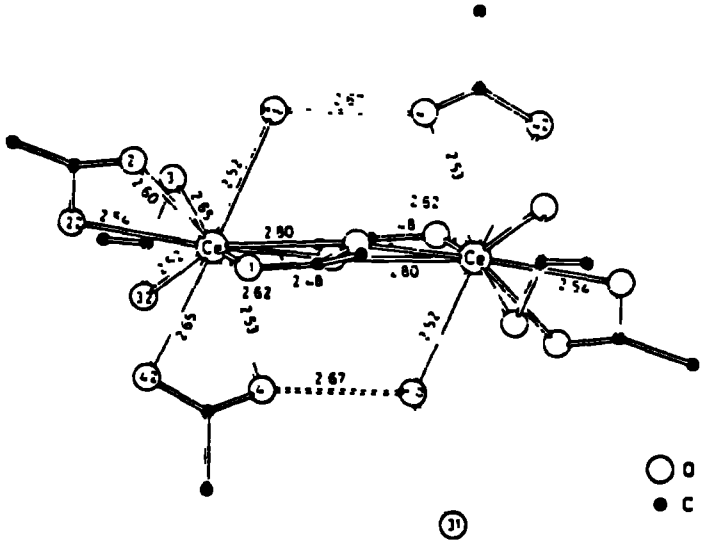

Figure 4.8 : Structure of the $[Ce_2(OAc)_8(H_2O)_2]^{2-}$ dianion

The crystal structure of the related polymeric neodymium cyanoacetato complex $[Nd(C_3H_2NO_2)_3(C_3H\text{-}NO)\text{-}(H_2O)].H_2O$ has a nine coordinate metal, bound by seven carboxylate oxygens, one dmf oxygen and one water molecule.[205] In contrast to many transition metal complexes with the cyanoacetato ligand there are no Nd-N bonds. The cyanoacetate ligands are either bridging didentate or unidentate.

$Ce(OAc)_4$ is made by dissolving Ce (III) acetate in acetic acid and acetic anhydride and oxidizing with ozone, to give a bright yellow, light sensitive solid.[206] Ce (IV) oxyacetates can be formed by thermally decomposing this material to give $[Ce_2O(OAc)_6]$ at 65°C and $[Ce_2O_2(OAc)_2]$ at 100°C.[207]

The trifluoroacetates of La to Tm may be made by dissolving the metal oxide in excess acid (often in the presence of trifluoroacetic anhydride), filtering any remaining oxide and evaporating off all excess acid.[208] Recrystallization from water gives $[M(tfa)_3.3H_2O]$. In the same way pentafluoropropionates, and heptafluorobutyrates can be formed but with differing degrees of hydration.[209] The pentafluoropropionates are noted to be isomorphous with each other. Lanthanum trifluoroacetate trihydrate has a nine coordinate metal in a tricapped trigonal prismatic geometry.[210] The metal is bound to four oxygen atoms from four bridging tfa groups, two oxygens from didentate tfa ligands, one oxygen from the didentate tfa on the neighbouring La, and two water molecules. The average La-O distance is 2.59Å.

In contrast the Pr complex is a nine coordinate dimer with four bridging and two unidentate tfa groups.[211] The average Pr-O bond length here is 2.45Å. Infrared data corroborates this, not only for lanthanum, but for other lanthanides too. In lanthanon mono- and trifluoroacetates, $\nu COO_{(asym)}$ increases from the value of the ionic ligand indicating its didentate bridging nature.

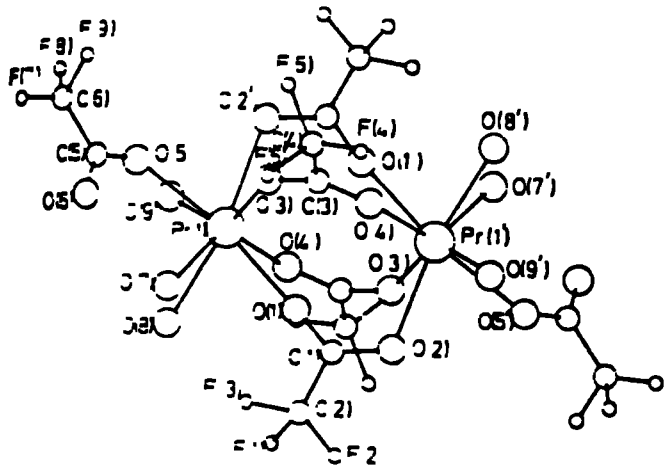

Figure 4.9 : X-ray crystal structure of $[Pr(tfa)_3.3H_2O]_2$

The thermochemistry of the tfa and pfp trihydrates of Pr, Sm and Er have been reported.[209] The TGA shows that they decompose in several stages; (i) the stepwise dehydration to the anhydrous state, (ii) decomposition of the salt to a stable intermediate, and (iii) decomposition to the final product. For $[Pr(tfa)_3.3H_2O]$ the decomposition proceeds as follows;

$$\underset{(25°C)}{[Pr(tfa)_3.3H_2O]} \text{ ----> } \underset{(110°C)}{[Pr(tfa)_3]} \text{ ----> } \underset{(250°C)}{PrF_3} \text{ ----> } \underset{(680 - 890°C)}{PrOF + Pr_6O_{11}} \quad \text{(xii)}$$

The three DSC endotherms observed correspond to the loss of the first two water molecules (105 and 120°C) and the loss of the third water molecule combined with solution effects (150°C). The volatile decomposition products of the above thermochemical reaction include CO, CO_2, COF_2, CF_3OF and $(CF_3CO)_2O$. This suggests that the decomposition of the anhydrous material goes via the anhydride, i.e.

$$2Ln(CF_3CO_2)_3 \text{ ----> } [2LnF_3 + 2(CF_3CO)_2O + 2CO_2 + 2CO] \text{ ----> } 2LnF_3 + 3CF_3COF + 3CO_2 + 3CO \quad \text{(xiii)}$$

Monofluoroacetates of the formula $[M(CH_2FCO_2)_3].xH_2O$ with M = Pr, Nd and Sm, were prepared by the reaction method reported above for the preparation of the La and Nd trifluoroacetates.[208] The dehydration was achieved either by heating the compounds to 60°C under reduced pressure or by keeping them in a vacuum desiccator over P_4O_{10}. The crystal structure of the neodymium monofluoroacetate dihydrate has been reported, the compound consisting of dimeric units.[210] The coordinating oxygens come from two bridging carboxylates (1 each), one didentate carboxylate (2 each), two triply bonded bridging cyclic ternary groups (1 and 2 each) and two water molecules. The Nd-O bonds to the carboxylate range from 2.36(1) - 2.70(3)Å.

Chlorinated carboxylates of the lanthanides are also known. Legendziewicz *et al.* have reported the crystal structures of Er and Nd trichloroacetates.[212] In the case of Nd (III), two different dimeric subunits exist in the polymeric chain. These units are bridged by oxygen atoms of water molecules and two carboxylic bridges of the Ln-O-C-O-Ln type. However, coordination numbers for Er (III) in the corresponding complex indicate a seven-nine coordinate (Er(2)) and an eight coordinate (Er(1)) metal.

Lanthanide monochloroacetates of the composition $[M(CH_2ClCO_2)_3.2H_2O]$ with La, Pr and Nd were prepared by dissolving the freshly prepared hydroxides in an excess of the acid, filtering and allowing the excess acid to evaporate off at R.T..[213] The solids obtained were air-dried and dehydrated by storage over P_4O_{10}. The trihydrates of the lighter lanthanides (La - Sm, excluding Pm) were prepared by a similar synthesis to that described above but starting with the respective carbonates.[214] Once again dehydration was by storage over P_4O_{10} or by heating at 60°C at reduced pressure. The IR spectra show that the antisymmetric and symmetric stretching wavenumbers increase with decreasing ionic radius, the difference between the two indicating a didentate structure for the ion.

Monochlorinated acetate species of the heavier lanthanides (Gd - Yb) have also been crystallographically studied. In the Yb complex $[Yb_3(ClCH_2CO_2)_9(H_2O)_4]_n$, there are three types of independent metal atoms, Yb(1) and Yb(2) are octacoordinated (square antiprism) while Yb(3) is enna coordinated (monocapped square antiprism).[215] The structures of these complexes are different to those of the lighter lanthanide complexes.[202] In the heavier complexes only one water molecule is coordinated to each metal, while all water molecules are coordinated in the lighter lanthanoid complexes. The coordination numbers in the heavier complexes are also lower (two eight and one nine coordinate as opposed to two nine and one ten coordinate).

Anhydrous propionates, butyrates, isobutyrates and isovalerates of La to Gd can be made either by dissolving the carbonates in the required acid then heating and evaporating off the remaining acid,[216] or by the acid interchange method with the acetates.[112,127,128] XPD suggests that the propionates are isomorphous with each other. The trihydrated complexes can be made using the oxides or carbonates, e.g. $[M(C_2H_5O_2)_3.xH_2O]$ (where M = Ce, Pr, Nd, Sm and Yb).[217] The Y (x = 1), Eu (x = 2) and Tm (x = 1) compounds have also been prepared using the oxide as the starting material.[218] Various coordination compounds of the propionates have been synthesized using ligands such as phenanthroline and urea. These complexes are discussed further in Chapter 6.

Finally two intriguing complexes utilizing pyridine-2,6-dicarboxylate (dipic), have only recently been synthesized.[219] Both are cation - anion complexes, the first being $Cs_3[Eu(dipic)_3].9H_2O$ and the second $[Co(sar)][Eu(dipic)_3].13H_2O$. In both cases the anion, $[Eu(dipic)_3]^{3-}$ is monomeric with the Eu enneacoordinated to the nitrogen and one of the carboxylate oxygens of each of the three dipic ligands. The ion is remarkably symmetrical in the former complex, approaching D_3 symmetry (the dihedral angles between planes being only 0.7°).

As is seen from the brief outline above there is a paucity of work relating to the cerium(IV) carboxylates and that which has been done is limited to the smaller carboxylates and the chlorinated species of the type $[Ce(RCO_2)Cl_3.H_2O]$. The aim of the research described in this Thesis was to define more clearly the synthesis, coordination chemistry and physicochemical properties of the Ce(IV) carboxylates.

Chapter five describes the synthesis and characterization of a range of novel cerium(IV) carboxylates using ligands which vary with respect to their chain length, degree of substitution and substituted group (see contents for a pictorial representation of many of the carboxylate ligands used in this Thesis). These compounds (and others which have been synthesized but not reported in this Thesis because of word limitations) form the basis to the rest of the work.

The reaction of these oxo-*bis* carboxylates with various neutral, e.g. multidentate glymes, crowns and sterically hindered amines, and potentially charged, e.g. alcohols and phenols, coordinating ligands has been investigated and the results are described in Chapters six and seven. The former Chapter relates to the hydrocarbyl carboxylate ligands, and the latter to the perfluoro carboxylate ligands, the very different chemistries of these compounds necessitating the division.

Cerium has two stable oxidation states (+3) and (+4), between which it can readily interchange. Chapter eight describes a variety of methods in which this redox reaction can be brought about. Firstly like many of the Ce(IV) alkoxides, the carboxylates are light sensitive, and photoreduce to Ce(III) species in the presence of either sunlight or monochromatic ultraviolet light. Secondly, the cyclic voltammetry of the Ce^{3+}/Ce^{4+} couple has been investigated for the oxo-*bis* carboxylates. Finally as has been discussed previously in this section, there are a number of Ce(III) carboxylates which have been prepared, oxidation of these with, for example, peracetic acid results in the formation of Ce(IV) species.

Chapter 5

OXO-BIS CERIUM(IV) CARBOXYLATES

5.1 Introduction

As was noted in the previous Chapter, the majority of the chemistry of lanthanide carboxylates has been limited to the smaller acids, e.g. formic, acetic and trifluoroacetic acids. This is especially true for cerium whose structurally characterized complexes are by no means boundless. Much of the literature has, understandably, concentrated on the chemistry of the tervalent lanthanides since they are more numerous and with cerium, significantly more stable. For example the ceric tetrahalides are much less stable than the trihalides.

Various thorium(IV) and cerium(IV) carbonates have been reported in the literature including the guadinium salt complex $[C(NH_2)_3]_6[Ce(CO_3)_5].4H_2O$ and the analogous sodium salt.[220] The cerium and thorium compounds are isomorphous, with all five carbonate groups in didentate coordination modes surrounding the ten coordinate metal in an irregular geometry.

Paul *et al.* employed an acid interchange method (i.e. the replacement of the lanthanide acetate with the corresponding longer chain and chlorinated acids) to synthesize cerous propionates, n-butyrates, iso-butyrates, iso-valerates and mono-, di- and trichloroacetates amongst others.[112, 127, 128] They discovered that, in line with the Pr(III), Sm(III), U(IV) and Th(IV) carboxylates, the cerium species were virtually insoluble in common organic solvents but were soluble in the parent acids at elevated temperatures. Thermal studies indicated that the cerium(III) compounds decompose directly to cerium(IV) dioxide without the formation of a meta-acetate and / or basic carbonate as is noted with many other lanthanides, (see Figure 5.1). The fact that the cerous compounds decompose to a ceric dioxide indicates a decomposition with concomitant oxidation of Ce(III) to Ce(IV). Further, molecular weight experiments on cerium(III) carboxylates synthesized from either the cerous nitrate or chloride salts indicate that they are monomeric in benzene.

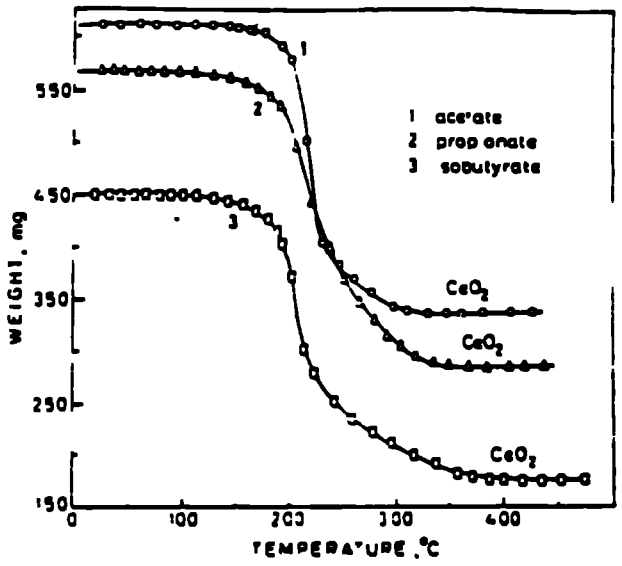

Figure 5.1 : Thermogravimetric analysis of cerium(III) carboxylates

The first reported long chain ceric carboxylates were the monocarboxylate chlorinated series [$Ce(O_2CR)Cl_3.xH_2O$] (where R = H, Me, Et, n-Pr and Ph), which were synthesized by Kapoor *et al.* in 1976.[198] Since then very few Ce(IV) carboxylate complexes have been reported in the literature. Those which have been reported include the homoleptic acetate, $Ce(OAc)_4$,[206] its thermally decomposed oxocarboxylate daughter products [$Ce_2O(OAc)_6$] and [$Ce_2O_2(OAc)_4$] and a few peroxyacetates, e.g. [$Ce_2(O_2)_3(OAc)_2$].[207] The latter peroxy complexes will be further discussed in Chapter 8. The homoleptic acetate is prepared by the reaction of Ce(III) nitrate with a mixture of glacial acetic acid and acetic anhydride to yield red crystals. Any traces of water change the colour of the complex to white, indicating a reduction to cerium(III). Another complication is that this light sensitive compound is isolated in only a 10-15% yield by this route.

In order to increase the yield, Hay and Kochi oxidized the cerium(III) acetate solution by bubbling ozone through the flask until slightly more than a quantitative amount of ozone was absorbed.[206] Due to the exothermic nature of the reaction it was noted to proceed at 70°C. As is often the case with cerium(IV) compounds, light, air and water were excluded from the reaction at all times. Further homoleptic cerium(IV) compounds may be made by exchanging the acetate for longer chain acids, as shown by Paul's example above. These compounds all have the molecular formula [$Ce(O_2CR)_4$] and have *ca.* 98% Ce(IV), unfortunately no crystal structures have been reported.[221]

In contrast, Kapoor's chlorinated species $[Ce(O_2CR)Cl_3.xH_2O]$, are synthesized by refluxing hexachloroceric acid (H_2CeCl_6), which itself requires a very involved synthesis, in the respective acid for up to 10 hours (until no further HCl was evolved).[198] The solution gradually turned from deep red to yellow. The solid carboxylates are obtained by distillation and washed in benzene and dried *in vacuo*. The chemistry of Ce(IV) carboxylates is, therefore, limited somewhat.

These materials also have a number of applications in the industrial community too. For instance cerium carboxylates can be used as fuel additives for reducing diesel particulate emissions in motor engines.[222] A recent study in France found that vehicles that run on diesel emit up to 80% more particulate matter than those with petrol engines.[223] These particles, produced by an incomplete combustion of the fuel, are less than 2.5 micrometres across and can penetrate deep into the lungs. They are linked to an increased death rate from respiratory disease and heart disease and may also carry carcinogens such as benzopyrene and other hydrocarbons.

The Hellenic Vehicle Industry together with Rhone-Poulenc Chemicals Ltd., have found a useful solution to this problem which is itself, based on a very simple idea. To burn the accumulated soot in the diesel engine one uses the excess oxygen given off in the exhaust, which, together with a fuel additive, acts as a catalytic regeneration supporter. The soot is, therefore, completely transformed into carbon dioxide. The trap continues to clean and filter gas exhaust. Part of the diesel particulate trap is shown below.

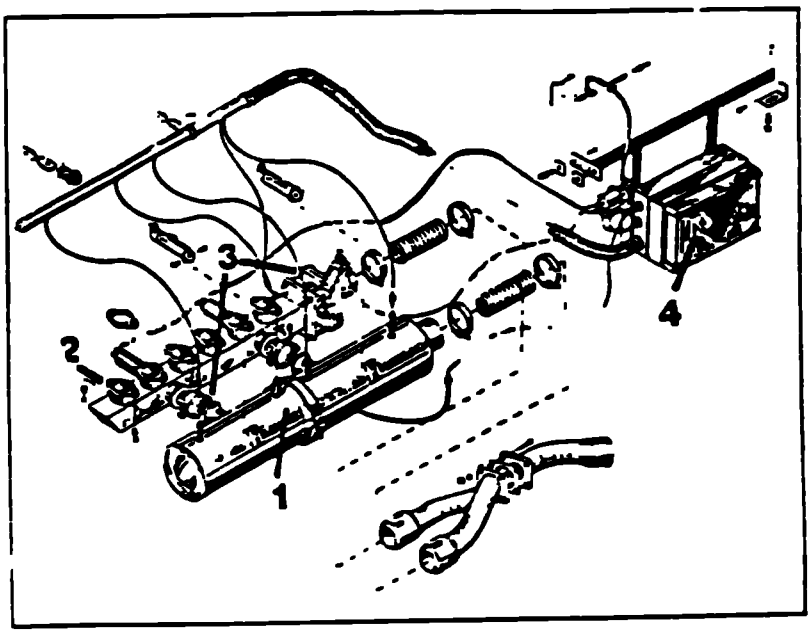

Figure 5.2 Diesel particulate trap

1. Principle ceramic filter. These are both small, efficient and easily replaced.
2. Steel exhaust collector (which collects all unoxidized particles).
3. Cooling system, which ensures regeneration and protection of ceramic filter.
4. Electronic regulating unit.

The carboxylates are hydrocarbon soluble and may, therefore, be added directly to the fuel to a concentration of about 100ppm by weight. The regenerative mechanism involves the oxidation of the carboxylate to leave a non-toxic, inert cerium dioxide by-product. Copper and manganese carboxylates have also been used, however, toxicity remains a problem for both of these materials.

Hydrocarbons, carbon monoxide and particulate matter are all reduced in diesel engines using this catalytic system, however, oxides of nitrogen are not reduced to any great extent. One possible consequence of adding a cerium compound to the diesel fuel is that cerium emissions into the atmosphere are likely to rise. The cerium emission is determined by fuel consumption, therefore, the concentration retained in the ceramic filter (*ca.*92%) is all important. The projected Ce concentration in air for the next 20 years if the addition of a cerium compound to diesel fuel were to become widespread, is estimated at 0.1-0.6$\mu g/m^3$ whereas the recognized personal acceptable level is 5.0$\mu g/m^3$.

Other patent literature relevant to cerium carboxylates includes the manufacture of high surface area cerium dioxide which can be used as a catalyst for the manufacture of methanol or in the treatment of waste gases.[224] The CeO_2 is prepared from Ce hydroxide by reacting cerium nitrate with a strong base in the presence of carboxylate ions such as 2-ethylhexanoate (eh), neodecanoate or stearate, or by reacting a cerous carboxylate with a strong base, separating and heat treating the precipitate. Also the discolouration of PTFE coatings can be prevented by the addition of either cerous nitrate or (eh), to a mixture of a fluorocarbon polymer (e.g. PTFE), pigment and a polymeric adjunct (e.g. an alkyl acrylate).[225] The important factor is that the cerium species decomposes in the range 100-500°C to an oxide containing >0.2% by weight of the metal. Silicon rubbers can be heat stabilized with the reaction product of cerous (eh) and an alkali metal siloxanolate.[226]

European patent number 0093627 refers to the synthesis of ceric carboxylates prepared by the oxidation of cerous carboxylates by H_2O_2 in a two-phase system.[227] Once again a cerous salt, such as the nitrate and neodecanoic acid may be used, this time in conjunction with ammonium hydroxide. After the addition of hydrogen peroxide the solution is heated to 70°C to decompose the Ce^{4+} / H_2O_2 complexes which are subsequently separated. A high yield (94%) of the Ce(IV) product is obtained.

5.2 Synthesis of oxo-*bis* cerium(IV) carboxylates

The synthesis of air and moisture stable Ce(IV) carboxylates has been investigated along with the physico-chemical properties and where appropriate, crystallographic characterization. It can be shown that when four molar equivalents of the required hydrocarbon carboxylic acid are added to a concentrated aqueous solution of ceric ammonium nitrate (CAN) in the presence of an appropriate base, the resultant product mixture is a yellow solid (or liquid) and an aqueous ammonium nitrate (and alkali metal nitrate if an alkali metal base is used) supernatant.

The mixture is then filtered, washed with water and extracted with benzene. On further drying and removal of all solvents, a yellow solid (or oil) results. Although this is a 'one pot' reaction there are two processes at work to form the Ce(IV) product, e.g.

$$(NH_4)_2Ce(NO_3)_6 + 4NaOH + 4RCO_2H \text{ -------> } \text{'}Ce(RCO_2)_4\text{'} + 4H_2O + 4NaNO_3 + 2NH_4NO_3 \quad \text{(i)}$$

$$\text{'}Ce(RCO_2)_4\text{'} \xrightarrow{\text{hydrolysed}} [OCe(RCO_2)_2]_n \quad \text{(ii)}$$

The product formula as written above in equation (ii) is the general formula for the shorter branched chain hydrocarbon carboxylic acids, however with some of the longer branched chain acids such as 2-ethylhexanoic acid and 2-methylvaleric acid, a liquid product results. The reason for this is that they have two further neutral organic residues associated, i.e. their formulae is more properly written as $[CeO(RCO_2)_2.2(RCO_2H)]_n$. Most of the above cerium compounds have good solubilities in a range of organic solvents.

Also it may be seen that in the case of perfluorinated carboxylic acids the general formula above does not hold. The compounds $[Ce(OH)_2(R_FCO_2)_2]_n$ are produced in slightly lower yields than for the hydrocarbon analogues. This is because the perfluorinated cerium intermediates have some solubility in the aqueous medium (in the case of trifluoroacetic acid, this solubility is appreciable), thus, rather more concentrated solutions of starting materials must be used in order to maximize yields.

These latter species are formulated as hydroxy rather than oxo compounds due to the nature of the substituents on the carboxylate ligand. During the reaction a H_2O-Ce bond is formed (see Figure 5.3). The first O-H bond is relatively weak and is therefore easily deprotonated, leaving a Ce-OH species. The second Ce-OH bond is now much stronger,

therefore, the carboxylate must be much more basic to remove the final proton. With the hydrocarbon carboxylates this is the case and the final proton is removed to leave the oxo compound. However, the fluorinated carboxylates are more acidic due to the electron withdrawing nature of the fluorine groups, and the O-H bond remains intact.

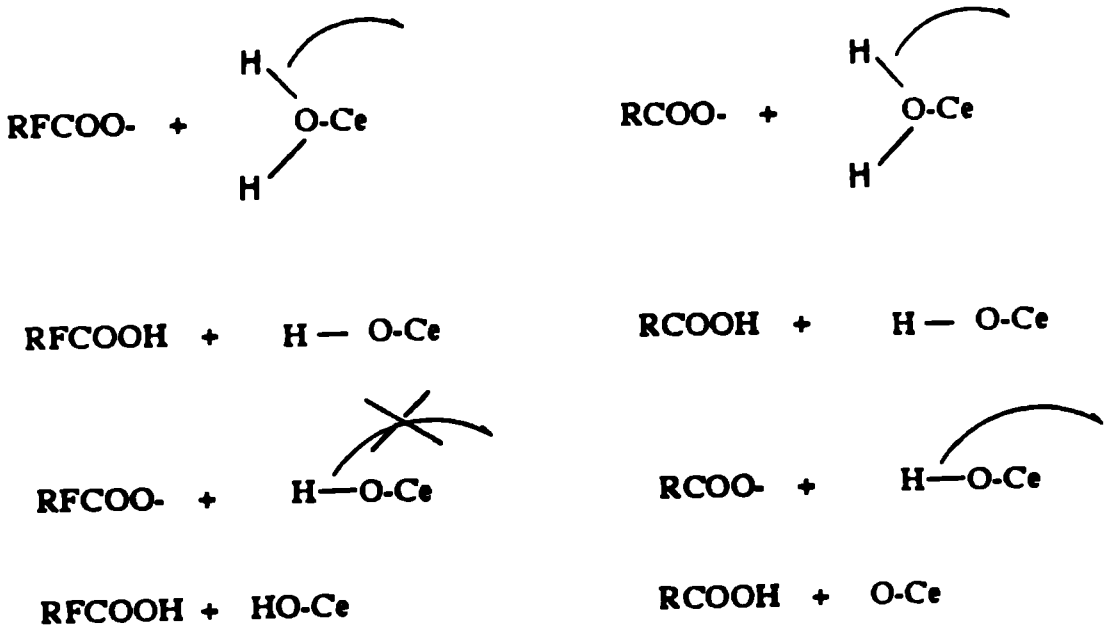

Figure 5.3 : Formation of hydroxy and oxo species

These novel organic solvent soluble (in many cases) cerium(IV) compounds are storage stable either in the pure solid / liquid form, or when dissolved in an appropriate solvent. The cerium(IV) content is generally ≥95% of the total cerium content. A huge variety of carboxylic acids may be used, differing in the number of carbon atoms, the type and size of any substituents, and the position of the substituents relative to the carboxylato group. The range of acids used within this Thesis is pictorially represented in the contents section.

The acids which may be used can have a pKa between *ca.* 0.1 and 5, and have between 2 and 12 carbon atoms, and may be straight or branched chain. Acids which are substituted on the α-, β- (or other) position, in relation to the carboxylic acid group often form cerium(IV) derivatives which have an advantageous degree of solubility, especially when there is only a single, small substituent. Aryl acids such as benzoic acid and p-tertbutylbenzoic acid may also be used, however these compounds are less soluble.

While increasing the number of carbon atoms tends to increase the solubility, it has the adverse effect of reducing the cerium weight content, and as such most of the

compounds described have medium sized acid (i.e. 4 to 8 carbon atoms). Mixtures of acids may also be used to form mixed carboxylate species.

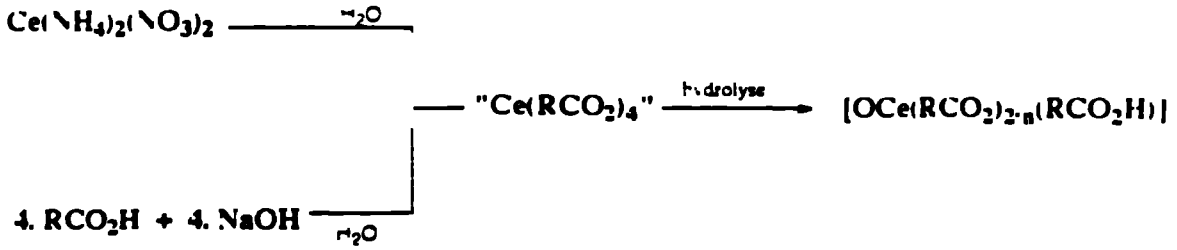

Figure 5.4 : Reaction scheme for compounds (23) to (33)

The following general reaction conditions were developed: A dilute aqueous solution of NaO_2CR was added dropwise to a concentrated aqueous solution of ceric ammonium nitrate (CAN) over a period of fifteen minutes. After 15 mins. stirring at R.T. a yellow solid (23), (24), (27) - (33), or yellow liquid (25) and (26) precipitated. The precipitate was either filtered or extracted with benzene or chloroform, washed with water, re-extracted at 40°C with benzene and dried with sodium sulphate then finally reduced to dryness.

Mixed carboxylate species may be synthesized using two equivalents of two carboxylic acids with similar pKa's, e.g. 2-ethylhexanoic and 2-ethylbutyric acids. Alternatively, a ligand with a lower pKa may be used to displace carboxylates within the structure. For instance the reaction between $[CeO(eb)_2]$ (23) and two equivalents of perfluorobutyric acid in chloroform gives a soluble yellow solution and an insoluble pale yellow precipitate. The precipitate analyses as $[Ce(OH)_2(pfb)_2]$ (31) while reducing the solution to dryness yields $[CeO(eb)_2]$ (23).

Repeated attempts to use CeO_2 and $Ce(OH)_4$ as starting compounds in similar experiments failed probably due to the former being insoluble in all common solvents. The hydroxide, however, gave pale yellow solid compounds on following the reaction procedure above. The resultant products are CeO_2 based, e.g. with pentafluoropropionic acid, cerium weight analysis of the product gives 56.8%, which corresponds to $CeO_{1.5}(pfp)_{0.5}$, and is a very insoluble solid.

The fluorinated homoleptic compound $Ce(tfa)_4$ has been synthesized using cerium(IV) hydroxide.[221] The salt is added to excess tfa-H and refluxed for a number of

hours until the solid dissolves. Any remaining acid is evaporated off in air to yield $[Ce(OH)_2(tfa)_2]$, which is reported here as complex (33) but formed from a different route. The tfa compound is then added to tfa-H and trifluoroacetic anhydride, then refluxed for two hours and stripped dry to yield a powdery yellow solid. This solid is light sensitive so the reaction must be undertaken with the exclusion of light. The reaction relies upon the acidity and the volatility of the requisite acid (and anhydride), therefore, this procedure is limited to the smaller fluorinated ligands such as pfb-H and pfp-H. Attempts to form the hydrocarbon species with isobutyric and 2-ethylhexanoic acids resulted in decomposed products as the temperatures involved in removing the 'volatiles' were too high.

Other straight chain and substituted carboxylic acids were also used to synthesize the homoleptic species, many of these were insoluble in organic and coordinating solvents making analyses difficult. The details of these compounds are not reported for reasons of economy. Carboxylic acids included 2,2-dimethylbutyric, isobutyric, pivalic, benzoic, p-tertbutylbenzoic, pentadecafluorooctanoic, propanoic, butyric, octanoic and nonanoic acids.

The compounds described within this Chapter are as follows:
(23) $[Ce_6H_2O_6(OH)_2(eb)_{12}]$, (24) $[CeO(mv)_2.2(mv\text{-}H])$, (25) $[CeO(eh)_2.2(eh\text{-}H)]$, (26) $[CeO(emb)_2]$, (27) $[Ce_6H_2O_6(OH)_2(dmp)_{12}.2(dmp\text{-}H)]$, (28) $[CeO(mb)_2]$, (29) $[CeO(iva)_2]$, (30) $[CeO(hept)_2.1.67(hept\text{-}H)]$, (31) $[Ce(OH)_2(pfb)_2)]$, (32) $[Ce(OH)_2(pfp)_2)]$ and (33) $[Ce(OH)_2(tfa)_2)]$.

Note 1: Although each of the above compounds is based on a hexameric cluster, the compounds are written as $[CeO(RCO_2)_2]$ for reasons of economy.

Note 2: eb = 2-ethylbutyrate, mv = 2-methylvalerate, eh = 2-ethylhexanoate, emb = 2-ethyl,2-methylbutyrate, dmp = 2,2-dimethylpentanoate, mb = 2-methylbutyrate, iva = isovalerate, hept = heptanoate, pfb = heptafluorobutyrate, pfp = pentafluoropropionate, tfa = trifluoroacetate.

5.3 Spectroscopic characterization

5.3.1 Infrared analysis

The most useful bands in the IR spectra for determining structure are the $\nu_{(asym)}COO$ and $\nu_{(sym)}COO$ stretching modes and their separation ($\Delta\nu$). This factor has already been discussed in Section 4.3.

When the carboxylate is unidentate a divergence of the two COO stretches, with respect to the free ion, is expected due to a decrease in the equivalence of the CO bonds. For instance $[Co(NH_3)_5(OAc)]^{2+}$ [133] has a $\Delta\nu$ of 223cm^{-1} compared with the ionic sodium acetate which has a $\Delta\nu$ of 153cm^{-1}.[228] However, a second unidentate acetate complex, $[Ni(H_2O)_4(OAc)_2]$, has a $\Delta\nu$ of only 107cm^{-1} due to intramolecular hydrogen bonding between the uncoordinated C=O and a water molecule, thereby making the two bonds more equivalent.[229]

When acting as a bridging entity, the COO stretching vibrations are not too dissimilar from the free ion, for example, the Ce(IV) complexes $Ce(O_2CR)Cl_3.xH_2O$ which all show $\nu_{(asym)}COO$ from 1625-1590cm^{-1} and $\nu_{(sym)}COO$ from 1465-1455cm^{-1}, i.e. the band positions and separations remain essentially constant, suggesting symmetrically bridging carboxylates.[198] However, crystallography has shown that the same kind of bridging groups can have separations between 80 and 200cm^{-1}, therefore, it is hazardous to use this separation alone to propose structures. As has already been indicated, Grigor'ev's studies on didentate acetates predict that due to the differences in O-C-O angles of the didentate and bridging species the $\Delta\nu$ is less in the didentate than it is in the bridging, this too can only be taken as a rough guideline.[138]

As well as the COO stretching vibrations the M-O bands can also reveal valuable information. Unfortunately, these lie in the *ca.* 400-150cm^{-1} range and thus have to be measured, in part, by either Raman or far IR techniques. A Raman study of a series of rare earth formates and acetates shows a clear increasing shift in the low frequency absorptions indicating that the M-O bond strength increases from Ce to Gd, indicating that the bonds have a higher covalent character.[230] Raman studies have been performed on a number of compounds in order to assign the MO vibrations.

Table 5.1 shows selected infrared data for the complexes described in this Chapter. The IR spectra of the oxo-*bis* ceric carboxylates have been assigned according to Ferraro

Table 5.1 : Selected Infrared Data (cm^{-1}) for Complexes (23) - (33) :

Compound	νOH	νCH[a]	$\nu COO_{(asym)}$	$\nu COO_{(sym)}$	πCH	δOCO	Δν
(23)	3627	2963, 2931	1547	1416	651	564	131
(24)	3636	2961, 2934	1563	1417	627	577	146
(25)	3635	2960, 2934	1559	1415	635	574	144
(26)	3624	2970	1531	1407	656, 612	569	124
(27)	3624	2963, 2934, 2873	1538	1412	654	577	126
(28)	3632	2967, 2935, 2876	1561	1414	655	568	147
(29)	3639, 3612	2957, 2928	1565[a]	1431[a]	643	564	132
(30)	3641	2933, 2858	1515	1413[a]	647	563	102
(31)	3688, 3627	----	1670	1441	----	587, 573	----
(32)	3667, 3621, 3606	----	1673, 1615	1442[a]	----	585, 559	173
(33)	3702, 3655, 3626, 3613	- --	1675, 1600	1472[a]	----	618, 545	128

Spectra recorded at R.T.as Nujol mulls, except (24) and (25) which are neat liquids, and [a] which are hexachlorobutadiene mulls.

and Becker's studies on deuterated carboxylates in 1970 and reveal a number of interesting points.[231] (N.B. This is only one of a number of studies concerning the infrared spectra of metal carboxylates, not all of which are in complete agreement).[232-4]

Firstly all the hydrocarbyl carboxylates show both the $\nu_{(asym)}COO$ and $\nu_{(sym)}COO$ stretches between 1563-1531 and 1431-1407cm^{-1} respectively. The separations between the two values ($\Delta\nu$) ranges from 147 (28) to 102cm^{-1} (30). All these values are in the correct region for the expected bridging or chelating modes of carboxylate ligands. Significant too is that the νCOO values are at higher frequencies for the fluorinated complexes (31) - (33); this shift to higher frequency is also noted in the free acids and is due to the electron withdrawing nature of the fluorine atoms thus making the C-O bonds stronger. There is also noted to be two peaks for the $\nu COO_{(asym)}$ vibration in the spectra of (32) and (33) separated by 60 - 70cm^{-1}. These are at *ca.* 1675 and 1610cm^{-1} while the corresponding symmetric stretch is at *ca.* 1440 for (31) and (32) and 1472cm^{-1} for (33). The $\Delta\nu$ values for the fluorinated species are slightly larger than the hydrocarbyl species (128 - 173cm^{-1}); however, the bonding modes are likely to be similar.

A second feature is the presence of a νC=O stretching vibration at 1710$\pm$25cm^{-1} corresponding to that of a free carboxylic acid. This feature, however, is not observed in the spectra of the fluorinated compounds (31) - (33). This stretching vibration would be expected in compounds (24), (25) and (27) which have either uncoordinated or unidentate acids. For the other compounds which do not have either free or unidentate ligands, such a band would not normally be expected. This vibration may be due to the fact that four equivalents of carboxylic acid are used in the synthesis, yet only two are coordinated. The peak may, therefore, be a result of having some residual free acid in association with the solid compounds.

All the compounds have a distinct arrangement of peaks in the 660-530cm^{-1} range, containing at least three and in many cases four or five separate bands (see Figure 5.5). These bands have been assigned according to Ferraro and Becker[231] as corresponding to the πCH (655-612cm^{-1}) and δOCO (618-545cm^{-1}) vibrations of the carboxylate ligands. The fluorinated species do not show the same shape for this set of vibrations because they do not posses the πCH vibrations although they do have the δOCO vibrations.

A very sharp OH peak is observed at *ca.* 3630cm^{-1} in all spectra. Indeed in the

fluorinated species 2-4 bands are observed in this immediate region although they are considerably weaker than the peaks in the hydrocarbyl species. This may be due to a number of factors such as the OH stretch of an uncoordinated carboxylic acid (i.e. in conjunction with the band at *ca.* 1710cm^{-1}), a coordinated water molecule or a coordinated Ce-OH. In order to determine the exact nature of this band deuterated studies were performed.

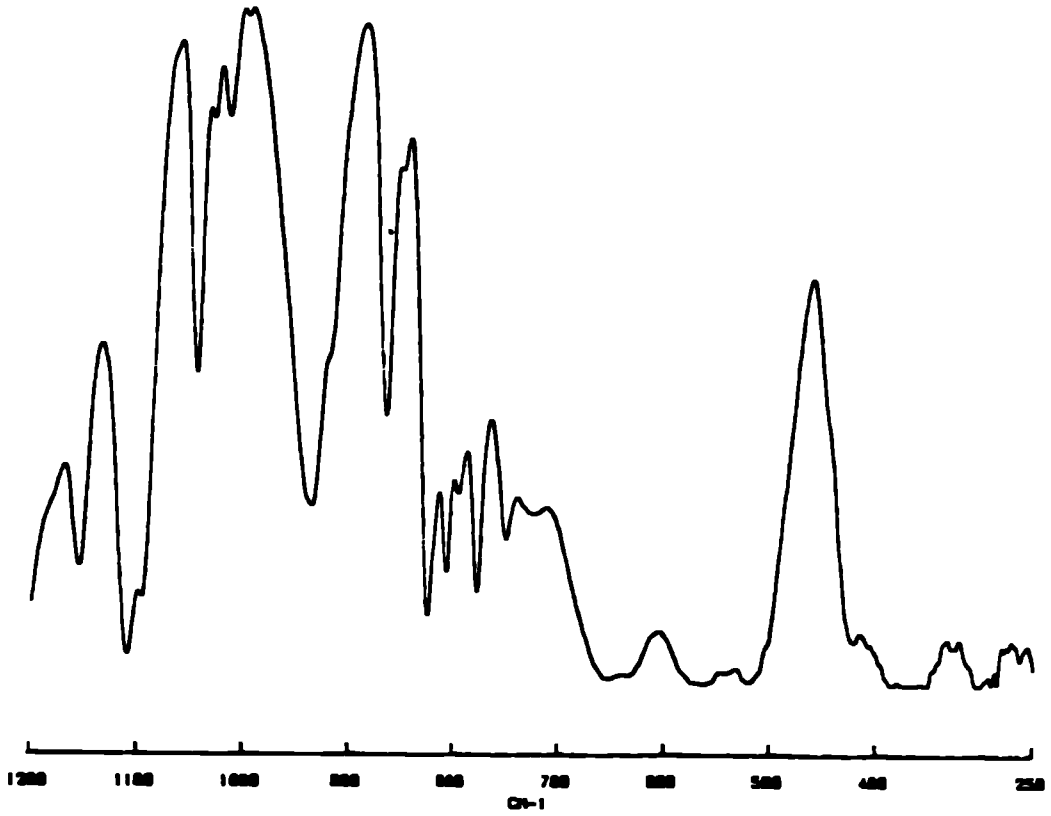

Figure 5.5 : Infrared spectrum of (23) (1200 - 250cm^{-1} KBr disc)

The deuterated compound (34), was synthesized according to the procedure described in section 5.7. The IR spectra shows a number of features in the 4000-2000cm^{-1} range. There are two peaks associated with the normal OH resonances at 3636 and 3153cm^{-1} which are sharp and broad respectively. Their deuterated analogues appear at 2681 and 2264cm^{-1} as a sharp and broader peak again. The sharp peaks are most likely to be due to the stretching vibrations of the OH and OD groups of the free carboxylic acid. In contrast the broader peaks are probably due to residual water and deuterated water retained by the aqueous route into these compounds.

Vratny *et al.* discovered that bands at 1040±15cm^{-1} and 930±20cm^{-1} were observed in metal acetates, this was attributed to the metal-acetate bonding.[235] The lower frequency band is observed in the ceric carboxylate complexes in a narrow range between 947 and 913cm^{-1}, however, the upper frequency has a much larger range (1091-1012cm^{-1}) and is not observed in (25). The latter may be due to the free acids masking this vibration. This latter effect is not surprising at it is observed that the spectra of the neat samples (24) and (25) give significantly broader peaks than those of either the Nujol or hexachlorobutadiene mulls. Also a weak peak at *ca.* 893cm^{-1} is noted in most spectra, this peak corresponds to a νC-C stretching vibration.

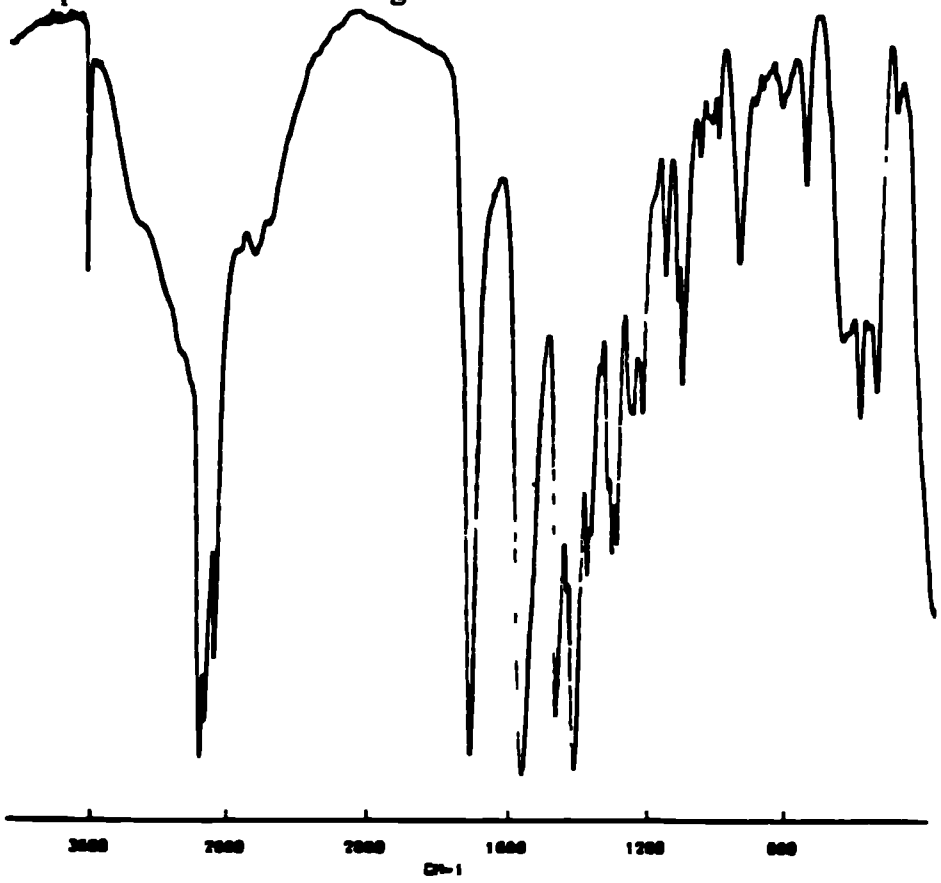

Figure 5.6 : Infrared spectrum of (24) in Nujol

One feature of the higher frequency CO stretching vibration is that the frequency increases very markedly with the electron withdrawing effect of the substituent group. The sequence is: tfa > pfp > pfb > iva = mv > mb > eh > eb > dmp > emb > hept, i.e. the most electron withdrawing group, CF_3 has the highest frequency vibration, whereas the more electron donating straight chain and α,α-disubstituted groups have lower frequency stretching vibrations. This sequence is very similar to that observed in the corresponding acids. In contrast the symmetric COO stretch is expected to decrease with increasing mass.

this is not observed. Spinner's results also corroborate this observation as the groups involving first row elements, i.e. C and F, are seen to vary irregularly.

An aspect of the fluorinated compounds (31) - (33) is the $\nu_{(asym)}$CF stretching vibrations at 1215±10cm^{-1} and 1170±5cm^{-1}, all of these bands are noted within a small frequency range. The absence of a third CF band in this region supports the chelating or bridging mode of coordination because in a monodentate ligand all three CF vibrations would be present. A further $\nu_{(sym)}$CF stretching vibration is also noted between 817-849cm^{-1} for the three species. This is in accord with the data reported by Spinner for Na(tfa) which shows three vibrations for the CF stretching modes at 1213, 1140 and 850cm^{-1}.[232] Also a broad OH peak is noted at *ca.* 3370cm^{-1} which probably corresponds to the νOH stretch of the OH coordinated to the metal centre for each of the fluorinated species.

The Raman spectra of compounds (23) and (33) have also been measured in the low frequency range in order to try and determine the Ce-O vibration modes. Previous researchers[231] have suggested that peaks in the region of 350 - 100cm^{-1} account for the MO vibrations of lanthanide carboxylates, with the higher frequency peaks being the MO stretching and the lower the OMO in plane bending vibrations. In this vein, compound (23) has peaks at 410 and 355cm^{-1}, both of which are likely to be νCeO resonances and also three well defined peaks at 220, 179 and 166cm^{-1} corresponding to δ OCeO vibrations. The tfa compound (33) shows only one low frequency peak at 167cm^{-1} (δ OCeO) but three at higher frequency at 357, 317 and 289cm^{-1} (νCeO). The large number of peaks corroborates the δOCO peak separations, once again suggesting that the carboxylate ligands are bridging units.

5.3.2 ^{1}H NMR spectroscopy

Cerium(IV) is diamagnetic ($Kr4d^{10}5s^{2}5p^{6}4f^{0}$) and as such is expected to give sharp lines in both proton and carbon NMR spectra. In complexes which are rigorously recrystallized, then the Ce(III) content is minimal and sharp NMR spectra are obtained. However, if spectra are recorded on samples prior to complete purification, then some broadening is observed due to traces of Ce(III) (paramagnetic; $Kr4d^{10}5s^{2}5p^{6}4f^{1}$).[236]

Each of the hydrocarbyl ligands (complexes (23) - (30) and (34)) have at least one terminal methyl group, this is observed, with only one exception (compound (29)), as a triplet, due to the splitting of the adjacent methylene group. The chemical shifts range between δ 0.83 (23) and (26) and 1.08 (25). Compound (29) shows only a broad singlet at δ 0.91 for both terminal methyls.

The peaks of the CH_2 groups are rather more diverse in nature. For example, compound (23) exhibits two multiplets at δ 1.42 and 1.51, while for essentially the same protons (25) shows only a single multiplet at δ 1.46. Multiplets are seen throughout, except, once again, for (29), which does not have a methylene group adjacent to a methyl group, only a CH, and as such is a doublet at δ 1.99. The CH_2 peaks have a much larger range than the terminal CH_3 groups, between δ 1.15 for (30) and 2.28 for (30). The latter being further downfield due to its close proximity to the CO_2 group. It is noticeable too that the α- branched methyl groups of (26) and (27) are further downfield than the terminal methyls.

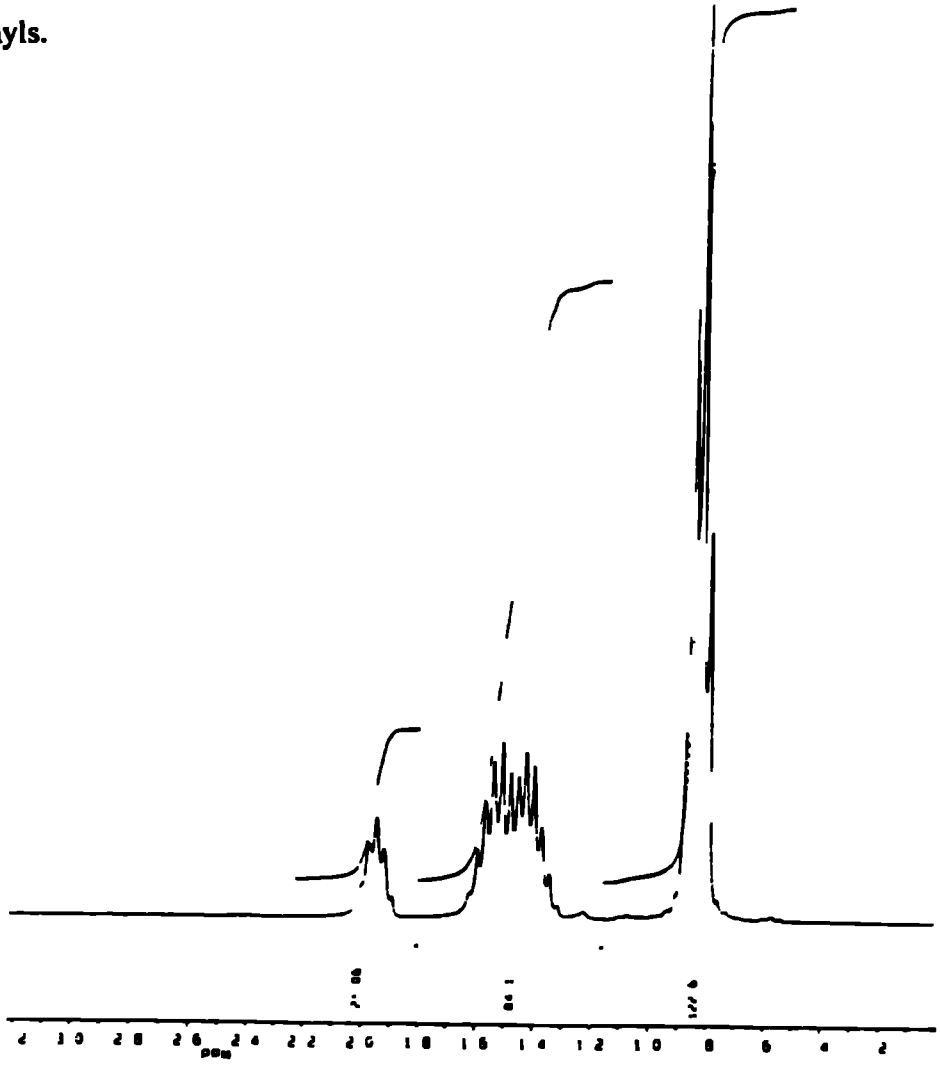

Figure 5.7 : ^1H NMR spectrum of (23) in $CDCl_3$

The CH proton is a complex, ill-defined multiplet in all cases except (23) where a clear quintet is discernable at δ 1.95. The observed splitting is because it is adjacent to two, essentially equivalent, methylene groups. It is difficult to determine whether coordination has taken place by looking simply at the respective chemical shifts of the free ligands and carboxylates, but in general the chemical shifts of methyl resonances increase, methylene decrease and methine decrease on coordination.

Compound (24) has an unusual spectrum in that it has two peaks for the CH_2 groups at δ 1.58 and 1.91, but in a 3 : 1 ratio. This suggests that the two CH_2 protons nearest to the CH group are inequivalent. A similar phenomenon is observed for (28) whose carboxylate is based on the same structure. This may be due to one of the CH_2 protons being shielded by the α-substituted methyl group thereby making them less equivalent.

The fluorinated carboxylates (31) - (33), show only one resonance, that of the hydroxy Ce-OH proton. This is a very broad peak between δ 3.42 (31) and 4.90 (33). An OH resonance is also observed for the liquid complexes (24) and (25). This is due to the uncoordinated carboxylic acids, and are thus weaker, broader and considerably further downfield at δ 11.50 (25) and 12.39 (24). These OH resonances are not observed for any of the other homoleptic carboxylates.

5.3.3 ^{13}C NMR spectroscopy

The important ^{13}C NMR data for complexes (23) - (30) are shown in Table 5.2 overleaf. The CO resonances are within a fairly small range, δ 180.9 (29) to 185.2 (27). However, two compounds have resonances noticeably further downfield, i.e. (26) and (27). This is because the carboxylate ligand of the latter two are both α,α- disubstituted and, therefore, much less acidic than the alternative α or β- monobranched and straight chain acids. This can be shown in a table of relative pKa's (see Table 5.4). In general, the higher the acidity (i.e. lower numbers) the more upfield the CO resonance.

The consistency of the CH resonance is much less apparent with a very broad range between δ 40.1 (24) and 50.1 (23). There is no apparent correlation other than that the two methyl substituted compounds (24) and (28) appear to have lower chemical shifts. The methylene groups all give the expected number of resonances for (23) - (30). A good example is the heptanoate compound (30), which shows five groups between δ 23.7 and

Table 5.2 : Selected ^{13}C NMR Data for Complexes (23) - (30) :

Compound	CH_3	CH_2	$\underline{C}CH_3$	CH	CO
(23)[a]	12.2	24.6	----	50.1	182.5
(24)[b]	13.6, 16.6	20.3, 35.7	----	40.1	183.1
(25)[b]	11.9, 13.6	22.5, 24.7, 29.6, 31.1	----	47.9	182.6
(26)[b]	9.11, 20.2	31.6	46.9	---	185.1
(27)[b]	15.1, 18.7	25.6	43.5	---	185.2
(28)[b]	11.9, 13.6	27.0	----	42.4	183.3
(29)[c]	23.9	26.8	----	46.6	180.9, 181.2
(30)[c]	15.1	23.7, 26.1, 30.3, 32.6, 36.4	----	----	181.4

[a] Spectra run at R.T., 67.94 MHz in $CDCl_3$, [b] Spectra run at R.T., 22.65 MHz in C_6D_6, [c] Spectra run at R.T., 22.65 MHz in $CDCl_3$

36.4 which detail the CH_2 groups as they become increasingly nearer to the COO group.

There are two types of methyl group, terminal and α-substituted (the latter includes the ethyl substituted compound (25)). The terminal resonances are noted to be upfield between δ 9.11 and 15.1, with the α-substituted further downfield, between δ 13.6 and 20.2. Only (29) does not follow this trend as its single methyl resonance appears at δ 23.9. Again as with ^1H NMR it is nearly impossible to tell whether coordination has occurred from ^{13}C NMR analysis, even the CO resonance in the free ligand and carboxylate complexes are similar, e.g. 2-ethylbutyric acid (CO = 183.7ppm) and cerium 2-ethylbutyrate (CO = 182.5ppm).

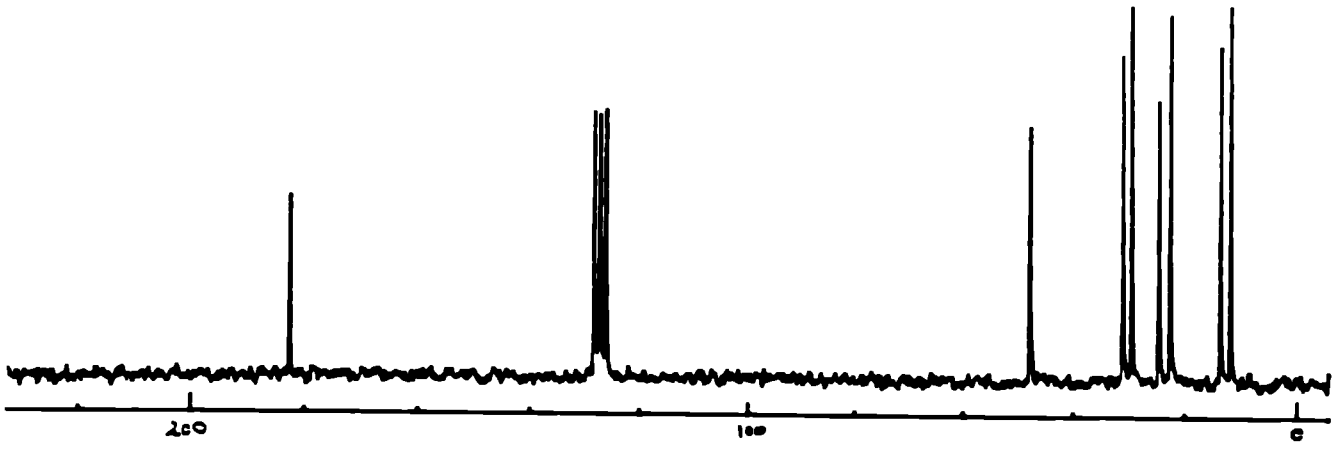

Figure 5.8 : ^{13}C NMR spectrum of (25) in C_6D_6

Compound (27) shows two different sets of peaks for its ^{13}C spectra corresponding to the unidentate and coordinated carboxyl groups, the resonances for the unidentate acid ligands being significantly smaller. The terminal methyl resonance of the free ligand is seen further upfield at δ 9.80 (coordinated = δ 15.1), whereas the α-substituted methyls and other CH_x resonances are seen further downfield for the free acid by δ 3-6ppm. The carbonyl resonance is noted to be equivalent for both. Solid state NMR of this complex also shows the two different environments for the dmp ligands with very similar chemical shifts to those in the solution spectra. Once again the carbonyl resonances are similar.

Table 5.3 : ^{13}C NMR Data for Complexes (31) - (33) :

Compound	$\underline{C}F_2CF_2CF_3$	$\underline{C}F_2CF_3$	CF_3	CO
(31)	108.3 (^1J – 266, ^2J = 38Hz)	108.9 (^1J = 268, ^2J = 37Hz)	117.9 (^1J = 287, ^2J = 34Hz)	158.9
(32)	-	107.2 (^1J = 264, ^2J = 37Hz)	118.7 (^1J = 286, ^2J = 35Hz)	159.1
(33)		- -	117.1 (^1J = 293 Hz)	159.1

Allspectra run at R.T., 22.65 MHz in D_6dmso.

Table 5.4 : pKa Values for Selected Carboxylic Acids :

Carboxylic acid	pKa	Carboxylic acid	pKa
perfluorobutyric	0.17	hexanoic	4.84
benzoic	4.20	octanoic	4.89
2 ethylbutyric	4.71	2,2 dimethylpentanoic	4.97
2 methylbutyric	4.76	2,2 dimethylbutyric	5.03

The principle ^{13}C NMR data for complexes (31) - (33) are summarized in Table 5.3. As usual the fluorine atoms cause a splitting of the carbon resonances to give, in some cases, very complex spectra. The CO resonances are all very similar, δ 158.9 - 159.1. Contrasting these values with the previous hydrocarbyl ligands, we note that the increased acidity is apparent (see Table 5.4). For (31) and (32) a broad singlet is noted for the CO resonance, however, a pronounced 1:3:3:1 quartet is observed for the CO resonance of (33) at δ 159.1 with a ^2J coupling constant of 35Hz. The CF_3 group of (33) is a simple quartet at δ 117.1 (^1J = 293Hz), but with the longer acids the splitting is more complex, both showing a quartet of triplets with similar coupling constants for the CF_3 group.

The CF_2 group for the pentafluoropropionate complex (32) is a triplet of quartets at δ 107.2, split by a ^1J coupling constant of 264Hz, and a ^2J of 37Hz. This region is much more complex for the perfluorobutyrate complex (31) where the $\underline{C}F_2CF_2$ and $\underline{C}F_2CF_2CF_3$ peaks are partially superimposed, see Figure 5.9. The combined complex splitting pattern can be best described as a triplet of multiplets and a triplet respectively. It is noteworthy, too, that the coupling constants for the CF_3 groups are notably larger than for the CF_2 groups. For example the ^1J couple of 264Hz for the CF_2 group of (32) is fairly typical while the ^1J couple of 293Hz for the CF_3 group of compound (33) is more usual.

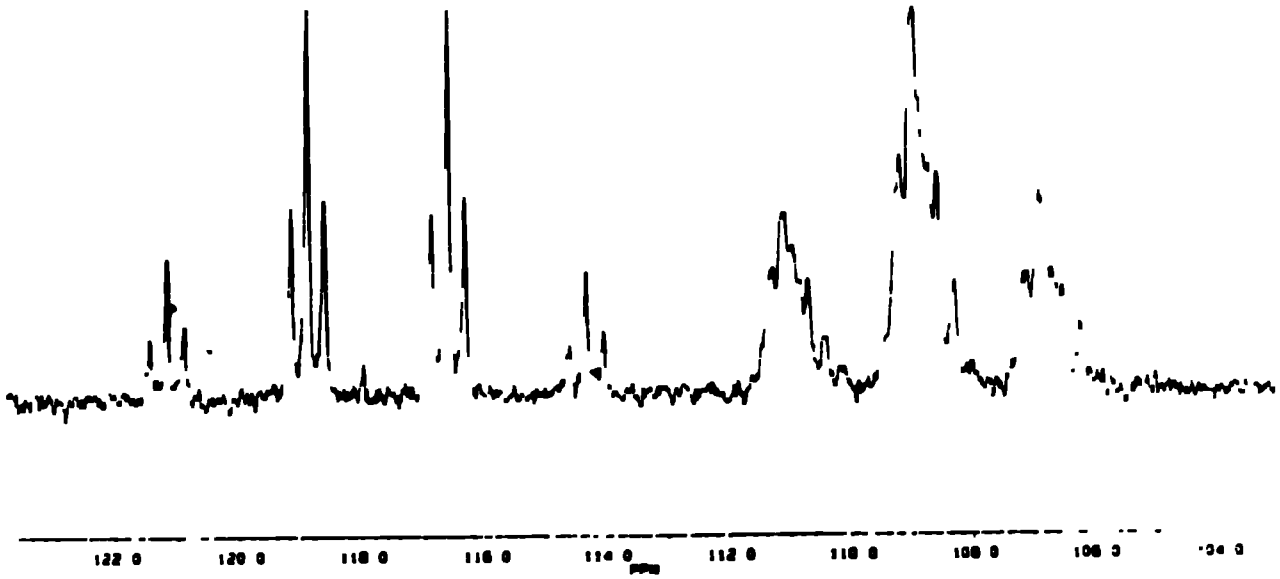

Figure 5.9 : ^{13}C NMR CF_x region of (31)

5.3.4 Mass spectrometry

Mass spectrometry can be very misleading when it comes to trying to characterize polynuclear carboxylates. 'Parent ions' appear in the spectrum indicating clusters that are smaller, larger and only very rarely, the true size. Transition metal carboxylates, in particular zinc, have been widely studied. For example Mead *et al.* found that a compound formed with a mixture of 2-ethylhexanoic and pivalic acids gave a range of intense peaks corresponding to $[(RCO_2)_{5-n}(R'CO_2)_nZn_4O]^+$, where n had all values from 5 to 0.[237] Furthermore Charalambous *et al.* performed an in depth study on numerous transition metal carboxylates and showed a sequential loss of fragments from the initial tetrameric vapour phase clusters.[238] The poor volatility of the metal carboxylates rarely give much useful information. However, fluorinated ligands, especially trifluoroacetate, appear to be more volatile and suitable for mass spectral studies, giving a wide range of ions.

The cerium carboxylates (23) - (34) show a wide range of ions, however, one particular type of ion is omnipresent. These are the Ce_xO_y ions, where x can take any value between 1 and 6 and y can take any value between 1 and 12. For example, compound (23) has five such ions, namely m/z 967 $[Ce_6O_8]$, 656 $[Ce_4O_6]$, 641 $[Ce_4O_5]$, 483 $[Ce_3O_4]$ and 329 $[Ce_2O_3]$. It is often the case too that the smaller of these ions are the most abundant, e.g. the ion at m/z 483 has a 34% abundance, almost twice the next most abundant ion. The liquid compounds (24) and (25) too show these ions but not to such a large degree, e.g. (25) shows only the ions at m/z 967 and 484. Both the α,α-disubstituted compounds (26) and (27) and the straight chain compound (30), show similar fragments. One noteworthy fact about these ions is that they are almost exclusively Ce (III) species. For instance (23) the ion at m/z 483 corresponds to a mono positive ion $[Ce_3O_4]^+$, while that at m/z 641 corresponds to a dipositive ion $[Ce_4O_5]^{++}$.

For many of the above compounds we are able to see a sequential loss of carboxylate ligands. This is often accompanied by the addition of an oxygen atom. For example, compound (26) shows a very interesting fragmentation pattern, *viz.*, m/z 1469 $[Ce_3(emb)_8O]$, 1337 $[Ce_3(emb)_7O]$, 1209 $[Ce_3(emb)_6O]$, 1096 $[Ce_3(emb)_5O]$, 1053 $[Ce_2(emb)_6]$, 925 $[Ce_2(emb)_5]$, 683 $[Ce_2(emb)_3O]$, 529 $[Ce(emb)_3]$, 397 $[Ce(emb)_2]$ and 286 [Ce(emb)O]. In the first instance we note the loss of carboxylate fragments from eight to five. At this point one of the metals is lost and a carboxylate is reclaimed to give the ion at m/z 1053. This ion then goes on to fragment in much the same way. Again at m/z 529 a further metal is lost and the procedure carries on as before. In this case the number of

oxygen atoms does not vary much, it is either one or none, however, in other cases, such as (29) it can vary from 0 to 5. A similar sequential loss is observed for compound (25) whose highest discernable peak is at m/z 1140 for $[Ce_2(eh)_6]$. A similar peak is seen for (23) and its deuterated analogue (34) whose pattern of degradation is almost identical, indicating that these species are very similar.

Another commonly observed group of ions are the $[(CeO)_x(O_2CR)_y]$ ions. This set of fragments is easy to envisage if we consider that the carboxylate ligands are bridging entities and are, therefore, capable of linking up numerous metal centres together with their coordinating ligands. This group of ions does not necessitate the breaking up of the hexameric structure, however, this may very well be the case. The extent to which these fragments aggregate can often be quite large, indicating a significant stability within the Ce-O structure in particular. Some examples of these ions are m/z 726 $[(CeO)_3(emb)_2]$, 571 $[(CeO)_2(emb)_2]$, 441 $[(CeO)_2(emb)]$ and 286 [Ce(emb)O].

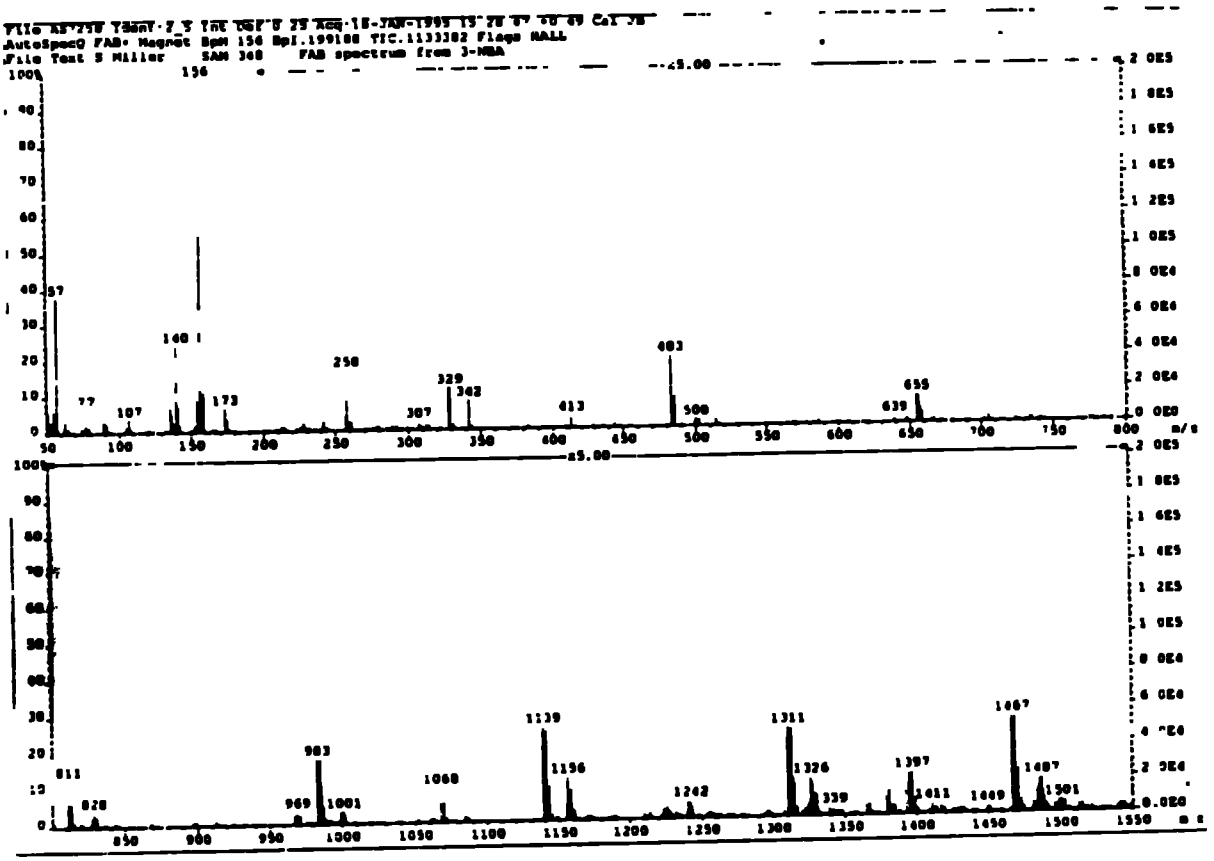

Figure 5.10 : FAB+ Mass spectrum of (28)

In contrast to that of the transition metal carboxylates[237,238] it is rare to be able to distinguish the breakdown of individual organic ligands, however, (27) is an exception to this rule. The fragments at m/z 1225 $[Ce_7O_{10}(O_2C_2(CH_3)_2)]$, 1096

$[Ce_6O_9(O_2C_2(CH_3)_2CH_2CH_3)]$ and 354 $[Ce(dmp)(O_2C_2(CH_3)_2)](2\%)$ are observed. This suggests that the 2,2-dimethylpentanoate ligand can fragment to lose either the terminal methyl or n-propyl groups. Secondly, another rarity is the observation of more than one or two $[Ce(RCO_2)_n]$ ions. Compound (30) shows a very diverse range of ions including $[OCe(hept)]$, $[Ce(hept)_2]$ and $[Ce(hept)_3]$ at m/z 286, 398 and 525 respectively. $[Ce(hept)_4]$ would be expected to be at m/z 656, however, there is a fairly large $[Ce_3O_4]$ ion at this point which may be masking the homoleptic carboxylate ion.

The three perfluorinated carboxylate complexes show exactly the same ions in exactly the same patterns indicating that there are few significant carbonaceous fragments in the ions. Figure 5.10 shows a typical mass spectrum for such a fluorinated complex. The most notable feature is the sequential loss of fragments of m/z *ca.* 19, this corresponds to the loss of fluorine ions. For example (32) shows a sequential loss of fluorine ions from m/z 724 $[Ce_4O_5F_4]$, 699 $[Ce_4O_5F_3]$, 677 $[Ce_4O_5F_2]$, 658 $[Ce_4O_5F]$, to the metal oxide at m/z 640 $[Ce_4O_5]$. All three compounds show this for varying metal-oxide ratios, e.g. Ce_3O_4, Ce_4O_5 and Ce_5O_8. Once again though, the fact that there are Ce_6O_x fragments does not necessarily mean that these are hexameric species. The perfluorobutyrate complex (31) also shows the presence of some $[(CeO)_x(pfb)_y]$ ions at m/z 1093 and 1073 for $[(CeO)_3(pfb)_3\text{-}F]$ and $[(CeO)_3(pfb)_3\text{-}F_2]$.

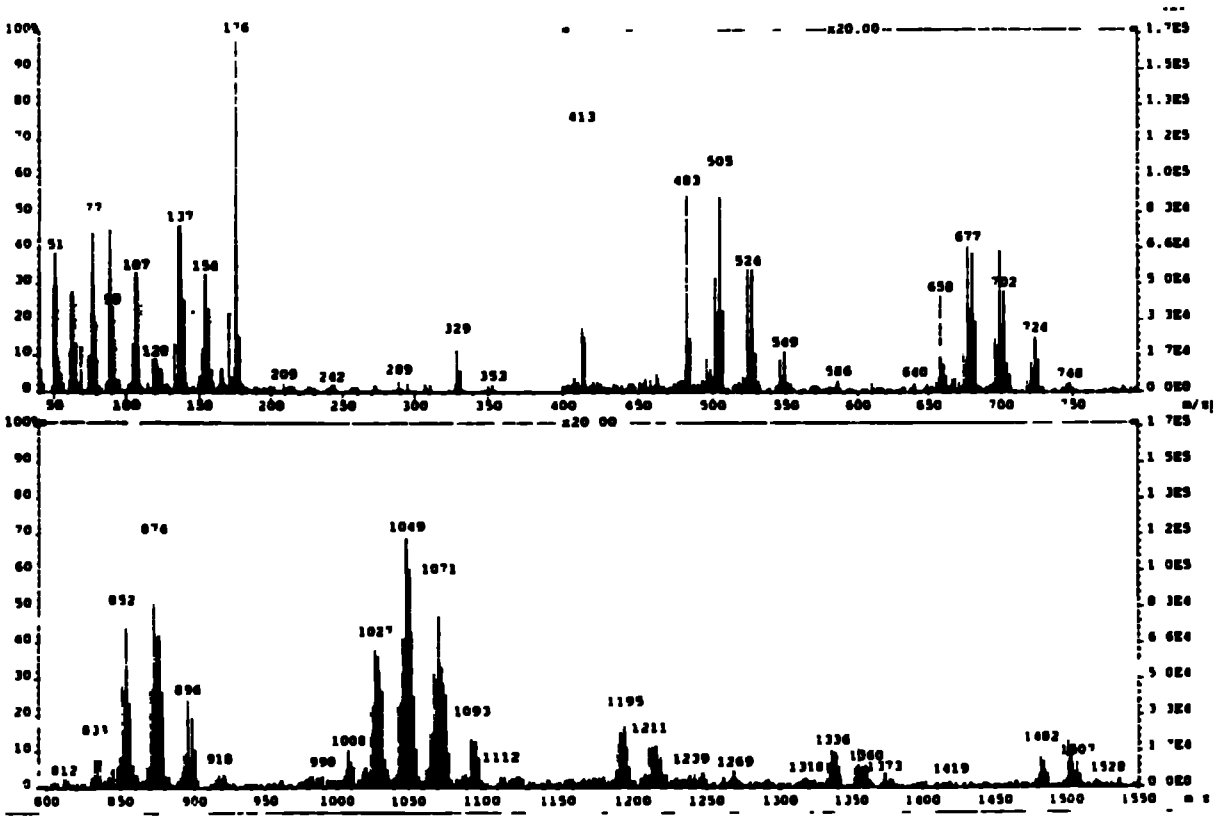

Figure 5.10 : FAB+ Mass spectrum of (32)

5.4 Physical properties

5.4.1 Solubilities and melting points

The overriding factor in determining the solubilities of the homoleptic cerium(IV) carboxylates described in this Chapter is the nature of the acid group itself. Evidence suggests that the degree of oligomerization is constant in all of the complexes, yet the solubilities change dramatically.

Of the compounds (23) - (34) there are four distinct types of carboxylic acid ligand, (i) α- or β-branched (23) - (25), (28), (29), (34), (ii) α,α-branched (26), (27), (iii) straight chain (30) and (iv) fluorinated straight chain (31) - (33). Broadly speaking these four groups show distinctive solubility patterns.

The α- or β- monobranched compounds (group (i)) show appreciable solubilities in the less polar solvents, e.g. hexane and benzene, whereas they are insoluble in more polar solvents e.g., dmso, water, alcohols and acetonitrile. It is noticeable too that solubility, or rather miscibility, is greatest in the case of the two liquid compounds (24) and (25). This group of acids has between 5 and 8 carbon atoms. Therefore, it is not simply the number of carbon atoms which determines solubility.

In contrast the α,α-disubstituted carboxylate complexes are less soluble in non-polar solvents. The added steric hinderance at the α-carbon causes compounds (26) and (27) to be insoluble in hexane and the more polar acetonitrile and alcoholic solvents. However, they remain soluble in benzene and chloroform. Notable too is their solubility in warm dmso. The straight chain hydrocarbyl compound (30), also shows similar solubilities (but it is generally less soluble) except in dmso where it remains insoluble. With other straight chain compounds we notice that the short chain ($n = \leq 4$) and long chain ($n = \geq 9$), (where n is the number of carbon atoms in the carboxylate chain) carboxylates show less solubility in organic solvents, the optimum solubility being when $n = 5 - 7$.

In summary the single most important factor with regards to solubility of the hydrocarbyl carboxylates is the number and relative size of substituent groups on the carboxylato ligands. The solubility data are summarized in Table 5.5. (where the hydrocarbon is toluene, benzene, heptane or hexane).

Table 5.5 : Solubilities of Ce(IV) Carboxylates :

Carboxylate chain structure	Minimum number of carbon atoms for product to be: Hydrocarbon miscible liquid	Hydrocarbon soluble solid
2-methyl branched	6	5
2-ethyl branched	8	6
2,2-dimethyl branched	10	6,7
straight chain	----	5-8

The fluorinated compounds are, as expected, insoluble in non-polar solvents. This is due to the increased polarities of the fluorinated substituents over their hydrocarbyl analogues. Only (31) shows some solubility in chloroform, this is accord with the straight chain hydrocarbon ligands, where the optimum solubility in 'organics' is in the mid range for 'n'. They are all especially soluble in oxygenated solvents (for example alcohols, thf and dmso) which probably coordinate to the metal centre, forming adducts. It can be difficult to remove these solvents making them of limited use as recrystallization solvents. Acetonitrile is a particularly useful solvent especially for (33).

The ceric carboxylates generally do not melt in the conventional sense, instead they tend to decompose to pale yellow solids over a fairly large temperature range. For example (26) decomposes very slowly over the range 135-160°C . Compounds (23) and (28) behave similarly. They both turn from a crystalline yellow solid to an orange solid before decomposing to a black / brown solid. Compound (23) does this almost instantaneously darkening at 163°C and decomposing at 166-171°C, whereas (28) has a much more drawn out process, as it begins to darken at 120°C but does not fully decompose until 198-205°C. The latter is similar to (29) in this respect which darkens at 115°C but does not fully decompose until 220-226°C.

The one exception to the rule (apart from the liquid complexes (24) and (25)) is compound (27) which melts at 81-86°C. This can be explained when one considers the X-ray structure of this compound which shows that there are two unidentate carboxylic acid molecules associated with it, $[Ce_6O_6(OH)_2(dmp)_{12}(dmp\text{-}H)_2]$. These two acids are likely

to be more labile, as they are unidentate, than the bridging carboxylate ligands, therefore, we may explain the low melting point if we postulate that the solid complex is actually dissolving in the free acid which is liberated as opposed to actually melting. A more probable temperature for the melting or more likely, decomposition point, is given by TGA analysis as 177°C.

The fluorinated complexes decompose to very pale yellow solids over a smaller temperature range and at higher temperatures than their hydrocarbyl analogues. Especially striking is the trifluoroacetate compound (33), which appears to explode at 263-265°C. In contrast to the decompositions of the hydrocarbyl species, the fluorinated compounds decompose directly to cerium(IV) dioxide. This can be shown by direct correlation with STA results where it is shown that the decomposition points correspond to the onset of decomposition as detailed in the TGA. For example, the second weight loss in the TGA plot of (33) is between 259-269°C, with a corresponding large exotherm in the DSC plot at 262°C, these values correspond well to the uncorrected decomposition point above.

5.4.2 STA discussion

Thermogravimetric studies of lanthanide carboxylates have tended to focus on the straight chain and aryl substituted acid ligands. However, studies by Paul *et al.*[112,127,128] in the late 1960's with numerous metals and acids have yielded useful information. Uranium(IV) acetate, propionate, butyrate, isobutyrate and isovalerate undergo thermal decomposition through the formation of the corresponding anhydrous carboxylates as intermediates, from whence they decompose to give UO_3 or a mixture of UO_3 and U_3O_8 as the final residue.

With thorium(IV), the same carboxylates decompose in a single step with similar patterns of decomposition. All give ThO_2, CO_2 and the corresponding ketone on final decomposition. e.g.

$$Th(O_2CCH_3)_4 \text{ ----> } ThO_2 + 2CO_2 + 2CH_3COCH_3 \qquad \text{(iii)}$$

Lanthanum carboxylates decompose *via* the formation of either a meta-carboxylate (e.g. acetate) or a basic carbonate (e.g. n-butyrate) to leave La_2O_3.

Cerium(III) carboxylates decompose on heating without the formation of any intermediates. Furthermore the end product is always CeO_2 (i.e. a Ce(IV) species), this being despite the fact that there is apparently no Ce_2O_3 (i.e. Ce(III)) intermediate. This suggests that the decomposition of these carboxylates proceeds with the concurrent oxidation of Ce(III) to Ce(IV). This pattern of decomposition is not necessarily the same

for halogenated species, e.g. $Ce(OCPh)Cl_3$.[198] Here a two step process is observed with a $Ce(CO_3)_2$ intermediate being formed at 230°C, before the compound finally decomposes to CeO_2 at *ca.* 485°C.

Compound (23) shows a TGA plot with three distinct steps. The first two between 84 and 120°C and 154 and 188°C are due to the loss of a small amount of residual solvent. The third between 435 and 495°C is the one step decomposition of the oxo-*bis* compound[$CeO(eb)_2$] to CeO_2 (Expected 44.5 , Found 43.8%). The two major DSC endotherms are at 329 and 482°C. The smaller, former peak is attributed to the onset of decomposition with the latter to the formation of the final CeO_2 product.

The liquid compound, (24) gives a rather more simple plot. The DSC shows just two endotherms at 139 and 472°C. The latter again is the decomposition to the residual CeO_2, whereas the former is attributed to the initial loss of the two weakly bound acid residues and the subsequent reformation to [$CeO(mv)_2$]. The TGA data upholds these findings, with two steps clearly observed. The first between 110 and 171°C is due to the loss of the two acid residues, and the second, between 454 and 482°C is due to the complete decomposition to CeO_2. Compounds (23) and (24) (amongst others) show a long horizontal plateau between steps in the TGA (see Figure 5.12). This is attributed to the stage between the loss of the uncoordinated acids, and the coordinated carboxylates. The related liquid complex (25) shows very similar results. This time, however, the two DSC endotherms are at 165 and 482°C, while the TGA data shows two steps between 124 and 220°C and secondly between 452 and 490°C. Both final residues indicate the formation of CeO_2 as the decomposition product.

Compound (28) undergoes two weight losses in the TGA, the first between 134 and 247°C (13.0%) and the second between 451 and 499°C (30.8%) with a final residue of 48.1%. The residue corresponds, as expected, to CeO_2 (Expected 48.0%). The first step corresponds to a weight loss of *ca.* 46.7g, this may be attributed to the fragmentation of one of the 2-methylbutyrate ligands to leave the corresponding acetate ligand, i.e. [CeO(OAc)(mb)], this conforms to the loss of 44g. It is also mathematically possible to lose the oxo and part of the carbon chain to form [$Ce(mb)(O_2CCHCH_3)$]. The second loss is between 451 and 499°C and is probably due to the removal of carbon fragments. The DSC also has some interesting peaks at lower temperatures. There are two endotherms at 108 and 154°C and an exotherm at 222°C. The final exotherm is probably a cause of the first observed weight loss and the subsequent formation of the new species.

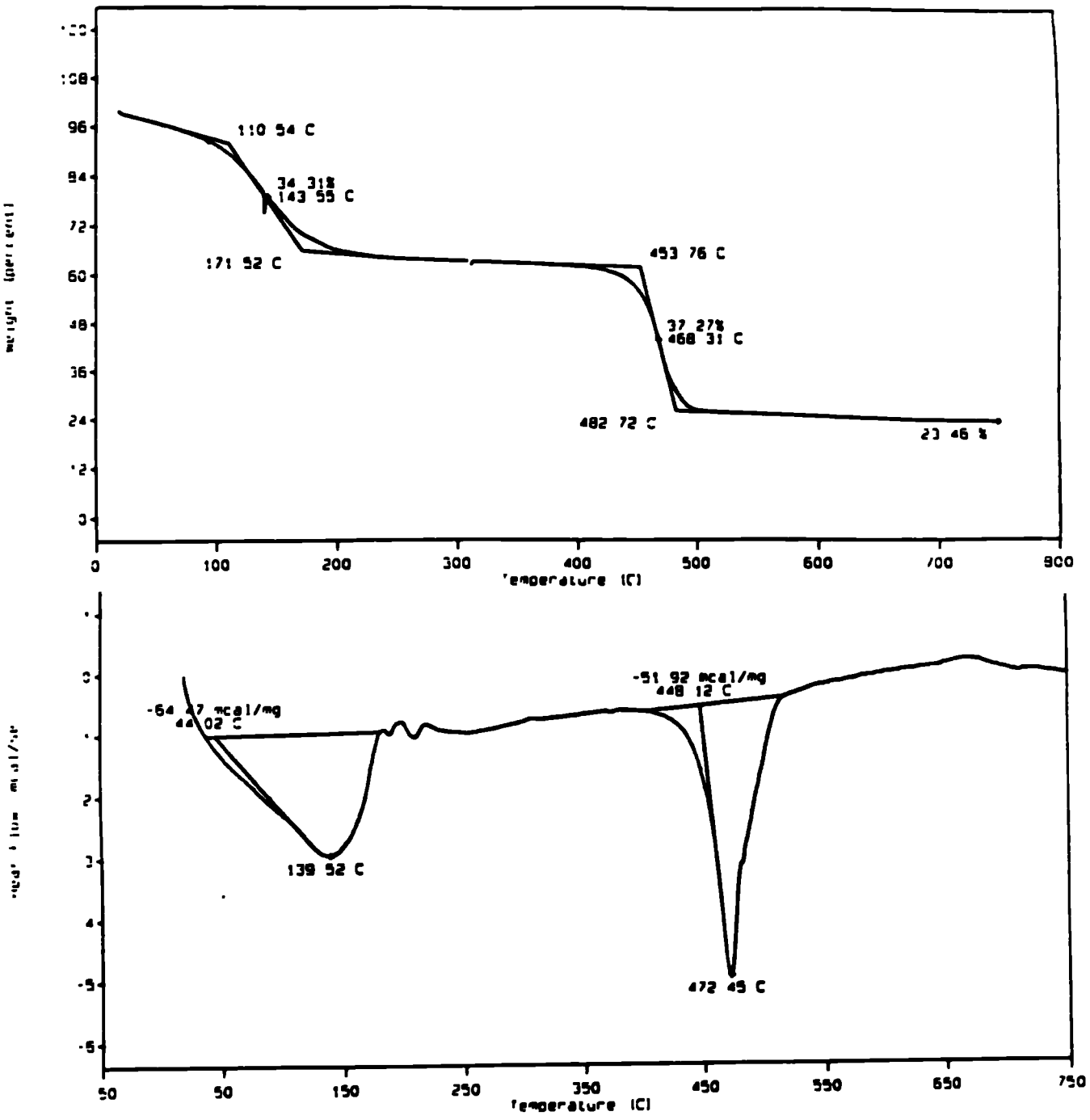

Figure 5.12 : TGA (top) and DSC (bottom) plots of compound (24)

As a result of the high temperatures involved we may surmise, therefore, that the hydrocarbon carboxylate complexes are relatively involatile, irrespective of whether they are solid or liquids, and that they also decompose to CeO_2 without exception. The solid

compounds do not form any stable (or otherwise) intermediates, whereas the liquid compounds lose two organic residues to form the equivalent solid carboxylate $[CeO(RCO_2)]_n$, and then go on to decompose in a similar fashion to the solid complexes.

The fluorinated complexes (31)-(33) have proved to be much more volatile than their hydrocarbon partners, at least the ligand themselves are more volatile. For example the $T_{50\%}$ for (31) is *ca.* 298°C whereas for (25) it is 460°C. This appears to be a general trend and is also noted in Chapter 2, where hfpd compounds are more volatile than their tmhd analogues. In the TGA of (31) two discernable weight losses are noted. The first between 193 and 220°C and the second between 268 and 327°C. The first is likely to be the loss of all fluorine atoms from one of the ligands (Expected 22.2, Found 22.4%), and the second the loss of the remaining fluorines and hydrocarbon fragments (Expected 43.5, Found 43.4%). These processes are almost directly concurrent and only a small plateau is noted between the two. The residue of 24.1% is consistent with its formulation as CeO_2. Two smallish peaks are observed in the DSC plot. The first is an endotherm at 220°C and the second an exotherm at 340°C. The latter is likely to be the formation of the CeO_2 end product, while the former corresponds to the first TGA step.

One noteworthy fact concerning (33) is that at 259-269°C a very sharp loss is observed in the TGA, corresponding to a very large exotherm in the DSC at 262°C. It is not immediately apparent what this corresponds to. Although an explosion cannot be physically observed in the TGA, the behaviour is consistent with the observation that the compound explodes on reaching 263-265°C. This is, however, a controlled explosion, since three STA runs were performed, each one giving a final residue between 9.05 and 9.25%.

5.5 Crystallization of liquid Ce(IV) carboxylates

Both compounds (24) and (25) have two organic residues closely associated such that the solid '$[CeO(RCO_2)_2]$' compound dissolves in the excess acid and forms '$[CeO(RCO_2)_2.2(RCO_2H)]$' as either an orange (24) or yellow (25) liquid. One effect of this is to lower the Ce% content of the compounds. For commercial uses, e.g. in paints[106] or in the promotion of combustion of hydrocarbon fuels,[222] they must be dissolved in a suitable solvent at the time of use. Therefore, one of the major criteria is that the compounds should have a high Ce% (preferably between 20 and 30%). In order to increase

the Ce% we may remove the excess uncoordinated acid residues from complexes (24) and (25). This is done *via* the following procedure, for example, in the related liquid complex [$CeO(cek)_2.2(cekH)$] (where cek = cekanoic acid or 3,5-dimethylheptanoic acid):

$CeO(cek)_2.2(cekH)$ (which was synthesized as for (24)) (4.33g, 5.50 mmol) was dissolved in heptane (30 mL) and stirred for 5 mins.. A 2 Molar equivalent solution of sodium bicarbonate was prepared by the dissolution of $NaHCO_3$ (1.64g, 19.68 mmol) in water (50 mL). The cerium solution was washed with the aqueous solution and left to settle giving a yellow / orange organic layer above a flocculent white layer. The organic layer was separated, dried over sodium sulphate and reduced to dryness to yield a yellow / brown solid. Yield 2.1g (76%).

The cerium weight percentage results are shown in Table 5.6 for three liquid compounds, [$CeO(mv)_2.n(mvH)$] (24), [$CeO(eh)_2.n(ehH)$] (25) and [$CeO(cek)_2.n(cekH)$]. The value of 'n' i.e. the number of free uncoordinated acids still associated is also shown. The analytical methods used to determine both Ce(IV) and Ce(III) contents are given in Appendices 1 and 2 respectively.

Table 5.6 : Ce % Before and After Sodium Bicarbonate Washing :

$NaHCO_3$ conc.	'$CeO(mv)_2.n(mvH)$'	'$CeO(eh)_2.n(ehH)$'	'$CeO(cek)_2.n(cekH)$'
0 Molar	22.6 (n = 2)	19.0 (n = 2)	17.8 (n = 2)
physical form	liquid	liquid	liquid
1/2 Molar	29.0 (n = 5/6)	23.4 (n = 7/6)	20.6 (n = 4/3)
physical form	oily solid	oily solid	oily solid
1 Molar	34.5 (n = 1/6)	26.9 (n = 1/2)	22.3 (n = 1)
physical form	solid	solid	oily solid
2 Molar	36.4 (n = 0)	31.7 (n = 0)	28.2 (n = 1/6)
physical form	solid	solid	solid

As noted in Section 5.3.3 above, that the carboxylate complexes, (24) and (25), corresponding to '[$CeO(RCO_2)_2.2(RCO_2H)$]', show a very broad downfield signal for the OH proton of the free acid. However, on washing these liquids with sodium bicarbonate solution we note that this resonance disappears, even when the concentration of the solution is only 1/2 molar. This is not so unlikely as the resonance is so broad that it is only just possible to see it in the initial compounds, especially for (25). From infrared studies we note that the band at *ca.* 3636cm^{-1} still exists for the maority of the above compounds.

Although the molar ratios of the sodium solution do not necessarily correspond exactly to the numerical removal of acid ligands (e.g. a 1/2 molar solution should remove only 1/2 mole of free acid, whereas in the case of (24) for instance, it removes 7/6 mole) it is notable that the more concentrated solutions remove more acid. It is observed that as more and more acid is removed, the compounds start to solidify, until there is about 1/2 mole of free acid remaining and the liquid complex becomes solid, and in some cases crystalline. The solubility of the 2 Molar washed '$CeO(eh)_2$' product was investigated and it was found that, in cold heptane the solubility was 837g/dm^3 while in hot heptane it was 834g/dm^3, i.e. the same.

Other methods for the removal of the free acid include washing with acetone; this, however, has two drawbacks. Firstly, there is always the chance of acetone coordination as cerium has a certain affinity for oxygen donors, and secondly it is not such a repeatable method as some of the parent compound may be soluble in acetone. Indeed a particular Ce% in the washed compounds can vary by 2-4%, whereas those in the sodium bicarbonate washing method tend to differ by less than 1%.

A related sodium bicarbonate washing was attempted on mixed carboxylate complexes of the form '[$CeO(RCO_2)(R'CO_2)$]' using various ligands of differing lengths (e.g. octanoic and 2-ethylbutyric). However there was no evidence (NMR in particular) that any one acid was removed in preference to another. It would appear that it is only the free uncoordinated acids which can be removed *via* this method and not any of the coordinated carboxylate ligands.

5.6 Ammoniacal route into cerium(IV) carboxylates

The crystal structures of compounds (23) and (27) (section 5.7) show them both to be hexameric structures based on a Ce_6O_8 core framework. The reaction scheme for their synthesis shows that the oxo groups are not formed directly from the first step, but are put in place by the subsequent hydrolysis of the homoleptic species, *viz.*;

$$(NH_4)_2Ce(NO_3)_6 + 4NaOH + 4RCO_2H \text{ -------> } \text{'}Ce(RCO_2)_4\text{'} \quad \text{(i)}$$

hydrolysed

$$\text{'}Ce(RCO_2)_4\text{'} \text{ ----------> } [OCe(RCO_2)_2]_n \quad \text{(ii)}$$

If this hydrolysis reaction is not allowed to occur, we would presumably be left with quite a different set of compounds, probably based on the true homoleptic cerium(IV) carboxylate species. This has been achieved with an ammoniacal base using Schlenk line techniques. This together with the use of pre-dried solvents ensures the absence both of water and air. The full experimental details are given in the experimental section. The reaction scheme for the formation of compound (35) is as follows,

$$4\ NH_4eb + (NH_4)_2Ce(NO_3)_6 \text{ ---------> } \text{'}Ce(eb)_4\text{'} + 6\ NH_4NO_3 \quad \text{(iii)}$$

Microanalyses on (35) shows the absence of nitrogen, either as ammonia or ammonium nitrate. From this and spectroscopic methods (see section 5.8) the most likely empirical formula of the compound is $[Ce(eb)_{3.5}(O)_{0.25}]$. This would necessitate a significant change in the structure, destroying the Ce_6O_8 core. Analysis of the $\Delta\nu$ in the infrared ($102cm^{-1}$) suggests a bridging or bidentate bonding mode for the carboxylates.

We may also go one step further. If we isolate the complex at the second filtration stage and open it up to air we may add water in order to determine whether this compound will hydrolyse to the same hexameric species formed in the aqueous route. This procedure was performed by removing the toluene solvent, redissolving completely in benzene and adding a stoichiometric amount of water (1 Ce : 1 water). The reaction is then heated to 60°C for 30 mins. and then all solvents were removed *in vacuo*. The resultant bright yellow solid has been characterized by spectroscopic, physical and analytical techniques and appears to be based on the same formula as (23), i.e. $[CeO(eb)_2]$. At this stage, however, we are unable to determine whether the hexameric structure persists, although it is likely.

5.7 X-ray crystallography

The previous sections have described a wide range of cerium carboxylates of the general type $[CeO(RCO_2)_2.n(RCO_2H)]$ and their spectroscopic properties. Single crystals of a number of these compounds were obtained and studied by X-ray diffraction techniques. Unfortunately many of them gave poor diffraction patterns and no more structural information could be obtained. Compounds (23) and (27) gave satisfactory diffraction patterns and the data sets obtained were sufficiently good for the structures to be solved. The relevant crystallographic collection data and Tables of bond lengths and angles appear in the Appendix. The structures of both (23) and (27) showed very similar skeletal geometries but the latter showed more disorder associated with the carboxylate ligand atoms.

5.7.1 Overview

The salient points of the crystal structures of the cerium(IV) carboxylates described in this Chapter is their central Ce_6O_8 core, with the oxygen atoms existing as either oxo- or hydroxo- ligands. This metal-oxygen core is not, however, specific to these carboxylates and has also been seen in two other compounds.

The first example was synthesized by the reaction of cerium isopropoxide with two equivalents of pd-H to yield $[Ce(O^iPr)_2(pd)_2]$ and the subsequent hydrolysis to yield $[Ce_6(\mu_3\text{-}O)_4(\mu_3\text{-}OH)_4(pd)_{12}]$. The pd ligands are didentate and outside the central core, screening the remaining hydroxo ligands, therefore, inhibiting further condensation.[239]

The mechanism for the formation of the hexamer has been proposed and confirmed by stepwise crystallographic data, it is illustrated in part below (see Figure 5.13). For a H_2O : Ce ratio of 2, all isopropoxide groups are cleaved but the pd is bound to yield a hydrolysed precursor (b). Two hydrolysed dimers then condense *via* olation, to a cyclic tetramer. This tetramer has an eight coordinate metal (square antiprism) and is bonded *via* double hydroxo bridges (c). This tetramer is isostructural with that of the zirconium complex, $[Zr_4(\mu_2\text{-}OH)_8(H_2O)_{16}Cl_8]$.[240] Two hydrolysed monomers condense with the tetramer *via* oxolation to give the observed hexamer. The six Ce atoms are at the vertices of an octahedron with the oxygens atoms surrounding the octahedron to form a cube. Each Ce is octacoordinated to four oxygen atoms of two pd molecules two oxo atoms and two hydroxo atoms. The three types of Ce-O bond lengths are easily differentiated, *viz*. Ce-O(μ_3-OH) = 2.45(1), Ce-O(μ_3-O) = 2.20(5) and Ce-O(pd) 2.33(3) - 2.38(2)Å.

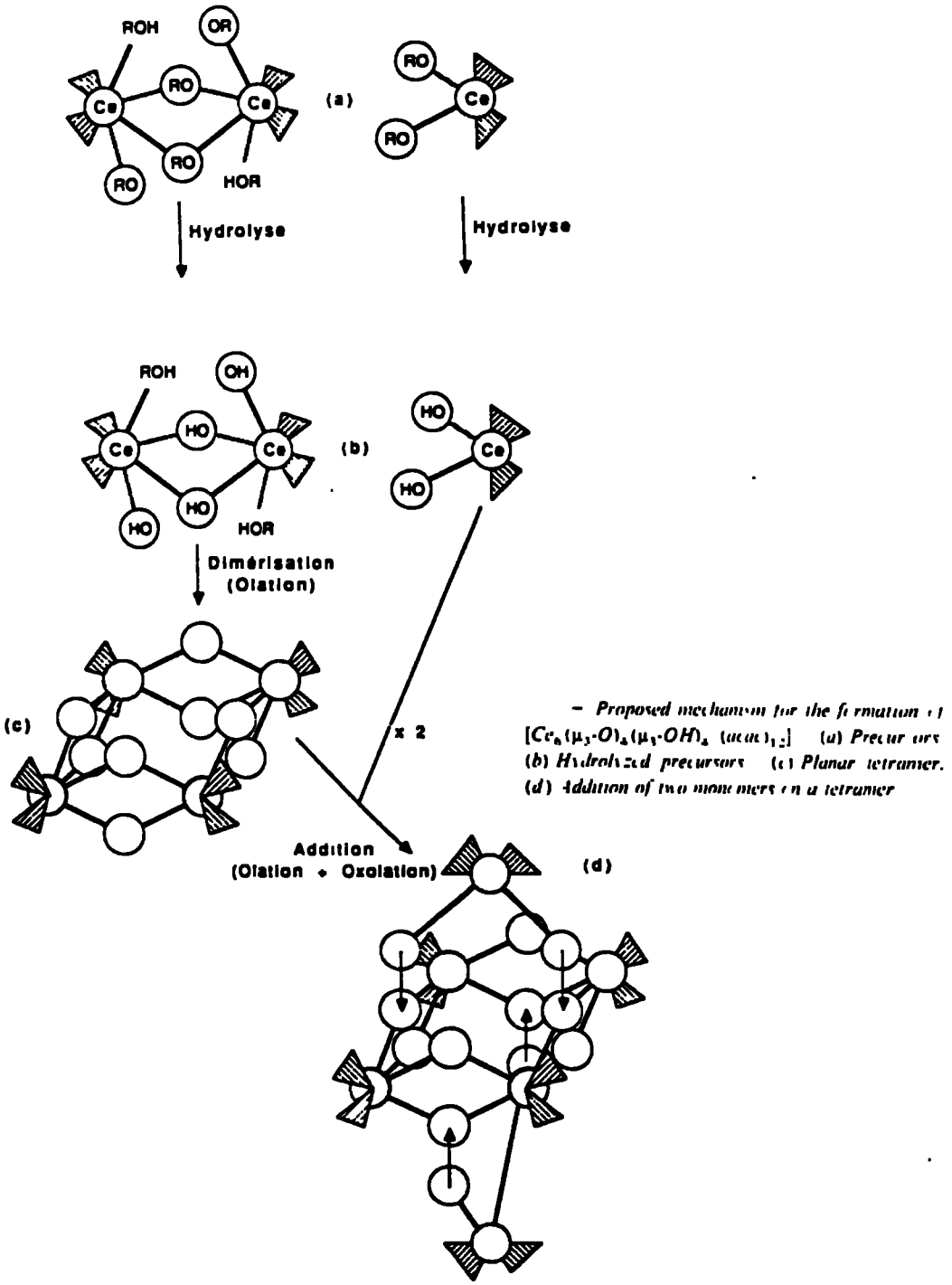

– *Proposed mechanism for the formation of* $[Ce_6(\mu_3\text{-}O)_4(\mu_3\text{-}OH)_4(acac)_{12}]$ (*a*) *Precursors* (*b*) *Hydrolyzed precursors* (*c*) *Planar tetramer.* (*d*) *Addition of two monomers on a tetramer*

Figure 5.13 : Mechanism of hexamer formation

This core is isostructural with that of the hexameric complex, $[Ce_6(\mu_3\text{-}O)_4(\mu_3\text{-}OH)_4(SO_4)_6]$. This compound is prepared by the hydrothermal hydrolysis of the sulphate at 200°C. The central $[Ce_6(\mu_3\text{-}O)_4(\mu_3\text{-}OH)_4]^{12+}$ core has six Ce atoms at the corners of an octahedron, surrounded by eight oxygen atoms, four of which are actually OH anions. The average Ce-O bond lengths are 2.33(6)Å which is similar to those of CeO_2.[241]

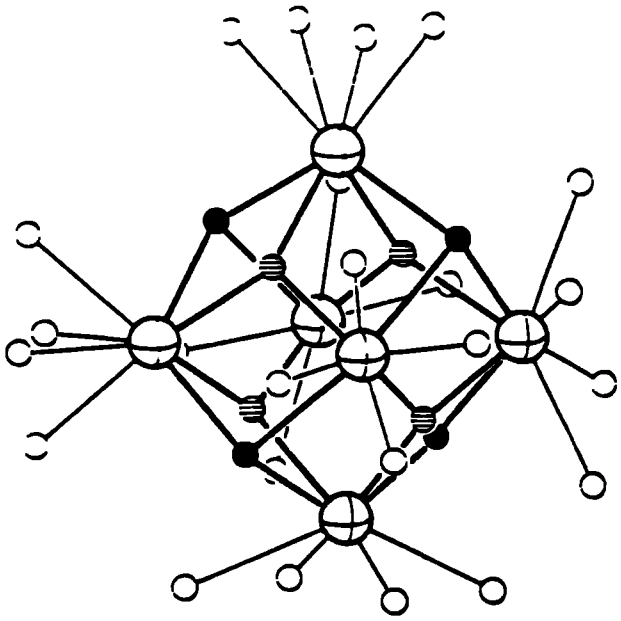

Figure 5.14 : X-ray crystal structure of the $[Ce_6(\mu_3\text{-}O)_4(\mu_3\text{-}OH)_4]^{12+}$ core of $[Ce_6(O)_4(OH)_4(pd)_{12}]$

5.7.2 $[Ce_6H_2O_6(OH)_2(dmp)_{12}(dmp\text{-}H)_2]$ (27)

The structure of (27) is based on the same overall structure of the rest of the solid hydrocarbyl cerium(IV) carboxylates described within this Chapter but with one major difference, that there are two unidentate carboxylic acids residues coordinated to two of the cerium metal centres.

The structure is related by mirror symmetry about the centre of the core framework, leading to three symmetrically distinct metal atoms. Ce(1) is nine coordinate, being

coordinated to four oxygen atoms of the cerium - oxo framework, four oxygens of the bridging carboxylate ligands and a single oxygen of a unidentate carboxylic acid residue. Both Ce(2) and Ce(3) are eight coordinate, being coordinated in a similar manner to Ce(1) without the added oxygen of the unidentate acid.

The central core can be considered in a number of ways. Firstly, the cerium atoms are arranged at the apexes of a regular octahedron with each of the eight faces capped by a triply bridging oxygen atom. We might also describe the core structure as a square prism containing a meridional hexagon. Alternatively we may consider the entire core as a rhombic dodecahedron. Analysis of both the bond lengths and angles of the cerium-oxygen core also allows us to determine which of the oxygen atoms are oxo- and which are hydroxo- molecules. The cerium oxygen framework is shown below in Figure 5.15.

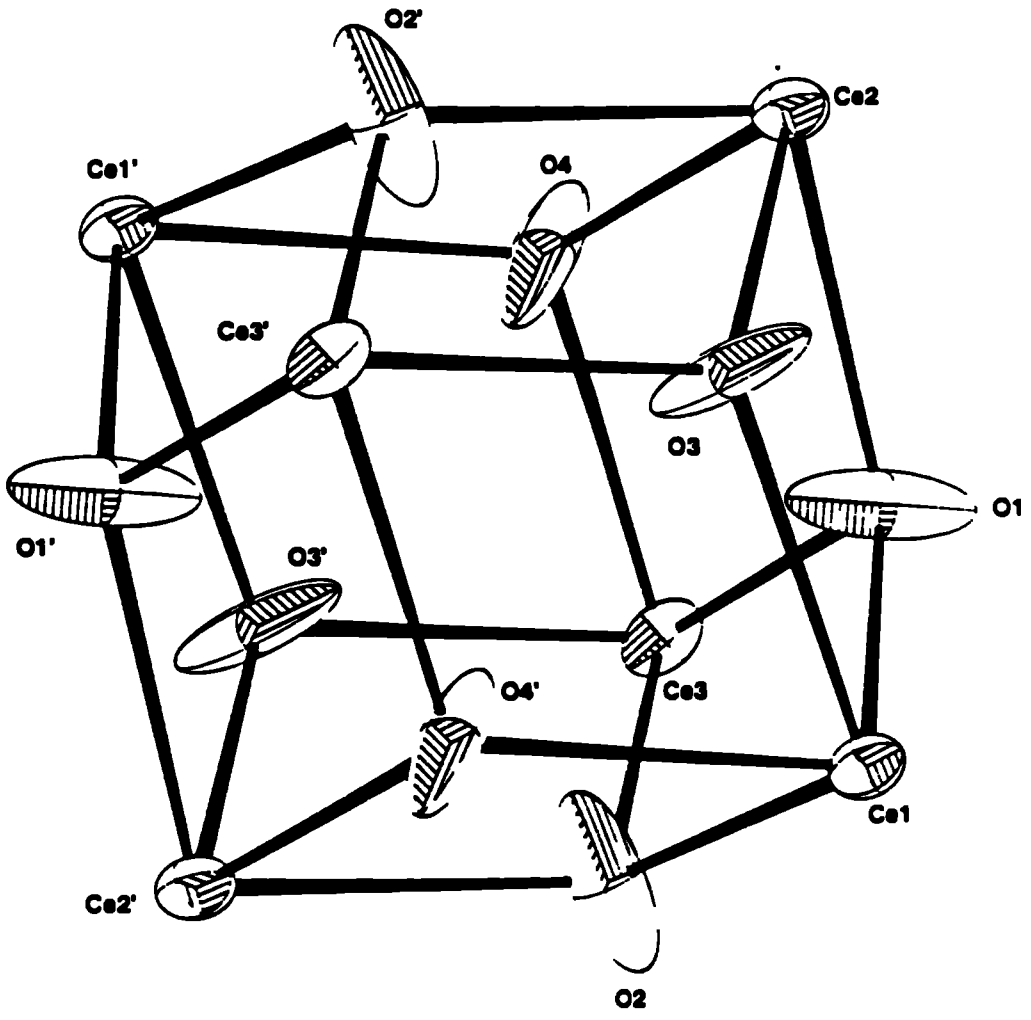

Figure 5.15 : Ce_6O_8 framework of (27)

The average Ce-O bond lengths within the core are 2.289(6) (O(1)), 2.290(6) (O(2)), 2.335(7) (O(3)) and 2.290(7)Å (O(4)). The fact that the average bond lengths are significantly longer to O(3) (by *ca.* 0.045Å) suggests that both O(3) and O(3') are in fact hydroxy groups while the other six are oxo groups. Thus the core structure is better described as $Ce_6O_6(OH)_2$. Analysis of the Ce-O-Ce bond angles too gives us direct confirmation of the fact that there are two OH groups within the core. Three angles are significantly smaller than the others, these are Ce(2)-O(3)-Ce(3') (106.8(2)°), Ce(3')-O(3)-Ce(1) (108.9(3)°) and Ce(2)-O(3)-Ce(1) (109.3(2)°). The average Ce-O-Ce bond angles of the other groups is 111.6(3)°. This too suggests that O(3) and O(3') are both OH groups.

These bond lengths and in particular, those within the core, can be correlated with those of the two other compounds containing this central core framework. The sulphate compound $[Ce_6(O)_4(OH)_4(SO_4)_6]$ has four μ_3 bridging oxo and hydroxy groups, with an overall Ce-O bond length of 2.33(6)Å.[241] Compound (27) has an overall core bond length average of 2.601(7)Å, i.e. it is considerably longer, this may due in part to the action of the bridging carboxylate groups. The related compound $[Ce_6(\mu_3\text{-}O)_4(\mu_3\text{-}OH)_4(pd)_{12}]$ also has a pattern of four hydroxy and four oxo groups, with average bond lengths of 2.45(1) and 2.20(5)Å respectively.[239] These are rather more similar to those within compound (27) presumably because the other ligands involved are involved in similar bonding modes, i.e. bidentate (pd) and bridging (dmp).

The twelve carboxylate ligands are arranged in bridging configurations along the edges of the octahedron and lead to metal-metal distances which average 3.791(9)Å, i.e. there is no evidence of any metal-metal bonding. This distance compares to that of the cerium oxo-pentanedionate complex above whose Ce-Ce bond distances are an average of 3.772(2)Å.[239] The average metal oxygen bond lengths can be split up into four distinct types. These are (i) those between Ce and core oxo groups (average 2.290(6)Å), (ii) those between Ce and core hydroxy groups (average 2.335(6)Å), (iii) those between Ce and bridging carboxylates (average 2.419(7)Å) and (iv) those between Ce and the unidentate carboxylic acid (2.702(7)Å). This increase in bond lengths through the series is as would be expected for the four groups. However, the carboxylates do not bridge to the two metal centres in a completely symmetrical fashion, the difference between the two Ce-O bond lengths of the same carboxylate group being about 0.03Å. For example, the bond between Ce(3) and O(12) is 2.396(7), while that between Ce(2) and O(11) is 2.363(6)Å.

Along with the twelve bridging carboxylate ligands are two unidentate carboxylic acid ligands which are coordinated to Ce(1) and Ce(1') respectively. These two ligands

have the oxygens atoms O(41), O(42) and O(41'), O(42'). These two residues are also related by a centre of symmetry at the centre of the cerium oxo core. The Ce-O(41) bond length is significantly longer than any of those to the other bridging carboxylate groups (by about 0.283Å) due to the fact that O(41) is protonated. This proton, however, has not been unambiguously located.

The bond lengths of the oxygens of the unidentate carboxylic acid group to the central carbon of the acetato group C(42), are quite different to those of the bridging carboxylates. In the latter, the two bond lengths are very similar although they are not completely symmetrical (the differences being about 0.019Å) and have an average bond length of about 1.272(11)Å, however, for the unidentate ligands the bond lengths are 1.206(11) (C(41)-O(41)) and 1.326(13) (C(41)-O(42)). This vast difference of 0.12Å clearly identifies the carboxylic uncoordinated oxygen O(42), and the protonated coordinated oxygen atom O(41).

The bond angles along the Ce-O-C groups of both the unidentate and bridging carboxylates also give us evidence of the different bonding nature of the respective ligands. The angle of the unidentate ligand, between Ce(1)-O(41)-C(41) is 140.6(7) is significantly longer than that between a typical bridging group, e.g. C(51)-O(52)-Ce(2) is 136.6(6)°. More obvious is the difference between the O-C-O bond angles. For instance for the unidentate ligand, the O(41)-C(41)-O(42) angle is 117.5(10) while that for O(12)-C(11)-O(11) is larger at 125.3(8)°. This larger angle for the bridging carboxylate must be expected as a specific constraint is put on this part of the carboxylate ligand in that it needs to arrange itself such that it can bond to two metal centres. Thus in order to satisfy the electronic requirements of this complex the structure must be considered as having two further protons which have not been found in the difference map, therefore, the complete structure is $[Ce_6H_2O_6(OH)_2(dmp)_{12}(dmp\text{-}H)_2]$ and is shown in Figure 5.16 overleaf.

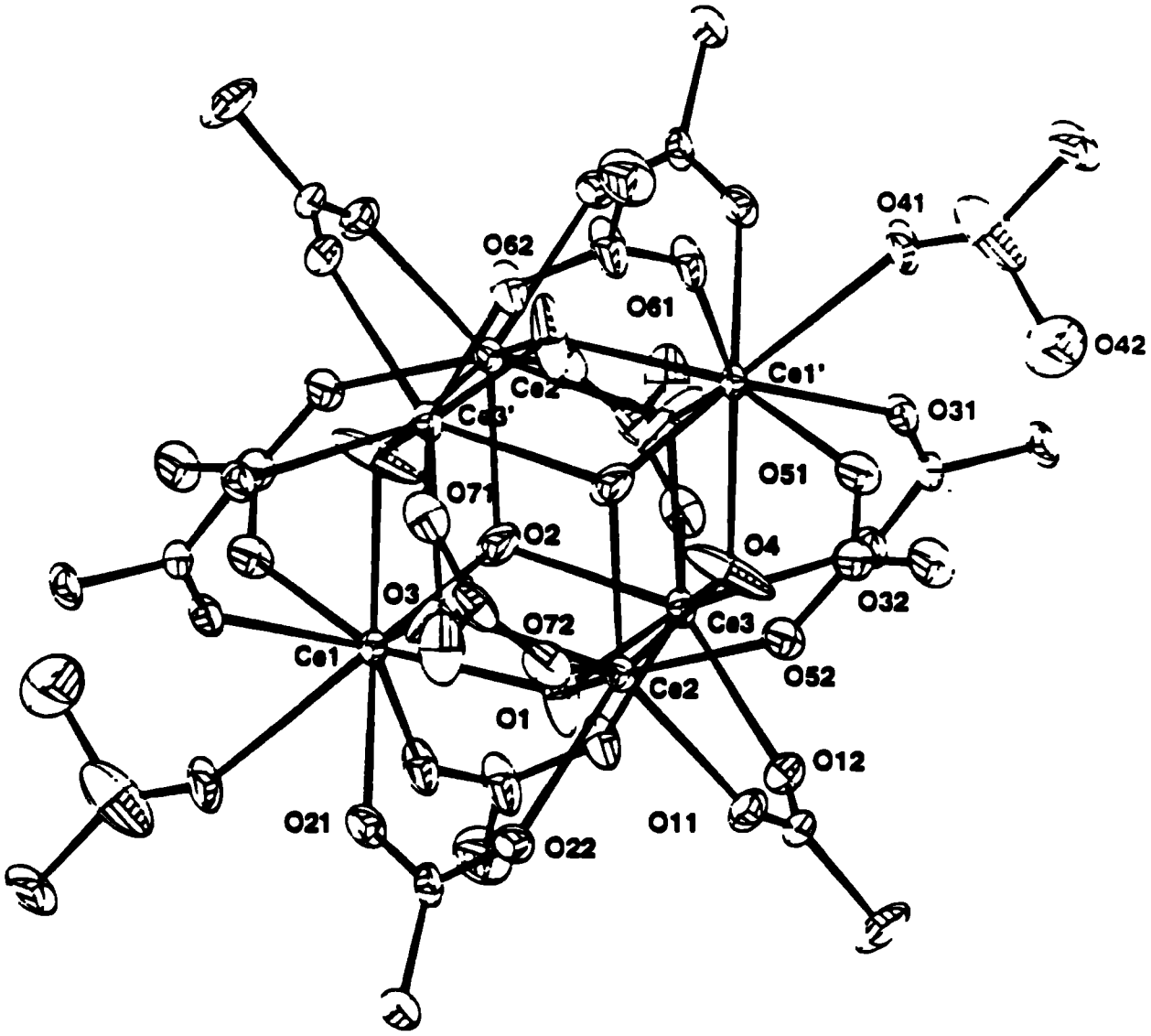

Figure 5.16 : X-ray structure of $[Ce_6H_2O_6(OH)_2(dmp)_{12}(dmp\text{-}H)_2]$ (27)

5.7.3 $[Ce_6H_2O_6(OH)_2(eb)_{1.2}(EtOH)_2]$ (23)

Compound (23) (*ca.* 3.0g) was dissolved in diethyl ether (10 mL) and ethanol (5 mL) added and the solution was left at 0°C to crystallize. Within a few days large yellow blocks, suitable for analysis by X-ray crystallography, were produced. Preliminary studies indicate that the core structure is based on the same framework as that of compound (27), i.e. $Ce_6O_6(OH)_2$. Again the metal atoms are arranged at the vertices of a regular octahedron with the oxo and hydroxo groups capping each of the eight faces in a triply bridging mode. The pattern of twelve bridging 2-ethylbutyrate ligands remains intact, however, there are a number of notable differences between this compound and (27).

Firstly we note that the two unidentate carboxylic acid residues are no longer observed, each of the twelve carboxylates being (i) deprotonated and (ii) bridging two metals. This might suggest that the coordination numbers of the metals within the complex might also differ (there are two nine coordinate and four eight coordinate in (27)), however, this is not the case. This is due to the presence of two ethanol molecules coordinated to two metal centres directly opposite each other, giving a pattern of two nine coordinate and four eight coordinate metal centres. Thus, in the majority of ways this structure can be considered to be very similar to that of (27) if we postulate that the crystallizing medium (ethanol and diethyl ether) removes any free carboxylic acid.

Unfortunately during the solution this structure the R factor has remained rather high due to disorder in the carboxylate ligands, therefore, any description of bond lengths and angles would be presumptuous.

5.8 Experimental section

Synthesis of $[Ce_6H_2O_6(OH)_2(eb)_{12}]$ (23)

Cerium ammonium nitrate (CAN) (5.0g, 9.03 mmol) was dissolved in distilled water (20 mL) at R.T., which was followed by the dropwise addition of a colourless solution of NaOH (1.45g, 36.12 mmol), 2-ethylbutyric acid (4.20g, 36.12 mmol) and water (50 mL). The solution rapidly turned from soluble orange, to insoluble yellow. The solution was stirred at R.T. for 30 mins., filtered, washed with water (2 x 20 mL) and dried under suction for 2 hours. To the yellow solid precipitate was added benzene (30 mL) and the partially soluble solution stirred at 60°C for 30 mins.. The solvent was removed under vacuo to leave a yellow solid. This solid was again dissolved in benzene (30 mL) at 60°C to yield a soluble yellow solution, to which was added magnesium sulphate (*ca.* 3.0g). The solution was filtered and stripped to dryness to yield a bright yellow crystalline solid. **Yield** 3.24g (93%) **M. Pt.** dec. 166-171°C

Microanalysis : Found, C, 39.3 ; H, 6.27 ; Calc. for $Ce_6O_{32}C_{72}H_{136}$, C 40.0 ; H, 6.30 %.

Infrared (Nujol ν cm^{-1}) : 3627(m), 1702(s), 1547(s), 1416(s), 1316(m), 1262(w), 1217(w), 1110(w), 885(w), 651(w), 564(m), 520(w).

Infrared (KBr disc ν cm^{-1}) : 2963(m), 2931(m), 1704(s), 1546(s), 1414(s), 1312(m), 1258(m), 1221(m), 1156(s), 1111(s), 1045(m), 1015(m), 936(s), 826(s), 807(s), 776(s), 749(m), 652(s), 563(s), 375(s), 304(s).

FT Raman (ν cm^{-1}) : 410(s), 355(w), 220(w), 179(w), 166(s).

^{1}H NMR (270 MHz, $CDCl_3$, 20°C) : δ 0.83 (6H, t, CH_3), 1.42, 1.51 (4H, m, CH_2), 1.95 (1H, quintet, CH).

^{13}C NMR (67.94 MHz, $CDCl_3$, 20°C) : δ 12.2 (s, CH_3), 24.6 (s, CH_2), 50.1 (s, CH), 182.5 (s, CO).

Mass Spectrometry (FAB +) : 1082 $[CeO(eb)]_4$(4%), 984 $[Ce_4O_5(eb)_3]$(2%), 967 $[Ce_6O_8]$(2%), 656 $[Ce_4O_6]$(2%), 641 $[Ce_4O_5]$(4%), 542 $[CeO(eb)]_2$(2%), 483 $[Ce_3O_4]$(34%), 427 $[(CeO)_2(eb)]$(21%), 370 $[Ce(eb)_2]$(4%), 329 $[Ce_2O_3]$(21%), 272 $[CeO(eb)]$(5%).

Solubility : Soluble in hexane, benzene and chloroform, insoluble in dmso, water and alcohols.

STA data : TGA : 84-120°C (9.8%), 154-188°C (11.6%), 435-495°C (43.8%), Res. 36.2%, $T_{50\%}$ 473°C. DSC : 60.7°C, 111.1°C, 164.8°C, 329.1°C, 482.3°C. (DSC peaks are endotherms unless otherwise stated).

Synthesis of $CeO(mv)_2.2(mv\text{-}H)$ (24)

CAN (5.0g, 9.03 mmol) was dissolved in distilled water (20 mL) at R.T., which was followed by the dropwise addition of a colourless solution of NaOH (1.45g, 36.12 mmol), 2-methylvaleric acid (4.20g, 36.12 mmol) and water (50 mL). The solution rapidly

turned from soluble orange, to insoluble yellow. The solution was stirred at R.T. for 30 mins. to yield an insoluble yellow liquid, which was separated and washed with water (2 x 20 mL). To the yellow liquid was added benzene (30 mL) and the partially soluble solution was stirred at 60°C for 30 mins.. The solvent was removed under vacuo to leave a yellow liquid. This was again dissolved in benzene (30 mL) at 60°C to yield a soluble yellow solution, to which was added magnesium sulphate (*ca.* 3.0g). The solution was filtered and stripped to dryness to yield an orange / yellow liquid. **Yield** 5.24g, (94%)

Microanalyses : Found, C, 45.3 ; H, 7.21 ; Calc. for $Ce_6O_{56}C_{144}H_{278}$, C, 46.2 ; H, 7.43 %.

Infrared (Neat ν cm^{-1}) : 3636(m), 2961(w), 2934(m), 1710(s), 1563(s), 1417(s), 1307(m), 1294(m), 1248(m), 1218(m), 1155(w), 1117(w), 1100(m), 1055(w), 1022(w), 937(m), 816(w), 743(w), 627(m), 577(m), 538(m), 478(w).

^{1}H NMR (90 MHz, C_6D_6, 20°C) : δ 1.13 (6H, t, terminal CH_3), 1.35 (6H, t, α-sub CH_3), 1.58 (3H, s, CH_2), 1.91 (1H, m, CH_2), 2.60 (1H, m, CH), 12.39 (1H, s, OH).

^{13}C NMR (22.65 MHz, C_6D_6, 20°C) : δ 13.6 (s, CH_3), 16.6 (s, CH_3), 20.3 (s, CH_2), 35.7 (s, CH_2), 40.1 (s, CH), 183.1 (s, CO).

Mass Spectrometry : 388 [Ce(mv)$_2$](5%), 329 [Ce_2O_3](5%), 289 [CeO(mv)](8%), 156 [CeO](100%), 140 [Ce](42%).

Solubility : Soluble in hexane, benzene and chloroform, insoluble in dmso, water and alcohols.

STA data : TGA : 110-171°C (34.3%), 454-482°C (37.3%), Res. 23.5%, $T_{50\%}$ 420°C. DSC : 139.5°C, 472.5°C.

Synthesis of $CeO(eh)_2.2(eh\text{-}H)$ (25)

CAN (5.0g, 9.03 mmol) was dissolved in distilled water (20 mL) at R.T., which was followed by the dropwise addition of a colourless solution of NaOH (1.45g, 36.12 mmol), 2-ethylhexanoic acid (5.21g, 36.12 mmol) and water (50 mL). The experimental details were as for (24). The resultant product was a yellow liquid. **Yield** 6.14g (93%)

Microanalyses : Found, C, 51.6 ; H, 8.5 ; Calc. for $Ce_6O_{56}C_{192}H_{374}$, C, 52.2 ; H, 8.46 %.

Infrared (Neat ν cm^{-1}) : 3635(m), 2960(s), 2934(s), 2874(s), 2861(s), 1708(s), 1559(s), 1460(s), 1415(s), 1380(m), 1347(m), 1318(m), 1296(m), 1230(m), 1205(w), 1151(w), 1103(m), 947(m), 801(w), 783(w), 730(w), 635(m), 574(m), 529(m), 365(m).

^{1}H NMR (90 MHz, C_6D_6, 20°C) : δ 1.08 (6H, t, CH_3), 1.46 (4H, m, CH_2), 1.68 (4H, m, CH_2), 2.28 (1H, m, CH), 11.50 (1H, br, OH).

^{13}C NMR (22.65 MHz, C_6D_6, 20°C) : δ 11.9 (s, terminal CH_3), 13.6 (s, α-sub CH_3), 22.5 (s, CH_2), 24.7 (s, CH_2), 29.6 (s, CH_2), 31.1 (s, CH_2), 47.9 (s, CH), 182.6 (s, CO).

Mass Spectrometry : 1140 [Ce_2(eh)$_6$](6%), 996 [Ce_2(eh)$_5$](100%), 967 [Ce_6O_8](5%), 868

$[Ce_2O(eh)_4]$(10%), 754 $[(CeO)_3(eh)_2]$(5%), 725 $[OCe_2(eh)_3]$(36%), 598 $[(CeO)_2(eh)_2]$(8%), 570 $[Ce(eh)_3]$(6%), 484 $[Ce_3O_4]$(23%), 455 $[(CeO)_2(eh)]$(32%), 426 $[Ce(eh)_2]$(21%).

Solubility : Soluble in hexane, benzene and chloroform, insoluble in dmso, water and alcohols.

STA data : TGA : 124-220°C (28.8%), 452-490°C (48.0%). Res. 19.4%, $T_{50\%}$ 460°C. DSC : 164.8°C, 481.6°C.

Synthesis of $CeO(emb)_2$ (26)

CAN (5.0g, 9.03 mmol) was dissolved in distilled water (20 mL) at R.T., which was followed by the dropwise addition of a colourless solution of NaOH (1.45g, 36.12 mmol), 2-ethyl-2-methylbutyric acid (4.69g, 36.12 mmol) and water (50 mL). The solution rapidly turned from soluble orange, to insoluble yellow. The solution was stirred at R.T. for 30 mins., filtered, washed with water (2 x 20 mL) and dried under suction for 2 hours. To the yellow solid was added benzene (30 mL) and chloroform (30 mL) and the partially soluble solution was stirred at 60°C for 30 mins.. The solvent was removed under vacuo to leave a yellow solid. This solid was again dissolved in chloroform (30 mL) at 60°C to yield a *ca.* 80% soluble yellow solution, to which was added magnesium sulphate (*ca.* 3.0g). The solution was filtered and stripped to dryness to yield a yellow solid. **Yield** 3.33g (89%). **M. Pt.** dec.135-60°C

Microanalyses : Found, C, 39.7 ; H, 6.10 ; Calc. for $Ce_6O_{32}C_{84}H_{158}$, C, 40.0 ; H, 6.27 %.

Infrared (Nujol ν cm^{-1}) : 3624(m), 1701(s), 1531(s), 1407(s), 1327(m), 1303(m), 1258(s), 1179(s), 1070(w), 1010(w), 913(m), 822(w), 789(w), 744(w), 656(m), 612(m), 569(s), 521(m), 395(m).

Infrared (hexachlorobutadiene ν cm^{-1}) : 3625(s), 2970(s), 1697(s), 1556(s), 1464(s), 1404(s), 1327(m), 1304(m), 1259(s), 1178(s), 1070(w), 1040(w), 612(m), 522(m), 396(m).

^{1}H NMR (90 MHz, C_6D_6, 20°C) : δ 0.83 (6H, t, CH_3), 1.04 (3H, s, $C(CH_3)$), 1.51 (4H, m, CH_2).

^{13}C NMR (22.65 MHz, C_6D_6, 20°C) : δ 9.11 (s, CH_3), 20.2 (s, $C(\underline{C}H_3)$), 31.6 (s, CH_2), 46.9 (s, $\underline{C}(CH_3)$), 185.1 (s, CO).

Mass Spectrometry : 1469 $[Ce_3(emb)_8O]$(2%), 1337 $[Ce_3(emb)_7O]$(2%), 1209 $[Ce_3(emb)_6O]$(3%), 1096 $[Ce_3(emb)_5O]$(4%), 1053 $[Ce_2(emb)_6]$(2%), 967 $[Ce_6O_8]$(5%), 925 $[Ce_2(emb)_5]$(5%), 726 $[(CeO)_3(emb)_2]$(5%), 683 $[Ce_3(emb)_3O]$(5%), 655 $[Ce_4O_6]$(2%), 571 $[(CeO)_2(emb)_2]$(5%), 529 $[Ce(emb)_3]$(1%), 483 $[Ce_3O_4]$(12%), 441 $[(CeO)_2(emb)]$(15%), 397 $[Ce(emb)_2]$(8%), 286 $[Ce(emb)O]$(3%).

Solubility : Soluble in dmso, chloroform and benzene, insoluble in hexane and alcohols.

Synthesis of $Ce_6H_2(OH)_2O_6(dmp)_{12}(dmpH)_2$ (27)

CAN (5.0g, 9.03 mmol) was dissolved in distilled water (20 mL) at R.T., which

was followed by the dropwise addition of a colourless solution of NaOH (1.45g, 36.12 mmol), 2,2-dimethylpentanoic acid (4.69g, 36.12 mmol) and water (50 mL). The experimental details were as for (26) to yield an orange crystalline solid product. **Yield** 3.18g (85%). **M. Pt.** 81-86°C

Microanalyses : Found C, 42.6, H, 6.81 ; Calc. for $Ce_6O_{36}C_{98}H_{190}$, C, 42.3, H, 6.79%.

Infrared (Nujol ν cm^{-1}) : 3624(m), 3190(m,br), 1738(w), 1699(m), 1651(w), 1645(w), 1634(w), 1538(m), 1412(m), 1311(w), 1262(m), 1239(m), 1183(m), 1091(w), 923(w), 892(w), 855(w), 823(w), 786(w), 740(w), 654(w), 577(m), 526(w), 398(m).

Infrared (hexachlorobutadiene ν cm^{-1}) : 3626(m), 3191(m,br), 2963(s), 2934(m), 2873(m), 1699(m), 1476(s), 1412(s), 1376(m), 1362(m), 1315(w), 1291(w), 1231(m), 1184(m), 1094(w), 892(w), 578(m), 526(w), 402(m), 323(w).

^{1}H NMR (90 MHz, C_6D_6, 20°C) : δ 1.01 (3H, t, CH_3), 1.29 (6H, s, $C(C\underline{H}_3)_2$), 1.57 (4H, m, CH_2).

^{13}C NMR (22.65 MHz, C_6D_6, 20°C) : δ 9.8 (s,CH_3 unidentate), 15.1 (s, CH_3), 18.7 (s, $C(\underline{C}H_3)_2$), 21.7 (s, $C(\underline{C}H_3)_2$ unidentate), 25.6 (s, CH_2), 31.7 (s, CH_2 unidentate), 43.5 (s, $\underline{C}(CH_3)$), 46.6 (s, $\underline{C}(CH_3)$ unidentate), 185.2 (s, CO).

Mass Spectrometry : 1225 $[Ce_7O_{10}(O_2C_2Me_2)]$(2%), 1141 $[Ce_7O_{10}]$(5%), 1096 $[Ce_6O_9(O_2C_2Me_2CH_2CH_2)]$(4%), 983 $[Ce_6O_9]$(5%), 967 $[Ce_6O_8]$(8%), 811 $[Ce_5O_7]$(3%), 724 $[(CeO)_3(dmp)_2]$(3%), 483 $[Ce_3O_4]$(7%), 441 $[(CeO)_2(dmp)]$(5%), 397 $[Ce(dmp)_2]$(3%), 354 $[Ce(dmp)(O_2C_2Me_2)]$(2%), 329 $[Ce_2O_3]$(3%), 286 [CeO(dmp)](2%).

Solubility : Soluble in dmso, chloroform and benzene, insoluble in hexane, alcohols and acetonitrile.

STA data : TGA : 143-210°C (22.9%), 477-517°C (46.6%), Res 25.4%, $T_{50\%}$ 480°C . DSC : 81, 177, 506°C.

Synthesis of $CeO(mb)_2$ (28)

CAN (5.0g, 9.03 mmol) was dissolved in distilled water (20 mL) at R.T., which was followed by the dropwise addition of a colourless solution of NaOH (1.45g, 36.12 mmol), 2-methylbutyric acid (3.65g, 36.12 mmol) and water (50 mL). The experimental details were as for (23) to yield a yellow crystalline solid. **Yield** 3.0g, (93%). **M. Pt.** dec. 198-205°C

Microanalyses : Found C, 32.5 , H, 5.12 ; Calc. for $Ce_6O_{32}C_{60}H_{110}$, C, 33.0, H, 5.04%.

Infrared (Nujol νcm^{-1}) : 3632(m), 1709(s), 1672(m), 1561(s), 1414(s), 1307(m), 1156(w), 1105(w), 1088(w), 1013(m), 983(m), 967(m), 944(m), 855(w), 796(w), 741(m), 724(w), 655(w), 568(m), 521(w), 400(m), 307(m).

Infrared (hexachlorobutadiene ν cm^{-1}) : 3633(m), 3436(m), 2967(m), 2935(m), 2876(m), 1708(m), 1667(w), 1561(m), 1467(s), 1417(s), 1367(m), 1309(m), 1274(w), 1172(m), 1106(w), 1089(w), 894(w).

^{1}H NMR (90 MHz, C_6D_6, 20°C) : δ 0.86 (3H, t, terminal CH_3), 1.04 (3H, s, α-sub CH_3), 1.38 (1H, m, CH_2), 1.61 (1H, m, CH_2), 2.16 (1H, m, CH).

^{13}C NMR (22.65 MHz, C_6D_6, 20°C) : δ 11.9 (s, CH_3), 13.6 (s, CH_3), 27.0 (s, CH_2), 42.4 (s, CH), 183.3 (s, CO).

Mass Spectrometry : 1467 [Ce_9O_{13}](32%), 1311 [Ce_8O_{12}](29%), 1139 [Ce_7O_{10}](29%), 1068 [Ce_2(mb)$_7O_5$](11%), 983 [Ce_6O_9](24%), 968 [Ce_6O_8](2%), 655 [Ce_4O_6](11%), 483 [Ce_3O_4](23%), 413 [$(CeO)_2$(mb)](5%), 342 [Ce(mb)$_2$](11%), 329 [Ce_2O_3](11%), 258 [CeO(mb)](18%).

Solubility : Soluble in hexane, benzene and chloroform, insoluble in dmso, water and alcohols.

STA data : TGA : 133-247°C (13.0%), 451-499°C (30.8%), Res 48.1%, $T_{50\%}$ 460°C . DSC : 155, 185, 219, 480°C.

Synthesis of $CeO(iva)_2$ (29)

CAN (5.0g, 9.03 mmol) was dissolved in distilled water (20 mL) at R.T., which was followed by the dropwise addition of a colourless solution of NaOH (1.45g, 36.12 mmol), isovaleric acid (3.65g, 36.12 mmol) and water (50 mL). The experimental details were as for (23) to yield a yellow crystalline solid. **Yield** 2.81g (87%) **M. Pt.** dec. 220-226°C

Microanalyses : Found C, 32.7, H, 4.94 ; Calc. for $Ce_6O_{32}C_{60}H_{110}$, C, 33.0, H, 5.04%.

Infrared (Nujol ν cm^{-1}) : 3639(w), 3612(w), 1711(w), 1265(m), 1311(w), 1265(m), 1169(w), 1124(w), 972(m), 935(w), 891(w), 840(w), 643(shoul), 564(m), 511(w), 432(w), 357(w), 274(w).

Infrared (hexachlorobutadiene ν cm^{-1}) : 3626(w), 2957(m), 2928(m), 1730(m), 1710(m), 1565(m), 1431(m), 1327(w), 1264(w), 1239(w), 1170(w), 1107(w), 1037(m), 893(w).

^{1}H NMR (90 MHz, $CDCl_3$, 20°C) : δ 0.91 (s, 6H, CH_3), 1.99 (s, 2H, CH_2), 2.01 (1H, m, CH).

^{13}C NMR (22.65 MHz, $CDCl_3$, 20°C) : δ 23.9 (s, CH_3), 26.8 (s, CH_2), 46.6 (s, CH), 180.9 (s, CO), 181.2 (s, CO).

Mass Spectrometry : 772 [$(CeO)_3$(iva)$_3$](5%), 701 [Ce_3O_5(iva)$_2$](5%), 530 [Ce_2O_3(iva)$_2$](4%), 483 [Ce_3O_4](3%), 461 [Ce_2O_5(iva)](3%), 410 [$(CeO)_2$(iva)](3%), 354 [$(CeO)_2(O_2C)$](35%), 329 [Ce_2O_3](6%), 258 [CeO(iva)](6%).

Solubility : Soluble in hexane, benzene and chloroform, insoluble in dmso, water and alcohols.

Synthesis of $CeO(heptanoate)_2.1.67$(heptanoic acid) (30)

CAN (5.0g, 9.03 mmol) was dissolved in distilled water (20 mL) at R.T., which was followed by the dropwise addition of a colourless solution of NaOH (1.45g, 36.12 mmol), isovaleric acid (3.65g, 36.12 mmol) and water (50 mL). The experimental details were as for (26) and yielded a very wet yellow solid. **Yield** 5.15g (84%)

Microanalyses : Found C, 48.2 , H, 7 27 ; Calc. for $Ce_6O_{52}C_{154}H_{298}$, C, 48.4 , H, 7.80 %.

Infrared (Nujol vcm^{-1}) : 3641(m), 3397(s), 1713(s), 1515(s,br), 1320(s), 1301(s), 1188(m), 1109(m), 1012(w), 938(m), 891(w), 793(m), 764(m), 694(m), 647(m), 563(s), 458(m), 398(m), 316(m).

Infrared (hexachlorobutadiene v cm^{-1}) : 3640(m), 3398(s), 2933(s), 2858(s), 1713(s), 1510(s,br), 1413(s,br), 1329(s), 1287(s), 1240(s), 1173(s), 1109(m), 892(m), 564(s), 458(m), 402(s).

^{1}H NMR (90 MHz, $CDCl_3$, 20°C) : δ 0.84 (3H, s, CH_3), 1.15 (6H, s, $C\underline{H_2}$), 1.48 (2H, s, $O_2CCH_2C\underline{H_2}$), 2.28 (2H, m, $O_2CC\underline{H_2}$).

^{13}C NMR (22.65 MHz, $CDCl_3$, 20°C) : δ 15.1 (s, CH_3), 23.7, 26.1, 30.0, 32.6, 36.4 (s, CH_2), 181.4 (s, CO).

Mass Spectrometry : 1039 [$(OCe)_5(hept)_2$](2%), 1008 [$O_3Ce_5(hept)_2$](2%), 984 [Ce_7O_9](2%), 963 [Ce_7O_8](2%), 908 [$(OCe)_5(hept)$](1%), 855 [$(OCe)_3(hept)_3$](2%), 829 [O_8Ce_5](2%), 823 [$OCe_3(hept)_3$](2%), 811 [Ce_5O_7](2%), 725 [$(OCe)_3(hept)$](4%), 656 [Ce_4O_6](5%), 570 [$(OCe)_2(hept)_2$](4%), 555 [$OCe_2(hept)_2$](2%), 525 [$Ce(hept)_3$](2%), 483 [Ce_3O_4](20%), 441 [$(OCe)_2(hept)$](11%), 398 [$Ce(hept)_2$](4%), 329 [Ce_2O_3](12%), 286 [$OCe(hept)$](6%).

Solubility : Soluble in benzene and chloroform, insoluble in dmso, water and alcohols.

STA data : TGA : 158-210°C (28.3%), 379-406°C (47.0%), Res. (21.5%), $T_{50\%}$ 384°C. DSC : 132, 197, 398°C.

Synthesis of $[Ce(OH)_2(pfb)_2]_n$ (31)

CAN (5.0g, 9.03 mmol) was dissolved in distilled water (20 mL) at R.T., which was followed by the dropwise addition of a colourless solution of NaOH (1.45g, 36.12 mmol), heptafluorobutyric acid (7.73g, 36.12 mmol) and water (40 mL). The experimental details were as for (26) to yield a pale yellow solid product. **Yield** 4.62g, (85%) **M. Pt.** dec. 275-280°C

Microanalyses : Found, C, 15.2 ; H, 0.34 ; Calc. for $CeF_{14}O_6C_8H_2$, C, 16.0 ; H, 0.33 %.

Infrared (Nujol v cm^{-1}) : 3688(m), 3627(w), 3363(w,br), 1733 (vw), 1670(w), 1570(shoul), 1441(s), 1277(m), 1219(m), 1170(m), 1121(m), 1087(m), 971(m), 938(m), 891(m), 817(m), 764(w), 741(w), 587(m), 573(m), 526(m), 457(w).

Infrared (hexachlorobutadiene v cm^{-1}) : 3687(m), 3667(m), 3618(w), 3408(m,br), 1671(m), 1441(m), 1385(m), 1346(m), 1230(s), 1170(s), 1122(m), 1088(w), 1039(w), 893(w), 719(w), 571(m).

^{1}H NMR (90 MHz, D_6dmso, 20°C) : δ 3.42 (br, OH).

^{13}C NMR (22.65 MHz, D_6dmso, 20°C) : δ 108.3 (triplet, $C\underline{F_2}CF_2$, ^1J = 266, ^2J = 38Hz), 108.9 (triplet of multiplets, $C\underline{F_2}CF_3$ ^1J = 268, ^2J = 37Hz), 117.9 (quartet of triplets, CF_3 ^1J = 287, ^2J = 34Hz), 158.9 (s, CO).

Mass Spectrometry : 1093 [$(CeO)_3(pfb)_3$-F](5%), 1073 [$(CeO)_3(pfb)_3$-F_2](4%), 895

[$(CeO)_3(pfb)_2$](6%), 874 [$(CeO)_3(pfb)_2$-F](6%), 699 [$Ce_4O_5F_3$](7%), 503 [Ce_3O_4F](5%), 350 [Ce_2O_3F](3%), 331 [Ce_2O_3](7%), 259 [$Ce(O_2CCF_2C_2)$](15%), 245 [$Ce(O_2CCF_2C)$](40%).

Solubility : Soluble in alcohols, chloroform and dmso, insoluble in benzene and hexane.

STA data : TGA : 193-220°C (22.4%), 268-327°C (43.4%), Res. 24.1%, $T_{50\%}$ 298°C. DSC : 210, 339°C(exotherm).

Synthesis of $[Ce(OH)_2(pfp)_2]_n$ (32)

CAN (10.8g, 19.50 mmol) was dissolved in distilled water (20 mL) at R.T., which was followed by the dropwise addition of a colourless solution of NaOH (3.12g, 78.05 mmol), pentafluoropropionic acid (12.80g, 78.05 mmol) and water (50 mL). The solution was stirred for 30 mins. to yield a pale yellow insoluble layer below a yellow soluble layer. The solid was filtered and washed with water (2 x 10 mL) and dried on a Buchner for 2 hours, to yield a pale yellow solid. **Yield** 7.31g, (78%) **M. Pt.** dec. 270-273°C

Microanalyses : Found, C, 13.8 ; H, 0.45 ; Calc. for $CeF_{10}O_6C_6H_2$, C, 14.4 ; H, 0.40 %.

Infrared (Nujol ν cm^{-1}) : 3667(m), 3621(m), 3606(m), 3278(m,br), 1673(s), 1615(w), 1571(shoul), 1330(s), 1221(m), 1176(m), 1038(m), 822(m), 778(w), 585(m), 559(m), 542(m), 426(m), 361(w).

Infrared (hexachlorobutadiene ν cm^{-1}) : 3685(w), 3605(w), 3368(m,br), 1674(m), 1442(m), 1330(m), 1219(m), 1173(s), 1036(s), 893(w), 734(w), 559(m), 542(m), 424(w), 388(w).

^{1}H NMR (90 MHz, D_6dmso, 20°C) : δ 3.61 (br, OH).

^{13}C NMR (22.65 MHz, D_6dmso, 20°C) : δ 107.2 (triplet of quartets, CF_2, ^1J = 264, ^2J = 37Hz), 118.7 (quartet of triplets, CF_3, ^1J = 286, ^2J = 35Hz), 159.1 (s, CO).

Mass Spectrometry : 1093 [$(CeO)_3(pfb)_3$-F](1%), 1071 [$(CeO)_3(pfb)_3$-F_2](3%), 1049 [$(CeO)_3(pfb)_3$-F_3](4%), 896 [$(CeO)_3(pfb)_2$](1%), 874 [$(CeO)_3(pfb)_2$-F](3%), 852 [$(CeO)_3(pfb)_2$-F_2](3%), 833 [$(CeO)_3(pfb)_2$-F_3](1%), 724 [$Ce_4O_5F_4$](2%), 699 [$Ce_4O_5F_3$](2%), 677 [$Ce_4O_5F_2$](2%), 658 [Ce_4O_5F](2%), 640 [Ce_4O_5](1%), 524 [$Ce_3O_4F_2$](2%), 505 [Ce_3O_4F](4%), 483 [Ce_3O_4](3%), 413 [$CeOH(pfp)(O_2C_2F_2)$](4%), 329 [Ce_2O_3](17%).

Solubility : Soluble in thf, alcohols and dmso, insoluble in chloroform, benzene and hexane.

STA data : TGA : 156-244°C (32.2%), 244-302°C (28.6%), Res. 27.4%, $T_{50\%}$ 296°C. DSC : 194.4°C, 289.7°C(exotherm).

Synthesis of $[Ce(OH)_2(tfa)_2]_n$ (33)

CAN (10.0g, 18.06 mmol) was dissolved in distilled water (20 mL) at R.T., which was followed by the dropwise addition of a colourless solution of NaOH (2.89g, 72.22

mmol), trifluoroacetic acid (8.23g, 72.22 mmol) and water (40 mL). The solution was stirred for 30 mins. to yield a pale yellow insoluble layer below a yellow soluble layer. The solid was filtered and washed with water (2 x 10 mL) and dried on a Buchner for 2 hours, to yield a pale yellow solid. **Yield** 4.84g (67%) **M. Pt.** dec. 263-265°C (explodes)

Microanalyses : Found, C, 11.7 ; H, 0.63 ; Calc. for $CeF_6O_6C_4H_2$, C, 12.0 ; H, 0.50 %.

Infrared (Nujol ν cm^{-1}) : 3702(m), 3655(m), 3626(m), 3613(m), 3578(m), 3480(w), 3361(w), 3158(m), 1675(s), 1600(m), 1409(m), 1206(s), 1132(s), 849(m), 795(m), 724(s), 618(m), 545(m), 448(m), 410(m), 318(m).

Infrared (hexachlorobutadiene ν cm^{-1}) : 3656(w), 3579(w), 3366(w), 2924(w), 1677(m), 1472(m), 1385(w), 1170(m), 894(w), 725(m), 617(m).

FT Raman (cm^{-1}) : 357(s), 317(w), 289(w), 167(s).

^{1}H NMR (90 MHz, D_6dmso, 20°C) : δ 4.90 (br, OH).

^{13}C NMR (22.65 MHz, D_6dmso, 20°C) : δ 117.1 (quartet, CF_3, ^1J = 293Hz), 159.1 (quartet, CO, ^2J = 35Hz).

Mass Spectrometry : 896 $[(CeO)_3(pfb)_2]$(1%), 874 $[(CeO)_3(pfb)_2\text{-}F]$(3%), 855 $[(CeO)_3(pfb)_2\text{-}F_2]$(3%), 699 $[Ce_4O_5F_3]$(3%), 677 $[Ce_4O_5F_2]$(4%), 658 $[Ce_4O_5F]$(3%), 525 $[Ce_3O_4F_2]$(3%), 506 $[Ce_3O_4F]$(4%), 484 $[Ce_3O_4]$(4%), 329 $[Ce_2O_3]$(7%).

Solubility : Soluble in dmso, acetonitrile, alcohols and thf, insoluble in chloroform, benzene and hexane.

STA data : TGA : 60-253°C (29.9%), 259-269°C (63.4%), Res. 9.21%, $T_{50\%}$ 261°C. DSC : 162°C, 225°C, 262.0°C(exotherm).

Synthesis of deuterated '$CeO(eb)_2$' (34)

CAN (5.0g, 9.03 mmol) was placed in a Schlenk tube and flame dried until it turned a deep red colour, indicating the removal of water impurities. This was then dissolved in D_2O (12 mL) and a solution of 2-ethylbutyric acid (4.19g, 36.12 mmol) and NaOH (1.44g, 36.12 mmol) in D_2O (25 mL) added dropwise. The mixture was stirred for 30 mins. at R.T. and the resultant yellow solid filtered, washed with D_2O (10 mL) and dried *in vacuo* at 70°C. The solid was redissolved in benzene (20 mL) and stirred for 30 mins. at 50°C, then stripped dry. This procedure was repeated to yield a yellow solid. **Yield** 2.26g (65%)

Microanalyses : Found, C, 36.9 ; H, 6.01 ; Calc. for $CeO_5C_{12}H_{22}$, C, 37.3 ; H, 5.70 %.

Infrared (Nujol ν cm^{-1}) : 1705(m), 1651(w), 1563(m), 1558(m), 1506(m), 1416(m), 1316(m), 1261(m), 1154(w), 1096(w), 1044(m), 974(w), 936(w), 845(w), 805(w), 674(w), 641(w), 616(w), 571(m), 523(w), 501(w).

Infrared (Hexachlorobutadiene v cm ^{1}) : 3636(m), 3153(w,br), 2963(s), 2933(m), 2875(w), 2681(m), 2264(w), 1704(m), 1683(w), 1653(m), 1558(s), 1463(m), 1415(s), 1385(m), 1329(w), 1316(w), 1292(w), 1260(w), 1248(w), 1170(m), 1137(w), 1097(w), 893(w), 572(m), 522(w).

^{1}H NMR (270 MHz, $CDCl_3$, 20°C) : δ 1.03 (6H, t, CH_3), 1.62 (4H, br, CH_2), 2.36 (1H, br, CH).

^{13}C NMR (67.94 MHz, $CDCl_3$, 20°C) : δ 12.8 (s, CH_3), 24.3 (s, CH_2), 50.2 (s, CH), 182.6 (s, CO).

Mass Spectrometry (FAB +) : 1083 $[CeO(eb)]_4$(5%), 984 $[Ce_4O_5(eb)_3]$(6%), 969 $[Ce_6O_8]$(4%), 811 $[Ce_5O_7]$(8%), 656 $[Ce_4O_6]$(2%), 641 $[Ce_4O_5]$(2%), 542 $[CeO(eb)]_2$(2%), 484 $[Ce_3O_4]$(31%), 427 $[(CeO)_2(eb)]$(15%), 329 $[Ce_2O_3]$(11%), 272 [CeO(eb)](5%).

Solubility : Soluble in hexane, benzene and chloroform, insoluble in dmso, water and alcohols.

Synthesis of $[Ce(O)_{0.25}(eb)_{3.5}]$ (35)

CAN (2.0g, 3.61 mmol) was placed in a Schlenk tube and flame dried until it turned a deep red colour, indicating the removal of water impurities. This was then dissolved in dme (25 mL) and a solution of 2-ethylbutyric acid (1.81 mL, 14.45 mmol) added. A steady stream of ammonia was added to the mixture for 30 mins. at R.T. to yield a soluble yellow solution and an insoluble cream solid. The ammonium nitrate residue was filtered and the solution stripped to dryness yielding an orange solid. This was then dissolved in toluene (15 mL) and heated to *ca.* 80°C whereupon it became soluble. Any remaining residues were filtered and the solution stripped dry to yield a yellow / brown solid. **Yield** 1.23g (62%)

Microanalyses : Found, C, 45.9 ; H, 7.15 ; Calc. for $CeO_{7.25}C_{21}H_{38.5}$, C, 46.1 ; H, 7.04 %.

Infrared (Nujol v cm^{-1}) : 3634(w), 1708(s), 1515(s), 1413(m), 1310(m), 1259(m), 1154(m), 1095(m), 1020(m), 939(m), 862(w), 811(m), 803(m), 655(w), 531(m), 376(m).

^{1}H NMR (270 MHz, $CDCl_3$, 20°C) : δ 1.17 (21H, t, CH_3), 2.04 (14H, br, CH_2), 3.11 (3.5H, br, CH), 12.13 (0.5H, br, OH).

^{13}C NMR (67.94 MHz, $CDCl_3$, 20°C) : δ 12.8 (s, CH_3), 24.3 (s, CH_2), 50.2 (s, CH), 182.6 (s, CO).

Mass Spectrometry (FAB +) : 484 $[Ce_3O_4]$(5%), 427 $[(CeO)_2(eb)]$(4%), 329 $[Ce_2O_3]$(4%).

Solubility : Partially soluble in hot toluene, soluble in chloroform and dmso, insoluble in hexane and benzene.

Chapter 6

COORDINATION CHEMISTRY OF HYDROCARBYL CERIUM (IV) CARBOXYLATES

A multitude of reactions has been performed to elucidate the coordination chemistry of the hydrocarbyl cerium(IV) carboxylates, including reactions with oxygen and nitrogen donor ligands, neutral and potentially charged ligands. The following Chapter describes some representative reactions and the characterization of the resultant products.

6.1 Introduction

Although the chemistry of lanthanide carboxylates is rather limited, that of the β-diketonates is far more diverse. In recent years, the electronic and ceramic industries have become increasingly interested in the properties of the rare earth metal complexes, especially the diketonates which have good solubilities and volatilities with transition metal and Group 2 metal chelates, often an important consideration. Indeed there are currently studies concerning the use of lanthanide diketonate complexes in the formation of thin mixed metal oxide films which have electronic properties.[242] Lanthanide diketonates are also widely used as laser chelates[179] and lanthanide shift reagents.[175]

Lanthanide β-diketonates have been combined with a large number of coordinating ligands including carboxylates.[243] In many cases these reactions form mixed diketonate / carboxylate species with a wide range of metals. However, once again, the chemistry is centred on the tervalent metals and no crystallographically characterized cerium(IV) compounds have been reported.

Much of the work in this area has involved the synthesis of new europium chelates. In 1964, Charles *et al.* prepared the mixed chelate-acetate compound $[Eu(dppd)_2(OAc).n(HOAc)]$ (n=0-1),[244] by mixing an aqueous solution of sodium acetate and europium chloride. An ethanolic solution of dppd-H was added to yield a yellow precipitate, which on separation and purification gave a solid with a melting point of 269-270°C. Sinha and co-workers have also synthesized the same product by a similar synthesis.[245] The analogous propionate and benzoates have also been prepared by Charles.[244]

In the IR of the above Eu compounds the wavenumber difference between the anti- and symmetric νOCO vibrating frequencies is 100-120cm^{-1}, indicating that the coordinated carboxylates are most likely to be bridging, thus the complexes have a dimeric or polymeric structure.[244] The carboxylate groups in these mixed ligand compounds are assumed to have a tridentate bridging cyclic function. The thermal behaviour of Charles' three compounds has been studied with the result that the heat stability of the complexes

decreases in the order: acetate > propionate > benzoate, as judged by the temperatures at which weight loss first became apparent. Various other compounds of the same form have been prepared using different diketonates with different substituent R groups, for example, R = Ph, R' = CH_3; R = Ph, R' = PhOH and R = CF_3, R' = C_4H_3S.[245] Infrared and solubility studies of these compounds suggest that they possess oligomeric structures.

The related mixed chelate complex $[Y_2(\mu\text{-OAc})_2(pd)_4(H_2O)_2]$ was prepared by Hubert-Pfalzgraf *et al.* by reacting yttrium isopropoxide $[Y_5(OPr^i)_{13}]$ with excess 2,4-pentanedione at R.T. under anhydrous conditions, giving a high yield (*ca.* 85%) compound.[246] The molecule is a centrosymmetric dimer with chelating tridentate acetato-groups in the bridging positions. The yttrium atoms are eight coordinate with a distorted square-antiprismatic geometry. There is intermolecular hydrogen bonding between the water and diketonate ligands. The origin of the acetato ligand is most likely the pentanedionate ligand, whose generation is a retro-Claisen type reaction,[247] induced by a trace amount of alkoxo or hydroxo anions (thus water may result from subsequent reactions) stabilized by a highly basic medium. The equivalent reaction with neodymium isopropoxide gives $[Nd(pd)_{10}(\mu_3\text{-OH})]$.[248] Similar reactions occur with fluorinated β-diketonates, however this will be further discussed in section 7.1.

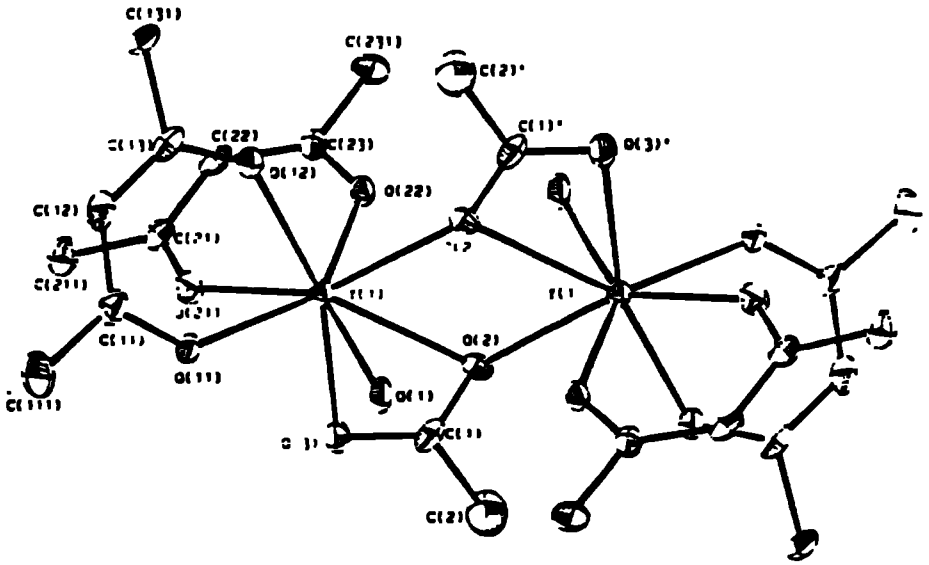

Figure 6.1 : X-ray crystal structure of $[Y_2(\mu\text{-OAc})_2(pd)_4(H_2O)_2]$

A further example of lanthanide carboxylates coordinated to oxygen donor ligands are the urea adducts.[249] The molecular structure of $[La(OAc)_3.2(CH_4N_2O)]$ involves a metal with a coordination polyhedron that consists of oxygen atoms from the acetate groups and one of the urea molecules, forming a ten coordinate metal centre.[250] The Pr[251] and Nd[252] analogues, $[M(OAc)_3.3urea.(H_2O)]$, are dimeric species with the metals in nine vertex polyhedra formed by oxygen donors from the acetate groups and two of the three urea molecules. The acetate ligands all bond in different ways, one is didentate bridging, one is didentate cyclic and one tridentate bridging cyclic. The coordination geometries of the metals are both singly capped square-antiprismatic.

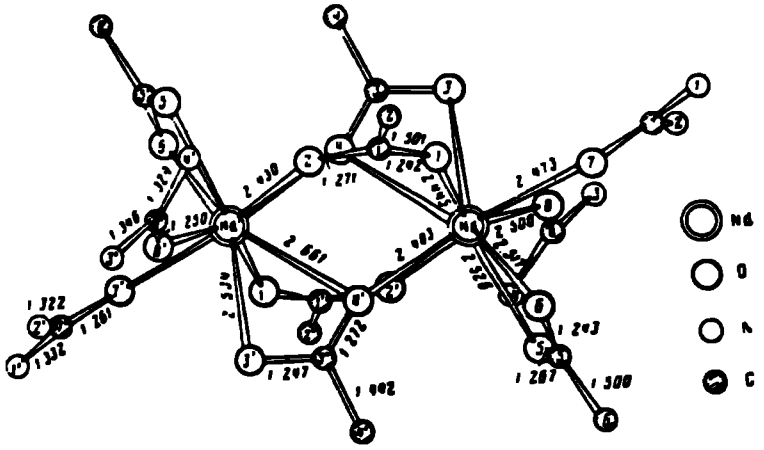

Figure 6.2 : X-ray crystal structure of $\{Nd(OAc)_3[CO(NH_2)_2]_2\}$

Lanthanide carboxylates also form coordination compounds with nitrogen donor ligands. An ethanolic solution of Ln(III) nitrate hexahydrate (Ln = all lanthanides except Pm and La) was treated with an ethanolic solution of sodium acetate trihydrate (1:3 molar ratio) and the sodium nitrate precipitate removed by filtration.[253] To the resultant solution an ethanolic solution of 1,10-phenanthroline (0.9 : 1 / ligand : metal ratio) was added to yield a crystalline complex after 24 hours. The yields of $[M(OAc)_3(phen)]$ varied from 80 (Pr) to 20%(Ce). The compounds are all insoluble in common organic solvents (as are the majority of Ln(III) compounds) but only sparingly soluble in hot water, they are also thermally stable, decomposing between 260 and 300°C. The coordination numbers are assumed to be eight, but IR data do not allow unambiguous assignment of the bonding mode of the acetate ligands, however, Δv values suggest they are unlikely to be unidentate.

The related diketonate compound, $[Eu(tmhd)_3(dmop)]$ (where dmop = 2,9-

dimethyl-1,10-phenanthroline) has been structurally characterized, the structure containing two geometric isomers in the unit cell, the metal is eight coordinate with the ligating atoms forming a distorted square antiprism.[254] The average Eu-O and Eu-N bond lengths are 2.363(5) and 2.678(5)Å, respectively.

The benzoate compound $[Eu(phen)_2(benz)_3]$ was prepared by the reaction of an aqueous solution of sodium benzoate with an aqueous solution of europium(III) chloride and 1,10-phenanthroline (3 : 1 : 2 molar ratio).[255] Alternatively the Gd, Eu and Tb acetates $[Ln(OAc)_3(phen)]$, are made by adding phen to a solution of lanthanide acetate in hot dmso.[256]

The 2,2-dipyridyl analogues of Pr, Nd and Yb have also been synthesized by Hart *et al.* in similar syntheses to those of the phenanthroline complexes.[257] Higher yields are observed for the bipy complexes (*ca.* 90%). All attempts to synthesize the La and Ce analogues resulted in the formation of impure products. The thermal stability of the bipy compounds is lower than that of the phen complexes, the decomposition points lying between 240 and 250°C.

Finally, the macrocyclic phthalocyaninato ligand has also been used to prepare mixed lanthanide acetato complexes.[258] The coordination geometry of the metal in $[Lu(III)Pc(OAc)(H_2O).H_2O.MeOH]$ is a distorted square antiprism. The eight donor atoms consist of four isoindole nitrogens of the Pc ring, two oxygens of an asymmetrically chelating acetate and two oxygens of two water molecules. The Lu-N bonds range between 2.333(3) and 2.359(3)Å, whereas the Lu-$O_{(OAc)}$ bonds are longer, 2.366(3) and 2.426(3)Å. Cerium(IV) compounds with this type of ligand are rare as the metal generally oxidizes the phthalocyaninato to phthalimide, unless the pc ligand is sulphonated.[259]

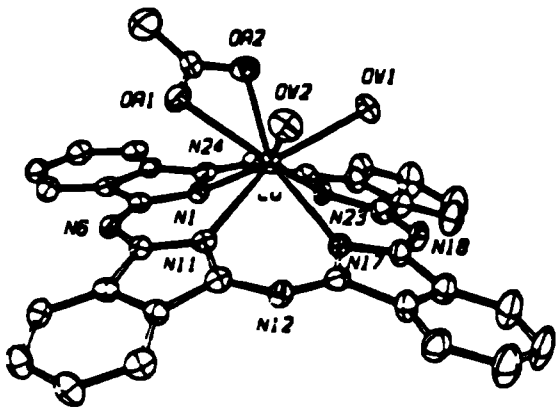

Figure 6.3 : X-ray crystal structure of $[LuPc(OAc)(H_2O)_2]$

6.2 Synthesis of hydrocarbyl carboxylate coordination compounds

The general synthetic procedure for the preparation of the hydrocarbyl cerium(IV) carboxylate coordination compounds described in this Chapter involves dissolving the oxo-*bis* carboxylate species in a suitable solvent. For the hydrocarbon mono-α-substituted compounds, e.g. (23) and (24) this solvent was either hexane or benzene, whereas for the di-α-substituted compounds such as (27) the solvent media used was usually chloroform. After dissolution of the cerium oxo-*bis* carboxylate species, the coordinating ligand was added and the reaction mixture refluxed for 2-9 hours, depending on the reactants. The solvent media were then removed *in vacuo* to yield the resultant product. Many crystalline products suitable for X-ray crystallographic analysis were grown, generally yielding either yellow or orange symmetrical blocks, ranging in size from *ca.* 0.2 - 5mm. However each of the crystals produced a very weak and poorly defined X-ray diffraction pattern from which no adequate data could be obtained.

The most likely reason for the ill-defined diffraction patterns is that there is such a large degree of ligand distortion over the entire structure due to the length and number of carboxylate groups. Attempts to make the carboxylates more 'rigid' by introducing possible hydrogen bonding sites on both the carboxylate and the coordinating ligand failed to give crystals which produced better diffraction patterns. Such ligands that were used included substituted dipyridyl and phenanthroline ligands and also hydroxy- and amino-substituted carboxylic acids. Using smaller carboxylic acids, such as pivalic and isobutyric acids, generally resulted in the formation of insoluble yellow powders.

Potentially charged coordination ligands included alcohols and phenols. The reactions with these ligands proved to be very different to those with the fluorinated carboxylates (see Chapter 7). Firstly, aliphatic primary, secondary and tertiary alcohols did not produce any coordinated alcoholic complexes; in fact none of the hydrocarbyl oxo-*bis* carboxylate compounds have any degree of solubility in alcohols. The alcohols were added in both stoichiometric and excess amounts; however, on removal of the solvent media, spectroscopic methods (most notably ^{13}C NMR) showed that the alcohol was absent.

In contrast, the reaction of the hydrocarbyl cerium(IV) carboxylates with phenols (including substituted phenols) produced somewhat different results. It is well known that phenol can be oxidized to the corresponding quinone giving a black glassy material. The reaction of (23) and (24) with phenol displays their oxidizing nature as the resultant

compounds are black insoluble glasses. These oxidized products are also yielded from the analogous reactions with 4-tertbutyl- and 3,5-ditertbutylphenol. However, with both (23) and (24), brightly coloured compounds (such as red, yellow and orange) are formed when sterically crowded disubstituted phenols are used. These phenols include 2,6-ditertbutyl-, 2,6-diisopropyl-, 2,4-ditertbutyl- and 2,4-diisopropylphenol. It is noteworthy that the phenols are not oxidized when there is a substituent at either the 2 or 6-position. This is most likely to be due to the steric encumbrance at the metal centre imposed by the large organic groups at the *ortho* positions, a factor which is not observed when there are only substituents at the *meta* and *para* positions. This factor precludes the oxidation of the phenol and results in the observed cerium(IV) phenoxide complexes.

On analysis of the brightly coloured metal species formed from the reaction of the sterically crowded phenols and $[CeO(eb)_2]$ (23), it was determined that they are no longer carboxylate species. In fact it appears that the carboxylate ligands are completely removed from the metal centre and are replaced by the substituted phenols, to give $[Ce(phenol')_4]_n$ type species (e.g. compounds (49) and (50)) as shown by spectroscopic analyses. This is, however, not necessarily the only scenario, however, as species such as $[CeO(mv)_2$(2,6-diPr^{i}phenol).(mv-H)] (51) may also be synthesized with the liquid cerium carboxylate complex (24).

The neutral 1,10-phenanthroline and 2,2-dipyridyl ligands readily form coordination compounds with the cerium(IV) carboxylates, as they do with the tervalent lanthanide carboxylates previously noted above.[253,257] These compounds often give crystalline products which, unfortunately, do not give sufficiently good diffraction patterns for X-ray analyses. These reactions also occur readily with oxide ligands such as pyridine-*N*-oxide (40) and triphenylphosphine oxide. Although cerium(IV) is quite a powerful oxidizing agent (as has been shown above with phenol), the carboxylates do not oxidize the macrocyclic amines to amine-oxides as might be suggested. However, with pmdeta, an aliphatic amine, an insoluble white solid is observed in a *ca.* 25% yield, along with the brown product (see compound (39)). This white residue is $[Ce(III)(eb)_3.2(H_2O)]$. The NMR spectra of the amine complexes, especially with the aliphatic amines, are often broader, inferring a higher proportion of Ce(III) with respect to Ce(IV) in the complex.

Two ways in which the liquid carboxylates (24) and (25) differ from their solid counterparts are shown when their coordination products are treated with pyridine and glyme ligands. Whereas the solid carboxylate compound (38) has half a coordinated pyridine molecule associated, the equivalent reaction with $CeO(eh)_2.2(ehH)$ (25) yields a

gummy solid which is formulated as $[CeO(eh)_2(ehH)_{0.75}]$ on the basis of microanalysis. Also, when the product from the reaction of $CeO(eh)_2.2(ehH)$ (25) and heptaglyme (0.5 equivalents) is washed with sodium nitrate solution, the heptaglyme is removed, leaving a yellow solid which would appear to have the formula $[CeO(eh)_2(ehH)_{0.16}]$.

6.2.1 Synthesis of mixed carboxylate / β-diketonates

A number of europium chelates have been synthesized, as discussed above, by preparing an aqueous solution of sodium acetate and europium(III) chloride and adding an ethanolic solution of dppd-H (or other diketonate such as bzpd-H or ttfa-H), c.f. the preparation of $[Eu(dppd)_2(OAc).n(HOAc)]$.[244] All of these syntheses have, however, concentrated on the tervalent metals and no mixed chelate complexes have been reported with Ce(IV). Also, direct comparisons with the tervalent chloride synthesis described above may not be drawn as cerium tetrachloride is unstable.

With the cerium carboxylates described in this Chapter the synthesis of the mixed chelate species can take many forms:

(i) The *tetrakis* β-diketonate may be preformed and an equimolar amount (by metal) of oxo-*bis* carboxylate $[CeO(RCO_2)]$ added.

(ii) The *tetrakis* β-diketonate may be preformed and an equimolar amount (by metal) of oxo-*bis* carboxylate $[CeO(RCO_2)]$ added together with two molar equivalents of carboxylic acid (i.e. giving equal amounts of both diketonate and carboxylate ligand).

(iii) The *tetrakis* β-diketonate may be preformed and 1-4 molar equivalents of carboxylic acid may be added.

(iv) The carboxylate $[CeO(RCO_2)]$, may be preformed and 1-4 molar equivalents of β-diketone may be added.

(v) A dilute aqueous (or alcoholic) solution of sodium hydroxide, carboxylic acid and β-diketone (4 : x : 4-x molar ratio) may be added, dropwise, to a concentrated aqueous (alcoholic) solution of CAN, at either R.T. or -70°C

The underlying problem with these syntheses is the preference for the formation of the *tetrakis* β-diketonates which are far more stable than are the carboxylate complexes. Their smaller, often monomeric, structure also makes them easier to form than the oligomeric structures likely to be formed by any mixed chelate species (the inclination of the carboxylate ion to bridge is likely to be very strong). This effect may be limited to a degree by the judicious choice of ligands with either similar, or very dissimilar pKa's. For example, hfpd-H and tfa-H are both very acidic due to the electron withdrawing nature of the fluorinated substituents, while pd-H and dmp-H are significantly less acidic due to the electron donating properties of their substituent groups. However, two separate compounds are almost always formed.

6.2.2 Reaction of cerium (IV) carboxylates with isocyanates

Around the turn of this century a considerable amount of information regarding the fundamental properties of organic isocyanates was amassed. However, it was not until some forty to fifty years later that practical uses of these compounds, in particular their reactivities, were studied in detail. Reactions with active hydrogen compounds, e.g. HX and ROH, are probably the most numerous; however, a number of polymerization reactions have also been studied.[260]

Several catalysts have been used to bring about different degrees of polymerization. In the presence of triethylphosphine most aromatic isocyanates dimerize, presumably to the structure illustrated below for phenyl isocyanate (see Figure 6.4).[261] Cryoscopic molecular weight measurements have been made, estimating the weight of the polymerized phenyl isocyanate to be between 222 and 231g ±16% (i.e. a dimer).[262]

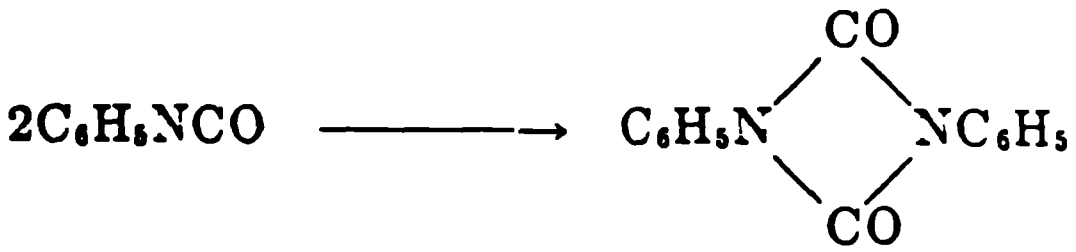

Figure 6.4 : The postulated dimerization of phenyl isocyanate

Using pyridine as the catalyst also produces a dimer,[263] whereas it has been reported that 2,4-toluene diioscyanate slowly forms a dimer on standing at R.T..[264]

In contrast, ethyl isocyanate, when brought into contact with triethylphosphine, trimerizes.[265] This phenomenon has also been shown to occur with other aromatic or aliphatic isocyanates in the presence of catalysts such as triethylamine,[266] peroxides,[264] sodium methoxide,[267] calcium[262] and potassium acetates[268] and sodium formate.[268] The trimerized product has a structure which is presumably based on that of the dimer above. Slotta and Tschesche have reported, however, that methyl isocyanate forms a different type of trimer when the catalyst used is triethylphosphine, i.e. 3,5-dimethyl-2-methylimino-4,6-diketo-1,3,5-trioxadiazine.[269]

Two noteworthy types of catalysts mentioned above are the Group 2 formates and acetates, i.e. carboxylates. The question may be asked, therefore, do cerium carboxylates perform the same catalytic task? Results of experiments in this Chapter have indicated that this is indeed the case. For instance, the reaction between phenyl isocyanate and cerium(IV) 2-ethylbutyrate in benzene (52), results in the precipitation of a white solid from a yellow / orange solution. On reducing the solution to dryness it was found to be the initial starting material, i.e. $[CeO(eb)_2]$, however, phenyl isocyanate is a powerful smelling colourless liquid, yet the precipitate is an innocuous smelling white solid. Different results were noted with the fluorinated carboxylate $[Ce(OH)_2(pfb)_2]$ (31) and phenyl isocyanate, where a dark purple solid was obtained (see Chapter 7).

This may be explained when one considers that the polymerization products of aromatic isocyanates, such as phenyl isocyanate, are medium - high melting solids (e.g. the dimeric form of phenyl isocyanate is observed to melt at 175-176°C).[263] The polymerized product, then, is the nature of the solid precipitates formed from these reactions. Although the extent of polymerization has not been established using the cerium carboxylates as catalysts it is unlikely to be a simple dimer. The melting point of the polymerized solid resulting from reaction (52) is 224-6°C, significantly higher than that observed for the dimeric form. This may be the trimeric form, therefore, synthesized using alkaline metal formates and acetates as catalysts.

Not only may phenyl isocyanate be polymerized in this fashion, but also other aliphatic and aryl isocyanates. For instance the reactions between (23) and (24) with isopropyl isocyanate also gives either white or pink insoluble residues together with the unreacted starting materials. These polymeric isocyanate compounds melt at slightly lower temperatures, *ca.* 160°C.

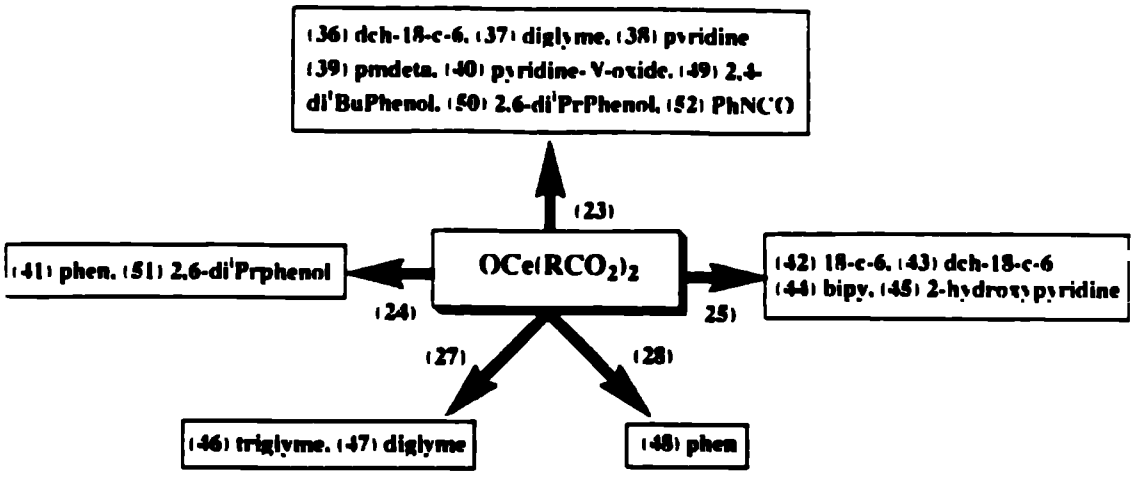

Figure 6.5 : Schematic representation of the synthesis of the hydrocarbyl carboxylate coordination compounds

Reaction conditions: The oxo-*bis* carboxylates were dissolved in hexane (23), benzene ((23), (24), (25), (28)) or chloroform (27) at R.T.. A stoichiometric amount of the coordinating ligand was added to the reaction and the mixture refluxed for 2-9 hours. Any residues were filtered and the resultant filtrate was dried under reduced pressure.

The compoundsdescribed within this Chapter are:
(36) $[CeO(eb)_2(dch18\text{-}crown\text{-}6)]$, (37) $[CeO(eb)_2(diglyme)_{0.5}]$, (38) $[CeO(eb)_2(py)_{0.5}]$, (39) $[CeO(eb)_2(pmdeta)]$, (40) $[CeO(eb)_2(pyNO)]$, (41) $[CeO(mv)_2(phen)](mvH)$, (42) $[CeO(eh)_2(18\text{-}crown\text{-}6)]$, (43) $[CeO(eh)_2(dch18\text{-}crown\text{-}6)]$, (44) $[CeO(eh)_2(bipy)]$, (45) $[CeO(eh)_2(py\text{-}OH)](ehH)$, (46) $[CeO(emb)_2(triglyme)_{1.5}]$, (47) $[CeO(emb)_2(diglyme)_{1.5}]$, (48) $[CeO(mb)_2(phen)]$, (49) $[Ce(2,4\text{-}di^tBuphenol)]_n$, (50) $[Ce(2,6\text{-}di^tPrphenol)]_n$, (51) $[CeO(mv)_2(2,6\text{-}di^tPrphenol)](mvH)$, (52) $[PhNCO]_n$.

6.3 Spectroscopic characterization

6.3.1 Infrared analyses

Selected infrared data of complexes (36) - (48) are summarized in Table 6.1 overleaf. All spectra were recorded at R.T. as Nujol or hexachlorobutadiene mulls, or as neat liquids.

The CH stretching vibrations show only two types of bands, namely those above *ca.* 3000cm^{-1} and those between *ca.* 2980 and 2870cm^{-1}. The higher frequency peaks are only observed in those spectra corresponding to compounds utilizing aromatic amine ligands. For example the bipy complex (44) shows two peaks at 3067 and 3009cm^{-1}, while the phen complex (41) shows one peak at 3066cm^{-1}. This is in accord with the spectra of the free ligands, both of which have CH stretching vibrations above 3000cm^{-1}. The pyridine oxide complex (40) also shows vibrations in this region corresponding to the CH groups on the aromatic amines. The other, lower frequency stretches are all observed in the spectra of the oxo-*bis* carboxylate species and are due to the CH groups of the carboxylates.

The sharp OH stretching vibrations observed at *ca.* 3630cm^{-1} in the spectra of the oxo-*bis* carboxylate compounds are once again observed in these coordination compounds. This band has already been identified as the OH stretching vibration of a small amount of residual carboxylic acid. Compound (40) actually shows two bands at 3640 and 3603cm^{-1} which might suggest that one of the OH groups associated with the complex is in closer proximity to the amine oxide.

The $\nu OCO_{(asym)}$ vibrations are all in a relatively small range, 1563 (39) - 1533cm^{-1} (41). These peaks are generally strong vibrations. The $\nu OCO_{(sym)}$ vibrations also lie within a narrow range, 1425 [(41) and (48)] - 1405cm^{-1} (46). Consequently the separation between the two differs by less than 40cm^{-1} throughout the series, suggesting that all the complexes are similarly structured with respect to the nature of the carboxylate bonding. From these observations it is most likely that the carboxylate groups adopt bridging bonding modes.

The collection of bands in the fingerprint region between *ca.* 650 and 500cm^{-1} previously assigned according to Ferraro and Becker as πCH and δOCO vibrations is also present in the coordination compounds.[231] One particularly well resolved spectrum is that of compound (37) (see Figure 6.6 below) which has four peaks in this region at 631, 592, 568 and 520cm^{-1}, the two higher frequency peaks presumably are due to the action of the CH out of plane bending vibrations.

Table 6.1 Selected Infrared Data (cm^{-1}) of Coordination Complexes (36) - (48) :

Compound	νOH	νCH[a]	$\delta OCO_{(asym)}$	$\delta OCO_{(asym)}$	Δν
(36)[b]	3636	2935, 2867	1550	1414	136
(37)	3635	2964, 2932, 2875	1558	1415	143
(38)	3637	2964, 2932, 2875	1559	1413	146
(39)[b]	3640	2959, 2873, 2815	1563	1409	154
(40)	3640, 3603	3075, 2961, 2933, 2874	1536	1409	127
(41)	----	3066, 2930, 2871	1533	1425	108
(42)[b]	3635	2960, 2933, 2874	1559	1415	144
(43)[b]	3633	2936, 2873	1561	1413	148
(44)	3635	3067, 3009, 2960, 2932, 2873	1561	1416	145
(45)[b]	3633	2959, 2934, 2874	1558	1417	141
(46)[b]	3636	2967	1537	1405	132
(47)[b]	3624	2978, 2932	1537	1407	130
(48)	----	2963, 2933, 2873	1548	1425	123

All spectra were recorded as Nujol mulls except ([a]) which were recorded as hexachlorobutadiene mulls and ([b]) which were neat liquids.

Figure 6.6 : Infrared spectrum of (37) (1000 - 300cm^{-1}, nujol mull)

In compliance with the findings of Misra *et al.*, regarding the coordination compounds of Pr, Nd and Sm carboxylates the infrared data of the complexes are rather similar to those of the homoleptic species.[270] However, with the bipy complex (44), for example, a coordinative shift is noted in the C=C and C=N stretching vibrations. The spectra of the free ligand of bipy has two doublets at 1579 and 1552cm^{-1} and 1450 and 1415cm^{-1}. On coordination these bands shift to 1584 and 1457cm^{-1}, respectively.

In contrast the phenolic compounds (49) - (51) exhibit completely different spectra. The spectrum of (51) still shows the sharp OH stretch at 3622cm^{-1} and the broader C=O stretch at 1705cm^{-1} that is observed in the spectra of the homoleptic, however there is now also a very strong broad OH peak at 3382cm^{-1} corresponding to the OH of the phenol ligand, its broadness possibly indicating some intermolecular hydrogen bonding. The usual $\nu OCO_{(asym)}$ and $\nu OCO_{(sym)}$ vibrations are also observed at 1538 and 1425cm^{-1}, respectively.

Neither the spectra of (49) or (50) show the presence of either of the OCO vibrations, similarly the peaks at *ca.* 1710 and 3630cm^{-1} have disappeared and are replaced with a sharp peak at *ca.* 3527cm^{-1}. This suggests an OH molecule with possible intramolecular hydrogen bonding, however, (50) also has a broad signal at 3506cm^{-1} corresponding to an intermolecular hydrogen bonded OH group. Both are possible as the tertbutyl methyl groups are likely to be relatively close together and, therefore, fairly close to the oxygen atoms of neighbouring phenol ligands. There are also peaks corresponding to CO stretching and OH in plane deformations at 1153, 1198 and 1385, 1363cm^{-1} respectively.

The infrared spectrum of the polymerized isocyanate complex (52) shows a number of marked contrasts to the spectrum of the free ligand. Consistent with the free ligand, there are a number of high frequency CH stretching vibrations between 3328 and 3037cm^{-1}, these are notably higher than those of the carboxylate ligand due to the considerable increase in aromaticity. However, the most obvious contrast lies in the NCO stretching vibration, which occurs at 2259cm^{-1} in the free ligand, but is not observed in the polymerized complex. This is probably due to the fact that the polymerized structure necessitates a rigid structure which places the NCO group in a completely different environment. The C=O stretching vibration at 1597cm^{-1} in (52) is in the same region as that of the free ligand (1599cm^{-1}) suggesting that this bond is not altered in any significant way. This is certainly the case when one considers that the most likely structure of the polymer (see Figure 6.4) links units *via* the carbon and nitrogen atoms of adjacent isocyanates.

6.3.2 ^{1}H NMR analyses

Selected ^{1}H NMR data of complexes (36) - (48) are shown in Table 6.2 overleaf. All spectra were recorded at R.T. at either 90 or 270MHz in either deuterated chloroform, benzene or toluene solvents.

The usual triplet of peaks is observed for the methyl group of the eb compounds (36) - (40) in all but one case, that of compound (39). This is not surprising as the pmdeta ligand in this reaction is oxidized to a degree (hence the formation of two reaction products, $[OCe^{IV}(eb)_2(pmdeta)]$ and $[Ce^{III}(eb)_3.2(H_2O)]$) with the consequent partial reduction of the metal to the lower valency state, a paramagnetic one, thus line broadening is observed. The range of chemical shifts is rather larger than might be expected, i.e. δ 1.14 (36) - 0.81 (37). In contrast to the CH_2 groups of the homoleptic species (23), we do not

Table 6.2 : Selected ^1H NMR Data of Coordination Complexes (36) - (48) :

Compound	CH_3	CCH_3	CH_2	$CHC\underline{H}_2$	CH
(36)[a]	1.14	----	1.65	----	2.20
(37)[b]	0.81	----	1.43	----	1.94
(38)[b]	1.10	----	1.81	----	2.28
(39)[a]	0.96	----	1.55	----	2.07
(40)[a]	0.82	----	1.40, 1.48	----	2.00
(41)[a]	0.81	1.09	1.31	1.61	2.40
(42)[a]	0.81	----	1.10	1.39	2.02
(43)[a]	0.77	----	1.18	1.37	2.05
(44)[b]	0.92	----	1.33	1.52	2.22
(45)[c]	1.20	----	1.74br.	----	2.58
(46)[a]	0.71	0.96	1.34	----	----
(47)[a]	0.77	1.03	1.54	----	----
(48)[a]	0.83	1.19	1.55	----	2.15

Spectra were recorded at R.T. at either 90 or 270MHz in ([a]) $CDCl_3$, or ([b]) C_6D_6, or ([c]) C_7D_8.

observe two resonances at *ca.* δ 1.4 and 1.5, but a single resonance just above these limits. Only for the amine oxide complex (40) are two distinct resonances observed at δ 1.40 and 1.48. The CH resonances also appear to follow the trend set by the methyl groups, namely compounds (36) and (38) having peaks at higher frequencies than the other compounds. However, they lie within a fairly small range.

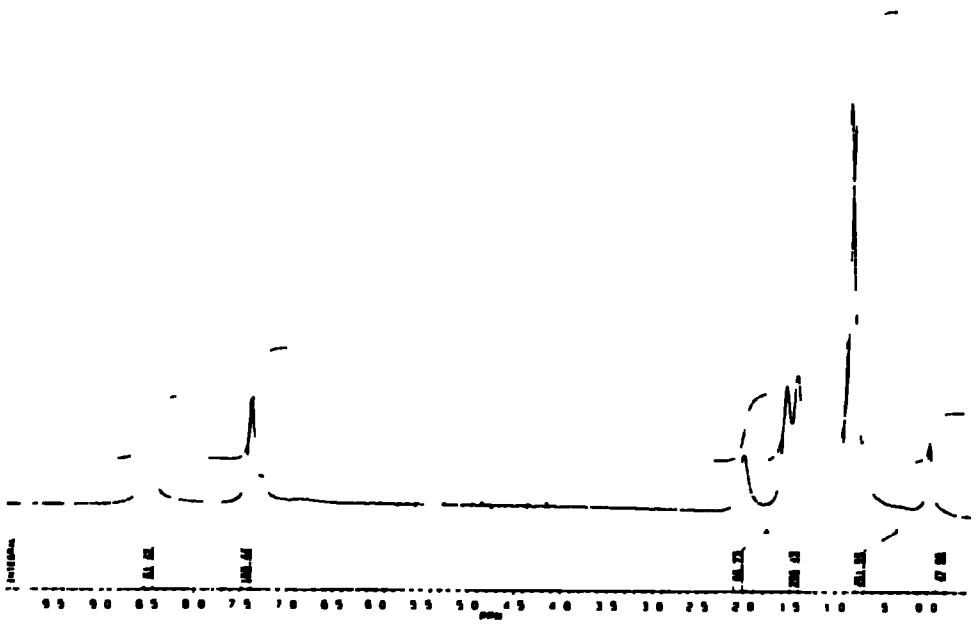

Figure 6.7 : ^{1}H NMR of (40) in $CDCl_3$

The spectrum of compound (37) shows a differentiation between OCH_2 groups of the diglyme ligand, however, they are very close together, two multiplets being resolved at δ 3.55 and 3.57. It is likely, therefore, that the same type of glyme coordination occurs in the cerium complexes as it does in the alkaline earth metal complexes described in Chapter 2, i.e. the outer two oxygens binding closer to the metal than the inner oxygens due to steric crowding. The pyridine complex (38) displays a shift of the amine resonances on coordination to the metal. In the free ligand the three resonances appear at δ 7.30, 7.61 and 8.58, however, in (38) the first two are shifted upfield to δ 6.77 and 7.09, respectively, while the latter is shifted downfield to δ 8.75.

As with the homoleptic 2-ethylhexanoate compound (25) the different types of methyl resonance are not readily distinguished by ^{1}H NMR techniques. The methyl resonances that are observed are once again triplets and lie in a narrow region, δ 0.77 - 1.20, the latter is notably higher due to the paramagnetism induced by the oxidation of the

hydroxypyridine ligand. The CH_2 groups give rise to two resonances, those at low frequency corresponding to the two methylene groups furthest from the CH group, and those at higher frequency which are directly adjacent to the CH group, and hence closer to the metal centre. The difference between the two resonances is between δ 0.2 and 0.3. As with (39) the spectrum of (45) is different, giving only one broad methylene resonance at δ 1.74.

The OCH_2 resonances of the two crown complexes (42) and (43) occur at roughly the same chemical shift, δ 3.40 and 3.43. In conjunction with this in (43) is a range of dicyclohexano peaks at δ 1.56, 1.70 and 1.92 for the $CHCH_2C\underline{H_2}$, $CHC\underline{H_2}$ and CH groups. The resonances of the bipy group in compound (44) do not shift to any large extent on coordination to the metal in contrast to those of the related pyridine ligand in (38). The peaks of the coordinated 2-hydroxypyridine ligand in compound (45) on the other hand do show a difference with respect to the spectra of the free ligand. In the free ligand a triplet and a doublet are observed at δ 6.14 and 6.33 with two other multiplets at δ 7.32 and 7.39. In the carboxylate compound, however, these resonances are broadened and have shifted to δ 6.20, 6.90, 7.38 and 7.60, respectively. This may either be a consequence of coordinative shifts or even a slight paramagnetic shift upon the introduction of the hydroxyamine.

Both the emb and mb carboxylates have two distinct types of methyl group, the terminal and the α-substituted. These are clearly differentiated with the terminal group appearing at low frequency (*ca.* δ 0.77± 0.06) and the α-substituted methyl group at higher frequency (*ca.* δ 1.00± 0.04 for the emb, and δ 1.19 for the mb). The emb α-substituted methyl resonance is at a lower frequency than the mb due to the added shielding imparted by the two α,α-substituents. Unlike the spectra of (37) the OCH_2 resonances of the glyme ligands in (46) and (47) are not resolved, a single multiplet being observed at δ 3.42 and 3.69, respectively.

Compounds (41) and (48) are both phenanthroline complexes and therefore the relative resonances of the amine ligand may be directly correlated. For (48) the spectra at 90MHz in $CDCl_3$ is not well resolved and only two broad peaks are observed at δ 7.47 and 8.15. However, the spectra of (41) at 270MHz in $CDCl_3$, gives us more information showing four peaks at δ 7.78(m), 7.85(s), 8.41(d) and 9.84(d). These resonances are at lower field than the corresponding peaks for (48) indicating a larger degree of electronegativity about the phenanthroline ligand in (41).

The ^{1}H NMR spectrum of the 2,4-ditertbutylphenol compound (49) clearly shows the two different ^{t}Butyl environments. The first singlet at δ 1.49 corresponds to the methyls of the ^{t}Butyl at the 4-position, while the second at δ 1.53 arise from the methyls of the ^{t}Butyl at the 2-position. The chemical shifts of these two resonances are altered from the free ligand, shifting them downfield by *ca.* δ 0.2. The phenyl resonances at δ 7.34 and 7.58 are also shifted to a higher frequency, but by an even greater amount, between δ 0.5 and 0.8. Although only two phenyl resonances are observed (as doublets) this is noted in the spectra of the free ligand also.

The spectrum of (50) shows a similar pattern of chemical shift on coordination. In the free ligand a pair of doublets (having a ^{2}J coupling constant of *ca.* 1.5Hz) occur at δ 1.21 and 1.29. In the spectrum of (50) these resonances keep a doublet structure but are shifted to δ 1.60 and 1.62. The CH resonance is also shifted by a similar amount from δ 3.32 (free ligand) to δ 3.56 (50); this also appears as a complex multiplet. In the free ligand only one broad signal is observed for the aromatic protons at δ 7.09; however, on complexation to the metal a greater amount of negative charge is donated to the ring resulting in three resonances being observed in (50) for the *ortho*, *meta*, and *para* protons. These resonances are shifted to δ 8.03, 7.51 and 7.32, respectively. In neither of the latter two compounds are any resonances corresponding to carboxylic acids observed. In contrast, however, compound (51) shows resonances for both the phenol and the 2-methylvalerate ligands.

The spectrum of (52) in D_6dmso gives three sets of peaks corresponding to the three aromatic proton environments of the phenyl isocyanate ligand. A multiplet at δ 6.94 integrates to one proton and is assigned as the *para* proton, further multiplets at δ 7.24 and 7.40 integrate to two protons each and are assigned as the *meta* and *ortho* protons respectively. The ^{1}H NMR spectrum of the free ligand also reveals a similar pattern; however, the peaks are closer together, between δ 7.00 and 7.20. These shifts are likely to arise from the change in structure and physical nature, i.e. the formation of a solid from a liquid precursor.

6.3.3 ^{13}C NMR analyses

Selected ^{13}C NMR data of complexes (36) - (48) are shown in Table 6.3 overleaf. All spectra were recorded at R.T. at either 22.65 or 67.94MHz in either deuterated chloroform, benzene or toluene solvents.

All four types of carbon atoms in the 2-ethylbutyrate complex are observed for each of compounds (36) - (40), each set of resonances being within a very narrow band, generally less than δ 2.0. This might indicate that their structures remain constant throughout. The consistency of the chemical shifts of these peaks is also observed throughout the rest of the carboxylate ligands, each differing by less than δ 2.0. The CH_2 groups of the 2-ethyl, 2-methylbutyrate complexes (46) and (47), are observed to be slightly further downfield, with respect to those of the other ligands. This is most likely to be due to the fact that they are adjacent to a quarternary carbon, whereas all the others are adjacent to a tertiary carbon.

The spectrum of (37) shows the different environments of the OCH_2 groups of the diglyme ligand at δ 71.5 (a) and 72.9 (b). Again a difference in metal-oxygen bond lengths may account for this. The related multidentate Lewis base compound (39) gives a remarkably good spectrum considering that the ^1H NMR spectrum is so broad. In it we can clearly see the NCH_3 and $N(CH_3)_2$ groups at δ 43.6 and 46.3 respectively, and also two different environments for the NCH_2 groups at δ 56.5 and 57.8. A similar argument as for the bonding mode of the Lewis base may also be put forward for this compound.

The two dicyclohexano-18-crown-6 complexes (36) and (43) show a whole host of resonances in the low frequency region corresponding to both the carboxylate and more especially, crown ligands. Each of the five different carbon environments in the ether ligand is discernible, it is even possible to differentiate between the two types of OCH_2 group, one being closer to the saturated ring than the other. The ether resonances of the two emb glyme complexes show a similar degree of splitting to (37). The triglyme complex (46) has two OCH_2 resonances at δ 72.1 for (a) and (b) and δ 73.2 for (c). The diglyme complex also shows two resonances at δ 71.3 and 72.9 for (a) and (b) respectively.

Each of the carbon environments in the bipy compound (44) can also be assigned from the ^{13}C NMR spectrum using non-decoupled NMR techniques. The relative peaks are assigned overleaf.

Table 6.3 : Selected ^{13}C NMR Data of Coordination Complexes (36) - (48) :

Compound	$CH_{3(ter)}$	$CH_{3(\alpha\ sub)}$	CH_2	CH	CO
(36)[a]	12.8	----	25.3	50.7	182.6
(37)[b]	13.3	----	25.7	51.1	182.3
(38)[b]	12.7	----	25.3	50.6	182.3
(39)[a]	13.1	----	25.7	49.1	184.2
(40)[a]	12.3	----	24.8	50.6	182.4
(41)[a]	14.1	16.8	20.5, 35.7	41.1	187.0
(42)[a]	12.5	15.0	22.1, 24.9, 30.3, 32.0	49.9	186.6
(43)[a]	12.3	15.3	22.1, 24.9, 30.2, 32.1	49.2	185.0
(44)[b]	12.2	15.1	22.0, 24.6, 30.1, 31.9	49.0	183.9
(45)[c]	12.5	14.4	23.8, 25.1, 30.8, 31.8	49.3	182.3
(46)[a]	9.90	21.6	31.8	----	185.2
(47)[a]	10.1	21.5	31.9	----	184.8
(48)[a]	13.0	17.8	27.9	48.6	183.2

Spectra were recorded at R.T. at either 22.65 or 67.94MHz in ([a]) $CDCl_3$, or ([b]) C_6D_6, or ([c]) C_7D_8.

Note: ter = terminal methyl ; α-sub = α-substituted methyl

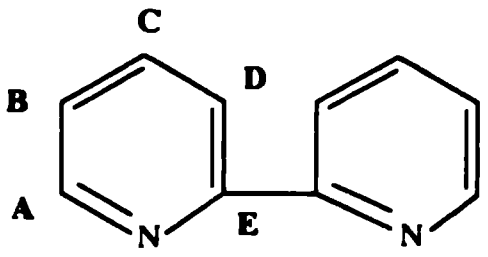

C	121.0
B	123.4
D	127.7
A	136.2
E	149.1

Figure 6.8 : ^{13}C NMR assignments of 2,2-dipyridyl in (44) ($CDCl_3$)

Compounds (50) and (51) produce similar patterns of resonances for the 2,6-diisopropylphenol ligand. A singlet at *ca.* δ 22.0 is observed for the methyl carbons with a smaller singlet at *ca.* δ 31.0 noted for the isopropyl group. The introduction of the carboxylate ligands does not appear to have altered the electronic situation of the phenyl groups to any significant extent either. The spectrum of (49) clearly shows the difference between the two tertbutyl groups at the 2- and 4-positions. The lower frequency resonances at δ 30.7 and 35.5 are assigned as the methyl and ^{t}Butyl carbons of the 4-position and those at δ 32.7 and 36.3, the 2-position carbons. Tentative assignments based on off resonance NMR experiments for the phenyl ring carbons have also been given in the experimental section. It would appear that the order of carbon resonances is:

δ 123.3 (3-position), 125.8 (5-position), 126.3 (6-position), 137.3 (4-position), 144.0 (2-position), 150.8 (1-position).

The ^{13}C NMR spectrum of compound (52) shows essentially the same pattern of peaks as the free ligand (as did the ^{1}H NMR previously); once again, however, the peaks are rather more spaced out than in the free ligand. Four peaks at δ 118.2, 121.8, 139.8 and 152.6 are observed in the spectrum of (52) suggesting that a greater degree of negative charge has been placed on the phenyl carbons with respect to the free ligand (whose peaks only range between δ 125 and 134). This is likely to have come from the oxygen atoms of adjacent isocyanate groups being in close proximity to the phenyl ring carbons.

6.3.4 Mass Spectrometry

All mass spectra were collected under FAB+ conditions, using 3-nitrobenzylalcohol as the supporting matrix. The 2-ethylbutyrate complexes (36) - (40) show a wide variety of ions in the vapour phase. In all cases the $[Ce_xO_y]$ ions are observed ranging up to $[Ce_7O_{10}]$ at m/z 1139 in complex (36). In (36) there are a number of ions containing the ether ligand, for instance, $[Ce(eb)_3(crown)]$ at m/z 856 and $[Ce(eb)_2(crown)]$ at m/z 742. The diglyme complex (37) shows no evidence of any such ether ions, however, it does show a particular group of ions which were not observed to any great extent in the spectra of the homoleptic complexes. These are the high mass $[Ce_x(eb)_y]$ ions, such as $[Ce_2(eb)_7]$ at m/z 1083 and $[Ce_2(eb)_5]$ at m/z 855. These ions are also observed in the spectrum of (38) but not so extensively. The $[(CeO)_x(eb)_y]$ type ions are also observed in a number of the eb compounds. For (37) and (38) x and y are equal only to two, giving an ion at m/z 427, however, a larger ion at m/z 698 is observed in the spectrum of (39) for $[(CeO)_3(eb)_2]$. No amine fragments are observed in this spectrum though.

The mass spectrum of (48) shows numerous ions containing both amine and carboxylate ligands, some of which have very high masses. A phenanthroline ligand is lost in each of the steps of the series, $[Ce_2(phen)_x(mb)_5]$, where x = 2 - 0, at m/z 1145, 965 and 785 respectively. Smaller mass ions that do not contain any carboxylate fragments are also observed, for example [CeO(phen)] at m/z 336. It is noteworthy that the majority of these ions have a very high abundance, three are over 90%. Compound (41) shows far fewer phenanthroline based ions.

The 2-ethylhexanoate complexes generally show ions corresponding to both types of coordinated ligand in the vapour phase. Crown ions are observed in both (42) and (43) at, for example m/z 690 for $[Ce(eh)_2(crown)]$ (42) and m/z 798 for (43). Both of these ions are in 100% abundance. Combined with this is the observation of an ion corresponding to the breakdown of the carboxylate ligand at m/z 397 for $[Ce(eh)_2\text{-}(CH_3)_2]$. The dicyclohexanocrown ligand in (43) also shows an ether ligand breakdown ion at m/z 1111 for $[Ce(eh)_2(crown)_2\text{-}(CH_2)_4]$. Compound (45) shows a number of ions containing the coordinating amine ligand. For instance, there is a steady loss of carboxylate loss in the series $[Ce_2(eh)_4(py\text{-}OH)]$, $[Ce_2(eh)_3(py\text{-}OH)_2]$, $[Ce_2(eh)_2(py\text{-}OH)]$, $[Ce_2(eh)(py\text{-}OH)]$ at m/z 947, 897, 521 and 377 respectively. An ion containing just the amine ligand at m/z 251 for [Ce(py-OH)O] is also observed. Both compounds (44) and (45) show the presence of the large mass $[Ce_x(eh)_y]$ ions (previously observed in the spectra of (37)), at m/z 995 for $[Ce_2(eh)_5]$. (44) also shows a couple of $[(CeO)_x(eh)_y]$ ions at m/z 598 and 455 for $[(CeO)_2(eh)_2]$ and $[(CeO)_2(eh)]$ respectively.

Compounds (46) and (47) show a similar pattern of ions in all respects, except one. They both show $[Ce_xO_y]$, $[Ce_2(emb)_5]$ and $[Ce(emb)_2]$ type ions, however, there are no peaks corresponding to the glyme ligand in the spectrum of the diglyme complex (47). Complex (46) shows an ion at m/z 576 corresponding to $[Ce(emb)_2(triglyme)]$ in 9% abundance. It would appear that the diglyme ligand prefers to 'fly' in the vapour phase, whereas the triglyme ligand remains coordinated.

The two 2,6-diisopropyl compounds (50) and (51) show only a very basic set of fragments in the vapour phase (see Figure 6.9). There are no metal ions, nor are there any carboxylate fragments in the case of (51), suggesting that the phenol groups are more volatile under these conditions than the carboxylates. All the ions are simply phenol ligands and various combinations of these. The ions range from $[(phenol')_6]$ at m/z 1069 to $[(phenol')_2)]$ at m/z 354. There are in fact larger ions at m/z 1234 corresponding to $[(phenol')_7]$, however, these are in such small amounts (< 1%) to be of little importance. Another observation is the loss of one isopropyl group in a number of cases, this appears to take place quite regularly, for example at m/z 706 $[(phenol')_4]$, 664 $[[(phenol')_4\text{-}(^iPr)]$ and at m/z 530 $[(phenol')_3]$, 488 $[[(phenol')_3\text{-}(^iPr)]$. By far the most abundant mass ion (100%) for both complexes is the ion at m/z 354 $[(phenol')_2]$. Compound (49) shows a similar pattern, with the loss of numerous ^{t}Butyl groups from the oligomeric ions.

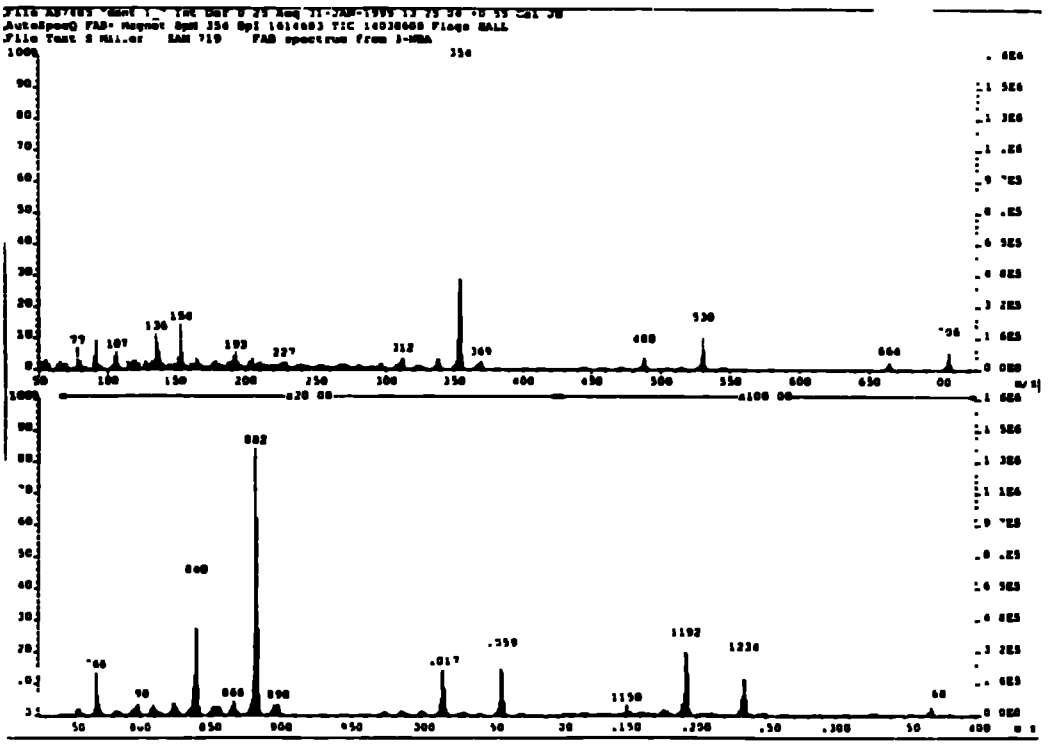

Figure 6.9 : FAB+ mass spectrum of $[Ce(2,6\text{-di}^iPrphenol)_4]_n$ (50)

The mass spectrum of (52) shows very few ions and only one in any great abundance. The mass ion at m/z 213 has an abundance of 100% and is assigned as $[(PhNCO)_2\text{-}CO]$, this suggests that at least a dimer is formed in the vapour phase. Unfortunately we can not transpose this fact directly to the solid state and affirm that a polymer exists at R.T. from these findings, although it seems likely. Larger ions are also observed up as far as m/z 578 corresponding to $[(PhNCO)_5\text{-}O]$, however, all of these have very small abundances. We also note with a number of ions that the phenyl group may lose some or all of its CH groups.

6.4 Physical properties

6.4.1 Solubilities and melting points

It was mentioned in Chapter 5 that the cerium(IV) carboxylates owe their relative solubilities to the nature of the carboxylate ligand itself. This factor is mirrored in the coordination compounds also. The 2-ethylbutyrate compounds are all soluble in hexane, benzene and chloroform but insoluble in dmso, water and alcohols. This is the case throughout, except for (40) which has only very limited solubility in hexane. This may be due in part to the cerium partially oxidizing the amine, however, since the ligand is pyridine-*N*-oxide, it results in little difference in the physical properties.

Much more pronounced is the formation of two compounds from the reaction between $[CeO(eb)_2]$ (23) and pmdeta. A mixture of products is obtained, one being a brown oily solid which is soluble in hexane, benzene and chloroform, the other being a white powder which is insoluble in these solvents. The former brown compound is a cerium(IV) complex whilst its paler coloured counterpart is a cerium(III) complex and as such shows significantly less solubility in organic and non-coordinating solvents. It would appear that the pmdeta ligand is much more susceptible to oxidation by the cerium(IV) metal than the aromatic amines.

The 2-ethylhexanoate compounds (42) and (43) are both very soluble (miscible) in isopentane, as is the oxo-*bis* starting material (25). The 2-ethylbutyrate complexes rarely show appreciable solubility in isopentane. Compounds (46) and (47) are both 2-ethyl,2-methylbutyrate complexes. The oxo-*bis* species (29) shows very limited solubility in hexane and only slightly more in benzene. It is however, very soluble in chloroform. In line with the 2-ethylbutyrate complex, it is insoluble in coordinating (e.g. water, alcohols

and dmso) solvents. The coordination compounds too show the same solubility patterns as the oxo-*bis* species.

The compounds synthesized from the reactions between the ceric carboxylates and substituted phenols all have very similar solubilities. They are observed to be very highly coloured and may almost be described as dyes. They generally give rise to yellow or orange colouration despite the fact that (51), for example, is black. They are all [(49) - (51)] observed to be soluble in isopentane, petroleum ether, hexane, benzene and chloroform but insoluble in dmso and alcohols. This solubility in organic solvents may suggest that there is an effective organic sheath surrounding the metal centres as there is in the oxo-*bis* carboxylate complexes, i.e. that there may be some aggregation.

Finally the reaction between $[CeO(eb)_2]$ (23) and phenyl isocyanate gives two distinctly different products. The first is a yellow solid, which analyses as the starting material, while the second is a white solid. It has been shown that this white solid is the polymerized isocyanate. The solubility of the yellow solid is the same as that described for the compound synthesized from CAN and the sodium carboxylate (23), whereas the polymerized compound shows no solubility in either hexane, benzene or chloroform. It is, however, soluble in coordinating solvents such as acetone, dmso, dmf and water.

The addition of coordinating ligands to the ceric carboxylate species appears to lower the melting point slightly. The oxo-*bis* 2-ethylbutyrate complex (23) is observed to decompose at *ca.* 166-71°C whereas its coordination complexes (38), (37) and (40) are observed to melt at 135-6 and 122-4 and 104-6°C, respectively. A similar drop in the melting point is noted for the 2-methylbutyrate complex (48), the starting material decomposing between 198 and 205°C whereas the phenanthroline complex melts at 96-9°C. The cerium(III) complex formed from the reaction between (32) and pmdeta has a very high decomposition point, 285-92°C, which is consistent with its formulation as a cerous carboxylate.

As was noted with the oxo-*bis* species the 2-ethylhexanoate complexes are generally liquids and as such have melting points beyond the scope of these findings. Compound (44), however, is a yellow solid with a melting point of 101-4°C. The related 2-methylvalerate complex (41) is also a solid having a melting point of 138-44°C, this is observed to be some 40°C higher than the 2-methylbutyrate analogue. The oxo-*bis* 2-ethyl,2-methylbutyrate complex $[CeO(emb)_2]$ (27) has a decomposition point of 135-60°C.

As is noted with the 2-ethylbutyrate complexes the addition of coordinating ligands lowers the melting (decomposition) points to 124-9 and 136-8°C for (46) and (47) respectively.

The polymerized isocyanate compound (52) has very unusual properties at elevated temperatures. Although the compound is a white solid at R.T. it is observed to melt to a purple liquid at 224-6°C. It is noteworthy too that many of the other compounds synthesized from reactions between similar isocyanates and ceric carboxylates are actually pale purple solids. Finally, the phenolic compounds (49) - (51) are all observed to melt to give either red or orange / brown liquids. Both (49) and (51) are observed to melt at relatively low temperatures (119-25 and 143-8 °C respectively) while compound (50) melts significantly higher, between 193 and 195°C. Compounds (50) and (51) both utilize the same phenol, namely 2,6-di^{i}Prphenol, but the presence of the free 2-methylvaleric acid residues in the latter appears to lower the respective melting points. This latter melting may, therefore, be due to the compound dissolving in liberated carboxylic acid.

6.5 X-ray crystallography

6.5.1 $[OCe(eh)_2(bipy)]$ (44)

As has already been discussed in the previous Chapter, the sheer size of the hexameric clusters and in particular the organic ligands, give rise to large unit cells and very poor diffraction patterns, making structural diagnoses almost impossible. Diffraction studies on all but one case, that of compound (44), gave no useful information. Indeed the information given for the yellow needles of (44) is limited to only the unit cell data, *viz.*

Space group	Monoclinic	**α (deg)**	90
a (Å)	12.439(3)	**β (deg)**	98.03(1)
b (Å)	18.825(2)	**γ (deg)**	90
c (Å)	20.591(3)	**Volume (Å^3)**	4774(1)

From this data we can only postulate about the extent to which the aggregation in the oxo-*bis* carboxylate species (25) is retained. If we consider the unit cell data of the two complexes which have been structurally characterized, (23) and (27) (see Chapter 5) it may

be noted that the unit cell dimension values are in the order of 18.090 (a), 17.558 (b) and 19.077Å(c) (monoclinic $P2_1/c$). These data are significantly larger than those of compound (44) which may suggest that the hexameric structure is not retained when the homoleptic is reacted with a neutral coordinating ligand such as 2,2-dipyridyl. This is only a cautious statement, however, as further structural analyses need to be obtained in order to irrefutably prove that the coordination compounds are generally smaller than the hexameric species. Although this holds for the dipyridyl ligand and is likely to be similar for related ligands (e.g. phenanthroline) it is not necessarily the case for other unrelated ligands such as glymes and crown ethers.

There is one further aside, however, that being that infrared data concerning the δOCO bending vibrations and their separations (Δν) suggest that all of the coordination compounds have similar carboxylate bonding modes, namely bridging or didentate. This might suggest that all the carboxylate coordination compounds have similar structures, possibly based on a smaller Ce_xO_y framework (see for example Figure 5.13 : Mechanism of hexamer formation).

6.5.2 Conclusions

The oxo-*bis* carboxylate species $[CeO(RCO_2).n(RCO_2H)]$ react with a wide range of ligands but unfortunately yield crystalline products which produce poor X-ray diffraction patterns. The spectroscopic and analytical data suggest that the compounds are formulated as $[CeO(RCO_2).n(RCO_2H)L_x]_m$ (where x = 0.5 - 1.5 depending on the nature of the ligand) i.e. that they are still cerium(IV) oxo-*bis* carboxylate species.

From the scant crystallographic data we might suggest that the hexameric configuration of the parent compounds does not remain intact on addition of the coordination ligands. This factor might be expected as the coordination sphere of the metals would have to alter significantly in order to allow the ligands to approach close enough to coordinate, this might also cause a disruption and possible breakdown of the Ce_6O_8 core framework.

6.6 Experimental section

Synthesis of $[CeO(eb)_2(dch18\text{-}crown\text{-}6)]$ (36)

$CeO(eb)_2$ (1.0 g, 2.60 mmol) (23) was dissolved in benzene (50 mL) to yield a soluble yellow solution, to which was added dicyclohexano-18-crown-6 (0.97 g, 2.60 mmol). The soluble solution was stirred for 2h at 45-50°C and then stripped to dryness to yield an orange oil which on cooling to 0°C produced a crystalline solid. **Yield** 1.56 g (79%) **M. Pt.** 156-8°C

Microanalyses : Found, C, 50.5 , H, 7.20 , Calc. for $CeO_{11}C_{32}H_{58}$, C, 50.7, H, 6.99 %.

Infrared (Neat ν cm^{-1}) : 3636(m), 2935(s), 2867(s), 1728(s), 1550(s), 1506(m), 1414(s), 1357(s), 1315(s), 1292(m), 1247(m), 1202(m), 1099(s), 993(s), 949(m), 935(m), 846(m), 808(m), 681(w), 602(m), 569(w), 522(m), 381(m), 370(m).

^1H NMR (270 MHz, $CDCl_3$, 20°C) : δ 1.14 (t, 6H, CH_3(eb)), 1.65 (m, 4H, CH_2(eb)), 1.89 (m, 8H, CH (crown)), 2.20 (m, 1H, CH (eb)), 3.47 (m, 8H, OCH_2 (crown)), 3.77 (m, 2H, CH_2 (crown)).

^{13}C NMR (67.94 MHz, $CDCl_3$, 20°C) : δ 12.8 (s, CH_3(eb)), 22.5 (s, CH_2 (crown)), 25.3 (s, CH_2(eb)), 28.3 (s, $CH\underline{C}H_2$ (crown)), 50.7 (s, CH (eb)), 68.8 (s, $O\underline{C}H_2CH_2OCH$ (crown)), 70.2 (s, $CHO\underline{C}H_2$ (crown)), 77.9 (s, OCH), 182.6 (s, CO).

Mass Spectrometry (FAB +) : 1139 $[Ce_7O_{10}]$(1%), 984 $[Ce_6O_9]$(1%), 856 [Ce(eb)$_3$(crown)](5%), 811 $[Ce_5O_9]$(1%), 742 [Ce(eb)$_2$(crown)](85%), 656 $[Ce_4O_6]$(3%), 643 [Ce(eb)(crown)O](3%), 564 $[Ce_3O_8]$(20%), 287 $[Ce(eb)O_2]$(17%).

Solubility : Soluble in hexane, benzene and chloroform, insoluble in dmso, water and alcohols.

Synthesis of $[CeO(eb)_2(diglyme)_{0.5}]$ (37)

$CeO(eb)_2$ (2.0 g, 5.20 mmol) (23) was dissolved in hexane (50 mL) to yield a soluble yellow solution, to which was added diglyme (0.37 mL, 2.60 mmol). The soluble solution was stirred for 3h at 45-50°C and then stripped to dryness to yield a yellow crystalline solid. **Yield** 1.97 g (84%) **M. Pt.** melts 122-4°C

Microanalyses : Found, C, 39.7 , H, 5.94 , Calc. for $CeO_{6.5}C_{15}H_{29}$, C, 39.7 , H, 6.40%.

Infrared (Nujol ν cm^{-1}) : 3635(m), 1708(m), 1558(s), 1415(s), 1329(m), 1314(m), 1247(m), 1225(m), 1201(m), 1111(m), 1044(m), 934(w), 861(w), 805(m), 631(m), 592(w), 568(m), 520(m), 375(m).

Infrared (Hexachlorobutadiene ν cm^{-1}) : 3636(m), 2964(s), 2932(s), 2875(m), 1709(m), 1558(s), 1417(s), 1384(m), 1352(m), 1329(m), 1316(m), 1294(m), 1248(m), 1223(m), 1200(w), 1169(m), 1111(m), 1028(m), 894(w), 569(m), 522(m), 378(m).

Note : numbering system for glymes are the same as those described in Chapter 2.

^{1}H NMR (90 MHz, C_6D_6, 20°C) : δ 0.81 (t, 12H, CH_3 (eb)), 1.43 (m, 8H, CH_2 (eb)), 1.94 (quintet, 2H, CH (eb)), 3.33 (s, 3H, OCH_3), 3.55 (m, 2H, OCH_2 a), 3.57 (m, 2H, OCH_2 b).

^{13}C NMR (22.65 MHz, C_6D_6, 20°C) : δ 13.3 (s, CH_3 (eb)), 25.7 (s, CH_2 (eb)), 51.1 (s, CH (eb)), 60.0 (s, OCH_3), 71.5 (s, OCH_2 a), 72.9 (s, OCH_2 b), 182.3 (s, CO).

Mass Spectrometry (FAB +) : 1083 [$Ce_2(eb)_7$](7%), 855 [$Ce_2(eb)_5$](5%), 812 [Ce_5O_9](4%), 657 [Ce_5O_7](8%), 484 [Ce_3O_4](42%), 427 [$(CeO)_2(eb)$](27%), 383 [$(CeO)_2(O_2CCHCH_3)$](10%), 329 [Ce_2O_3](19%)), 272 [Ce(eb)O](8%).

Solubility : Soluble in hexane, benzene and chloroform, insoluble in dmso, water and alcohols.

Synthesis of $[CeO(eb)_2(py)_{0.5}]$ (38)

$CeO(eb)_2$ (2.0 g, 5.20 mmol) (23) was dissolved in benzene (50 mL) to yield a soluble yellow solution, to which was added pyridine (0.42 mL, 5.20 mmol). The soluble solution was stirred for 6h at 45-50°C and then stripped to dryness to yield a yellow crystalline solid. **Yield** 1.88 g (85%) **M. Pt.** melts 135-6°C

Microanalyses : Found, C, 41.3, H, 5.57, N, 1.27, Calc. for $CeO_5C_{14.5}H_{24.5}N_{0.5}$, C, 40.9, H, 5.76, N, 1.64%.

Infrared (Nujol ν cm^{-1}) : 3637(m), 1709(m), 1559(s), 1413(s), 1315(m), 1222(m), 1155(m), 1096(m), 1035(m), 935(m), 861(w), 803(m), 700(m), 563(m), 517(m), 376(m), 301(m), 248(m).

Infrared (Hexachlorobutadiene ν cm^{-1}) : 3637(m), 2964(s), 2932(s), 2875(m), 1708(s), 1563(s), 1462(s), 1446(m), 1416(s), 1385(m), 1350(m), 1329(m), 1316(m), 1293(m), 1248(m), 1221(m), 1171(m), 1110(m), 1097(m), 1035(m), 894(w), 750(w), 701(m), 620(m), 602(m), 566(m), 519(m), 376(m).

^{1}H NMR (90 MHz, C_6D_6, 20°C) : δ 1.10 (t, 12H, CH_3 (eb)), 1.81 (m, 4H, CH_2 (eb)), 2.28 (quintet, 2H, CH (eb)), 6.77 (br, 0.5H, *para* Ph-H), 7.09 (br, 1H, *meta* Ph-H), 8.75 (br, 1H, *ortho* Ph-H).

^{13}C NMR (22.65 MHz, C_6D_6, 20°C) : δ 12.7 (s, CH_3 (eb)), 25.3 (s, CH_2 (eb)), 50.6 (s, CH (eb)), 124.3 (s, p-Ph) 136.0 (s, m-Ph), 149.8 (s, o-Ph), 182.3 (s, CO).

Mass Spectrometry (FAB +) : 855 [$Ce_2(eb)_5$](5%), 811 [Ce_5O_9](2%), 656 [Ce_5O_7](4%), 483 [Ce_3O_4](12%), 427 [$(CeO)_2(eb)$](17%), 383 [$(CeO)_2(O_2CCHCH_3)$](10%), 329 [Ce_2O_3](17%)), 272 [Ce(eb)O](8%).

Solubility : Soluble in hexane, benzene and chloroform, insoluble in dmso, water and alcohols.

Synthesis of [CeO(eb)$_2$(pmdeta)] (39)

$CeO(eb)_2$ (4.0 g, 10.34 mmol) (23) was dissolved in benzene (50 mL) to yield a soluble yellow solution, to which was added pmdeta (2.04 g, 10.34 mmol). The soluble solution was stirred for 2h at 45-50°C and then stripped to dryness to yield an oily brown solid and a white solid. The product mixture was separated by washing with benzene (2 x 15 mL). **Yield (brown oily solid)** 3.92g (68%). **Yield (white solid)** 1.24g (23%) **M. Pt.** dec. 285-92°C

Microanalyses (brown oily solid) : Found, C, 44.8 , H, 7.89 , N, 7.01 , Calc. for $CeO_5C_{21}H_{45}N_3$, C, 45.1 , H, 8.05 , N, 7.51%.

Microanalyses (white solid) : Found, C, 41.1 , H, 6.68 , Calc. for $CeO_8C_{18}H_{37}$, C, 41.5 , H, 7.1%. Note, white solid analyses to [Ce(eb)$_3$.2(H_2O)]

Infrared (brown oily solid) (Neat ν cm^{-1}) : 3640(s), 2959(s), 2873(s), 2815(s), 1714(m), 1680(m), 1563(m), 1409(m), 1313(m), 1206(w), 1123(m), 1029(m), 936(m), 861(m), 805(m), 781(m), 676(m), 572(m), 515(s), 381(s).

^{1}H NMR (brown oily solid) (90 MHz, $CDCl_3$, 20°C) : δ 0.96 (v.br, 6H, CH_3 (eb)), 1.55 (v.br, 4H, CH_2 (eb)), 2.07 (v.br, 1H, CH (eb)), 2.29 (br, 15H, NCH_3), 2.48 (br, 8H, NCH_2).

^{13}C NMR (brown oily solid) (22.65 MHz, $CDCl_3$, 20°C) : δ 13.1 (s, CH_3 (eb)), 25.7 (s, CH_2 (eb)), 43.6 (s, NCH_3), 46.3 (s, $N(CH_3)_2$), 49.1 (s, CH (eb)), 56.5, 57.8 (s, NCH_2), 184.2 (s, CO).

Mass Spectrometry (brown oily solid) (FAB +) : 1126 [Ce_7O_9](10%), 1110 [Ce_7O_8](1%), 811 [Ce_5O_9](1%), 698 [$(CeO)_3(eb)_2$](3%), 656 [Ce_4O_6](3%), 641 [Ce_4O_5](7%), 484 [Ce_3O_4](6%), 427 [$(CeO)_2$(eb)](10%), 272 [Ce(eb)O](7%).

Solubility (brown oily solid) : Soluble in hexane, benzene and chloroform, insoluble in dmso, water and alcohols.

Synthesis of [CeO(eb)$_2$(py-NO)] (40)

$CeO(eb)_2$ (1.90 g, 4.92 mmol) (28) was dissolved in benzene (50 mL) to yield a soluble yellow solution, to which was added pyridine-*N*-oxide (0.47 g, 4.92 mmol). The solution turned orange / yellow and became soluble as soon as refluxing temperatures were attained. The solution was stirred for 6h at 60°C and then stripped to dryness to yield an orange solid. **Yield** 1.95 g (82%) **M. Pt.** melts 104-6°C

Microanalyses : Found, C, 42.1 , H, 5.43 , N, 2.81 , Calc. for $CeO_6C_{17}H_{27}N$, C, 42.4, H, 5.61, N, 2.91 %.

Infrared (Nujol ν cm^{-1}) : 3640(m), 3603(w), 1709(m), 1536(s), 1409(s), 1314(m), 1222(m), 1143(w), 1095(w), 1016(m), 934(m), 838(m), 763(s), 672(m), 552(m), 514(m), 463(m), 374(m).

Infrared (Hexachlorobutadiene ν cm $^{-1}$) : 3640(m), 3625(m), 3075(m), 2961(s), 2933(s), 2874(m), 1708(m), 1609(m), 1545(s), 1470(m), 1412(s), 1316(m), 1232(s), 1173(m), 1107(m), 1017(m), 772(m), 673(m), 556(s), 522(m), 464(m), 377(m).

^{1}H NMR (270 MHz, $CDCl_3$, 20°C) : δ 0.82 (s, 12H, CH_3), 1.40, 1.48 (s, 8H, CH_2), 2.00 (br, 2H, CH), 7.38 (br, 3H, m- and p-phenyl (py-OH)), 8.47 (br, 2H, o-phenyl (py-OH)).

^{13}C NMR (67.94 MHz, $CDCl_3$, 20°C) : δ 12.3 (s, CH_3), 24.8 (s, CH_2), 50.6 (s, CH), 126.2 (s, m-Ph), 127.4 (s, p-Ph), 140.0 (s, o-Ph), 182.4 (s, CO).

Mass Spectrometry (FAB +) : 855 $[(CeO)_4(eb)_2]$(32%), 699 $[(CeO)_3(eb)_2]$(7%), 640 $[(CeO)_2(eb)_2(pyNO)]$(14%), 542 $[(CeO)_2(eb)_2]$(4%), 484 $[Ce_3O_4]$(32%), 427 $[(CeO)_2(eb)]$(36%), 329 $[Ce_2O_3]$(22%).

Solubility : Soluble in benzene and chloroform, insoluble in dmso, water and alcohols.

Synthesis of $[CeO(mv)_2(phen)](mvH)$ (41)

$CeO(mv)_2.2mvH$ (0.79 g, 1.26 mmol) (24) was dissolved in chloroform (50 mL) to yield a soluble orange solution, to which was added 1,10-phenanthroline (0.23 g, 1.26 mmol). The solution was stirred for 9h at 50°C and then stripped to dryness to yield a yellow / orange semi crystalline solid. **Yield** 0.76g (88%) **M. Pt.** melts 138-44°C

Microanalyses : Found, C, 53.4, H, 6.26, N, 3.76, Calc. for $CeO_7C_{30}H_{42}N_2$, C, 52.8, H, 6.16, N, 4.10%.

Infrared (Nujol n cm^{-1}) : 1708(s), 1579(m), 1533(s), 1515(m), 1425(m), 1305(w), 1260(m), 1187(m), 1093(m), 937(m), 894(w), 847(m), 799(m), 730(m), 646(m), 551(m), 414(m), 382(w), 338(m).

Infrared (Hexachlorobutadiene ν cm^{-1}) : 3066(w), 2930(s), 2871(s), 1723(m), 1706(m), 1571(m), 1464(m), 1415(m), 1366(m), 1306(s), 1293(m), 1220(w), 1099(s), 893(w), 729(w), 720(m), 713(m), 688(w), 649(m), 551(m).

^{1}H NMR (90 MHz, $CDCl_3$, 20°C) : δ 0.81 (t, 3H, CH_3), 1.09 (d, 3H, $CHC\underline{H}_3$), 1.31 (s, 3H, CH_2), 1.61 (m, 1H, CH_2), 2.40 (m, 1H, CH), 7.78 (m, 1H, phenH), 7.85 (s, 1H, phenH), 8.41 (d, 1H, phenH), 9.84 (d, 1H, phenH), 11.97 (br, 1H, OH).

^{13}C NMR (22.65 MHz, $CDCl_3$, 20°C) : δ 14.1 (s, CH_3), 16.8 (s, $CH\underline{C}H_3$), 20.5 (s, CH_2), 35.7 (s, $CHCH_2$), 41.1 (s, CH), 124.1 (s, $NCC\underline{C}H$), 126.5 (s, $NCHCH\underline{C}H$), 129.4 (s, $NCH\underline{C}H$), 138.2 (s, $NC\underline{C}$), 144.9 (s, NCH), 151.0 (s, $N\underline{C}$), 187.0 (s, CO).

Mass Spectrometry (FAB +) : 855 $[Ce_2(mv)_5]$(9%), 641 $[Ce_4O_5]$(13%), 550 $[Ce_3O_7]$(5%), 427 $[(CeO)_2(eb)]$(23%), 336 [CeO(phen)](45%).

Solubility : Soluble in benzene and chloroform, insoluble in dmso, water and alcohols.

Synthesis of [CeO(eh)$_2$(18-crown-6)] (42)

CeO(eh)$_2$.2ehH (1.96 g, 2.68 mmol) (25) was dissolved in benzene (50 mL) to yield a soluble orange / yellow solution, to which was added 18-crown-6 (0.71 g, 2.68 mmol). The soluble solution was stirred for 2h at 55-60°C and then stripped to dryness to yield an orange oil. **Yield** 1.63 g (86%)

Microanalyses : Found, C, 47.9 , H, 7.52 , Calc. for $CeO_{11}C_{28}H_{54}$, C, 47.6, H, 7.64%.

Infrared (Neat ν cm^{-1}) : 3635(m), 2960(s), 2933(s), 2874(s), 1733(m), 1708(m), 1559(s), 1460(m), 1415(s), 1381(m), 1353(s), 1297(m), 1252(m), 1182(m), 1114(s), 1039(w), 952(m), 839(w), 811(w), 731(w), 679(m), 634(w), 577(w), 531(w).

^{1}H NMR (270 MHz, $CDCl_3$, 20°C) : δ 0.81 (t, 12H, CH_3), 1.10 (s, 8H, CH_2), 1.39 (s, 8H, $C(CH_2)$), 2.02 (s, 2H, CH), 3.43 (s, 12H, OCH_2 (crown)).

^{13}C NMR (67.94 MHz, $CDCl_3$, 20°C) : δ 12.5 (s, CH_3), 15.0 (s, $CHCH_2\underline{C}H_3$), 22.1 (s, $CHCH_2CH_2\underline{C}H_2$), 24.9 (s, $CHCH_2\underline{C}H_2$), 30.3 (s, $CH\underline{C}H_2$), 32.0 (s, $CH\underline{C}H_2CH_3$), 49.9 (s, CH), 72.1 (OCH_2 (crown)), 186.6 (s, CO).

Mass Spectrometry (FAB +) : 690 [Ce(eh)$_2$crown](100%), 618 [Ce(eh)$_3$O$_3$](5%), 397 [Ce(eh)$_2$-(CH_3)$_2$](20%).

Solubility : Soluble in 2-methylbutane, hexane, benzene and chloroform, insoluble in dmso, water and alcohols.

Synthesis of [CeO(eh)$_2$(dch18-crown-6)] (43)

CeO(eh)$_2$.2ehH (1.56 g, 2.13 mmol) (25) was dissolved in benzene (50 mL) to yield a soluble yellow solution, to which was added dicyclohexano-18-crown-6 (0.79 g, 2.13 mmol). The soluble solution was stirred for 3h at 55-60°C and then stripped to dryness to yield an orange oil. **Yield** 1.60 g (92%)

Microanalyses : Found, C, 53.4 , H, 8.56 , Calc. for $CeO_{11}C_{36}H_{66}$, C, 53.1 , H, 8.11 %.

Infrared (Neat ν cm^{-1}) : 3633(m), 2936(s), 2873(s), 1713(m), 1561(s), 1461(m), 1413(s), 1380(m), 1358(s), 1341(m), 1316(m), 1248(m), 1202(m), 1100(s), 983(w), 949(m), 935(m), 846(w). 808(w), 773(m), 731(w), 679(m), 631(w), 603(w), 575(w), 530(w).

^{1}H NMR (270 MHz, $CDCl_3$, 20°C) : δ 0.77 (t, 12H, CH_3), 1.18 (s, 8H, CH_2), 1.37 (s, 8H, $CHC\underline{H}_2$), 1.56 (br, 8H, $CCH_2\underline{C}H_2$ (crown)), 1.70 (br, 8H, CCH_2 (crown)), 1.92 (br, 4H, CH (crown)), 2.05 (s, 2H, CH), 3.40 (s, 12H, OCH_2 (crown)).

^{13}C NMR (67.94 MHz, $CDCl_3$, 20°C) : δ 12.3 (s, CH_3), 15.3 (s, $CHCH_2\underline{C}H_3$), 21.8 (s, $OCHCH_2\underline{C}H_2$ (crown)), 22.1 (s, $CHCH_2CH_2\underline{C}H_2$), 24.9 (s, $CHCH_2\underline{C}H_2$), 29.0 (s, $OCH\underline{C}H_2$ (crown)), 30.2 (s,

$CH\underline{C}H_2$), 32.1 (s, $CH\underline{C}H_2CH_3$), 49.2 (s, CH), 69.4 (s, $O\underline{C}H_2CH_2OCH$ (crown)), 71.5 (s, $\underline{C}H_2OCH$ (crown)), 78.2 (s, OCH (crown)), 185.0 (s, CO).

Mass Spectrometry (FAB +) : 1111 [$Ce(eh)_2(crown)_2$-$(CH_2)_4$](2%), 1084 [$Ce(eh)_4$(crown)](1%), 810 [Ce_5O_9](2%), 798 [$Ce(eh)_2$(crown)](100%), 671 [Ce(eh)(crown)O](6%), 484 [Ce_3O_4](7%), 426 [$Ce(eh)_2$](6%).

Solubility : Soluble in 2-methylbutane, hexane, benzene and chloroform, insoluble in dmso, water and alcohols.

Synthesis of $[CeO(eh)_2(bipy)]$ (44)

$CeO(eh)_2.2eh$ (1.44 g, 1.97 mmol) (23) was dissolved in hexane (50 mL) to yield a soluble yellow solution, to which was added 2,2-dipyridyl (0.31 g, 1.97 mmol). The solution was stirred for 6h at 45-50°C and then stripped to dryness to yield a yellow oil which on cooling to 0°C separated, yielding a semi crystalline solid. **Yield** 1.01g (86%) **M. Pt.** 101-4°C

Microanalyses : Found, C, 52.0 , H, 6.19 , N, 4.39 , Calc. for $CeO_5C_{26}H_{38}N_2$, C, 52.2, H, 6.35, N, 4.68%.

Infrared (Nujol ν cm^{-1}) : 3635(w), 1708(w), 1584(m), 1561(m), 1418(m), 1378(m), 1315(w), 1255(w), 1230(w), 1147(w), 1091(w), 1040(w), 1011(w), 993(m), 949(m), 757(s), 741(w), 676(w), 620(m), 397(w), 310(w).

Infrared (Hexachlorobutadiene ν cm^{-1}) : 3635(m), 3067(w), 3009(w), 2960(s), 2932(s), 2873(m), 1706(m), 1584(s), 1558(m), 1457(m), 1419(s), 1382(m), 1315(m), 1255(m), 1231(w), 1171(m), 1091(m), 1068(w), 1040(w), 894(w), 621(m), 574(w).

^1H NMR (90 MHz, C_6D_6, 20°C) : δ 0.92 (t, 12H, CH_3), 1.33 (s, 8H, CH_2), 1.52 (s, 8H, $CHC\underline{H}_2$), 2.22 (s, 2H, CH), 7.31, 7.83, 8.49, 8.69 (s, 8H, phenyl (bipy)).

^{13}C NMR (22.65 MHz, C_6D_6, 20°C) : δ 12.2 (s, CH_3), 15.1 (s, $CHCH_2\underline{C}H_3$), 22.0 (s, $CHCH_2CH_2\underline{C}H_2$), 24.6 (s, $CHCH_2\underline{C}H_2$), 30.1 (s, $CH\underline{C}H_2$), 31.9 (s, $CH\underline{C}H_2CH_3$), 49.0 (s, CH), 121.0 (s, $NCCH\underline{C}H$), 123.4 (s, $NCH\underline{C}H$), 127.7 (s, $NC\underline{C}H$), 136.2 (s, $N\underline{C}H$), 149.1 (s, $N\underline{C}$), 183.9 (s, CO).

Mass Spectrometry (FAB +) : 995 [$Ce_2(eh)_5$](43%), 725 [$Ce_2(eh)_3O$](21%), 598 [$(OCe)_2(eh)_2$](4%), 484 [Ce_3O_4](34%), 455 [$(OCe)_2(eh)$](44%), 426 [$Ce(eb)_2$](6%), 329 [Ce_2O_3](13%).

Solubility : Soluble in hexane, benzene and chloroform, insoluble in dmso, water and alcohols.

Synthesis of $[CeO(eh)_2(py\text{-}OH)](eh\text{-}H)$ (45)

$CeO(eh)_2.2ehH$ (1.44 g, 1.95 mmol) (28) was dissolved in benzene (50 mL) to yield a soluble yellow solution, to which was added 2-hydroxypyridine (0.19 g, 1.95 mmol). The solution turned orange and became soluble as soon as refluxing temperatures were attained. The solution was stirred for 6h at 60°C and then stripped to dryness to yield a viscous dark orange oil. **Yield** 1.24 g (93%)

Microanalyses : Found, C, 50.2 , H, 7.39, N, 1.96 , Calc. for $CeO_8C_{29}H_{51}N$, C, 51.1 , H, 7.49, N, 2.06%.

Infrared (Neat ν cm $^{-1}$) : 3633(s), 2959(s), 2934(s), 2874(s), 1707(s), 1648(m), 1610(m), 1558(s), 1460(s), 1417(s), 1318(s), 1264(s), 1230(m), 1155(w), 1101(m), 996(w), 893(m), 868(m), 776(m), 729(m), 640(m), 620(m), 568(m), 523(m), 457(w), 389(m).

^{1}H NMR (90 MHz, C_7D_8, 20°C) : δ 1.20 (br, s, 18H, CH_3), 1.74 (br, m, 24H, CH_2 and $CHC\underline{H}_2$), 2.58 (br, 3H, CH), 6.20, 6.90, 7.38, 7.60 (br, 4H, phenyl (py-OH)).

^{13}C NMR (22.65 MHz, C_7D_8, 20°C) : δ 12.5 (s, CH_3), 14.4 (s, $CHCH_2\underline{C}H_3$), 23.8 (s, $CH_3\underline{C}H_2$), 25.1 (s, $CH_3CH_2\underline{C}H_2$), 30.8 (s, $CHCH_2\underline{C}H_2$), 31.8 (s, $CH\underline{C}H_2$), 49.3 (s, CH), 107.7 (s, $NCHCH\underline{C}H$), 120.1 (s, $NCH\underline{C}H$), 137.3 (s, $NC\underline{C}H$), 141.9 (s, $N\underline{C}H$), 166.0 (s, $N\underline{C}OH$), 182.3 (s, CO).

Mass Spectrometry (FAB +) : 995 $[Ce_2(eh)_5]$(6%), 947 $[Ce_2(eh)_4(py\text{-}OH)]$(9%), 897 $[Ce_2(eh)_3(py\text{-}OH)_2]$(5%), 725 $[Ce_2(eh)_3O]$(4%), 676 $[Ce_2(eh)_2(py\text{-}OH)O]$(4%), 521 $[Ce(eh)_2(py\text{-}OH)]$(2%), 484 $[Ce_3O_4]$(9%), 377 [Ce(eh)(py-OH)](8%), 328 $[Ce_2O_3]$(5%), 251 [Ce(py-OH)O](5%).

Solubility : Soluble in benzene and chloroform, insoluble in dmso, water and alcohols.

Synthesis of $[CeO(emb)_2(triglyme)_{1.5}]$ (46)

$CeO(emb)_2$ (1.00 g, 2.42 mmol) (26) was dissolved in chloroform (50 mL) to yield a (90%) soluble, yellow solution, to which was added triglyme (0.44 mL, 2.42 mmol). The solution was stirred for 8h at 55-60°C and then stripped to dryness to yield a yellow oil which on cooling formed a semi crystalline solid. **Yield** 1.23 g (75%) **M. Pt.** 124-8°C

Microanalyses : Found, C, 45.9 , H, 7.82 , Calc. for $CeO_{11}C_{26}H_{53}$, C, 45.8 , H, 7.78%.

Infrared (Neat ν cm^{-1}) : 3636(w), 2967(s), 1728(m), 1700(m), 1537(s), 1405(s), 1304(m), 1247(m), 1200(m), 1110(s), 1029(m), 944(m), 853(m), 817(m), 756(s), 666(w), 604(m), 585(m), 396(m).

^{1}H NMR (90 MHz, $CDCl_3$, 20°C) : δ 0.71 (t, 12H, CH_3), 0.96 (s, 6H, $C(CH_3)$), 1.34 (m, 8H, CH_2), 3.15 (s, 9H, OCH_3), 3.42 (m, 18H, OCH_2).

^{13}C NMR (22.65 MHz, $CDCl_3$, 20°C) : δ 9.90 (s, CH_3), 21.6 (s, $C(\underline{C}H_3)$), 31.8 (s, CH_2), 48.0 (s, CR_3), 59.6 (s, OCH_3), 72.1 (s, OCH_2 a,b), 73.2 (s, OCH_2 c), 185.2 (s, CO).

Mass Spectrometry (FAB +) . 1011 [$(CeO)_4(emb)_3$](3%), 925 [$Ce_2(emb)_5$](6%), 797 [$Ce_2(emb)_4$](4%), 726 [$(CeO)_3(emb)_2$](5%), 576 [$Ce(emb)_2$(triglyme)](9%), 483 [Ce_3O_4](16%), 441 [$(CeO)_2(emb)$](8%), 397 [$Ce(emb)_2$](6%), 329 [Ce_2O_3](7%).

Solubility : Soluble in hot benzene and chloroform, insoluble in dmso, water and alcohols.

Synthesis of [$CeO(emb)_2(diglyme)_{1.5}$] (47)

$CeO(emb)_2$ (0.74 g, 1.79 mmol) (26) was dissolved in chloroform (50 mL) to yield a (90%) soluble yellow solution, to which was added diglyme (0.26 mL, 1.79 mmol). The soluble solution was stirred for 8h at 55-60°C and then stripped to dryness to yield a yellow oil which on cooling formed a semi crystalline solid. **Yield** 1.01 g (92%) **M. Pt.** 136-9°C

Microanalyses : Found, C, 45.5 , H, 7.46 , Calc. for $CeO_{9.5}C_{23}H_{47}$, C, 44.9 , H, 7.64%.

Infrared (Neat ν cm^{-1}) : 3624(s), 2978(s), 2932(m), 1729(m), 1697(m), 1537(s), 1407(s), 1328(m), 1304(m), 1282(m), 1244(m), 1200(m), 1177(m), 1110(s), 1012(m), 979(m), 912(m), 856(m), 822(m), 806(m), 789(s), 745(w), 657(w), 612(m), 569(m), 521(m), 474(w).

^1H NMR (90 MHz, $CDCl_3$, 20°C) : δ 0.77 (br, 12H, CH_3), 1.03 (s, 6H, $C(CH_3)$), 1.54 (m, 8H, CH_2), 3.34 (s, 9H, OCH_3), 3.69 (m, 12H, OCH_2).

^{13}C NMR (22.65 MHz, $CDCl_3$, 20°C) : δ 10.1 (s, CH_3), 21.5 (s, $C(\underline{C}H_3)$), 31.9 (s, CH_2), 47.6 (s, CR_3), 63.0 (s, OCH_3), 71.3 (s, OCH_2 a), 72.9 (s, OCH_2 b), 184.8 (s, CO).

Mass Spectrometry (FAB +) : 925 [$Ce_2(emb)_5$](16%), 726 [$(CeO)_3(emb)_2$](5%), 683 [$Ce_2O(emb)_3$](7%), 484 [Ce_3O_4](25%), 441 [$(CeO)_2(emb)$](18%), 397 [$Ce(emb)_2$](9%), 327 [Ce_2O_3](7%).

Solubility : Soluble in hot benzene and chloroform, insoluble in dmso, water and alcohols.

Synthesis of [$CeO(mb)_2(phen)$] (48)

$CeO(mb)_2$ (0.40 g, 1.11 mmol) (28) was dissolved in benzene (50 mL) to yield a soluble yellow solution, to which was added 1,10-phenanthroline (0.20 g, 1.11 mmol). The solution was stirred for 6h at 45-50°C and then stripped to dryness to yield a yellow solid. **Yield** 0.57 g (95%) **M. Pt.** melts 96-99°C.

Microanalyses : Found, C, 49.5 , H, 5.42, N, 5.01 , Calc. for $CeO_5C_{22}H_{26}N_2$, C, 49.1 , H, 4.83, N, 5.20%.

Infrared (Nujol ν cm^{-1}) : 1710(m), 1623(m), 1548(m), 1515(m), 1425(m), 1306(m), 1261(w), 1140(w), 1102(m), 1020(m), 964(m), 902(m), 861(w), 845(m), 801(w), 772(w), 732(m), 634(w), 571(w), 523(w), 503(w), 417(w).

Infrared (Hexachlorobutadiene ν cm $^{-1}$) : 2963(m), 2933(m), 2873(w), 1708(w), 1516(m), 1466(m), 1423(m), 1364(w), 1345(m), 1307(w), 1261(w), 1229(w), 1170(m), 1139(m), 1102(m), 1017(m), 893(w), 732(m), 719(w), 634(w), 575(w), 472(w).

^{1}H NMR (90 MHz, $CDCl_3$, 20°C) : δ 0.83 (br, 6H, CH_3 (mb)), 1.19 (br, 6H, $CHC\underline{H}_3$ (mb)), 1.55 (br, 4H, CH_2 (mb)), 2.15 (s, 2H, CH (mb)), 7.47, 8.15 (br, 8H, phenyl (phen)).

^{13}C NMR (22.65 MHz, $CDCl_3$, 20°C) : δ 13.0 (s, CH_3 (mb)), 17.8 (s, $CH\underline{C}H_3$ (mb)), 27.9 (s, CH_2 (mb)), 48.6 (s, CH (mb)), 123.8 (s, NCHCH$\underline{C}$H), 124.1 (s, NCH$\underline{C}$H), 127.3 (s, N$\underline{C}$H), 129.9 (s, N$\underline{C}$C), 136.7 (s, N$\underline{C}$), 183.2 (s, CO).

Mass Spectrometry (FAB +) : 1145 [Ce_2(phen)$_2$(mb)$_5$](10%), 965 [Ce_2(phen)(mb)$_5$](100%), 785 [Ce_2(mb)$_5$](90%), 522 [Ce(mb)$_2$(phen)](100%), 413 [(CeO)$_2$(mb)](44%), 336 [CeO(phen)](31%), 329 [Ce_2O_3](10%)) 258 [CeO(mb)](8%).

Solubility : Soluble in benzene and chloroform, insoluble in dmso, water and alcohols.

Synthesis of [Ce(2,4-di^{t}Buphenol)$_4$]$_n$ (49)

$CeO(eb)_2$ (2.42 g, 6.26 mmol) (23) was dissolved in toluene (50 mL) and heated to 80°C to yield a soluble yellow solution, to which was added 2,4-ditertbutylphenol (1.29g, 6.26 mmol). The soluble solution was refluxed for 8 hours and then stripped to dryness to yield a bright yellow / orange solid. **Yield** 4.67 g (78%) **M. Pt.** melts 119-25°C

Microanalyses : Found, C, 70.8 , H, 9.37 , Calc. for $CeO_4C_{56}H_{84}$, C, 70.0 , H, 8.75%.

Infrared (Nujol ν cm^{-1}) : 3527(s), 1773(w), 1662(w), 1550(m), 1365(s), 1333(s), 1282(m), 1239(m), 1201(m), 1168(m), 1094(m), 1065(w), 1024(w), 967(w), 934(w), 882(w), 829(w), 814(w), 792(w), 770(w), 651(w), 510(w), 441(w), 386(w).

Infrared (Hexachlorobutadiene ν cm^{-1}) : 3527(s), 2964(s), 2908(m), 2871(m), 1783(vw), 1661(w), 1476(m), 1463(m), 1437(m), 1418(m), 1393(m), 1363(m), 1332(m), 1282(m), 1235(m), 1201(m), 1169(s), 1095(m), 1064(w), 1025(w), 886(m), 551(m), 510(w).

^{1}H NMR (90 MHz, $CDCl_3$, 20°C) : δ 1.49 (9H, d, CH_3 (4-position)), 1.53 (9H, d, CH_3 (2-position)), 7.34, 7.58 (3H, d, phenyl).

^{13}C NMR (22.65 MHz, $CDCl_3$, 20°C) : δ 30.7 (s, CH_3 (4-position)), 32.7 (s, CH_3 (2-position)), 35.5 (s, $\underline{C}(CH_3)_3$ (4-position)), 36.3 (s, $\underline{C}(CH_3)_3$ (2-position)), 123.3 (s, (3-position)), 125.8 (s, (5-position)), 126.3 (s, (6-position)), 137.3 (s, (4-position)), 144.0 (s, (2-position)), 150.8 (s, CO).

Mass Spectrometry (FAB +) : 758 [(phenol')$_4$-^{t}Bu](10%), 423 [(phenol')$_2$O](11%), 408 [(phenol')$_2$](43%), 395 [(phenol')$_2$-(CH_3)](12%), 367 [(phenol')$_2$-(CH_3)$_3$](4%), 241 [(phenol')$_2$-(^{t}Bu)$_3$](8%).

Solubility : Soluble in petroleum ether, hexane, benzene and chloroform, insoluble in water and alcohols.

Synthesis of [Ce(2,6-di^{i}Prphenol)$_4$]$_n$ (50)

$CeO(eb)_2$ (2.27 g, 5.87 mmol) (23) was dissolved in toluene (50 mL) and heated to 80°C to yield a soluble yellow solution, to which was added 2,6-diisopropylphenol (1.04g, 5.87 mmol). The solution was refluxed for 8 hours and then stripped to dryness to yield a bright orange solid. **Yield** 4.02 g (82%) **M. Pt.** melts 193-5°C

Microanalyses : Found, C, 69.1 , H, 7.35 , Calc. for $CeO_4C_{48}H_{68}$, C, 68.6 , H, 7.14%.

Infrared (Neat ν cm^{-1}) : 3525(w), 3506(s, br), 3033(w), 2963(s), 2871(m), 1633(m), 1588(s), 1461(s), 1441(s), 1385(m), 1363(m), 1309(m), 1258(m), 1198(m), 1153(m), 1109(m), 1077(m), 1061(m), 1046(m), 993(m), 967(m), 935(m), 899(m), 871(m), 825(m), 793(m), 766(m), 748(m), 673(w), 646(w), 580(w), 499(m).

^{1}H NMR (90 MHz, $CDCl_3$, 20°C) : δ 1.60 (6H, d, CH_3), 1.62 (6H, d, CH_3), 3.56 (2H, m, CH), 7.32, 7.51, 8.03 (3H, s, phenyl).

^{13}C NMR (22.65 MHz, $CDCl_3$, 20°C) : δ 21.1 (s, CH_3), 32.3 (s, CH), 120.9 (s, p-Ph), 125.2 (s, m-Ph), 135.9 (s, o-Ph), 149.8 (s, CO).

Mass Spectrometry (FAB +) : 1069 [(phenol')$_6$](2%), 882 [(phenol')$_5$](4%), 840 [(phenol')$_5$-(^{i}Pr)](2%), 706 [(phenol')$_4$](11%), 664 [[(phenol')$_4$-(^{i}Pr)](5%), 530 [(phenol')$_3$](18%), 488 [[(phenol')$_3$-(^{i}Pr)](10%), 354 [(phenol')$_2$](100%), 312 [[(phenol')$_2$-(^{i}Pr)](6%).

Solubility : Soluble in petroleum ether, hexane, benzene and chloroform, insoluble in water and alcohols.

Synthesis of [CeO(2,6-di^{i}Prphenol)(mv)$_2$](mv-H) (51)

$CeO(mv)_2.2mvH$ (2.20 g, 3.56 mmol) (24) was dissolved in toluene (50 mL) and heated to 80°C to yield a soluble yellow solution, to which was added 2,6-diisopropylphenol (0.63g, 3.56 mmol). The soluble solution was refluxed for 8 hours and then stripped to dryness to yield a black oily solid. **Yield** 2.14 g (89%) **M. Pt.** melts 143-8°C

Microanalyses : Found, C, 54.4 , H, 7.25 , Calc. for $CeO_8C_{30}H_{51}$, C, 54.5 , H, 7.27%.

Infrared (Neat ν cm^{-1}) : 3622(m), 3382(br), 2961(s), 2933(s), 2872(s), 1705(m), 1538(s), 1468(s), 1425(s), 1379(m), 1300(m), 1259(m), 1201(m), 1151(m), 1100(m), 1047(w), 1002(w), 938(m), 899(m), 871(m), 861(m), 826(m), 790(w), 747(m), 702(m), 661(m), 551(m), 413(w), 350(m).

^{1}H NMR (270 MHz, $CDCl_3$, 20°C) : δ 0.50 (9H, br, CH_3 (mv)), 0.82 (9H, br, $CHC\underline{H}_3$ (mv)), 0.94 (12H, br, CH_2 (mv)), 1.27, 1.33 (6H, m, CH_3 (phenol')), 1.65 (3H, br, CH (mv)), 3.21 (2H, m, CH (phenol')), 6.98, 7.05, 7.20 (3H, s, phenyl).

^{13}C NMR (67.94 MHz, $CDCl_3$, 20°C) : δ 13.9 (s, CH_3 (mv)), 15.7 (s, $CH\underline{C}H_3$ (mv)), 20.2 (s, CH_2 (mv)), 22.8 (s, CH_3 (phenol')), 32.0 (s, CH (phenol')), 35.2 (s, CH_2 (mv)), 47.1 (br, CH (mv)), 120.7 (s,

m-Ph), 133.9 (s, o-Ph), 150.1 (s, CO (phenol')), 189.4 (s, CO (mv)).

Mass Spectrometry (FAB +) : 882 [(phenol')$_5$](5%), 840 [(phenol')$_5$-(^{i}Pr)](1%), 706 [(phenol')$_4$](22%), 530 [(phenol')$_3$](35%), 488 [(phenol')$_3$-Pr^i](5%), 354 [(phenol')$_2$](100%), 312 [(phenol')$_2$-(^{i}Pr)](3%).

Solubility : Soluble in petroleum ether, hexane, benzene and chloroform, insoluble in water and alcohols.

Synthesis of $[PhNCO]_n$ (52)

$CeO(eb)_2$ (3.0 g, 7.76 mmol) (243 was dissolved in benzene (70 mL) to which was added phenyl isocyanate (0.92g, 7.76 mmol). The partially soluble solution / suspension was refluxed for 30 mins. whereupon a precipitate formed, the mixture was refluxed for a further 6 hours and filtered to give a white solid and a yellow / brown solution. The solution was then stripped to dryness to yield a yellow solid. **Yield (white solid)** 0.85 g (92% of carboxylate) **M. Pt.** dec. 166°C. **Yield (yellow solid)** 2.74 g (91% of isocyanate) **M. Pt.** melts to purple liquid 224-6 °C. Note the yellow solid analyses as $CeO(eb)_2$. A similar reaction was observed to occur using phenyl isocyanate and $CeO(mv)_2.2$(mv-H) (24) yielding a grey solid and an orange liquid. Once again the starting cerium carboxylate and the polymerized isocyanate were obtained.

Microanalyses (white solid) : Found, C, 70.0 , H, 4.68 , N, 12.2 , Calc. for OC_7H_5N, C, 70.6 , H, 4.20 , N 11.8%.

Infrared (white solid) (Nujol ν cm^{-1}) : 3268(m), 1745(w), 1597(m), 1544(m), 1314(m), 1232(m), 1156(m), 1052(m), 1026(w), 985(w), 914(w), 894(m), 753(m), 696(m), 641(w), 561(w), 525(w), 509(w), 499(w), 377(w).

Infrared (white solid) (Hexachlorobutadiene ν cm^{-1}) : 3328(m), 3278(m), 3131(w), 3065(w), 3037(w), 1744(w), 1498(m), 1440(m), 1390(w), 1315(m), 1296(m), 1260(m), 1233(m), 1172(s), 1083(w), 1052(w), 1027(w), 895(m), 754(m), 697(m).

^{1}H NMR (white solid) (90 MHz, $CDCl_3$, 20°C) : δ 6.94 (1H, s, p-PhH), 7.24 (2H, s, m-PhH), 7.40 (2H, s, o-PhH).

^{13}C NMR (white solid) (22.65 MHz, $CDCl_3$, 20°C) : δ 118.2 (s, p-Ph), 121.8 (s, m-Ph), 128.8 (s, o-Ph), 139.8 (s, i-Ph), 152.6 (s, CO).

Mass Spectrometry (white solid) (FAB +) : 578 [(PhNCO)$_5$-O](1%), 519 [(PhNCO)$_4$+NCO](1%), 461 [(PhNCO)$_4$-O](1%), 425 [(PhNCO)$_4$-(CH)$_4$](8%), 290 [(PhNCO)$_3$-(CH)$_5$](6%), 213 [(PhNCO)$_2$-CO](100%).

Solubility (white solid) : Soluble in dmso and dmf, insoluble in benzene and hexane.

Chapter 7

COORDINATION CHEMISTRY OF PERFLUORINATED CERIUM(IV) CARBOXYLATES

7.1 Introduction

The chemistry of the halogenated carboxylates has been studied primarily for the smaller carboxylate ligands, i.e. where $n \leq 4$ (n = number carbon atoms in the chain). Very few crystal structures have been solved and those of the lanthanides are extremely rare.

Hara and Cady have described the synthesis of a number of trifluoroacetates.[271] Group 1, 2, Ag, Co, Ni, Cu and Th trifluoroacetates were all made by dissolving the corresponding carbonates in aqueous trifluoroacetic acid. After filtration, the solutions were evaporated to dryness and dried under vacuum at 100°C. La, Ce(III), Pr, Nd and Hg(II) trifluoroacetates have been made by the dissolution of the metal oxides and hydroxides in aqueous trifluoroacetic acid. Crystalline trifluoroacetates are obtained on evaporation.

The thermal decomposition of both the Nd and La trifluoroacetates in air were studied by Roberts and were seen to decompose according to the following equation.[208]

$$2Nd(tfa)_3 \text{ ----------> } 2NdF_3 + 3CF_3COF + 3CO + 3CO_2 \quad \text{(i)}$$

At 110°C the compounds decomposed to give a solid which gave a cloudy solution in water; this turned out to be the rare earth fluoride. Above 110°C the decomposition accelerated becoming very rapid between 250 and 300°C, the anhydrous fluoride being the final product. However, further heating in air to 700°C caused a further weight loss giving LnOF.

Using the preparative method of Roberts,[208] Singh *et. al.* examined the spectral and magnetic properties of a range of lanthanon trifluoroacetates[272] From IR data they discovered that in lanthanon trifluoroacetates $\nu COO_{(asym)}$ increased from the value of the ionic sodium analogue, indicating the bridging nature of the monofluoroacetate group. In these trifluoroacetates both oxygens of the carboxylic group appeared to be coordinating, resulting in a bidentate structure with a concomitant decrease in $\nu COO_{(sym)}$. This was also confirmed by molecular weight studies in glacial acetic acid which showed that the molecular complexity of these species lay between two and three. Magnetic studies involving band shapes for hypersensitive transitions were correlated with other coordination numbers and ligand geometries about lanthanide ions,[273] from this they postulated that the metal ions were nine coordinate. However, no crystallographic evidence has been reported to confirm the structures in the solid state.

Although most simple salts of the lanthanides are insoluble in liquid ammonia both the samarium(III) acetate and trifluoroacetate are soluble and in the case of the fluorinated species, not ammonolysed at, or below -33.5°C. The subsequent reduction of the $Sm(tfa)_3$ with potassium in the ammonical solvent provided evidence for the transitory existence of Sm(II).[274] During the reaction unstable brown products, indicative of Sm(II) species, were noted; however, all of the samarium containing products isolated (principally $[Sm(tfa)_3.2NH_3]$), were Sm(III) in nature.

$[Ln(tfa)_3(phen)]$ and $[Ln(tfa)_3(bipy)]$ complexes (where M = Pr, Nd and Sm) were synthesized by Misra *et. al.* by dissolving the lanthanide trifluoroacetates in a mixture of ethyl acetate and benzene and refluxing the solutions for 5-10 hours.[270] A solution of the amine (1.5 equiv.) in benzene was added slowly to the mixture. A further 15 mins. refluxing gave a microcrystalline solid precipitate which was soluble in dmf and ethanol but insoluble in water. This difference in solubility is in contrast to the oxo-*bis* trifluoroacetates which are highly soluble in water.[272] This indicates an increase in the organic periphery of the complexes on addition of the amines.

The infrared data of the complexes were found to be rather similar to the oxo-*bis* carboxylate species, but with a number of differences. In the free bipy ligand, strong interaction between C=C and C=N vibrations gives rise to two doublets at 1578, 1552 and 1450, 1415cm^{-1}. These bands have a considerable shift when coordinated to the Ln metals, notably to *ca.* 1595 and *ca.* 1465cm^{-1}. The variation of the tfa group vibrations may be attributed to the coordination mode. The lanthanon trifluoroacetates show bands at *ca.* 1650 and *ca.* 1540cm^{-1} for COO^- anti- and symmetric stretching vibrations respectively.

In comparison to the ionic sodium trifluoroacetate[228] the antisymmetric stretch of the amine complexes decreases, while the symmetric stretch increases (in line with the oxo-*bis* carboxylates) indicating the bidentate structure of the carboxylate ligands. The number of CF stretching vibrations in the region 1220-1135cm^{-1} (only two being observed) also indicates that the ligands have either a bidentate or bridging bonding mode (see section 5.3.1). The M-N vibrations have been assigned at *ca.* 200 for the phen and *ca.* 280, 270, 250 and 230cm^{-1} for the bipy complexes. The M-O bands for both sets of complexes are between *ca.* 475 and 325cm^{-1}.

Heller synthesized the related compound $[Nd(pfp)_3(phen)]$ by mixing ethanolic solutions of neodymium chloride and sodium pentafluoropropionate (1 : 3 molar ratio) and removing the precipitated NaCl by filtration.[275] An ethanolic solution of phen was then

added (1 equivalent) to yield the ethanol solvated complex. Heating this solvate at 60°C *in vacuo* yielded the non-solvated product.

The mixed ligand chelates $[Ln(hfpd)_2(tfa)].2H_2O$, (Ln = La - Lu) were obtained as the major byproducts (yield = 5-10%) of the *tris* chelate preparations.[188] The yield of these chelates was increased by the addition of ammonium trifluoroacetate to the ethereal ammonium hexafluoropentanedionate reaction solution. The chelates are extremely soluble in oxygenated organic solvents, slightly soluble in benzene and insoluble in hexane and water. The reaction of hexafluoropentanedione with water to give trifluoroacetic acid and trifluoroacetone is essentially the reverse of the condensation reaction used to prepare hexafluoropentanedione. These mixed chelates are analogous to the lanthanide complexes which are often formed when 2,4-pentanedione is used (see Chapter 6).[246]

The authors suggest that the trifluoroacetate ester could form in the present system because of the absence of alcohol, but the trifluoroacetic acid produced could react with the *tris* chelate to give the observed complex. Also Fry and Pirie have found that heat and light decompose ethanolic europium benzoylpentanedionate (bzpd), the ultimate reaction products being ethyl acetate and acetophenone.[276]

Work by the Drake research group into rare earth β-diketonate species has brought a number of interesting results. The reaction between $[TbCl_3.6H_2O]$ and Na(hfpd) (1:3 molar ratio) in aqueous media gives a crystalline green compound with three entities in the unit cell, one dimer and two monomers. Both the dimer $[Tb_2(hfpd)_4(\mu_2\text{-}O_2CCF_3)_2(H_2O)_4]$ and the monomer $[Tb(hfpd)_3(H_2O)_2]_2$ are eight coordinate.[191] The dimeric structure has bridging tfa groups with enlarged O-C-O angles (128.3(12)°) (see Figure 7.1), however, the Tb-O bond lengths are remarkably similar for both the hfpd and tfa ligands. In the mass spectrum the compound dissociates to give both a volatile $[Tb(hfpd)_3]$ fragment and a poorly volatile $[Tb_2(hfpd)_4(tfa)_2]$ fragment.

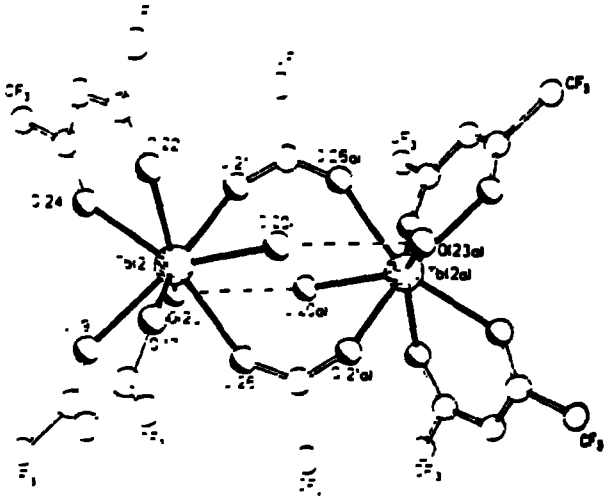

Figure 7.1 : X-ray structure of $[Tb_2(hfpd)_4(\mu_2\text{-}O_2CCF_3)_2(H_2O)_4]$

Paul's method for the preparation for the U and Th tetrapositive and La and Ce tripositive acetates in near quantitative yield may also be used for mono-, di- and trichloroacetates.[112,127,128] For instance the required chlorocarboxylic acid is added to cerium(III) acetate and the mixture refluxed at reduced pressure (*ca.* 10mm) for 2 hours and the replaced acetic acid removed. The cerium chloroacetate was precipitated by the addition of ether and further purified by evacuation at 50°C (5mm pressure) for 2 hours.

Although the syntheses are the same, the thermal behaviour of the chlorinated species differ from that of the hydrocarbon analogues. U(IV) acetate undergoes thermal decomposition *via* the formation of anhydrous acetate as an intermediate product, then decomposes very rapidly to give UO_3 or a mixture of UO_3 and U_3O_8.[128] U(IV) di- and trichloroacetates decompose through the formation of a mixture of U(IV) chloride and uranyl chloride, until a constant weight level is obtained for UO_3. The Th(IV) di- and trichloroacetates also decompose in a similar fashion, however, the intermediary products do not correspond directly to $ThCl_4$, but to $ThCl_{3.4}$ and $ThCl_{3.5}$ respectively.[127] On further heating they too convert to ThO_2 at *ca.* 550°C. The thermal behaviour of both U and Th monochloroacetate is unclear.

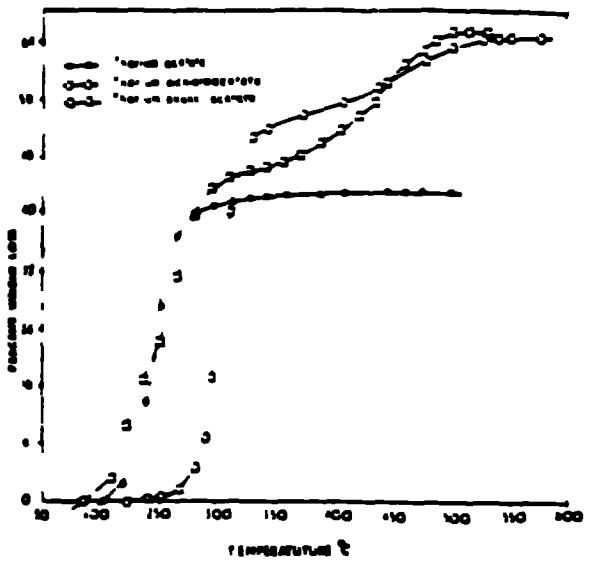

Figure 7.2 : Thermal decomposition of thorium (IV) carboxylates

The majority of the coordination compounds of lanthanide chlorocarboxylates are those containing nitrogen donor ligands and in particular the larger cyclic groups, $[M(terpy)(CCl_xH_{3-x}CO_2)_3]$ (where M = Nd, Eu and Er and x = 1-3) is one such example.[277] All three chlorocarboxylates may be prepared by the addition of an ethanolic solution of terpyridyl to a hot ethanolic solution of lanthanide chloroacetate. The precipitate is separated, thoroughly washed and dried to give the resultant product. The compounds are thermally stable to 350-400°C. They have low solubilities in ethanol, acetone, chloroform and nitromethane, but are slightly soluble in dmso and dmf.

The 2,2-dipyridyl complexes are synthesized by the direct addition of bipy to an ethanolic solution of rare earth chloroacetate (1:1 molar ratio).[278] After stirring and allowing to stand for a number of hours, a crystalline precipitate, $[M(bipy)((CCl_xH_{3-x}CO_2)_3].nH_2O$ (M = Sm, Eu, Er, x = 2, 3; M = Dy, x = 1, 2, 3) is formed. The complexes are insoluble in benzene and dioxane and only slightly soluble in ethanol. Thermal studies show the loss of water at 80°C followed by the loss of the amine at 200°C.

The analogous o-phenanthroline compounds $[M(phen)((CCl_xH_{3-x}CO_2)_3]$ have also been synthesized by Spacu *et. al.* (M = La, Ce, Pr, Sm, Eu, Dy and Er for x = 1-3).[279] The syntheses mirror those of the bipy compounds. The phenanthroline complexes are all insoluble in benzene and dioxane but soluble in hot pyridine and piperidine. The TGA

indicated the loss of the amine at 200°C, however, this process was complicated by an almost simultaneous decomposition of the chloroacetate ion.

The trichloroacetato compounds $(\mu\text{-}O_2CCl_3)_4[M(O_2CCl_3)(EtOH)(phen)]_2$ (where M = Pr, Nd and Er), have been studied by X-ray crystallography.[280] Each lanthanide ion is octacoordinated by four bridging didentate trichloroacetate ligands, one monodentate trichloroacetate ligand, one ethanol ligand and one phen, yielding a distorted square antiprismatic configuration. The two lanthanide ions are connected by the four bridging didentate trichloroacetate ligands to form a dimer containing a centre of symmetry.

Figure 7.3 : Stereoscopic view of the crystal structure of $(\mu\text{-}O_2CCl_3)_4[Er(O_2CCl_3)(EtOH)(phen)]_2$

7.2 Synthesis of coordination compounds of perfluorinated cerium (IV) carboxylates

Broadly speaking we might, from experimental considerations, suggest that the chemistry of the perfluorinated cerium(IV) carboxylates is similar to that of the hydrocarbon carboxylates only when the coordinated ligands involved are essentially neutral. This is somewhat of an over-simplification, however.

Neutral ligands such as 2,2-dipyridyl, pyridine, o-phenanthroline and crowns are all observed to coordinate in similar stoichiometries to the compounds described in Chapter 6. This might suggest that the cerium atoms have similar spatial environments in both types of oxo-*bis* carboxylate compounds. Their reactions with potentially charged ligands, such as alcohols, are rather different, suggesting that the electronic nature of the metal itself is different in the two carboxylates. This factor has been partially discussed in Chapter 5, with similar arguments being used as the reason for the fluorinated complexes forming hydroxy- compounds while the hydrocarbons form oxo- compounds (see section 5.1).

One of the noteworthy features of the hydrocarbyl carboxylates is their reactivity with isocyanates, e.g. compound (52). The hydrocarbyl carboxylates are observed to polymerize the isocyanates from colourless liquids to pale coloured (usually white or pink) medium - high melting solids. The degree of polymerization in these compounds has been suggested to be either two or three. The cerium compounds act as effective catalysts and the carboxylate is essentially retained. However, with the fluorinated species $[Ce(OH)_2(O_2CR_F)]$, we do not observe specific polymerization, but coordination, yielding, for example $[Ce(OH)_2(pfb)_2(PhNCO)]$ (55). These compounds, in contrast, are very highly coloured solids, usually dark purple.

Both simple and more complicated aliphatic alcohols have been used to some effect. Isopropyl alcohol (IPA) has been reacted with in compound (57) giving the product $[(OH)Ce(pfb)_2(IPA)_{0.5}]$. This compound can be made either by adding stoichiometric amounts of alcohol, or by dissolving the compound in neat alcohol. All of the perfluorinated compounds have appreciable solubilities in alcohols. Triethylene glycol monomethyl ether (tgme) has also been used as negatively charged ligand to give $[(OH)Ce(pfb)_2(tgme)]$ (59). Only stoichiometric equivalents of this ligand have been used to achieve coordination. These reactions occur with the loss of a hydroxy- ligand (presumably as water) giving a 1 : 1 / hydroxy : alkoxy ratio. A possible structure of these

compounds is one with bridging hydroxy- groups and terminal alkoxy- groups, i.e. $[Ce(\mu_2\text{-}OH)(pfb)_2(\eta_1\text{-}OR)]_n$, thereby relieving the steric crowding.

In complete contrast to the compounds described in Chapter 6, the perfluorinated carboxylates fail to coordinate with substituted phenols to give $[Ce(OPh)_4]$ species, e.g. (50). This may be due in part to the steric crowding at the acidic hydrogen of the phenol making it impossible to get close enough to the Ce-OH bond to replace it. It may also be due to the Ce-OCR_F bond being significantly weaker in the fluorinated species due to the increased electron withdrawing nature of the carboxylate ligands, thereby strengthening the Ce-OH bond. With phenols that are not substituted at the 2- or 6- position, e.g. phenol itself, the fluorinated carboxylates react in the same fashion as the hydrocarbyl carboxylates, oxidizing the ligands to the respective quinones.

Finally, considering the oxygenated pyridine ligands employed, i.e. 2-hydroxypyridine in compound (54) and pyridine-*N*-oxide in compound (63) we note one major difference. One of the hydroxy groups is lost in the coordination compound of the former with pfb. This is to be expected as cerium(IV) is very oxophilic (especially when there are electron withdrawing groups surrounding the metal centre) and thus the pyridine-N-oxide is able to act as a neutral ligand. This factor also means that the cerium metal in the oxo-*bis* carboxylate compound can bind to the 2-hydroxypyridine by removing the acidic proton, thus requiring the loss of one of the hydroxy groups. This might indicate a change in the structure of complex (54) in comparison to the other coordination compounds.

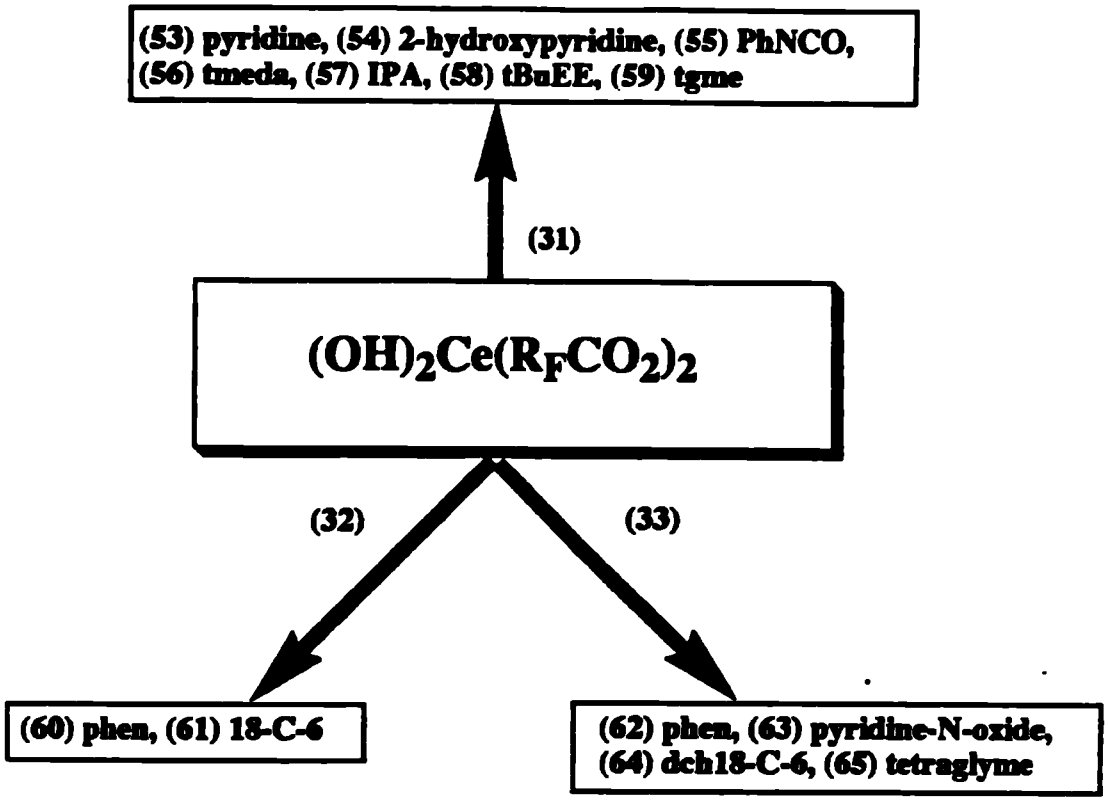

Figure 7.4 : Schematic representation of the synthesis of the perfluorinated cerium (IV) carboxylate coordination compounds

Reaction conditions: The oxo-*bis* carboxylates were dissolved in chloroform (31), (32) and (33) or acetonitrile (33) at R.T.. A stoichiometric amount of ligand was added to the solution and the mixture refluxed for 4-24 hours. Any residues were filtered and the resultant soluble filtrate was stripped to dryness.

This procedure led to the isolation of the following compounds:
$[Ce(OH)_2(pfb)_2(py)_{0.5}]$ (53), $[(OH)Ce(pfb)_2(2\text{-}pyO)]$ (54), $[Ce(OH)_2(pfb)_2(PhNCO)]$ (55), $[Ce(OH)_2(pfb)_2(tmeda)_{0.33}]$ (56), $[Ce(OH)_2(pfb)_2(IPA)_{0.5}]$ (57), $[Ce(OH)_2(pfb)_2(^tBuEE)_{0.25}]$ (58), $[(OH)Ce(pfb)_2(tgme)]$ (59), $[Ce(OH)_2(pfp)_2(phen)]$ (60), $[Ce(OH)_2(pfp)_2(18\text{-}C\text{-}6)]$ (61), $[Ce(OH)_2(tfa)_2(phen)]$ (62), $[Ce(OH)_2(tfa)_2(pyNO)]$ (63), $[Ce(OH)_2(tfa)_2(dch18\text{-}C\text{-}6)]$ (64) and $[Ce(OH)_2(tfa)_2(tetraglyme)]$ (65).

7.3 Spectroscopic characterization

7.3.1 Infrared analyses

The vibrational spectra exhibited by the tfa groups have been the subject of much discussion[272] and their assignment has only recently been clarified by matrix isolation studies.[234] The spectra of the tfa groups are often very similar to those of the acetates and other hydrocarbyl species which have been previously discussed. In carboxylates, specific attention has centred on the separations of the anti and symmetric carboxylate stretching modes the results indicating that the positions of the stretching frequencies do not afford a general distinction between the various types of tfa group.[150] For instance, $\Delta\nu$ values for bridging tfa groups range between 133 and 312cm^{-1} while those for unidentate tfa groups range between 271 and 404cm^{-1}. This overlap may lead to confusion and misinterpretation. However, in situations where the nature and oxidation state of the metal are unchanged, the C-O stretching frequencies of a trifluoroacetate group may differentiate between unidentate coordination on the one hand and either ionic, or bridging on the other.[150]

The infrared spectra of compounds (53) - (65) were measured as either Nujol or hexachlorobutadiene mulls or as neat liquids at R.T., specific details are given with the experimental section of this Chapter. Pertinent data are recorded in Table 7.1.

One feature of the fluorinated oxo-*bis* carboxylate compounds (31) - (33) is the $\nu_{(asym)}$CF stretching vibrations at 1215$\pm$10cm^{-1} and 1170$\pm$5cm^{-1}. All of these bands are observed within a small frequency range. The absence of a third CF band in this region supports the chelating or bridging mode of coordination because for a monodentate ligand all three CF vibrations would be present. A further $\nu_{(sym)}$CF stretching vibration is also noted between 817-849cm^{-1} for the three species. These CF stretches are also noted in the spectra of the coordination compounds (53) - (65). The $\nu_{(asym)}$CF stretching vibrations occur between 1215$\pm$15cm^{-1} and 1160$\pm$15cm^{-1}appearing to be at lower frequency in both cases for the tfa compounds. These tfa stretching frequencies range between 1207 - 1201 and 1152 - 1144cm^{-1} for the two resonances. The $\nu_{(sym)}$CF stretching vibration again is noted between a fairly narrow frequency range, 810 (54) - 849cm^{-1} (62). Once again the tfa complexes appear to be slightly anomalous in the fact that they have slightly higher frequencies, 841 - 849cm^{-1}. In both cases neither the pfp nor the pfb compounds appear to have significantly different CF bands.

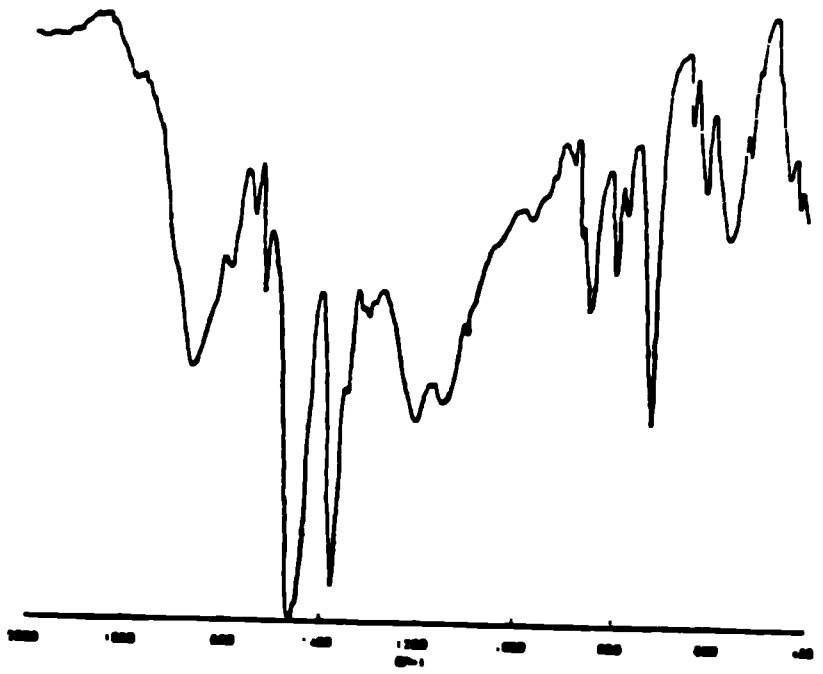

Figure 7.5 : Infrared spectrum of (62) (2000 - 400cm^{-1} nujol mull)

A broad OH band is observed in all cases due to the Ce-OH group. In the oxo-*bis* carboxylate compounds this band is observed at *ca.* 3370cm^{-1}. The range in the coordination compounds appears to be much larger, however, being between 3391 [(53) and (55)] and 3127cm^{-1} (63). In general this peak is at lower frequencies for the four tfa compounds. Also in the oxo-*bis* carboxylate compounds, we note that the $\nu COO_{(asym)}$ stretching vibrations are all very similar, this being also the case for the coordination compounds. In line with the oxo-*bis* carboxylate compounds there is no peak at *ca.* 1720±20cm^{-1} as there was in the hydrocarbyl oxo-*bis* carboxylate species. This band has been equated to the $\nu C{=}O_{(asym)}$ of free carboxylic acids. The dominant band at *ca.*3630cm^{-1} corresponding to the OH stretch of the free acid observed in all hydrocarbyl carboxylate complexes is, as is noted in the fluorinated oxo-*bis* carboxylates, rarely seen in these coordination compounds.

The $\nu COO_{(asym)}$ stretching frequency is observed to be in a very small range, *viz.* 1681 (55) - 1664cm^{-1} (60). As with the oxo-*bis* carboxylate compounds, in a number of cases, two bands are observed for this vibration. This may be an overall indication that the bonding of the carboxylate group is similar in strength throughout the series. The

$\nu COO_{(sym)}$ stretching frequencies are all in similar regions to those observed in the oxo-*bis* carboxylate compounds, however, their range is somewhat larger than that observed for the corresponding antisymmetric stretch. The separation between the two values ($\Delta\nu$) remains in the region generally reserved to indicate the presence of bridging or didentate carboxylate ligands, i.e. 234-105cm^{-1}. Although the larger separation often indicates unidentate carboxylates, this is unlikely to be the case.

Table 7.1 : Infrared data (cm^{-1}) of coordination compounds (53) - (65) :

Compound	νCe-OH	$\nu COO_{(asym)}$	$\nu COO_{(sym)}$	$\nu CF_{(asym)}$	$\nu CF_{(sym)}$
(53)	3391	1669	1493[a]	1223, 1170	815
(54)	3440[a]	1679, 1644	1463	1223, 1158	810
(55)	3391[a]	1681, 1605	1500	1212, 1171[a]	815
(56)	3373	1674, 1652	1471	1227, 1171	815
(57)	3331[a]	1669	1443	1222, 1170	818
(58)	3235[a]	1669[a]	1435[a]	1231[a], 1174[a]	818
(59)[b]	3405	1674	1456[a]	1230, 1172	812
(60)	3389[a]	1664	1520	1219, 1167	816
(61)	3354	1672	1473	1215, 1168	812
(62)	3320	1666	1455	1203, 1152	849
(63)	3127	1674	1470	1201, 1151	843
(64)[b]	3225	1679	1455	1207, 1147	841
(65)[b]	3256	1680	1456	1207, 1144	842

All spectra recorded as nujol mulls except ([a]) which were recorded as hexachlorobutadiene mulls and ([b]) which were recorded as neat liquids.

7.3.2 ^{1}H NMR analyses

The ^{1}H NMR of compounds (53) - (65) were measured in either deuterated chloroform or dmso and at either 90 or 270MHz at R.T.. Specific details are given with the experimental section of this Chapter. Bearing in mind that there are no protons on the carboxylate ligands themselves we are not able to glean much information about their nature from this spectroscopic technique, however, we may learn a great deal of information concerning both the coordination ligands and their ratio to the coordinated hydroxo ligands.

The Ce-OH resonance is usually observed as a broad peak, however, its position varies dramatically from compound to compound. For instance in compound (54) it appears as a broad singlet at δ 3.40 while in compound (60) it is considerably further downfield at δ 5.56. In general the ratio between the Ce-OH proton and the coordinating ligand is 2 : 1, however, when alcohols such triethylene glycol monomethyl ether (59) and 2-hydroxypyridine (54) are employed the ratio becomes 1 : 1, i.e. these reactions are accompanied by the loss of a hydroxyl group. This could suggest that the structures of these compounds are radically different from those with the neutral coordinating ligands such as phen, although from IR data there is no evidence of an alteration in the bonding nature of the pfb ligands. There appears to be no direct correlation between the position of the Ce-OH resonance and either the nature of the carboxylate or the coordinating ligand. For example the two phenanthroline compounds have Ce-OH resonances at δ 5.56 (60) and δ 4.23 (62), while the two pfp compounds have Ce-OH resonances at δ 5.56 (60) and δ 3.45.

The phen compounds (60) and (62) have very similar chemical shifts for the amine ligand suggesting similar coordination geometries. In general the respective resonances differ by only *ca.* δ 0.1. The 18-crown-6 compound (61) has a remarkably straight forward spectrum, having only two resonances. The first at δ 3.21 is a sharp singlet and corresponds to the OCH_2 resonances of the ether ligand, while the other is a broad singlet at δ 3.45 and is due to the Ce-OH proton. The ratio between the two is 1 ether : 2 hydroxyl groups.

Compound (56) has very broad peaks throughout its spectrum. The coordinating ligand in this particular compound is tmeda, a multidentate amine ligand. The spectrum is similar in many respects to that of compound (39) which employs a similar amine ligand, pmdeta. The reason for the line broadening is once again due to the amine being partially oxidized to the amine oxide, with the direct consequence of reducing the metal to Ce(III).

As has been previously discussed, Ce(III) compounds tend to give rather broad lines in the NMR spectrum due to their paramagnetic nature. Compound (63) has only two resonances for the pyridine-*N*-oxide ligand, at δ 7.49 and 8.36. The integration shows that there are three protons (the *meta* and *para*) at high field and two (presumably the *ortho* protons) at low field.

The ^{1}H NMR spectrum of compound (65) is remarkably similar to that of compound (8) in terms of chemical shifts and the pattern of resonances of the polyether ligand. A sharp singlet is noted at *ca.* δ 3.2 for the OCH_3 resonance followed by OCH_2 resonances at δ 3.40 (a), 3.42 (b), 3.47 (c) and 3.48 (d). These shifts may be compared with those of compound (8) whose OCH_2 resonances are at 3.41, 3.42, 3.48 and 3.51 respectively. This may indicate that the nature of the bonding of the glyme ligand is similar in both compounds. This might, however, necessitate the breaking up of any polymeric structure in the starting material.

Finally compound (55) has a very unusual spectrum (see Figure 7.7). The ^{1}H NMR of free phenyl isocyanate has two sharp doublets centred at *ca.* δ 7.1 and 7.2 in a ratio of 2 : 3, presumably due to the two *ortho* protons and the three *meta* and *para* protons respectively. When this ligand is reacted with $[Ce(OH)_2(pfb)_2]$ (31) we observe a dramatic change in the resonance pattern. Two doublets with a coupling constant of 8Hz are observed at δ 6.52 and 7.49, due to the nature of the splitting, these resonances are most likely to be due to the two *ortho* protons. Two triplets with coupling constants of 7Hz are also observed at δ 6.97 and 7.23, these are most likely to be due to the *meta* protons. Each of these four resonances has an integral of 1. Finally two smaller triplets with coupling constants of 7Hz are also observed at δ 6.45 and 6.91. Both of these triplets integrate to 1/2 proton each. These two resonances are most likely to be due to the *para* proton.

One possible reason for this inequality in aromatic proton resonances is that the phenyl isocyanate ligand has partially polymerized, but also coordinated to the cerium metal centre. The close proximity of the phenyl rings to each other might cause them to twist about the NC bond so as to relieve some of the steric crowding, this would have the effect of altering the respective proton resonances. A possible partial structure could be similar to the one shown below.

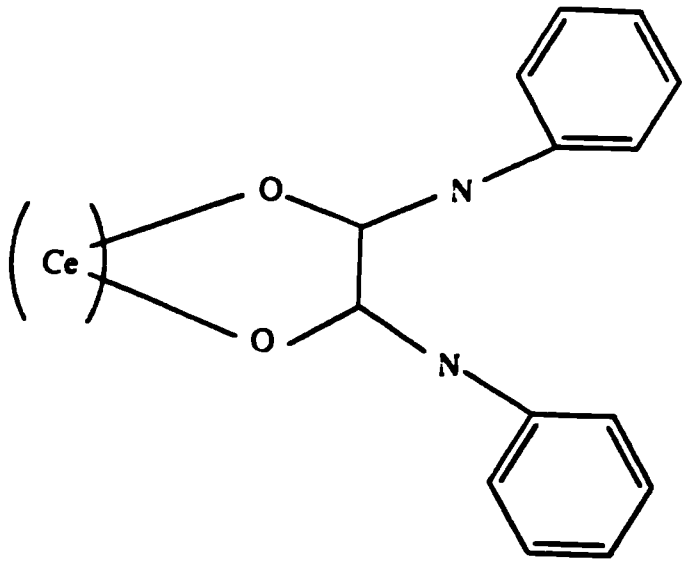

Figure 7.6 : Postulated partial structure for (55)

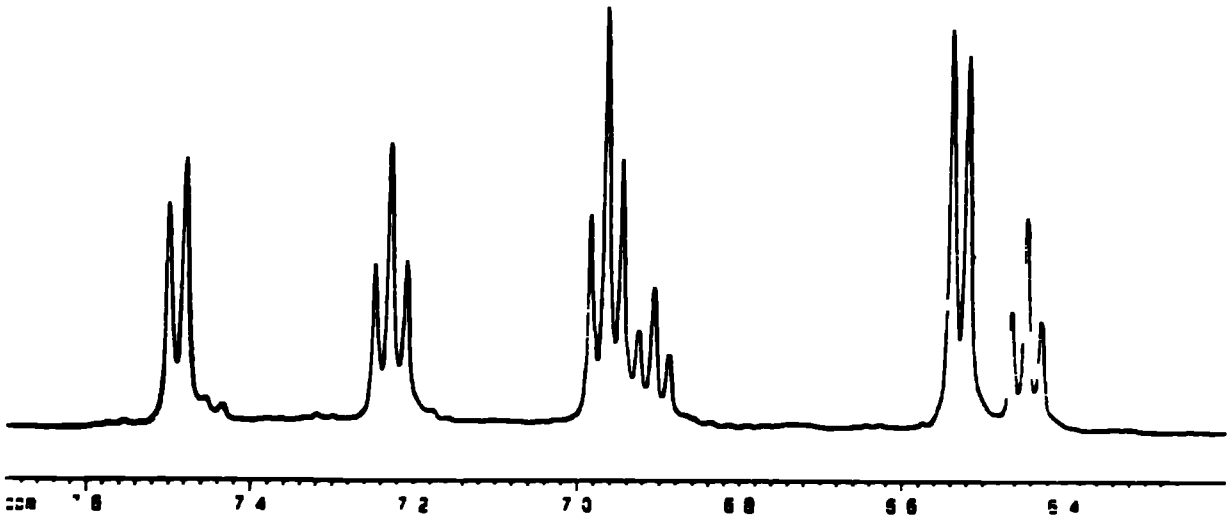

Figure 7.7 : ^{1}H NMR spectrum of (55) in D_6-dmso (aromatic region)

The apparent shift in the signals of the isocyanate ligand in the ^{1}H NMR leads one to investigate the magnetic properties of compound (55). The results using a magnetic susceptibility balance are shown below:

$$X = C(R - R')l / W$$

where l is the length of the sample in mm

W is the sample mass in g

R' is the empty tube reading

C is the calibration constant (1.19×10^{-12})

R was measured to be 88

therefore $X = 1.85 \times 10^{-8}\ m^3Kg^{-1}$

therefore $X_m = 1.85 \times 10^{-8} \times 0.719\ (M_r) = 1.33 \times 10^{-8}\ m^3mol^{-1}$

diamagnetic correction = $-0.186 \times 10^{-8}\ m^3mol^{-1}$

therefore $X_m' = (1.33 + 0.186) \times 10^{-8} = 1.516 \times 10^{-8}\ m^3mol^{-1}$

$\mu_{eff} = 796\ (298 \times 1.516 \times 10^{-8})^{1/2} =$ <u>1.69 BM</u>

Compound (55) is, therefore, paramagnetic which accounts for the proton resonances being shifted in the NMR spectrum. The expected values are considerably higher (2.46 - 2.54 BM), however, this discrepancy may be due to the size of the oligomer.

7.3.3 ^{13}C NMR analyses

The ^{13}C NMR spectra of the oxo-*bis* carboxylates (31) - (33), show a complex pattern for the CF resonances, especially with the larger carboxylates containing fluorine atoms in different environments. For instance complex (33) is a tfa compound and shows only one quartet at δ 117.9 for the CF_3 group and a further quartet for the CO group at δ 158.9. This contrast with the pfb compound (31) which also shows the CF_3 and CO resonances with similar chemical shifts, but also shows a triplet and a multiplet of triplets for the CF_2 groups. These latter resonances are upfield of the CF_3 resonance at *ca.* δ 108-9.

These patterns are observed in the majority of the coordination compounds of the perfluorinated cerium carboxylates. Very small chemical shift ranges are noted for the CF resonances in most cases. For example, the range of CF_3 resonances in the tfa compounds is only δ 117.6 - 118.8, a quartet being observed in each case. The coupling constants are approximately equal to those observed in the oxo-*bis* carboxylate complexes, *ca.* 290 - 300Hz. The CO resonance for the tfa compounds also lies within a very narrow band, between δ 158.4 and 159.4, the coupling constant being *ca.* 32 - 34Hz are similar to those noted for the oxo-*bis* carboxylates too. The resonances for the tfa compounds are relatively simple, however, the complex nature of the pfp and pfb ligands may account for why the CF resonances are not always observed. For example the pfp complexes (60) and (61) show no carboxylate ligand resonances at all. Alternatively an intermolecular exchange process could account for this lack of signals.

Table 7.2 shows the CF_3 and the CO resonances for the oxo-*bis* carboxylate species and the coordination compounds of the tfa ligand.

Table 7.2 : Selected ^{13}C NMR data for tfa compounds (31) and (62) - (65)

Compound	δ CF_3	δ CO
(31)	117.1 (^1J = 293Hz)	159.1 (^2J = 35Hz)
(62)	117.7 (^1J = 296Hz)	159.4 (^2J = 34Hz)
(63)	117.6 (^1J = 298Hz)	158.9 (^2J = 33Hz)
(64)	118.8 (^1J = 299Hz)	158.4 (^2J = 32Hz)
(65)	117.7 (^1J = 294Hz)	159.2 (^2J = 34Hz)

The CF_x and CO resonances of the pfb ligands also appear to lie within a very narrow range, generally between δ 1.0 - 2.0 of the values observed for the oxo-*bis* carboxylate compound. The resonances are particularly well resolved in complex (55). Here there is a triplet of quartets at δ 109.0 attributed to the $CF_3\underline{C}F_2$ carbons, and a further triplet of triplets at δ 110.3 corresponding to the $CO\underline{C}F_2$ groups. A final quartet of triplets is observed at δ 117.9 for the CF_3 carbons.

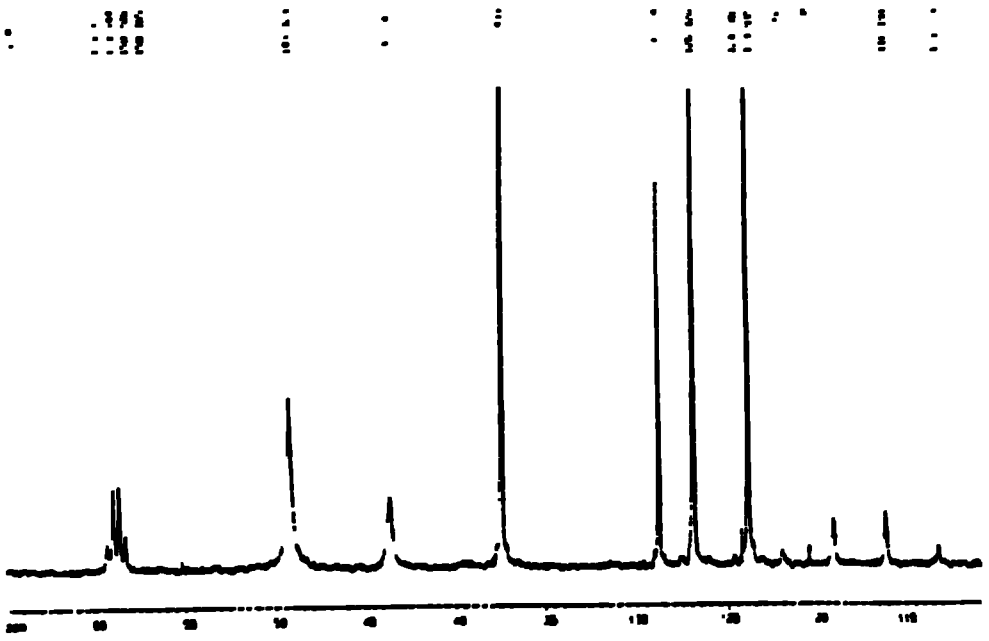

Figure 7.8 : ^{13}C NMR of (62) in D_6dmso

As was previously noted for the ^{1}H NMR spectra the two phenanthroline complexes (60) and (74) have very similar chemical shifts for the coordinating ligand in the ^{13}C NMR. The shifts differ by only δ 0.2 in each case except for the NC<u>C</u> and N<u>C</u>H carbon atoms which differ by between δ 1 - 2. Compound (59) has a long chain etheric alcohol as its coordinating ligand (tgme). From ^{13}C NMR analysis we are able to differentiate between the different OCH_2 groups in the same way that we are able to differentiate in the glyme complexes described in Chapter 2 and also compound (65). In compound (59) there is a large difference between the OCH_2 resonances. e.g. OCH_2 (a) is at δ 60.3 while the other three resonances appear in the more usual position between δ 69.0 and 72.0. This may suggest that the OCH_2 (a) group is not actually coordinated to the metal centre. presumably due to steric factors. In contrast the tetraglyme complex (65) has four OCH_2 resonances in the more usual region between δ 69.6 and 71.3 and corroborates the conclusions from the ^{1}H NMR analysis.

Once again compound (55) shows an intriguing spectrum. It was noted that in the ^{1}H NMR spectrum each of the protons on the isocyanate ring had a different chemical shift. and the *para* proton was split into two triplets. A similar phenomenon occurs in the ^{13}C

NMR spectrum where six resonances are noted for the ring carbons instead of the expected four. The *para* carbon is at highest field at δ 114.0, while the two *meta* carbons are at δ 115.7 and 118.2. The two *ortho* carbons are at δ 121.7 and 128.9 with the *ipso* carbon at lowest field at δ 140.3. This inequality in carbon atom environments may be due to the same reason described in section 7.3.2 above.

7.3.4 Mass spectrometry

The perfluorinated compounds (31) - (33) tend to show only a few types of ion in the mass spectrum. All three compounds show both $[Ce_xO_y]$ and $[Ce_xO_yF_z]$ ions. Compound (31) shows a further set of ions, namely $[(CeOH)_x(pfb)_y]$ together with the fragments caused by the loss of a number of fluorine atoms. This type of ion is also seen in the mass spectra of the hydrocarbyl carboxylates. The coordination compounds of this Chapter also show these three types of ions.

Many of the pfb compounds including, (53) and (54), show an ion at m/z 525 for $[(CeO)_2(pfb)]$. This fragment is easy to imagine bearing in mind that the carboxylate ligands are all likely to be bridging. In contrast to the mass spectrum of the oxo-*bis* carboxylates there are no larger ions of this type. For the pfb compounds an ion is often noted at m/z 353 for [Ce(pfb)], this ion is observed as only a weak fragment in (54) (2%) but is a somewhat more important ion in the spectra of compounds (55) and (58) (<10%). Two related ions are also observed for compound (55) at m/z 547 and 938, which correspond to $[Ce(pfb)_2\text{-}F]$ and $[Ce_2(pfb)_3F]$ respectively. Once again the propensity for the perfluorinated ligands to either lose or gain fluorine atoms almost at will is rife.

This factor is reproduced well in compounds (56) and (53) which show ions illustrating the loss of a number of fluorine atoms. A very large ion at m/z 259 (100%), which corresponds to $[Ce(O_2CCF_2C)]$ which depicts the loss of a CF_3 group and two further fluorine atoms from the pfb ligand, is observed in the spectrum of (53). Similarly, compound (56) has an ion corresponding to $[Ce(O_2CCF_2)]$ at m/z 245, this is basically the same ion but with the complete loss of a C_2F_5 group.

Both compounds (58) and (59) show a wide range of ions consisting of both pfb and coordinating ligand. For instance (59) has peaks at very high molecular weight, m/z 1244 and 1050 for $[Ce_2(pfb)_3\text{-}F(tgme)_2(OH)]$ and $[Ce_2(pfb)_2(tgme)_2(OH)]$ respectively. These ions are also observed to be very abundant (75 and 21%) despite their size. Compound (57) shows the same pattern as for the 'oxo-*bis* carboxylate' species, this is not that surprising as the coordinated alcohol is likely to be vaporized prior to the decomposition of the rest of the sample.

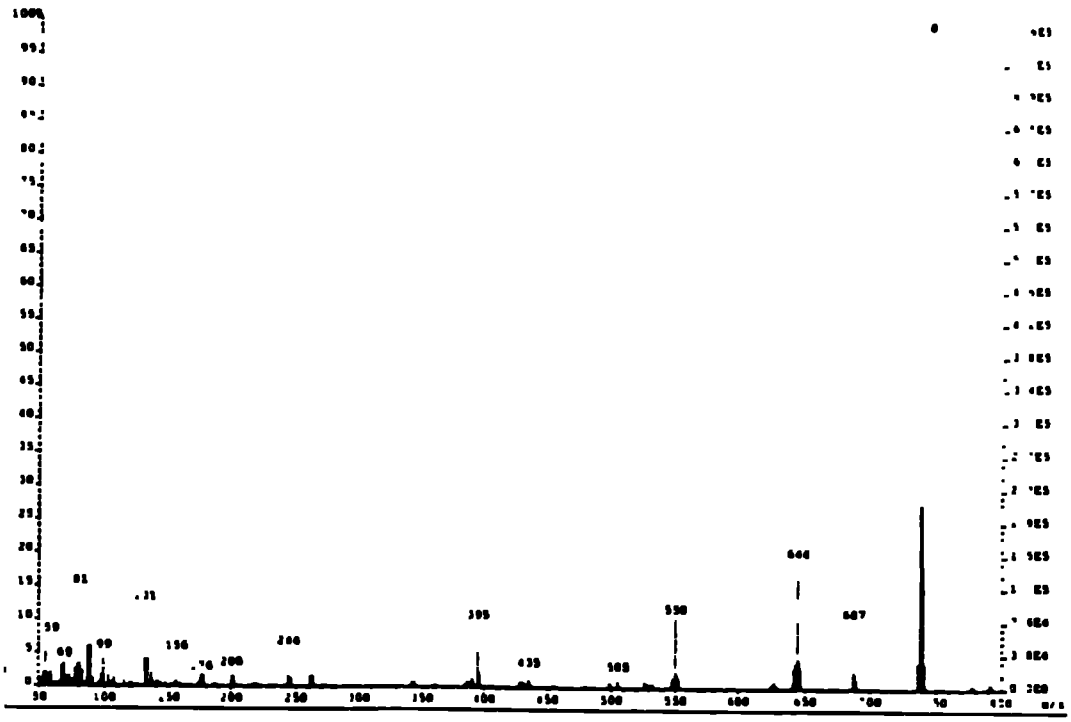

Figure 7.9 : FAB+ mass spectrum of (64)

The pentafluoropropionate compounds (60) and (61) do not show any $[(CeOH)_x(pfp)_y]$ ions under FAB+ conditions. They do, however, show a number of peaks associated with the coordinating ligands. Compound (61) shows numerous ether containing ions at m/z 730, 586 and 442 for [Ce(pfp)$_2$(crown)], [Ce(pfp)(crown)F] and [Ce(crown)F$_2$]. Similar peaks have also been noted in the dicyclohexano-18-crown-6 and tetraglyme complexes (64) (see Figure 7.9) and (65). The spectrum of (60) shows a number of peaks which are duplicated in the spectrum of (62), therefore, they are likely to consist only of cerium, oxygen and phen fragments. Large peaks at m/z 505, 358 and 181 correspond to [Ce(phen)$_2$(OH)-C], [Ce(phen)NCC] and [(phen)]. The spectrum of (63) shows a number of interesting ions. $[ML_x]$ ions appear at m/z 658 [Ce$_2$(tfa)$_3$F$_2$], 368 [Ce(tfa)$_2$] and 273 [Ce(tfa)F]. There is also an $[(CeOH)_x(tfa)_y]$ type ion at m/z 556 for [Ce$_2$O$_3$(tfa)$_2$] and a coordinated pyridine-*N*-oxide ion at m/z 462 for [Ce(tfa)$_2$(PyNO)].

7.4 Physical properties

7.4.1 Solubilities and melting points

In common with the compounds described in Chapter 6, the solubilities of the perfluorinated carboxylate coordination compounds are more dependent on the nature of the carboxylate itself than with the properties of the coordinating ligand. The oxo-*bis* carboxylate compounds themselves show extensive solubilities in polar solvents, such as alcohols, dmso, dmf and acetonitrile but are insoluble in non polar solvents such as benzene and toluene. The longer chain carboxylates, (31) and (32), however, show some solubility in chloroform.

The mixed coordination compounds show similar solubilities to the oxo-*bis* carboxylate compounds. For example the perfluorobutyrate compounds are all soluble in chloroform, acetonitrile, dmso and thf, whereas the analogous tfa compounds are soluble only in the more polar solvents, e.g. acetonitrile, dmso and thf. However, neither are soluble in water to any significant degree (unlike the oxo-*bis* tfa compound which shows appreciable solubility in water). This is not unexpected in view of the solubility properties of the oxo-*bis* carboxylate species (see Chapter 5) where it was noted that the optimum number of carbon atoms in the chain for solubility is between four and seven (pfb having four carbon atoms while tfa has only two). As with the oxo-*bis* carboxylates the pfp compounds show solubility properties intermediate between those of the other two carboxylates.

None of the coordination compounds show any solubility in non-polar solvents such as petroleum ether, hexane or benzene, however, the compounds containing coordinated ethers (including crowns) e.g. (61), (64) and (65) show appreciable solubilities in diethyl ether. Employing a ligand which is essentially a sterically crowded substituted alcohol, 2-hydroxypyridine, appears to lower the solubilities of the carboxylate complex somewhat more dramatically than the majority of the other ligands. The perfluorobutyrate complex (54), is only partially soluble in boiling chloroform but completely soluble in more polar solvents. The fact that the solubilities of the coordination compounds are similar to those of the oxo-*bis* carboxylate species may indicate similar structures, i.e. coordination of the ligand does not break up the hexamer to any significant degree.

There appears to be no distinct patterns concerning the melting points of the coordination compounds of the perfluorinated cerium(IV) carboxylate species, either with

respect to the carboxylate ligand or the organic coordination ligand. For instance, compounds (60) and (62) are both phenanthroline compounds but with different carboxylates. The pfp compound is observed to partially melt at 173-7°C but remains stable until boiling at 250-2°C. In contrast the tfa compound (62) has a much higher partial melting point, namely 260-2°C and does not decompose until the temperature reaches 280-5°C.

This cannot be explained simply by considering the size of the carboxylate ligand as the pfp oxo-*bis* carboxylate is observed to decompose at a higher temperature than the tfa oxo-*bis* carboxylate compound, i.e. (270-3 and 263-5°C respectively). This factor is also noted for the related compounds (54) and (63). Once again the organic ligands are similar and the compounds differ only in the size of the carboxylate ligand. However, the pfb complex (54) is observed to melt at a relatively low temperature, 158-72°C while the tfa compound (63) only begins to partially melt at 248-55°C and decomposes at 280-5°C.

Considering too, the perfluorobutyrate compounds (53) - (59) we note a wide range of melting and decomposition points, which cannot be easily explained. A number of coordination compounds of this group are observed to melt between *ca.* 155 and 172°C, for example compounds (54), (56) and (58), however, the only link between these compounds is the carboxylate ligand. One noteworthy compound is (55), $[Ce(OH)_2(pfb)_2(PhNCO)]$, which has a remarkably low melting point of only 75-8°C. This compound has already been shown to have many different properties to the other coordination compounds of this group (e.g. being a deep purple colour as opposed to the more usual yellow or orange and its consequent uv/vis spectrum). This melting point value is also considerably lower (almost 100°C lower in fact) than those observed for the residual polymeric products yielded from the reactions between the hydrocarbyl carboxylate complexes and either alkyl or aryl isocyanates, for example compound (693). This too supports the observation that $[Ce(OH)_2(pfb)_2]$ (31) does not polymerize phenyl isocyanate to the same extent.

7.4.2 STA analyses

The TGA plot of $[Ce(OH)_2(tfa)_2]$ (33) is very straightforward showing only one very sharp weight loss between 259 and 269°C. This loss was observed to be due to controlled explosion, one which is also noted in the melting point measurement, this time occurring at 263-265°C. A similar phenomenon is observed for $[Ce(OH)_2(tfa)_2(pyNO)]$ (63), which shows just one very sharp weight loss between 264.0 and 288.2°C (75.2%). This too is likely to be due to an explosion under these conditions. However, there is not such a vigorous explosion observed in the melting point measurement. The final residue of 24.2% is less than expected for CeO_2 (35.0%), however, this is also the case with the oxo-*bis* carboxylate species and is not surprising given the explosive nature of the weight loss. The DSC plot, too, is very simple, just a single very sharp endotherm observed at 279.9°C due to the observed explosion.

The TGA plot of $[Ce(OH)_2(pfp)_2(phen)]$ (60) also initially appears very simple with only two clearly discernible weight losses being observed. The first between 167.3 and 234.5°C most likely corresponds to the loss of two fluorine atoms from the carboxylate ligand (found 5.42% ; expected 5.59%). Secondly there is a larger weight loss (58.9%) between 270.3 and 294.4°C. This may correspond to the loss of a combination of the phenanthroline ligand, the C_2F_3 fragment of the initial pfp ligand and the whole of the second pfp ligand (expected 62.3%). Between this temperature and the final horizontal plateau at 750°C there is a further steady weight loss of *ca.* 6% which may correspond to the loss of some of the remaining carbon and oxygen fragments. The final residue of 35.7% is higher than expected for CeO_2 (expected 25.6%) suggesting that much of residue is carbonaceous (and even possibly oxyfluoro) deposits.

The DSC plot of (60) shows two endotherms, the first being a broad one at 214.9°C corresponding to the loss of the fluorine atoms, while the second is much more sharp at 286.3°C this is most likely to be due to the loss of the amine and pfp ligand. Following this is a very broad and shallow endotherm which mirrors the slow loss of the remaining carbon and oxygen atoms shown in the TGA plot. Taken together these data suggest that the coordination compounds of the fluorinated carboxylates have similar volatilities to those of the oxo-*bis* carboxylate perfluorinated materials and are considerably more volatile than the hydrocarbon carboxylates (23) - (30).

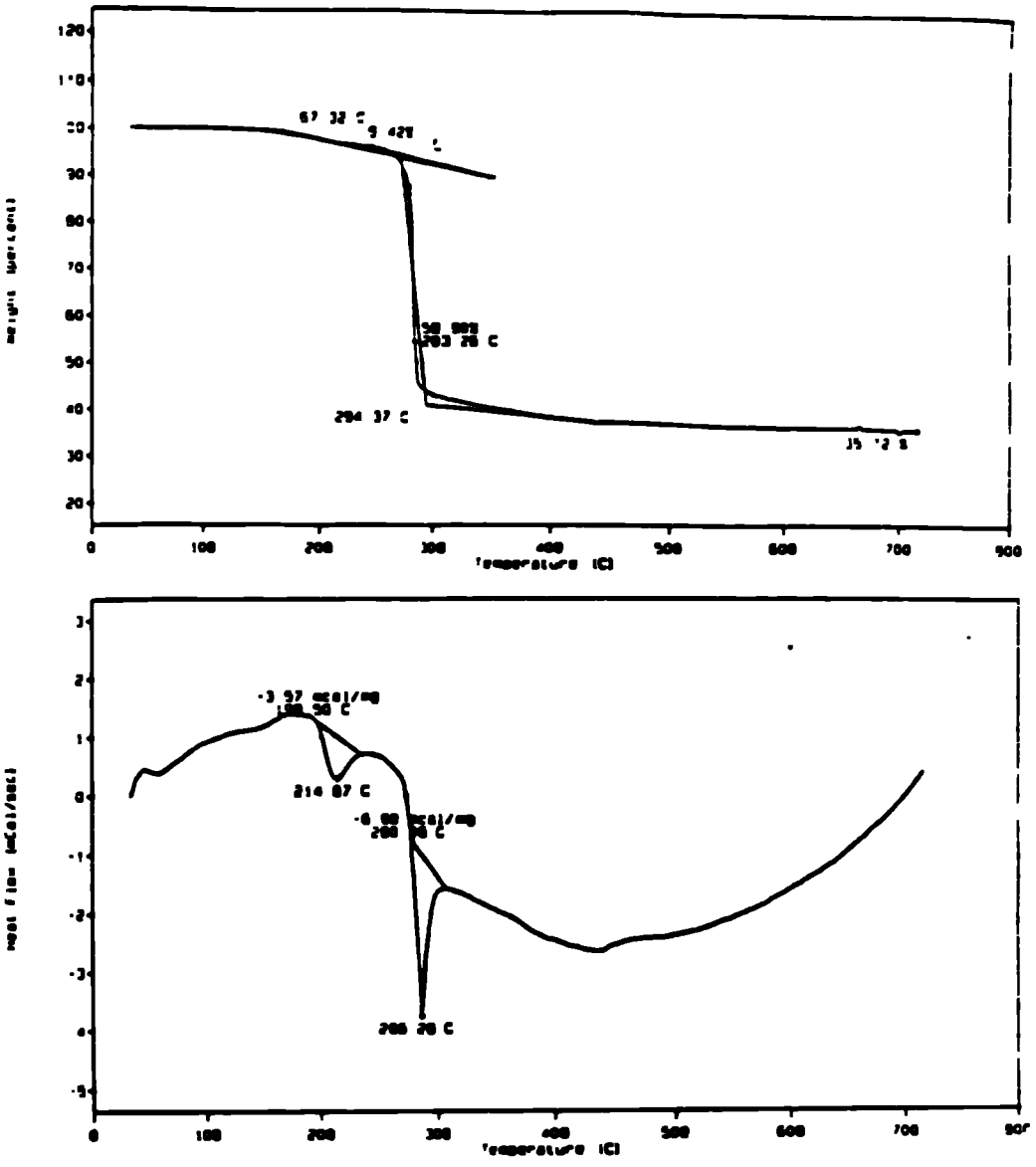

Figure 7.10 : TGA (top) and DSC (bottom) plots of (60)

7.4.3 Conclusions

The perfluorinated cerium (IV) carboxylate species react with a wide range of coordinating ligands to yield, generally, non crystalline products of the general formula $[Ce(OH)_2(RCO_2)_2L_x]$ (where x = 0.25 - 1 depending on the nature of the ligand). Again we are unable to ascertain from spectroscopic and analytical data whether the coordination of the ligands causes the hexameric cluster to break down into smaller units. The difference in reactivity of these halogenated species to the hydrocarbyl species described in the previous Chapter is often apparent from analysis of the ratios of the carboxylate ligand to the coordinating ligand.

7.5 : Experimental Section

Synthesis of $[Ce(OH)_2(pfb)_2(py)_{0.5}]$ (53)

$Ce(OH)_2(pfb)_2$ (0.35g, 0.59 mmol) (31) was dissolved in chloroform (50 mL) to yield a soluble yellow solution, to which was added pyridine (0.05g, 0.59 mmol). The soluble solution was stirred for 16h at 60°C and then stripped to dryness to yield a pale yellow solid. **Yield** 0.23 g (62%) **M. Pt.** dec. 260-3°C

Microanalyses : Found, C, 19.3 ; H, 0.78 ; N, 0.89 ; Calc. for $CeO_6C_{10.5}F_{14}H_{4.5}N_{0.5}$, C, 19.7 ; H, 0.70 ; N, 1.09%.

Infrared (Nujol ν cm^{-1}) : 3391(br), 1669(w), 1550(w), 1347(m), 1223(m), 1170(w), 1120(w), 1086(w), 970(w), 937(m), 815(m), 679(w), 583(m), 468(w), 415(w).

Infrared (Hexachlorobutadiene ν cm^{-1}) : 3433(w, br), 2924(w), 1672(m), 1493(w), 1426(m), 1341(m), 1229(m), 1171(m), 1121(m), 1067(m), 893(w), 718(w), 581(m).

^1H NMR (90 MHz, $CDCl_3$, 20°C) : δ 4.12 (2H, br, Ce-OH), 7.59 (1H, br, NCHC<u>H</u>), 7.88 (0.5H, br, NCHCHC<u>H</u>), 8.57 (1H, br, NC<u>H</u>).

^{13}C NMR (22.65 MHz, $CDCl_3$, 20°C) : δ 108.8 (m, CF_2 , ^1J = 288Hz, ^2J = 35Hz), 117.7 (q of t, CF_3, ^1J = 265Hz, ^2J = 31Hz), 124.1 (s, NCHCH<u>C</u>H), 136.7 (s, NCH<u>C</u>H), 149.2 (s, N<u>C</u>H), 158.4 (br, CO).

Mass Spectrometry (FAB +) : 525 [$(CeO)_2(pfb)$](3%), 328 [Ce_2O_3](5%), 259 [$Ce(O_2CCF_2C)$](100%).

Solubility : Soluble in chloroform, dmso and thf, insoluble in water, hexane and benzene.

Synthesis of $[Ce(OH)(pfb)_2(2\text{-}pyO)]$ (54)

$Ce(OH)_2(pfb)_2$ (0.45 g, 0.77 mmol) (31) was dissolved in chloroform (50 mL) to yield a soluble yellow solution, to which was added 2-hydroxypyridine (0.07g, 0.77 mmol). The soluble yellow solution was stirred for 24h at 60°C and then stripped to dryness to yield a dark yellow solid. **Yield** 0.41 g (79%) **M. Pt.** melts 158-72°C

Microanalyses : Found, C, 23.0 ; H, 0.75 ; N, 2.17 ; Calc. for $CeO_6C_{13}F_{14}H_5N$, C, 23.0 ; H, 0.74 ; N, 2.07%.

Infrared (Nujol ν cm^{-1}) : 1678(m), 1644(s), 1597(m), 1541(m), 1341(s), 1223(m), 1158(m), 1118(m), 1083(m), 999(m), 967(m), 935(m), 859(m), 810(m), 775(m), 624(w), 566(m), 501(w), 498(m), 480(w), 464(w), 408(m), 338(w).

Infrared (Hexachlorobutadiene ν cm^{-1}) : 3440(m, br), 1679(m), 1645(s), 1463(m), 1411(m), 1338(m), 1230(m), 1171(m), 1118(m), 1084(m), 898(w), 716(w), 566(m), 490(m), 465(w).

^1H NMR (90 MHz, D_6-dmso, 20°C) : δ 3.40 (2H, br, Ce-OH), 6.19 (2H, m, NCHC<u>H</u> and NCHCHC<u>H</u> (py-O)), 7.33 (2H, m, NC<u>H</u> and NCC<u>H</u> (py-O)).

^{13}C NMR (22.65 MHz, D_6-dmso, 20°C) : δ 106.3 (s, NCHCHCH), 120.7 (s, NCHCH), 136.2 (s, NCCH), 141.2 (s, NCH), 165.4 (br, NCO).

Mass Spectrometry (FAB +) : 525 [$(CeO)_2$(pfb)](2%), 353 [Ce(pfb)](2%), 328 [Ce_2O_3](5%), 259 [$Ce(O_2CF_2CC)$](100%).

Solubility : Soluble in dmso and thf, partially soluble in hot chloroform, insoluble in water, hexane and benzene.

Synthesis of $[Ce(OH)_2(pfb)_2(PhNCO)]$ (55)

$Ce(OH)_2(pfb)_2$ (0.62g, 1.03 mmol) (31) was dissolved in chloroform (50 mL) yielding a yellow solution, to which was added phenyl isocyanate (0.12g, 1.03 mmol). Immediately the solution became purple / black and soluble. The reaction mixture was stirred for 6h at 60°C and on completion stripped to dryness to yield a purple solid. **Yield** 0.60 g (83%) **M. Pt.** melts 75-8°C

Microanalyses : Found, C, 25.3 ; H, 1.21 ; N, 2.20 ; Calc. for $CeO_7C_{15}H_7F_{14}N$, C, 25.0 ; H, 0.97 ; N, 1.95%.

Infrared (Nujol ν cm^{-1}) : 3606(w), 3299(m), 1681(m), 1605(m), 1539(m), 1500(m), 1339(m), 1212(s), 1118(m), 1083(m), 1029(m), 968(m), 935(m), 815(m), 741(m), 693(m), 588(m), 526(w).

Infrared (Hexachlorobutadiene ν cm^{-1}) : 3585(w), 3391(m), 1682(m), 1500(m), 1430(m), 1341(m), 1214(m), 1171(s), 1119(w), 1085(w), 1028(w), 894(w), 720(w), 693(w).

^1H NMR (270 MHz, D_6-dmso, 20°C) : δ 3.42 (2H, br, Ce-OH), 6.45 (0.5H, t, p-CH (PhNCO)), 6.52 (1H, d, o-CH (PhNCO)), 6.91 (0.5H, t, p-CH (PhNCO)), 6.97 (1H, t, m-CH (PhNCO)), 7.23 (1H, t, m-CH (PhNCO)), 7.49 (1H, d, o-CH (PhNCO)).

^{13}C NMR (67.94 MHz, D_6-dmso, 20°C) : δ 109.0 (t of q, CF_3CF_2, ^1J = 273Hz, ^2J = 36Hz), 110.3 (t of t, $COCF_2$, ^1J = 266Hz, ^2J = 32Hz), 114.0 (s, p-Ph), 115.7 (s, m-Ph), 117.9 (q of t, CF_3, ^1J = 288Hz, ^2J = 34Hz), 118.2 (s, m-Ph), 121.7 (s, o-Ph), 128.9 (s, o-Ph), 140.3 (s, i-Ph), 157.6 (t, CO, ^2J = 33Hz).

Mass Spectrometry (FAB +) : 938 [$Ce_2(pfb)_3F$](38%), 547 [$Ce(pfb)_2F$](14%), 353 [Ce(pfb)](18%).

Solubility : Soluble in acetone, chloroform, dmso and thf, insoluble in water, hexane and benzene.

Synthesis of $[Ce(OH)_2(pfb)_2(tmeda)_{0.33}]$ (56)

$Ce(OH)_2(pfb)_2$ (0.56g, 0.96 mmol) (31) was partially dissolved in chloroform (50 mL) yielding a yellow solution, to which was added tmeda (0.12g, 0.96 mmol). The brown solution was stirred for 16h at 65°C whereupon it became soluble, on completion the mixture was stripped to dryness to yield a brown oily solid. **Yield** 0.50 g (82%) **M. Pt.**

partial dec. 115-22, melts 155-57°C

Microanalyses : Found, C, 18.8 ; H, 1.46 ; N, 1.50 ; Calc. for $CeO_6C_{10}H_{7.33}F_{14}N_{67}$, C, 18.8 ; H, 1.14 ; N, 1.46%.

Infrared (Nujol ν cm^{-1}) : 3373(w, br), 1738(w), 1674(m), 1652(m), 1227(m), 1169(m), 1116(m), 1083(m), 969(w), 935(m), 811(m), 762(w), 588(m), 453(m), 410(w).

Infrared (Hexachlorobutadiene ν cm^{-1}) : 3391 (m, br), 1674(m), 1652(w), 1471(m), 1423(m), 1339(m), 1230(m), 1170(s), 1118(m), 1086(m), 893(w), 717(m), 579(m).

^{1}H NMR (90 MHz, D_6-dmso, 20°C) : δ 2.03 (4H, br, NCH_3), 2.40 (1.3H, br, NCH_2), 3.56 (2H, br, Ce-OH).

^{13}C NMR (22.65 MHz, D_6-dmso, 20°C) : δ 44.13 (s, NCH_3), 54.28 (s, NCH_2).

Mass Spectrometry (FAB +) : 377 [Ce(O_2CF_2C)(tmeda-O)](8%), 245 [Ce(O_2CCF_2)](14%), 133 [(tmeda-O)](11%), 117 [(tmeda)](100%).

Solubility : Soluble in chloroform, dmso and thf, insoluble in water, hexane and benzene.

Synthesis of $[Ce(OH)_2(pfb)_2(IPA)_{0.5}]$ (57)

$Ce(OH)_2(pfb)_2$ (0.89g, 1.48 mmol) (31) was suspended in toluene (50 mL) and heated to 75°C whereupon iso-propyl alcohol (0.22 mL, 1.48 mmol) was added. At this juncture there was no observable reaction. The reaction mixture was stirred for 6h at 100°C to yield a soluble yellow solution which was stripped to dryness to yield a pale yellow solid. Yield 0.73 g (78%) M. Pt. dec. 232-40°C

Microanalyses : Found, C, 17.5 ; H, 0.98 ; Calc. for $CeO_{6.5}C_{9.5}H_{5.5}F_{14}$, C, 18.1 ; H, 0.87 %.

Infrared (Nujol ν cm^{-1}) : 3686(m), 3618(m), 1669(m), 1585(w), 1303(m), 1222(m), 1170(m), 1123(w), 1087(w), 972(m), 938(m), 892(w), 818(m), 765(m), 653(m), 570(m), 536(m), 460(m), 399(m), 338(w).

Infrared (Hexachlorobutadiene ν cm^{-1}) : 3698(w), 3619(w), 3331(br), 1671(m), 1443(w), 1343(w), 1279(w), 1231(m), 1172(m), 1123(w), 1089(m), 1037(w), 894(w), 743(m), 719(w).

^{1}H NMR (90 MHz, D_6-dmso, 20°C) : δ 0.97, 1.04 (3H, m, CH_3 (IPA)), 3.75 (0.5H, septet, CH (IPA)), 4.97 (2H, br, Ce-OH).

^{13}C NMR (22.65 MHz, D_6-dmso, 20°C) : δ 25.6 (s, CH_3 (IPA)), 62.3 (s, CH (IPA)).

Mass Spectrometry (FAB +) : 724 [$Ce_4O_5F_4$](3%), 699 [$Ce_4O_5F_3$](4%), 677 [$Ce_4O_5F_2$](4%), 658 [Ce_4O_5F](3%), 640 [Ce_4O_5](2%), 524 [$Ce_3O_4F_2$](2%), 505 [Ce_3O_4F](4%), 483 [Ce_3O_4](4%), 329 [Ce_2O_3](17%).

Solubility : Soluble in acetone, chloroform, dmso and thf, insoluble in water, hexane and benzene.

Synthesis of $[Ce(OH)_2(pfb)_2(^tBuEE)_{0.25}]$ (58)

$Ce(OH)_2(pfb)_2$ (2.00 g, 3.43 mmol) (31) was dissolved in chloroform (80 mL) to yield a soluble yellow solution, to which was added tertbutoxy-ethoxyethane (0.50g, 3.43 mmol). The soluble yellow solution was stirred for 4h at 60°C and then stripped to dryness to yield a yellow oily solid. **Yield** 1.50g (69%) **M. Pt.** melts 162-5°C

Microanalyses : Found, C, 19.3 ; H, 1.13 ; Calc. for $CeO_{6.5}C_{10}F_{14}H_{6.5}$, C, 18.9 ; H, 1.02%

Infrared (Hexachlorobutadiene ν cm^{-1}) : 3626(s), 3235(s, br), 2982(s), 2881(s), 1669(s), 1435(s), 1373(s), 1339(s), 1276(s), 1231(s), 1174(s), 1122(m), 1088(m), 1055(m), 899(w), 763(m), 583(m), 538(m), 459(w), 425(m), 417(m).

^1H NMR (90 MHz, $CDCl_3$, 20°C) : δ 1.20 (2.25H, s, $C(CH_3)$), 1.32 (0.75H, s, $CH_2\underline{CH_3}$), 3.51 (1.5H, m, OCH_2), 3.84 (2H, br, Ce-OH).

^{13}C NMR (22.65 MHz, $CDCl_3$, 20°C) : δ 16.2 (s, $C(\underline{C}H_3)$), 28.1 (s, $CH_2\underline{C}H_3$), 62.3 (s, $O\underline{C}H_2CH_3$), 67.4 (s, OCH_2), 72.1 (s, $O\underline{C}(CH_3)$).

Mass Spectrometry (FAB +) : 527 ($[(CeO)_2(pfb)]$(5%), 483 $[Ce_3O_4]$(9%), 353 [Ce(pfb)](12%), 331 [Ce(^{t}BuEE)(OCH_2CH_3)](14%), 286 [Ce(^{t}BuEE)](10%).

Solubility : Soluble in chloroform, diethyl ether, dmso and thf, insoluble in water, hexane and benzene.

Synthesis of $[Ce(OH)(pfb)_2(tgme)]$ (59)

$Ce(OH)_2(pfb)_2$ (0.58 g, 0.99 mmol) (31) was dissolved in chloroform (50 mL) to yield a soluble yellow solution, to which was added triethylene glycol monomethyl ether (0.16g, 0.99 mmol). The soluble yellow solution was stirred for 6h at 60°C whereupon it became orange, the solution was then stripped to dryness to yield a yellow oily solid. **Yield** 0.52 g (69%) **M. Pt.** dec. 227-32°C

Microanalyses : Found, C, 24.4 ; H, 2.50 ; Calc. for $CeO_5C_{15}F_{14}H_{16}$, C, 24.1 ; H, 2.14%.

Infrared (Neat ν cm^{-1}) : 3638(m), 3405(s, br), 2927(s), 1674(m), 1456(m), 1423(m), 1338(m), 1230(s), 1120(m), 1084(m), 969(m), 936(m), 891(w), 856(m), 812(w), 763(w), 741(m), 717(m), 585(w), 542(m), 529(m), 456(w), 410(w), 383(m).

Numbering scheme for tgme: $CH_3OCH_2(a)CH_2(a)OCH_2(b)CH_2(b)OCH_2(c)CH_2(d)O$

^1H NMR (90 MHz, $CDCl_3$, 20°C) : δ 1.99 (3H, s, OCH_3), 2.91 (12H, br, OCH_2), 4.44 (1H, br, Ce-OH).

^{13}C NMR (22.65 MHz, $CDCl_3$, 20°C) : δ 57.9 (s, OCH_3), 60.3 (s, OCH_2 a), 69.0 (s,OCH_2 b), 71.2 (s, OCH_2 c), 72.0 (s, OCH_2 d).

Mass Spectrometry (FAB +) : 1244 $[Ce_2(pfb)_3\text{-}F(tgme)_2(OH)]$(75%), 1050

$[Ce_2(pfb)_2(tgme)_2(OH)]$(21%), 560 [Ce(pfb)(OAc)(tgme)](22%), 516 [Ce(pfb)(tgme)](41%), 353 [Ce(pfb)](12%), 322 [CeF(tgme)](100%), 278 [Ce(pfb)-F_4](42%).

Solubility : Soluble in chloroform, diethyl ether, dmso and thf, insoluble in water, hexane and benzene.

Synthesis of $[Ce(OH)_2(pfp)_2(phen)]$ (60)

$Ce(OH)_2(pfp)_2$ (0.64g, 1.28 mmol) (32) was partially dissolved in chloroform (50 mL) yielding a yellow solution, to which was added 1,10-phenanthroline (0.23g, 1.28 mmol). The solution was stirred for 6h at 60°C whereupon it became soluble, on completion the mixture was stripped to dryness to yield a pale yellow solid. **Yield** 0.69 g (79%) **M. Pt.** partial melt 173-7, boils 250-2°C

Microanalyses : Found, C, 31.0 ; H, 1.29 ; N, 4.38 ; Calc. for $CeO_6C_{18}H_{10}F_{10}N_2$, C, 31.8 ; H, 1.47 ; N, 4.12%.

Infrared (Nujol ν cm^{-1}) : 1664(m), 1599(w), 1543(w), 1520(w), 1327(m), 1219(m), 1167(m), 1104(w), 1034(m), 886(w), 865(w), 847(m), 816(w), 790(w), 775(w), 642(w), 622(w), 587(w), 562(m), 542(w), 419(w).

Infrared (Hexachlorobutadiene ν cm^{-1}) : 3389(w, br), 1667(m), 1521(w), 1429(m), 1327(m), 1219(m), 1169(s), 1104(w), 1034(m), 894(w), 728(m).

^1H NMR (90 MHz, D_6-dmso, 20°C) : δ 5.56 (2H, br, Ce-OH), 7.85 (2H, d of d, NCHC<u>H</u>), 8.11 (2H, s, NCCCH), 8.65 (2H, d of d, NCHCHC<u>H</u>), 9.14 (2H, br, NCH).

^{13}C NMR (22.65 MHz, $CDCl_3$, 20°C) : δ 124.3 (s, NCC<u>C</u>H), 127.1 (s, NCHCH<u>C</u>H), 129.0 (s, NCH<u>C</u>H), 138.6 (s, NC<u>C</u>), 141.2 (s, N<u>C</u>H), 149.1 (s, N<u>C</u>), 159.4 (br, CO).

Mass Spectrometry (FAB +) : 1458 [$(CeO)_5(pfp)_4F$](33%), 825 [Ce_5O_8](11%), 505 [$Ce(phen)_2(OH)$-C](24%), 358 [Ce(phen)NCC](100%), 181 [(phen)](45%).

Solubility : Soluble in chloroform, dmso and thf, insoluble in water, hexane and benzene.

STA data : TGA : 167.3-234.5°C (5.42%), 270.3-294.4°C (58.9%), Res. 35.7%, $T_{50\%}$ 288°C. DSC : 214.9, 286.3°C.

Synthesis of $[Ce(OH)_2(pfp)_2(18\text{-crown-}6)]$ (61)

$Ce(OH)_2(pfp)_2$ (0.63 g, 1.26 mmol) (33) was dissolved in chloroform (50 mL) to yield a soluble yellow solution, to which was added 18-crown-6 (0.33g, 1.26 mmol). The soluble yellow solution was stirred for 6h at 60°C then stripped to dryness to yield a yellow solid. **Yield** 0.81 g (84%) **M. Pt.** melts 183-8°C

Microanalyses : Found, C, 28.3 ; H, 3.36 ; Calc. for $CeO_{12}C_{18}F_{10}H_{26}$, C, 28.3 ; H, 3.40%.

Infrared (Nujol ν cm^{-1}) : 3647(m), 3354(m, br), 2926(s), 2855(s), 1672(m), 1354(w), 1326(w), 1215(m), 1168(m), 1109(m), 1030(m), 959(m), 837(w), 812(m), 582(m), 540(w), 414(w), 307(w).

Infrared (Hexachlorobutadiene ν cm^{-1}) : 3647(m), 3363(m, br), 1671(s), 1473(m), 1423(m), 1394(m), 1354(m), 1327(m), 1215(m), 1169(s), 1109(s), 1031(s), 894(w), 731(m), 586(m), 542(m), 415(m).

^{1}H NMR (90 MHz, D_6-dmso, 20°C) : δ 3.21 (12H, s, OCH_2), 3.45 (2H, br, Ce-OH).

^{13}C NMR (22.65 MHz, D_6-dmso, 20°C) : δ 70.0 (s, OCH_2).

Mass Spectrometry (FAB +) : 730 [Ce(pfp)$_2$(crown)](100%), 586 [Ce(pfp)(crown)F](42%), 442 [Ce(crown)F_2](20%), 303 [Ce(pfp)](11%).

Solubility : Soluble in chloroform, diethyl ether, dmso and thf, insoluble in water, hexane and benzene.

Synthesis of $[Ce(OH)_2(tfa)_2(phen)]$ (62)

$Ce(OH)_2(tfa)_2$ (1.20g, 3.0 mmol) (33) was partially dissolved in acetonitrile (50 mL) yielding a yellow solution, to which was added 1,10-phenanthroline (0.54g, 3.0 mmol). The solution was stirred for 6h at 60°C whereupon it became soluble, on completion the mixture was stripped to dryness to yield a pale yellow solid. **Yield** 1.35 g (78%) **M. Pt.** partial melt 260-2, dec. 268°C

Microanalyses : Found, C, 32.9 ; H, 1.53 ; N, 4.76 ; Calc. for $CeO_6C_{16}H_{10}F_6N_2$, C, 33.1 ; H, 1.72 ; N, 4.83%.

Infrared (Nujol ν cm^{-1}) : 3320 (w, br), 1666(m), 1542(w), 1519(m), 1302(w), 1203(m), 1152(m), 885(w), 849(m), 795(w), 775(m), 641(w), 613(m), 561(m), 522(w), 440(m), 417(m).

Infrared (Hexachlorobutadiene ν cm^{-1}) : 3329(w, br), 3100(m), 1668(m), 1520(m), 1498(w), 1455(m), 1427(m), 1377(m), 1344(w), 1317(w), 1186(s), 1103(w), 1037(w), 723(m), 613(m).

^{1}H NMR (270 MHz, D_6-dmso, 20°C) : δ 4.23 (2H, br, Ce-OH), 7.81 (2H, d of d, NCHC<u>H</u>), 8.02 (2H, s, NCCC<u>H</u>), 8.58 (2H, d of d, NCHCHC<u>H</u>), 9.07 (2H, br, NC<u>H</u>).

^{13}C NMR (270 MHz, D_6-dmso, 20°C) : δ 117.7 (q, CF_3 ^1J = 296Hz), 123.9 (s, NCC<u>C</u>H), 126.9 (s, NCHCH<u>C</u>H), 128.8 (s, NCH<u>C</u>H), 137.5 (s, NC<u>C</u>), 143.6 (s, N<u>C</u>H), 149.3 (s, N<u>C</u>), 159.4 (q, CO ^2J = 34Hz).

Mass Spectrometry (FAB +) : 505 [Ce(phen)$_2$(OH)-C](17%), 358 [Ce(phen)NCC](100%), 181 [(phen)](95%).

Solubility : Soluble in acetonitrile, dmso and thf, insoluble in water, hexane and benzene.

Synthesis of $[Ce(OH)_2(tfa)_2(pyNO)]$ (63)

$Ce(OH)_2(tfa)_2$ (1.20g, 3.0 mmol) (33) was partially dissolved in acetonitrile (50 mL) yielding a yellow solution, to which was added pyridine-*N*-oxide (0.29g, 3.0 mmol). The solution was stirred for 6h at 60°C whereupon it became a soluble orange colour, on completion the mixture was stripped to dryness to yield a pale orange solid. **Yield** 1.09 g (73%) **M. Pt.** partial melt 248-55, dec. 280-5°C

Microanalyses : Found, C, 22.3 ; H, 1.23 ; N, 3.01 ; Calc. for $CeO_7C_9H_7F_6N$, C, 21.8 ; H, 1.41 ; N, 2.83%.

Infrared (Nujol ν cm^{-1}) : 3127 (w, br), 1674(m), 1410(m), 1304(m), 1201(m), 1151(m), 1026(w), 972(m), 843(w), 794(m), 770(w), 670(m), 612(m), 540(w), 462(w), 414(w).

Infrared (Hexachlorobutadiene ν cm^{-1}) : 3125(w, br), 2925(w), 2854(m), 1674(s), 1476(s), 1457(m), 1430(m), 1171(s), 1026(m), 893(w), 723(m), 671(m), 613(m).

^1H NMR (270 MHz, D_6-dmso, 20°C) : δ 3.67 (2H, br, Ce-OH), 7.49 (s, 3H, NCHC<u>H</u>C<u>H</u>), 8.36 (s, 2H, NC<u>H</u>).

^{13}C NMR (270 MHz, D_6-dmso, 20°C) : δ 117.6 (q, CF_3 ^1J = 298Hz), 126.7 (s, NCH<u>C</u>HCH), 128.1 (br, NCHCH<u>C</u>H), 139.3 (s, N<u>C</u>), 158.9 (q, CO ^2J = 33Hz).

Mass Spectrometry (FAB +) : 658 $[Ce_2(tfa)_3F_2]$(12%), 556 $[Ce_2O_3(tfa)_2]$(36%), 462 $[Ce(tfa)_2(PyNO)]$(44%), 368 $[Ce(tfa)_2]$(43%), 273 [Ce(tfa)F](56%).

Solubility : Soluble in acetonitrile, dmso and thf, insoluble in water, hexane and benzene.

STA data : TGA : 264.0-288.2°C (75.2%), Res. 24.2%, $T_{50\%}$ 275°C. DSC : 279.9°C.

Synthesis of $[Ce(OH)_2(tfa)_2(dch\text{-}18\text{-}crown\text{-}6)]$ (64)

$Ce(OH)_2(tfa)_2$ (0.93 g, 2.33 mmol) (33) was dissolved in acetonitrile (50 mL) to yield a soluble yellow solution, to which was added dicyclohexano-18-crown-6 (0.87g, 2.33 mmol). The soluble yellow solution was stirred for 6h at 60°C then stripped to dryness to yield a yellow solid. **Yield** 1.23 g (68%) **M. Pt.** melts 194-9°C

Microanalyses : Found, C, 37.7 ; H, 4.79 ; Calc. for $CeO_{12}C_{24}F_6H_{38}$, C, 37.3 ; H, 4.92%.

Infrared (Neat ν cm^{-1}) : 3225(s, br), 2928(s), 1679(s), 1506(m), 1455(s), 1359(s), 1342(m), 1268(m), 1207(s), 1147(s), 1099(s), 993(s), 976(m), 933(w), 841(m), 796(m), 734(m), 615(m), 560(m), 523(w), 441(w), 409(m).

^1H NMR (270 MHz, D_6-dmso, 20°C) : δ 1.15 (4H, m, $CHCH_2C\underline{H}_2$), 1.35 (4H, m, $CHCH_2C\underline{H}_2$), 1.44 (4H, m, $CHC\underline{H}_2$), 1.71 (4H, br, $CHC\underline{H}_2$), 3.37 (4H, s, OCH), 3.47 (2H, br, Ce-OH), 3.51 (16H, m, OCH_2).

^{13}C NMR (67.94 MHz, D_6-dmso, 20°C) : δ 21.4 (s, $CHCH_2\underline{C}H_2$), 26.9 (s, $CH\underline{C}H_2$), 67.0 (s, OCH_2).

67.1 (s, OCH_2), 69.5 (s, OCH_2), 69 8 (s, OCH_2), 76.1 (s, OCH), 118.8 (q, CF_3 ^1J = 299Hz), 158 4 (q, CO ^2J = 32Hz).

Mass Spectrometry (FAB +) : 738 [Ce(tfa)$_2$(crown)](100%), 687 [Ce$_2$(OH)$_2$(crown)](11%), 644 [Ce(tfa)$_2$(crown)-F$_5$](20%), 550 [Ce(tfa)$_3$(OH)$_2$F$_2$](11%), 435 [CeOH(crown)F-(CH$_2$)$_8$](4%).

Solubility : Soluble in chloroform, diethyl ether, dmso and thf, insoluble in water, hexane and benzene.

Synthesis of [Ce(OH)$_2$(tfa)$_2$(tetraglyme)] (65)

Ce(OH)$_2$(tfa)$_2$ (0.98g, 2.45 mmol) (32) was partially dissolved in chloroform (50 mL) yielding a yellow solution, to which was added tetraglyme (0.54g, 2.45 mmol). The solution was stirred for 8h at 60°C whereupon it became slightly orange, on completion the mixture was stripped to dryness to yield a yellow oily liquid. Yield 1.29 g (85%)

Microanalyses : Found, C, 26.7 ; H, 3.73 ; Calc. for $CeO_{11}C_{14}H_{24}F_6$, C, 27.0 ; H, 3.86%.

Infrared (Neatv cm^{-1}) : 3256(br, s), 2898(s), 1680(s), 1550(m), 1456(s), 1351(m), 1291(m), 1207(m), 1144(s), 1028(m), 985(w), 948(m), 842(m), 796(m), 722(m), 615(m), 559(m), 523(w), 439(w), 409(m), 356(w), 307(m).

^{1}H NMR (270 MHz, D_6-dmso, 20°C) : δ 3.22 (6H, s, OCH_3), 3.40 (4H, s, OCH_2 a), 3.42 (4H, s, OCH_2 b), 3.47 (4H, s, OCH_2 c), 3.48 (4H, s, OCH_2 d), 3.79 (2H, br, Ce-OH).

^{13}C NMR (67.94 MHz, $CDCl_3$, 20°C) : δ 62.8 (s, OCH_3), 69.6 (s, OCH_2 a), 69.7 (s, OCH_2 b), 69.8 (s, OCH_2 c), 71.3 (s, OCH_2 d), 117.7 (q, CF_3 ^1J = 294Hz), 159.2 (q, CO ^2J = 34Hz).

Mass Spectrometry (FAB +) : 1195 [Ce$_2$(tfa)$_4$F[(glyme)$_2$](5%), 973 [Ce$_2$(tfa)$_4$F(glyme)](6%), 630 [](11%), 588 [Ce(tfa)$_2$(glyme)](100%), 537 [(OHCe)$_2$(glyme)](13%), 494 [Ce(tfa)F(glyme)](47%), 400 [Ce(OH)$_2$(tfa)$_2$](35%).

Solubility : Soluble in acetonitrile, diethyl ether, dmso and thf, insoluble in water, hexane and benzene.

Chapter 8

REDOX STUDIES ON THE CERIUM (IV) OXO-BIS-CARBOXYLATES

This chapter is divided into three parts, each of which is concerned with the relatively facile Ce^{3+}/Ce^{4+} reduction - oxidation process. This exchange may be brought about by both chemical and physical means. Firstly by the action of ultraviolet light on the ceric carboxylates which causes a photochemical reduction to leave Ce(III) or mixed Ce(IV) / Ce(III) species. Secondly by electrochemical processes using cyclic voltammetry and finally by chemical oxidation of the cerous species using a suitable oxidizing agent.

8.1 The oxidation states of cerium

The strong similarity in the properties of the lanthanide elements is due, in part, to their common existence in the trivalent state. The fact that the trivalent state is virtually ubiquitous is a result of the relative energies of the 4f, 5d, 6p and 6s electron orbitals in the range of z = 57 - 71 (i.e. La - Lu). The ionizations of the elemental atoms. Ln^0, to form the uni- and dipositive gaseous ions, Ln^+ and Ln^{2+}, have a fairly constant energy requirement (see Figure 8.1).

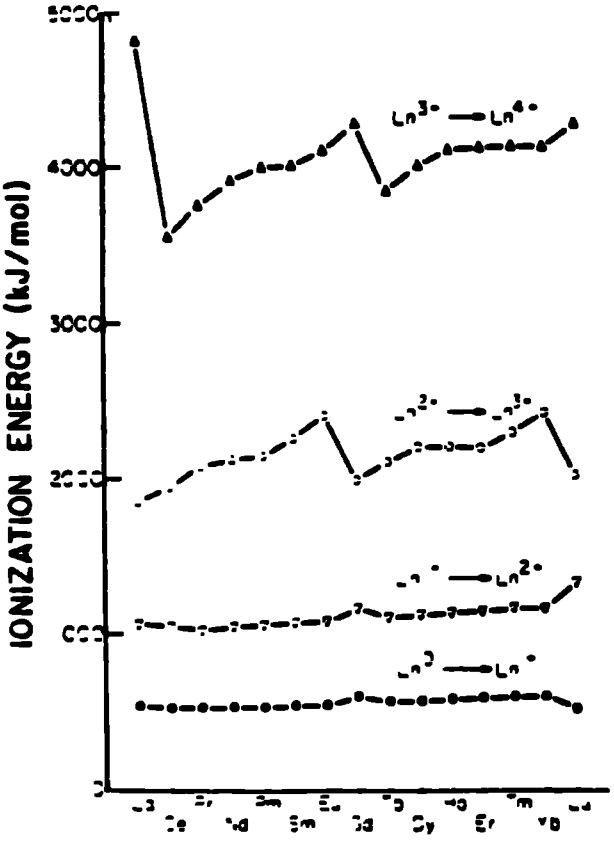

Figure 8.1 : Ionization energies for the ionization steps of lanthanides[281]

For the Ln^{2+} - Ln^{3+} and the Ln^{3+} - Ln^{4+} processes, the ionization energies are more variable. Examination of the electronic configuration of the lanthanides shows a number of points; (i) Ln^{+} and Ln^{2+} are formed by the ionization of the electrons in the 6s orbital, (ii) the ionization of the third electron results in the removal of a 5d electron, implying that the 4f orbitals are lower in energy than either the 5d or 6s, and (iii) that the successive trivalent ions differ in a regular pattern of successive electron occupation of the 4f orbitals as the atomic number increases. This is the basis of the lanthanide contraction which states that the ionic radii decrease as the atomic number increases because of an increase in the pull of the nuclear charge on the unchanging number of electrons in the two outer shells. The stabilizing effect of the f^0 and f^7 configurations (as set out by Hund's rules) are noted to occur with the lowest energy ionizations of the fourth electron, i.e. for Ce^{4+} and Tb^{4+} which are the most stable lanthanide elements in the(IV) state.

Qualitative calculations show that in solution all 4+ states revert to the 3+ state (except possibly Ce^{4+} as it is difficult to reduce Ce^{4+} ($4f^0$) to Ce^{3+} ($4f^1$)), i.e. the tripositive state also owes its stability to a fortuitous combination of ionization and hydration energies. With the solid compounds, it is the ionization energy and the lattice energy which combine to give the resultant 3+ compounds. The energy conditions are more favoured for the existence of non-tripositive species in the solid state than in solution. Pr, Nd, Tb and Dy all have tetrapositive states but require trapping in a crystal lattice for their stabilization, in solution they revert to Ln^{3+}. These Ln^{4+} species are all oxidizing but not to such a large extent as Ce^{4+}.

A few solid compounds exemplifying the tetrapositive state have been synthesized. However, with the tetrapositive lanthanides only Ce^{4+} has a sufficiently long half-life with respect to reduction so as to be of importance in solution. Lanthanide complexes have been obtained in the dipositive state by trapping in solid alkaline earth halide matrices (e.g. $CeCl_2$)[282] but dissolution into aqueous systems results in rapid oxidation to the tripositive state, for all species except Eu (II).

There are numerous differences, in both chemical and physical terms, between the coordination compounds of Ce(III) and Ce(IV), taking as an example, the carboxylates which are pertinant to this Thesis. Firstly, Ce(III) carboxylates are appreciably soluble in polar solvents such as water and insoluble in hydrocarbon solvents. In contrast the analogous Ce(IV) compounds have shown to have extensive solubility in non-polar hydrocarbon solvents and little or no solubility in water. Thermal behaviour is very similar for both species, the compounds generally decomposing to the tetrapositive CeO_2 residue.

Ce(III) is paramagnetic and, therefore, its compounds do not give sharp NMR spectra, while on the other hand the magnetic spectrum may be measured. For instance the calculated value for Ce^{3+} at R.T. is 2.54B.M.[283] with measured values in the order of 2.37B.M. for $Ce_2(SO_4)_3.8H_2O$ for example.[284] Ce(IV), being diamagnetic, has the converse properties. The electronic spectra of both species are somewhat different, as is to be expected seeing that the tetrapositive compounds are yellow or orange in colour whilst the tripositive compounds are white. The normal absorption bands for Ce(III) compounds are in the ultraviolet region, between 210 - 250nm whereas for the Ce(IV) they are often broader and nearer 350 - 400nm (see section 8.2).

8.2 The photoreduction of Ce(IV) carboxylates

8.2.1 Overview of the photolytic processes of cerium

The relative ease with which cerium can alternate between its two most prominent oxidation states (3+ and 4+) has been the centre of some attention for many years. For instance, $Ce^{4+}OH^-$ has proven to be an active photosensitizer in the polymerization of vinyl compounds[285] and Ce(IV) has also been employed in the photolytic splitting of water to give Ce(III), O_2 and H^+.[286] The ceric ion has also been reported to exist in perchloric acid solution as Ce^{4+}, $CeOH^{3+}$ and a dimer, most probably $(Ce\text{-}O\text{-}Ce)^{6+}$. A spectral study between 395-430nm giving the values of the equilibrium ratios along with the molar extinction coefficients (ε) of each ion over this wavelength range has been undertaken. The ε value for each ion is observed to decrease with increasing wavelength.[287] Similarly the photochemical reduction of cerium(IV) salts, particularly nitrates and sulphates, in aqueous and acidic solutions has been extensively studied in, for instance, the work of Martin *et al.* with CAN in glacial acetic acid.[288]

Photochemical reduction of Ce(IV) as $CeCl_6^{2-}$ has also been studied by uv/vis spectrophotometry in acetonitrile.[289] The hexachloro complex displays two bands at 255 and 375nm. Upon irradiation into these bands (at 254, 333 and 365nm) Ce(IV) undergoes photoreduction accompanied by spectral changes.

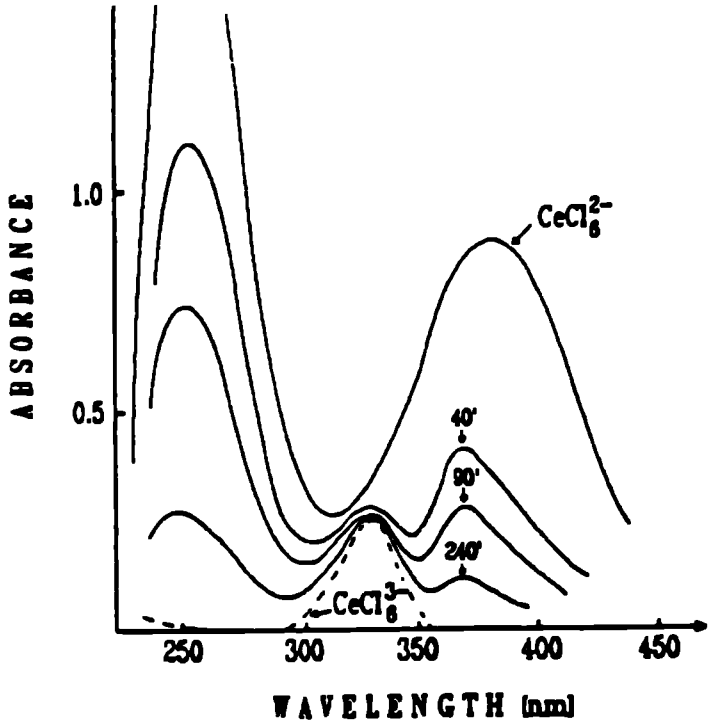

Figure 8.2 : Changes in the absorption spectra of $CeCl_6^{2-}$ obtained at various irradiation times in the presence of $[(C_2H_5)_4NCl]$ (λ = 254nm)

Sheldon and Kochi examined the photolysis of Ce(IV) carboxylates at 350nm, a wavelength at which Ce(III) species do not absorb.[290] The carboxylic acids chosen were acetic, n-butyric, isobutyric and pivalic acids, giving the homoleptic species $[Ce(RCO_2)_4]$. These homoleptics were synthesized by first preparing the acetate complex *via* Hay and Kochi's method,[206] and then replacing the acetate with the larger carboxylates by refluxing them and distilling off the more volatile acetic acid. Both thermal and photochemical reduction to the cerium(III) species were accompanied by decarboxylation and the liberation of alkyl radicals. For instance, the n-butyrate complex photolysed to give principally CO_2 and propane, however, propylene (2%) and propyl esters (trace) were also detected. The other carboxylates all gave similar decomposition products, e.g.

$$Ce(IV)(O_2CCH_2CH_2CH_3)_4 \text{ -------> } Ce(III)(O_2CCH_2CH_2CH_3)_3 + CH_3CH_2CH_3 + CO_2 \quad (i)^*$$

*note the equation is not balanced as propane is the major product

When perchloric acid was added to a solution of Ce(IV) acetate in butyric acid, the rate of photochemical reduction at 350nm increased dramatically. The addition of pyridine, tfa-H and lithium acetate, however, resulted in little increment. Perchloric acid, too, increased the rate of thermal decarboxylation, however, these thermal reactions produced only partial reduction. It was found that Ce(IV) in acidic media is a stronger oxidant than elemental chlorine and is exceeded in strength only by species such as O_3, F_2, persulphate and XeO_3.[290]

The detection by esr of alkyl radicals generated during the photodecomposition of charge-transfer complexes between $CeOH^{3-}$ ion and tertiary alcohols and carboxylic acids has been reported.[291] The photochemical processes proceed by the following concerted mechanisms:

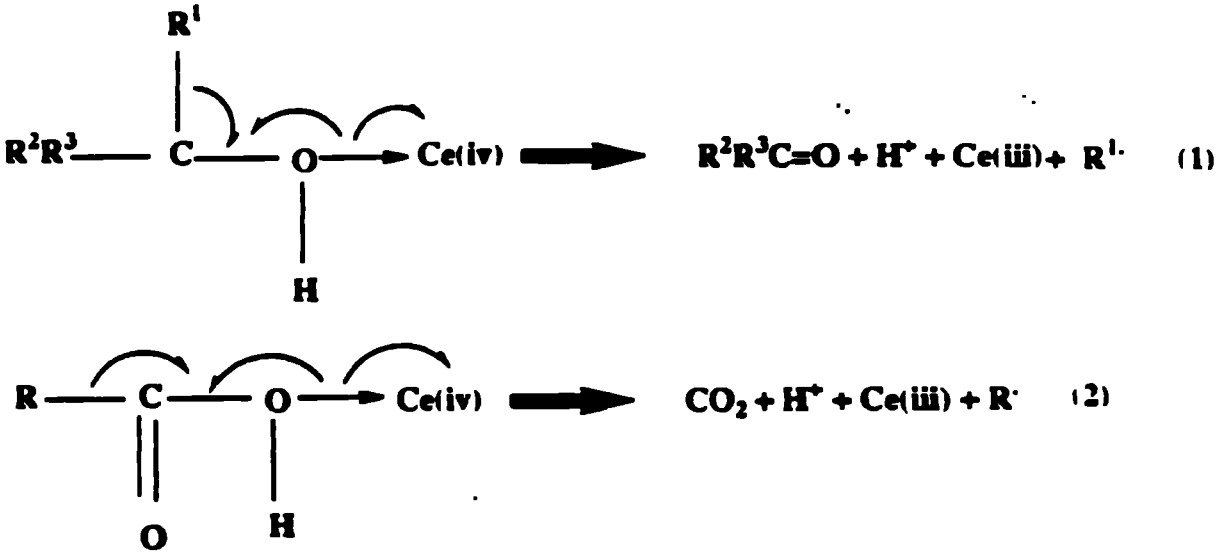

Figure 8.3 : Photo-oxidation of tertiary alcohols and carboxylic acids

The mechanism of the carboxylic acid photo-oxidation is identical to that suggested for the Ce(IV) thermal and photo-oxidation by Sheldon and Kochi.[290]

Probably the only 'mixed cerium$^{3-,4+}$ complex' that has successfully been isolated in the solid state and structurally characterized is that of $[Ce_4O(O^iPr)_{13}(^iPrOH)]$.[292] This compound was synthesized by the visible irradiation of cerium isopropoxide, $[Ce_2(O^iPr)_8(^iPrOH)_2]$. A solution of the isopropoxide in IPA and dme was exposed to sunlight for 50 hours, whereupon the colour changed from olive green to orange brown. The crystal structure is described as $[Ce_4(\mu_4\text{-}O)(\mu_3\text{-}O^iPr)_2(\mu_2\text{-}O^iPr)_4(O^iPr)_5(^iPrOH)]$, with the $Ce_4(\mu_4\text{-}O)$ core having a butterfly form possessing a C_2 axis. The metal centres have

coordination numbers of either six (wingtip metals) or seven (hinge metals) which are satisfied by bridging oxo- and isopropoxy- ligands. Crystallographic analysis of Ce-O bonds reveals that only one bond is significantly longer than the others, indicating that only one isopropanol is protonated. The symmetry in the solid state of this mixed valent compound rules out a localized $Ce^{III}Ce^{IV}_3$ formulation. The compound must, therefore, have a delocalized $Ce^{IV}_2(Ce_2^{7+})$ assignment, or else Ce_4^{15+}.

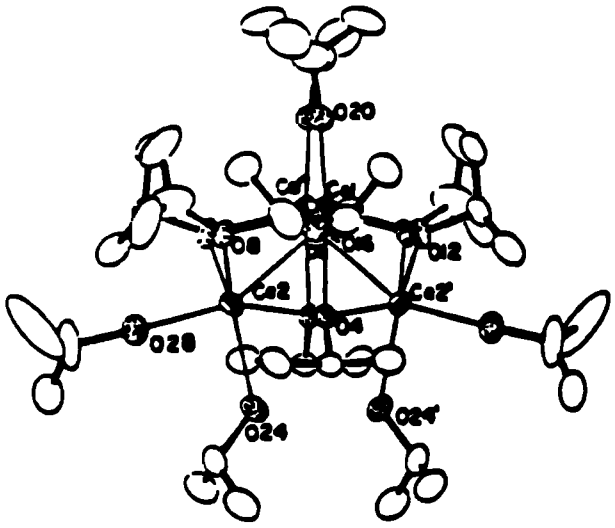

Figure 8.4 : X-ray crystal structure of $[Ce_4O(O^iPr)_{13}(^iPrOH)]$

8.2.2 Photochemical reduction of cerium(IV) carboxylates

One of the properties of lanthanide metals is their ability to attain different electronic configurations, the transitions between which may be studied by electronic spectroscopy. Cerium(IV) carboxylates are no exception to this rule. The electronic spectra of the oxo-*bis* carboxylate compounds have been studied using both ultraviolet and visible light wavelengths (between 700 and 200nm). Results have been complicated by the large carboxylate transition in the 350-200nm region which tends to mask the metal transitions. However, in a number of cases the metal transitions appear as a weak shoulder to the strong metal carboxylate absorbances. Table 8.1 summarizes a number of observed peaks for various cerium(IV) carboxylates in a variety of solvents.

Table 8.1 : Electronic spectra for some cerium(IV) carboxylates

Compound	λ_{max}(nm)	solvent
CAN	379	water
$CeO(eb)_2$ (23)	385	chloroform
$CeO(mv)_2.2mvH$ (24)	386	thf
$CeO(mb)_2$ (28)	381	thf
$Ce(OH)_2(pfb)_2$ (31)	360	thf
$Ce(OH)_2(pfp)_2$ (32)	312	thf
$Ce(OH)_2(tfa)_2$ (33)	342	thf
$Ce(OH)(pfb)_2PhNCO$ (55)	556, 389(weak)	acetone

In all cases an electronic transition is observed below 400nm. For the hydrocarbyl species (23), (24) and (28) this transition is in a very small range (381 - 386nm) and is in a similar position to that of CAN. The perfluorinated species have transitions at lower wavelengths (312 - 360nm) but tend to be more distinct than the weak shoulders observed for their hydrocarbon counterparts. The purple coloured complex, (55) also has a large peak maximum at 556nm.

If one of the cerium(IV) carboxylates described in Chapter 5 is left open to sunlight in a pyrex sample tube as either a pure solid (liquid) or as a solution it will turn paler until it eventually turns white, indicating a photoreduction to a cerium(III) complex. Generally this change is quicker for the pure oxo-*bis* carboxylate solids and liquids than it is for the solutions, the former taking only a few days in bright sunlight, whereas the latter take considerably longer, typically over a week.

The type of carboxylate ligand also appears to have a direct effect on the rapidity of the photodecomposition. For example, the 2,2-dimethylpentanoic compound (27), photoreduces in direct sunlight from a crystalline yellow / orange solid to a semi-crystalline colourless solid in less than 24 hours. The liquid compound (24), however, takes over 2 weeks to photoreduce to a colourless / grey liquid.

8.2.3 Experimental procedure

An ultraviolet lamp was employed to induce the photoreduction of the oxo-*bis* carboxylate cerium(IV) species.

The lamp has a wavelength of about 360nm and is placed within a vessel which is surrounded in turn by a water cooled jacket. Outside this is a third vessel which contains the cerium carboxylate solution, this vessel is fitted with nitrogen inlets which allow the apparatus to be flushed with nitrogen before the experiment is carried out to ensure that no oxygen radicals from the air can alter the measurements.

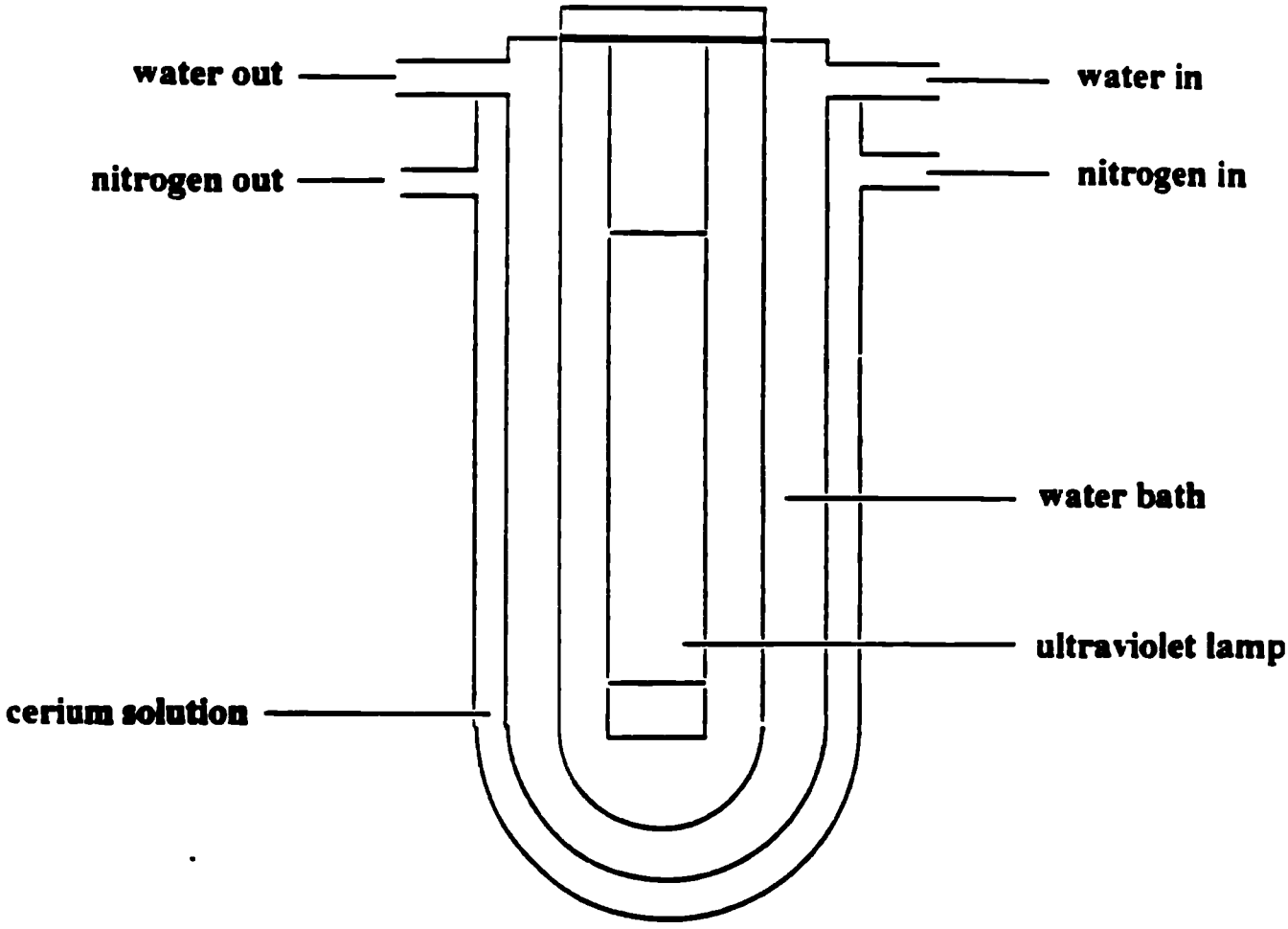

Figure 8.5 : Ultraviolet light reaction vessel

A typical photochemical experiment was performed thus:

1.0 - 2.0g of the cerium oxo-*bis* carboxylate was dissolved in 85 - 95 mL chloroform at R.T.. The solution was added to the outer vessel, connected to the nitrogen supply and flushed with the inert gas. The whole reaction vessel was then covered and the ultraviolet light illuminated. After periods of 30, 60, 90, 120 minutes and 24 hours a small portion (*ca.* 10 mL) of the solution was removed and the solvent removed. The samples were then analyzed by the titration method described in Appendix 2 so as to determine the amount of Ce(III) with respect to Ce(IV) each sample contained.

8.2.4 Results

The results for a number of the cerium (IV) carboxylate species are shown below in both tabular and graphical form.

Compound	[OCe(eb)$_2$]	Total Ce% = 36.3%	
Time	Appearance of solution	Appearance of solid	% Ce(III) wrt Ce(IV)
30 mins	yellow brown soluble	yellow brown solid	12
60 mins	tan part soluble	brown solid	25
90 mins	brown part soluble	brown solid	34
120 mins	brown part soluble	brown solid	49
24 hours	white insoluble	white solid	92

Compound	[OCe(mv)$_2$.2mvH]	Total Ce% = 22.7%	
Time	Appearance of solution	Appearance of solid	% Ce(III) wrt Ce(IV)
30 mins	orange soluble	orange oil	10
60 mins	orange soluble	orange oil	23
90 mins	orange soluble	orange oily solid	15
120 mins	orange soluble	orange oily solid	44
24 hours	brown insoluble	brown solid	82

Tables 8.2 and 8.3 : Photodecomposition of OCe(eb)$_2$ (23) and OCe(mv)$_2$.2mvH (24)

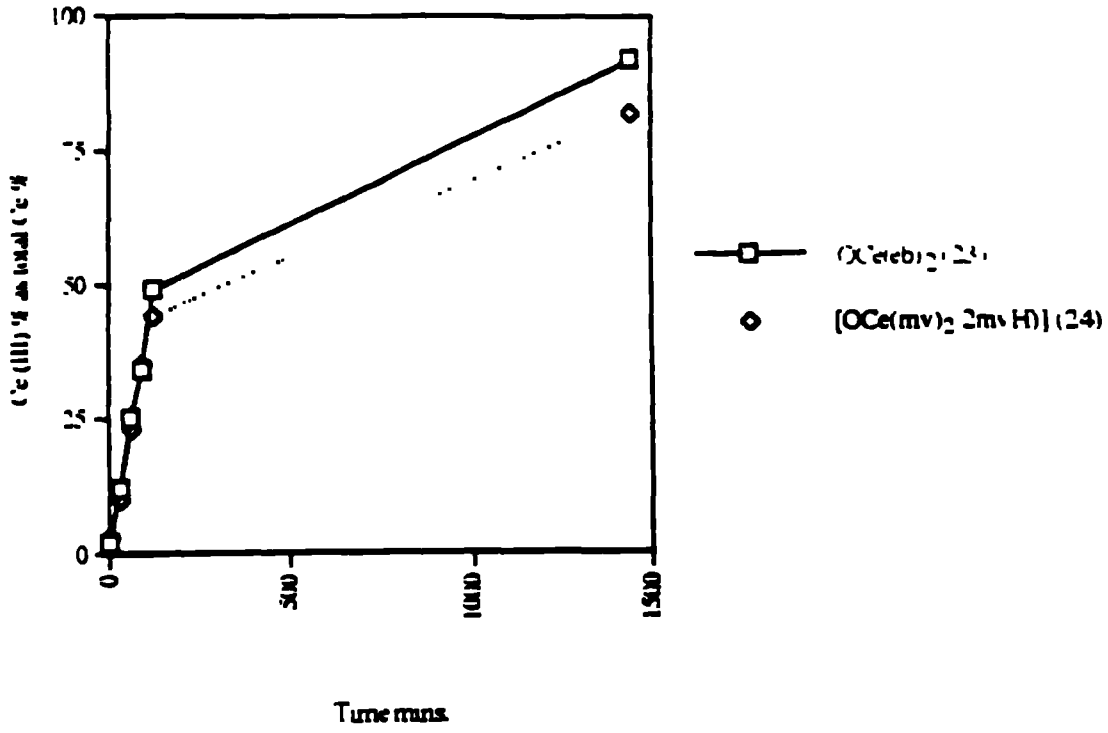

Figure 8.6 : Graphical plot of photodecomposition of (23) and (24)

The photoreduction reactions of compounds (23) and (24) are shown above. Compound (23) is observed to lose its bright yellow colour very quickly, becoming a pale brown colour within half an hour of the introduction of the ultraviolet light. This brown colour persists for a number of hours. After 24 hours (1440 mins) the cerium carboxylate is completely insoluble in the chloroform solvent and a white colour, indicating a very high degree of Ce(III).

Compound (24), $CeO(mv)_2.2mvH$, follows a very similar pattern, however, the rate of photodecomposition is notably slower than for (23) (and also (28) and (31)). Once again the chloroform solution remains soluble for the first few hours, but after 24 hours a brown insoluble solid is obtained. The Ce(III) % of 82% is consistent with the observation that the liquid carboxylates photodecompose slower in sunlight, giving greyish oils. It is also noted that leaving (23) in the reaction vessel for 4 days results in a white solid which analyses as $[Ce(OH)_{2.5}(eb)_{0.5}]$ (Found, C, 14.9, H, 3.2, Expected, C, 15.0, 3.3%).

Compound	[O	Total	
Time	Appearance of solution	Appearance of solid	
30 mins	orange brown soluble	orange brown solid	13
60 mins	tan soluble	brown solid	23
90 mins	tan soluble	brown solid	34
120 mins	tan soluble	brown solid	45
24 hours	tan insoluble	brown solid	98

Compound	[OH	Total	
Time	Appearance of solution	Appearance of solid	
30 mins	yellow brown soluble	yellow green solid	-
60 mins	yellow green soluble	green solid	29
90 mins	yellow green soluble	green brown solid	42
120 mins	yellow green soluble	green brown solid	47
24 hours	white insoluble	white solid	94

Tables 8.4 and 8.5 : Photodecomposition of $CeO(mb)_2$ (28) and $Ce(OH)_2(pfb)_2$ (31)

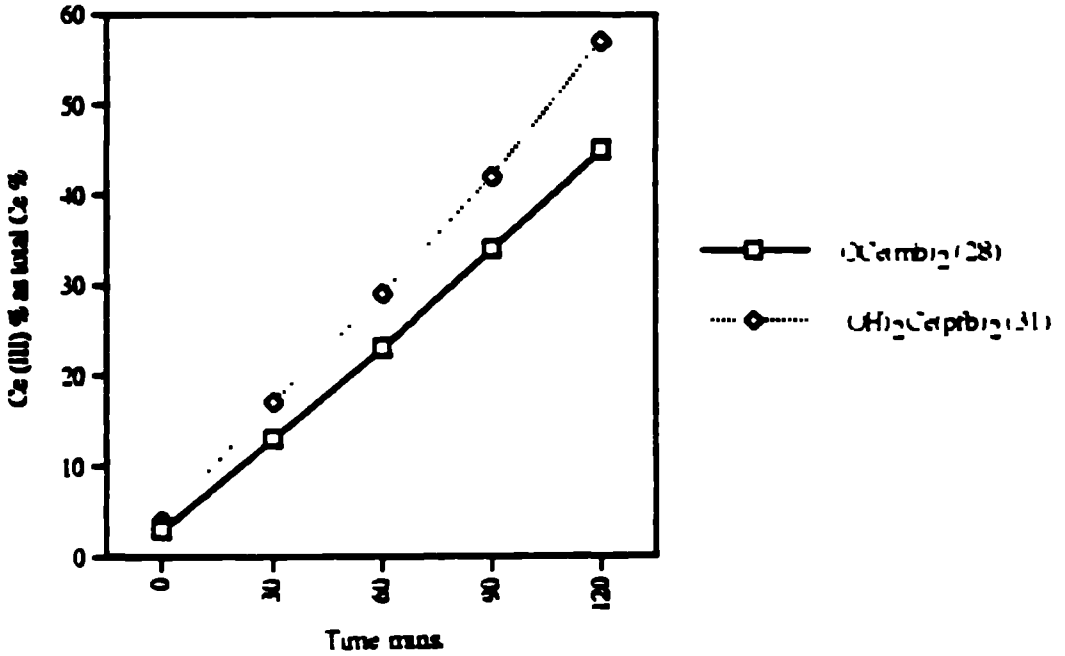

Figure 8.7 : Graphical plot of photodecomposition of (28) and (31)

The photoreduction of compounds (28) and (31) are shown above. Both plots show that the photodecomposition is a fairly linear process. Compound (28) follows a similar path to that of the hydrocarbyl compounds, (23) and (24), above with a similar final cerium(III) percentage. The carboxylate remains soluble throughout the first few hours, but once again after 24 hours the solid has dropped out of solution and is a much paler colour. As with compound (23) the bright yellow colour of the starting material is lost within the first few minutes.

The perfluorinated compound (31) has a slightly different decomposition pathway. Firstly, the decomposition is observed to be at a faster rate than for any of the hydrocarbyl species, secondly the final Ce(III) percentage is considerably higher and finally a bright green colour is observed during the energy process. The first two phenomena are due to the effects of the electron withdrawing fluorine atoms, which have a tendency to stabilize the lower oxidation state (i.e. fluorinated substituents prefer a Ce(III) metal centre, this factor is also clearly shown in section 8.4). The green colour of the solid compounds isolated between 30 and 120 mins is also observed in the photodecomposition $[Ce_4O(O^iPr)_{13}(^iPrOH)]$[292]; this colouration may be due either to a mixed Ce(III) / Ce(IV) or a Ce_4^{n+} species (where n = 13 -15).

It is also noted that leaving the analogous trifluoroacetate complex (33) in the reaction vessel in acetonitrile for 4 days results in a white solid which appears to be $[Ce_2O_3]$, showing only trace amounts of carbon, nitrogen and hydrogen in the microanalyses, which are presumably due to the presence of a small amount of acetonitrile solvent.

8.3 Cyclic Voltammetry of Cerium(IV) Carboxylates

8.3.1 Principles of cyclic voltammetry

The set up for typical cyclic voltammetry experiments involves a cell (of which there are many types) containing various electrodes which dip into a solution of the sample to be measured and a supporting electrolyte. There are three electrodes in the cell, the working, counter and reference electrodes.

The working electrode can be constructed of a variety of materials with the prerequisite that the electrode does not dissolve either anodically or cathodically. For example Pt, Au, noble metals, Fe and Ni may be used. The reference electrode has a simple general requirement in that its potential should not vary when an external potential is applied. Cu, Ag, Pt, Al and ferrocene reference electrodes have all been employed. In cyclic voltammetry, the current flows between the working and the counter electrode, therefore, neither must complicate proceedings by dissolving in the solvent medium for example. Also to avoid large currents passing between the electrodes (and thus perturbing the equilibrium of the system) a larger Pt counter electrode is employed.

The solvent used should have sufficient solubility for ionic substances to form conducting electrolytes and must also have a wide enough potential region for the redox study. Water, acetonitrile, dmf, dmso, dcm and hmpa are all employed. The supporting electrolytes impart conductivity to the solvent and enable continuous flow. Typical examples include KCl, KCN, edta and tetrabutyl ammonium (TBA) salts.

The cell usually consists of a vessel that can be sealed to prevent air entering the solution, with inlet and outlet ports to allow saturation of the solution with an inert gas (e.g. nitrogen). The removal of O_2 is necessary to prevent currents due to the reduction of O_2 interfering with the response from the system.

In linear sweep voltammetry (LSV) and cyclic voltammetry (CV) a large periodic potential change is imposed on the system. In LSV the potential is ramped between two chosen limits at a steady rate and the current monitored, a plot of current versus potential may then be drawn. CV is the same except that the potential is swept back and forth between the two chosen limits (known as switching potentials) numerous times and the current monitored.

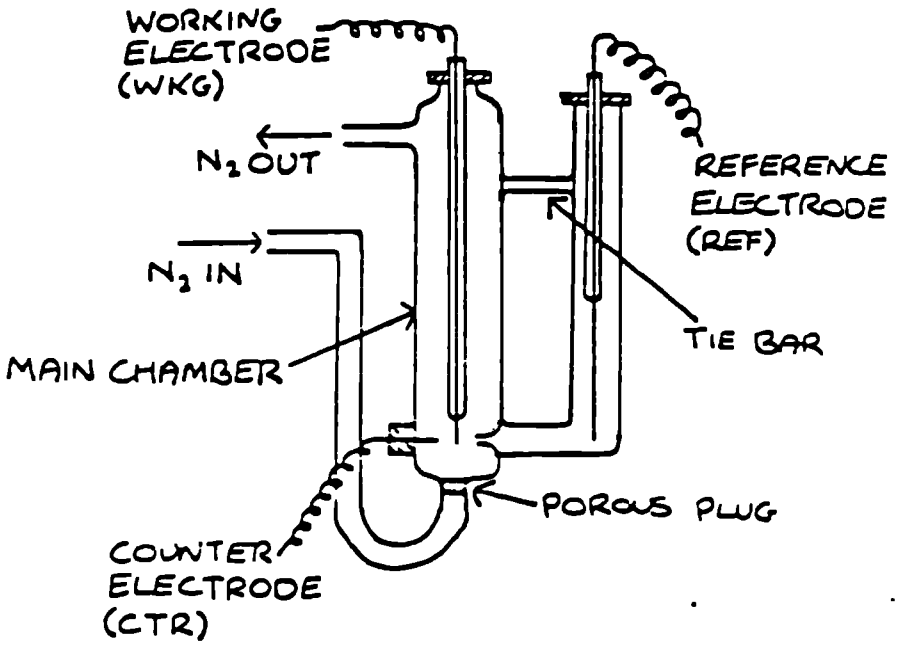

Figure 8.8 : The cyclic voltammetry cell

8.3.2 Types of cyclic voltammetry processes

There are three basic types of electronic charge transfer noted in cyclic voltammetry, reversible, irreversible and quasi-reversible. With a reversible charge transfer process, the oxidized species, Ox, is reduced at the inert electrode surface according to the equation;

$$Ox + ne^- \leftrightharpoons R \qquad (ii)$$

If the potential is taken at least (35/n) mV past the peak potential (E_p) in the negative direction (anodic scan) before reversing the potential, it is ensuring that the surface concentration of Ox = 0, therefore, the surface concentration of R at this potential equals the initial concentration of Ox: $C_r = C_{ox}$. When one moves the potential to positive (cathodic scan), R slowly gets oxidized. The cyclic voltammagram for a typical one electron reversible charge transfer process is shown in Figure 8.9. Thus, reversibility can be summarized as a process in which the redox reaction is sufficiently fast to maintain the concentration of oxidized and reduced forms in equilibrium with each other at the electrode surface.

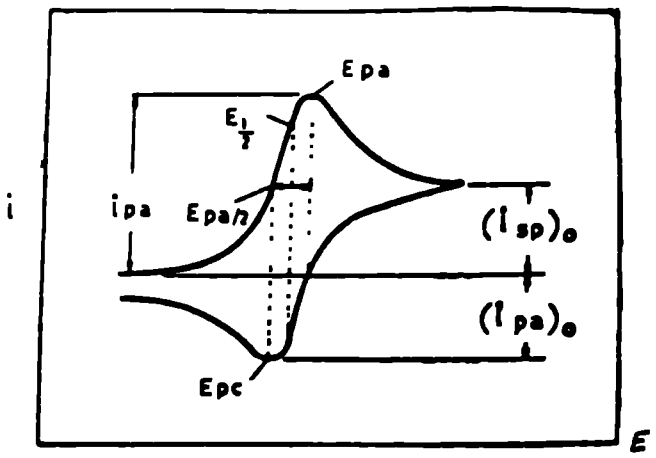

Fig. 8.9 : A typical cyclic voltammagram for reversible charge transfer. The measurable parameters are also indicated in the figure.

When the charge transfer is reversible, O/R has sufficiently fast kinetics that the electron transfer process at the surface appears to be in equilibrium. When a reaction with poor kinetics is performed, the peak shapes are altered by being more drawn out and one does not notice any anodic peak in the reverse direction. The CV waves are, therefore, irreversible because of the reactivity of the anions or cations formed during the electron transfer process. A further type of wave is the quasi-reversible charge transfer wave, which is, as its name implies, part way between the other two processes.[293-5]

8.3.3 Experimental results

The cyclic voltammetry apparatus used was an Oxford Portable Potentiostat which was connected to a Phillips PM 8043 X-Y plotter. The voltammetry cell used in each experiment is shown above in Figure 8.8. The solutions were flushed with nitrogen for *ca.* two minutes before any measurements were taken. About 1 mmol of each of the carboxylate materials to be measured was dissolved in dichloroethane (*ca.* 10 mL) to which was added 10 mmol. of supporting electrolyte (n-tertbutyl ammonium hexafluorophosphate ($TBAPF_6$)) at R.T.. This procedure was repeated for the voltammagram of the free carboxylic acid ligand. The voltammagram of CAN was measured in water (10 mL) using a KCl supporting electrolyte (1 mmol CAN : 10 mmol KCl) The specific procedure for the use of this apparatus is given in references 296-8

There are two recognized couples which may occur when a cerium complex is subjected to an electrochemical process such as cyclic voltammetry. The first between Ce (IV) and Ce (III), (iii), has a electrode potential of about +1.72V. The second couple (iv) has a very negative electrode potential of -2.34V and is, therefore, rarely observed in cyclic voltammetry (as the number of solvents which conduct in this region is severely limited).

$$Ce\ (IV) + e^- \longrightarrow Ce\ (III) \qquad (iii)$$

$$Ce\ (III) + 3e^- \longrightarrow Ce\ (0) \qquad (iv)$$

Firstly a number of measurements were made in order to determine whether either the carboxylic acid ligand or the chosen solvent had any electrochemical properties so that they could be removed from the plots. A voltammagram of CAN was also measured in order to determine an approximate value for the two Ce couples.

(a) The voltammagram of CAN in water between +0.5 and +1.5V gives a single reversible peak at +1.05V for $E_{p,c}$. This peak is most likely to be the Ce (IV) - Ce (III) oxidation process. Unfortunately water does not conduct much beyond +1.2V, therefore, no anodic peak ($E_{p,c}$) is observed and only an approximate value for the formal electrode potential can be estimated at *ca.* 1.2V. Also no Ce (III) - Ce metal couple was observed in the expected region. The formal electrode potential (E^f) is given by;

$$E^f = (E_{p,a} + E_{p,c}) / 2 \qquad (v)$$

(where $E_{p,a}$ is the anodic peak potential and $E_{p,c}$ the cathodic peak potential)

However since no $E_{p,a}$ value is observed this value is only an approximation. The ratio of the peak currents is also a criterion of electrochemical reversibility (see equation (vii)) however, this value could not be measured for the same reason as for E^f.

$$i_{p,a} / i_{p,c} = 1 \qquad (vi)$$

(where $i_{p,a}$ is the anodic peak current and $i_{p,c}$ the cathodic peak current)

(b) The voltammagram of dichloroethane with 10 mmol supporting electrolyte ($TBAPF_6$) was also measured, no significant peaks were observed, however, cut off potentials at *ca.* -2.0V and + 1.75V indicates that limited data can be collated from beyond these potentials, this, therefore, mans that we are unlikely to see any peaks corresponding

these potentials, this, therefore, means that we are unlikely to see any peaks corresponding to the Ce(III) - Ce(0) couple. Chlorinated solvents such as dichloroethane are often considered the best solvents in which a large potential range may be observed, therefore, no other solvents were employed in order to locate this couple.

(c) The voltammagram of 2-ethylbutyric acid (1 mmol) in dichloroethane (10 mL) with a $TBAPF_6$ supporting electrolyte (10 mmol) was also measured. This voltammagram gave a number of interesting peaks. The voltammagram between +2.0V and -0.5V is shown below in Figure 8.10.

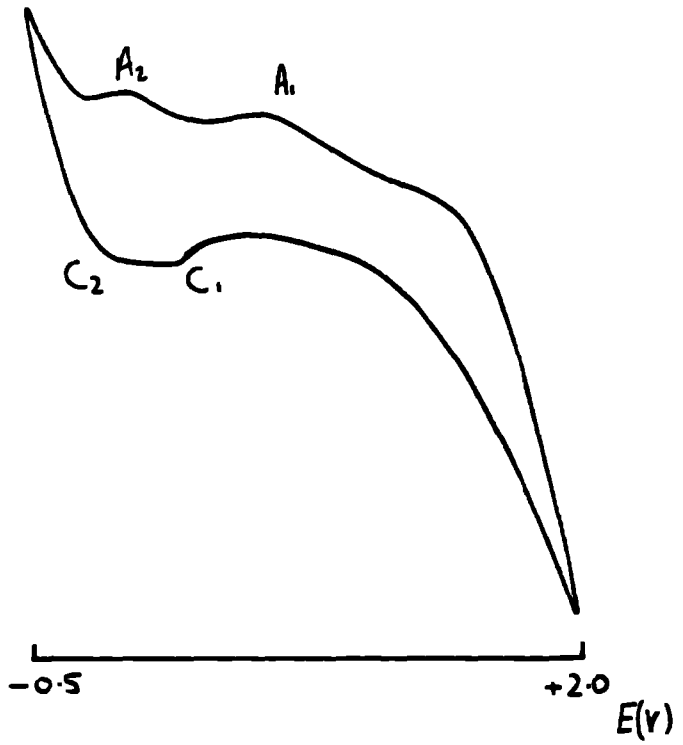

Figure 8.10 : CV of 2-ethylbutyric acid in dichloroethane (+2.0V -> -0.5V)

Starting from positive potential (right hand side) and sweeping towards negative potential there are two clear anodic peaks at 0.72 (A_1) and 0.04V (A_2). There is also a broader peak at *ca.* 1.6V, however, this is due to the solvent approaching its 'cut off' point. On reversing the potential from negative to positive, the corresponding cathodic peaks are observed but are closer together and less obvious, appearing at +0.18 (C_1) and -0.24V (C_2), indicating a degree of reversibility. The second is not easily observed in this voltammagram as the negative potential was not taken sufficiently far to allow the surface concentration of the oxidant to become zero. Thus a second voltammagram was measured

between +1.5 and -1.0V giving only one peak in the anodic and cathodic directions, the strong anodic peak being observed at -0.30V (C_2).

The formal electrode potentials (E^f) of these two processes given by equation (v) are +0.45 and -0.13V for A_1 / C_1 and A_2 / C_2 respectively. However, the shape of the curves using these restricted potential ranges makes analysis of the peak currents very approximate, and therefore, no analysis of these was made for the ligand system.

(d) The voltammagram of $[Ce(OH)_2(tfa)_2]$ (33) in acetonitrile with a $TBAPF_6$ supporting electrolyte, between +2.5 and -2.5V is shown in Figure 8.11 overleaf. A large cathodic peak ($E_{p,c}$) is observed at +0.65V (C_1) with the corresponding anodic peak ($E_{p,a}$) observed at +1.05V (A_1). The E^f value for this couple is 0.85V and is likely to be due to the action of the Ce(IV) - Ce(III) process. The fact that only one large peak is observed for the Ce(IV) - Ce(III) couple suggests that each of the metals in the structure of the compound is in the same environment; this is observed to be the case if one considers the structures of (23) and (27) (see Chapter 5) in which each of the six metals is surrounded by oxo and carboxylate groups. The added ethanol molecules in (23) and unidentate carboxylic acid ligands in (27) appear to have little or no effect on the electrochemical process.

The shape is a clear indication that this process is reversible. The peaks at -1.85 (C_2) and +2.0V (C_3) are both due to the solvent nearing the 'cut off' point. There are also a number of smaller peaks in both the anodic and cathodic directions which most likely correspond to the trifluoroacetate ligand, these appearing at +1.20 (C_4) and +1.85V (A_2). Using a restricted potential range did not produce any further data by which the peak currents could be analyzed.

(e) The voltammagram of $CeO(eb)_2$ (23) in dichloroethane with a $TBAPF_6$ supporting electrolyte, between +3.0 and -3.0V gives a very complex plot with numerous peaks in the cathodic and anodic directions. The majority of these can be assigned to ligand (three in each direction) and solvent (two in each direction corresponding to the voltage nearing the 'cut off' potentials) processes. If one restricts the potential range to +2.5V -> -1.0V (see Figure 8.12) the Ce couple becomes more obvious.

Beginning from the negative potential and following the lower plot we observe a peak at +0.34V which is the $E_{p,c}$ for the Ce(III) - Ce(IV) couple; in this process the metal is being oxidized from the 3+ to the 4+ state. At the higher switching potential (+2.5V) the scan returns and the applied potential (E_{appl}) approaches the E^f for the redox couple from the other side. Electrons are taken up by the complex and the metal is reduced from Ce(IV)

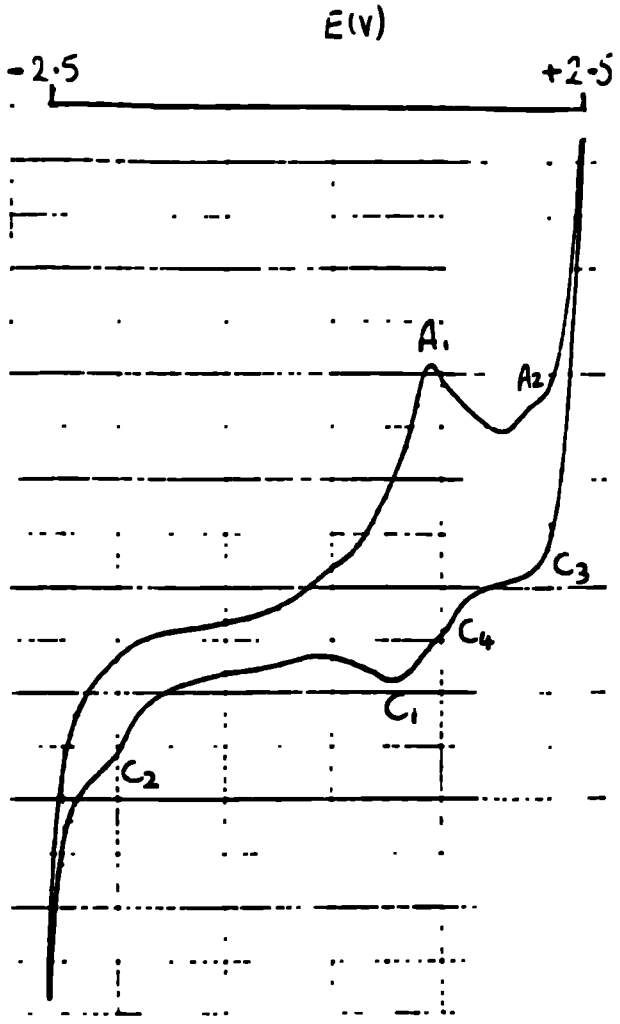

Figure 8.11 : CV of $[Ce(OH)_2(tfa)_2]$ (33) in acetonitrile (+2.5 -> -2.5V)

to Ce(III). The $E_{p,a}$ for this process is observed at +1.08V, therefore, the E^f equates to 0.71V (see equation (v)). A further peak is noted at *ca.* 2.2V, this is due to the solvent 'cut off'. This potential range also enables the direct correlation of $i_{p,a}$ and $i_{p,c}$, the observed ratio (see equation (vi)) is 0.97, indicating that this process is reversible between these two potential limits. Once again no Ce(III) - Ce (0) couple was observed at negative potential.

The voltammagram of $[CeO(mv)_2.2mvH]$ (24) shows similar plots to those described for (23). The E_f values for (33) and (23) of 0.85 and 0.71V, respectively are significantly lower than either that of the observed couple for CAN in water (*ca.* 1.2V) or the electrode potential of +1.72V. These differences may be due in part to the solvent and carboxylate ligand processes.

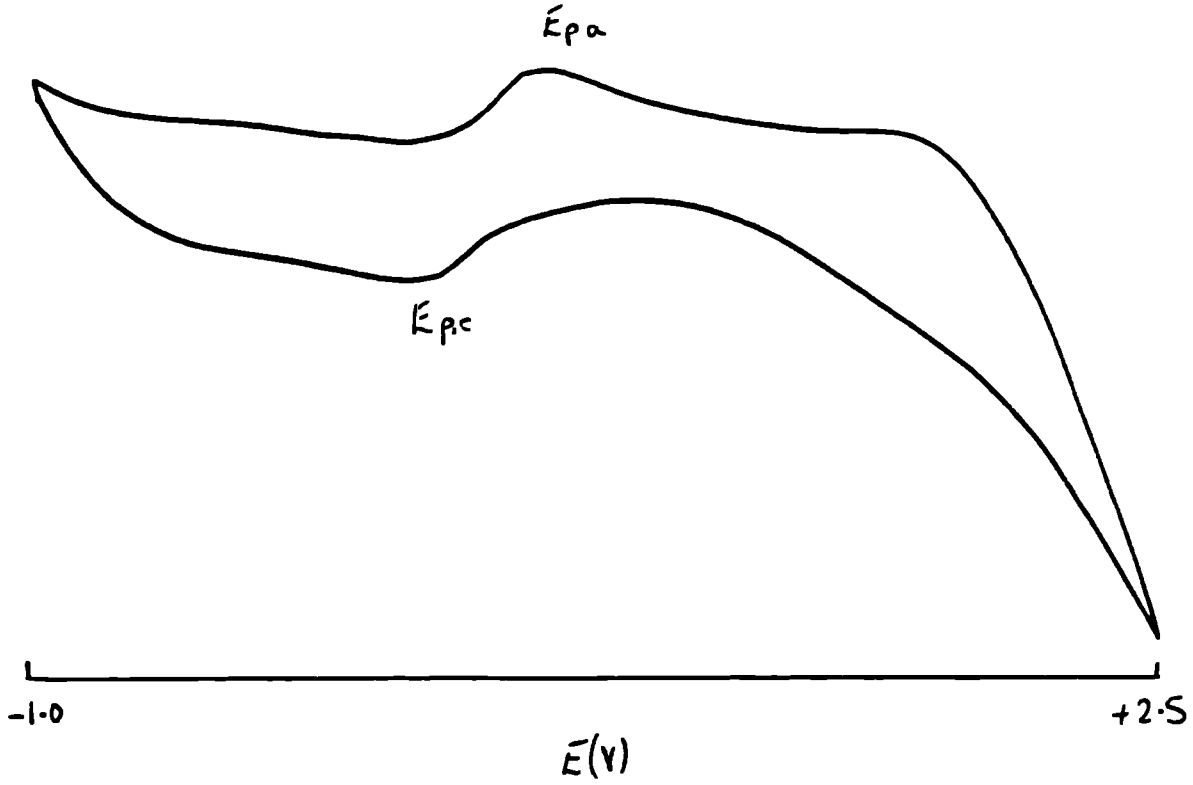

Figure 8.12 : CV of $[CeO(eb)_2]$ (23) in dichloroethane (+2.5 -> -1.0V)

8.3.4 Conclusions

The complex voltammagram of the carboxylic acid ligands in the solvent media (see Figure 8.10) makes the task of identifying any Ce-Ce couples more difficult. However, in general it would appear that the cerium (IV) carboxylate complexes produce a voltammagram which shows one principal set of peaks, namely those concerned with the Ce(III) - Ce(IV) couple between 0.85 and 0.71V. No Ce(III) - Ce(0) couple (at very negative voltage) is observed. Also, the fact that only one set of peaks is observed for this couple is an indication that the cerium metals all have similar dispositions within the structure.

8.4 Chemical oxidation of Ce(III) carboxylates

8.4.1 Cerium(IV) 'oxo' compounds

Ceric carboxylates may be prepared by the oxidation of cerous carboxylates by hydrogen peroxide in a two-phase system. For instance cerium(III) nitrate (0.25 mol) and neodecanoic acid (1 mol) in Amsco 140 solvent was treated dropwise with 1 molar aqueous solution of ammonium hydroxide. After two hours 30% aqueous hydrogen peroxide (0.25 mol) was added and the mixture heated to 70°C to decompose the Ce^{4+} / H_2O_2 complexes, and the two layers separated. A 94% yield of Ce(IV) product was obtained. 2-ethylhexanoic, naphthenic and octanoic acids were also used in the above synthesis.[227]

Barnes *et al.* have taken the seminal work of Melloche[299] and studied many of the compounds described therein by X-ray crystallography. The compound, $[K_4Ce(CO_3)_3O_2.6H_2O]$ is synthesized by dissolving CAN in water and a saturated solution of ammonium carbonate in 30% H_2O_2, to give a dark red perceric ammonium carbonate to which potassium carbonate is slowly added.[300] The structure consists of the anion $[(CO_3)_3Ce(O_2)Ce(CO_3)_3]^{8-}$ which is centrosymmetric. The Ce atoms are symmetrically bridged by edge-on doubly bidentate peroxide groups. Each Ce is ten coordinate with all four peroxide oxygens atoms between 2.331(4) - 2.373(3)Å from the Ce atom (mean 2.354(3)Å) and three bidentate carbonates, Ce-O 2.390(4) - 2.458(4)Å. The carbonate groups are all planar.

The corresponding sodium compound $Na_8[(Ce(O_2)(CO_3)_3]_2.18H_2O$ has also been crystallographically characterized.[301] The dimeric anion is closely related to the potassium compound described above with only minor differences, the average Ce-O distances are, Ce-(O_2) 2.350(17) and Ce-(CO_3) 2.433(20)Å and are very similar to the potassium compound.

A third compound with a guadinium salt $\{[C(NH_2)_3]_8^+[(CO_3)_3Ce(O_2)_2Ce(CO_3)_3]^{8-}.2H_2O\}$ was prepared by Butman *et al.*[302] The structure is again a centrosymmetric binuclear complex. The cerium atom is surrounded by six oxygens of three chelating carbonates and four oxygens of two bridging peroxo groups. The coordination number is ten, however, the peroxo ligands are often considered as just one entity, thus the geometry is a dodecahedron. Once again the Ce-O bond lengths are similar to those above [Ce-(O_2) 2.342(8) and Ce-(CO_3) 2.439(9)Å]. The two peroxo groups form a flat triangle, perpendicular to the line Ce-Ce. More often, dimeric peroxo complexes adopt a 'zig-zag' chain structure similar to those observed in a number of transition metal complexes.[303-4]

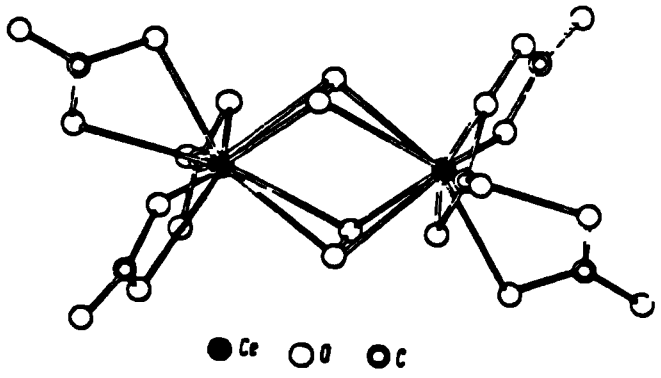

Figure 8.13 : X-ray Structure of the anion $[(CO_3)_3Ce(O_2)_2Ce(CO_3)_3]$

The different bonding may be due to the peroxo ligands of the lanthanides being more ionic than in the transition metals. Also the dimensions of the lanthanides are greater and, therefore, the peroxo ligand tends to act more as an independent unit.

The $[Ce(O_2)_2Ce]^{4+}$ unit with bridging doubly bidentate peroxy groups found in the above carbonate salts is also found in $\{K_2Na_2[(edta)Ce(O_2)_2Ce(edta)].13H_2O\}$ which is synthesized by dissolving the above potassium salt in saturated $Na_4(edta)$.[ref] The edta complex has an average Ce-O bond length of 2.418(3) and average Ce-N bond length of 2.716(3)Å, the ligands fitting neatly as caps over the metal atoms of the $[Ce_2(O_2)_2]$ core allowing the coordination of four oxygens and two nitrogen atoms, giving a ten coordinate polyhedron for Ce.

Peroxy carboxylates have also been prepared. Ce(IV) peroxy acetate, $[Ce_2(O_2)_3(OAc)_2]$ was precipitated from an aqueous solution containing acetic acid, cerium(III) nitrate, sodium nitrate and hydrogen peroxide, in 97% yield.[305] The complex was unstable and lost both oxygen and acetic acid on standing in air at R.T. The composition of the freshly prepared material depends to some extent on the reaction conditions used in the preparation. Studies over a few days show that the material decomposes from an original ratio of 1.5 peroxide groups per cerium atom to 0.75 in 69 hours.

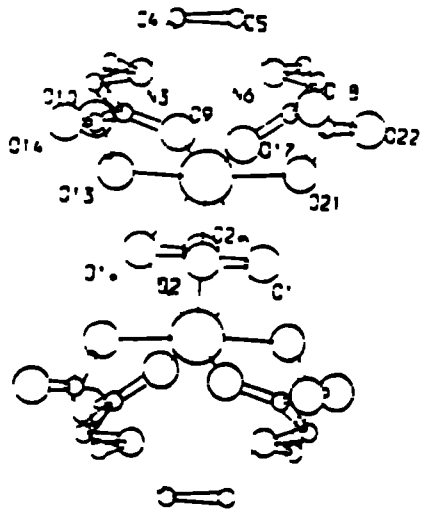

Figure 8.14 : View of the $[(edta)Ce(O_2)_2Ce(edta)]^{4-}$ anion showing the edta ligands capping the Ce atom

Finally the oxoacetates of cerium carboxylates may be prepared by decomposing anhydrous ceric acetate in a vacuum.[207] At 65°C, $[Ce_2O(OAc)_6]$ is reported to form and at 100°C $[Ce_2O_2(OAc)_4]$. These formulations are based on Ce(IV) and acetate analyses.

8.4.2 Synthesis of Ce(IV) carboxylates from Ce(III) salts

The cerium(III) carboxylates may be synthesized from a variety of tripositive salts (see section 4.6), however, when the syntheses are performed according to the method described for the synthesis of the cerium(IV) carboxylates of Chapter 5, it would appear that particular salts should be used for specific carboxylic acids. When the carboxylic acid in question has a low pKa, cerium carbonate appears to be the best salt, however, with the less acidic carboxylates, cerium chloride is a more profitable starting material.

The perfluorinated acids are the most acidic and may be added directly (in diluted concentrations) to a solution of the cerium(III) carbonate in water according to equation

(vii). This addition is accompanied by a release of carbon dioxide which is observed as 'frothing'. Once all the acid has been added the solution becomes virtually clear (having been an insoluble white colour before the addition). Filtration and evaporation to dryness yields white powdery solids (>90%), which analyze to give $[Ce(R_FCO_2)_3.xH_2O]$ (where x = 0-3).

$$Ce_2(CO_3)_3 + 6\ R_FCO_2H \text{ ----------> } 2\ Ce(R_FCO_2)_3.xH_2O + 3\ CO_2 + 3\text{-}x.H_2O \quad \text{(vii)}$$

In contrast the acids with a lower pKa, i.e. the hydrocarbyl acids, give insoluble suspensions when added directly to cerium carbonate, also very little' frothing' is observed indicating low reactivity. Subsequent filtration and evaporation results in a yield of *ca.* 10-20%. Therefore, the sodium salts of the acids are added dropwise to an aqueous solution of cerium(III) chloride heptahydrate according to equation (viii), giving insoluble white solids. These solids are then filtered, washed with water and dried. These compounds similarly analyze to $[Ce(RCO_2)_3.xH_2O]$ (where x = 0-4). When the perfluorinated acids are added either directly, or as sodium salts, to the cerium chloride solution, the solution becomes completely insoluble. However, the cerium carboxylate proves to be difficult to separate from the NaCl which is also in solution. Precise experimental details are given for three examples in section 8.4.6.

$$CeCl_3.7H_2O + 3\ Na(RCO_2) + H_2O \text{ ---------> } Ce(RCO_2)_3.xH_2O + 3\ NaCl + xs.H_2O \quad \text{(viii)}$$

These cerium(III) carboxylates may then be oxidized with peracetic acid in a variety of different ways. Firstly the carboxylates may be either suspended (hydrocarbyl) or dissolved (perfluoro-) in acetonitrile and one equivalent of peracetic acid added. The solution is observed to darken immediately to either insoluble brown (hydrocarbyl) or soluble yellow (perfluoro-). The reaction mixtures are then stirred for 2-48 hours. Once complete the solutions are stripped to dryness on a rotary evaporator to yield either yellow (hydrocarbyl) or white (perfluoro-) solids. The general equation for these reactions is:

$$Ce(RCO_2)_3.xH_2O + CH_3CO_3H \text{ ---------> } CeO(RCO_2)_2.(RCO_2H) + HOAc + H_2O \quad \text{(ix)}$$

The perfluorinated compounds, although turning yellow immediately on addition of the peracetic acid, indicating that they have changed from Ce(III) to Ce(IV), appear to give a product which is cerium(III) in nature. On close examination it transpires that there is actually a small amount of yellow cerium(IV) product also but only in *ca.* 5-15% yield. This is not surprising as the electron withdrawing perfluoro- acids render the metal more susceptible to lower oxidation states, i.e. Ce(III) is preferred to Ce(IV). When the solvent used in the preparation is diethyl ether and the reaction mixture stirred at R.T. until all the solvent has evaporated, a larger amount of Ce(IV) product is recovered, however, it is impure, being contaminated by the water and acetic acid in the peracid.

Similar procedures are employed for the hydrocarbyl carboxylates. Once the oily yellow solids are recovered from the evaporation of the solvent, it is noted that they still contain some acetic acid (peracetic acid is supplied by the manufacturers as a 38% solution in dilute aqueous acetic acid). The excess acetic acid may be removed by dissolving the solid in benzene (25 mL) and washing with water (2x20 mL). The organic phase is then separated, dried over magnesium sulphate and stripped to dryness to give a yellow oil which on cooling yields yellow crystals which may be separated from the oil. Analysis of these crystals shows that they are based on the same formulation as those compounds synthesized by the aqueous method described in Chapter 5, *viz.* $[CeO(RCO_2)_2]$. The oil is the free carboxylic acid which is removed from the starting material to give the product.

The excess acetic acid may also be removed in some cases by stirring the heated solution under vacuum on a Schlenk line. This procedure also gives an oily yellow solid. When the acids employed are those which tend to give liquid products from the aqueous route (e.g. 2-ethylhexanoic and 2-methylvaleric acids) it is noticed that they do not analyze to give the same materials as prepared by the aqueous route. In fact they appear to lose some of the external uncoordinated acid. For example, the analogue of compound (24) $[CeO(mv)_2.2mv\text{-}H]$, is synthesized as $[CeO(mv)_2.mv\text{-}H]$ (73) by this route and that of $[CeO(eh)_2.2eh\text{-}H]$ (25), $[CeO(eh)_2.1.5eh\text{-}H]$ (72). This is also the case for (71) and (74) which have rather less uncoordinated acid residues associated.

The compounds described within this Chapter are:
(66) $[Ce(eb)_3.H_2O]$, (67) $[Ce(dmp)_3.3H_2O]$, (68) $[Ce(pfp)_3.2.5H_2O]$, (69) $[CeO(eb)_2]$, (70) $[CeO(dmb)_2]$, (71) $[CeO(dmp)_2](dmpH)_{0.33}$, (72) $[CeO(eh)_2](ehH)_{1.5}$, (73) $[CeO(mv)_2](mvH)$ and (74) $[CeO(oct)_2](octH)_{0.33}$.

8.4.3 Spectroscopic characterization

8.4.3.1 Infrared analysis

The infrared spectra of compounds (66) - (74) were measured as either Nujol or hexachlorobutadiene mulls, or as neat liquids at R.T.. Pertinent data are tabulated in Table 8.6 below.

Table 8.6 : Selected infrared data (cm^{-1}) for compounds (66) - (74) :

Compound	νOH	$\nu COO_{(asym)}$	$\nu COO_{(sym)}$
(66)	3334	1528	1421[a]
(67)	3340[a]	1520	1409[a]
(68)	3450	1647	1443
(69)	3626	1541	1417
(70)	3636	1544	1412
(71)	3624	1538	1410
(72)[b]	3628	1557	1417
(73)[b]	3635	1557	1417
(74)	3345	1538	1408[a]

All spectra recorded as Nujol mulls, except [a] which were recorded as hexachlorobutadiene mulls and [b] as neat liquids.

Again one of the most interesting features of the infrared spectra concerns the COO carboxylate stretching vibrations. Firstly the asymmetric stretch for compound (68) is found to be considerably higher than the other peak values; this is in accordance with the findings for the cerium(IV) compounds discussed in Chapter 5. This factor was previously explained to be due to the increased electron withdrawing effect imparted by the fluorinated carboxylate ligands. However, in this compound the peak is at $1647cm^{-1}$ whereas in the cerium(IV) compound it is at $1571cm^{-1}$. This shift may indicate a shift from a bridging carboxylate towards a more unidentate one as the low frequency symmetric stretch [1442 (32) - $1443cm^{-1}$ (68)] remains the same.

The separations between $\nu COO_{(asym)}$ and $\nu COO_{(sym)}$ are notably different for the Ce(III) and Ce(IV) species. The general separation ($\Delta\nu$) for the ceric carboxylates (69) - (74) is in the order of *ca.* 135cm $^{-1}$, however, for the cerous compounds it is markedly different. For the fluorinated species (68) it is 204cm^{-1}, while for the hydrocarbyl species (66) and (67) it is 107 and 111cm^{-1}, respectively. It is unlikely that these changes in $\Delta\nu$ have any significant effects on their relative structures. It is also noteworthy that the hydrocarbyl cerous compounds appear to have $\nu COO_{(asym)}$ stretches at lower frequencies (by *ca.* 10 -15cm^{-1}) than compounds (69) - (74). These COO stretching vibrations are all in the same region as those observed in the oxo-*bis* carboxylate species synthesized from the CAN route.

The OH stretching frequencies are also a source of information. For the three cerous carboxylates (66) - (68), a very broad peak is noted at *ca.* 3340cm^{-1} for (66) and (67) and 3450cm^{-1} for (68). These are both due to the associated water molecules. A similar peak is observed in the spectra of (74). For the cerium(IV) species, however, no such broad resonance is noted and instead a single sharp peak at *ca.* 3630cm^{-1} is observed. This peak is also observed in the hydrocarbyl oxo-*bis* carboxylate species described in Chapter 5 and has been assigned as the νOH stretching vibration of the free carboxylic acid residues.

The infrared spectrum of (68) shows a number of additional bands corresponding to the νCF stretching vibrations. These occur at 1214 and 1167 for the asymmetric and 820cm^{-1} for the symmetric stretch. These bands are also noted in the ceric pfp oxo-*bis* carboxylate compound (32) at 1221, 1176 and 822cm^{-1}, respectively. The hydrocarbyl species show a similar pattern in the 700-500cm^{-1} region compared with that of the oxo-*bis* carboxylate species synthesized from the CAN route; these vibrations have been assigned to a combination of πCH and δOCO vibrations.

8.4.3.2 Multinuclear NMR analyses

The ^{1}H NMR spectra of compounds (66) - (68) were run at R.T. in D_6-dmso at 90MHz with the corresponding solid-state spectra being run under ^{13}C CPMAS conditions. The spectra of compounds (69) - (74) were run at R.T. in $CDCl_3$ using either a 90 or 270MHz instrument.

Cerium(III) compounds, being paramagnetic, rarely give good quality NMR spectra, generally giving broad signals. This line broadening is seen in the ^{1}H and ^{13}C NMR spectra of compounds (66) - (68). The ^{1}H NMR of (66) and (67) give the expected proton signals with adequate integration and also show the presence of the water molecules

at δ 4.02 and 3.30, respectively. The solid-state ^{13}C NMR of the three compounds also gives broad lines but again in the expected regions. The spectra of (68) does not show the expected quartets for either the CF_3 or the CO groups, only a broad resonance being observed.

The ^{1}H NMR spectra of the ceric compounds (69) - (74) also show some line broadening effects, but not to the extent displayed by the cerous compounds. This is most likely to be due to a small amount of Ce(III) remaining in the products. The CH_3 resonances are all within a fairly small range as was noted for the compounds described in Chapter 5 [δ 0.69 (70) - 0.95 (72)]. Both (70) and (71) have two sets of methyl resonance corresponding to the terminal and the α-substituted groups. The terminal resonances are at lower frequency (δ 0.69 - 0.88) than the α-substituted resonances (δ 1.05 - 1.15).

The CH_2 resonances are all in the expected regions with acceptable integrations, but once again are rather broad. In the ^{1}H NMR spectrum of the 2-ethylbutyrate compound (23), two CH_2 resonances are observed at δ 1.42 and 1.51; similarly two resonances are observed for (69) at δ 1.45 and 1.56. The CH resonances are in the expected positions, commensurate with the oxo-*bis* carboxylate species.

The 2,2-dimethylpentanoic compound (27) has been characterized by X-ray crystallography and its structure discussed in section 5.7. The structure consists of a central Ce_6O_8 core with twelve bridging and two unidentate carboxylic acid ligands. The unidentate ligands were also noted to possess their OH protons. It would appear from ^{1}H NMR analysis that the same (or very similar) compound has been synthesized from the chemical oxidation of the cerous carboxylates. This is because a small resonance at δ 8.10 is observed in the spectrum of (71), probably being due to the OH proton of the unidentate protonated acid. Subsequent integration of the peaks suggests that the compound is actually $[CeO(dmp)_2(dmp\text{-}H)_{0.33}]$.

The ^{13}C NMR spectra also confirm that these compounds are largely the same as those synthesized in Chapter 5. One noteworthy feature concerns the CO resonances at high frequency. These are all observed to be in a similar region, however, it is notable that the most acidic ligand of the hydrocarbyl carboxylates, 2-methylvalerate (on account of this ligand being mono α-substituted whereas the others are all di α-substituted) has its CO resonance furthest downfield at δ 186.6. Compound (74) is only sparingly soluble and does not provide any useful ^{13}C NMR information.

8.4.3.3 Mass spectrometric analysis

The mass spectrometric data were collected under FAB+ conditions using 3-nitrobenzyl alcohol as the supporting matrix. Although the ceric carboxylates have given many large mass ions, in some cases over 1500 a.m.u., their cerous counterparts appear to be significantly less volatile under the same conditions. In fact for the three cerous compounds there are no ions exceeding 500 a.m.u..

Compound (66) shows a large number of ions which are directly related to each other through the loss of either water or carbonaceous fragments. For example the fragments at m/z 461 and 309 for $[Ce(eb)_2(O_2CCHCH_2)(H_2O)]$ and $[Ce(eb)O_2(H_2O)]$ lose a water molecule each to give ions at 443 and 290, respectively. There is also an interesting breakdown of the eb ligand which steadily loses hydrocarbon fragments to give the series m/z 260 $[Ce(eb)]$, 242 $[Ce(O_2C_2(CH_3)_2CH_2)]$, 228 $[Ce(O_2C_2(CH_3)_2]$ and 196 $[Ce(O_2CC)]$. Compound (67) also shows similar losses of water and hydrocarbon fragments. In conjunction with these are a number of $[Ce_xO_y]$ fragments at m/z 483 and 329 for $[Ce_3O_4]$ and $[Ce_2O_3]$, respectively.

The pfp compound (68) shows the previously observed ions corresponding to the loss of numerous fluorine atoms, however, there are considerably more carbonaceous fragments than in the ceric oxo-*bis* carboxylate (32). For instance, ions at m/z 464 $[Ce(pfp)_2]$, 376 $[Ce(pfp)(O_2C_2)(H_2O)]$ and 263 $[Ce(O_2C_3F_2)(H_2O)]$ are observed. An ion at m/z 202 for $[Ce(OAc)(H_2O)]$ also shows the complete loss of all fluorine atoms. A noteworthy feature of the mass spectrometry of the cerous compounds is that they very rarely have any ions of large abundance.

In contrast to the cerous species, the ceric carboxylates (69) - (74) tend to show larger mass ions but not as many ligand fragmentation ions. For example the eb ligand remains intact throughout for compound (69) giving ions such as $[Ce_4O_5(eb)_2]$ and $[(CeO)_4(eb)_2]$ at m/z 870 and 855, respectively. Both the dmb and the dmp complexes (70) and (71) show a similar disinclination to ligand fragmentation. In the case of the latter this is in contrast to the spectrum of compound (27) where numerous hydrocarbon ligand fragmentations are observed. The ions assigned as $[(CeO)_x(O_2CR)_y]$ are also prevalent in these spectra. For instance compound (71) shows ions such as m/z 855 $[(CeO)_3(dmp)_3]$, 770 $[(CeO)_3(dmp)_2(OAc)]$ and 726 $[(CeO)_3(dmp)_2]$.

However, the breakdown of the carboxylate ligand is observed in the spectra of both (72) and (74) giving rise to very similar ions. The complete carboxylate ion $[Ce(oct)_2O]$ is observed at m/z 443 for (74), whereupon the ion begins to lose hydrocarbon

fragments at the expense of obtaining oxygen atoms. These are then steadily lost in conjunction with more carbonaceous fragments, eventually giving rise to $[Ce(O_2C(CH_2)_3]$ at m/z 443. Compound (73) gives a very poor mass spectrum showing only two weak ions.

8.4.4 Physical properties

8.4.4.1 Solubilities and melting points

Cerous carboxylates are generally less soluble than their ceric counterparts, especially in non-aqueous media. For instance, the solubility of $[Ce(OAc)_3.H_2O]$ in water at R.T. is appreciable (22.44 g/100 g water).[306] It also has some solubility in methanol, aminoethanol and ethylene glycol, however, it is insoluble in non-polar solvents. This is not surprising as the structure of the compound reveals it to consist of extended chains. The homoleptic ceric acetate, $[Ce(OAc)_4]$, is also soluble in water, but in contrast, has some solubility in benzene.[206]

Compounds (66) and (67) show little solubility in water (in fact their syntheses rely on the fact that they drop out of aqueous media), or any other solvent. They are completely insoluble in aliphatic (e.g. hexane), aromatic (e.g. benzene) and non-coordinating (e.g. chloroform) solvents, but do show some solubility in coordinating solvents such as dmso and dmf. The third cerous carboxylate described within this Chapter, *viz.* (68) has completely different solubility properties.

Due to the electron withdrawing nature of the substituent groups of the halogenated compounds, the oxo-*bis* carboxylate perfluorinated species are soluble in alcohols and acetonitrile, whereas the hydrocarbyl species are soluble in benzene and petroleum ether. Compound (68) is insoluble in non polar solvents such as benzene and chloroform but very soluble in polar solvents including acetone, dmso, acetonitrile and water. The synthesis of (68) using cerium(III) carbonate relies on the fact that the product is soluble in aqueous media whereas the carbonate starting material is not.

The compounds synthesized from the oxidation by peracetic acid of the corresponding hydrated cerous carboxylates have quite different solubilities to their starting materials. Compounds (69) and (71) have the same solubilities as compounds (23) and (28), respectively, i.e. they are both soluble in benzene and chloroform but insoluble in alcohols, water and dmso. Compounds (23) and (69) are also soluble in hexane. This factor also lends support to the fact they are one and the same complex, i.e. they have the

same molecularities. Compound (70) also shows similar solubility.

The liquid cerium carboxylates, compounds (24) and (25) were observed to be extremely miscible with organic solvents such as petroleum ether, isopentane and hexane. However, the compounds synthesized from this preparation show quite different solubilities. These compounds are no longer yellow / orange liquids but yellow oily solids and are observed to be less soluble than the complexes made from CAN. Compounds (72) and (73) are both appreciably soluble in benzene and chloroform but insoluble in polar solvents. The final compound in this section, (74), shows very limited solubility in any solvent; in fact it only shows any degree of solubility in hot chloroform. This lack of solubility is also noted in the corresponding compound synthesized from CAN. It is only from microanalytical studies and physical observations that we are able to confirm compounds (72) and (73) as having less than two organic residues associated with their structures.

The melting points of the hydrocarbon cerium(III) carboxylates (66) and (67) are significantly higher than their Ce(IV) counterparts. Both are observed to decompose (or melt) above 300°C, whereas the Ce(IV) species either decompose or melt at 166-8 or 85-9°C, respectively (see compounds (69) and (71)). In line with the findings for the ceric compounds, however, we note that the perfluorinated compounds (68) melts at a much lower temperature, i.e. 233-9°C. The cerium(IV) oxo-*bis* carboxylate analogue of this compound (32) is observed to decompose with an explosion at 263-5°C.

The cerium(IV) species synthesized from the aqueous route appear to have similar melting points to the compounds synthesized from this peracid route, *viz*. compounds (23) and (69) and also (27) and (71). The majority of the other compounds in this series appear to decompose at relatively high temperatures (*ca.* 240°C) except for (74) which melts at 86-9°C. This low melting point is possibly due to the same reason that compounds (27) and (71) have low melting points in that the coordinated unidentate carboxylic acid 'drops off' at relatively low temperatures and the rest of the compound dissolves within the liberated liquid.

8.4.4.2 STA analysis

The thermal decompositions of the cerium(IV) oxo-*bis* carboxylates and some of their coordination compounds have already been discussed in previous chapters; therefore, it is only the cerous carboxylates which are considered here. The pertinent data are illustrated in Table 8.6 below.

Table 8.6 : TGA / DSC results for compounds (66) - (68) :

Compound	TGA1(C)	TGA2(C)	DSC1(°C)	DSC2(°C)	$T_{50\%}$
(66)	48.9-82.0	464.9-518.5	77.2	512.8	487
(67)	85.2-221.9	272.4-520.4	115.0	277.4, 511.8	350
(68)	162.5-173.9	314.2-350.2	166.3	340.5	330

The TGA of the 2-ethylbutyrate complex (66), shows a very simple plot comprising of two steps. The first,between 48.9 and 82.0°C, is most likely to be due to the loss of the coordinated water molecule to give the dehydrated carboxylate. This is then stable until 465°C where there is a further weight loss (56.4%), before stabilizing once again at 518.5°C. This step corresponds to the loss of the carboxylate fragments with the exception of two oxygen atoms. The final residue of 29.6% at 700°C is most likely cerium dioxide. It is noteworthy that the CeO_2 is not yellow as is more usual, but white. This indicates that the oxide is very pure, the yellow colour only being observed when the sample has been left in the atmosphere for several hours. The DSC curve is similarly straightforward, showing just two inflexions at 77.2°C and 512.8°C, corresponding to the loss of the water and carboxylate fragments, respectively.

In contrast, the TGA plot of (67) has a small initial step between 85.2 and 221.9°C which corresponds to the loss of the water molecules and a second very drawn out weight loss between 272.4 and 520.4°C (Found 59.1, Expected 61.1%) corresponding to the loss of the hydrocarbon carboxylate fragments, to leave a white CeO_2 residue of 36.3% at 700°C. Therefore, although the decomposition process involving the loss of the carboxylate ligands begins at a lower temperature than for (66), the temperature at which the weight loss is complete is approximately the same. Therefore, the $T_{50\%}$ of 350°C should not be taken as an indication that the volatility of this complex is considerably better than that of (66). The DSC shows three inflexions at 115.0, 277.4 and 511.8°C, corresponding to (i) the loss of the water molecules, (ii) the initiation of the loss of the carboxylate fragments and (iii) the final decomposition temperature and the subsequent

formation of the CeO_2 residue.

The TGA plot of compound (68) is similar to that of (66) in that it shows just two steps, however, the latter is at a significantly lower temperature. This factor is in accord with the data previously noted for both the alkaline earth metal complexes and the cerium carboxylates, where fluorinated substituents on the organic ligands tend to produce more volatile species. The initial weight loss at 162.5°C (5.1%) corresponds to the loss of the water molecules (expected 6.6%) and is essentially complete by 174°C. The second weight loss is between 314.2 and 350.2°C and corresponds to the loss of the carboxylate fragments with the exception of two oxygen atoms. The final residue is 27.5% at 700°C; this again corresponds to CeO_2 (expected 25.8%).

As was previously noted it is shown that the decomposition of the fluorinated species is complete at significantly lower temperatures than the hydrocarbyl species, in this case almost 170°C lower although it is observed to be somewhat higher than that of the corresponding cerium(IV) compound (32) which has a $T_{50\%}$ of 296°C. The DSC curve shows two inflexions at 166.3°C and 340.5°C corresponding to the loss of the water and carboxylate fragments, respectively. The related cerous tfa compound has similar plots for both the TGA and DSC analyses, however, the decomposition is complete at an even lower temperature, the final weight loss being essentially complete by 287°C. Once again the residue is CeO_2 (found 37.9 ; calculated 34.4%).

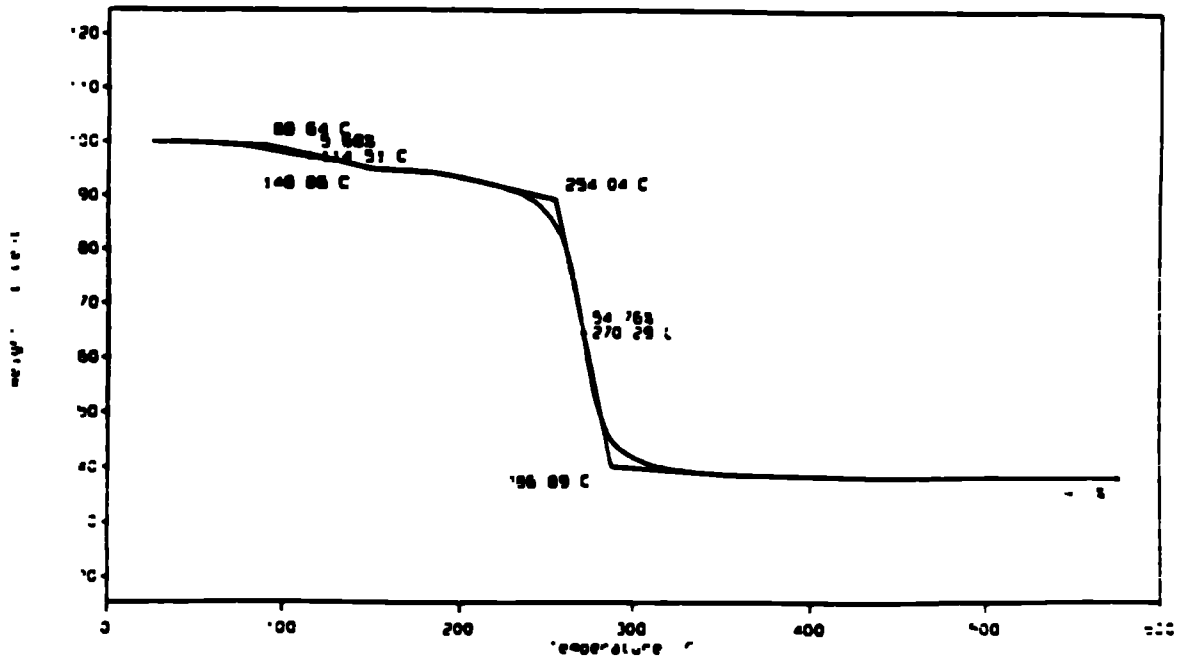

Figure 8.15 : TGA plot of $Ce(tfa)_3.1.5H_2O$

8.4.5 Summary

Cerium(IV) oxo-*bis* carboxylate compounds have been synthesized from the addition of an aqueous solution of the sodium carboxylate to a concentrated aqueous solution of cerium ammonium nitrate (CAN). The products obtained are of the general formula $[CeO(RCO_2).n(RCO_2H)]$. Infrared analysis suggests that the carboxylate ligands are either chelating or bridging (from $\Delta\nu$ values). Crystallographic determinations of compounds (23) and (27) shows that the structures are based on a $Ce_6(OH)_2O_6$ core framework, with twelve bridging carboxylate ligands surrounding it. Compound (27) also has two unidentate carboxylic acid ligands coordinated giving overall metal coordination numbers of either eight or nine.

The hydrocarbyl cerium(IV) carboxylates are soluble in hydrocarbon solvents such as hexane and benzene, while the perfluorinated carboxylate are soluble in more polar solvents such as chloroform, ethers and alcohols. The $[CeO(RCO_2).n(RCO_2H)]$ products appear to be formed only in aqueous media because the exclusion of water and the employment of inert atmosphere conditions gives oxo species of the form $[Ce(O)_{0.25}(eb)_{3.5}]$ (35), which is unlikely to be hexameric

The addition of neutral and potentially charged coordinating ligands has also been investigated. Infrared analysis again suggests that the carboxylate ligands are either bridging or chelating, however, it is only really with X-ray techniques that we can tell for sure whether the hexameric oligomers persist when these ligands are added. The unit cell of $[CeO(eb)_2(bipy)]$ (44) is significantly smaller than that of the oxo-*bis* carboxylate compound (27) (both of which are monoclinic), which may suggest that the hexamer does not persist in the coordination compounds. However, further crystallographic evidence is needed to qualify this.

The redox chemistry of the cerium(IV) carboxylates has shown that by three completely different routes (physical and chemical) the Ce(III) and Ce(IV) carboxylates are able to exchange. This is testament to Hund's rules which allow both the ubiquitous tripositive lanthanide complexes and the tetrapositive complexes which utilize the stability of the f^0 configuration to exist both in the solid state and in solution.

8.4.6 Experimental section

Synthesis of $Ce(eb)_3.H_2O$ (66)

$CeCl_3.7H_2O$ (3.0g, 7.80 mmol) was dissolved in distilled water (20 mL) at R.T., which was followed by the dropwise addition of a colourless solution of NaOH (0.94g, 23.40 mmol), 2-ethylbutyric acid (2.93g, 23.40 mmol) and water (50 mL). The solution rapidly turned from a partially soluble white solution, to an insoluble one. The suspension was stirred at R.T. for 10 mins., filtered, washed with water (2 x 20 mL) and dried under vacuum for 2 hours. The white solid was further dried for 2 hours at *ca.* 80°C. **Yield** 3.39g (86%). **M. Pt.** dec. >300°C

Microanalysis : Found, C, 42.9 ; H, 6.84 ; Calc. for $CeO_7C_{18}H_{35}$, C, 42.9 ; H, 6.95 %.

Infrared (Nujol ν cm^{-1}) : 3334(br), 1704(w), 1528(m), 1317(m), 1250(w), 1214(m), 1214(m), 1111(m), 939(w), 865(w), 811(m), 655(w), 529(w), 369(w).

Infrared (hexachlorobutadiene ν cm^{-1}) : 3345(br), 2964(m), 2936(m), 2876(m), 1703(w), 1508(m), 1466(m), 1421(m), 1383(m), 1352(m), 1318(m), 1250(w), 1215(w), 1170(m), 1111(w), 893(w), 809(m), 527(w).

^1H NMR (90 MHz, D_6-dmso, 20°C) : δ 1.46 (br, 18H, CH_3), 2.72 (br, 12H, CH_2), 2.95 (br, 3H, CH), 4.02 (br, 2H, OH).

Solid State ^{13}C NMR : CPMAS: δ 13.8 (br, CH_3), 25.8 (br, CH_2), 61.0 (br, CH), 191.2 (br, CO).

Mass Spectrometry : 461 [$Ce(eb)_2(O_2CCHCH_2)(H_2O)$](15%), 443 [$Ce(eb)_2(O_2CCHCH_2)$](15%), 329 [$Ce_2O_3$](8%), 309 [$Ce(eb)O_2(H_2O)$](12%), 290 [$Ce(eb)O_2$](24%), 273 [Ce(eb)O](29%), 260 [Ce(eb)](24%), 242 [$Ce(O_2C_2(CH_3)_2CH_2)$](22%), 228 [$Ce(O_2C_2(CH_3)_2$](16%), 196 [$Ce(O_2CC)$](9%).

Solubility : Partially soluble in dmso, insoluble in hexane, alcohols, chloroform and benzene.

STA data : TGA: 48.9-82.0°C (7.4%), 464.9-518.5°C (56.4%), Residue (29.6%), $T_{50\%}$ (487°C); DSC: 77.2(exotherm), 512.8(exotherm)°C.

Synthesis of $Ce(dmp)_3.3H_2O$ (67)

$CeCl_3.7H_2O$ (3.0g, 7.80 mmol) was dissolved in distilled water (20 mL) at R.T., which was followed by the dropwise addition of a colourless solution of NaOH (0.94g, 23.40 mmol), 2,2-dimethylpentanoic acid (3.04g, 23.40 mmol) and water (50 mL). The reaction proceeded as for (66). The white solid was further dried for 2 hours at *ca.* 80°C. **Yield** 3.48g (77%). **M. Pt.** dec. >300°C

Microanalysis : Found, C, 42.8 ; H, 6.91 ; Calc. for $CeO_9C_{21}H_{45}$, C, 43 4 ; H, 7.74 %.

Infrared (Nujol ν cm^{-1}) : 1520(m), 1313(m), 1263(w), 1181(m), 982(m), 943(m), 922(w), 886(w),

855(m), 791(m), 655(w), 607(w), 555(w), 399(w).

Infrared (hexachlorobutadiene ν cm^{-1}) 3340(br), 2959(m), 2928(m), 2873(m), 1478(m), 1409(m), 1375(m), 1314(m), 1291(w), 1265(w), 1180(m), 887(w), 608(m), 555(w), 399(m).

^{1}H NMR (90 MHz, D_6-dmso, 20°C) : δ 1.23 (br, 9H, CH_3), 2.52 (br, 12H, CH_2), 2.74 (br, 18H, CCH_3), 3.30 (br, 6H, OH).

^{13}C NMR (22.65 MHz, D_6-dmso, 20°C) : δ 15.7 (s, CH_3), 19.1 (s, $C(\underline{C}H_3)$), 27.6 (s, $CH_3\underline{C}H_2$), 45.4 (s, $C\underline{C}H_2$), 51.8 (s, $\underline{C}(CH_3)_2$), 184.5 (s, CO).

Solid State ^{13}C NMR : CPMAS: δ 15.2 (s, CH_3), 18.3 (s, $C(\underline{C}H_3)$), 26.8 (s, $CH_3\underline{C}H_2$), 45.8 (s, CH_2), 46.8 (s, $\underline{C}(CH_3)_2$), 197.0 (s, CO).

Mass Spectrometry : 483 $[Ce_3O_4]$(17%), 441 $[Ce(dmp)_2(OAc)]$(15%), 397 $[Ce(dmp)_2]$(7%), 329 $[Ce_2O_3]$(12%), 290 $[Ce(dmp)(H_2O)]$(16%), 260 $[Ce(O_2C_2CH_2CH_2)(H_2O)_2]$(8%), 242 $[Ce(O_2C_2CH_2CH_2)(H_2O)]$(8%), 228 $[Ce(O_2C_2CH_2)(H_2O)]$(5%), 214 $[Ce(O_2C_2)(H_2O)]$(4%), 192 $[CeO_2(H_2O)]$(64%).

Solubility : Partially soluble in dmso, insoluble in hexane, alcohols, chloroform and benzene.

STA data : TGA : 85.2-221.9°C (3.64%), 272.4-520.4°C (59.1%), Res. 36.3%, $T_{50\%}$ 350°C. DSC : 115.0, 277.4(exotherm), 511.8(exotherm)°C.

Synthesis of $Ce(pfp)_3.2.5H_2O$ (68)

$Ce_2(CO_3)_3$ (3.0g, 6.52 mmol) was dissolved in distilled water (50 mL) at R.T., which was followed by the dropwise addition of pentafluoropropionicic acid (6.41 g, 39.10 mmol) in water (40 mL). The reaction mixture was stirred for 30 mins. until all CO_2 had evolved, the solution turning from insoluble white to soluble colourless. Any remaining residues were filtered and the resultant solution stripped to dryness yielding a powdery white solid. **Yield** 8.01g (95%). **M. Pt.** melts 233-9°C

Microanalysis : Found, C, 15.9 ; H, 0.78 ; Calc. for $CeO_{8.5}C_9H_5F_{15}$, C, 16.0 ; H, 0.74 %.

Infrared (Nujol ν cm^{-1}) : 3692(w), 3661(w), 3450(br), 1717(m), 1647(m), 1328(m), 1214(m), 1167(s), 1037(m), 820(m), 775(w), 602(m), 584(w), 541(w), 523(w), 420(w).

Infrared (hexachlorobutadiene ν cm^{-1}) : 3447(w,br), 3155(m,br), 1507(w), 1443(m), 1408(m), 1331(m), 1229(m), 1165(m), 1036(m), 892(w), 731(m), 544(m), 421(w).

^{13}C NMR (solid state MAS decoupling) : δ 117.4 (br, CF), 179.5 (br, CO).

Mass Spectrometry : 464 $[Ce(pfp)_2]$(15%), 376 $[Ce(pfp)(O_2C_2)(H_2O)]$(19%), 263 $[Ce(O_2C_3F_2)(H_2O)]$(12%), 244 $[Ce(O_2C_3F)(H_2O)]$(32%), 202 $[Ce(OAc)(H_2O)]$(12%).

Solubility : Soluble in dmso, alcohols, acetonitrile and acetone, insoluble in hexane, chloroform and benzene.

STA data : TGA: 162.5-173.9°C (5.06%), 314.2-350.2°C (66.1%), Residue (27.5%), $T_{50\%}$ (330°C), DSC: 166.3(exotherm), 340.5°C.

Synthesis of $CeO(eb)_2$ (69)

$Ce(eb)_3.H_2O$ (66) (1.50g, 2.98 mmol) was suspended in acetonitrile (40 mL) and stirred for 10 mins. to give an insoluble white suspension. Peracetic acid (0.53 mL, 2.98 mmol) was added whereupon the solution immediately turned brown. The insoluble suspension was stirred for 24 hours at R.T., eventually yielding a yellow / brown solution. The solvent was removed *in vacuo* to yield an oily yellow solid. The excess acetic acid (peracetic acid is supplied as a dilute solution in acetic acid) was removed by dissolving the solid in benzene (25 mL) and washing with water (2x20 mL). The organic phase was separated, dried over magnesium sulphate and stripped to dryness to give a yellow oil which on cooling, yielded crystalline yellow solid. **Yield** 0.91g (79%). **M. Pt.** dec. 166-8°C

Microanalysis : Found, C, 38.0 , H, 5.93 ; Calc. for $CeO_5C_{12}H_{22}$, C, 37.3 , H, 5.70 %.

Infrared (Nujol ν cm^{-1}) : 3626(m), 1708(s), 1541(s), 1417(m), 1316(m), 1246(m), 1216(m), 1155(w), 1110(w), 1096(m), 1046(w), 938(m), 885(m), 825(w), 777(w), 653(w), 583(m), 518(m), 381(m), 301(w).

Infrared (hexachlorobutadiene ν cm^{-1}) : 3635(m), 2965(s), 2935(m), 2876(m), 1707(m), 1462(s), 1416(s), 1316(m), 1293(m), 1247(m), 1229(m), 1170(m), 1110(w), 1097(w), 894(w), 566(m), 520(m).

^1H NMR (270 MHz, $CDCl_3$, 20°C) : δ 0.85 (br, 6H, CH_3), 1.45, 1.56 (br, 4H, CH_2), 2.11 (br, 1H, CH).

^{13}C NMR (67.94 MHz, $CDCl_3$, 20°C) : δ 11.9 (s, CH_3), 24.6 (s, CH_2), 50.5 (s, CH), 182.8 (s, CO).

Mass Spectrometry : 870 $[Ce_4O_5(eb)_2]$(8%), 855 $[(CeO)_4(eb)_2]$(4%), 483 $[Ce_3O_4]$(17%), 419 $[Ce(eb)_2O_3]$(11%), 329 $[Ce_2O_3]$(44%), 272 [Ce(eb)O](12%).

Solubility : Soluble in hexane, benzene and chloroform, insoluble in alcohols, water and dmso.

Synthesis of $CeO(dmb)_2$ (70)

$Ce(dmb)_3.3H_2O$ (1.16g, 2.15 mmol) was suspended in acetonitrile (40 mL) and stirred for 10 mins. to give a white suspension. Peracetic acid (0.38 mL, 2.15 mmol) was added whereupon the solution immediately turned brown. The reaction proceeded as for (69) to give a yellow oil which on cooling, yielded a crystalline yellow solid. **Yield** 0.63g (76%). **M. Pt.** dec. 245-8°C

Microanalysis : Found, C, 38.1 , H, 5.79 ; Calc. for $CeO_5C_{12}H_{22}$, C, 37.3 , H, 5.70 %.

Infrared (Nujol ν cm^{-1}) : 3636(m), 1544(s), 1412(m), 1289(m), 1262(m), 1205(m), 1186(m), 1097(w).

1053(w), 1020(m), 944(w), 885(w), 801(m), 667(m), 619(m), 579(m), 527(w), 398(m), 310(w).

Infrared (hexachlorobutadiene ν cm^{-1}) 3639(m), 2967(m), 2927(m), 1478(m), 1462(m), 1412(m), 1374(m), 1360(m), 1289(m), 1231(w), 1205(m), 1171(m), 893(m), 619(w), 579(m), 527(m), 396(m), 316(m).

^{1}H NMR (270 MHz, $CDCl_3$, 20°C) : δ 0.69 (t, 3H, CH_3), 1.05 (s, 6H, $C(CH_3)_2$), 1.51 (br, 2H, CH_2).

^{13}C NMR (22.65 MHz, $CDCl_3$, 20°C) : δ 10.7 (s, CH_3), 25.9 (s, $C(\underline{C}H_3)_2$), 34.5 (s, CH_2), 43.9 (s, $\underline{C}(CH_3)_2$), 182.3 (s, CO).

Mass Spectrometry : 813 $[Ce_5O_7]$(6%), 697 $[(CeO)_3(dmb)_2]$(6%), 655 $[Ce_4O_6]$(4%), 483 $[Ce_3O_4]$(19%), 445 $[Ce_2(dmb)O_3]$(5%), 427 $[(CeO)_2(dmb)]$(11%), 328 $[Ce_2O_3]$(14%), 289 $[Ce(dmb)O_2]$(7%).

Solubility : Soluble in benzene and chloroform, insoluble in alcohols, water and dmso.

Synthesis of $CeO(dmp)_2(dmp\text{-}H)_{.33}$ (71)

$Ce(dmp)_3.3H_2O$ (67) (1.10g, 1.89 mmol) was suspended in acetonitrile (40 mL) and stirred for 10 mins. to give a white suspension. Peracetic acid (0.34 mL, 1.89 mmol) was added whereupon the solution immediately turned brown. The reaction proceeded as for (69) to give a yellow oil which on cooling, yielded a crystalline yellow solid. **Yield** 0.65g (75%). **M. Pt.** melts 85-9°C

Microanalysis : Found, C, 42.8 , H, 7.09 ; Calc. for $CeO_{5.67}C_{16.33}H_{30.67}$, C, 42.9 , H, 6.71 %.

Infrared (Nujol ν cm^{-1}) : 3624(s), 1538(s), 1410(m), 1306(s), 1289(s), 1261(s), 1240(s), 1185(s), 1091(w), 1067(m), 1041(m), 1007(m), 962(m), 923(m), 892(m), 855(m), 823(w), 804(w), 786(m), 763(m), 740(m), 654(m), 577(s), 525(s), 401(m), 377(s).

Infrared (hexachlorobutadiene ν cm^{-1}) : 3626(m), 2962(s), 2934(s), 2874(s), 1699(s), 1651(m), 1476(s), 1434(m), 1376(m), 1362(m), 1313(w), 1289(m), 1262(m), 1184(s), 1091(m), 891(m), 741(m), 578(m), 527(m), 404(m), 379(m).

^{1}H NMR (270 MHz, $CDCl_3$, 20°C) : δ 0.88 (t, 6H, CH_3), 1.15 (s, 12H, $C(CH_3)_2$), 1.46 (br, 8H, CH_2), 8.10 (br, 0.33H, OH).

^{13}C NMR (22.65 MHz, $CDCl_3$, 20°C) . δ 15.5 (s, CH_3), 18.9 (s, $C(\underline{C}H_3)_2$), 26.5 (s, CH_2), 44.1 (s, $\underline{C}(CH_3)_2$), 184.3 (br, s, CO)

Mass Spectrometry : 1099 $[Ce_3(dmp)_5O_2]$(9%), 925 $[Ce_2(dmp)_5]$(7%), 855 $[(CeO)_3(dmp)_3]$(5%), 811 $[Ce_5O_7]$(6%), 770 $[(CeO)_3(dmp)_2(OAc)]$(25%), 726 $[(CeO)_3(dmp)_2]$(6%), 484 $[Ce_3O_4]$(35%), 441 $[(CeO)_2(dmp)]$(33%), 397 $[Ce(dmp)_2]$(20%), 329 $[Ce_2O_3]$(8%).

Solubility : Soluble in benzene and chloroform, insoluble in alcohols, water and dmso.

Synthesis of $CeO(eh)_2(eh\text{-}H)_{1.5}$ (72)

$Ce(eh)_3.2H_2O$ (2.00g, 3.30 mmol) was suspended in acetonitrile (80 mL) and stirred for 10 mins. in a round bottomed flask covered with silver foil, to give a white suspension. Peracetic acid (0.59 mL, 3.30 mmol) was added whereupon the solution immediately turned brown. The reaction proceeded as for (69) to give a yellow oil. **Yield** 1.88g (86%). **M. Pt.** dec. 245-50°C

Microanalysis : Found, C, 50.5 , H, 8.01 ; Calc. for $CeO_8C_{28}H_{54}$, C, 51.0 , H, 7.97 %.

Infrared (Neat ν cm^{-1}) : 3628(m), 2960(s), 2934(s), 2874(s), 1706(m), 1557(s), 1417(s), 1316(m), 1231(m), 1150(m), 1104(m), 1075(w), 1021(w), 949(m), 918(m), 900(m), 812(m), 781(m), 732(m), 640(m), 568(m), 391(m), 366(m), 310(w).

^1H NMR (90 MHz, $CDCl_3$, 20°C) : δ 0.95 (br, 6H, CH_3), 1.75 (br, 8H, CH_2), 2.49 (br, 1H, CH).

^{13}C NMR (22.65 MHz, $CDCl_3$, 20°C) : δ 12.9 (s, CH_3), 14.9 (s, $CHCH_2\underline{C}H_3$), 23.9 (s, $CHCH_2CH_2\underline{C}H_2$), 25.8 (s, $CHCH_2\underline{C}H_2$), 30.7 (s, $CH\underline{C}H_2CH_2$), 32.2 (s, $CH\underline{C}H_2CH_3$), 52.4 (s, CH), 185.6 (s, CO).

Mass Spectrometry : 442 $[CeO(eh)_2]$(22%), 289 $[CeO_3(O_2C(CH_2)_4)]$(21%), 259 $[CeO_2(O_2C(CH_2)_3)]$(11%), 242 $[CeO(O_2C(CH_2)_3)]$(17%), 227 $[Ce(O_2C(CH_2)_3)]$(13%).

Solubility : Soluble in benzene and chloroform, insoluble in alcohols, water and dmso.

Synthesis of $CeO(mv)_2(mv\text{-}H)$ (73)

$Ce(mv)_3.H_2O$ (1.90g, 3.77 mmol) was suspended in acetonitrile (80 mL) and stirred for 10 mins. in a round bottomed flask covered with silver foil, to give a white suspension. Peracetic acid (0.67 mL, 3.77 mmol) was added whereupon the solution immediately turned brown. The reaction proceeded as for (69) to give a yellow oily solid. **Yield** 1.66g (88%). **M. Pt.** dec. 236-41°C

Microanalysis : Found, C, 43.6 , H, 6.52 ; Calc. for $CeO_7C_{18}H_{34}$, C, 43.0 , H, 6.76 %

Infrared (Neat ν cm^{-1}) : 3635(m), 2960(s), 2874(s), 1711(m), 1557(s), 1470(s), 1417(s), 1379(m), 1308(s), 1260(m), 1156(m), 1100(m), 1054(w), 1022(w), 1004(m), 939(m), 900(m), 861(m), 809(m), 786(m), 744(m), 658(m), 550(m), 474(w), 376(m), 356(m), 316(w).

^1H NMR (90 MHz, $CDCl_3$, 20°C) δ 0.78 (br, 6H, CH_3), 1.33 (br, 4H, CH_2), 2.65 (br, 1H, CH).

^{13}C NMR (22.65 MHz, $CDCl_3$, 20°C) : δ 15.0 (s, CH_3), 17.5 (s, $CH\underline{C}H_3$), 21.3 (s, $CHCH_2\underline{C}H_2$), 36.6 (s, $CH\underline{C}H_2$), 45.8 (s, CH), 186.6 (s, CO).

Mass Spectrometry : 483 $[Ce_3O_4]$(12%), 329 $[Ce_2O_3]$(5%).

Solubility : Soluble in benzene and chloroform, insoluble in alcohols, water and dmso.

Synthesis of $CeO(oct)_2(oct\text{-}H)_{.33}$ (74)

$Ce(octanoate)_3.H_2O$ (422) (1.25g, 2.13 mmol) was suspended in acetonitrile (80 mL) and stirred for 10 mins. in a round bottomed flask covered with silver foil, to give a white suspension. Peracetic acid (0.38 mL, 2.13 mmol) was added whereupon the solution gradually turned orange / yellow over 5 mins.. The reaction proceeded as for (69) to give a very pale yellow solid. **Yield** 0.87g (83%). **M. Pt.** melts 86-9°C

Microanalysis : Found, C, 45.4 , H, 7.21 ; Calc. for $CeO_{5.67}C_{18.67}H_{35.33}$, C, 45.6 , H, 7.21 %

Infrared (Nujol νcm^{-1}) : 3345(br), 1714(m), 1662(m), 1538(s), 1303(m), 1256(m), 1211(m), 1184(m), 1104(m), 1066(m), 1020(m), 943(m), 891(w), 836(w), 774(m), 675(m), 539(w), 500(w), 479(w), 446(w), 392(w), 317(w).

Infrared (hexachlorobutadiene $\nu\ cm^{-1}$) : 3361(br), 2957(s), 2925(s), 2852(m), 1712(m), 1661(m), 1451(m), 1408(m), 1341(m), 1304(m), 1256(w), 1231(w), 1212(w), 1171(m), 1105(w), 893(w), 723(m), 549(m), 446(w).

^1H NMR (90 MHz, $CDCl_3$, 20°C) : δ 0.81 (br, 3H, CH_3), 1.37 (br, 12H, CH_2).

Mass Spectrometry : 443 $[CeO(oct)_2]$(12%), 309 $[CeO_3(O_2C(CH_2)_4(H_2O))]$(16%), 290 $[CeO_3(O_2C(CH_2)_4)]$(26%), 273 $[CeO_2(O_2C(CH_2)_4)]$(22%), 259 $[CeO_2(O_2C(CH_2)_3)]$(17%), 242 $[CeO(O_2C(CH_2)_3)]$(9%), 226 $[Ce(O_2C(CH_2)_3)]$(16%).

Solubility : Partially soluble in hot chloroform, insoluble in organic aliphatics, organic aromatics, alcohols, water and dmso.

Chapter 9

REFERENCES

Part 1: Stabilized Group II β-diketonates

1. M. Bouquet and J. *Ann. Chim. Phys.*, 1846, 17, 54.
2. H. K. Bowen and H. Okamura, *Ceram. Inter.*, 1986, 12, 161.
3. D. C. Bradley, *Chem. Rev.*, 1989, 89, 1317.
4. L. G. Hubert-Pfalzgraf, *App. Organomet. Chem.*, 1992, 6, 627.
5. I. M. Thomas, *US Patent 3799 909*, 26 March 1974.
6. C. J. Lynch, K. S. Mazdiyasni and J. S. Smith, *J. Am. Chem. Soc.*, 1972, 55, 548.
7. L. G. Hubert-Pfalzgraf, M. C. Massiani, R. Papiernek and O. Poncelet, *J Physique*, 1989, 50, C5-981.
8. M. L. Hoppe, R. A. Kennish, R. M. Laine, J. Ray, K. A. Youngdahl and Z. F. Zhang, *J. Mater. Res.*, 1991, 5, 895.
9. J. Coupeck, D. Lim and L. Lochmann, *Ger Patent. 2035260*, 1971.
10. D. T. Dolloff, K. S. Mazdyasni and J. S. Smith, *J. Am. Ceram. Soc.*, 1969, 52,523.
11. D. T. Dolloff, K. S. Mazdyasni and J. S. Smith, *J. Am. Ceram. Soc.*, 1970, 53,91.
12. V. C. Arunasalam, S. R. Drake, M. B. Hursthouse, K. M. A. Malik and D. J. Otway, *J. Am. Chem. Soc.*, manuscript in preparation.
13. V. G. Kessler, Y. T. Struckov, E. P. Turevskaya, N. Y. Turova and A. I. Yanovsky, *J. Chem. Soc. Chem. Commun.*, 1993, 21.
14. J. H. Gladstone and A. Tribe, *J. Chem. Soc.*, 1881, 39, 4.
15. C. T. Lynch, K. S. Mazdiyasni and J. S. Smith, *Inorg. Chem.*, 1966, 5, 342.
16. R. C. Mehrotra and I. D. Verma, *J. Chem. Soc.*, 1960, 2966.
17. See for example; T. Colclough, W. Gerrard and M. F. Lappert, *J. Chem. Soc.*, 1966, 3006. D. C. Bradley, R. C. Mehrotra and W. Wardlaw, *J. Chem. Soc.*, 1952, 5020. J. R. Van Wazer, *Phosphorus and its compounds*, Vols. 1, 2, Interscience Publishers, New York, 1958.
18. R. C. Mehrotra, S. N. Misra and T. N. Misra, *J. Indian Chem. Soc.*, 1965, 42, 351.
19. J. Nelles, *US Patent 2187721*, 1940.
20. D. C. Bradley and W. Wardlaw, *Nature*, 1950, 75, 163.
21. See for example; H. Schiff, *Ann. Suppl.*, 1867, 5, 154. O. L. Hughes and G. E. M. Jones, *J. Chem. Soc.*, 1934, 1197. Sasin, G.S., *J. Org. Chem.*, 1953, 18, 1142.

22. J. A. Connor, *Top. Curr. Chem.*, 1971, 71, 71.
23. See for example; G. E. Coates and A. H. Fishwick, *J. Chem. Soc. (A)*, 1968, 1118. B. J. Wakefield, *Organometal. Chem. Rev.*, 1966, 1, 131. G. E. Coates, and D. Ridley, *J. Chem. Soc.*, 1965, 1970.
24. H. Noeth and H. Suchy, *Z. Anorg. Allg. Chem.*, 1968, 358, 44.
25. S. R. Drake, P. Hall and D. J. Otway, manuscript in preparation.
26. L. M. Brown, K. S. Mazdiyasni, *Inorg. Chem*, 1970, 9, 2783.
27. R. H. Backer, *J. Am. Chem. Soc.*, 1938, 60, 2673.
28. L. Malatesta, *Gazz. Chim. Ital.*, 1948, 78, 753.
29. L. Atwood, B. Cetinkaya, I. Gumiukcu and M. F. Lappert,*J. Am. Chem. Soc.*, 1980, 102, 2086.
30. M. H. Chisholm, F. A. Cotton, M. W. Extine and R. L. Kelly, *J. Am. Chem. Soc.*, 1978, 100, 5764.
31. V. C. Arunasalam, I. Baxter, M. B. Hursthouse, K. M. A. Malik, D. M. P. Mingos and J. C. Plakatouras, *Polyhedron*, 1995, 14, 1105.
32. M. H. Chisholm,and I. Rothwell, *Comp. Organomet. Chem.*, 1984, 2, 335.
33. V. C. A. Arunasalam, S. R. Drake, M. B. Hursthouse, K. M. A. Malik, S. A. Miller and D. J. Otway, unpublished results.
34. T. P. Hanusa, C. J. Huffman, J. C. Huffman and K. F. Tesh, *Inorg. Chem.*, 1991, 31, 5572.
35. K. G. Caulton, M. H. Chisholm, S. R. Drake and W. E. Strieb, *Inorg. Chem.*, 1990, 29, 2708.
36. R. Bohra, D. P. Gaur and R. C. Mehrotra, *Metal Alkoxides*, Academic Press Inc., London, 1978.
37. R. C. Mehrotra and R. K. Mehrotra, *Can. J. Chem.*, 1961, 39, 795.
38. R. C. Young, *Inorg. Synth.*, 1946, 2, 25.
39. See for example; W. Dilthey, *Annalen.*, 1903, 344, 300. H. D. K. Drew and D. T. Morgan, *J. Chem. Soc.*, 1921, 119, 1058.
40. R. Sahai and P. R. Singh, *Inorg. Chim. Acta* , 1968, 2, 102.
41. J. P. Collman, S. D. Goldby, R. A. Moss and W. S. Trhanovsky, *Chem. and Ind.*, 1960, 1213.
42. H. S. Booth and D. G. Pierce, *J. Phys. Chem.*, 1933, 37, 59.
43. F. P. Dwyer and A. M. Sargeson, *Proc. Roy. Soc. N. S. Wales*, 1956, 90, 29.
44. D. E. Fenton, R. Newmann and B. L. Vickery, *Chem. Commun.*, 1971, 93.
45. K. Isobe, S. Kawaguchi, Y. Nakamura and K. Noda, *Bull. Chem. Soc. Japan*, 1973, 46, 1699.

46. K. Isobe, S. Kawaguchi, Y. Nakamura and K. Takeda, *Inorg. Nucl. Chem. Soc.*, 1973, 9, 1283.

47. E. M. Brainina, R. Kh. Friedlina and A. N. Nesemayanov, *Izv. Akad. Nauk SSSR Otdel. Khim. Nauk*, 1957, 43. *ibid.*, 1958, 937,

48. J. C. Daran, L. G. Hubert-Pfalzgraf, O. Poncelet and C. Sirio, *Ultrastructure, Processing of Ceramics*, Wiley Interscience, 1992, chap 26.

49. F. Ribot, C. Sanchez and P. Toledano, *Chem. Mater.*, 1991, 3 759.

50. F. J. Hollander, D. H. Templeton and A. Zalkin, *Acta Cryst.*, 1973, B29, 1313.

51. S. R. Drake, M. H. Chisholm, K. G. Caulton and K. Folting, *J. Chem. Soc., Chem. Commun.*, 1990, 1349.

52. H. K. Shin, M. J. Hampden-Smith, E. N. Duesler and T. T. Kodas, *Can. J. Chem.*, 1992, 70, 2954.

53. D. W. Brown, R. Gardiner and P. S. Kirlin, *Chem. Mater.*, 1991, 3, 1053.

54. M. Becht, K. H. Dahmen and T. Gerfin, *Chem. Mater.*, 1993, 5, 137.

55. See for example ; H. A. Meinma and K. Timmer, *Inorg. Chim. Acta*, 1991, 187, 99. J. A. T. Norman and G. P. Pez, *J. Chem. Soc., Chem. Commun.*, 1991, 971. J. A. T. Norman and G. P. Pez, 'Volatile Crown Ligand β-Diketonate Alkaline Earth Metal Complexes'; *Eur. Pat. Appl. EP. 460,627.*

56. A. R. Barron, J. M. Buriak, L. K. Cheatham, R. G. Gordon and J. J. Graham, *Eur. J. Solid State Inorg. Chem.*, 1992, 29, 43.

57. S. I. Bridge, N. I. Dunhill and J. O. Williams, *Chemtronics*, 1989, 4, 266.

58. R. Belcher, C. R. Cranley, J. R. Majer, W. I. Stephen and P. C. Uden, *Anal. Chem. Acta.*, 1972, 60, 109.

59. K. H. Dahmen, C. R. Kannewurf, H. O. Marcy, T. J. Marks, L. M. Tonge, B. W. Wessels and J. Zhao, *Appl. Phys. Lett.*, 1988, 53, 31.

60. R. Bohra, D. P. Gaur and R. C. Mehrotra, *Metal β-diketonates*, Academic press, London, 1978.

61. R. M. Barkely, R. E. Sievers and S. B. Turnipseed, *Inorg. Chem.*, 1991, 30, 1164.

62. S. R. Drake, M. B. Hursthouse, K. M. A. Malik, and D. J. Otway, *J. Chem. Soc. Dalton Trans.*, 1993, 2283 .

63. V. C. Arunasalam, S. R. Drake, M. B. Hursthouse, K. M. A. Malik and D. J. Otway, Unpublished results.

64. A. D. Berry, M. Fatemi, D. K. Gaskill, R. T. Holm and A. P. Purdy, *Inorg. Chem.*, 1989, 28, 2799.

65. D. C. Bradley, M. Hasan, M. B. Hursthouse, O. F. Z. Khan, M. Motevalli,

R. G. Pritchard and J. O. Williams, *J. Chem. Soc., Chem. Commun.*, 1992, 575.

66. P. F. Benetiollo, M. Porchia, G. Rosetto and P. Zanella, *Polyhedron*, 1992, 11, 979.
67. D. A. Meinema, P. van der Sluis, A. L. Spek and K. Timmer, *Acta Cryst.*, 1990, C46, 1741.
68. B. J. Hinds, T. J. Marks, D. L. Schulz and C. L. Stern, *Inorg. Chem.*, 1993, 32, 249.
69. W. Becker and S. Wiedlich, *Eur.Pat. 0 508 345 A2.*
70. A. Mackor, H. A. Meinema, K. I. M. A. Spee and K. Timmer, *Inorg. Chim. Acta*, 1991, 190, 109.
71. A. Drozdov, N. Kuzmina, L. Martynenko and S. Troyanov, *Mater. Sci. Eng.*, 1993, B18, 139.
72. See for example ; I. L. Fragala, B. J. Hinds, G. Malandrino, T. J. Marks, D. A. Neumayer and C. L. Stern, *J. Mater. Chem.*, 1994, 4, 1061. S. L. Cook, M. L. Hitchman, B. C. Richards and S. H. Shamilan, *J. Mater. Chem.*, 1994, 4, 81.
73. R. E. Sievers, *Appl. Phys.*, 1990, 76, 1542.
74. R. W. Moshier, J. E. Schwarberg and R. E. Sievers, *Anal. Chem.*, 1970, 42, 1828.
75. K. Kikuchi Y. Shiohara, K. Sugawara, M .Yoshida and S. Yuhya, *Mol. Cryst. Liq. Cryst.*, 1990, 184, 231.
76. C. H. Cho, J. S. Chun, S. H. Kim and K. S. No, *J. Mater. Res.*, 1991, 6, 704.
77. A. A. Danoupoulos, M. B. Hursthouse, B. Hussain-Bates and G. Wilkinson, *J. Chem. Soc. Dalton Trans.*, 1991, 1855.
78. D. Stuart and N. P. C. Walker, *Acta. Cryst.*, 1983, A39, 1980, adapted for FAST geometry by A. Karuaulov, University of Wales, College of Cardiff, 1991.
79. G. M. Sheldrick, 1980. Scattering factor data is included in the SHELX-S program, (G. M. Sheldrick, University of Gottingen, FRG, 1986).
80. W. R. Jr. Rees and M. W. Carris, *Inorg. Chem.*. 1991, 30, 4479.
81. K. Davies, SNOOPI program for Crystal Structure Drawing, Univ. Of Oxford, 1983.
82. G. M. Sheldrick, SHELXL-93 program system, *J. Appl. Cryst.*, 1994, in press.
83. S. R. Drake, A. Lyons, D. J. Otway, A. M. Slawin and D. J. Williams, *J. Chem. Soc., Chem. Commun.*, 1993, 2378.
84. K. G. Caulton, M. H. Chisholm, S. R. Drake, K. Folting and J. C. Huffman, *Inorg. Chem.*, 1993, 33, 2974

85. Z. Pang, K. D. L. Smith, S. Wang and M. J. Wagner, *J. Chem. Soc. Chem. Commun.*, 1992, 1594.
86. M. P. Bernstein and D. B. Collum, unpublished results.
87. D. B. Collum, *Acc. Chem. Res.*, 1992, 25, 448.
88. M. Becht, K. H. Dahmen and T. Gerfin, *Chem. Mater.*, 1993, 5, 137.
89. J. L. Atwood, F. C. Lee, C. L. Raston and K. D. Robinson, *J. Chem. Soc. Dalton Trans.*, 1993, 2019.
90. Y. Fukuda, J. Kotaki, N. Shintani and K. Sone, *Bull. Chem. Soc. Japan*, 1993, 66, 789.
91. J. R. Hall, S. Wang and J. C. Zheng, *Polyhedron*, 1994, 13, 1039.
92a. D. E. Fenton and R. Newman, *J. Chem. Soc. Dalton Trans.*, 1974, 655.
92b. M. R. Truter and B. L Vickery, *J. Chem. Soc. Dalton Trans.*, 1972, 395.
93. R. M. Barkely, R. C. Haltiwanger, L. Huang and R. E. Sievers, *Inorg. Chem.*, 1994, 33, 798.
94. A. R. Barron, J. M. Buriak and R. Gordon, *US Patent (pending).*
95. A. R. Barron, *Strem Chemiker*, 1990, 13, 1.
96. L. G. Hubert-Pfalzgraf and F. Labrize, unpublished results.
97. A. Drozdov, N. Kuzmina, L. Martynenko and S. Troyanov, *Polyhedron*, 1993, 12, 2973.

Part 2 : Cerium (IV) Carboxylates

98. R. S. Coffey, *J. Chem. Soc. Chem. Commum.*, 1967, 923.
99. British Petroleum Co., *Chem. Abstr.*, 1970, 72, 2995, 31226, 100035.
100. S. B. Elliott, *The Alkaline Earth and Heavy Metal Soaps*, Reinhold, New York, 1946.
101. J. W. McBain, *Colloid Science*, Reinhold, New York, 1950.
102. V. Amirthalingam and V. M. Padmanabhan, *Acta Cryst.*, 1958, 11, 896.
103. J. Lifschitz and E. Rosenbohm, *Z. Electrochem.*, 1915, 21, 499.
104. R. Tsuchida and S. Yamada, *Nature (London)*, 1955, 176, 1171.
105. B. N. Figgis and R. L. Martin, *J. Chem. Soc.*, 1956, 3837.
106. R. Bohra and R. C. Mehrotra, *Metal Carboxylates*, Academic Press, London, 1983.
107. J. G. Bailar and J. H. Baltthis, *Inorg. Synth.*, 1939, 1, 123.
108. M. R. Hatfield, *Inorg. Synth.*, 1950. 3, 148.

109. R. C. Mehrotra, S. N. Misra and T. N. Misra, *J. Inorg. Nucl. Chem.*, 1963, 25, 195.
110. T. N. Misra, *Ph. D. Thesis*, Rajasthan University Jaipur, India, 1963.
111. S. N. Misra, *Ph. D. Thesis*, Rajasthan University Jaipur, India, 1964.
112. M. S. Bains, J. S. Ghotra and R. C. Paul, *Indian J. Chem.*, 1969, 7, 514.
113. Kh. A. Cherches, M. Ya. Lazarev and S. S. Stanovaya *Izv. Vyssh. Uche. Zaved. Khim. Khim. Tekhnol*, 1974, 17, 464.
114. R. C. Mehrotra and B. C. Pant, *Indian J. Chem.*, 1963, 1, 380.
115. S. J. Peachey and W. J. Pope, *Proc. Chem. Soc.*, 1900, 16, 42.
116. S. J. Peachey and W. J. Pope, *Proc. Chem. Soc.*, 1900, 16, 116.
117. R. C. Mehrotra, S. N. Misra and T. N. Misra, *J. Inorg. Nucl. Chem.*, 1963, 25, 201.
118. B. D. Jain, B. L. Kalsotra and R. K. Multani, *J. Chin. Chem. Soc.*, 1971, 18, 189.
119. E. W. Bohres, *Ber. Kernforschungangslange Juelich, Jul. 1080-NC*, 1974.
120. G. A. Razuvaev, V. N. Latyaeva and A. N. Lineva, *Zh. Obshch. Khim.*, 1970, 40, 1804.
121. A. Saitow, D. Seyferth and E. G. Rochow, *J. Org. Chem.*, 1958, 23, 116.
122. V. Peruzzo, G. Plazzogna and G. Tagliavini, *J. Organometal. Chem.*, 1970, 24, 347.
123. O. W. Kolling and E. W. Mawdsley, *Trans. Kans. Acad. Sci.*, 1971, 74, 38.
124. J. Kleinwachter and F. D. Nerdel, *Chem. Ber.*, 1957, 90, 598.
125. G. H. Cady, R. Dev and P. V. Radheshwar, *J. Inorg. Nucl. Chem.*, 1927, 34, 3913.
126. R. C. Mehrotra and R. P. Narain, *J. Indian Chem. Soc.*, 1964, 41, 755.
127. M. S. Bains, J. S. Ghotra and R. C. Paul, *Indian J. Chem.*, 1969, 7, 384.
128. M. S. Bains, J. S. Ghotra and R. C. Paul, *Indian J. Chem.*, 1969, 7, 381.
129. A. Miyasit and A Yamamoto, *J. Organomet. Chem.*, 1973, 49, C57; *ibid*, 1976, 113, 187.
130. W. H. Zachariasen, *J. Am. Chem. Soc.*, 1940, 62, 1011.
131. E. Spinner, *J. Chem. Soc.*, 1967, B, 879.
132. G. M. Brown and R. Chidambaram, *Acta Cryst..*, 1973, B29, 2393.
133. M. Linhard and B. Rau, *Z. Anorg. Allg. Chem.*, 1953, 271, 121.
134. C. D. Garner and B. Hughes, *Inorg. Chem.*, 1975, 14, 1722.
135. H. A. Plettinger and W. H. Zachariasen, *Acta.Cryst.*, 1959, 12, 526.
136. J. N. van Niekerk, F. R. L. Schoenig and J. H. Talbot, *Acta Cryst.*, 1953, 6, 720.

137. N. W. Alcock, V. M. Tracy and T. C. Waddington, *J. Chem. Soc. Dalton Trans.*, 1976, 2243.
138. A. I. Grigorev, *Russ. J. Inorg. Chem.*, 1963, 8, 409.
139. Q. Fernando, R. D. Mounts and T. Ogura, *Inorg. Chem.*, 1974, 13, 820.
140. G. A. Burney and J. A. Porter, *Inorg. Nucl. Chem. Lett.*, 1967, 3, 79.
141. J. Besson and H. D. Hardt, *Z. Anorg. Allg. Chem.*, 1954, 277, 188.
142. G. M. Kurdyumov and K. N. Semenko, *Zh. Neorg. Khim.*, 1962, 7, 1512.
143. A. I. Grigorev, A. V. Novaselova and E. G. Pogodilova, *Zh. Neorg. Khim.*, 1965, 10, 772.
144. A. I. Grigorev and A. V. Novaselova, *Dokl. Akad. Nauk., Chem. Sect.*, 1966, 167, 342.
145. A. I. Grigorev, E. G. Pogodilova and V. A. Sipachev, *Zh. Neorg. Khim.*, 1970, 15, 1757.
146. R. C. Mehrotra and A. K. Rai, *Polyhedron*, 1991, 10, 1967.
147. G. M. Tanner, D. C. Tuck and E. G. Wells, *Can. J. Chem.*, 1974, 52, 3950.
148. N. W. Alcock and R. E. Timms, *J. Chem. Soc. A*, 1968, 1873.
149. J. D. Donaldson, J. F. Khifton and S. D. Ross, *Spectrochim. Acta*, 1965, 21, 1043.
150. C. D. Garner and B. Hughes, *Adv. in Inorg. Chem. and Radiochem.*, 1975, 17, 1.
151. R. S. P. Coutts, R. L. Martin and P. C. Wailes, *Aust. J. Chem.*, 1973, 26, 941.
152. G. G. Aleksandrov, V. T. Kallinnikov, N. E. Kolobova, G. M. Larin, A. A. Pasnskii and Yu. T. Struchkov, *Z. Strukt. Khim.*, 1972, 13, 880.
153. K. Anzenhofer and J. J. de Boer, *Rec. Trav. Chim. Pays.-Bas*, 1969, 88, 286.
154. M. B. Hursthouse, D. B. New, C. E. Pellatt and P. Thornton, unpublished results.
155. S. C. Chang and G. A. Jeffrey, *Acta Cryst.*, 1970, B26, 673.
156. C. Calvo, N. C. Jayadevan and C. J. L. Lock, *Can. J. Chem.*, 1969, 47, 4213.
157. F. A. Cotton, C. Oldham and R. A. Walton, *Inorg. Chem.*, 1967, 6, 214.
158. A. S. Ancyskina, *Acta Cryst.*, 1966, A21, 135.
159. J. Catterick, M. B. Hursthouse, P. Thornton and A. J. Welch, *J. Chem. Soc. Dalton Trans.*, 1977, 223.
160. H. Koyama and Y. Saito, *Bull. Chem. Soc. Japan*, 1954, 27, 113.
161. A. A. Eliseev, O. M. Ivanova and A. K. Molodkin, *Russ. J. Inorg. Chem.*, 1967, 12, 1507.
162. A. Bezjek, D. Grdenic and I. Jelenic, *Acta Cryst.*, 1964, 17, 758.
163. K. W. Bagnall and O. V. Lopez, *J. Chem. Soc. Dalton Trans.*, 1976, 1109.
164. A. Muller, *Z. Anorg. Allg. Chem.*, 1920, 109, 235.

165. *Ullmann's Encyclopedia of Industrial Chemistry*, Vol. A5, p.235.
166. P. M. Maitlis, *The Organic Chemistry of Palladium*, Vol. II, Academic Press, New York and London, 1971.
167. R. C. Poller., *The Chemistry of Organotin Compounds*, Logos Press, Great Britain, 1970.
168. R. D. Gorsich, *U.S. Patent*, 1974, 3, 824, 187; *Chem. Abstr.*, 1974, 81, 917302.
169. E. J. Bulten, *Ger. Offern.*, 1978, 2, 801, 700; *Chem Abstr.*, 1978, 89, 180157a.
170. Rhone-Poulenc Chemicals Ltd., personal communication.
171. R. M. Dessau and E. I. Heiba, *J. Am. Chem. Soc.*, 1971, 93, 995.
172. J. K. M. Sanders and D. H. Williams, *J. Chem. Soc. Chem. Commun.*, 1970, 422.
173. T. Imamoto, *Lanthanides in Organic Synthesis*, Academic press, London, 1994.
174. T. Sugiyama, *Chem. Lett.*, 1987, 1013.
175. C. C. Hinckley, *J. Am. Chem. Soc.*, 1969, 91, 5160.
176. J. K. M. Sanders and D. H. Williams, *J. Chem. Soc. Chem. Commun.*, 1970, 428.
177. R. E. Rondeau and R. E. Sievers, *Anal. Chem.*, 1973, 45, 2145.
178. C. A. Burgett and P. Warner, *J. Magn. Resonance*, 1972, 8, 87.
179. A. Lempicki and H. Samelson, *Phys. Lett.*, 1963, 2, 152.
180. S. J. Weissman, *J. Chem. Phys.*, 1942, 10, 214.
181. I. Kraitzer, K. McTaggart and G. Winter, *J. Oil and Colour Chemists Assocn.*, 1948, 31, 405.
182. D. R. Caramody and R. J. Speer, *Ind. Eng. Chem.*, 1950, 42, 251.
183. H. W. Chatfield, *Paint Manuf.*, 1950, 20, 5.
184. W. Grimme and F. Josten, *Germ. Patent*, 1950, 801,154.
185. D. C. Bradley, A. K. Chatterjee and W. Wardlaw, *J. Chem. Soc.*, 1956, 2260.
186. D. C. Bradley, M. A. Saad and W. Wardlaw, *J. Chem. Soc.*, 1954, 3488.
187. S. Dubey, M. Hasan, K. Kumar and S. N. Misra, *Bull. Chem. Soc. Japan*, 1958, 41, 2619.
188. M. F. Richardson, D. E. Sands and W. F. Wagner, *J. Inorg. Nucl. Chem.*, 1968, 30, 1275.
189. D. Grdenic and B. Matkovic, *Acta Cryst.*, 1963, 16, 456.
190. H. Titze, *Acta Chem. Scand.*, 1969, 23, 399.
191. S. R. Drake, A. Lyons, D. J. Otway and D. J. Williams, *Inorg. Chem.*, 1994, 6, 1230.
192. I. Baxter, S. R. Drake, M. B. Hursthouse, A. Lyons, K. M. A. Malik, D. J.

Otway and J. C. Plakatouras, *Inorg. Chem.*, submitted for publication.

193. G. P. Kuznetsova, G. V. Nadezhdina,V. E. Plyushchev, L. P. Shklover and L. M. Shkolnikova, *Dokl. Akad. Nauk. SSSR*, 1965, 160, 366.
194. C. James and J. E. Robinson, *J. Am. Chem. Soc.*, 1913, 35, 754.
195. G. P. Kuznetsova, V. E. Plyushchev, P. Shklorev and T. Trushina, *Zh. Neorgan. Khim.*, 1965, 10, 1121.
196. A. S. Antsyshkina, I. V. Arkangelskii, L. Butman and M. A. Porai-Koshits, *Koord. Khim.*, 1976, 2, 565.
197. N. V. Belov, N. G. Furmanova, L. I. Khapeva and L. V. Soboleva, *Krystallografiya*, 1983, 28, 62.
198. S. K. Gupta, B. L. Kalsotra and R. N. Kapoor, *Transition Metal Chem.*, 1976, 1, 158.
199. E. Spath, *Montash. Chem.*, 1912, 243, 235.
200. L. F. Audrieth and B. S. Hopkins, *Trans. Electrochem. Soc.*, 1934, 66, 139.
201. R. C. Mehrotra, S. N. Misra and T. N. Misra, *J. Indian Chem. Soc.*, 1966, 43, 6.
202. G. A. Kukina, M. A. Porai-Koshits and G. G. Sadikov, *Zh. Strukt. Khim.*, 1967, 8, 551.
203. I. K. Abdulminev, L. A. Aslanov, V. I. Ivanov and M. A. Porai-Koshits, *Dokl. Akad. Nauk. SSSR*, 1972, 205, 343.
204. L. A. Pospelova and T. F. Zaitseva, *Zh. Neorgan. Khim.*, 1965, 10, 1097.
205. V. I. Przemyslaw and S. Starynowiz, *Acta Cryst.*, 1993, C49, 1621.
206. N. E. Hay and J. K. Kochi, *J. Inorg. Nucl. Chem.*, 1968, 30, 884.
207. C. G. Warren, *J. Inorg. Nucl. Chem.*, 1964, 26, 1391.
208. J. E. Roberts, *J. Am. Chem. Soc.*, 1961, 83, 1087.
209. K. V. Rillings and J. E. Roberts, *Thermochem. Acta*, 1974, 10, 285.
210. L. A. Aslanov, V. M. Ionov and I. D. Kiekbaev, *Koord. Khim.*, 1976, 2, 1674.
211. S. P. Bone and D. B. Sowerby, *J. Chem. Soc. Dalton Trans.*, 1978, 1544.
212. J. Legendziewicz and G. Oczko, *Polyhedron*, 1991, 10, 1921.
213. S. S. Krishnamurthy and S. Soundararajan, *J. Less. Common Metals*, 1968, 16, 1.
214. S. N. Misra and M. Singh, *Syn. Reactiv. Inorg. Metal-Org. Chem.*, 1978, 8, 389.
215. A. Ouchi and Y. Sugita, *Bull. Chem. Soc. Japan*, 1987, 60, 171.
216. I. Ya. Evtushenk, Yu. G. Sakharov and N. N. Sakharova, *Zh. Neorgan. Khim.*, 1970, 15, 2602.
217. P. T. Cleeve, *Bull. Chem. Soc. Japan*, 1885, 43, 162.

218. G. V. Nadezhdina, G. L. Loseva and V. E. Plyushchev, *Izv. Vysshik. Uchebn. Zavedenii Khim. Khim. Tekhnol*, 1971, 14, 656.
219. P. A. Brayshaw, J. C. G. Bunzli, P. Froidevaux, J. M. Harrowfield, Y. Kim and A. N. Sobolev, *Inorg. Chem.*, 1995, 34, 2068.
220. A. Rimsky and P. S. Voliotis, *Acta Cryst.*, 1975, B31, 2607, 2612, 2615, 2620.
221. R. O. C. Norman, C. B. Thomas and P. J. Ward, *J. Chem. Soc. Perkin 1*, 1973, 2914.
222. European Patent Appl. Rhone-Poulenc Chemicals, Ltd.
223. Hellenic Vehicle Industry and Rhone-Poulenc Chemicals, Ltd., company report. See also T. Patel, *New Scientist*, 22nd April 1995.
224. C. David, C. Magnier and B. Latourrette, *French. Patent, FR 2608583.*
225. E. Vasiliou and W. Van Hoeven Jr., *US Patent, US 4145325.*
226. Y. Koda, Y. Koda and S. Sasaki, *US Patent, US 388490*
227. P. Gradeff and V. J. Charte, *Eur. Patent, EP 93627.*
228. H. J. Bernstein and K. Ito, *Can. J. Chem.*, 1956, 34, 170.
229. T. C. Downie, W. Harrison, M. A. Hepworth and E. S. Raper, *Acta. Cryst.*, 1971, B26, 706.
230. V. B. Kartha and T. S. Sugandhi, *Indian. J. Phys.*, 1976, 50, 115.
231. M. Becker and J. R. Ferraro, *J. Inorg. Nucl. Chem.*, 1970, 32, 1495.
232. See for example ; D. G. Karraker, *J. Inorg. Nucl. Chem.*, 1969, 31, 2815. E. Spinner, *J. Chem. Soc.*, 1964, 4217. J. TH. M. de Hosson, *J. Inorg. Nucl. Chem.*, 1975, 37, 2350.
233. D. A. Edwards and R. N. Howard, *Can. J. Chem.*, 1968, 46, 3443.
234. K. C. Lin and R. L. Reddington, *Spectrochim. Acta*, 1971, 27A, 2445.
235. C. N. R. Rao and F. Vratny, *Anal. Chem. Acta*, 1961, 33, 1455.
236. J. Catterick and P. Thornton, *Adv. in Inorg. Chem. and Radiochem.*, 1977, 20, 291.
237. W. L. Mead, W. K. Reid and H. B. Silver, *J. Chem. Soc. Chem. Commun.*, 1968, 573.
238. J. Charalambous, R. G. Copperthwaite, S. W. Jeffs and D. E. Shaw, *Inorg. Chim. Acta*, 1975, 14, 53.
239. F. Ribot, C. Sanchez and P. Toledano, *C. R. Acad. Sci. Paris. Ser II*, 1990, 311, 1315.
240. A. Clearfield and P. A. Vaughan, *Acta Cryst.*, 1956, 9, 555.
241. G. Lungnan, *Recl. Trav. Chem. Pays-Bas*, 1956, 75, 585.
242. J. A. Darr, J. McAleese and J. C. Plakatouras, Unpublished results.

243. 'Rare Earth Elements', *Gmelin Handbook*, 1981, D3, 85, 180, 207, 210, 217 and 232.
244. R. G. Charles, *J. Inorg. Nucl. Chem.*, 1964, 26, 2195.
245. V. Janardhanarao and A. P. B. Sinha, *Indian J. Chem.*, 1966, 4, 196.
246. J. C. Daran, L. G. Hubert-Pfalzgraf and O. Poncelet, *Polyhedron*, 1990, 9, 1305.
247. M. March, *Advanced Organic Chemistry : reactions, mechanisms and structure*, 2nd edition McGraw-Hill. New York (1977).
248. L. G. Hubert-Pfalzgraf and O. Poncelet, *Polyhedron*, 1989, 8, 2183.
249. See for example ; I. Ya. Evtushenko, L. F. Firsova, N. N. Sakharova and Yu. G. Sakharova, *Z. Neorg. Khim.*, 1973, 18, 656. T. I. Bogoduklova, O.G. Popotova and Yu. G. Sakharova, *Z. Neorg. Khim.*, 1978, 48, 2543. T. I. Bogoduklova, V. I. Loginov, N. N. Sakharova and Yu. G. Sakharova, *Z. Neorg. Khim.*, 1977 22, 100. T. I. Bogoduklova, N. N. Sakharova and Yu. G.Sakharova, *Zh. Obshch. Khim.*, 1978, 23, 2341. I. Ya. Evtushenko, *Z. Neorg. Khim.*, 1978, 23, 2953. V. I. Loginov, *Z. Neorg. Khim.*, 1978, 23, 2341. T. I. Bogoduhkova, V. I. Loginov and Yu. G. Sakharova, *Zh. Obshch. Khim.*, 1979, 49, 1590.
250. N. V. Belov, V. V. Ilyukin, V. I. Kusov, L. V. Soboleva and E. N. Treushnikov, *Dokl. Akad. Nauk SSSR*, 1978, 239, 594.
251. V. V. Bakakin, N. V. Podberezskaya and G. V. Romanenko, *Dokl. Akad. Nauk SSSR*, 1979, 248, 1337.
252. N. G. Furmanova, A. I. Gusev, N. I. Kirillova and L. V. Soboleva, *Kristallografiya*, 1983, 28, 886.
253. F. A. Hart and F. P. Laming, *J. Inorg. Nucl. Chem.*, 1965, 27, 1605.
254. R. C. Holz and L. C. Thompson, *Inorg. Chem.*, 1993, 32, 3231.
255. E. Butter and S. P. Sinha, *Mol. Phys.*, 1969, 16, 285.
256. S. Choi and M. Kleinerman, *J. Chem Phys.*, 1968, 49, 3901.
257. F. A. Hart and F. P. Laming, *J. Inorg. Nucl. Chem.*, 1965, 27, 1825.
258. A. De Cian, J. Fischer, M. Moussavi and R. Weiss, *Inorg. Chem.* 1985, 24, 3162.
259. I. S. Kirin and P. N. Moskalev, *Zh. Neorg. Khim.*, 1971, 16, 110.
260. See for example ; J. H. Saunders and R. J. Slocombe, *Chem Rev.*, 1948, 203. E. Pinner, *Plastics*, London, 1947, 11, 206.
261. J. R Bailey and A. T. McPherson, *J. Am. Chem. Soc.*, 1917, 39, 1322.
262. W. Frentzel, *Ber.*, 1888, 21, 411.

263. L. C. Raiford and H. B. Freyermuth, *J. Org. Chem.*, 1943, 8, 230.
264. B.I.O.S. Final Report No. 719, Interview with Professor Otto Bayer.
265. A. W. Hofmann, *Ber.*, 1870, 3, 765.
266. A. W. Hofmann, *Jahrb. Fortschritte Chem.*, 1862, 355.
267. A. Michael, *Ber.*, 1905, 38, 22.
268. A. W. Hofmann, *Ber.*, 1885, 18, 765.
269. K. H. Slotta and R. Tschesche, *Ber.*, 1927, 60, 295.
270. S. N. Misra and M. Singh, *J. Indian Chem. Soc.*, 1983, 60, 115.
271. G. H. Cady and R. Hara, *J. Am. Chem. Soc.*, 1954, 76, 4285.
272. S. N. Misra, M. Singh and R. D. Verma, *J. Inorg. Nucl. Chem.*, 1978, 40, 1939.
273. D. G. Karraker, *Inorg. Chem.*, 1968, 7, 473.
274. M. L. Muga and G. W. Watt, *J. Inorg. Nucl. Chem.*, 1959, 9, 166.
275. A. Heller, *J. Am. Chem. Soc.*, 1967, 89, 167.
276. F. H. Fry and W. R. Pirie, *J. Chem. Phys.*, 1965, 43, 3761.
277. E. Antonescu and P. Spacu, *Rev. Roumanie Chim.*, 1971, 16, 373.
278. E. Antonescu and P. Spacu, *Rev. Roumanie Chim.*, 1969, 14, 201.
279. E. Antonescu and P. Spacu, *Z. Chem.*, 1967, 7, 163.
280. R. J. Barton, N. Dong, B. E. Robertson and H. Wang, *J. Coord. Chem.*, 1990, 22, 191.
281. J. C. G. Bunzli and G. R. Choppin, *Lanthanide Probes in Life, Chemical and Earth Sciences*, Elsevier Publishing, New York, 1989.
282. P. N. Yocom, *Lanth. and Actin. Chem.*, 1967, 71, 51.
283. F. Hund, *Z. Physik.*, 1925, 33, 855.
284. J. Ziernecke and C. James, *J. Am. Chem. Soc.*, 1926, 48, 2827.
285. *Nature*, 164, 404
286. A. W. Adamson and P. D. Fleischauer, *Concepts of Inorganic Photochemistry*, Wiley, New York, 1975.
287. T. J. Hardwick and E. Robertson, *Can. J. Chem.*, 1951, 29, 818.
288. J. M. Burk, A. Henshall and T. W Martin, *J. Am. Chem. Soc.*, 1966, 88, 1097.
289. O. Horvath and K. L. Stevenson, *Charge Transfer Photochemistry of Coordination Compounds*, VCH Publishers Inc, New York, 1993.
290. J. K. Kochi and R. A. Sheldon, *J. Am. Chem. Soc.*, 1968, 90, 6688.
291. D. Greatorex and T. J. Kemp, *J. Chem. Soc. Chem. Commun.*, 1969, 383.
292. K. G. Caulton, N. Edelstein, P. S. Gradeff, W. Kot, G. Shalimoff, W. E. Streib, B. A. Vaartstra and K. Yunlu, *Inorg. Chem.*, 1991, 30, 2317.
293. M. Noel and K. I. Vasu, *Cyclic Voltammetry and the Frontiers of*

Electrochemistry, Aspect Publications Ltd., London, 1990.

294. P. A. Christiansen and A. Hamnett, *Techniques and Mechanisms in Electrochemistry*, Blackie Academic and Professional Press, Glasgow, 1994.
295. D. Pletcher, *A First Course in Electrochemistry*, Alresford Press, England, 1991.
296. D. H. Evans, K. M. O'Connel, R. A. Petersen and M. J. Kelly, *J. Chem. Ed.*, 1983, 60, 290.
297. P. T. Kissinger and W. R. Heineman, *J. Chem. Ed.*, 1983, 60, 702.
298. C. J. Edwards and W. P. Griffith, *J. Chem. Soc. Chem. Commun.*, 1990, 1523.
299. C. G. Melloche, *J. Am. Chem. Soc.*, 1915, 37, 2339, 2645.
300. J. C. Barnes and C. S. Blyth, *Inorg. Chim. Acta.*, 1985, 110, 133.
301. J. C. Barnes, C. S. Blyth, and D. Knowles, *Inorg. Chim. Acta.*, 1987, 126, L3.
302. L. A. Butman, M. A. Porai-Koshits and V. I. Sokol, *Sov. J. Coord. Chem.*, 1976, 12, 265.
303. R. E. Marsh and W P. Schaefer, *Acta. Cryst.*, 1968, B24, 246.
304. R. E. Marsh and W P. Schaefer, *Acta. Cryst.*, 1966, 21, 735.
305. J. C. Barnes, C. S. Blyth, J. D. Paton and G. B. Smith, *Lanth. and Actin. Res.*, 1990, 3, 181
306. N. N. Sakharova and Yu. G. Sakharova, *Zh. Neorgan. Khim.*, 1967, 12, 1007.

APPENDICES

Appendix 1 : Determination of Ce(IV) in cerium carboxylates :

N.B. This method calculates the total lanthanide percentage in the sample, and as such may be used for all lanthanides. It can not be used to differentiate between different oxidation states of lanthanide elements, e.g. Ce(IV) and Ce(III).

Materials:

HCl solution - 0.1M in propan-2-ol

Complexing solution - Diaminocyclohexane tetraethanoic acid (18.22g) and 50% NaOH (*ca.* 5-8 mL) in 1 L water.

Indicator solution - Xylenol orange (0.1g dissolved in 50 mL 0.1M aqueous NaOH solution)

Buffer solution - Hexamethylene tetramine (800g), NaCl (400g) and conc. HCL (280 mL) are made up to 4 L with water.

Zinc solution - Zinc (*ca.* 3.3g) metal is accurately weighed and dissolved in conc. HCl (20 mL), the solution is diluted to 1 L with water. Zinc factor = actual weight zinc / 3.2685.

Procedure:

About 0.1 - 0.5g of sample (W) is accurately weighed to a 250 mL conical flask. HCl (10 mL) is added and the solution is boiled briefly. Water (10 mL) is added and the solution is briefly reboiled, this should result in a clear solution. 50 mL of complexing solution is added and the solution boiled for 5 mins.. In order that a sharp end point may be given, all alcohol should be boiled off. The solution is cooled and 100 mL of buffer solution and 1 mL of indicator is added. The solution is then titrated with standard zinc solution, until it turns a permanent purple colour.

Calculation:

$$\% \text{ Rare Earth} = (B - T) \times \text{zinc factor} \times F / W$$

(where F = 0.7006 for Ce, and B = blank titre)

Appendix 2 : Ce(III) carboxylate in Ce(IV) carboxylate matrix titration :

$(RCO_2)_3Ce + 3\,HCl$ ----------> $3\,RCO_2H + Ce^{3+} + 3\,Cl$

(bold type indicates species in organic phase)

The Ce(IV) carboxylate remains in the organic phase while the Ce(III), with the addition of a low HCl concentration, is quickly transferred to the aqueous phase. The variation of aqueous phase pH is plotted against volume of HCl added. The point of inflexion corresponds to three times the Ce(III) content.

Procedure:

About 1g of sample (e) is accurately weighed into a 50 mL beaker and dissolved in 5 mL toluene (or other organic solvent). Water (35 mL) is added and the solution stirred. HCl (0.1 M solution) is added in 0.1mL portions and the pH noted for each addition. This is continued until the pH reaches 2. A graph of pH against volume of HCl added may then be plotted.

Calculation:

V is the volume (mL) corresponding to the point of inflexion

X is the Ce (iii) content (in mol/kg)

T is the %(w/w) ratio of Ce (iii) in raw material.

$$X = V \times 0.1 / e \times 3$$

$$T\,\% = X \times 140.12 \times 100 / 1000 = X \times 14.$$

Appendix 3 : Crystallographic collection data and tables of all bond lengths and angles for complexes (1) - (3), (5) - (9), (11), (13) - (16), (22), and (27) not within the text.

Crystal data and details of data collection and refinement for $[Ba(C_{11}H_{19}O_2)_2(C_{10}H_{22}O_5)]$ (1)

Formula	$[Ba(C_{11}H_{19}O_2)_2(C_{10}H_{22}O_5)]$
M.W.	726.15
Crystal system	Triclinic
a/Å	10.596(5)
b/Å	14.620(2)
c/Å	15.455(2)
α/°	115.38(1)
β/°	97.82(1)
γ/°	105.13(2)
V/Å^3	1974.59
θ range for cell/°	2.6-25
Space group	$P\bar{1}$
z	2
D_c/gcm^{-3}	1.221
$F(000)$	768
μ(Mo Kα)/cm^{-1}	10.4
T/K	298
Crystal size/mm^3	0.30x0.18x0.15
θ range for data/°	2.1-28.7
h_{min}, h_{max}	-9,11
k_{min}, k_{max}	-14,18
l_{min}, l_{max}	-19,16
Total data measured	12524
Total unique	8667
R_{int}	0.0368
Total observed	6105
Significance test	$Fo>3\sigma(Fo)$
Absorption correction factors, min, max	0.781,1.277
No. of parameters	407
ρ_{min}, ρ_{max}/eÅ^{-3}	0.33,0.65
$(\Delta/\sigma)_{max}$	0.036
Weighting scheme	unit weight
R	0.0418
wR	0.0493

Bond lengths (Å) and angles (deg.) for $[Ba(C_{11}H_{19}O_2)_2(C_{10}H_{22}O_5)]$ (1)

O(1)-Ba	2.675(8)	O(2)-Ba	2.667(8)
O(3)-Ba	2.723(7)	O(4)-Ba	2.656(7)
O(5)-Ba	2.863(8)	O(6)-Ba	2.895(9)
O(7)-Ba	2.959(9)	O(8)-Ba	2.918(9)
O(9)-Ba	2.872(9)		
O(2)-Ba-O(1)	64.3(2)	O(3)-Ba-O(1)	139.8(1)
O(3)-Ba-O(2)	153.7(1)	O(4)-Ba-O(1)	142.9(2)
O(4)-Ba-O(2)	89.9(2)	O(4)-Ba-O(3)	64.3(2)
O(5)-Ba-O(1)	116.4(3)	O(5)-Ba-O(2)	70.3(3)
O(5)-Ba-O(3)	97.5(3)	O(5)-Ba-O(4)	75.7(3)
O(6)-Ba-O(1)	83.8(3)	O(6)-Ba-O(2)	93.4(3)
O(6)-Ba-O(3)	99.0(3)	O(6)-Ba-O(4)	127.5(3)
O(6)-Ba-O(5)	56.8(3)	O(7)-Ba-O(1)	72.3(3)
O(7)-Ba-O(2)	129.6(3)	O(7)-Ba-O(3)	76.1(3)
O(7)-Ba-O(4)	140.4(2)	O(7)-Ba-O(5)	110.6(3)
O(7)-Ba-O(6)	56.5(3)	O(8)-Ba-O(1)	73.4(3)
O(8)-Ba-O(2)	127.0(3)	O(8)-Ba-O(3)	68.6(3)
O(8)-Ba-O(4)	106.3(3)	O(8)-Ba-O(5)	162.1(2)
O(8)-Ba-O(6)	112.7(3)	O(8)-Ba-O(7)	56.3(3)
O(9)-Ba-O(1)	76.4(3)	O(9)-Ba-O(2)	81.2(3)
O(9)-Ba-O(3)	94.0(3)	O(9)-Ba-O(4)	72.1(3)
O(9)-Ba-O(5)	136.6(2)	O(9)-Ba-O(6)	159.9(2)
O(9)-Ba-O(7)	112.8(3)	O(9)-Ba-O(8)	58.3(3)
C(1)-O(1)-Ba	139.0(4)	C(3)-O(2)-Ba	139.7(4)
C(6)-O(3)-Ba	133.8(4)	C(8)-O(4)-Ba	134.5(4)
C(11)-O(5)-Ba	120.8(6)	C(12)-O(5)-Ba	116.9(6)
C(13)-O(6)-Ba	117.9(7)	C(14)-O(6)-Ba	118.5(7)
C(15)-O(7)-Ba	116.0(8)	C(16)-O(7)-Ba	116.8(8)
C(17)-O(8)-Ba	119.2(8)	C(18)-O(8)-Ba	115.3(7)
C(19)-O(9)-Ba	115.9(8)	C(20)-O(9)-Ba	119.8(7)
C(1)-O(1)	1.225(9)	C(3)-O(2)	1.229(8)
C(6)-O(3)	1.244(8)	C(8)-O(4)	1.243(8)
C(2)-C(1)	1.404(10)	C(4)-C(1)	1.548(12)
C(3)-C(2)	1.390(10)	C(5)-C(3)	1.546(11)
C(41) C(4)	1.437(14)	C(42)-C(4)	1.477(14)
C(43)-C(4)	1.440(16)	C(51)-C(5)	1.528(14)
C(52)-C(5)	1.472(13)	C(53)-C(5)	1.527(14)
C(7)-C(6)	1.409(10)	C(9)-C(6)	1.548(10)
C(8)-C(7)	1.407(9)	C(10)-C(8)	1.559(11)
C(91)-C(9)	1.505(12)	C(92)-C(9)	1.509(12)
C(93)-C(9)	1.546(13)	C(101)-C(10)	1.533(17)
C(102)-C(10)	1.537(20)	C(103)-C(10)	1.547(20)
C(104)-C(10)	1.562(21)	C(105)-C(10)	1.504(20)
C(106)-C(10)	1.568(25)	C(11)-O(5)	1.420(10)
C(12)-O(5)	1.380(10)	C(13)-O(6)	1.340(13)
C(14)-O(6)	1.408(12)	C(15)-O(7)	1.274(14)
C(16)-O(7)	1.350(13)	C(17)-O(8)	1.332(12)
C(18)-O(8)	1.354(13)	C(19)-O(9)	1.377(13)
C(20)-O(9)	1.392(12)	C(13)-C(12)	1.357(15)
C(15) C(14)	1.305(16)	C(17)-C(16)	1.299(17)
C(19)-C(18)	1.306(16)		
C(2) C(1)-O(1)	126.0(8)	C(4)-C(1)-O(1)	116.4(7)
C(4)-C(1)-C(2)	117.6(8)	C(3)-C(2)-C(1)	125.3(8)
C(2)-C(3)-O(2)	125.6(7)	C(5)-C(3)-O(2)	114.5(7)
C(5)-C(3)-C(2)	119.9(7)	C(41)-C(4)-C(1)	116.4(8)
C(42)-C(4)-C(1)	110.2(8)	C(42) C(4)-C(41)	108.2(12)
C(43) C(4)-C(1)	107.3(10)	C(43)-C(4)-C(41)	110.2(11)
C(43)-C(4)-C(42)	103.9(11)	C(51)-C(5)-C(3)	109.2(8)
C(52)-C(5)-C(3)	108.3(8)	C(52)-C(5)-C(51)	109.1(10)
C(53)-C(5)-C(3)	113.9(8)	C(53)-C(5)-C(51)	105.6(9)
C(53)-C(5)-C(52)	110.6(11)	C(7)-C(6)-O(3)	125.5(7)
C(9)-C(6)-O(3)	116.7(7)	C(9)-C(6)-C(7)	117.8(7)
C(8) C(7)-C(6)	125.5(7)	C(7)-C(8)-O(4)	125.2(7)
C(10)-C(8)-O(4)	116.1(7)	C(10)-C(8)-C(7)	118.7(7)
C(91) C(9) C(6)	113.6(7)	C(92)-C(9)-C(6)	110.2(7)
C(92) C(9) C(91)	109.5(9)	C(93)-C(9)-C(6)	105.2(7)
C(93)-C(9)-C(91)	109.4(8)	C(93)-C(9)-C(92)	108.9(9)
C(101)-C(10)-C(8)	108.4(9)	C(102)-C(10)-C(8)	111.1(9)
C(102) C(10) C(101)	110.7(12)	C(103)-C(10)-C(8)	104.9(9)
C(103)-C(10) C(101)	107.1(13)	C(103)-C(10)-C(102)	114.3(12)
C(104) C(10)-C(8)	106.2(10)	C(105)-C(10)-C(8)	116.1(10)
C(105)-C(10)-C(104)	114.1(15)	C(106)-C(10)-C(8)	107.9(11)
C(106) C(10) C(104)	96.9(14)	C(106)-C(10)-C(105)	113.9(15)
C(12)-O(5)-C(11)	115.6(8)	C(14)-O(6)-C(13)	123.4(9)
C(16)-O(7)-C(15)	126.2(10)	C(18)-O(8)-C(17)	124.5(10)
C(20)-O(9)-C(19)	113.3(11)	C(13)-C(12)-O(5)	117.1(9)
C(12) C(13) O(6)	122.1(11)	C(15)-C(14)-O(6)	118.6(11)
C(14)-C(15) O(7)	127.7(13)	C(17)-C(16)-O(7)	122.6(12)
C(16)-C(17)-O(8)	122.8(11)	C(19)-C(18)-O(8)	124.5(11)
C(18)-C(19)-O(9)	121.6(12)		

formula	$C_{28}H_{56}BaO_8$
mol wt	682.1
color and habit	clear blocks
cryst size/mm	0.12 × 0.23 × 0.4)
cryst syst	monoclinic
a/Å	10.668(2)
b/Å	23.614(4)
c/Å	15.630(3)
α/deg	
β/deg	109.11(2)
γ/deg	
V/Å^3	3725.8(14)
space group	$P2_1/c$
Z	4
D_{calc} (g cm^{-3})	1.216
λ/Å	0.71073 (Moα)
μ/cm^{-1}	11.1
F(000)	1424
transm factors max., min	
no. of unique data	6561
no. of obsd data with $F > 4\sigma(F)$	3926
scan type	ω
2θ range/deg	4–50
final $\Delta\rho$/(e Å^{-3})	1.12
final Δ/σ	0.000
$R = \sum w(F_o - F_c)^2$	5.02
R_w	4.71[a]
temp/K	293

[a] The form of the weighting function is $w^{-1} = \sigma^2(F) + 0.0005F^2$.

Crystal data and details of data collection and refinement for (2)
Bond lengths and angles for [Ba(tmhd)$_2$(triglyme)] (2)

Ba-O(2)	2.854(9)	Ba-O(5)	2.814(6)	C(13)-C(14)	1.543(11)	C(14)-O(14)	1.342(9)
Ba-O(8)	2.809(5)	Ba-O(11)	2.900(6)	C(14)-C(15)	1.395(10)	C(15)-C(16)	1.412(10)
Ba-O(14)	2.634(5)	Ba-O(16)	2.621(5)	C(16)-O(16)	1.343(9)	C(16)-C(17)	1.534(10)
Ba-O(19)	2.622(5)	Ba-O(21)	2.643(5)	C(17)-C(171)	1.525(14)	C(17)-C(172)	1.515(13)
C(1)-O(2)	1.264(13)	C(2)-C(3)	1.325(15)	C(17)-C(173)	1.522(15)	C(18)-C(181)	1.444(18)
C(3)-C(4)	1.402(15)	C(4)-O(5)	1.426(14)	C(18)-C(182)	1.495(15)	C(18)-C(183)	1.490(16)
O(5)-C(6)	1.432(10)	C(6)-C(7)	1.495(15)	C(18)-O(19)	1.532(11)	C(19)-O(19)	1.256(9)
C(7)-O(8)	1.421(12)	O(8)-C(9)	1.422(12)	C(19)-C(20)	1.383(11)	C(20)-C(21)	1.378(10)
C(9)-C(10)	1.478(14)	C(10)-O(11)	1.404(10)	C(21)-O(21)	1.257(8)	C(21)-C(22)	1.534(11)
O(11)-C(12)	1.418(11)	C(11)-C(131)	1.483(16)	C(222)-C(221)	1.548(17)	C(222)-C(222)	1.463(13)
C(13)-C(132)	1.513(16)	C(13)-C(133)	1.490(13)	C(222)-C(223)	1.509(12)		

O(2)-Ba-O(5)	56.8(2)	O(2)-Ba-O(8)	109.8(2)	Ba-O(11)-C(12)	118.5(5)	C(10)-O(11)-C(12)	111.8(6)
O(5)-Ba-O(8)	58.0(2)	O(2)-Ba-O(11)	144.7(2)	C(131)-C(13)-C(132)	108.0(9)	C(131)-C(13)-C(133)	108.8(12)
O(5)-Ba-O(11)	114.7(2)	O(8)-Ba-O(11)	57.8(2)	C(132)-C(13)-C(133)	108.0(10)	C(131)-C(13)-C(14)	108.3(9)
O(2)-Ba-O(14)	75.2(2)	O(5)-Ba-O(14)	97.3(2)	C(132)-C(13)-C(14)	107.3(8)	C(133)-C(13)-C(14)	113.2(7)
O(8)-Ba-O(14)	89.9(2)	O(11)-Ba-O(14)	72.1(2)	C(13)-C(14)-O(14)	114.9(6)	C(13)-C(14)-C(15)	120.2(7)
O(2)-Ba-O(16)	94.4(2)	O(5)-Ba-O(16)	150.2(2)	O(14)-C(14)-C(15)	124.8(7)	Ba-O(14)-C(14)	137.8(4)
O(8)-Ba-O(16)	139.2(2)	O(11)-Ba-O(16)	83.8(2)	C(14)-C(15)-C(16)	126.0(7)	C(15)-C(16)-O(16)	123.9(6)
O(14)-Ba-O(16)	65.1(1)	O(2)-Ba-O(19)	76.0(2)	C(15)-C(16)-C(17)	119.8(7)	O(16)-C(16)-C(17)	116.3(6)
O(5)-Ba-O(19)	89.8(2)	O(8)-Ba-O(19)	126.2(2)	Ba-O(16)-C(16)	137.8(5)	O(16)-C(17)-C(171)	114.6(7)
O(11)-Ba-O(19)	139.0(2)	O(14)-Ba-O(19)	139.8(2)	C(16)-C(17)-C(172)	106.6(7)	C(171)-C(17)-C(172)	109.8(8)
O(16)-Ba-O(19)	89.9(2)	O(2)-Ba-O(21)	132.1(2)	C(16)-C(17)-C(173)	108.4(7)	C(171)-C(17)-C(173)	109.1(9)
O(5)-Ba-O(21)	93.8(2)	O(8)-Ba-O(21)	75.4(1)	C(172)-C(17)-C(173)	108.9(8)	C(181)-C(18)-C(182)	108.3(11)
O(11)-Ba-O(21)	79.8(2)	O(14)-Ba-O(21)	151.9(2)	C(181)-C(18)-C(183)	109.8(10)	C(182)-C(18)-C(183)	107.1(8)
O(16)-Ba-O(21)	111.8(2)	O(19)-Ba-O(21)	65.1(2)	C(181)-C(18)-C(19)	109.8(7)	C(182)-C(18)-C(19)	109.6(8)
Ba-O(2)-C(1)	113.9(8)	Ba-O(2)-C(3)	115.3(8)	C(183)-C(18)-C(19)	113.0(8)	C(18)-C(19)-O(19)	115.3(7)
C(1)-O(2)-C(3)	121.6(1)	O(2)-C(3)-C(4)	116.5(12)	C(18)-C(19)-C(20)	120.8(7)	O(19)-C(19)-C(20)	123.9(6)
C(3)-C(4)-O(5)	110.1(10)	Ba-O(5)-C(4)	121.6(5)	Ba-O(19)-C(19)	139.8(5)	C(19)-C(20)-C(21)	128.3(6)
Ba-O(5)-C(6)	121.3(6)	C(4)-O(5)-C(6)	112.8(7)	C(20)-C(21)-O(21)	123.7(7)	C(20)-C(21)-C(22)	120.7(6)
O(5)-C(6)-C(7)	107.8(7)	C(6)-C(7)-O(8)	108.4(7)	O(21)-C(21)-C(22)	115.7(6)	Ba-O(21)-C(21)	139.3(5)
Ba-O(8)-C(7)	108.0(4)	Ba-O(8)-C(9)	108.7(4)	C(21)-C(22)-C(221)	108.6(7)	C(21)-C(22)-C(222)	107.5(8)
C(7)-O(8)-C(9)	114.5(7)	O(8)-C(9)-C(10)	108.4(7)	C(221)-C(22)-C(222)	107.8(9)	C(21)-C(22)-C(223)	114.7(7)
C(9)-C(10)-O(11)	110.1(7)	Ba-O(11)-C(10)	118.8(6)	C(221)-C(22)-C(223)	105.8(9)	C(222)-C(22)-C(223)	112.2(8)

Bond lengths (Å) for [Ba2(thd)4(diglyme)2] (3)

(1) Ba	2.679(6)	(2) Ba	2.578(6)
(3) Ba	2.574(7)	(4) Ba	2.630(6)
(5) Ba	2.888(6)	O(5') Ba'	3.173(6)
(6) Ba	2.819(6)	(7) Ba	2.870(7)
C(2) O(1)	1.247(6)	C(4) O(2)	1.271(6)
C(13) O(3)	1.259(6)	C(15) O(4)	1.263(6)
(23)-O(5)	1.437(9)	C(24) O(5)	1.440(7)
C(25)-O(6)	1.425(7)	C(26) O(6)	1.434(9)
C(27) O(7)	1.435(8)	C(28) O(7)	1.410(8)
C(2)-C(1)	1.551(8)	C(6) C(1)	1.530(10)
C(7) C(1)	1.521(8)	C(8) C(1)	1.531(8)
C(3)-C(2)	1.414(7)	C(4) C(3)	1.387(8)
C(5)-C(4)	1.555(7)	C(9) C(5)	1.533(9)
C(10)-C(5)	1.523(11)	C(11)-C(5)	1.526(10)
C(13)-C(12)	1.545(9)	C(17) C(12)	1.516(10)
C(18)-C(12)	1.532(10)	C(19) C(12)	1.520(9)
C(14)-C(13)	1.404(7)	C(15)-C(14)	1.414(8)
C(16)-C(15)	1.544(8)	C(20) C(16)	1.517(9)
C(21) C(16)	1.521(10)	C(22) C(16)	1.534(8)
C(25)-C(24)	1.496(10)	C(27)-C(26)	1.500(10)

* The primed atom belongs to one and the same dimer and related to the unprimed one by the symmetry (-x, 1-y, -z).

Bond angles (deg) for [Ba2(thd)4(diglyme)2] (3)

O(2)-Ba-O(1)	66.2(2)	O(3)-Ba O(1)	86.2(2)
O(3)-Ba-O(2)	103.4(2)	O(4)-Ba-O(1)	141.3(1)
O(4)-Ba-O(2)	92.2(2)	O(4) Ba O(3)	66.9(2)
O(5)-Ba-O(1)	74.9(2)	O(5) Ba O(2)	138.4(1)
O(5)-Ba-O(3)	87.5(2)	O(5) Ba O(4)	128.4(2)
O(5')-Ba-O(1)*	138.0(2)	O(5') Ba O(2)	155.8(2)
O(5') Ba-O(3)	82.2(2)	O(5') Ba O(4)	68.1(2)
O(5')-Ba-O(5)	64.4(2)	O(6) Ba O(1)	78.1(2)
O(6) Ba-O(2)	97.6(2)	O(6) Ba O(3)	146.9(1)
O(6) Ba-O(4)	139.1(1)	O(6) Ba O(5)	74.4(2)
O(6) Ba O(5')	89.4(2)	O(7) Ba O(1)	76.8(2)
O(7) Ba-O(2)	76.0(2)	O(7) Ba O(3)	152.9(1)
O(7) Ba O(4)	86.1(2)	O(7) Ba O(5)	71.2(2)
O(7) Ba O(5')	88.4(2)	O(7) Ba O(6)	68.5(2)

Bond angles for (3)

Ba [5] Ba	115.6(3)	C(2) O(1) Ba	129.2(4)
C(4) O(2) Ba	126.0(4)	C(13) O(3) Ba	131.9(3)
C(15) C(4) Ba	134.4(3)	C(23) O(5) Ba	107.3(3)
C(24) O(5) Ba	107.7(3)	C(24) O(5) C(23)	110.3(5)
C(25) O(6) Ba	119.5(4)	C(26) O(6) Ba	120.5(4)
C(26) O(6) C(5)	113.2(5)	C(27) O(7) Ba	109.1(4)
C(28) O(7) Ba	111.1(5)	C(28) O(7) C(27)	112.4(6)
C(6) C(1) C(2)	109.6(5)	C(7) C(1) C(2)	110.4(4)
C(7) C(1) C(6)	108.7(5)	C(8) C(1) C(2)	110.1(5)
C(8) C(1) C(6)	109.0(5)	C(8) C(1) C(7)	109.0(5)
C(1) C(2) O(1)	117.9(4)	C(3) C(2) O(1)	124.8(5)
C(3) C(2) O(1)	117.3(4)	C(4) C(3) C(2)	120.5(5)
C(3) C(4) O(2)	124.7(5)	C(5) C(4) O(2)	114.4(5)
C(5) C(4) C(3)	120.9(5)	C(9) C(5) C(4)	113.7(5)
C(10) C(5) C(4)	108.5(5)	C(10) C(5) C(9)	109.9(5)
C(11) C(5) C(4)	106.1(4)	C(11) C(5) C(9)	109.2(6)
C(11) C(5) C(10)	109.4(6)	C(17) C(12) C(13)	107.5(5)
C(18) C(12) C(13)	107.1(6)	C(18) C(12) C(17)	108.3(6)
C(19) C(12) C(13)	114.6(5)	C(19) C(12) C(17)	109.4(6)
C(19) C(12) C(18)	109.8(5)	C(12) C(13) O(3)	115.3(5)
C(14) C(13) O(3)	124.8(6)	C(14) C(13) C(12)	119.8(5)
C(15) C(14) C(13)	126.3(5)	C(14) C(15) O(4)	124.6(5)
C(16) C(15) O(4)	115.7(5)	C(16) C(15) C(14)	119.7(5)
C(20) C(16) C(15)	114.6(5)	C(21) C(16) C(15)	108.3(5)
C(21) C(16) C(20)	108.9(5)	C(22) C(16) C(15)	107.6(4)
C(22) C(16) C(20)	108.8(5)	C(22) C(16) C(21)	108.5(6)
C(25) C(24) O(5)	109.5(5)	C(24) C(25) O(6)	109.0(5)
C(27) C(26) O(6)	107.8(5)	C(26) C(27) O(7)	108.4(5)

H(21B) C(21) H(21A)	110.9(71)	H(21C) C(21) C(16)	106.6(61)
H(21C) C(21) H(21A)	117.9(59)	H(21C) C(21) H(21B)	107.1(71)
H(22A) C(22) C(16)	110.2(26)	H(22B) C(22) C(16)	110.7(24)
H(22B) C(22) H(22A)	112.6(43)	H(22C) C(22) C(16)	111.1(44)
H(22C) C(22) H(22A)	106.3(51)	H(22C) C(22) H(22B)	105.8(51)
H(23A) C(23) O(5)	105.0(42)	H(23B) C(23) O(5)	115.2(44)
H(23B) C(23) H(23A)	108.5(49)	H(23C) C(23) O(5)	114.2(38)
H(23C) C(23) H(23A)	105.1(49)	H(23C) C(23) H(23B)	108.1(48)
H(24A) C(24) O(5)	106.4(31)	H(24A) C(24) C(25)	110.8(36)
H(24B) C(24) O(5)	114.1(42)	H(24B) C(24) C(25)	110.1(46)
H(24B) C(24) H(24A)	105.9(46)	H(25A) C(25) O(6)	112.6(30)
H(25A) C(25) C(24)	109.4(35)	H(25B) C(25) O(6)	105.1(33)
H(25B) C(25) C(24)	114.6(42)	H(25B) C(25) H(25A)	105.9(45)
H(26A) C(26) O(6)	105.9(40)	H(26A) C(26) C(27)	108.2(32)
H(26B) C(26) O(6)	109.1(41)	H(26B) C(26) C(27)	107.2(31)
H(26B) C(26) H(26A)	118.3(47)	H(27A) C(27) O(7)	112.2(30)
H(27A) C(27) C(26)	100.5(26)	H(27B) C(27) O(7)	110.9(27)
H(27B) C(27) C(26)	107.4(25)	H(27B) C(27) H(27A)	116.5(41)
H(28A) C(28) O(7)	113.8(45)	H(28B) C(28) O(7)	113.1(44)
H(28B) C(28) H(28A)	100.2(72)	H(28C) C(28) O(7)	106.9(48)
H(28C) C(28) H(28A)	110.5(67)	H(28C) C(28) H(28B)	112.4(76)

Bond lengths (A) and angles (deg) involving the H atoms (3)

H(3) C(3)	0.984(46)	H(6A) C(6)	0.976(55)
H(6B) C(6)	0.983(53)	H(6C) C(6)	0.993(60)
H(7A) C(7)	1.072(58)	H(7B) C(7)	0.965(60)
H(7C) C(7)	0.912(86)	H(8A) C(8)	0.970(63)
H(8B) C(8)	0.949(66)	H(8C) C(8)	0.982(52)
H(9A) C(9)	1.106(55)	H(9B) C(9)	0.946(65)
H(9C) C(9)	0.991(55)	H(10A) C(10)	0.921(46)
H(10B) C(10)	0.877(57)	H(10C) C(10)	1.008(64)
H(11A) C(11)	0.943(74)	H(11B) C(11)	1.008(65)
H(11C) C(11)	0.925(64)	H(14) C(14)	0.889(54)
H(17A) C(17)	0.937(59)	H(17B) C(17)	0.938(88)
H(17C) C(17)	0.947(57)	H(18A) C(18)	1.041(79)
H(18B) C(18)	1.028(64)	H(18C) C(18)	0.979(63)
H(19A) C(19)	0.972(64)	H(19B) C(19)	1.038(58)
H(19C) C(19)	0.982(55)	H(20A) C(20)	1.074(52)
H(20B) C(20)	0.949(73)	H(20C) C(20)	0.991(68)
H(21A) C(21)	0.906(72)	H(21B) C(21)	0.913(85)
H(21C) C(21)	0.881(72)	H(22A) C(22)	1.057(57)
H(22B) C(22)	1.134(53)	H(22C) C(22)	0.900(75)
H(23A) C(23)	0.884(55)	H(23B) C(23)	0.934(52)
H(23C) C(23)	1.041(58)	H(24A) C(24)	1.018(46)
H(24B) C(24)	1.013(65)	H(25A) C(25)	0.974(52)
H(25B) C(25)	0.975(53)	H(26A) C(26)	0.886(54)
H(26B) C(26)	0.983(52)	H(27A) C(27)	1.063(48)
H(27B) C(27)	1.053(62)	H(28A) C(28)	0.982(80)
H(28B) C(28)	0.976(100)	H(28C) C(28)	0.875(70)

H(3) C(3) C(2)	117.3(37)	H(3) C(3) C(4)	115.0(38)
H(6A) C(6) C(1)	114.2(32)	H(6B) C(6) C(1)	118.0(44)
H(6B) C(6) H(6A)	101.5(44)	H(6C) C(6) C(1)	110.8(37)
H(6C) C(6) H(6A)	108.6(49)	H(6C) C(6) H(6B)	102.6(47)
H(7A) C(7) C(1)	108.3(26)	H(7B) C(7) C(1)	104.5(31)
H(7B) C(7) H(7A)	114.6(51)	H(7C) C(7) C(1)	109.8(43)
H(7C) C(7) H(7A)	106.9(56)	H(7C) C(7) H(7B)	112.6(56)
H(8A) C(8) C(1)	107.1(28)	H(8B) C(8) C(1)	107.1(38)
H(8B) C(8) H(8A)	110.0(51)	H(8C) C(8) C(1)	112.9(36)
H(8C) C(8) H(8A)	104.5(52)	H(8C) C(8) H(8B)	115.1(48)
H(9A) C(9) C(5)	111.6(30)	H(9B) C(9) C(5)	113.9(29)
H(9B) C(9) H(9A)	98.5(47)	H(9C) C(9) C(5)	110.0(38)
H(9C) C(9) H(9A)	103.8(43)	H(9C) C(9) H(9B)	117.8(52)
H(10A) C(10) C(5)	111.3(32)	H(10B) C(10) C(5)	111.3(50)
H(10B) C(10) H(10A)	103.6(51)	H(10C) C(10) C(5)	107.6(45)
H(10C) C(10) H(10A)	111.4(48)	H(10C) C(10) H(10B)	111.8(52)
H(11A) C(11) C(5)	112.3(36)	H(11B) C(11) C(5)	112.1(39)
H(11B) C(11) H(11A)	108.0(53)	H(11C) C(11) C(5)	106.3(42)
H(11C) C(11) H(11A)	114.7(61)	H(11C) C(11) H(11B)	103.2(56)
H(14) C(14) C(13)	119.1(39)	H(14) C(14) C(15)	114.6(39)
H(17A) C(17) C(12)	112.6(39)	H(17B) C(17) C(12)	112.7(41)
H(17B) C(17) H(17A)	115.1(66)	H(17C) C(17) C(12)	109.1(38)
H(17C) C(17) H(17A)	112.2(46)	H(17C) C(17) H(17B)	93.6(61)
H(18A) C(18) C(12)	116.1(39)	H(18B) C(18) C(12)	118.1(53)
H(18B) C(18) H(18A)	101.3(55)	H(18C) C(18) C(12)	100.9(36)
H(18C) C(18) H(18A)	110.8(51)	H(18C) C(18) H(18B)	109.7(56)
H(19A) C(19) C(12)	113.9(30)	H(19B) C(19) C(12)	112.1(31)
H(19B) C(19) H(19A)	104.3(51)	H(19C) C(19) C(12)	112.5(36)
H(19C) C(19) H(19A)	103.8(46)	H(19C) C(19) H(19B)	109.7(46)
H(20A) C(20) C(16)	115.8(32)	H(20B) C(20) C(16)	114.1(35)
H(20B) C(20) H(20A)	99.3(48)	H(20C) C(20) C(16)	111.9(44)
H(20C) C(20) H(20A)	105.4(47)	H(20C) C(20) H(20B)	111.5(56)
H(21A) C(21) C(16)	101.8(49)	H(21B) C(21) C(16)	111.3(48)

Crystal data and details of data collection and refinement for $[Sr(C_{11}H_{19}O_2)_2(C_8H_{16}O_4)]$. (5)

Formula	$[Sr(C_{11}H_{19}O_2)_2(C_8H_{16}O_4)]$
M.W.	632.39
Crystal system	Monoclinic
a/Å	11.986(5)
b/Å	19.705(3)
c/Å	15.490(2)
α/°	90
β/°	96.26(2)
γ/°	90
V/Å^3	3636.62
θ range for cell/°	2.5-25
Space group	$P2_1/c$
Z	4
D_c/gcm^{-3}	1.155
F(000)	1352
μ(Mo-Kα)/cm^{-1}	14.7
T/K	298
Crystal size/mm^3	0.42×0.28×0.26
θ range for data/°	2.2-29.6
h_{min}, h_{max}	-15,12
k_{min}, k_{max}	-23,26
l_{min}, l_{max}	-20,13
Total data measured	22439
Total unique	8588
R_{int}	0.054
Total observed	2469
Significance test	Fo>3σ(Fo)
Absorption correction factors, min, max	0.849,1.132
No. of parameters	353
ρ_{min},ρ_{max}/eÅ^{-3}	0.45,0.76
$(\Delta/\sigma)_{max}$	0.054
Weighting scheme	unit weight
R	0.0510
wR	0.0558

Bond lengths (Å) and angles (deg.) for $[Sr(C_{11}H_{19}O_2)_2(C_8H_{16}O_4)]$ (5)

O(1)-Sr	2.501(10)	68.6(3)	O(1)-Sr-O(11)	144.1(2)	C(3)-O(12)	1.269(12)	C(4)-C(11)-O(11)	115.5(10)
O(3)-Sr	2.519(10)	146.9(3)	O(1)-Sr-O(12)	147.4(2)	C(8)-O(14)	1.248(13)	C(3)-C(12)-O(12)	124.7(10)
O(5)-Sr	2.628(10)	79.8(3)	O(1)-Sr-O(13)	68.4(3)	C(12)-O(15)	1.430(15)	C(5)-C(13)-O(12)	115.6(11)
O(7)-Sr	2.703(10)	85.1(3)	O(1)-Sr-O(14)	90.1(4)	C(14)-O(16)	1.429(14)	C(4)-C(14)-C(11)	105.9(10)
O(2)-Sr	2.468(9)	97.2(3)	O(1)-Sr-O(15)	87.2(4)	C(16)-O(17)	1.408(15)	C(4)-C(14)-C(142)	111.6(11)
O(4)-Sr	2.488(9)	74.8(3)	O(1)-Sr-O(16)	135.3(2)	C(18)-O(18)	1.442(14)	C(4)-C(14)-C(141)	107.8(10)
O(6)-Sr	2.715(10)	74.8(3)	O(1)-Sr-O(17)	127.7(3)	C(4) C(1)	1.559(15)	C(11)-C(14)-C(142)	108.2(11)
O(8)-Sr	2.650(10)	61.5(3)	O(1)-Sr-O(18)	73.0(3)	C(5)-C(1)	1.548(15)	C(141)-C(14)-C(142)	113.8(11)
		125.6(4)	O(2)-Sr-O(11)	76.1(3)	C(42)-C(14)	1.547(17)	C(14)-C(142)-C(141)	108.9(15)
		135.9(3)	O(2)-Sr-O(12)	129.6(3)	C(51)-C(15)	1.483(18)	C(14)-C(142)-C(143)	105.8(15)
		62.7(3)	O(2)-Sr-O(13)	95.9(3)	C(53)-C(15)	1.476(18)	C(141)-C(142)-C(143)	122.4(12)
		85.7(3)	O(2)-Sr-O(14)	84.0(3)	C(9)-C(16)	1.541(16)	C(142)-C(143)-C(141)	121.8(12)
		89.4(4)	O(2)-Sr-O(15)	175.0(2)	C(10)-C(18)	1.468(19)		
		123.4(4)	O(2)-Sr-O(16)	61.3(4)	C(101)-C(110)	1.536(17)		
		133.6(3)	O(2)-Sr-O(17)	134.7(3)	C(103)-C(10)	1.528(17)		
		134.1(3)	O(2)-Sr-O(18)	134.2(3)	C(15)-C(14)	1.480(15)		
		119.7(3)	O(4)-Sr-O(11)	119.6(3)				
		112.6(3)	O(4)-Sr-O(12)	112.8(3)	C(3)-O(12)	1.256(12)	C(4)-C(11)-O(11)	124.3(10)
		118.8(3)	O(4)-Sr-O(13)	113.2(3)	C(8)-O(14)	1.265(13)	C(3)-C(12)-O(12)	120.8(11)
		68.6(3)	O(4)-Sr-O(14)	118.8(3)	C(12)-O(15)	1.430(13)	C(5)-C(13)-O(12)	125.4(9)
		146.9(3)	O(4)-Sr-O(15)	68.4(3)	C(14)-O(16)	1.407(14)	C(4)-C(14)-C(11)	108.8(11)
		79.8(3)	O(4)-Sr-O(16)	90.1(4)	C(16)-O(17)	1.414(14)	C(4)-C(14)-C(142)	107.7(10)
		85.1(3)	O(4)-Sr-O(17)	87.2(4)	C(18)-O(18)	1.408(15)	C(4)-C(14)-C(141)	114.2(10)
		97.2(3)	O(4)-Sr-O(18)	135.3(2)	C(4) C(1)	1.411(14)	C(11)-C(14)-C(142)	109.7(11)
		74.8(3)	O(6)-Sr-O(11)	127.7(3)	C(5)-C(1)	1.394(14)	C(141)-C(14)-C(142)	108.9(12)
		74.8(3)	O(6)-Sr-O(12)	73.0(3)	C(42)-C(14)	1.552(16)	C(53)-C(15)-C(52)	110 8(12)
		61.5(4)	O(6)-Sr-O(13)	76.1(3)	C(51)-C(15)	1.531(16)	C(7)-C(16)-O(13)	109.8(12)
		125.6(4)	O(6)-Sr-O(14)	129.6(4)	C(53)-C(15)	1.452(18)	C(9)-C(16)-C(7)	115.8(10)
		135.9(3)	O(6)-Sr-O(15)	95.9(3)	C(9)-C(16)	1.397(14)		
		62.7(3)	O(6)-Sr-O(16)	84.0(3)	C(10)-C(18)	1.364(14)	C(7)-C(18)-O(14)	123.2(13)
		85.7(3)	O(6)-Sr-O(17)	175.0(2)	C(92)-C(9)	1.529(16)	C(10)-C(18)-C(7)	111.0(11)
		89.4(4)	O(6)-Sr-O(18)	61.3(4)	C(101)-C(110)	1.503(17)	C(92)-C(9)-C(16)	115.5(10)
		123.4(4)	O(8)-Sr-O(11)	134.7(3)	C(103)-C(10)	1.501(17)	C(101)-C(110)-C(102)	106.7(10)
		133.6(3)	O(8)-Sr-O(12)	134.2(3)	C(15)-C(14)	1.482(18)	C(103)-C(10)-C(18)	109.7(12)
		134.1(3)	O(8)-Sr-O(13)	119.6(3)			C(102)-C(101)-C(110)	112.5(10)
		119.7(3)	O(8)-Sr-O(14)	112.8(3)			C(101)-C(110)-C(102)	107.2(12)
		112.6(3)	O(8)-Sr-O(15)	113.2(3)			C(101)-C(110)-C(18)	108.9(12)
		118.8(3)	O(8)-Sr-O(16)	118.8(3)			C(102)-C(110)-C(18)	110 8(12)
							C(112)-C(13)-O(16)	109.8(12)
							C(14)-C(15)-O(17)	107.8(12)
							C(16)-C(17)-O(18)	107.7(13)
							C(14) O(16) C(13)	113.9(10)
							C(14) O(16) C(13)	112 8(11)

Bond lengths (Å) and angles (deg.) for [Sr(C11H1902)2(C6H1403)]2. H20(6)

O(1)-Sr	2.520(7)	O(2)-Sr	2.460(6)
O(3)-Sr	2.515(7)	O(4)-Sr	2.459(6)
O(5)-Sr	2.686(7)	O(6)-Sr	2.692(7)
O(7)-Sr	2.664(7)	O(8)-Sr	2.967(7)

O(2)-Sr-O(1)	69.3(2)	O(3)-Sr-O(1)	147.4(1)
O(3)-Sr-O(2)	86.6(2)	O(4)-Sr-O(1)	91.2(2)
O(4)-Sr-O(2)	95.7(2)	O(4)-Sr-O(3)	68.9(2)
O(5)-Sr-O(1)	72.5(2)	O(5)-Sr-O(2)	141.5(1)
O(5)-Sr-O(3)	125.7(2)	O(5)-Sr-O(4)	80.2(2)
O(6)-Sr-O(1)	86.5(2)	O(6)-Sr-O(2)	118.3(2)
O(6)-Sr-O(3)	125.1(2)	O(6)-Sr-O(4)	142.3(1)
O(6)-Sr-O(5)	63.2(2)	O(7)-Sr-O(1)	116.2(2)
O(7)-Sr-O(2)	80.5(2)	O(7)-Sr-O(3)	79.2(2)
O(7)-Sr-O(4)	148.1(1)	O(7)-Sr-O(5)	121.9(2)
O(7)-Sr-O(6)	60.5(2)	O(8)-Sr-O(1)	147.3(2)
O(8)-Sr-O(2)	143.3(2)	O(8)-Sr-O(3)	59.3(2)
O(8)-Sr-O(4)	84.9(2)	O(8)-Sr-O(5)	74.9(2)
O(8)-Sr-O(6)	77.3(2)	O(8)-Sr-O(7)	80.1(2)
C(1)-O(1)-Sr	133.2(3)	C(3)-O(2)-Sr	134.1(4)
C(6)-O(3)-Sr	133.0(3)	C(8)-O(4)-Sr	132.9(4)
C(11)-O(5)-Sr	115.9(5)	C(12)-O(5)-Sr	110.9(4)
C(13)-O(6)-Sr	114.2(4)	C(14)-O(6)-Sr	116.1(4)
C(15)-O(7)-Sr	121.0(5)	C(16)-O(7)-Sr	120.2(5)
Sr-O(8)-Sr(a)*	151.2(2)		

C(1)-O(1)	1.250(7)	C(3)-O(2)	1.255(7)
C(6)-O(3)	1.263(7)	C(8)-O(4)	1.255(7)
C(11)-O(5)	1.420(8)	C(12)-O(5)	1.425(8)
C(13)-O(6)	1.428(8)	C(14)-O(6)	1.437(8)
C(15)-O(7)	1.406(8)	C(16)-O(7)	1.424(9)
C(2)-C(1)	1.400(9)	C(4)-C(1)	1.557(9)
C(3)-C(2)	1.396(9)	C(5)-C(3)	1.543(9)
C(41)-C(4)	1.482(10)	C(42)-C(4)	1.514(12)
C(43)-C(4)	1.496(10)	C(51)-C(5)	1.499(11)
C(52)-C(5)	1.512(11)	C(53)-C(5)	1.511(12)
C(7)-C(6)	1.387(8)	C(9)-C(6)	1.546(10)
C(8)-C(7)	1.405(9)	C(10)-C(8)	1.558(9)
C(91)-C(9)	1.529(10)	C(92)-C(9)	1.522(10)
C(93)-C(9)	1.537(10)	C(101)-C(10)	1.493(10)
C(102)-C(10)	1.497(10)	C(103)-C(10)	1.502(11)
C(13)-C(12)	1.484(10)	C(15)-C(14)	1.487(10)

C(12)-O(5)-C(11)	113.7(6)	C(14)-O(6)-C(13)	111.8(6)
C(16)-O(7)-C(15)	112.7(6)	C(2)-C(1)-O(1)	125.4(6)
C(4)-C(1)-O(1)	116.1(6)	C(4)-C(1)-C(2)	118.4(6)
C(3)-C(2)-C(1)	125.5(6)	C(2)-C(3)-O(2)	124.9(6)
C(5)-C(3)-O(2)	116.8(6)	C(5)-C(3)-C(2)	118.3(6)
C(41)-C(4)-C(1)	113.8(6)	C(42)-C(4)-C(1)	110.5(7)
C(42)-C(4)-C(41)	108.3(8)	C(43)-C(4)-C(1)	106.7(6)
C(43)-C(4)-C(41)	109.4(8)	C(43)-C(4)-C(42)	107.9(9)
C(51)-C(5)-C(3)	110.5(7)	C(52)-C(5)-C(3)	113.2(6)
C(52)-C(5)-C(51)	108.7(8)	C(53)-C(5)-C(3)	107.0(7)
C(53)-C(5)-C(51)	110.3(8)	C(53)-C(5)-C(52)	107.1(9)
C(7)-C(6)-O(3)	124.5(6)	C(9)-C(6)-O(3)	114.9(6)
C(9)-C(6)-C(7)	120.5(6)	C(8)-C(7)-C(6)	125.9(6)
C(7)-C(8)-O(4)	124.5(6)	C(10)-C(8)-O(4)	114.8(6)
C(10)-C(8)-C(7)	120.7(6)	C(91)-C(9)-C(6)	108.4(6)
C(92)-C(9)-C(6)	113.8(6)	C(92)-C(9)-C(91)	109.9(6)
C(93)-C(9)-C(6)	106.8(6)	C(93)-C(9)-C(91)	108.4(7)
C(93)-C(9)-C(92)	109.4(7)	C(101)-C(10)-C(8)	107.1(6)
C(102)-C(10)-C(8)	108.4(6)	C(102)-C(10)-C(101)	107.9(8)
C(103)-C(10)-C(8)	114.0(7)	C(103)-C(10)-C(101)	108.1(8)
C(103)-C(10)-C(102)	111.2(8)	C(13)-C(12)-O(5)	108.5(6)
C(12)-C(13)-O(6)	108.6(6)	C(15)-C(14)-O(6)	108.5(6)
C(14)-C(15)-O(7)	108.8(6)		

* Key to symmetry: (a) -x, y, 0.5-z

Crystal data, data collection and bond lengths and angles for [Ca(tmhd)$_2$(triglyme)] (7)

formula	$C_{38}H_{70}CaO_8$
mol wt	686.8
color and habit	clear blocks
cryst size/mm	0.32 × 0.37 × 0.50
cryst syst	triclinic
a/Å	10.378(3)
b/Å	11.601(4)
c/Å	15.483(3)
α/deg	84.03(3)
β/deg	71.75(2)
γ/deg	82.61(3)
V/Å^3	1751.7(10)
space group	P-1
Z	2
D_{calc} (g cm^{-3})	1.189
λ/Å	1.54178 (Cu)
μ/cm^{-1}	18.8
F(000)	640
transm factors, max, min	0.5004, 0.6066
no. of unique data	4716
no. of obsd data with $F > 4\sigma(F)$	4146
scan type	ω
2θ range/deg	0-116
final $\Delta\rho$/(e Å^{-3})	0.49
final Δ/σ	0.112
$R = \Sigma w(F_o-F_c)^2$	5.41
R_w	5.96[a]
temp/K	291

[a] The form of the weighting function is $w^{-1} = \sigma^2(F) + 0.0005F^2$.

Ca-O(7)	2.471(3)	Ca-O(5)	2.394(3)	C(14)-C(15)	1.399(4)	C(15)-C(16)	1.405(4)
Ca-O(8)	2.378(2)	Ca-O(11)	2.492(3)	C(16)-O(16)	1.260(3)	C(16)-C(17)	1.549(4)
Ca-O(14)	2.365(2)	Ca-O(16)	2.355(2)	C(17)-C(171)	1.519(4)	C(17)-C(172)	1.518(5)
Ca-O(19)	2.348(2)	Ca-O(21)	2.379(2)	C(17)-C(173)	1.509(7)	C(18)-C(181)	1.464(9)
C(1)-O(2)	1.416(4)	O(2)-C(3)	1.419(4)	C(18)-C(182)	1.515(7)	C(18)-C(183)	1.545(7)
C(3)-C(4)	1.491(5)	C(4)-O(5)	1.416(5)	C(18)-C(184)	1.388(31)	C(18)-C(185)	1.524(26)
O(5)-C(6)	1.416(4)	C(6)-C(7)	1.472(6)	C(18)-C(186)	1.586(30)	C(18)-C(19)	1.549(4)
C(7)-O(8)	1.412(4)	O(9)-C(9)	1.413(5)	C(19)-O(19)	1.237(3)	C(19)-C(20)	1.402(4)
C(9)-C(10)	1.472(7)	C(10)-O(11)	1.421(5)	C(20)-C(21)	1.381(4)	C(21)-O(21)	1.253(3)
O(11)-C(12)	1.406(6)	C(13)-C(131)	1.531(4)	C(21)-C(22)	1.549(4)	C(22)-C(221)	1.528(6)
C(13)-C(132)	1.529(6)	C(13)-C(133)	1.516(4)	C(22)-C(222)	1.515(5)	C(22)-C(223)	1.520(4)
C(13)-C(14)	1.542(4)	C(14)-O(14)	1.250(3)				

O(7)-Ca-O(5)	64.8(1)	O(7)-Ca-O(8)	127.1(1)	C(132)-C(13)-C(133)	108.9(3)	C(131)-C(13)-C(14)	107.3(2)
O(5)-Ca-O(8)	64.2(1)	O(7)-Ca-O(11)	169.8(1)	C(132)-C(13)-C(14)	107.7(3)	C(133)-C(13)-C(14)	114.6(3)
O(5)-Ca-O(11)	126.7(1)	O(8)-Ca-O(11)	63.8(1)	C(13)-C(14)-O(14)	115.6(2)	C(13)-C(14)-C(15)	120.3(2)
O(7)-Ca-O(14)	85.9(1)	O(5)-Ca-O(14)	74.8(1)	O(14)-C(14)-C(15)	124.0(3)	Ca-O(14)-C(14)	133.7(2)
O(8)-Ca-O(14)	71.7(1)	O(11)-Ca-O(14)	99.8(1)	C(14)-C(15)-C(16)	126.5(3)	C(15)-C(16)-O(16)	124.5(3)
O(7)-Ca-O(16)	87.6(1)	O(5)-Ca-O(16)	137.3(1)	C(15)-C(16)-C(17)	119.3(3)	O(16)-C(16)-C(17)	116.2(2)
O(8)-Ca-O(16)	126.3(1)	O(11)-Ca-O(16)	84.7(1)	Ca-O(16)-C(16)	135.7(2)	C(16)-C(17)-C(171)	113.1(3)
O(14)-Ca-O(14)	71.9(1)	O(7)-Ca-O(19)	85.1(1)	C(16)-C(17)-C(172)	109.8(3)	C(171)-C(17)-C(172)	108.0(3)
O(5)-Ca-O(19)	138.2(1)	O(8)-Ca-O(19)	137.0(1)	C(16)-C(17)-C(173)	107.7(3)	C(171)-C(17)-C(173)	110.4(4)
O(11)-Ca-O(19)	85.4(1)	O(14)-Ca-O(19)	146.7(1)	C(172)-C(17)-C(173)	107.7(4)	C(181)-C(18)-C(182)	111.5(5)
O(16)-Ca-O(19)	75.7(1)	O(2)-Ca-O(21)	98.5(1)	C(181)-C(18)-C(183)	109.9(5)	C(182)-C(18)-C(183)	104.6(5)
O(5)-Ca-O(21)	72.8(1)	O(8)-Ca-O(21)	75.2(1)	C(184)-C(18)-C(185)	103.2(18)	C(184)-C(18)-C(186)	112.8(15)
O(11)-Ca-O(21)	83.9(1)	O(14)-Ca-O(21)	141.2(1)	C(185)-C(18)-C(186)	109.1(13)	C(181)-C(18)-C(19)	109.1(4)
O(16)-Ca-O(21)	146.4(1)	O(19)-Ca-O(21)	72.8(1)	C(182)-C(18)-C(19)	109.8(3)	C(183)-C(18)-C(19)	112.7(3)
Ca-O(7)-C(1)	120.5(3)	Ca-O(2)-C(3)	120.0(2)	C(184)-C(18)-C(19)	110.9(10)	C(185)-C(18)-C(19)	113.0(10)
C(1)-O(2)-C(3)	111.3(3)	O(2)-C(3)-C(4)	107.6(4)	C(186)-C(18)-C(19)	107.8(8)	C(18)-C(19)-O(19)	116.6(2)
C(3)-C(4)-O(5)	107.0(3)	Ca-O(5)-C(4)	112.4(2)	C(18)-C(19)-C(20)	118.9(2)	O(19)-C(19)-C(20)	124.4(3)
Ca-O(5)-C(6)	113.6(2)	C(4)-O(5)-C(6)	112.1(3)	Ca-O(19)-C(19)	135.9(2)	C(19)-C(20)-C(21)	124.9(3)
O(5)-C(6)-C(7)	108.3(3)	C(6)-C(7)-O(8)	108.4(3)	C(20)-C(21)-O(21)	124.9(3)	C(20)-C(21)-C(22)	120.2(2)
Ca-O(8)-C(7)	114.3(2)	Ca-O(8)-C(9)	114.5(2)	O(21)-C(21)-C(22)	115.0(2)	Ca-O(21)-C(21)	133.3(2)
C(7)-O(8)-C(9)	112.3(3)	O(8)-C(9)-C(10)	107.3(3)	C(21)-C(22)-C(221)	107.9(3)	C(21)-C(22)-C(222)	107.6(3)
C(9)-C(10)-O(11)	107.0(4)	Ca-O(11)-C(10)	110.3(3)	C(221)-C(22)-C(222)	109.4(3)	C(21)-C(22)-C(223)	114.4(2)
Ca-O(11)-C(12)	120.3(2)	C(10)-O(11)-C(12)	113.2(3)	C(221)-C(22)-C(223)	108.2(3)	C(222)-C(22)-C(223)	109.2(3)
C(131)-C(13)-C(132)	109.4(3)	C(131)-C(13)-C(133)	108.8(3)				

Crystal data and details of data collection and refinement for [Sr(dppd)$_2$(tetraglyme)] (8)

Formula	$C_{61}H_{98}SrO_8$
Molecular weight	1062.474
Colour, habit	Clear blocks
Crystal size (mm)	0.50 × 0.30 × 0.20
Crystal system	Monoclinic
a (Å)	12.950(2)
b (Å)	27.008(4)
c (Å)	12.373(7)
α (°)	90
β (°)	112.55(3)
γ (°)	90
V (Å^3)	3996.64
Temperature (K)	150
Space group	$P2_1/c$
Z	4
D_{calc} (g cm^{-3})	1.334
λ(Mo-K_α) (Å)	0.71069
μ(Mo-K_α) (cm^{-1})	13.6
F(000)	1676
θ range (°)	1.9–24.8
Total data measured	12,086
Absorption correction factors, min, max	0.945, 1.085
No. of unique data	5877
R_{int}	0.049
Observed data with $F > 3\sigma(F)$	4118
No. of parameters	506
Final $\Delta\rho$ (e Å^{-3})	0.49
Final Δ/σ	0.15
$R = \Sigma(\Delta F)/\Sigma(F_o)$	0.0378
R_w	0.0477[a]

[a] $Rw = [\Sigma\{w(\Delta F)^2\}/\Sigma_w(F_o)^2\}]^{0.5}$ ($w = 1$)

Bond lengths (Å) for (8)

O(1)—Sr	2 563(6)	O(2)—Sr	2 500(6)
O(3)—Sr	2 534(6)	O(4)—Sr	2 564(6)
O(5)—Sr	2 708(6)	O(6)—Sr	2 770(6)
O(7)—Sr	2 755(6)	O(8)—Sr	2 718(6)
O(9)—Sr	2 791(7)	C(7)—O(1)	1 258(6)
C(9)—O(2)	1 261(6)	C(22)—O(3)	1 263(6)
C(24)—O(4)	1 270(7)	C(31)—O(5)	1 443(8)
C(32)—O(5)	1 423(7)	C(33)—O(6)	1 423(8)
C(34)—O(6)	1 443(7)	C(35)—O(7)	1 406(8)
C(36)—O(7)	1 455(8)	C(37)—O(8)	1 444(8)
C(38)—O(8)	1 433(8)	C(39)—O(9)	1 430(8)
C(40)—O(9)	1 424(8)	C(2)—C(1)	1 396(8)
C(6)—C(1)	1 388(8)	C(7)—C(1)	1 536(8)
C(3)—C(2)	1 395(8)	C(4)—C(3)	1.386(9)
C(5)—C(4)	1 376(9)	C(6)—C(5)	1 407(8)
C(8)—C(7)	1 408(7)	C(9)—C(8)	1 409(7)
C(10)—C(9)	1 526(8)	C(11)—C(10)	1 404(8)
C(15)—C(10)	1 401(8)	C(12)—C(11)	1 383(8)
C(13)—C(12)	1 394(9)	C(14)—C(13)	1 377(9)
C(15)—C(14)	1.404(8)	C(17)—C(16)	1 374(8)
C(21)—C(16)	1 408(8)	C(22)—C(16)	1 519(8)
C(18)—C(17)	1.403(8)	C(19)—C(18)	1 376(9)
C(20)—C(19)	1 368(9)	C(21)—C(20)	1 398(8)
C(23)—C(22)	1 415(8)	C(24)—C(23)	1.403(8)
C(25)—C(24)	1 514(9)	C(26)—C(25)	1 407(8)
C(30)—C(25)	1 396(8)	C(27)—C(26)	1.385(9)
C(28)—C(27)	1 394(10)	C(29)—C(28)	1.384(10)
C(30)—C(29)	1.388(9)	C(33)—C(32)	1.498(9)
C(35)—C(34)	1.502(11)	C(37)—C(36)	1.408(10)
C(39)—C(38)	1 466(9)		

Table 3 Bond angles (°) for (8)

O(2)—Sr—O(1)	67 6(2)	O(3)—Sr—O(1)	150 6(1)
O(3)—Sr—O(2)	86 6(2)	O(4)—Sr—O(1)	139 8(1)
O(4)—Sr—O(2)	139 8(1)	O(4)—Sr—O(3)	69 4(2)
O(5)—Sr—O(1)	88.1(2)	O(5)—Sr—O(2)	76 8(2)
O(5)—Sr—O(3)	71 9(2)	O(5)—Sr—O(4)	121 8(2)
O(6)—Sr—O(1)	102.6(2)	O(6)—St—O(2)	136 8(1)
O(6)—Sr—O(3)	86 3(2)	O(6)—Sr—O(4)	75 2(2)
O(6)—Sr—O(5)	60 5(2)	O(7)—Sr—O(1)	70 3(2)
O(7)—Sr—O(2)	137 7(1)	O(7)—Sr—O(3)	135 2(1)
O(7)—Sr—O(4)	75 4(2)	O(7)—Sr—O(5)	106 3(2)
O(7)—Sr—O(6)	57 9(2)	O(8)—Sr—O(1)	71 6(2)
O(8)—Sr—O(2)	99 6(2)	O(8)—Sr—O(3)	129 0(2)
O(8)—Sr—O(4)	74.3(2)	O(8)—Sr—O(5)	158 9(1)
O(8)—Sr—O(6)	117 6(2)	O(8)—Sr—O(7)	62 3(2)
O(9)—Sr—O(1)	106 6(2)	O(9)—Sr—O(2)	69 1(2)
O(9)—Sr—O(3)	75 0(2)	O(9)—Sr—O(4)	73 6(2)
O(9)—Sr—O(5)	133.2(1)	O(9)—Sr—O(6)	147 7(1)
O(9)—Sr—O(7)	120 5(2)	O(9)—Sr—O(8)	61 0(2)
C(7)—O(1)—Sr	134.9(3)	C(9)—O(2)—Sr	139 2(3)
C(22)—O(3)—Sr	136.4(3)	C(24)—O(4)—Sr	136 2(3)
C(31)—O(5)—Sr	117 5(4)	C(32)—O(5)—Sr	112 2(4)
C(32)—O(5)—C(31)	110 9(5)	C(33)—O(6)—Sr	118 1(4)
C(34)—O(6)—Sr	120 3(4)	C(34)—O(6)—C(33)	112 6(5)
C(35)—O(7)—Sr	111 9(4)	C(36)—O(7)—Sr	111 1(4)
C(36)—O(7)—C(35)	119 5(6)	C(37)—O(8)—Sr	115 7(4)
C(38)—O(8)—Sr	116 1(4)	C(38)—O(8)—C(37)	109 0(6)
C(39)—O(9)—Sr	113 2(4)	C(40)—O(9)—Sr	119 6(4)
C(40)—O(9)—C(39)	111 9(5)	C(6)—C(1)—C(2)	119 5(5)
C(7)—C(1)—C(2)	117 8(5)	C(7)—C(1)—C(6)	122 7(5)
C(3)—C(2)—C(1)	120.0(6)	C(4)—C(3)—C(2)	120 4(6)
C(5)—C(4)—C(3)	119 7(6)	C(6)—C(5)—C(4)	120 5(6)
C(5)—C(6)—C(1)	119 8(6)	C(1)—C(7)—O(1)	116 5(5)
C(8)—C(7)—O(1)	126 4(5)	C(8)—C(7)—C(1)	117 0(5)
C(9)—C(8)—C(7)	123 3(5)	C(8)—C(9)—O(2)	125 0(5)
C(10)—C(9)—O(2)	115 9(5)	C(10)—C(9)—C(8)	119 0(5)
C(11)—C(10)—C(9)	123 9(5)	C(15)—C(10)—C(9)	117 8(5)
C(15)—C(10)—C(11)	118 2(5)	C(12)—C(11)—C(10)	121 6(6)
C(13)—C(12)—C(11)	119 2(6)	C(14)—C(13)—C(12)	120 6(6)
C(15)—C(14)—C(13)	120 1(6)	C(14)—C(15)—C(10)	120 2 6)
C(21)—C(16)—C(17)	118 5(5)	C(22)—C(16)—C 17)	119 6(5)
C(22)—C(16)—C(21)	121 9(5)	C(18)—C(17)—C(16)	120 7(6)
C(19)—C(18)—C(17)	120 0(6)	C(20)—C(19)—C(18)	120 5(6)
C(21)—C(20)—C(19)	119 8(6)	C(20)—C(21)—C(16)	120 5(6)
C(16)—C(22)—O(3)	116.5(5)	C(23)—C(22)—O(3)	126 2(5)
C(23)—C(22)—C(16)	117 2(5)	C(24)—C(23)—C(22)	126 4(5)
C(23)—C(24)—O(4)	124 9(5)	C(25)—C(24)—O(4)	116 5(5)
C(25)—C(24)—C(23)	118 6(5)	C(26)—C(25)—C 24)	123 4(6)
C(30)—C(25)—C(24)	118 8(5)	C(30)—C(25)—C(26)	117 8(6)
C(27)—C(26)—C(25)	120 8(6)	C(28)—C(27)—C(26)	120 3(6)
C(29)—C(28)—C(27)	119 5(6)	C(30)—C(29)—C 28)	120 1 7)
C(29)—C(30)—C(25)	121 4(6)	C(33)—C(32)—O(5)	108 9(5)
C(32)—C(33)—O(6)	108 8(5)	C(35)—C(34)—O(6)	109 0(6)
C(34)—C(35)—O(7)	105 9(6)	C(37)—C(36)—O(7)	1 4 4(7)
C(36)—C(37)—O(8)	108 6(7)	C(39)—C(38)—O(8)	109 1 6)
C(38)—C(39)—O(9)	108 9(6)		

formula	$C_{28}H_{24}CaO_8F_{12}$
mol wt	676 5
color and habit	clear blocks
cryst size/mm	0 21 × 0 33 × 0 33
cryst syst	triclinic
a/Å	9 453(2)
b/Å	12 600(3)
c/Å	13 215(4)
α/deg	70 30(2)
β/deg	83 09(2)
γ/deg	76 49(2)
V/Å^3	1439.2(7)
space group	P-1
Z	2
D_{calcd} (g cm^{-3})	1.561
λ/Å	1 54178 (Cu)
μ/cm^{-1}	30 3
F(000)	688
transm factors: max, min	
no. of unique data	3857
no. of obsd data with $F > 4\sigma(F)$	3616
scan type	ω
2θ range/deg	0–116
final $\Delta\rho$/(e Å^{-3})	0.61
final Δ/σ	0 045
$R = \sum w(F_o - F_c)^2$	7 07
R_w	8 43[a]
temp/K	291

[a] The form of the weighting function is $w^{-1} = \sigma^2(F) + 0.0005F^2$.

Crystal data and details of data collection and refinement for [Ca(hfpd)$_2$(tetraglyme)] (9)

Bond lengths and angles for (9)

Ca–O(2)	2.434(3)	Ca–O(5)	2.497(3)	C(16)–C(17)	1.526(6)	C(17)–O(17)	1 239(5)
Ca–O(8)	2 493(3)	Ca–O(11)	2.449(3)	C(17)–C(18)	1.370(5)	C(18)–C(19)	1.369(6)
Ca–O(17)	2.401(3)	Ca–O(19)	2.402(3)	C(19)–O(19)	1.240(6)	C(19)–C(20)	1.540(5)
Ca–O(22)	2.410(3)	Ca–O(24)	2.395(3)	C(20)–F(201)	1.306(5)	C(20)–F(202)	1 315(7)
C(1)–O(2)	1 428(7)	O(2)–C(3)	1.423(7)	C(20)–F(203)	1.309(5)	C(20)–F(204)	1 306(12)
C(3)–C(4)	1.465(7)	C(4)–O(5)	1.436(6)	C(20)–F(205)	1.304(6)	C(20)–F(206)	1 306(7)
O(5)–C(6)	1 439(5)	C(6)–C(7)	1.490(8)	C(21)–F(211)	1.307(5)	C(21)–F(212)	1 302(5)
C(7)–O(8)	1.438(5)	O(8)–C(9)	1.429(6)	C(21)–F(213)	1.303(6)	C(21)–F(214)	1.301(7)
C(9)–C(10)	1 467(6)	C(10)–O(11)	1.423(5)	C(21)–F(215)	1.308(8)	C(21)–F(216)	1 298(8)
O(11)–C(12)	1 439(5)	C(12)–C(13)	1.513(9)	C(21)–C(22)	1.515(6)	C(22)–O(22)	1 251(5)
C(13)–O(14)	1 366(6)	O(14)–C(15)	1 404(10)	C(22)–C(23)	1.373(5)	C(23)–C(24)	1 385(7)
C(16)–F(161)	1 278(7)	C(16)–F(162)	1.284(8)	C(24)–O(24)	1.234(6)	C(24)–C(25)	1 525(6)
C(16)–F(163)	1.285(7)	C(16)–F(164)	1.283(14)	C(25)–F(251)	1.293(8)	C(25)–F(252)	1.318(6)
C(16)–F(165)	1.285(8)	C(16)–F(166)	1.280(8)	C(25)–F(253)	1.340(7)		
O(2)–Ca–O(5)	65.5(1)	O(2)–Ca–O(8)	131.8(1)	F(162)–C(16)–C(17)	112.1(6)	F(163)–C(16)–C(17)	111 3(4)
O(5)–Ca–O(8)	67.4(1)	O(2)–Ca–O(11)	162.4(1)	F(164)–C(16)–C(17)	112.0(5)	F(165)–C(16)–C(17)	110.7(5)
O(5)–Ca–O(11)	131 9(1)	O(8)–Ca–O(11)	65 7(1)	F(166)–C(16)–C(17)	118.1(5)	C(16)–C(17)–O(17)	113 7(3)
O(2)–Ca–O(17)	82.4(1)	O(5)–Ca–O(17)	125 7(1)	C(16)–C(17)–C(18)	117.7(4)	O(17)–C(17)–C(18)	128 6(4)
O(8)–Ca–O(17)	135.5(1)	O(11)–Ca–O(17)	83.5(1)	Ca–O(17)–C(17)	134.3(3)	C(17)–C(18)–C(19)	122.1(4)
O(2)–Ca–O(19)	103 3(1)	O(5)–Ca–O(19)	74.8(1)	C(18)–C(19)–O(19)	128.1(4)	C(18)–C(19)–C(20)	117 8(4)
O(8)–Ca–O(19)	73.1(1)	O(11)–Ca–O(19)	82.1(1)	O(19)–C(19)–C(20)	114.0(3)	Ca–O(19)–C(19)	134.4(2)
O(17)–Ca–O(19)	71.5(1)	O(2)–Ca–O(22)	84.8(1)	C(19)–C(20)–F(201)	110.7(3)	C(19)–C(20)–F(202)	110.6(3)
O(5)–Ca–O(22)	74.4(1)	O(8)–Ca–O(22)	73.6(1)	F(201)–C(20)–F(202)	107.2(4)	C(19)–C(20)–F(203)	113.0(3)
O(11)–Ca–O(22)	101.7(1)	O(17)–Ca–O(22)	147.2(1)	F(201)–C(20)–F(203)	105.9(4)	F(202)–C(20)–F(203)	104 9(4)
O(19)–Ca–O(22)	141 1(1)	O(2)–Ca–O(24)	83.7(1)	C(19)–C(20)–F(204)	105.9(7)	C(19)–C(20)–F(205)	115.8(6)
O(5)–Ca–O(24)	135 8(1)	O(8)–Ca–O(24)	126 4(1)	F(204)–C(20)–F(205)	98.2(8)	C(19)–C(20)–F(206)	111 7(5)
O(11)–Ca–O(24)	82.9(1)	O(17)–Ca–O(24)	76 9(1)	F(204)–C(20)–F(206)	94.6(7)	F(205)–C(20)–F(206)	128.8(8)
O(19)–Ca–O(24)	146.2(1)	O(22)–Ca–O(24)	71 8(1)	F(211)–C(21)–F(212)	108.3(4)	F(211)–C(21)–F(213)	103 4(4)
Ca–O(2)–C(1)	123.6(3)	Ca–O(2)–C(3)	120 1(3)	F(212)–C(21)–F(213)	106 9(5)	F(214)–C(21)–F(215)	102.5(9)
C(1)–O(2)–C(3)	114 4(4)	O(2)–C(3)–C(4)	109 4(4)	F(214)–C(21)–F(216)	99 2(7)	F(215)–C(21)–F(216)	114 9(8)
C(3)–C(4)–O(5)	108 7(5)	Ca–O(5)–C(4)	112 8(2)	F(211)–C(21)–C(22)	110.4(4)	F(212)–C(21)–C(22)	113 5(4)
Ca–O(5)–C(6)	112.6(2)	C(4)–O(5)–C(6)	111.2(4)	F(213)–C(21)–C(22)	115.6(3)	F(214)–C(21)–C(22)	106 9(6)
O(5)–C(6)–C(7)	107.6(4)	C(6)–C(7)–O(8)	107 4(3)	F(215)–C(21)–C(22)	116.0(6)	F(216)–C(21)–C(22)	114 6(7)
Ca–O(8)–C(7)	112.5(2)	Ca–O(8)–C(9)	113 9(2)	C(21)–C(22)–O(22)	113.6(3)	C(21)–C(22)–C(23)	118.0(4)
C(7)–O(8)–C(9)	112.3(3)	O(8)–C(9)–C(10)	107 6(4)	O(22)–C(22)–C(23)	128.3(4)	Ca–O(22)–C(22)	132.2(3)
C(9)–C(10)–O(11)	108 9(3)	Ca–O(11)–C(10)	117.8(3)	C(22)–C(23)–C(24)	122.0(4)	C(23)–C(24)–O(24)	128 3(4)
Ca–O(11)–C(12)	123 1(2)	C(10)–O(11)–C(12)	115 1(3)	C(23)–C(24)–C(25)	117.5(4)	O(24)–C(24)–C(25)	114.2(4)
O(11)–C(12)–C(13)	109.2(4)	C(12)–C(13)–O(14)	107.4(4)	Ca–O(24)–C(24)	133.7(3)	C(24)–C(25)–F(251)	115 4(5)
C(13)–O(14)–C(15)	111 2(4)	F(161)–C(16)–F(162)	105 4(6)	C(24)–C(25)–F(252)	111.9(4)	F(251)–C(25)–F(252)	107 7(5)
F(161)–C(16)–F(163)	104 0(6)	F(162)–C(16)–F(163)	107 0(5)	C(24)–C(25)–F(253)	110.4(4)	F(251)–C(25)–F(253)	106.6(4)
F(164)–C(16)–F(165)	106 6(7)	F(164)–C(16)–F(166)	105 9(7)	F(252)–C(25)–F(253)	104.1(5)		
F(165)–C(16)–F(166)	102.6(6)	F(161)–C(16)–C(17)	116.4(4)				

Table 4 Bond lengths [A] and angles [deg] for (1)

Ca-O 4	2 354 2
Ca-O(3	2 396 2
Ca-O 2	2 398 2
Ca-O 1	2 413 2
Ca-O 7	2 464 2
Ca-O 6	2.478 2)
Ca-O 5	2.502 2
Ca-O 8	2.542 2
O 1 -C 2	1 236 3
O 2 -C 4	1.249 3)
O 3 -C 7	1.242 3
O 4 -C 9	1 243 3
O 5 -C 12	1.428 3
O 5 -C 11	1.430 3)
O 6 -C 13	1.423(3)
O 6 -C 14	1.428(3)
O 7 -C 15	1 428'3
O 7 -C 16	1 431 3
O 8 -C 17	1.438 3
O 8 -C 18	1.438 3)
C 1 -F 1'	1.108(13)
C 1 -F 1	1.276 4)
C 1 -F 2'	1.327 12)
C 1 -F 3	1.319 4)
C 1 -F 3'	1.32 2)
C 1 -F 2	1 333 4)
C 1 -C 2	1.535 4)
C 2 -C 3	1.400 4)
C 3 -C 4	1.383 4)
C 3)-H 3	0.93
C 4)-C 5)	1.540(3)
C 5)-F 5)	1.311(3)
C 5 -F 4	1.319 3)
C 5 -F 6	1.327(3)
C 6 -F 9'	1.19(5)
C 6 -F 8'	1 22(3)
C 6 -F 7'	1.26 3)
C 6)-F 8	1.319 3)
C 6)-F 9)	1.325(4)
C'6)-F(7)	1.329 4)
C 6)-C(7)	1.537 4)
F 8')-F(9')	1.65 6)
C 7 -C 8)	1.383(4)
C 8)-C(9)	1.391 4
C 8 -H 8)	0.93
C 9 -C 10	1.543(4)
C 10 -F 12'	1.24 2)
C 10 -F 11')	1.26 2)
C 10)-F 11)	1.308 4)
C 10)-F(10)	1.313 4)
C 10)-F(10')	1.32 2
C 10)-F(12)	1.317 4
C 11)-H(11A)	0 96
C 11)-H(11B)	0.96
C'11)-H(11C)	0.96
C 12)-C(13)	1 501(3)
C 12)-H(12A)	0.97
C 12 -H 12B	0 97
C 13 -H 13A	0 97
C 13 -H 13B	0 97
C 14 -C 15	1 496 3
C 14 -H 14A	0 97
C 14 -H 14B	0.97
C 15 -H 15A)	0 97
C 15)-H 15B	0 97
C 16)-C(17)	1 495 3
C 16)-H(16A	0 97
C 16)-H 16B	0 97
C 17 -H 17A	0.97
C 17 -H 17B	0.97
C 18)-C 18 #1	1.515 4
C 18)-H 18A)	0 97
C(18)-H(18B)	0.97
O(4)-Ca-O(3)	72 01 6
O 4)-Ca-O 2)	81 36 6
O(3)-Ca-O 2	147 66 6
O 4 -Ca-O 1	146 41 6
O 3)-Ca-O(1)	140 05 6
O 2)-Ca-O 1	70 56 6
O 4)-Ca-O 7	138.20 6
O(3)-Ca-O(7)	72.66'6
O(2)-Ca-O(7)	121.07 6
O 1)-Ca-O 7	74.20 6
O 4 -Ca-O 6'	122.76 6
O 3 -Ca-O(6	75 18 6
O 2)-Ca-O 6	136 29 6
O 1)-Ca-O 6	71 82 6
O 7)-Ca-O 6	67 23 5
O(4)-Ca-O'5)	77 06 6
O(3)-Ca-O 5)	102.57 6
O 2)-Ca-O'5	88 62 6
O 1 -Ca-O 5	84 04 6
O 7 -Ca-O 5	142 55 5
O 6)-Ca-O 5	66 03 5
O 4)-Ca-O 8)	87 24 5
O 3)-Ca-O 8	82.51 6
O 2)-Ca-O 8	78 11 5
O(1)-Ca-O 8)	104.06 6
O(7)-Ca-O(8	66.60 5
O 6)-Ca-O 8	132 83 5
O 5)-Ca-O 8	160 85 5
C 2)-O(1 -Ca	134 6 2
C 4)-O 2)-Ca	134 4 2
C 7)-O(3)-Ca	134 2 2
C 9)-O(4)-Ca	135 3 2
C(12)-O(5)-C(11)	110.7 2
C(12)-O(5)-Ca	116 37 13
C 11)-O(5)-Ca	123 49 14
C 13 -O 6 -C 14	112 2 2
C 13 -O 6)-Ca	114 11 13
C 14 -O 6 -Ca	113 91 12
C 15 -O 7)-C 16	112 3 2
C 15 -O 7)-Ca	114 74 13
C 16)-O 7 -Ca	113 97 13
C 17 -O 8 -C 18	109 9 2
C 17 -O 8 -Ca	113 80 12
C 18 -O 8 -Ca	126 40 12
F 1 -C 1 -F 2	106 9 14
F 1 -C 1 -F 3	109 1 4
F 1' -C 1 -F 3'	112 6 14
F 2' -C 1 -F 3	105 1 11
F 1)-C 1 -F 2	106 7 4
F 3 -C 1 -F 2	102 3 3

F 2' -C 1 -C 2	115 1 6
F 1 -C 1)-C 2	112 4 3
F 2' -C 1)-C 2	109 0 5
F 3 -C 1)-C 2	113.8 3
F(3')-C 1)-C 2)	107 7 5)
F 2 -C 1 -C 2)	112 9 2)
O 1 -C 2 -C 3	127.7 2)
O 1 -C 2 -C 1	114.9 2)
C 3 -C 2 -C 1	117 3 2
C 4 -C 3 -C 2	120.7 2
C 4 -C 3 -H 3	119 67 14
C 2 -C 3 -H 3	119.67 14
O 2 -C 4 -C 3	128 2 2)
O 2 -C 4 -C 5)	114.4 2)
C 3 -C 4 -C 5	117.4 2)
F 5 -C 5 -F(4	108.2 3)
F 5 -C 5 -F 6	107.0 3)
F 4 -C 5 -F 6	104.8 2)
F 5 -C 5 -C 4	111.3 2)
F 4 -C 5 -C 4	113.9 2)
F 6 -C 5 -C 4)	111.2(2)
F 9' -C 6 -F 8')	86 3)
F 9' -C 6)-F 7')	115(2)
F 8')-C 6 -F 7')	106 2)
F 8 -C 6 -F 9)	107.4(3)
F 8 -C 6 -F 7	105.0(3)
F 9 -C 6 -F 7	107.5 4)
F 9')-C 6 -C 7	118(2)
F 8' -C'6 -C 7)	114.6 11)
F 7' -C 6)-C 7)	113.7(12)
F 8 -C 6)-C(7)	115.1(3)
F 9 -C 6)-C(7)	111.2(2)
F 7 -C 6)-C 7)	110.2(3)
C 6 -F 8' -F 9')	46 2)
C 6 -F 9' -F 8'	48 2)
O 3 -C 7 -C 8)	128.6 2)
O 3 -C 7 -C 6)	113.9(2)
C 8 -C 7 -C 6	117.5(2)
C 7 -C(8)-C'9)	120.2(2)
C(7)-C(8)-H 8)	119.9(2)
C 9 -C'8 -H 8)	119.88(14)
O 4 -C(9)-C(8)	129.0(2)
O 4)-C(9)-C 10)	114.8(2)
C 8 -C 9)-C 10)	116.2(2)
F 12')-C'10)-F(11')	120(2)
F 11)-C 10)-F(10)	106.4(3)
F 12')-C(10)-F(10')	102(2)
F(11')-C(10)-F(10')	107(2)
F 11)-C(10)-F(12)	105.8(4)
F 10)-C 10)-F(12)	105.7(3)
F 12' -C'10)-C 9)	111.5(7)
F 11')-C(10)-C(9)	109.8(8)
F(11)-C(10)-C(9)	113.7(3)
F 10)-C(10)-C(9)	111.5 3)
F 10')-C(10)-C(9)	105.3(7)
F(12)-C(10)-C(9)	113.0(3)
O 5)-C(11)-H(11A)	109.47(12)
O 5)-C(11)-H(11B)	109.47(13)
H 11A)-C(11)-H(11B)	109.5
O 5 -C'11)-H(11C)	109.47 12)
H 11A -C 11 -H 11C)	109 5
H 11B -C 11 -H 11C)	109 5
O 5 -C 12 -C 13)	108 5(2
O 5 -C 12 -H 12A)	110.00 12)
C 13)-C(12)-H(12A	109.99 13
O 5)-C 12)-H(12B)	110.00 12
C'13)-C(12)-H(12B	110.00 14
H(12A)-C(12)-H(12B)	108.4
O 6)-C 13)-C'12)	107 6 2
O(6)-C(13)-H'13A)	110.19 12
C(12)-C(13)-H 13A)	110 19 12
O(6)-C(13)-H(13B)	110.19 12
C(12)-C(13)-H(13B	110.19 14
H(13A)-C 13 -H 13B)	108.5
O 6 -C(14 -C'15	108 1 2
O 6 -C 14)-H 14A	110.07 12
C 15)-C 14)-H 14A	110.07 14
O 6)-C(14)-H 14B	110.07 11
C 15)-C'14)-H 14B	110.07 13
H(14A)-C 14 -H(14B)	108.4
O(7)-C(15)-C(14)	107.9'2
O(7)-C 15)-H(15A	110.12 12
C(14)-C'15)-H 15A)	110.12 14
O(7)-C(15)-H 15B	110.12 12
C 14)-C 15 -H 15B	110 12 13
H 15A)-C'15 -H 15B	108.4
O 7)-C 16 -C(17	107 6 2
O 7)-C(16 -H 16A	110.19 12
C 17)-C 16)-H 16A)	110.19 13
O 7)-C 16)-H(16B	110.19 13
C 17 -C 16 -H 16B)	110 19 14
H 16A -C 16 -H 16B)	108.5
O 8)-C 17 -C 16	108 7 2
O 8)-C 17 -H 17A	109 95 12
C 16 -C 17 -H 17A	109 95 13
O 8 -C 17 -H 17B	109 96 13
C(16 -C 17 -H 17B	109 96 14
H 17A)-C 17)-H(17B)	108 3
O(8)-C 18 -C 18)#1	108 0 2
O 8 -C 18 -H 18A	110 10 12
C 18 #1-C 18 -H 18A	110 1 2
O 8 -C 18 -H 18B	110 10 11
C 18 #1-C 18 -H 18B	110 1 2
H 18A)-C 18 -H 18B	108 4

Symmetry transformations used to generate equivalent atoms.
#1 -x,-y,-z

Bond lengths (A) for (13)

O(1)-Ca	1.875(7)	O 2)-Ca	1.882 7
O(3)-Ca	1.881(7)	O(4)-Ca	1 882(7)
O(5)-Ca	1.869(7)	O(6)-Ca	1.858(7)
C(7)-O(1)	1.291(9)	C(9)-O(2)	1.278 8)
C'2 -C(1)	1.389(11)	C(6)-C(1)	1.403(11
C(7)-C(1)	1.498(10)	C(3)-C(2)	1 386(11)
C 4 -C 3)	1.381(14)	C(5)-C(4)	1.383(14)
C(6)-C(5)	1.373(11)	C(8)-C(7)	1.387(10)
C(9)-C(8)	1.387(9)	C(10)-C(9)	1.501(11)
C(11)-C(10)	1.388(11)	C(15)-C(10)	1.387(11)
C(12)-C(11)	1.382(11)	C(13)-C(12)	1.374(12)
C(14)-C(13)	1.381(13)	C(15)-C(14)	1.404(11)
C(22)-O(3)	1.275(8)	C(24)-O(4)	1.276(8)
C(17)-C(16)	1.392(10)	C(21)-C(16)	1.388(11)
C(22)-C(16)	1.493(10)	C(18)-C(17)	1.379(10)
C(19)-C(18)	1.395(12)	C(20)-C(19)	1.381(12)
C(21)-C(20)	1.392(11)	C(23)-C(22)	1.391(10)
C(24)-C(23)	1.393(10)	C(25)-C(24)	1.482(10)
C(26)-C(25)	1.386(10)	C(30)-C(25)	1.407(10)
C(27)-C(26)	1.381(11)	C(28)-C(27)	1.374(12)
C(29)-C(28)	1.373(12)	C(30)-C(29)	1.395(11)
C(37)-O(5)	1.287(8)	C(39)-O(6)	1.286(8)
C(32)-C(31)	1.396(11)	C(36)-C(31)	1.387(10)
C(37)-C(31)	1.494(10)	C(33)-C(32)	1.385(11)
C(34)-C(33)	1.397(12)	C(35)-C(34)	1.374(12)
C(36)-C(35)	1.371(11)	C(38)-C(37)	1.386(10)
C(39)-C(38)	1.404(10)	C(40)-C(39)	1.485(10)
C(41)-C(40)	1.387(10)	C(45)-C(40)	1.392(10)
C(42)-C(41)	1.383(10)	C(43)-C(42)	1.394(11)
C(44)-C(43)	1.374(12)	C(45)-C(44)	1.387(11)

Bond angles (deg.) for (13)

O(2)-Ca-O(1)	89.3(3)	O(3)-Ca-O(1)	91.2(3)
O(3)-Ca-O(2)	88.9(3)	O(4)-Ca-O(1)	91.1(3)
O(4)-Ca-O(2)	179.1(2)	O(4)-Ca-O(3)	90.3(3)
O(5)-Ca-O(1)	176.2(2)	O(5)-Ca-O(2)	87.2(3)
O(5)-Ca-O(3)	87.3(3)	O(5)-Ca-O(4)	92.4(3)
O(6)-Ca-O(1)	90.5(3)	O(6)-Ca-O(2)	92.9(3)
O(6)-Ca-O(3)	177.5(2)	O(6)-Ca-O(4)	87.9(3)
O(6)-Ca-O(5)	91.1(3)	C(7)-O(1)-Ca	128.4(5)
C(9)-O(2)-Ca	129.4(5)	C(22)-O(3)-Ca	127.5(5)
C(24)-O(4)-Ca	127.8(5)	C(37)-O(5)-Ca	127.9(5)
C(39)-O(6)-Ca	129.3(5)	C(6)-C(1)-C(2)	119.4(7)
C(7)-C(1)-C(2)	122.2(7)	C(7)-C(1)-C(6)	118.2(7)
C(3)-C(2)-C(1)	120.1(8)	C(4)-C(3)-C(2)	120.2(9)
C(5)-C(4)-C(3)	119.8(8)	C(6)-C(5)-C(4)	120.8(9)
C(5)-C'6)-C(1)	119.7(8)	C(1)-C(7)-O(1)	115.0(7)
C(8)-C(7)-O(1)	124.0(7)	C(8)-C(7)-C(1)	120.9(7)
C(9)-C(8)-C(7)	121.6(7)	C(8)-C(9)-O(2)	124.1(7)
C(10)-C(9)-O(2)	115.3(7)	C(10)-C(9)-C(8)	120.6(7)
C(11)-C(10)-C(9)	118.4(7)	C(15)-C(10)-C(9)	122.1(7)
C(15)-C(10)-C(11)	119.4(7)	C(12)-C(11)-C(10)	120.4(8)
C(13)-C(12)-C(11)	120.0(8)	C(14)-C(13)-C(12)	121.0(8)
C(15)-C(14)-C(13)	119.0(8)	C(14)-C(15)-C(10)	120.2(8)
C(21)-C(16)-C(17)	119.4(7)	C(22)-C(16)-C(17)	121.7(7)
C(22)-C(16)-C(21)	118.9(7)	C(18)-C(17)-C(16)	120.6(8)
C(19)-C(18)-C(17)	119.7(7)	C(20)-C(19)-C(18)	120.1(8)
C(21)-C(20)-C(19)	120.0(8)	C(20)-C(21)-C(16)	120.2(8)
C(16)-C(22)-O(3)	116.6(7)	C(23)-C(22)-O(3)	124.2(7)
C(23)-C(22)-C(16)	119.2(7)	C(24)-C(23)-C(22)	122.7(7)
C 23)-C(24)-O(4)	123.1(7)	C(25)-C(24)-O(4)	116.3(6)
C(25)-C(24)-C(23)	120.6(6)	C(26)-C(25)-C(24)	118.9(7)
C(30)-C(25)-C(24)	122.3(7)	C(30)-C(25)-C(26)	118.9(7)
C(27)-C(26)-C(25)	121.1(8)	C(28)-C(27)-C(26)	119.8 8)
C(29)-C(28)-C(27)	120.4(8)	C(30)-C(29)-C(28)	120.7 8)
C(29 -C(30)-C(25)	119.1(8)	C(36)-C(31)-C(32)	118.4(8)
C 37 -C(31)-C 32)	118.6(7)	C(37)-C(31)-C(36)	122.8(7)
C'33)-C 32)-C(31)	120.4(8)	C(34)-C(33)-C(32)	120.0(8)
C 35)-C(34)-C(33)	119.3(8)	C(36)-C(35)-C(34)	120.6(8)
C(35)-C(36)-C(31)	121.3(8)	C(31)-C(37)-O(5)	115.0(7)
C 38)-C 37)-O 5)	123.0(7)	C(38)-C(37)-C(31)	122.0(7)
C(39)-C 38)-C(37)	122.9(7)	C(38)-C(39)-O(6)	123.0(7)
C 40)-C(39)-O 6)	115.7(7)	C(40)-C(39)-C(38)	121.3(7
C 41)-C 40)-C 39)	118.0(7)	C(45)-C(40)-C(39)	122.3(7)
C 45)-C 40)-C 41)	119.7(7)	C(42)-C(41)-C(40)	120.3(7)
C 43)-C(42)-C(41)	119.7(8)	C(44)-C(43)-C(42)	119.9(8)
C(45)-C(44)-C(43)	120.6(8)	C(44)-C(45)-C(40)	119.7(8)

Erpirical Formula	$C_{28}H_{40}CaF_{14}O_8$	Radiation	MoKα (λ = 0.71073 Å)
Color; Habit	Clear platey rhombs	Temperature (K)	293
Crystal size (mm)	.17 x .47 x .50	Monochromator	Highly oriented graphite crystal
Crystal System	Monoclinic	2θ Range	4.0 to 50.0°
Space Group	P2/n	Scan Type	ω
Unit Cell Dimensions	a = 11.894(9) Å	Scan Speed	Variable; 2.00 to 29.00° min. .n =
	b = 10.699(6) Å	Scan Range (ω)	0.80°
	c = 14.837(8) Å	Background Measurement	Stationary crystal and stationary counter at beginning and end of scan, each for 40.0% of total scan time
	β = 97.02(2)°		
Volume	1874(2) Å^3		
Z	2	Standard Reflections	2 measured every 50 reflections
Formula weight	810.7	Index Ranges	$0 \le h \le 14$, $0 \le k \le 12$
Density(calc.)	1.437 Mg/m^3		$-17 \le l \le 17$
Absorption Coefficient	0.279 mm^{-1}	Reflections Collected	3460
F(000)	836	Independent Reflections	3299 (R_{int} = 1.95%)
		Observed Reflections	1964 ($F > 4.0\sigma(F)$)

Weighting Scheme	$w^{-1} = \sigma^2(F) + 0.0006F^2$
Number of Parameters Refined	244
Final R Indices (obs. data)	R = 6.01 %, Rw = 6.36 %
R Indices (all data)	R = 9.79 %, wR = 7.70 %
Goodness-of-Fit	1.78
Largest and Mean Δ/σ	0.052, 0.003
Data-to-Parameter Ratio	8.0:1
Largest Difference Peak	0.31 eA^{-3}
Largest Difference Hole	-0.28 eÅ^{-3}

Crystal data and details of data collection and refinement for [Ca(fod)$_2$(triglyme)] (14)

Bond lengths (Å) (14)

Ca-O(2)	2.491 (4)	Ca-O(5)	2.514 (4)
Ca-O(8)	2.365 (3)	Ca-O(10)	2.374 (3)
Ca-O(2A)	2.491 (4)	Ca-O(5A)	2.514 (4)
Ca-O(8A)	2.365 (3)	Ca-O(10A)	2.374 (3)
C(1)-O(2)	1.437 (8)	O 2)-C(3)	1.423 (7)
C(3)-C(4)	1.487 (9)	C 4)-O(5)	1.416 (7)
O(5)-C(6)	1.394 (6)	C 6)-C(6A)	1.599 (12)
C(7)-C(71)	1.497 (7)	C(7)-C(72)	1.502 (9)
C(7)-C(73)	1.495 (7)	C(7)-C(71')	1.496 (15)
C(7)-C(72')	1.496 (12)	C(7)-C(73')	1.497 (24)
C(7)-C(8)	1.550 (6)	C(71)-C(71')	1.132 (24)
C(71)-C(73')	1.624 (23)	C(72)-C(71')	1.654 (26)
C(72)-C 72')	1.272 (27)	C(73)-C(72')	1.488 (22)
C(73)-C(73')	1.307 (23)	C 8)-O(8)	1.241 (5)
C 8)-C(9)	1.401 (6)	C(9)-C(10)	1.379 (7)
C(10)-O(10)	1.241 (5)	C(10)-C(11)	1.533 (6)
C(11)-C(12)	1.533 (9)	C 11)-F(1)	1.337 (5)
C(11)-F(2)	1.339 (6)	C(12)-C(13)	1.430 (12)
C(12)-F(3)	1.356 (7)	C(12)-F(4)	1.435 (7)
C(13)-F 5)	1.296 (11)	C 13)-F(6)	1.374 (13)
C 13)-F 7)	1.352 (12)		

Bond lengths (A) for (15)

O(1)-Ca(1)	2.323(5)	O(2)-Ca(1)	2.311(5)
O(3)-Ca(1)	2.311(5)	O(4)-Ca(1)	2.323(5)
N(1)-Ca(1)	2.645(7)	N(2)-Ca(1)	2,585(7)
N(3)-Ca(1)	2.671(8)	O(5)-Ca(2)	2.297(5)
O(6)-Ca(2)	2.327(5)	N(4)-Ca(2)	2.648(7)
N(5)-Ca(2)	2.607(8)		
C(7)-O(1)	1.255(6)	C(9)-O(2)	1.266(6)
C(22)-O(3)	1.264(6)	C(24)-O(4)	1.265(6)
C(2)-C(1)	1.382(8)	C(6)-C(1)	1.391(8)
C(7)-C(1)	1.509(8)	C(3)-C(2)	1.382(7)
C(4)-C(3)	1.370(8)	C(5)-C(4)	1.382(9)
C(6)-C(5)	1.374(9)	C(8)-C(7)	1.405(7)
C(9)-C(8)	1.395(7)	C(10)-C(9)	1.501(8)
C(11)-C(10)	1.382(8)	C(15)-C(10)	1.376(7)
C(12)-C(11)	1.384(8)	C(13)-C(12)	1.367(9)
C(14)-C(13)	1.367(8)	C(15)-C(14)	1.386(7)
C(17)-C(16)	1.385(7)	C(21)-C(16)	1.387(8)
C(22)-C(16)	1.500(8)	C(18)-C(17)	1.377(8)
C(19)-C(18)	1.378(8)	C(20)-C(19)	1.374(8)
C(21)-C(20)	1.386(7)	C(23)-C(22)	1.407(7)
C(24)-C(23)	1.396(7)	C(25)-C(24)	1.507(8)
C(26)-C(25)	1.394(8)	C(30)-C(25)	1.385(7)
C(27)-C(26)	1.386(7)	C(28)-C(27)	1.381(8)
C(29)-C(28)	1.372(8)	C(30)-C(29)	1.393(7)
C(31)-N(1)	1.466(8)	C(32)-N(1)	1.470(9)
C(33)-N(1)	1.480(7)	C(34)-N(2)	1.484(13)
C(34')-N(2)	1.566(14)	C(35)-N(2)	1.363(12)
C(36)-N(2)	1.421(17)	C(37)-N(3)	1.460(8)
C(38)-N(3)	1.477(9)	C(39)-N(3)	1.462(8)
C(34)-C(33)	1.609(14)	C(34')-C(33)	1.552(18)
C(37)-C(36)	1.839(20)		
C(46)-O(5)	1.261(6)	C(48)-O(6)	1.267(7)
C(41)-C(40)	1.383(7)	C(45)-C(40)	1.388(8)
C(46)-C(40)	1.505(9)	C(42)-C(41)	1.393(9)
C(43)-C(42)	1.366(8)	C(44)-C(43)	1.363(9)
C(45)-C(44)	1.388(10)	C(47)-C(46)	1.402(7)
C(48)-C(47)	1.402(8)	C(49)-C(48)	1.501(8)
C(50)-C(49)	1.378(8)	C(54)-C(49)	1.404(8)
C(51)-C(50)	1.386(8)	C(52)-C(51)	1.378(9)
C(53)-C(52)	1.371(9)	C(54)-C(53)	1.384(8)
C(55)-N(4)	1.466(9)	C(56)-N(4)	1.479(8)
C(57)-N(4)	1.481(8)	C(58)-N(5)	1.545(15)
C(59)-N(5)	1.428(11)	C(58)-C(57)	1.684(16)

Bond angles (°) (14)

O(2)-Ca-O(5)	65.2(1)	O(2)-Ca-O(8)	84.4(1)
O(5)-Ca-O(8)	135.3(1)	O(2)-Ca-O(10)	85.5(1)
O(5)-Ca-O(10)	73.9(1)	O(8)-Ca-O(10)	71.7(1)
O(2)-Ca-O(2A)	163.5(2)	O(5)-Ca-O(2A)	131.3(1)
O(8)-Ca-O(2A)	82.7(1)	O(10)-Ca-O(2A)	100.1(1)
O(2)-Ca-O(5A)	131.3(1)	O(5)-Ca-O(5A)	66.8(2)
O(8)-Ca O(5A)	126.8(1)	O(10)-Ca-O(5A)	73.6(1)
O(2A)-Ca-O(5A)	65.2(1)	O(2)-Ca-O(8A)	82.7(1)
O(5)-Ca-O(8A)	126.8(1)	O(8)-Ca-O(8A)	76.6(1)
O(10)-Ca-O(8A)	147.1(1)	O(2A)-Ca-O(8A)	84.4(1)
O(5A)-Ca-O(8A)	135.3(1)	O(2)-Ca-O(10A)	100.1(1)
O(5)-Ca-O(10A)	73.6(1)	O(8)-Ca-O(10A)	147.1(1)
O(10)-Ca-O(10A)	140.9(2)	O(2A)-Ca-O(10A)	85.5(1)
O(5A)-Ca-O(10A)	73.9(1)	O(8A)-Ca-O(10A)	71.7(1)
Ca-O(2)-C(1)	121.2(3)	Ca-O(2)-C(3)	117.2(3)
C(1)-O(2)-C(3)	113.7(4)	O(2)-C(3)-C(4)	107.9(5)
C(3)-C(4)-O(5)	107.0(4)	Ca-O(5)-C(4)	112.9(3)
Ca-O(5)-C(6)	114.6(3)	C(4)-O(5)-C(6)	111.0(4)
O(5)-C(6)-C(6A)	107.0(4)	C(71)-C(7)-C(72)	108.7(5)
C(71)-C(7)-C(73)	109.6(5)	C(72)-C(7)-C(73)	109.1(5)
C(71')-C(7)-C(72')	109.5(14)	C(71')-C(7)-C(73')	109.4(13)
C(72')-C(7)-C(73')	109.3(13)	C(71)-C(7)-C(8)	110.3(3)
C(72)-C(7)-C(8)	110.4(4)	C(73)-C(7)-C(8)	108.8(4)
C(71')-C(7)-C(8)	111.3(10)	C(72')-C(7)-C(8)	117.3(10)
C(73')-C(7)-C(8)	99.5(10)	C(71)-C(71')-C(72)	120.7(10)
C(7)-C(72')-C(72)	65.1(9)	C(7)-C(8)-O(8)	117.6(3)
C(7)-C(8)-C(9)	119.6(4)	O(8)-C(8)-C(9)	122.7(4)
Ca-O(8)-C(8)	139.1(3)	C(8)-C(9)-C(10)	123.8(4)
C(9)-C(10)-O(10)	128.5(4)	C(9)-C(10)-C(11)	118.5(4)
O(10)-C(10)-C(11)	112.9(4)	Ca-O(10)-C(10)	134.1(3)
C(10)-C(11)-C(12)	115.5(4)	C(10)-C(11)-F(1)	113.0(4)
C(12)-C(11)-F(1)	107.4(4)	C(10)-C(11)-F(2)	110.4(4)
C(12)-C(11)-F(2)	103.8(4)	F(1)-C(11)-F(2)	105.9(4)
C(11)-C(12)-C(13)	119.2(7)	C(11)-C(12)-F(3)	109.3(5)
C(13)-C(12)-F(3)	108.9(7)	C(11)-C(12)-F(4)	109.3(5)
C(13)-C(12)-F(4)	102.7(6)	F(3)-C(12)-F(4)	106.6(5)
C(12)-C(13)-F(5)	113.2(8)	C(12)-C(13)-F(6)	104.9(7)
F(5)-C(13)-F(6)	111.0(9)	C(12)-C(13)-F(7)	110.7(9)
F(5)-C(13)-F(7)	106.1(7)	F(6)-C(13)-F(7)	111.2(8)

Bond angles (deg.) for (15)

O(2)-Ca(1)-O(1)	76.0(2)	O(3)-Ca(1)-O(1)	75.4(2)
O(3)-Ca(1)-O(2)	98.3(2)	O(4)-Ca(1)-O(1)	98.6(2)
O(4)-Ca(1)-O(2)	173.3(1)	O(4)-Ca(1)-O(3)	76.4(2)
N(1)-Ca(1)-O(1)	147.2(1)	N(1)-Ca(1)-O(2)	92.3(2)
N(1)-Ca(1)-O(3)	76.3(2)	N(1)-Ca(1)-O(4)	90.4(2)
N(2)-Ca(1)-O(1)	141.8(1)	N(2)-Ca(1)-O(2)	96.2(2)
N(2)-Ca(1)-O(3)	142.6(1)	N(2)-Ca(1)-O(4)	90.5(2)
N(2)-Ca(1)-N(1)	68.8(2)	N(3)-Ca(1)-O(1)	74.0(2)
N(3)-Ca(1)-O(2)	92.0(2)	N(3)-Ca(1)-O(3)	144.2(1)
N(3)-Ca(1)-O(4)	90.1(2)	N(3)-Ca(1)-N(1)	137.8(1)
N(3)-Ca(1)-N(2)	68.9(2)	O(6)-Ca(2)-O(5)	77.0(2)
N(4)-Ca(2)-O(5)	92.4(2)	N(4)-Ca(2)-O(6)	75.0(2)
N(5)-Ca(2)-O(5)	95.7(2)	N(5)-Ca(2)-O(6)	142.4(1)
N(5)-Ca(2)-N(4)	68.4(2)	O(5)-Ca(2)-O(5a)*	168.6(2)
O(6)-Ca(2)-O(5a)*	93.9(2)	N(4)-Ca(2)-O(5a)*	91.8(2)
O(6)-Ca(2)-O(6a)*	75.2(2)	N(4)-Ca(2)-O(6a)*	147.3(2)
N(4)-Ca(2)-N(4a)*	136.8(2)	C(7)-O(1)-Ca(1)	133.2(3)
C(9)-O(2)-Ca(1)	132.4(3)	C(22)-O(3)-Ca(1)	127.1(4)
C(24)-O(4)-Ca(1)	129.3(4)	C(6)-C(1)-C(2)	118.0(5)
C(7)-C(1)-C(2)	124.2(5)	C(7)-C(1)-C(6)	117.8(5)
C(3)-C(2)-C(1)	121.2(5)	C(4)-C(3)-C(2)	120.1(6)
C(5)-C(4)-C(3)	119.5(6)	C(6)-C(5)-C(4)	120.4(6)
C(5)-C(6)-C(1)	120.8(6)	C(1)-C(7)-O(1)	115.9(5)
C(8)-C(7)-O(1)	124.2(5)	C(8)-C(7)-C(1)	119.9(5)
C(9)-C(8)-C(7)	125.9(5)	C(8)-C(9)-O(2)	126.1(5)
C(10)-C(9)-O(2)	116.1(5)	C(10)-C(9)-C(8)	117.8(5)
C(11)-C(10)-C(9)	122.1(5)	C(15)-C(10)-C(9)	120.2(5)
C(15)-C(10)-C(11)	117.7(5)	C(12)-C(11)-C(10)	120.9(6)
C(13)-C(12)-C(11)	120.7(6)	C(14)-C(13)-C(12)	119.0(5)
C(15)-C(14)-C(13)	120.5(6)	C(14)-C(15)-C(10)	121.2(6)
C(21)-C(16)-C(17)	118.3(5)	C(22)-C(16)-C(17)	118.3(5)
C(22)-C(16)-C(21)	123.4(5)	C(18)-C(17)-C(16)	121.1(5)
C(19)-C(18)-C(17)	120.0(6)	C(20)-C(19)-C(18)	119.7(6)
C(21)-C(20)-C(19)	120.3(6)	C(20)-C(21)-C(16)	120.6(5)
C(16)-C(22)-O(3)	115.9(4)	C(23)-C(22)-O(3)	124.6(5)
C(23)-C(22)-C(16)	119.5(5)	C(24)-C(23)-C(22)	126.4(5)
C(23)-C(24)-O(4)	125.0(5)	C(25)-C(24)-O(4)	116.0(5)
C(25)-C(24)-C(23)	119.0(5)	C(26)-C(25)-C(24)	122.8(5)
C(30)-C(25)-C(24)	119.5(5)	C(30)-C(25)-C(26)	117.7(5)
C(27)-C(26)-C(25)	121.1(5)	C(28)-C(27)-C(26)	120.0(6)
C(29)-C(28)-C(27)	119.8(5)	C(30)-C(29)-C(28)	120.0(5)
C(29)-C(30)-C(25)	121.2(5)	C(31)-N(1)-Ca(1)	106.0(4)
C(32)-N(1)-Ca(1)	111.0(4)	C(32)-N(1)-C(31)	108.3(5)
C(33)-N(1)-Ca(1)	111.6(4)	C(33)-N(1)-C(31)	110.3(5)
C(33)-N(1)-C(32)	109.5(5)	C(34)-N(2)-Ca(1)	105.6(5)
C(34')-N(2)-Ca(1)	101.7(6)	C(35)-N(2)-Ca(1)	115.7(6)
C(35) N(2) C(34)	126.4(9)	C(35)-N(2)-C(34')	73.9(11)
C(36) N(2) Ca(1)	106.3(6)	C(36)-N(2)-C(34)	97.2(9)
C(36)-N(2)-C(34')	150.3(7)	C(36)-N(2)-C(35)	102.1(11)
C(37)-N(3)-Ca(1)	110.5(5)	C(38)-N(3)-Ca(1)	110.8(4)
C(38) N(3)-C(37)	110.2(6)	C(39)-N(3)-Ca(1)	106.3(4)
C(39)-N(3)-C(37)	110.1(5)	C(39)-N(3)-C(38)	108.9(6)
C(34)-C(33) N(1)	107.3(6)	C(34')-C(33)-N(1)	109.4(7)
C(33)-C(34) N(2)	107.0(7)	C(33)-C(34')-N(2)	105.8(9)
C(37) C(36) N(2)	99.1(8)	C(36)-C(37)-N(3)	111.7(7)

Crystal data and details of data collection and refinement for $[Ba(C_5H_4F_3O_2)_2(C_{12}H_{30}N_4)]$ (16)

Formula	$[Ba(C_5H_4F_3O_2)_2(C_{12}H_{30}N_4)]$
M.W.	673.89
Crystal system	Orthorhombic
a/Å	16.607(7)
b/Å	17.155(6)
c/Å	25.507(9)
α/°	90
β/°	90
γ/°	90
V/Å^3	5890.46
θ range for cell/°	2.5-25
Space group	*Pbca*
Z	8
D_c/gcm^{-3}	1.520
$F(000)$	2720
μ(Mo-Kα)/cm^{-1}	14.1
T/K	150
Crystal size/mm^3	0.30x0.20x0.18
θ range for data/°	2.0-24.8
h_{min}, h_{max}	-15,16
k_{min}, k_{max}	-9,19
l_{min}, l_{max}	-23,24
Total data measured	9140
Total unique	3608
R_{int}	0.040
Total observed	2208
Significance test	Fo>3σ(Fo)
Absorption correction factors, min, max	0.930,1.115
No. of parameters	334
ρ_{min},ρ_{max}/eÅ^{-3}	-0.50, 1.00
$(\Delta/\sigma)_{max}$	0.016
Weighting scheme	unit weight
R*	0.0384
wR*	0.0417

* $R = \Sigma(\Delta F)/\Sigma(Fo)$; $wR = [\Sigma(w(\Delta F)^2)/\Sigma(w(Fo)^2)]^{1/2}$

Bond lengths (A) and angles (deg) for [Ba(C5H4F3O2)2(C12H30N4] (16)

O(1)-Ba	2.687(9)	O(2)-Ba	2.669(10)
O(3)-Ba	2.665(9)	O(4)-Ba	2.688(10)
N(1)-Ba	2.972(10)	N(2)-Ba	2.975(11)
N(3)-Ba	3.022(10)	N(4)-Ba	2.963(11)
C(5)-F(1)	1.323(12)	C(5)-F(2)	1.334(13)
C(5)-F(3)	1.330(13)	C(10)-F(4)	1.296(14)
C(10)-F(5)	1.319(15)	C(10)-F(6)	1.316(14)
C(2)-O(1)	1.242(12)	C(4)-O(2)	1.258(12)
C(7)-O(3)	1.256(12)	C(9)-O(4)	1.261(13)
C(11)-N(1)	1.465(15)	C(12)-N(1)	1.476(13)
C(13)-N(1)	1.451(13)	C(14)-N(2)	1.466(13)
C(15)-N(2)	1.474(13)	C(16)-N(2)	1.459(14)
C(17)-N(3)	1.455(14)	C(18)-N(3)	1.478(14)
C(19)-N(3)	1.487(13)	C(20)-N(4)	1.481(13)
C(21)-N(4)	1.467(13)	C(22)-N(4)	1.476(13)
C(2)-C(1)	1.524(15)	C(3)-C(2)	1.411(14)
C(4)-C(3)	1.362(14)	C(5)-C(4)	1.532(15)
C(7)-C(6)	1.488(15)	C(8)-C(7)	1.419(15)
C(9)-C(8)	1.353(16)	C(10)-C(9)	1.532(17)
C(14)-C(13)	1.512(16)	C(17)-C(16)	1.505(16)
C(20)-C(19)	1.479(16)		
O(2)-Ba-O(1)	65.2(3)	O(3)-Ba-O(1)	79.5(3)
O(3)-Ba-O(2)	104.4(3)	O(4)-Ba-O(1)	94.7(3)
O(4)-Ba-O(2)	159.1(2)	O(4)-Ba-O(3)	64.1(3)
N(1)-Ba-O(1)	72.9(3)	N(1)-Ba-O(2)	97.3(3)
N(1)-Ba-O(3)	133.3(2)	N(1)-Ba-O(4)	81.3(3)
N(2)-Ba-O(1)	134.5(2)	N(2)-Ba-O(2)	124.4(3)
N(2)-Ba-O(3)	127.9(3)	N(2)-Ba-O(4)	73.5(3)
N(2)-Ba-N(1)	62.1(3)	N(3)-Ba-O(1)	131.8(2)
N(3)-Ba-O(2)	71.7(3)	N(3)-Ba-O(3)	133.1(2)
N(3)-Ba-O(4)	129.1(3)	N(3)-Ba-N(1)	92.8(3)
N(3)-Ba-N(2)	59.7(3)	N(4)-Ba-O(1)	129.3(3)
N(4)-Ba-O(2)	82.5(3)	N(4)-Ba-O(3)	71.7(3)
N(4)-Ba-O(4)	108.1(3)	N(4)-Ba-N(1)	153.1(2)
N(4)-Ba-N(2)	95.7(3)	N(4)-Ba-N(3)	61.4(3)
C(2)-O(1)-Ba	138.9(6)	C(4)-O(2)-Ba	135.4(5)
C(7)-O(3)-Ba	141.4(7)	C(9)-O(4)-Ba	136.0(6)
C(11)-N(1)-Ba	111.4(7)	C(12)-N(1)-Ba	103.4(6)
C(12)-N(1)-C(11)	109.5(9)	C(13)-N(1)-Ba	113.0(6)
C(13)-N(1)-C(11)	110.8(9)	C(13)-N(1)-C(12)	108.5(9)
C(14)-N(2)-Ba	107.8(7)	C(15)-N(2)-Ba	104.0(7)
C(15)-N(2)-C(14)	108.8(9)	C(16)-N(2)-Ba	115.7(7)
C(16)-N(2)-C(14)	110.5(9)	C(16)-N(2)-C(15)	109.7(9)
C(17)-N(3)-Ba	112.5(7)	C(18)-N(3)-Ba	107.0(7)
C(18)-N(3)-C(17)	110.7(9)	C(19)-N(3)-Ba	107.5(6)
C(19)-N(3)-C(17)	111.5(9)	C(19)-N(3)-C(18)	107.5(9)
C(20)-N(4)-Ba	113.9(6)	C(21)-N(4)-Ba	114.6(7)
C(21)-N(4)-C(20)	109.9(9)	C(22)-N(4)-Ba	100.5(7)
C(22)-N(4)-C(20)	109.1(9)	C(22)-N(4)-C(21)	108.2(8)
C(1)-C(2)-O(1)	116.6(10)	C(3)-C(2)-O(1)	125.6(10)
C(3)-C(2)-C(1)	117.8(10)	C(4)-C(3)-C(2)	123.8(10)
C(3)-C(4)-O(2)	130.8(9)	C(5)-C(4)-O(2)	111.5(9)
C(5)-C(4)-C(3)	117.7(10)	F(2)-C(5)-F(1)	107.2(10)
F(3)-C(5)-F(1)	106.1(9)	F(3)-C(5)-F(2)	105.2(9)
C 4)-C 5)-F(1)	112.0(9)	C(4)-C(5)-F(2)	114.4(9)
C 4)-C(5)-F(3)	111.4(9)	C(6)-C(7)-O(3)	118.1(12)
C(8)-C(7)-O(3)	122.8(10)	C(8)-C(7)-C(6)	119.1(11)
C(9)-C(8)-C(7)	124.9(10)	C(8)-C(9)-O(4)	129.7(11)
C(10)-C(9)-O(4)	112.0(11)	C(10)-C(9)-C(8)	118.3(11)
F(5)-C(10)-F(4)	104.9(11)	F(6)-C(10)-F(4)	109.4(13)
F(6)-C(10)-F(5)	103.8(11)	C(9)-C(10)-F(4)	112.5(11)
C(9)-C(10)-F(5)	111.6(11)	C(9)-C(10)-F(6)	114.0(11)
C(14)-C(13)-N(1)	115.1(9)	C(13)-C(14)-N(2)	114.7(9)
C(17)-C(16)-N(2)	113.4(9)	C(16)-C(17)-N(3)	113.7(9)
C(20)-C(19)-N(3)	114.1(9)	C(19)-C(20)-N(4)	115.3(9)

Table 1. Crystal data and structure refinement for **27**

Identification code	94SRD001
Empirical formula	C84 H168 Ce6 O30
Formula weight	2498.9
Temperature	150(2) K
Wavelength	0.71069 A
Crystal system	Monoclinic
Space group	P21/n
Unit cell dimensions	a = 18.090(4) A alpha = 90 deg. b = 17.558(3) A beta = 94.780(6) deg. c = 19.077(3) A gamma = 90 deg.
Volume	6038(2) A^3
Z	2
Density (calculated)	1.374 Mg/m^3
Absorption coefficient	2.274 mm^-1
F(000)	2520
Crystal size	0.28 x 0.22 x 0.17 mm
Theta range for data collection	1.89 to 25.10 deg.
Index ranges	-19<=h<=21, -17<=k<=20, -22<=l<=22
Reflections collected	25061
Independent reflections	9124 [R(int) = 0.0481]
Refinement method	Full-matrix-block least-squares on F^2
Data / restraints / parameters	9124 / 0 / 905
Goodness-of-fit on F^2	0.976
Final R indices [I>2sigma I)]	R1 = 0.0465, wR2 = 0.1198
R indices (all data)	R1 = 0.0554, wR2 = 0.1226
Largest diff. peak and hole	3.007 and -0.889 e.A^-3

ff

Bond lengths and angles for (27)

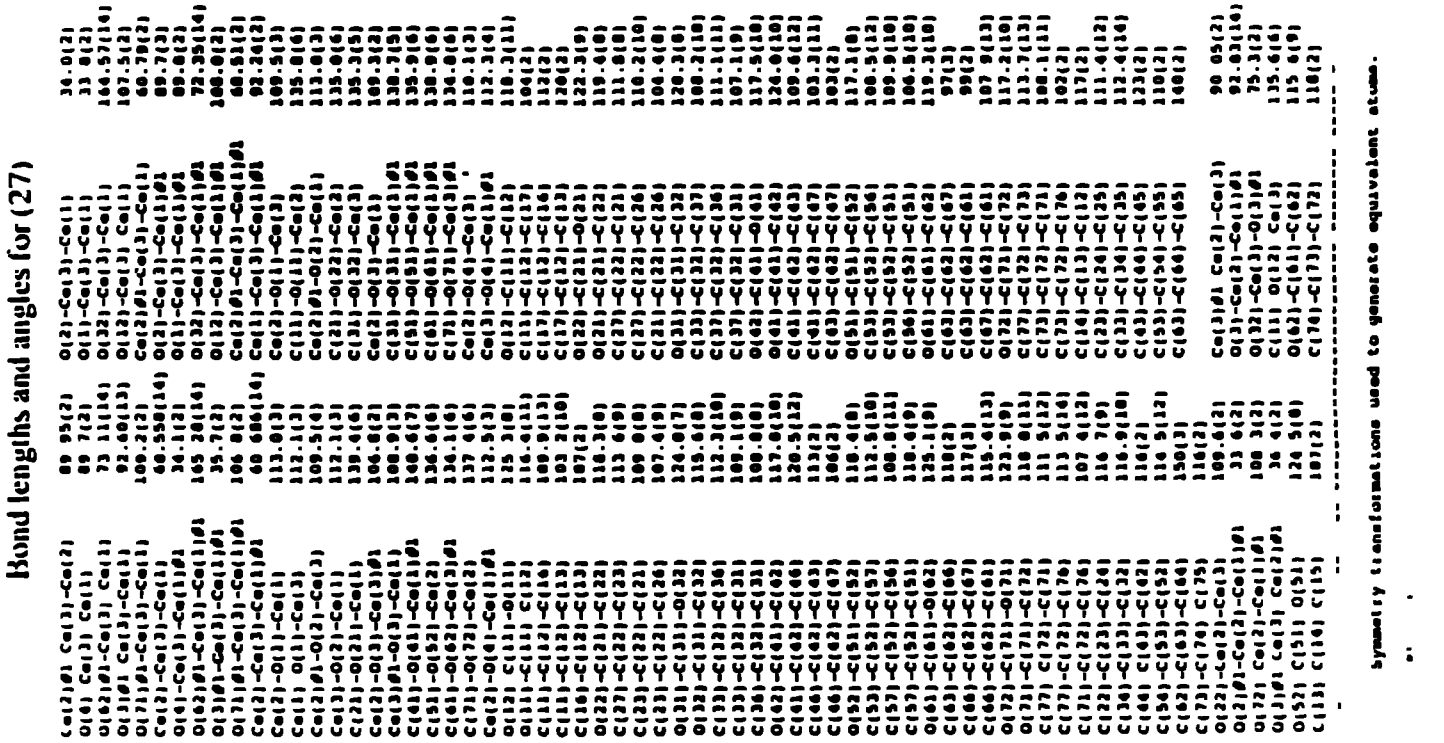

Symmetry transformations used to generate equivalent atoms.

Table 4. Bond lengths [A] and angles [deg] for (27)

Ce(1)-O(1)	2.290(7)	Ce(1)-O(2)	2.297(7)
Ce(1)-O(4)#1	2.313(8)	Ce(1)-O(3)	2.352(7)
Ce(2)-O(4)	2.278(6)	Ce(1)-O(31)#1	2.415(6)
Ce(2)-O(3)	2.313(6)	Ce(1)-O(21)	2.416(6)
Ce(1)-O(61)#1	2.421(6)	Ce(1)-O(51)#1	2.422(6)
Ce(1)-O(41)#1	2.702(7)	Ce(1)-Ce(2)	3.8056(9)
Ce(1)-Ce(3)	3.8098(10)	Ce(1)-Ce(3)#1	3.8170(8)
Ce(2)-O(1)	2.275(7)	Ce(2)-O(2)#1	2.279(8)
Ce(2)-O(72)	2.353(6)	Ce(2)-O(11)	2.363(6)
Ce(2)-O(52)	2.370(6)	Ce(2)-O(22)	2.381(6)
Ce(2)-Ce(3)#1	3.7366(8)	Ce(2)-Ce(3)	3.7377(9)
Ce(2)-Ce(1)#1	3.8170(8)	Ce(3)-O(2)	2.293(7)
Ce(3)-O(4)	2.282(7)	Ce(3)-O(1)	2.301(6)
Ce(3)-O(62)#1	2.343(6)	Ce(3)-O(32)	2.344(5)
Ce(3)-O(3)#1	2.340(7)	Ce(3)-O(12)	2.396(7)
Ce(3)-O(71)#1	2.422(7)	Ce(3)-Ce(2)#1	3.7366(8)
Ce(3)-Ce(1)#1	3.8170(8)	O(11)-C(11)	1.259(13)
O(12)-C(11)	1.255(13)	O(2)-Ce(2)#1	2.279(8)
O(22)-C(21)	1.270(11)	O(21)-C(21)	1.263(11)
O(32)-C(31)	1.273(10)	O(3)-Ce(3)#1	2.340(7)
O(31)-C(31)	1.253(10)	O(31)-Ce(1)#1	2.415(6)
O(41)-C(41)	1.206(11)	O(41)-Ce(1)#1	2.702(7)
O(42)-C(41)	1.326(13)	O(51)-C(51)	1.287(11)
O(51)-Ce(1)#1	2.422(6)	O(52)-C(51)	1.263(11)
O(61)-C(61)	1.251(12)	O(61)-Ce(1)#1	2.421(6)
O(62)-C(61)	1.269(12)	O(62)-Ce(3)#1	2.343(6)
O(71)-C(71)	1.283(13)	O(71)-Ce(3)#1	2.422(7)
O(72)-C(71)	1.261(13)	O(4)-Ce(1)#1	2.313(8)
C(11)-C(12)	1.525(14)	C(12)-C(17)	1.57(4)
C(12)-C(16)	1.56(2)	C(13)-C(13)	1.70(2)
C(21)-C(22)	1.521(13)	C(22)-C(27)	1.48(2)
C(22)-C(23)	1.530(14)	C(22)-C(26)	1.57(2)
C(31)-C(32)	1.533(12)	C(32)-C(33)	1.50(2)
C(32)-C(37)	1.52(2)	C(32)-C(36)	1.53(2)
C(41)-C(42)	1.512(13)	C(42)-C(46)	1.50(2)
C(42)-C(43)	1.50(2)	C(42)-C(47)	1.59(3)
C(51)-C(52)	1.529(13)	C(52)-C(53)	1.51(2)
C(52)-C(57)	1.53(2)	C(52)-C(56)	1.56(2)
C(61)-C(62)	1.53(2)	C(62)-C(63)	1.36(3)
C(62)-C(66)	1.47(2)	C(62)-C(67)	1.52(3)
C(71)-C(72)	1.541(14)	C(72)-C(77)	1.50(2)
C(72)-C(73)	1.50(2)	C(72)-C(76)	1.54(3)
C(13)-C(14)	1.39(3)	C(16)-C(15)	1.50(3)
C(23)-C(24)	1.51(2)	C(24)-C(25)	1.53(2)
C(33)-C(34)	1.50(2)	C(34)-C(35)	1.55(2)
C(43)-C(44)	1.42(3)	C(44)-C(45)	1.55(3)
C(53)-C(54)	1.52(2)	C(54)-C(55)	1.55(2)
C(63)-C(64)	1.25(3)	C(64)-C(65)	1.42(3)
C(73)-C(74)	1.32(3)	C(74)-C(75)	1.65(3)

O(1)-Ce(1)-O(2)	67.8(3)	O(1)-Ce(1)-O(4)#1	102.7(3)
O(2)-Ce(1)-O(4)#1	66.7(3)	O(1)-Ce(1)-O(3)	68.4(2)
O(2)-Ce(1)-O(3)	106.1(3)		
O(4)#1-Ce(1)-O(3)	69.0(3)	O(1)-Ce(1)-O(21)	74.6(3)
O(2)-Ce(1)-O(21)	139.7(2)	O(4)#1-Ce(1)-O(21)	137.9(2)
O(3)-Ce(1)-O(21)	71.3(2)	O(1)-Ce(1)-O(31)#1	138.1(2)
O(2)-Ce(1)-O(31)#1	138.4(2)	O(4)#1-Ce(1)-O(31)#1	74.6(2)
O(3)-Ce(1)-O(31)#1	72.0(2)	O(21)-Ce(1)-O(31)#1	80.5(2)
O(1)-Ce(1)-O(61)#1	75.0(3)	O(2)-Ce(1)-O(61)#1	73.5(3)
O(4)#1-Ce(1)-O(61)#1	137.2(2)	O(3)-Ce(1)-O(61)#1	139.8(2)
O(21)-Ce(1)-O(61)#1	83.7(2)	O(31)#1-Ce(1)-O(61)#1	135.1(2)
O(1)-Ce(1)-O(51)#1	141.4(2)	O(2)-Ce(1)-O(51)#1	76.1(3)
O(4)#1-Ce(1)-O(51)#1	73.9(3)	O(3)-Ce(1)-O(51)#1	137.7(2)
O(21)-Ce(1)-O(51)#1	133.6(2)	O(31)#1-Ce(1)-O(51)#1	78.2(2)
O(61)#1-Ce(1)-O(51)#1	82.2(3)	O(1)-Ce(1)-O(41)#1	126.0(3)
O(2)-Ce(1)-O(41)#1	128.6(3)	O(4)#1-Ce(1)-O(41)#1	131.3(3)
O(3)-Ce(1)-O(41)#1	125.6(2)	O(21)-Ce(1)-O(41)#1	65.7(2)
O(31)#1-Ce(1)-O(41)#1	69.3(2)	O(61)#1-Ce(1)-O(41)#1	65.9(2)
O(51)#1-Ce(1)-O(41)#1	68.2(2)	O(1)-Ce(1)-Ce(2)	33.6(2)
O(2)-Ce(1)-Ce(2)	86.6(2)	O(4)#1-Ce(1)-Ce(2)	86.8(2)
O(3)-Ce(1)-Ce(2)	35.00(14)	O(21)-Ce(1)-Ce(2)	88.81(14)
O(31)#1-Ce(1)-Ce(2)	105.9(2)	O(61)#1-Ce(1)-Ce(2)	106.8(2)
O(51)#1-Ce(1)-Ce(2)	157.3(2)	O(41)#1-Ce(1)-Ce(2)	134.6(2)
O(1)-Ce(1)-Ce(3)	34.0(2)	O(2)-Ce(1)-Ce(3)	33.9(2)
O(4)#1-Ce(1)-Ce(3)	86.8(2)	O(3)-Ce(1)-Ce(3)	88.95(12)
O(21)-Ce(1)-Ce(3)	106.8(2)	O(31)#1-Ce(1)-Ce(3)	156.51(14)
O(61)#1-Ce(1)-Ce(3)	88.37(14)	O(51)#1-Ce(1)-Ce(3)	108.3(2)
O(41)#1-Ce(1)-Ce(3)	136.19(14)	Ce(2)-Ce(1)-Ce(3)	58.79(2)
O(1)-Ce(1)-Ce(3)#1	86.1(2)	O(2)-Ce(1)-Ce(3)#1	86.0(2)
O(4)#1-Ce(1)-Ce(3)#1	33.6(2)	O(3)-Ce(1)-Ce(3)#1	35.5(2)
O(21)-Ce(1)-Ce(3)#1	105.5(2)	O(31)#1-Ce(1)-Ce(3)#1	88.74(14)
O(61)#1-Ce(1)-Ce(3)#1	156.1(2)	O(51)#1-Ce(1)-Ce(3)#1	105.1(2)
O(41)#1-Ce(1)-Ce(3)#1	138.88(14)	Ce(2)-Ce(1)-Ce(3)#1	58.672(14)
Ce(3)-Ce(1)-Ce(3)#1	87.76(2)	O(4)-Ce(2)-O(1)	70.3(3)
O(4)-Ce(2)-O(2)#1	67.6(3)	O(1)-Ce(2)-O(2)#1	106.5(4)
O(4)-Ce(2)-O(3)	109.7(3)	O(1)-Ce(2)-O(3)	69.3(2)
O(2)#1-Ce(2)-O(3)	72.2(3)	O(4)-Ce(2)-O(72)	140.3(2)
O(1)-Ce(2)-O(72)	140.2(2)	O(2)#1-Ce(2)-O(72)	77.2(3)
O(3)-Ce(2)-O(72)	74.7(2)	O(4)-Ce(2)-O(11)	76.9(3)
O(1)-Ce(2)-O(11)	77.3(3)	O(2)#1-Ce(2)-O(11)	139.7(2)
O(3)-Ce(2)-O(11)	140.5(2)	O(72)-Ce(2)-O(11)	125.8(2)
O(4)-Ce(2)-O(52)	77.2(3)	O(1)-Ce(2)-O(52)	142.7(2)
O(2)#1-Ce(2)-O(52)	76.3(3)	O(3)-Ce(2)-O(52)	141.5(2)
O(72)-Ce(2)-O(52)	77.1(2)	O(11)-Ce(2)-O(52)	77.9(2)
O(4)-Ce(2)-O(22)	141.9(2)	O(1)-Ce(2)-O(22)	77.0(3)
O(2)#1-Ce(2)-O(22)	143.8(2)	O(3)-Ce(2)-O(22)	75.1(2)
O(72)-Ce(2)-O(22)	77.8(2)	O(11)-Ce(2)-O(22)	77.3(2)
O(52)-Ce(2)-O(22)	123.4(2)	O(4)-Ce(2)-Ce(3)#1	88.3(2)
O(1)-Ce(2)-Ce(3)#1	88.3(2)	O(2)#1-Ce(2)-Ce(3)#1	35.4(2)
O(3)-Ce(2)-Ce(3)#1	36.9(2)	O(72)-Ce(2)-Ce(3)#1	72.2(2)
O(11)-Ce(2)-Ce(3)#1	162.8(2)	O(52)-Ce(2)-Ce(3)#1	108.9(2)
O(22)-Ce(2)-Ce(3)#1	110.2(2)	O(4)-Ce(2)-Ce(3)	35.0(2)
O(1)-Ce(2)-Ce(3)	35.5(2)	O(2)#1-Ce(2)-Ce(3)	88.2(2)
O(3)-Ce(2)-Ce(3)	91.30(14)	O(72)-Ce(2)-Ce(3)	162.2(2)
O(11)-Ce(2)-Ce(3)	72.8(2)	O(52)-Ce(2)-Ce(3)	109.6(2)
O(4)-Ce(2)-Ce(1)	89.8(2)	O(1)-Ce(2)-Ce(1)	33.6(2)
O(2)#1-Ce(2)-Ce(1)	98.2(2)	O(3)-Ce(2)-Ce(1)	35.7(2)
O(72)-Ce(2)-Ce(1)	108.7(2)	O(11)-Ce(2)-Ce(1)	108.5(2)
O(52)-Ce(2)-Ce(1)	166.8(2)	O(22)-Ce(2)-Ce(1)	72.5(2)
Ce(3)#1-Ce(2)-Ce(1)	60.82(2)	Ce(3)-Ce(2)-Ce(1)	60.65(2)
O(4)-Ce(2)-Ce(1)#1	36.1(2)	O(1)-Ce(2)-Ce(1)#1	90.2(2)
O(11)-Ce(2)-Ce(1)#1	108.2(2)	O(52)-Ce(2)-Ce(1)#1	71.7(2)
O(22)-Ce(2)-Ce(1)#1	166.8(2)	Ce(3)#1-Ce(2)-Ce(1)#1	60.57(2)
Ce(3)-Ce(2)-Ce(1)#1	60.686(13)	Ce(1)-Ce(2)-Ce(1)#1	92.29(2)
O(2)-Ce(3)-O(4)	106.0(4)	O(2)-Ce(3)-O(1)	67.6(3)
O(4)-Ce(3)-O(1)	69.8(3)	O(2)-Ce(3)-O(62)#1	77.4(3)
O(4)-Ce(3)-O(62)#1	143.6(3)	O(1)-Ce(3)-O(62)#1	78.8(3)
O(2)-Ce(3)-O(32)	142.6(2)	O(4)-Ce(3)-O(32)	77.3(2)
O(1)-Ce(3)-O(32)	141.8(2)	O(62)#1-Ce(3)-O(32)	122.3(2)
O(2)-Ce(3)-O(3)#1	71.5(3)	O(4)-Ce(3)-O(3)#1	69.7(3)
O(1)-Ce(3)-O(3)#1	109.4(3)	O(62)#1-Ce(3)-O(3)#1	140.8(3)
O(2)-Ce(3)-O(12)	139.7(2)	O(4)-Ce(3)-O(12)	76.4(3)
O(1)-Ce(3)-O(12)	76.3(3)	O(62)#1-Ce(3)-O(12)	78.6(3)
O(32)-Ce(3)-O(12)	77.7(2)	O(3)#1-Ce(3)-O(12)	140.4(2)
O(2)-Ce(3)-O(71)#1	77.6(3)	O(4)-Ce(3)-O(71)#1	138.9(2)
O(1)-Ce(3)-O(71)#1	141.3(2)	O(62)#1-Ce(3)-O(71)#1	77.6(2)
O(32)-Ce(3)-O(71)#1	76.8(2)	O(3)#1-Ce(3)-O(71)#1	73.1(2)
O(12)-Ce(3)-O(71)#1	127.4(2)	O(2)-Ce(3)-Ce(2)#1	35.1(2)
O(4)-Ce(3)-Ce(2)#1	88.2(2)	O(1)-Ce(3)-Ce(2)#1	88.2(2)
O(62)#1-Ce(3)-Ce(2)#1	109.3(2)	O(32)-Ce(3)-Ce(2)#1	109.9(2)
O(12)-Ce(3)-Ce(2)#1	161.1(2)	O(71)#1-Ce(3)-Ce(2)#1	71.5(2)
O(2)-Ce(3)-Ce(2)	88.1(2)	O(4)-Ce(3)-Ce(2)	34.9(2)
O(1)-Ce(3)-Ce(2)	35.0(2)	O(62)#1-Ce(3)-Ce(2)	111.2(2)
O(32)-Ce(3)-Ce(2)	109.6(2)	O(3)#1-Ce(3)-Ce(2)	91.20(14)
O(12)-Ce(3)-Ce(2)	71.2(2)	O(71)#1-Ce(3)-Ce(2)	161.6(2)

Appendix 4 : List of papers published and in progress

1. "The Synthesis and X-ray Structure Characterisation of the volatile complexes $[Sr(tmhd)_2\{Me(OCH_2CH_2)_3OMe\}]$ and $[Sr_2(tmhd)_4\{Me(OCH_2CH_2)_2OMe\}_2(\mu\text{-}H_2O)]$ (Htmhd = 1,1,1,6,6,6-Tetramethylheptane-2,4-dione", Simon R. Drake, Michael B. Hursthouse, K. M. Abdul Malik and Stewart A. S. Miller, *J. Chem. Soc., Chem. Commun*, 1993, 478.

2. "Monomeric Group IIa Metal β-diketonates Stabilized by Multidendate Glymes", Simon R. Drake, Stewart A. S. Miller and David J. Williams, *Inorg. Chem*, 1993, 32, 3227.

3. "Monomeric Strontium and Barium β-diketonate adducts with Polyethers; the X-ray crystal structures of $[Sr(dppd)_2(tetraglyme)]$ and $[Ba(tmhd)_2(tetraglyme)]$", Simon R. Drake, Michael B. Hursthouse, K. M. Abdul Malik and Stewart A. S. Miller, *Polyhedron*, 1993, 12, 1621.

4. "Oxygen or Nitrogen Chelates Stabilising Barium and Yttrium β-diketonates", Simon R. Drake, Michael B. Hursthouse, K. M. Abdul Malik, Stewart A. S. Miller, and David J. Otway, *Inorg. Chem.*, 1993, 32, 4464.

5. "Synthesis and Single Crystal X-ray Structure of the Diglyme bridged Barium Complex $[Ba(tmhd)_2(diglyme)]_2$", Simon R. Drake, Michael B. Hursthouse, K. M. Abdul Malik and Stewart A. S. Miller, *Inorg. Chem.*, 1993, 32, 4653.

Papers currently in progress:

1. "A simple route to stabilised monomeric calcium and strontium β-diketonates, and the X-ray structures of $[M(fod)_2(triglyme)]$ (where M = Ca and Sr)." Submitted to Polyhedron.

2. "Monomeric Group IIA Metal β-diketonates Stabilised by Protonated Amine Ligands as Tight Cation-Anion Pairs; and the X-ray Crystal Structure of $[Sr(tfpd)_4(H\text{-}tmeda)_2]$." Submitted to Dalton Transactions.

3. "A Facile Synthesis of Alkaline Earth Metal β-Diketonates and the X-ray Structure of the Loose Dimer $[\{Ca(hfpd)_2\}_2(heptaglyme)]$." Journal of the Chemical Society, Dalton Transactions.

4. "The Synthesis and Characterisation of the First Monomeric Homoleptic Calcium β-diketonate Complex; and the X-ray structures of $[HCa(dppd)_3]$, and $[Ca(dppd)_2(PMDETA)]$." Journal of the Chemical Society, Chemical Communication.

5. "Soluble Hexanuclear Cerium (iv) Carboxylates, the X-ray Crystal Structures of $[Ce_6H_2(OH)_2O_6(eb)_{12}(EtOH)_2]$ and $[Ce_6H_2(OH)_2O_6(dmp)_{12}(dmp\text{-}H)_2]$ (where eb = 2-ethylbutyrate and dmp = 2,2-dimethylpentanoate)." Journal of the Chemical Society, Dalton Transactions.